U N I V E R S I T Y O F S T R A T H C L Y D E

SCHOOL OF

MECHANICAL AND CHEMICAL

ENGINEERING

AND NAVAL ARCHITECTURE

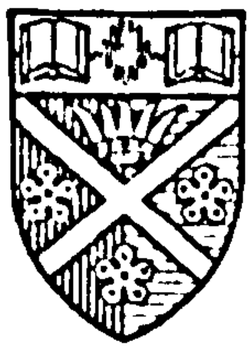

BIOMECHANICAL EVALUATION OF PROSTHETIC FEET

by

James C. H. Goh, BSc(Hons)

Thesis submitted for the Degree of

Doctor of Philosophy in Bioengineering

Bioengineering Unit

September 1982

"I will lift up my eyes to the mountains;
From whence shall my help come?
My help comes from the Lord,
Who made heaven and earth.

He will not allow your foot to slip;
He who keeps you will not slumber.
Behold, He who keeps Israel
Will neither slumber nor sleep."

Psalm 121:1-4

To

Monica, Evangeline and Jared-James

ACKNOWLEDGEMENT

I wish to sincerely thank Professor J.P. Paul for giving me the opportunity to undertake the work described in this thesis. To this extent, the University of Strathclyde for making the Open Postgraduate Studentship Award available to me.

I am deeply indebted to Mr. S.E. Solomonidis, my supervisor, for his constructive criticism, invaluable advice and the encouragement given to me throughout this project.

I would also like to express my appreciation to the assistance given to me by the staff of the Bioengineering Unit, in particular, Mrs. S. Nicol (Computer Programmer), Mr. W. Spence (Prosthetist), Mr. R. Donaldson (Prosthetic Technician), Mr. H. Beveridge, Dr. J. Courtney and Mr. M.S. Zahedi (Research Assistant). Thanks are also due to Mr. N. Govan (Prosthetist) and Ms C. Sclater(Librarian) of the National Centre. The kind participation of the patients is also acknowledged with thanks.

I am extremely grateful to Johnny and Gina Goh, for their understanding and kind assistance during the final stages of this project. Words fail to express my thankfulness to my beloved wife, Monica, for not only typing this thesis but also for her perseverance and trust in me.

A B S T R A C T

An evaluation method was developed which can be used generally for the assessment of any prosthetic feet. The two most common prosthetic feet prescribed to below-knee and above-knee amputees are the Uniaxial and SACH feet. A review of prescription practices shows that in the United Kingdom about 80% of the below-knee and above-knee amputees are fitted with a Uniaxial foot, whereas in the United States about 80% are fitted with the SACH foot.

These contradictory prescription practices between the two countries, prompted the project to be concentrated on the evaluation of the SACH and Uniaxial feet. The method developed includes a subjective assessment procedure and a biomechanical evaluation on the function of the two prosthetic feet and their effects on whole body gait kinematics and lower limb kinetics.

A review of the methods used in gait analysis is presented in the thesis. This forms a basis for the selection of a suitable gait recording system for the project. A background study of lower limb prosthetics in general and a review of prosthetic ankle/foot assemblies in particular are also presented.

The methodology and instrumentation used in the project are given. Altogether, six below-knee and five above-knee amputees were tested. Due to insufficient supply of heel bumper stiffness by the manufacturer for the Uniaxial foot, heel bumpers of varying stiffnesses had to be made in the Bioengineering Unit.

The development of the analytical procedure for the three-dimensional analysis is presented. A suite of computer programs was written to facilitate the handling of the large amount of data, details of which are included in the Appendix.

Results from the analysis of the tests performed are discussed. Although some apparent differences were observed between the SACH and Uniaxial feet, no conclusion can be drawn as to which is better for the function of the amputee.

CONTENTS

CHAPTER 1

Introduction

Introduction

A large number of ankle/foot assemblies has been designed, some incorporating ingenious mechanisms capable of reproducing certain functions and movements of the normal foot. However, the complexity of the designs, the excessive maintenance required and their unacceptably high mass have prevented their wide use.

By far the most common type of prosthetic foot used has been the Uniaxial foot, in which limited plantar flexion and dorsiflexion is permitted. This foot is relatively simple to fit to the patient and to maintain. However, it has several disadvantages; the moving parts can cause noise and wear; furthermore the appearance of the junction line between the prosthetic foot and the shank could be objectionable. The change in resistance that arises at the ankle joint during locomotion could also cause problems for some patients.

The development of the Solid Ankle Cushion Heel (SACH) foot in the 1950s, was the result of an attempt to overcome some of these problems. The SACH foot functions without the use of an articulated ankle joint. A wedge of cushioning materal at the heel provides the shock absorption during heel strike and a wooden keel shaped at the ball of the foot provides a rolling action. The foot requires minimal maintenance, has good appearance and is quiet during operation. Its main disadvantages are that it has no adjustment in plantar/dorsiflexion and a shorter life.

Prescription criteria for prosthetic foot and ankle units have been derived from experience gained by the clinician and the prosthetist. They tend to vary depending on the country and particular limb fitting centre. In the United Kingdom about 80% of the prosthetic

feet prescribed for the below- and above-knee amputees are Uniaxial feet, whereas in the United States about 80% of the prosthetic feet prescribed for the same groups of patients are SACH feet. The reason for this drastic difference in prescription practice is not readily clear.

In 1955, New York University was contracted by the Veterans Administration to determine the performance of the SACH foot as compared with the Uniaxial foot. A high level of acceptance of the SACH foot was indicated in their clinical analysis. Their engineering evaluation with force plate data showed that the above-knee amputees had smoother transition from heel to toe with the SACH foot. Following on, in the 1960s, clinical experiences showed a high percentage of preference for the SACH foot and that it was already in widespread use throughout the United States. There was no report of such a nature in the United Kingdom to indicate the preference of the Uniaxial foot, although it had been suggested that better knee stability could be achieved with the Uniaxial foot.

In reviewing existing literature and in conversation with experienced prosthetists, it is believed that in general a high percentage of SACH feet should be prescribed for the unilateral below-knee amputee, since the intact knee on the prosthetic side is capable of control. For the above-knee amputees, both the Uniaxial and SACH feet should be used, depending on the activity level of the patient, SACH being used for the active type and Uniaxial for the geriatric and enfeebled patient. This however is a broad rule of thumb and to date has not been backed up by scientific studies. Furthermore, the choice of the stiffness of the bumpers of the Uniaxial foot or heel of the SACH foot is decided subjectively. It is evident therefore that there is a lack of objective information and it was thus decided firstly to

perform a biomechanical evaluation on the function of the two prosthetic feet and secondly to investigate their effects on whole body gait kinematics and lower limb kinetics.

The below- and above-knee amputees form more than 80% of the amputation population and are prime users of prosthetic feet. Therefore, these two groups of amputees were considered in the project. Altogether, 6 below-knee and 5 above-knee amputees were tested. In order to keep variables which can influence the results down to a minimum, it was necessary to provide each patient with an experimental prosthesis which is flexible enough to accommodate either the SACH or Uniaxial foot. The Otto Bock Modular System was found to be very suitable for this purpose.

An evaluation method was developed, which can be used generally for the assessment of any prosthetic feet. It is however applied to the evaluation of the SACH and Uniaxial feet, for reasons already mentioned. The method includes a subjective assessment procedure and a quantitative assessment technique.

The quantitative assessment was done by recording the patient's gait by means of three cine-cameras and measuring the ground load actions using two force plates. This permitted three-dimensional analysis on the contralateral sides of the subject. The analytical procedure for the experimental system was designed to perform whole body gait kinematics and lower limb kinetics during locomotion. A suite of computer programs was written in the Fortran IV language to facilitate the handling of the large amount of data. Repeatability tests were performed on the system with one normal subject and one above-knee amputee, so as to check and compare the range of scatter inherent in the methodology.

CHAPTER 2

Review of Analytical Methods in Human Locomotion Studies

2.1 Body Segment Parameters

It is a fundamental requirement in the study of human locomotion, especially when performing kinetic analysis to determine the physical properties of the limb segments under consideration. Those body segment parameters required are: (1) mass of segment, (2) location of the centre of mass, and (3) mass moment of inertia.

The history and measurement techniques(both in-vivo and in-vitro) used in determining these body segment parameters are well documented in Drillis et al (1964), Miller and Nelson(1973) and Chandler et al (1975). Only a brief discourse on investigations that are of interest to this project is presented.

Harless(1860) reported on data collected from two male cadavers and introduced the method of coefficients in determining body segment parameters. They are :

C1 - ratio of body segment mass to total body mass,

C2 - ratio of distance between proximal joint and centre of mass of segment to total segment length,

C3 - ratio of radius of gyration to total segment length.

However, Harless only produced data concerning body segment mass and the position of the centre of mass.

Meeh(1884) was perhaps the first to report on data obtained from living subjects(eight males and two females). However, only the mass of the body segments was investigated.

Braune and Fischer(1889) presented information on three male cadavers. The coefficients C1, C2 and C3 derived from these data were even used by researchers of

the 1960s in their kinetic analysis.

Bernstein and his associates(1936) realising the inadequacy of the data used by Harless and by Braune and Fischer, performed a study on 152 living subjects of both sexes(76 males and 76 females). However, the investigation did not include the head, hands and feet.

Dempster(1955) obtained and presented results based on eight male cadavers. The coefficients derived from these results are still widely used and recommended for use in human motion studies by Plagenhoef (1971) and Winter(1979).

The team in New York University(NYU) conducted two series of studies. The first one was reported by Drillis and Contini(1966), where 12 live subjects were used. In their presentation, they combined all the coefficients obtained from previous investigators and produced weighted averages of the coefficients. The second study was reported by Contini(1972), where results of 17 live subjects (9 males and 8 females) were presented. However, not all data were recorded for every subject. Data on 19 additional subjects, with either hemiplegia or an amputation were also presented.

Several other studies had been conducted in the 1960s and 1970s besides those at NYU. Most of them were initiated by the Aerospace Medical Research Laboratory in the U.S.A., Chandler et al (1975). However, most of the data are not available for comparison, except for the work of Clauser et al (1969) who performed their study on 13 male cadavers. The derived coefficients were cited in Miller and Nelson(1973). Chandler et al (1975) also used the same method and technique as Clauser et. al. in their "Investigation of the inertial properties of the human body". Six male cadavers were used to obtain the information required.

	C1	C2	C3
		M E A N (± 1 S.D.)	
ONE THIGH	0.1027 (±0.0119)	0.4169 (±0.0325)	0.2912 (±0.0384)
ONE SHANK & FOOT	0.0632 (±0.0036)	0.4673 (±0.0455)	0.3467 (±0.0639)
ONE SHANK	0.0453 (±0.0035)	0.4030 (±0.0260)	0.2890 (±0.0134)
ONE FOOT	0.0152 (±0.0019)	0.5000 -	0.4750 -

Table 2.1. Coefficients of Body Segment Properties

The availability of additional information on body segment parameters obtained after 1966, enabled this author to include them in those presented by Drillis and Contini (1966). Table 2.1 gives the "new" set of coefficients of the lower limb segments, which are relevant to the analysis. Only data derived from male subjects were used. The standard deviation of the data is also presented, this could be used as an indication of the error inherent in the prediction. The details of the derivation are given in Appendix (A).

2.2 Kinematic Measurement

Human locomotion has been a subject of interest for a very long time. Ancient ruins from archaelogical excavations suggest this concern/interest either in art form or for communication. Greek philosophers, like Hippocrates(c.450 BC), Aristotle (c.350 BC) and Archimedes(c.250 BC), out of curiosity applied themselves to the understanding of it. Leonardo da Vinci (c.1500 AD), in his 'Notes on the human body' was perhaps the first to make systematic but still subjective observations of human movement.

The first indication of a scientific(theoretical) approach was in the seventeenth century. Borelli (1680) applied the sciences of mathematics, physics and anatomy to the understanding of human locomotion. This stimulated and accelerated greater interest in this field of combined sciences. In 1836, the Weber brothers presented a theory of locomotion which concluded that the swing phase of gait was a pure pendulum motion. This was however repudiated by successive investigators.

The state of the art was purely subjective and theoretical until the introduction of objective recording instruments. The following sections will be devoted to

Figure 2.2.1(a) One of Marey's subjects
(from Bernstein, 1967)

the development of these objective recording instruments for human locomotion, which allow quantitative analysis to be performed.

2.2.1 Photographic Techniques

Photography is by far the oldest method used in recording human motion yet it is the most widely used. There are basically two types of recording methods :

(a) recording of the entire movement on a single photographic plate,(or multiple exposure technique) and;

(b) recording each instant of movement in time on separate photographic negatives (or cinematography).

(a) Multiple exposure technique

This method in its earliest form was introduced by Marey (1873). His subject was dressed in black with bright reflective strips and spots to define the limb segments and joints, respectively, see Figure 2.2.1(a). These identifiers when illuminated showed up the movements of the subject and were photographed as a series of images on a single plate. This is called cyclography or cyclogrammetry and it has a limitation, in that the relative displacement of the joints and segments cannot be readily discerned. Hence, in 1886, he improved the technique by including a rotating shutter in the camera to overcome the problem. The images produced were in the form of 'sticks' and are called 'stick diagrams'. This inclusion of the sense of time in cyclography is termed chronocyclography.

This method has since then been modified and the quality improved. Braune and Fischer (1895) replaced the passive identifiers by "Geisler" tubes, which emit light intermittently at a frequency of 26 flashes per second. Using 4 open lens cameras in the layout as shown in

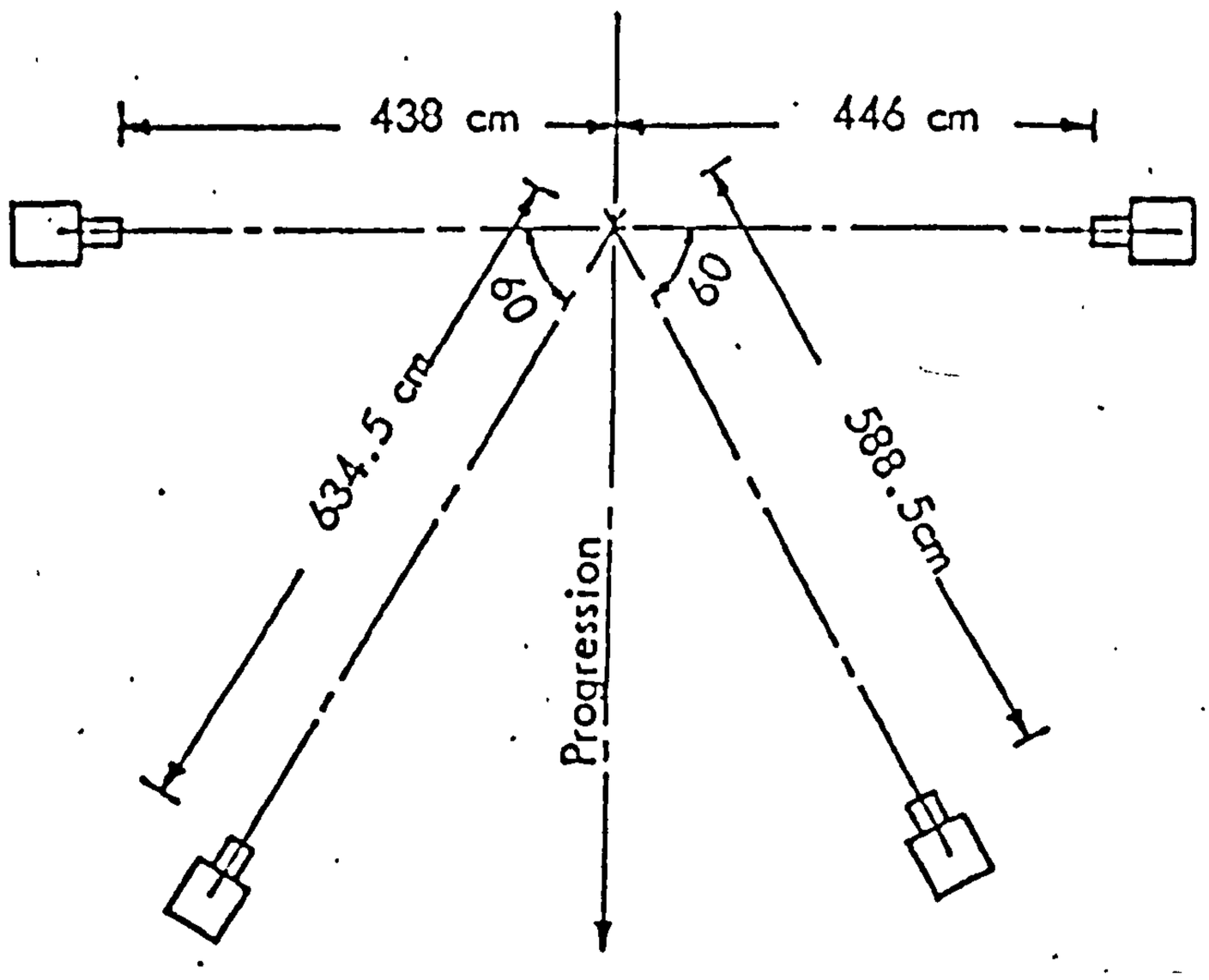

Figure 2.2.1(b) Braune and Fischer's arrangement for photographic recording of gait
(redrawn from Braune and Fischer, 1895)

Figure 2.2.1(b), they were able to perform 3 dimensional analysis. Calculating the velocities and accelerations from displacement data, and together with the body segmental parameters, some force actions on the body were evaluated.

In order to overcome the undifferentiable trajectories of overlapping movement in cyclography, Bernstein (1927) introduced kymocyclography or gliding cyclography (Drillis 1958). Instead of using a stationary plate, cyclographic exposures were taken on a slowly and evenly moving plate. This method was used in recording activities involving repetitive movement of the arms such as metal filing, sawing and hammering etc. It is rarely if ever, used nowadays especially in human gait recording.

Bernstein and Popova (1929) experimented with the chronocyclographic method, using even smaller electric light bulbs (approximately 1 mm filament length). A rotating shutter was positioned in front of an open lens camera and they claimed a frequency of up to 600 per second. However, most of their work was done using between 60 and 190 exposures per second.

Eberhart and Inman (1947) reported their extensive studies on human locomotion and related information on the design of artificial limbs. One of the methods they used in gait recording was interrupted light photography which is essentially chronocyclography. This was accomplished by the use of a rotating shutter in front of the open lens camera and opthalmic electric light bulbs were used as body markers. The speed of the rotating shutter was 30 rev/s and the slit on the shutter disc was 18 degrees, thus giving an exposure of 1/600 second. A 35 mm cinecamera was used to obtain the frontal view. They later concluded that interrupted light photography was "not particularly useful in the evaluation of gait"

(Eberhart et al ,1954). This was perhaps due to the difficulties they encountered in trying to obtain an accurate third dimension from their system.

Two methods of three dimensional recording using an interrupted light technique were described by Bernstein (1934). One involves the use of a large plane mirror placed at a known angle to the main optical axis of the camera. Only a single camera is required to obtain the direct, as well as the reflected images. From these the three spatial coordinates of a marker can be derived. The second method involves the use of a pair of stereoscopic cameras, either with parallel or convergent optical axes. The parallel axes type is limited by their fields of view. The convergent axes type is much more versatile and is popularly known as stereo-photogrammetry.

Murray et al (1964) mounted a mirror at an angle of 25^{o} over the walkpath, such that the overhead projection of the transverse movement could be recorded on the same photographic plate. The interrupted light source comes from a stroboscope, flashing at 20 times per second at the reflective markers. The camera lens was kept open and the test was performed in semi-darkness.

Lippert (1973) used a stereocamera system (i.e. two "calibrated" still cameras connected by a base of known length) to study the mobility of fracture fragments of the tibia. Reflective markers with a stainless steel stem were inserted into the bone and tests were performed in a darkened environment under stroboscopic lighting. The author claimed a measurement resolution of 1 to 1.5mm for the stereoscopic field of $(2.0 \times 2.0 \times 0.5)\ m^{3}$.

Cappozzo (1981) used stereophotogrammetry to study the linear movement of the head and trunk. Yellow light

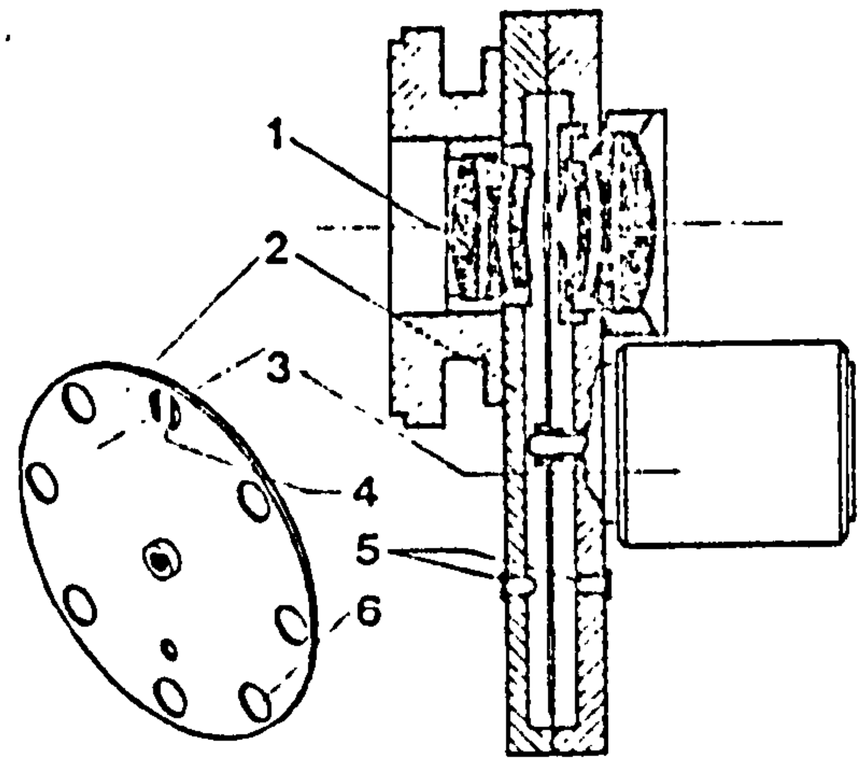

1) Lens - Symmar f. 5.6/100mm, stopped down to f/22.

2) Rotary shutter - 0.3mm aluminum sheet.

3) Stepping down motor - 7.5deg. per step, 90-120 steps per sec. to 1,200 steps per sec.

4) Partially masked hole

5) Photoelectric cell

6) Shutter apertures - equidistance accurate to nearest 1/100mm.

The casting is made of aluminum and can be matched to most single-lens reflex cameras up to maximal size of 6.5 x 9cm.

Figure 2.2.1(c) Baumann's chronocyclographic device (from Baumann, 1974)

emitting diodes (LED) were used as markers; their frequency range was from 30 to 60 impulses per second. Four 35 mm still cameras (with open shutters) were placed in stereoscopic pairs with convergent optical axes. Filming was carried out in a laboratory illuminated with green lighting, so as to "guarantee" a sufficient contrast with the yellow light LEDs. An accuracy of $\pm$2.5 mm for the 'X' and 'Z' displacements and $\pm$8mm for the "Y" displacement was claimed at the periphery of the stereoscopic field of (2.2 x 1.9 x 0.3) m^3.

Several disadvantages are inherent in interrupted light photographic technique. One of them is identification problems, i.e. when movements overlap and when a point remains more or less stationary. Baumann (1974) described several constructional features in his chronocyclographic system, which attempt to overcome this difficulty. One of the eight holes on the rotating shutter disc was partially masked, this was to produce shorter images in the plate for identification. A photocell was used to detect the partially masked hole and produce an output pulse to synchronise the two planar stereoscopic pictures, see Figure 2.2.1(c). For indoor filming, high intensity miniature filament bulbs were used as markers, with normal indoor lighting. While for outdoor filming, infra-red LEDs were used. The accuracy claimed by the author, was in the order of $\pm$ of 1 mm for 'X' and 'Z' displacements and $\pm$3 mm for 'Y' displacement for the stereoscopic field of (6 x 6 x 1.8) m^3.

The multiple exposure technique already described has the advantage of producing all the information on a single photographic picture, which can be obtained instantly by using polaroid cameras, Milner et al (1973). Results obtained from this method have been claimed to be fairly accurate. However, it has several disadvantages. The stroboscopic flashing, associated with one of the

interrupted light method, could produce a hypnotic effect on the subject and alter his gait pattern. Other methods which require filming in semi-darkness or "strange" lighting could also influence the natural gait pattern of the subject especially that of pathological subjects. Furthermore, wiring attachment of either electric bulbs or LEDs may restrict movement. The stereophotogrammetry method requires very precise alignment of the stereoscopic pair of cameras, in order to obtain accurate results. The stereocamera itself is limited by its critical distance between the two camera lenses, such that the field of view is restricted.

(b) Cinematography

This method was first used by Muybridge (1882) in the recording of racing horses. In further investigation, in 1901, human movements were recorded. Successive phases of motion were filmed by 24 cameras, with shutters operated by an electrical device of his own design. To allow for quantitative assessment, pictures were taken with a huge grid board in the background.

Marey (1885) devised a "photographic gun" which was able to film at 12 frames per second and had an exposure of 1/720 second. This in effect was the predecessor of cinephotography or cinematography. However, this technique did not gain popularity among researchers in human locomotion at this early stage because of the low filming rate and the difficulties involved in data reduction.

Elftman (1939) studied several aspects of the human gait using only one cinecamera. Filming was made in the saggittal plane to obtain displacement data in two dimensions.

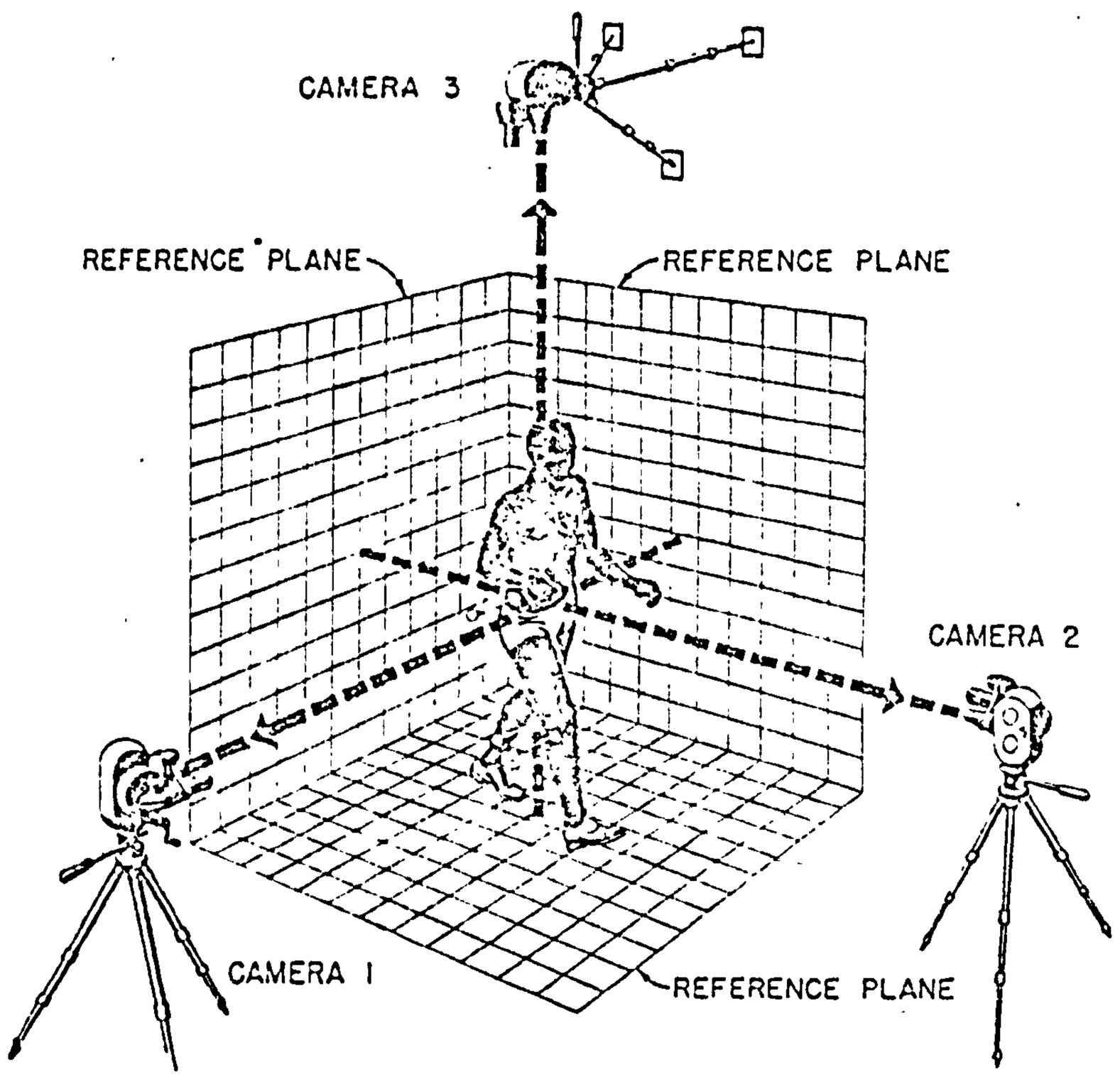

Figure 2.2.1(d) Arrangement of cinephotographic system of Eberhart and Inman(1947)

Eberhart and Inman (1947), as previously mentioned, presented two other methods incorporating the use of 35 mm cine cameras operating at 48 frames per second. The first method involved using three such cameras positioned 25 feet from the subject on the principal axes, so that the front, side and top views were obtained, see Figure 2.2.1(d). Wooden markers were attached to stainless steel screws driven into bony prominences. This was used to determine the transverse rotation of the lower extremity during locomotion (also described in Levens et al ,1948). The second method used a glass walkway with an inclined mirror underneath. One cinecamera was positioned normal to the saggittal plane, taking the lateral view as well as the view from the mirror. Another cinecamera was used to film the frontal view. Besides adhesive tape markers, a special pelvic girdle with an anterior extension and a 'U' shaped ankle bracket with three locating pins were used on the subject. The results for these two methods are questionable, due to the uncomfortable marking system which may have influenced the natural gait. However, the arrangement of the cameras does allow three dimensional analysis.

Bresler and Frankel (1950) presented a three dimensional analysis of the lower extremity, utilising two 35 mm cinecameras (front and side) operating at 40 frames per second. Skin markers, in the form of small white targets on black background tapes were used to indicate the hip, knee and ankle joint centres. Data reduction was done by projecting the image to half scale. There was no indication of any correction for parallax errors being performed.

Paul (1967) used the same method as Bresler and Frankel, except that the cinecameras were 16 mm and operated at 50 frames per second. The films were re-exposed to superimpose a grid board of 5 in. squares

as a reference. This improved the accuracy of data reduction and parallax errors were corrected. Ishai (1975) extended the method to include an additional side camera, so that the whole body movement (i.e. the contralateral lower extremities, and head, arm and trunk (HAT))could be analysed in 3-dimensions.

One question associated with cinematography is the frame rate. The sampling theorem states that the sampling frequency must be at least twice as high as the highest frequency in the signal. However, it must also be high enough to define the movement. Simon (1981) tried out several sampling rates and concluded that 50 frames per second was perhaps the best for analysing the walking movement.

One major setback in cinematography is the time consuming effort required in data reduction. However, Pepoe(1970) introduced an automated system for digitising cine films. The system comprises of three sheets of fibre optics interfaced to a mini-computer. The film is then projected onto the fibre ends and is scanned one line at a time for any light spots. The limitation of the system is that markers cannot be placed close together, otherwise erroneous coordinates will result if they fall on the same scanning line. The process rate of 2 frames per second is quoted. Further processing is required to relate the coordinates to the particular marker. Kasvand et al (1971) developed a computer-based system to process cine films automatically also. A computer controlled flying spot scanner was used to analyse each frame. An initial coarse scan of the first frame was performed to identify the code and marker dot, as well as a neighbourhood for each dot. Subsequently, the computer reads the code and locates the specified dots from frame to frame and produces continuous on-line displays. Without operator intervention, the processing

speed for one frame with 5 dots is about 15 seconds.

These are initial attempts to design and develope a fully automated system for data reduction of cine films. Further investigations are required in this area to produce an efficient, versatile and low cost system, which will definitely revolutionise the cinematographic technique in human locomotion. An added advantage of the cine films is that they provide a permanent visual record of the event.

2.2.2 Optoelectric Techniques

In an effort to overcome the tedious and time consuming manual data reduction procedures of the photographic methods, and to provide in addition an on-line gait analysis system suitable for clinical use, several optoelectric systems have been designed and developed over the years. They are as follows :

(a) The Television/computer systems
(b) The 'SELSPOT' system
(c) The 'CODA' system

These systems were introduced either in the late 1960s or early 1970s. Most of them are still undergoing modification and trials to improve performance in data collection. The following describe briefly the development of each system.

(a) The Television/comouter systems

Several television based systems for human motion recording have been developed independently. However, all the systems used the same basic principle in acquiring the two dimensional cartesian coordinates of the marker images. That is, through the scanning action of the television camera, the detected marker image is referenced

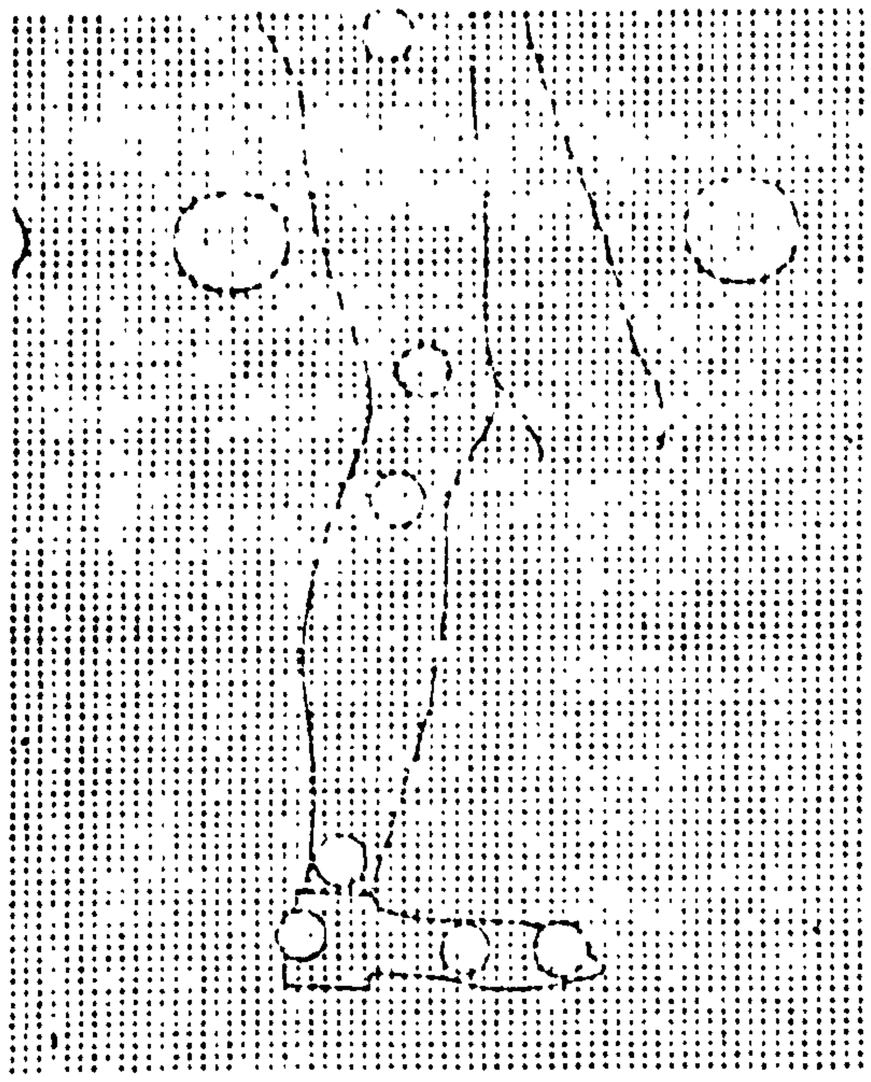

Computer print-out of one converted T.V. field. One bit resolution is required (0 for black, 1 for bright) Contour of leg is drawn in merely to indicate the position of the markers. Background markers are larger and easily identified, and serve as an absolute spatial reference in the plane of progression

Figure 2.2.2(a) Diagrammatic representation of video signals from TV-computer system
(from Winter et al,1974)

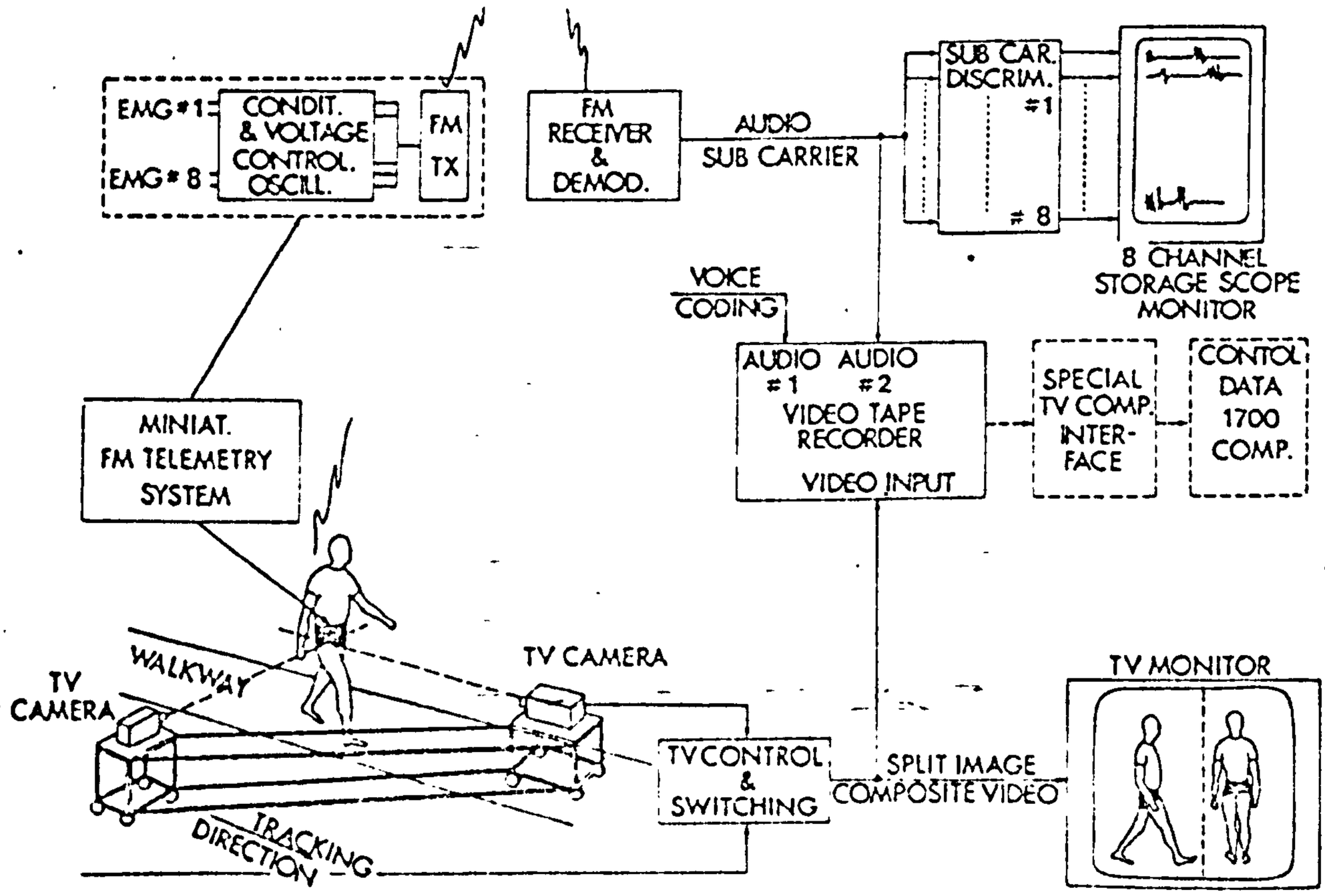

Figure 2.2.2(b) Schematic view of TV-computer-EMG recording system
(from Letts et al,1975)

to the scan line and the position on this line.

Furnee (1967) was perhaps the first to utilise a television based system for measuring human movement. Small electric light bulbs were used as markers to define the anatomical landmarks on the arm. Digitising of the video signals was carried out by digital counters. This was further improved by incorporating buffer memories into the system which allowed data to be transferred to the computer during the field blanking period. A synchronous rotary shutter, operating at 50 cycles per second, was also introduced into the system to provide simultaneous sampling of the markers. The exposure was 1/508 of a second. Due to design criteria, only 5 markers can be used. Furthermore, only one camera was used in the system, thus restricting their studies to two dimensions.

Waas (1969) developed a three dimensional television based system, using two cameras to provide bi-planar views of the electric bulbs. Digital counters were used to provide the coordinates, which were transferred immediately to the magnetic tape. This transfer time imposes restriction on marker arrangement, i.e. at any time during locomotion, the markers must not come within 9 scan lines of each other. Moreover, a maximum of only 4 markers could be used.

Winter et al (1972) described a system, which employed a general purpose computer interface developed by Dinn et al (1970) to perform the analogue to digital conversion of video signals. The interface was set to give a sampling matrix of 96 by 96 points for each television field. See Figure 2.2.2(a). This resulted in a very high data rate and therefore required a fairly large computer. Relatively large reflective hemispherical markers of 38 mm in diameter (i.e. half a ping pong ball)

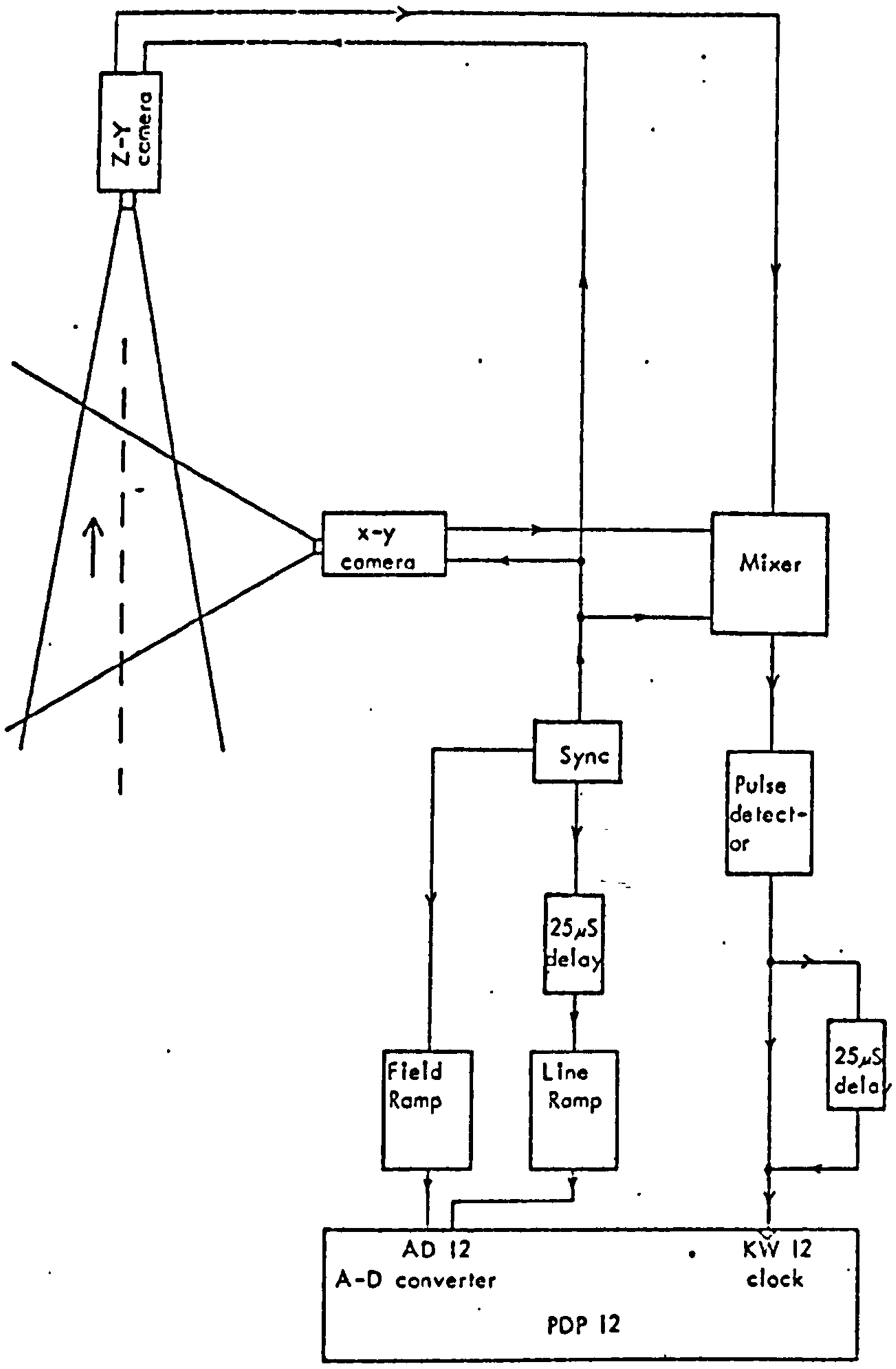

Figure 2.2.2(c). Block diagram of 3-D TV-computer system.

(from Jarrett,1976)

were used. This is because they found that the more sampling points there are within the marker image boundary, the more accurately the marker centre can be calculated. It was claimed that a diameter of 4 sample points gives a mean error of 3% of the marker diameter, i.e. about 1 mm. In order to maintain this accuracy from the relatively coarse sample matrix, a small field of view is needed, thus making it necessary for the television camera to track the walking subject. A later development includes a second camera to obtain the frontal view, Letts et al (1975), making it possible for three dimensional recording. Figure 2.2.2(b) shows their set up which also records EMG signals simultaneously.

Cheng (1974) used an on-line mini-computer to obtain data from one television camera. This system is in some ways similar to the one developed in Delft University. Digital counters were used to obtain the coordinates, which were then stored in a buffer register and transferred to the computer under program control. On transfer the data were checked and evaluated. The system is limited to detecting a maximum of one marker on any line due to the long processing time taken in transferring and evaluating a single marker. This effectively restricts the use of more than one marker on the same vertical height.

Jarrett (1976) working at the University of Strathclyde developed a system, which could incorporate up to six television cameras to acquire 3 dimensional kinematic information. However, only a two-camera system was installed, see Figure 2.2.2(c). Digital counters were used to obtain the coordinates, which were stored in buffer memories and transferred to the computer during the line blanking period. Up to six horizontal coordinates can be digitised and stored in a single scan line. The sampling rate was 50 Hz. Passive

retro-reflective markers, made from 7 mm diameter beads, were used. A tungsten halogen lamp positioned close beneath the camera, provides a light source for the reflection of the markers. This poses a limitation to the system in that other cameras have to avoid getting the lighting in their field of view. Therefore, simultaneous recording of the contralateral sides of the body is not possible with the present camera layout. Furthermore, the bright and intense light source is directed toward the subject and tends to cause temporary blindness thus affecting his natural walking pattern. It was claimed that the system has a resolution of 0.1% and 0.3% for the horizontal and vertical data respectively.

Jarrett (1980) recently developed a new interface for the PDP11 computer. It is now commercially available under the trade-name "Vicon" through Oxford Medical Computers, U.K. (1981).

Andrews et al (1981) in their attempt to overcome some of the problems in the Strathclyde T.V./Computer system, introduced an infra-red illuminator together with a rotary shutter. This they claimed also improved the spatial accuracy. However, the complete system is still under development at the time of writing.

(b) The 'SELSPOT' system

The 'SELSPOT' (an acronym for 'selective light spot recognition') is a commercially available system from Selcom AB of Partille, Sweden (1975). This system was originally developed at the Chalmers Institute of Technology, Gotëburg by Lindholm (1974). It is based on a continuous light spot position sensitive, silicon photodiode sensor. A light spot impinging on the surface of the sensor, varies the current in the load resistances,

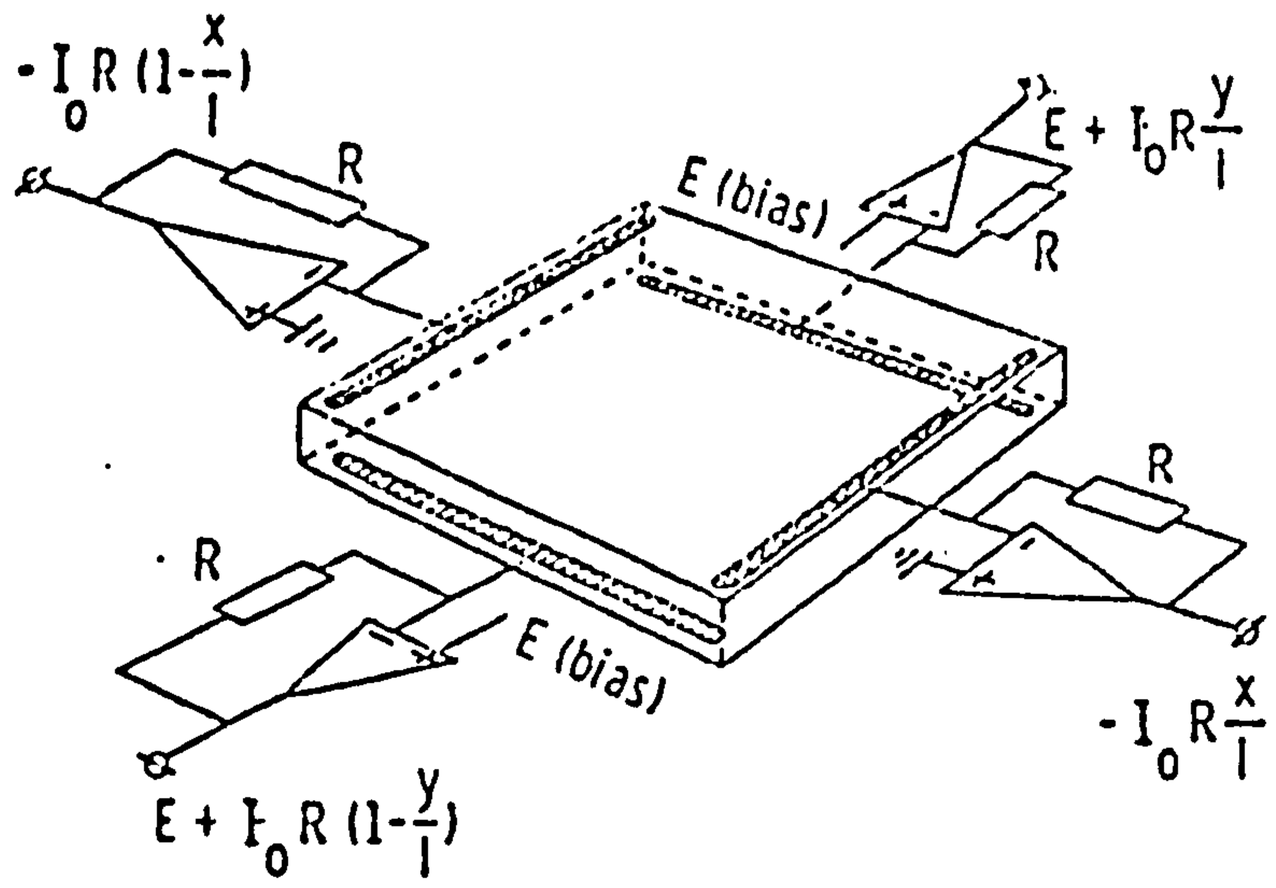

Figure 2.2.2(d). Dual-axis, duo-lateral, position sensitive photodiode.

(from Woltring, 1975)

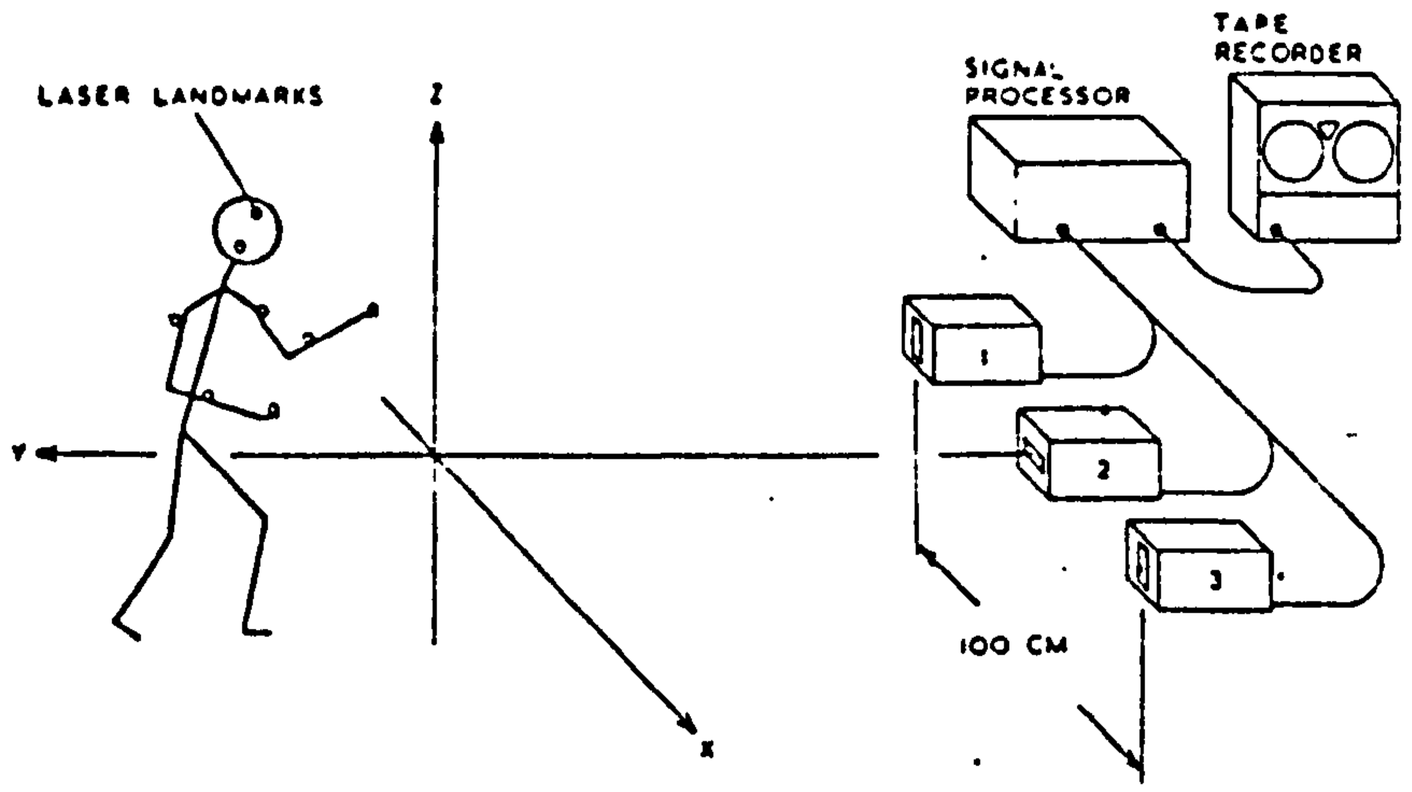

Figure 2.2.2(e). Schematic representation of the CODA system arrangement.

(from Mitchelson, 1975)

giving its position. A dual axes sensor will provide the 2 dimensional coordinates of the incident light spot. See Figure 2.2.2(d). Infra-red light emitting diodes are being used as markers. By time-multiplexing technique, up to 30 markers could be tracked at a sampling frequency of 312.5 Hz. For three dimensional recording, two of the specially designed cameras are used. Each LED marker is sampled sequentially, hence there is no problem in coordinate-markers identification. However, one unavoidable disadvantage is that the IR-LED markers have to be mounted on the body together with their circuitry and power supply.

The resolution of the system is largely dependent on the signal to noise ratio of the signal processor and detector, hence the power of the light source on the detector. This was demonstrated by Woltring and Marsolais (1980), when they varied the distance between the LED and the camera. The signal to noise ratio decreases when the LED is moved further away from the camera. They obtained a resolution of $\pm$3 mm per axis for a field width of 3 m and an observation distance of 6 m from a camera with a standard 50 mm lens.

Although the 'SELSPOT' system is potentially viable for clinical use because of its on-line and real time features in 3 dimensional kinematic data acquisition, it has significant limitations. Woltring and Marsolias(1980) and Paul and Nicol (1981) in their independent evaluation of the system found that background light interference is significant, "stray" reflection errors due to the power of the IR-LED used are very substantial and peripheral images are unstable because of the curvature of the lens.

(c) <u>The 'CODA' system</u>

The Cartesian Optoelectronic Dynamic Anthropometer

(i.e. CODA) system was developed by Mitchelson (1975) at Loughborough University of Technology.

This system consists of three specially designed cameras, specifically arranged,(see Figure 2.2.2(e)) so that the two outercameras are sensitive to horizontal movement (viz the 'Z' direction) and the middle one is sensitive to vertical movement (viz the 'Y' direction). From the stereoscopic arrangement of the two outer cameras, the 'depth' of the target (viz in the 'X' direction) can be computed. This is performed electronically within the camera system. The analogue or digital output produced is free from parallax errors.

Each camera consists of a cylindrical lens doublet, which is used to focus a point light source, (in this case a miniature infra-red gallium arsenide laser), into a line image in the focal plane. An array of silicon photodetectors, with an encoded optical mask in front, is positioned in this plane to detect the line image position. Up to eight markers can be used.

The resolution of the system is largely dependent on the signal to noise ratio at the sensors. The signal level from the laser target at the sensor follows the inverse square law, therefore an increase in distance from light source to cameras reduces the resolution. A distance of 2 m gives an accuracy of 0.25 mm while at 7 m an accuracy of 10 mm is obtained.

Mitchelson (1981) presented a vastly improved version, which is now commercially available as "CODA-3" under Movement Techniques Limited. Passive prism markers made from glass and mirror in the shape of a pyramid replace the infra-red laser. Each one is claimed to have an effective angular range of 220 degrees. Furthermore, each of the markers is uniquely identified by a colour

filter which is recognised by an optoelectronic colour decoding system. This automatically establishes and maintains marker identification upon start-up or after a marker is temporarily obscured. It also claimed that resolution of 0.2 mm and 1 mm can be achieved over a 1 m cube and 10 m cube field of view respectively. The sampling rate of each marker is 600 Hz. The field of view is 40 degrees, that is a 0.8 field width to distance ratio. Non-linearity of 0.2% over the total field of view is quoted.

To date there is no report of a fully operational CODA-3 system, therefore no data are available to confirm the claims of the manufacturer. However, it is understood that several systems are being installed, Mitchelson(1982) and their performances are awaited with interest.

2.2.3 Goniometry

Goniometry is a direct measurement method that has been used fairly extensively in human motion study. It offers the advantages of being fairly cheap and easy to operate. Moreover, a large amount of directly measured angular displacement data can be obtained instantaneously without tedious data reduction procedure.

Several types of goniometers have been developed. The simplest form is the protractor goniometer used in orthopaedic examination. Only passive movement can be measured fairly accurately. Carlson (1981) introduced a mechanical "Peak-reading" goniometer, which consists of a dial gauge and a pair of arms. Each arm is firmly at attached to the adjacent segments of the joint and only the maximum angular displacement during motion is measured. This type of device is not particularly useful in comprehensive gait studies. The following is a brief description of the development of continuous recording

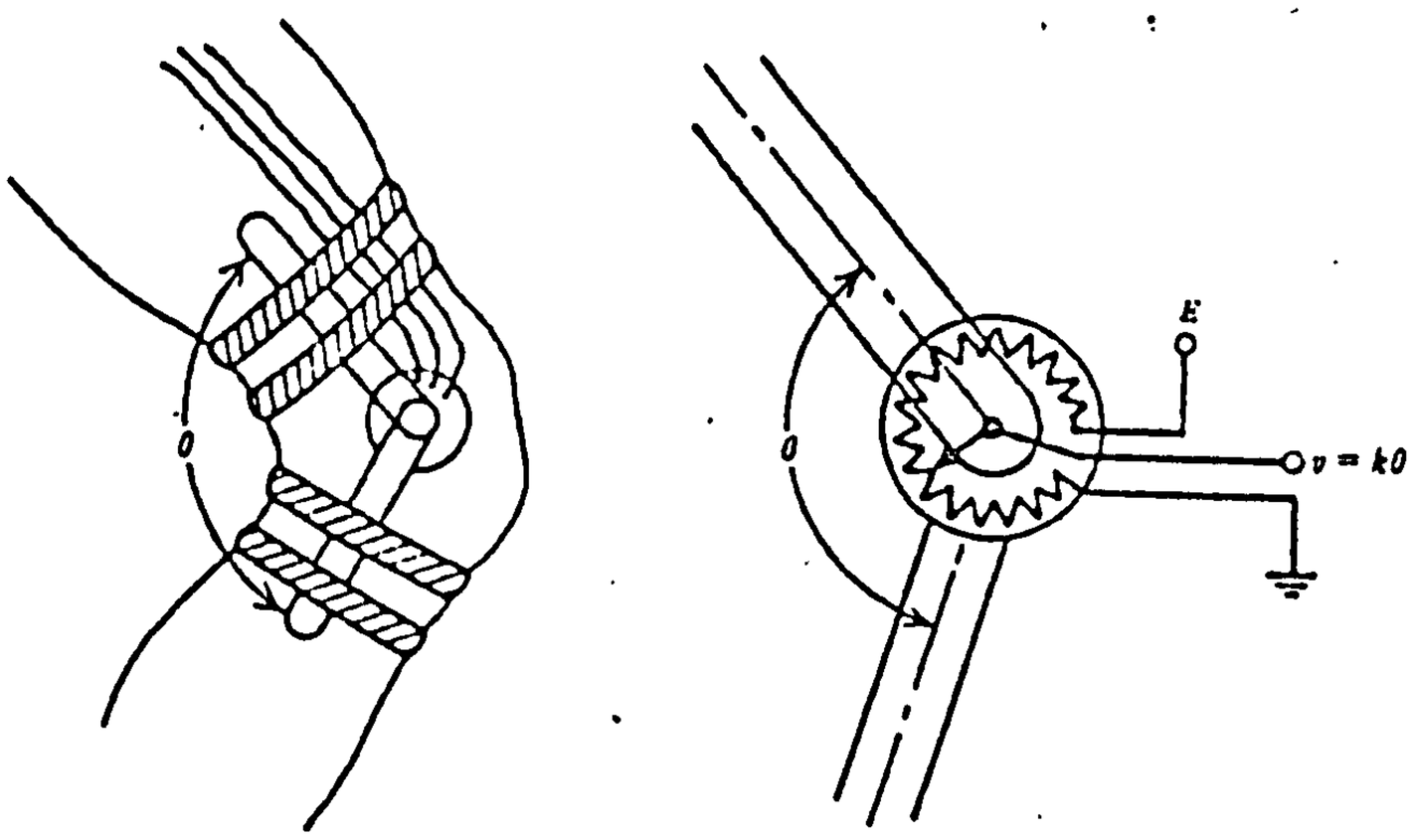

Figure 2.2.3(a). A simple planar electrogoniometer.
(from Winter, 1980)

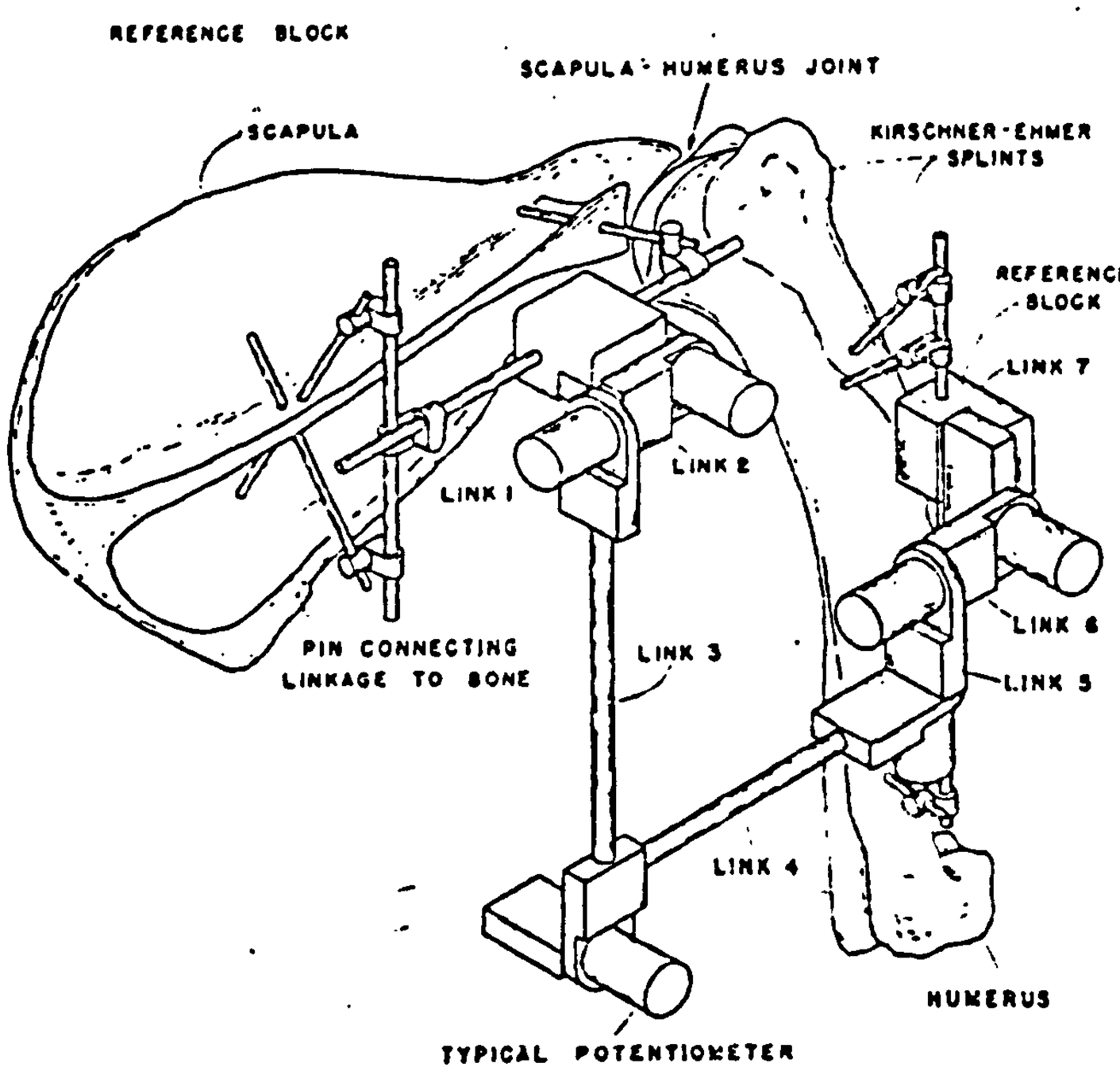

Figure 2.2.3(b). An electrogoniometric system with six degrees of freedom.
(from Kinzel et al,1972)

goniometers.

Karpovich and Karpovich (1959) presented an electrogoniometer (or Elgon) to record relative angular motion during locomotion. This device consists of an electrical potentiometer fixed to an arm with its spindle fixed to another arm. When used for measuring, the axis of the potentiometer is aligned to the joint axis and the arms are firmly attached to the adjacent segments. See Figure 2.2.3(a). Only saggital plane motion can be measured. Wright et al (1964) had two potentiometers built into their electrogoniometer. It was used to measure the ankle and subtalar rotations.

Johnston and Smidt (1969) developed a triaxial electrogoniometer, capable of measuring the saggital, coronal and transverse rotations about the hip joint. Three potentiometers were used, each one being aligned and orientated in one of the three principal axes of motion. The proximal arm was firmly fixed to the proximal segment, while the distal arm was allowed to slide in and out of a metal collar attached to the distal segment. This device was adapted by Kettelkamp et al (1970) to measure the three planes of motion about the knee. Errors due to "cross-talk" among the potentiometers were corrected by a 4 x 4 matrix method applied to the linkage system, Chao et al (1970).

To overcome the cumbersome configuration of the original device, Chao (1977) introduced a modified version. Using miniature potentiometers (viz 12 mm diameter and 14 mm length), he was able to construct a much smaller and lighter electrogoniometric system, thereby minimizing inertial effects and are less obstructive. The device was applied to the hip, knee and ankle for on-line and real time joint motion measurement. Precise alignment is necessary, to prevent errors caused

by the difference between the joint axes system and that of the goniometer. A telemetry system is currently being designed to transmit data from the device thus eliminating the need of cables.

Lamoreux (1971) designed and constructed an exoskeletal system for the pelvis and the right leg. It was used to measure the relative rotations about the hip, knee and ankle simultaneously. An external axes system was set up in the pelvic frame and was carefully aligned so that itsorigin is coincidental with the centre of the hip joint. Parallelogram linkages, which only transmit two out of the three components of spatial motion (absorbing the third one), were used for the knee and ankle. Two such linkages were used at the ankle to record all the three angular displacements. The knee had one such linkage, therefore only two angular displacements (i.e. flexion-extension and axial rotation) can be measured. Due to the self-aligning feature of the parallelogram linkages, precise alignment of the apparatus is not crucial to accurate measurement. However, the exoskeleton seems to be very bulky and cumbersome and the total weight of the whole assembly is approximately 6 lbs. These factors would undoubtedly affect the gait of the subject. It would be very difficult, if not impossible, to apply this system to patients. Furthermore, the tests were performed on a treadmill, which would also cause deviation of normal level walking gait pattern, Whittle (1980).

Cousins (1975) designed a moulded polyurethane parallelogram chain used in conjunction with an electrogoniometer. This device is now commercially available. The parallelogram chain is connected proximal to a triaxial electrogoniometer. The self-aligning feature does not require exact alignment of the device. Continuous data recordings are stored in a small portable

cassette recorder worn by the subject, hence, eliminating long and restrictive cables.

Jansen and Orbaek (1980) examined the reliability and reproducibility of gait data measured with a planar electrogoniometer. The device includes the Lamoreux's self-aligning parallelogram linkage and a sliding rod. They reported a standard deviation of 5% and 10% for the hip and knee respectively. Measurements were taken from only the saggital plane and tests were performed on a treadmill.

All the above systems described could at the most measure up to three degrees of freedom, i.e. assuming that all the joints are spherical or "ball and socket" type. However, some joints have six degrees of freedom; 3 rotations and 3 translation. The sliding rod present in some of the devices could absorb only a small magnitude of the translational movement. Hence, errors would inevitably be generated in the measuring system.

Kinzel et al (1972) presented an instrumented linkage system with six poteniometers capable of measuring the six degrees of freedom. This system was used in their study of the scapular-humerus joint of Alsatian dogs. See Figure 2.2.3(b). The linkage system was anchored securely with pins inserted into the bones, making exact measurement possible. However, for it to be viable for use in human subjects, the anchoring method has to be non-invasive. Townsend et al (1977) presented a similar system to measure the total knee motion. Attachment of the linkage system to the body segments was by means of cuffs. The angular recordings from the six potentiometers generate the (3 x 3) transformation matrix which describes the motion totally.

The use of cuffs or belts to fasten the device to

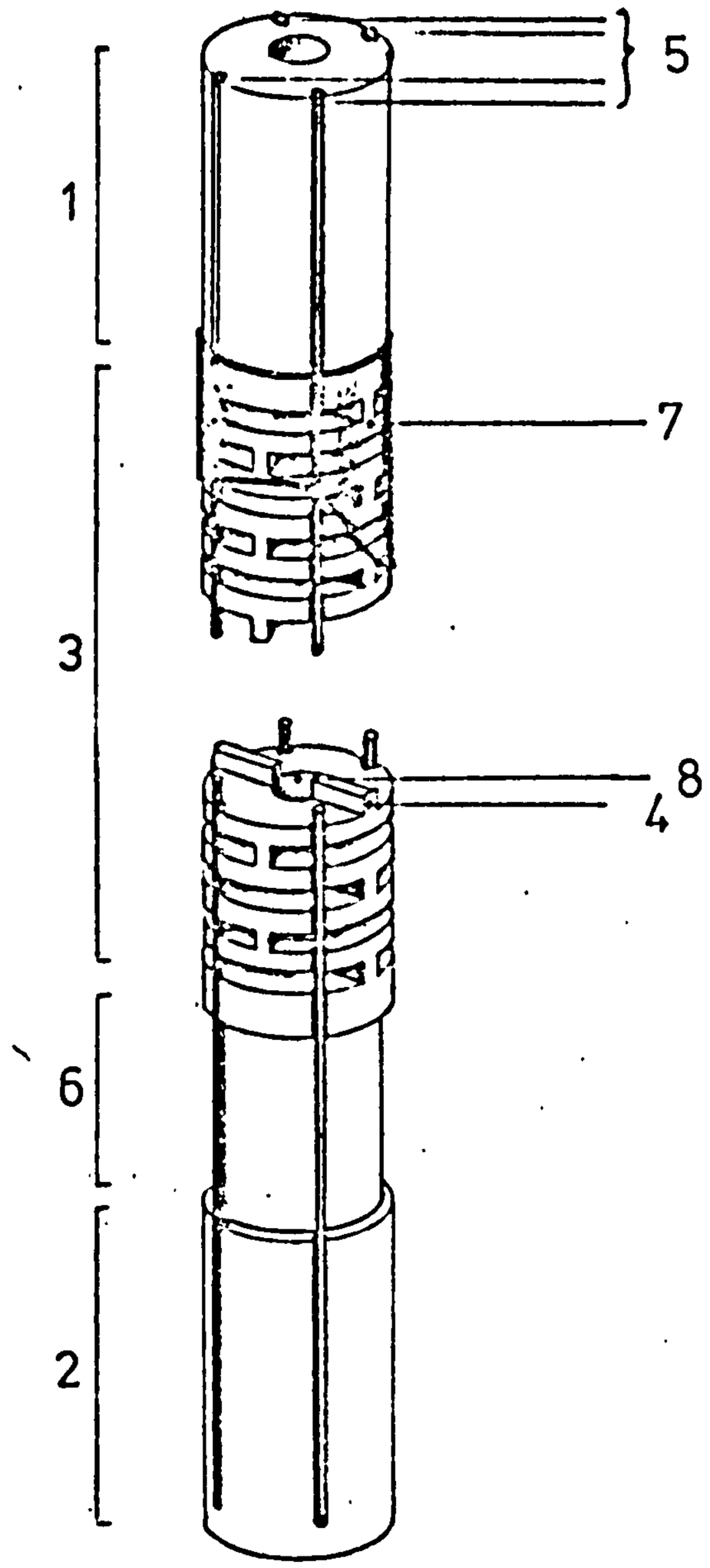

1&2) Rigid sections - duplicate limb segments' movements.

3) Flexible section

4) Web or hinge of slot

5) Grooves for mercury-in-rubber strain gauges.

6) Reduced diameter section for axial rotation.

7) Flexible elastic covering

8) Hole for carrying wire connections.

Figure 2.2.3(c). A flexible electrogoniometer.
(from Dewar et al,1981)

the body segments gives rise to the problem of relative movement between the linkage system and the underlying skeletal structure. This is due to the interposition of soft-tissues and also muscular contraction. This undesirable movement would cause substantial error which may be more significant than the translational components of joint motion. This then defeats the purpose of having an accurate instrument such as those described by the two latter investigators.

Another limitation of the electrogoniometric system described so far is that they are confined to the laboratory. Furthermore, the rigid mechanical linkages can be quite obstructive and could cause the subject to alter his gait pattern to adapt to the attachment.

Johnson et al (1981) described a recent development called the flexible electrogoniometer. It is a mercury-in-rubber strain gauge, 200 mm long with 0.2 mm bore and 0.5 mm outside diameter. Platinum wires (0.91 mm diameter) are used to seal the ends of the tubing. The gauge is fixed to the anterior of the knee with its ends taped to the skin. The goniometer is prevented from slipping off by a sleeve, taped over the most prominent part of the patella. The goniometer has to be calibrated for each knee undergoing measurement. It was observed that a temperature change of $10^{o}C$ produced a resistance change of 1%. Therefore, to obtain accurate measurement, some form of temperature compensation is required. The gauge is pre-stretched by 10% during attachment to overcome the initial lengthening problem. This device has been used in conjunction with a 24 hours portable monitoring system. Normal clothing can be worn over the goniometer, hence making it viable for recording outside the laboratory.

Dewar et al (1981) developed a more complicated

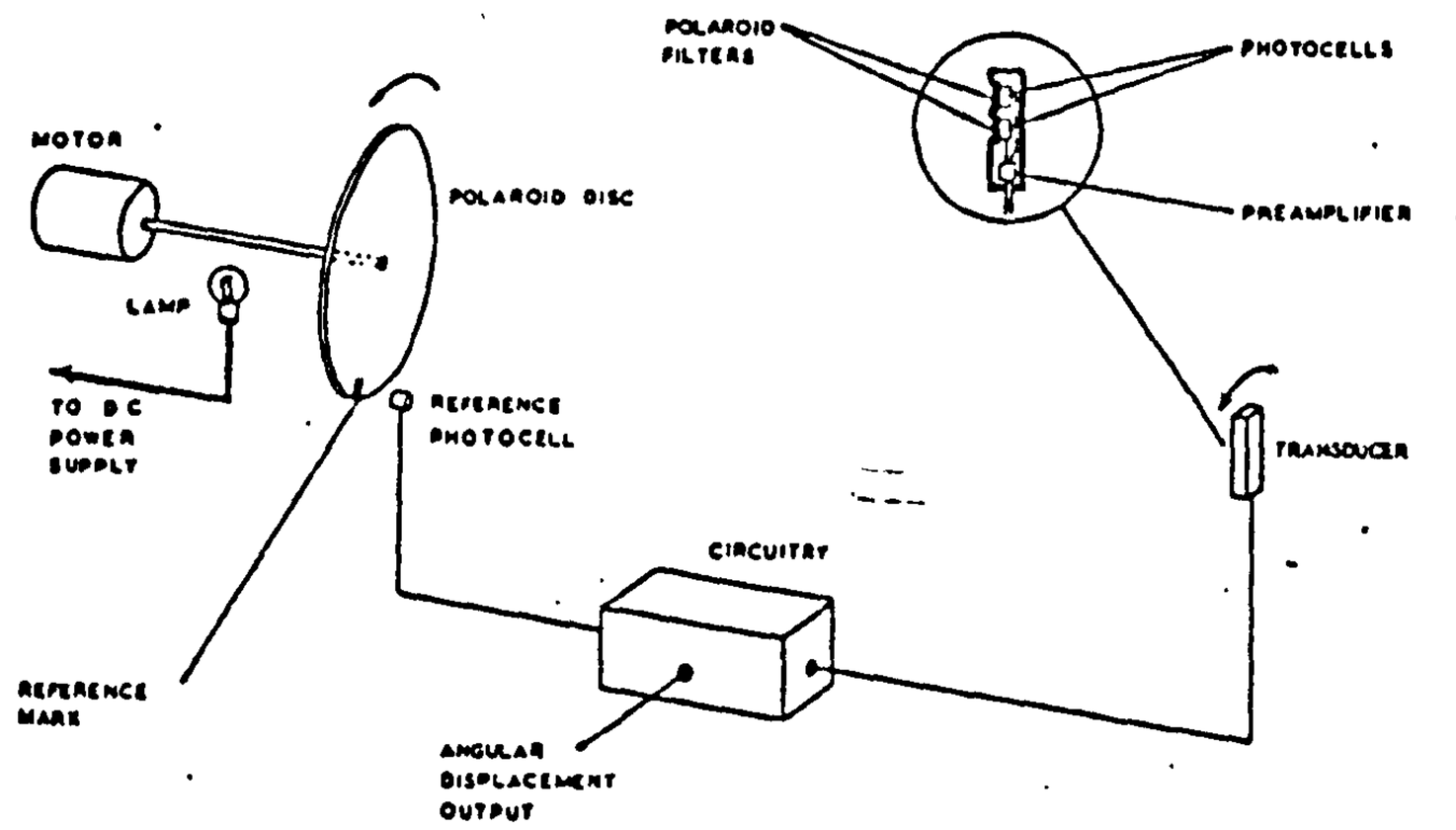

Figure 2.2.3(d). Schematic diagram of the Polarised Light Goniometer.

(from Mitchelson,1975)

flexible electrogoniometer, which is capable of measuring the three components of rotation. It comprises a nylon rod 1 cm in diameter. The mid-section has a large number of pairs of slots cut across it, each pair leaving a web-hinge across the diameter. See Figure 2.2.3(c). These allow the section to be flexible to bending in any direction except axial rotation. Four equally spaced grooves around the circumference hold the mercury-in-rubber strain gauges. Diametrically opposite pairs of gauges measure the two bending motions. One end of the goniometer is free to rotate axially. That section has a reduced diameter, such that the gauges are no longer held by the grooves. Any axial rotation can be measured by the increase in length of the gauges experiencing the spiral action. One problem inherent in this method is the determination of the direction of the axial rotation. The authors are still in the process of refining the device and a search is going on to determine the best method of attaching it to the body segments.

Flexible electrogoniometers seem to have the potential to replace the conventional ones. However, it is still in its infancy and more rigorous evaluation of the device is required to show its full potential.

Grieve (1969) and Reed and Reynold (1969) introduced a totally different type of goniometer, which makes use of polarised light. This device was termed "Polgon" by Grieve. A similar device was also developed at the Loughborough University of Technology in 1970, (Mitchelson, 1975). It consists of a polarised light generator that transmits light of rotating planes of polarisation and transducers sensitive to this light, receiving it as sinusoidal signals. See Figure 2.2.3(d). A reference mark on the polaroid disc is used to generate a reference pulse through the photocell. Passing the reference pulse and the sinusiodal signal into the

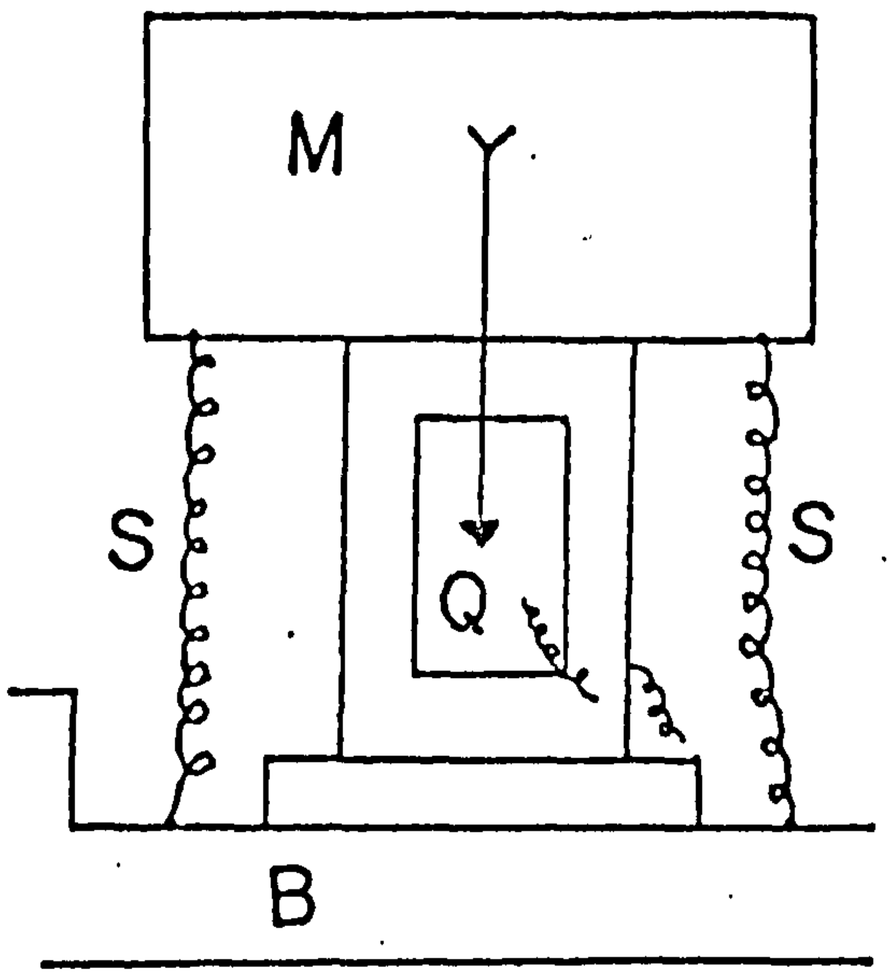

—Piezoelectric quartz accelerograph in which M designates mass; Q, quartz, B, base; and S, springs. The wires shown on the quartz are connected to an amplifier which in turn is connected to an ink-writing galvanometer. The arrow indicates the direction of the pressure during acceleration.

Figure 2.2.4(a). Piezo-electric accelerometer
(from Liberson, 1936)

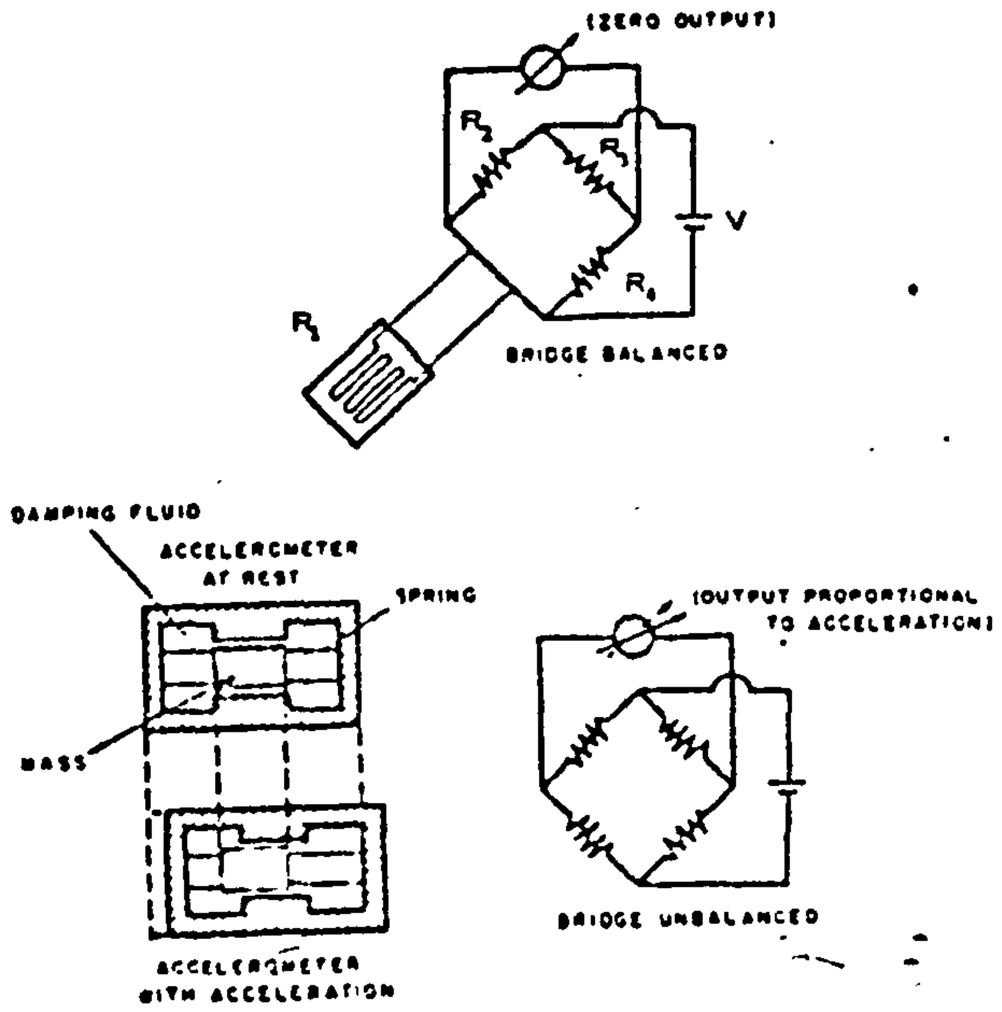

Figure 2.2.4(b). Unbonded resistance wire accelerometer
(from Contini & Drillis, 1966)

electronic circuit, the angular displacement is calculated. Although, angular velocity can be obtained by analogue processing of the angular displacement output, the effects of "white noise" must be taken into careful consideration. The linearity of the system was cited as $\pm$0.1% over 180^{o} range. It was shown that significant output errors can arise from transducers undergoing two additional rotations in planes mutually perpendicular to the plane of interest. In order to minimise this error, the transducers have to be carefully positioned on the body segments.

The goniometric systems described so far can only measure angular displacements between two adjacent segments. Therefore, they cannot be used in conjunction with force platform for kinetic analysis of normal human subjects unless simultaneous recording of an inertial reference is made. However, a knee goniometer with a pylon force transducer (see Section 2.3.2) on a prosthetic shank is capable of performing a kinetic analysis on the artificial limb, as demonstrated by Lowe (1969).

2.2.4 Accelerometry

Acceleration is one of the most important parameters in gait analysis. Direct measurement of this quantity is possible by means of accelerometers.

Liberson (1936) was perhaps the first to make use of this technique in human locomotion study. He described a piezo-electric accelerometer that consisted of a mass, a quartz crystal and a spring system, see Figure 2.2.4(a). As the device undergoes acceleration, the inertial force due to the mass will apply pressure on the quartz. The electrical potential developed from the quartz will be proportional to the force, which is also proportional to the acceleration. The output is recorded on an

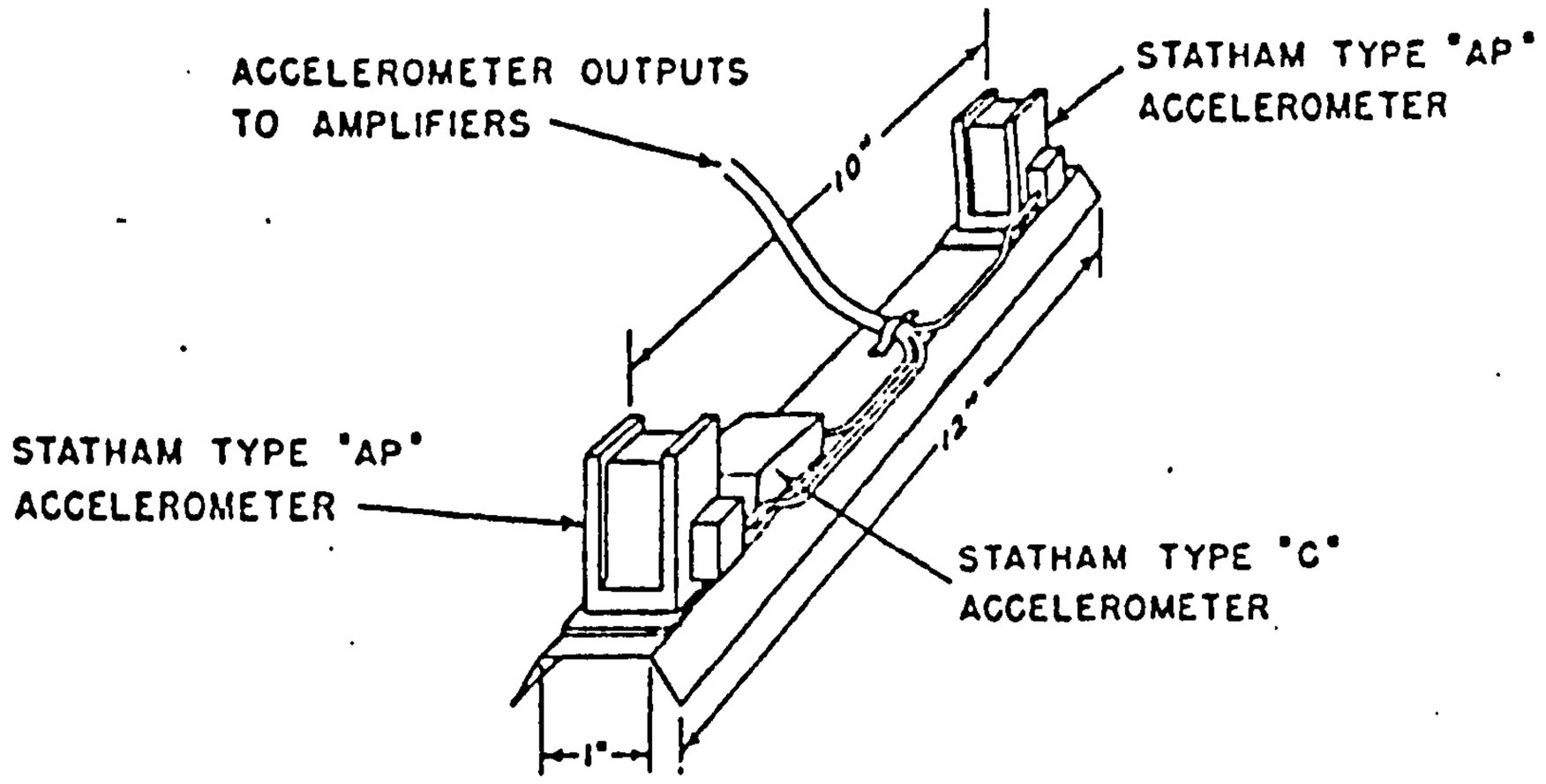

(a) ACCELEROMETER MOUNTING ASSEMBLY

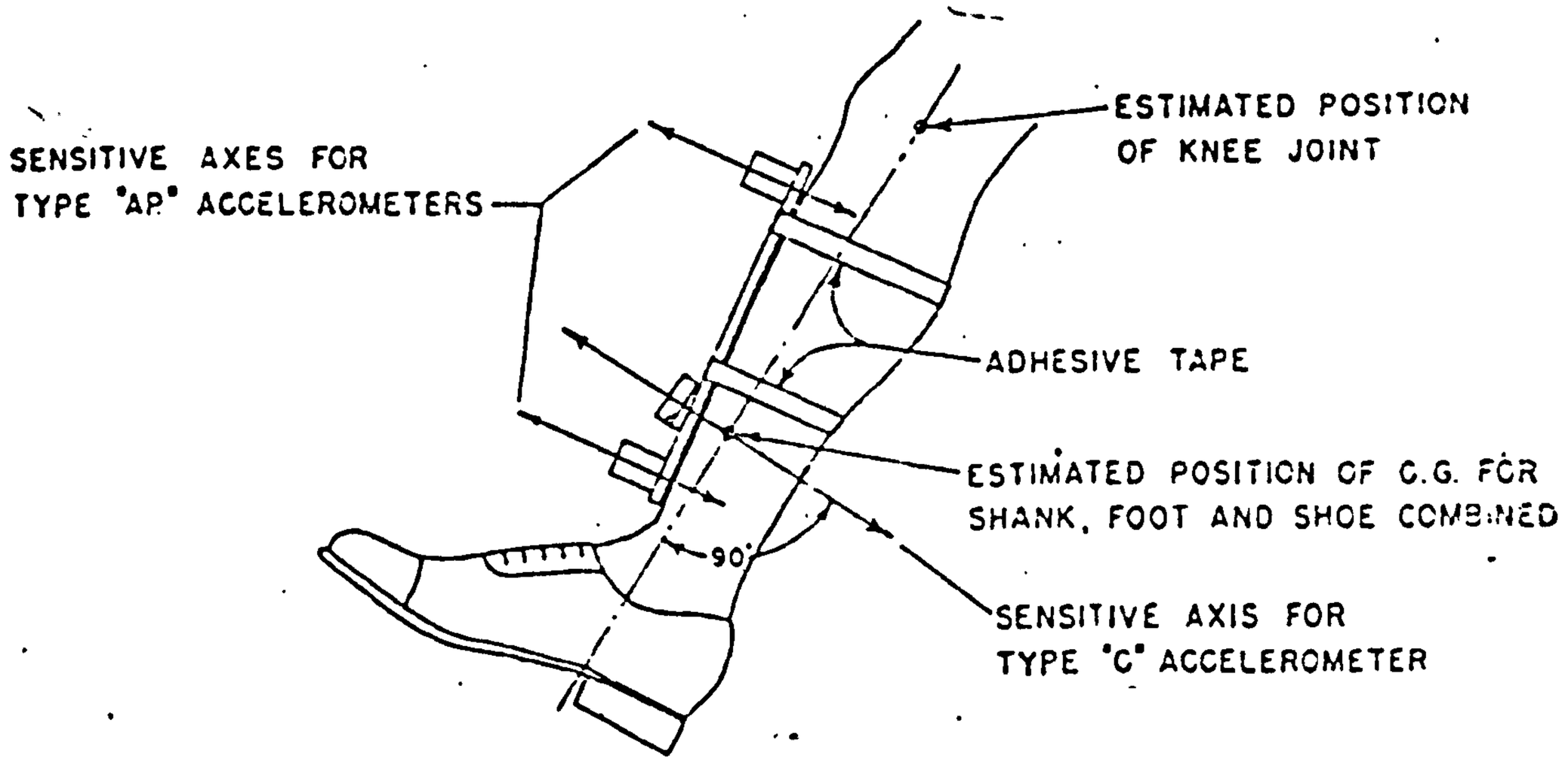

(b) ACCELEROMETER MOUNTING ASSEMBLY ON SHANK

Figure 2.2.4(c). Arrangement of accelerometers on shank.
(from Ryker and Bartholomew,1951)

oscillograph but only linear acceleration can be measured.

Eberhart and Inman (1947) reported the use of accelerometers to verify the numerical differentiation technique that was used to derive acceleration from displacement data of human locomotion. The procedure was described in detail by Ryker and Bartholomew (1951). Three linear accelerometers were used. The basic elements of these accelerometers are a mass, a spring system and a damping system, see Figure 2.2.4(b). The springs are in effect unbonded resistance wire strain gauges. Resistance changes occur when the mass, due to its own inertia, moves and thus strains the springs. This will cause an unbalance in the wheatstone bridge, giving an electrical analogue output that is proportional to the acceleration. An individual linear accelerometer can only measure linear acceleration parallel to its sensitive axis. However, by arranging two linear accelerometers in the same plane as shown in Figure 2.2.4(c), the angular acceleration can be obtained, which is proportional to the difference between the two linear accelerations. The third accelerometer is positioned normal to the long axis of the shank at the estimated centre of combined mass of the shank, foot and shoe. This will give the linear acceleration of the body segment at the centre of mass, normal to the shank's long axis. The shortcomings of this system are : (1) the excessive weight of the whole device, (2) relative movement of device and skeletal structure, due to cuff attachments, (3) the assumption that the shank moves in the saggital plane, thus ignoring the cross-sensitivity effects, and (4) the resultant linear acceleration of the shank cannot be directly determined.

Cavagna et al (1961) introduced an accelerometric system for human locomotion study. Each accelerometer was constructed of a plate (30 x 5 x 0.1 mm), pivoted at

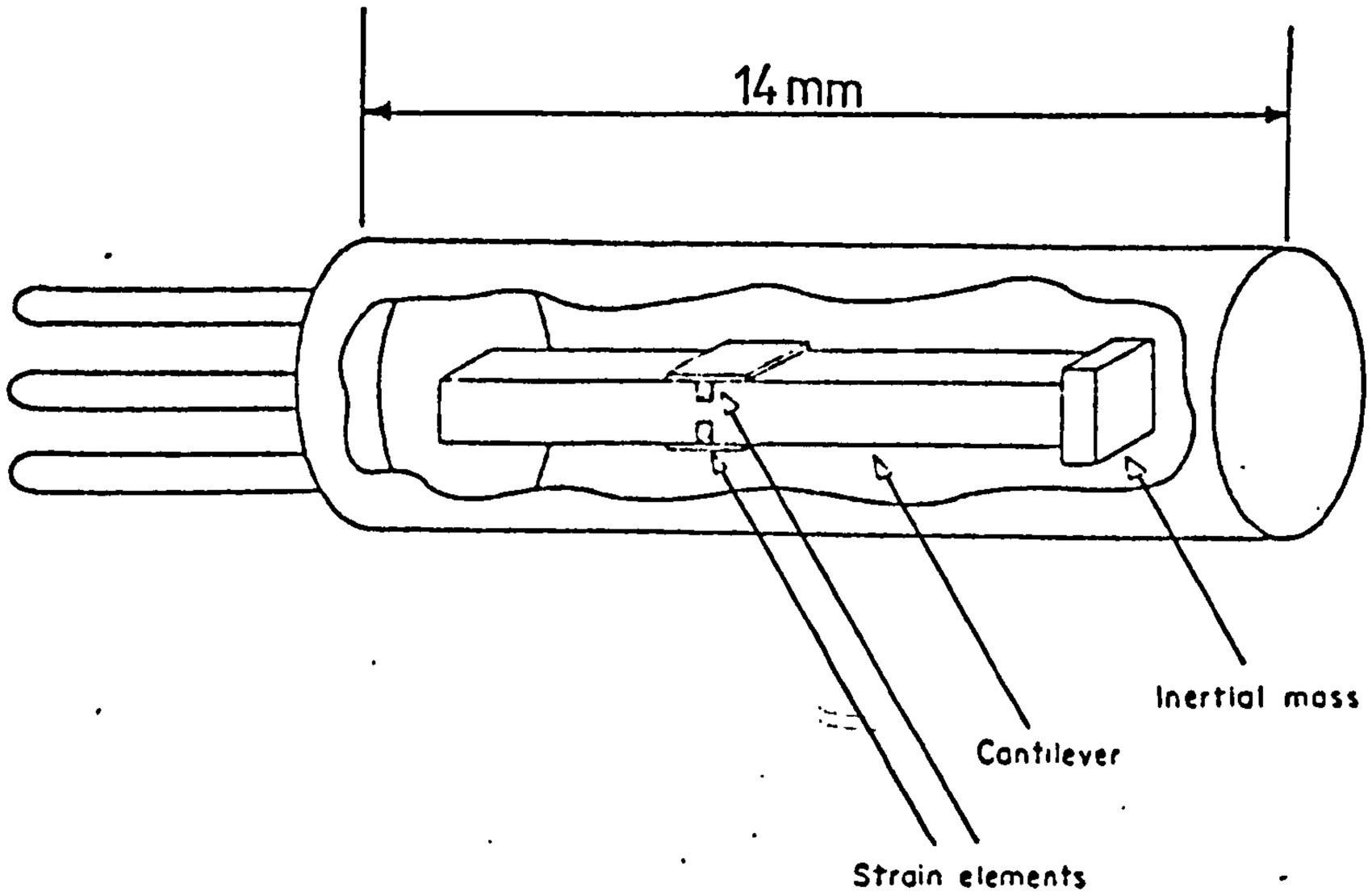

Figure 2.2.4(d) Strain-gauged Cantilever type accelerometer (from Morris, 1973)

both ends with a mass clamped at the centre. Four foil strain gauges were firmly attached to both sides of the mass on the two faces of the plate. The gauges were arranged into a full wheatstone bridge to measure the deflection of the plate. The mass can be varied according to the desired sensitivity. The whole setup was fairly light (about 50 grams) and relatively small, i.e. 40 x 40 x 15 mm. The device was firmly attached to the back at the lumbrasacral level of the spinal column; approximately at the centre of gravity of the body. The three linear accelerations obtained during walking enabled the investigators to calculate the instantaneous energy levels at the centre of gravity.

Gage (1964) mounted a pair of strain-gauged accelerometers with their axes mutually perpendicular at the level of the second sacral vertebra. This enabled him to record the vertical and forward accelerations of the approximated centre of gravity of the body. At the same time, the angular acceleration of the shank was measured by another pair of accelerometers mounted in tandem on the leg, as per Ryker and Bartholomew (1951), see Figure 2.2.4(c). The author realised the restriction imposed by the use of cables and so proposed a telemetry system for future work. Another problem faced by the author was the weight and inertia of the linear accelerometer platform. This caused over-shooting of the peaks and troughs producing erroneous results. Smaller instruments were suggested for future study.

Morris (1973) introduced a mathematical model for a six-accelerometers system to define the complete movement of the body in space. The mathematical procedure begins by solving for the angular velocity vector, followed by the direction cosine matrix and subsequently the absolute acceleration vector of a body point. Double integration of the absolute acceleration vector will

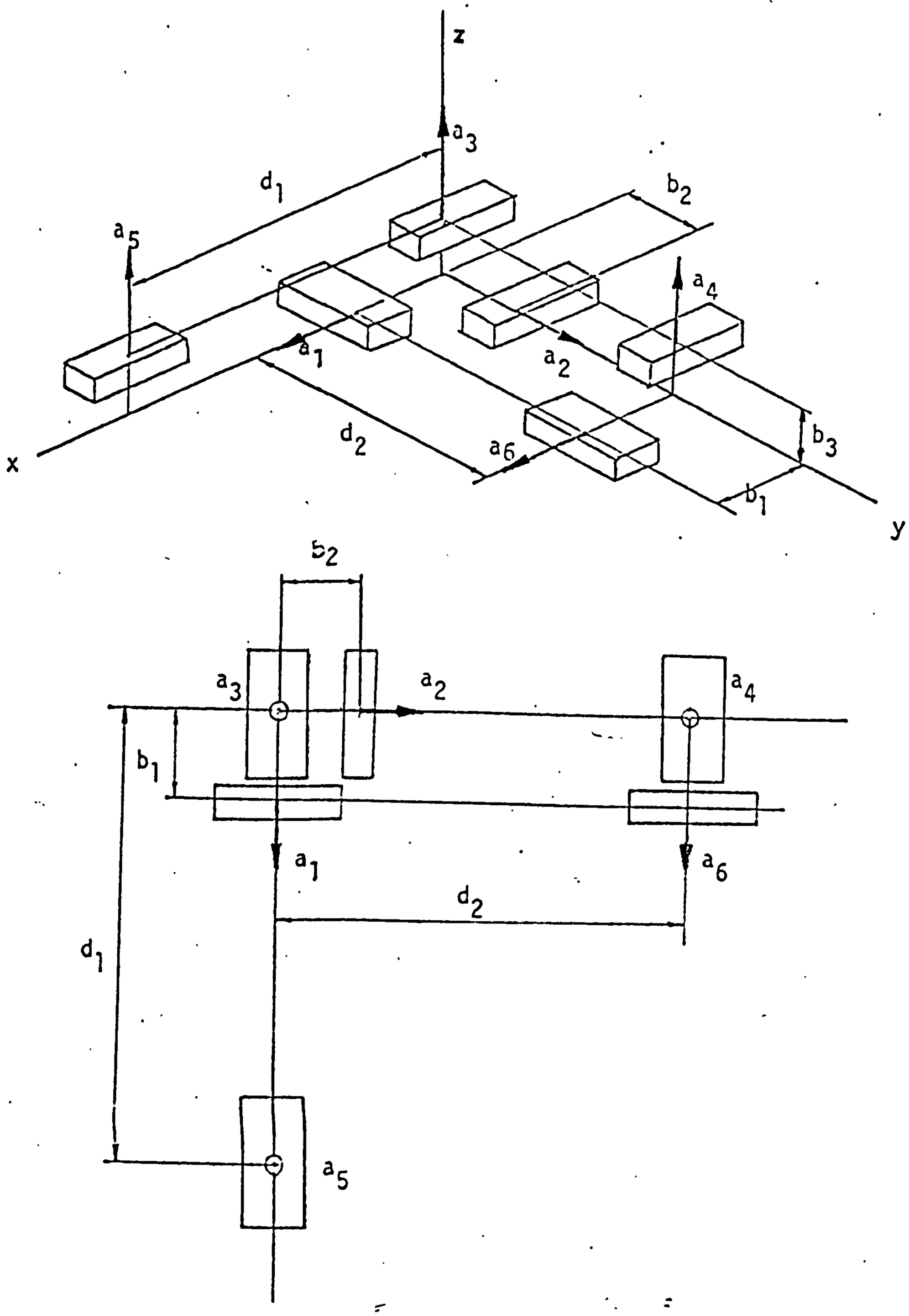

Figure 2.2.4(e). Six-accelerometer system .
(from Ishai,1975)

give the spatial position of that point. This new approach was applied to determine the kinematics of the shank. The author assumed that there is no transverse rotation of the shank and therefore developed a five-accelerometer system. Strain-gauged cantilever type accelerometers were used, see Figure 2.2.4(d). The accelerometric platform was mounted over the flat antero-medial surface of the tibia and held by means of a moulded "plastazote" cast and velero straps. Acceleration data can either be recorded on a portable cassette recorder or on a fixed recorder via light weight cables.

Ishai (1975) described a six-accelerometer system taking into account the transverse rotation of the shank. The arrangement of the accelerometers on the platform is as shown in Figure 2.2.4(e). The mathematical approach adopted was similar to that of Morris, except for the initial conditions. Morris considered the walking process to be cyclic and so marked off the beginning and end of a cycle visually, whereas, Ishai recorded zero initial conditions for the angular velocity vector during the standing position and took the direction cosine matrix of the platform to be coincident with the reference axes system.

The accelerometric method has the advantage of providing direct analogue data without tedious reduction procedure and it eliminates the use of potentially erroneous differentiation techniques. Numerical integration is much more exact. Outdoor recording is possible with the portable cassette recorder system, although drift could present problems. High precision accelerometers tend to be rather fragile, an alternative would be to use low precision accelerometers. Padgaonkar et al (1975) presented a system using nine piezoelectric accelerometers instead of six to minimise error due to cross sensitivity of such accelerometers. However the

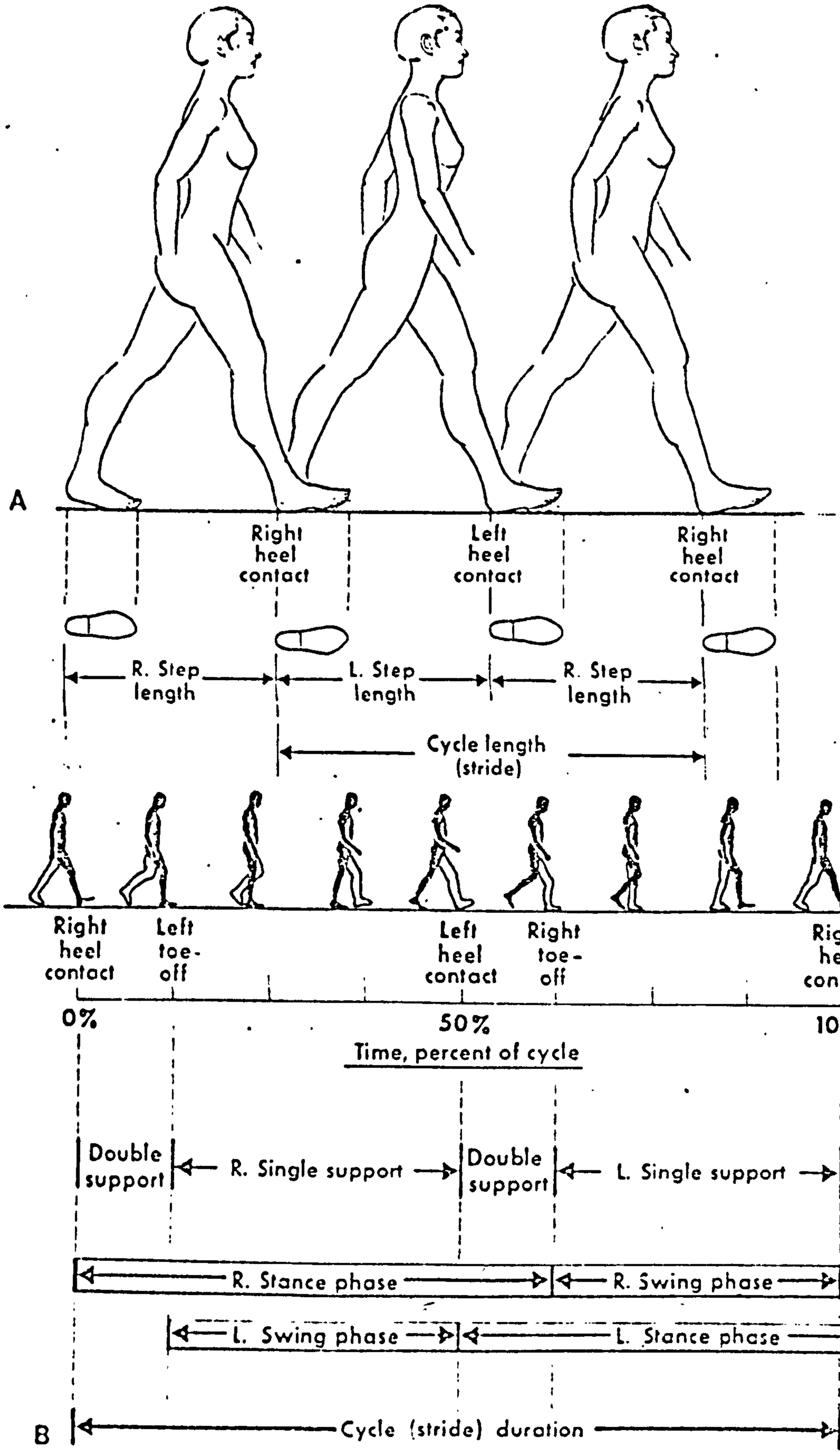

Time Dimensions of Walking Cycle

Distance and time dimensions of walking cycle. A, distance (length). B, time

Figure 2.2.5 (a) Temporal/Distance Parameters of Walking Cycle (from Inman et al,1981)

physical size and weight of this system present problems in attachment and produce possible errors due to its inertial effects.

Several limitations are inherent in this method. The attachment of the device to the skin introduces noise and artifacts to the results, especially the soft tissues of the thigh. The instrument noise, drift and hardware errors can cause significant problems in the reliability and resolution of the data produced. The procedure used by Morris to obtain displacement data requires operator intervention to determine the constant of integration. Extending this approach to the whole body gait study would not only present hardware problems but an enormous amount of time would be spent in analysis. This would defeat its purpose of being a direct and convenient method.

2.2.5 Temporal/Distance Factors Recording System

Walking is a highly repetitive activity, similar patterns of movement are repeated over and over again. The basic element in this cyclic motion is the stride, that is the interval between two successive occurrences of any identifiable event on one of the legs (for example, left heel strike to left heel strike). The two main phases of walking, making up the strike are the stance phase and the swing phase. Another important parameter is the step, which is the interval between the occurrence of an identifiable event in the cycle of one leg and the occurrence of the corresponding event on the other. Phases of walking are illustrated in Figure 2.2.5(a).

One simple and "crude" way of measuring these quantities is by taking footprints of the subject during walking. Shore (1980) suggested using "temporal" paint,

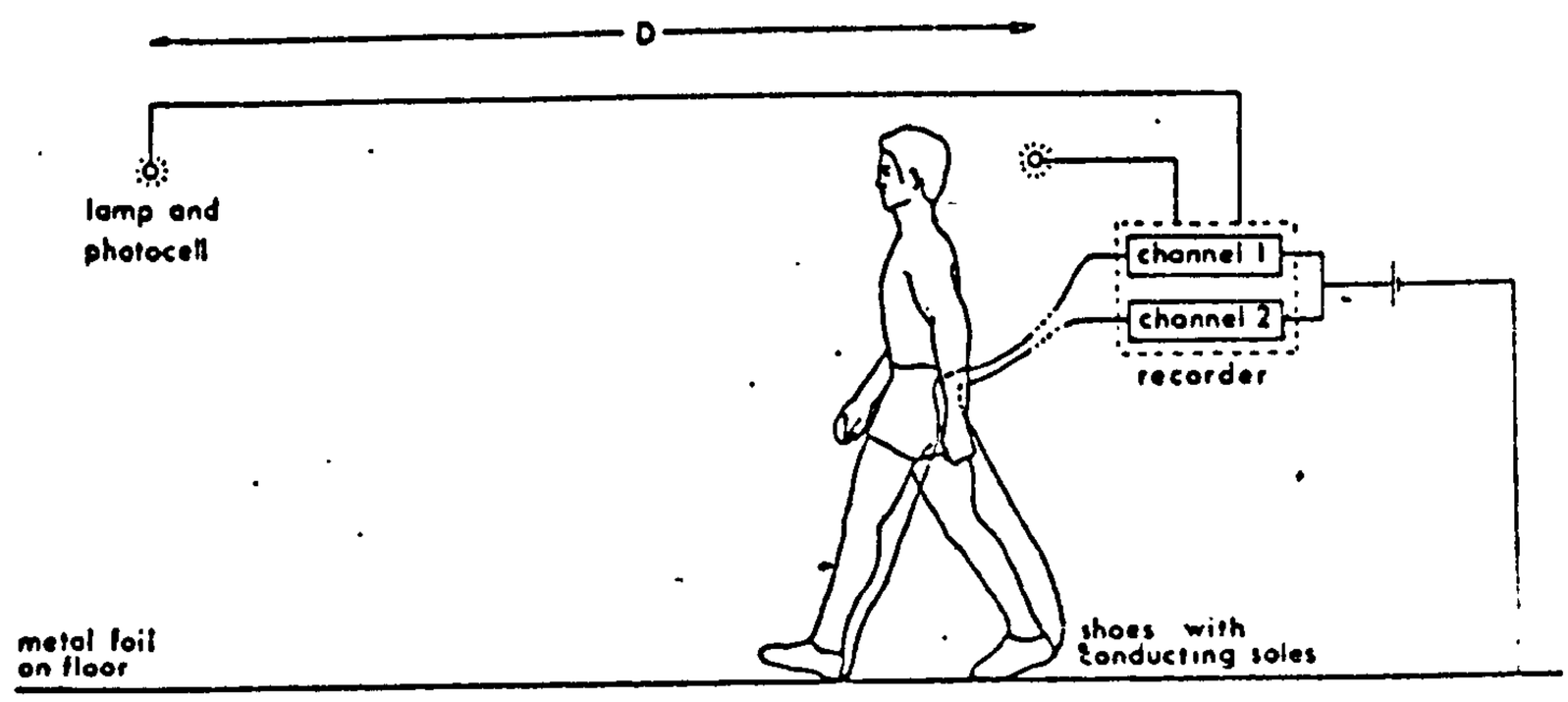

Figure 2.2.5(b). Typical temporal/distance factors walkway.

(from Wall et al,1976)

applied to the sole of the subject's feet and letting him walk over an unrolled paper. Stride and step length, base support and foot angle can be measured from the footprints. With a stopwatch, velocity and cadence were also derived. Although this method has the advantage of being very inexpensive, it does present certain problems. Walking on paper with painted soles would create a sense of insecurity, especially for pathological subjects. There is no way this technique can be on line to give immediate results.

Numerous devices have been developed over the years to measure these parameters directly. They can be broadly classified under these two categories :

a) Temporal/Distance Factors walkway (or Electro-basography)

This class of measuring system has been described by Schwartz et al(1933), Drillis (1958), Smith et al(1960) and Chantinier et al (1970).

The typical features of this system are as follows : The walkway consists of two long strips of conductive material affixed to the floor. Strips of pressure-sensitive conductive tape are fastened to the soles of the the subject's shoes. The power supply, recording device and the conductive strips are connected as shown in Figure 2.2.5(b). The conductive tape on the sole of the shoe acts as a switch. The interruption of the electrical circuit, as the feet step on and off the walkway during walking, facilitates the recording of the temporal factors.

To determine the distance factors, a pair of photoelectric cells was positioned at a known distance apart. The disruption of the light source of the first

photoelectric cell as the subject walks past it, signals the start of recording and as the subject passes the second cell, the recording stops. Dividing the distance between the photoelectric cells by the number of strides(or steps) recorded, will give the stride length(or step length). Speed of walking and cadence (i.e. steps per min) can also be derived from the recorded parameters.

One problem associated with this method is the trailing wire attached to the subject. This could be irksome especially for pathological subjects. One way around it, is to have some kind of a telemetry system. However, Wall et al (1976) introduced an instrumented mat that does not require trailing wires from the foot. Only self-adhesive conductive tape is applied to the sole of the subject's shoes. The mat consists of conducting rods set in grooves which are connected between resistors. As the foot makes contact with the mat, the conductive tape shorts-out the rods. Since current flows through the path of least resistance, stance progression pattern can be detected. Wall et al (1978) coupled this device to a mini-computer to produce an automated on-line system.

Gabel et al (1979) developed an instrumented walkway that consists of flat linear pressure-sensitive parallel switches in multiples of sixteen to complement sixteen channel multiplexers. A walkway of 3.6 m long has 240 sensors. The subject is not required to wear any apparatus. The walkway is coupled to a micro-processor which computes thirteen temporal/distance parameters of gait and also the foot position. Audible tones relating to step length are used for gait training.

Limitations inherent in this method are :(1) tests can only be carried out in specified areas and (2) traces from the system alone may not be representative of non-typical temporal factors, especially for pathological subjects with no distinct pattern of walking.

b) Foot Switches

The overview of existing gait laboratories presented by Milner (1977) shows a great number of laboratories having footswitches as part of their set up.

Most designs have only heel and toe contact switch switches, Bajd and Kralj (1980). Some have an additional switch at mid-foot, Zuniga and Leavitt (1974). These devices are sufficient to acquire and record data on the temporal factors of walking.

Perry et al (1978) and Blanc and Vadi (1981) presented a system with footswitches distributed underfoot to acquire information regarding time-space sequences which occur during stance phase. They also used telemetry to transmit footswitch signals.

To determine the distance factors, the length traversed has to be defined. This is usually determined by a pair of photoelectric cells, as described previously. Bajd and Kralj used a pulley-disc with non-elastic cord. The cord is attached to the subject's trunk and as he walks away, the disc will rotate and the photoelectric cell or potentiometer records the number of rotations. Multiplication of this number by the circumference of the disc gives the distance travelled by the subject.

One disadvantage of footswitches is that they could cause discomfort to the subject and hence alter his gait. To overcome this, Bontrager (1980) designed a very thin footswitch based on the membrane switch concept. Figure 2.2.5(c) shows the cross-section of the design that was claimed to have functioned satisfactorily.

Instruments developed for measuring ground reactions, foot-floor contact pressure distribution and

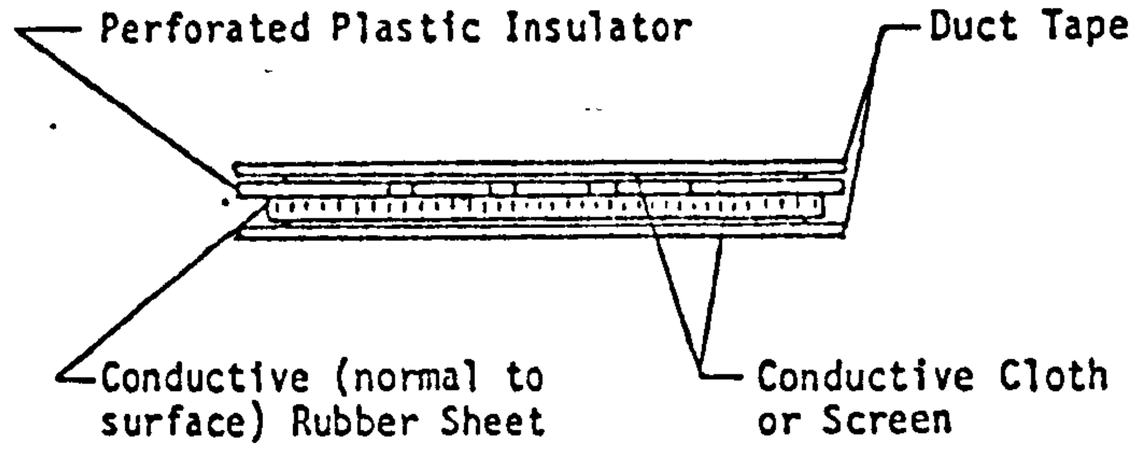

Figure 2.2.5(c) Cross section of footswitch based on membrance switch concept
(from Bontrager, 1980)

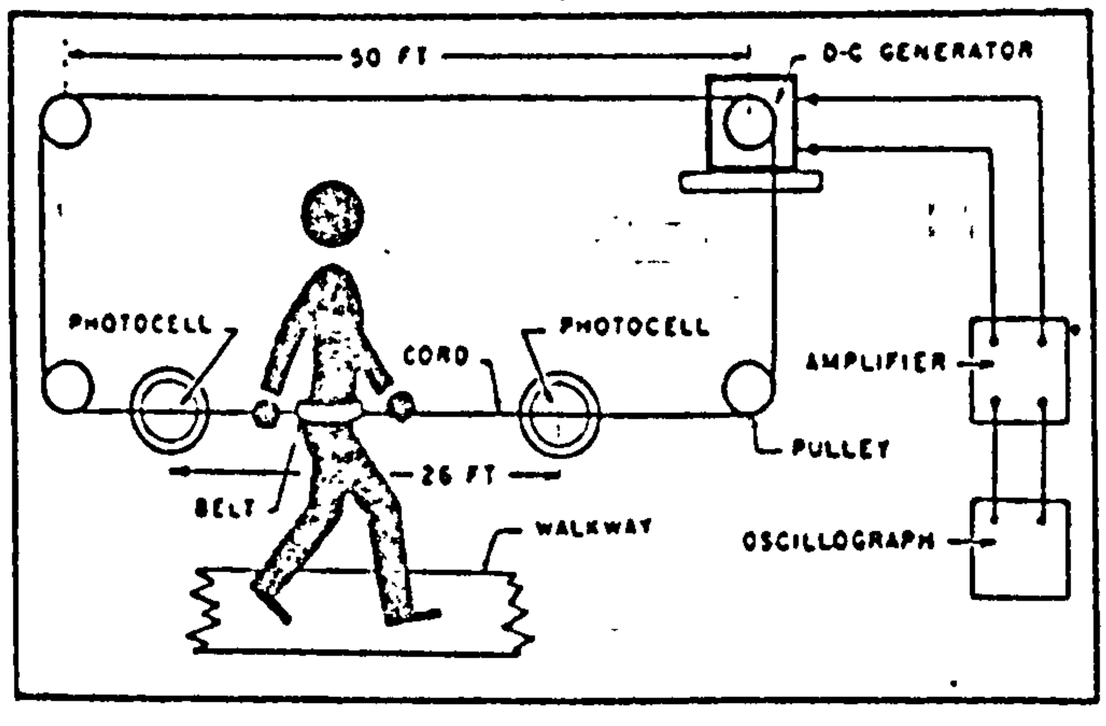

Figure 2.2.5(d) The tachograph
(from Drillis, 1958)

prosthetic or orthotic loadings etc. have the capability to give temporal/distance factors as well. These devices are described in Section 2.3. Displacement data obtained through photographic methods could also be used to derive temporal/distance parameters, Murray et al (1964) and Grieve and Gear (1966). As a matter of fact, all the kinematic recording systems described previously have the capability to produce these parameters. However, most of them would only give an approximate value and as such would not be as accurate as those produced directly.

Another temporal/distance parameter that can be measured directly is the instantaneous forward velocity of the approximate position of the centre of gravity during walking. Drillis (1958) was first to introduce the tachograph, see Figure 2.2.5(d). It consists of a small D.C. generator activated by the cable cord passing over the pulley coaxial with the rotor. The amplitude of the output signal is directly proportional to the instantaneous velocity of the subject's approximated centre of gravity.

Ganguli and Mukerjee (1973) employed this technique as their clinical gait recording system, the only difference from that of Drillis was the recording device. An ECG recorder was used instead of the cathode-ray oscilloscope suggested by Drillis. The major problem experienced was in aligning the pulleys. Tibarewala et al (1979) modified the system, using only three pulleys. They advocated that the instantaneous velocity is a vector and that the parameter measured is only a component of the velocity in the direction of progression. They therefore introduced the term "Differential of Progressive Displacement" and subsequently described a sub-transducing system comprising of a disc with equidistant holes around the circumference to produce this parameter. The distance between two adjacent holes

divided by the corresponding time interval of the two recorded pulses is the "Differential of Progressive Displacement". The output is in digital form.

Mohen and Boon (1972) developed a slightly different type of device; instead of cable cord, a magnetic tape with pre-recorded pulses is used. The subject stretches the tape while it runs through the play back head. The frequency of the signals recorded is therefore proportional to the momentary walking speed of the subject.

Bajd and Kralj (1980) presented analogue and digital versions of their instantaneous velocity measuring device. It basically comprised a thin light-weight non-elastic thread connected to the subject's trunk. For the analogue version, the thread drives the tachometer as the walking subject stretches it. The digital version has a toothed wheel and an optical transducer instead of the tachometer. The method of obtaining the instantaneous velocity is similar to that of Tibarewala et al.

2.2.6 Ultrasonic Tracking System

This technique utilises ultrasonic instrumentation to track fixed points on body segments in space. Transducers capable of producing ultrasonic pulses are positioned on anatomical features of interest. Three linear microphone sensors orientated orthogonally are used to receive the short ultrasonic pulses. The transit time of each pulse provides distance measurements which are converted to X, Y and Z coordinates by trigonometric calculation.

Finley et al (1972) reported on an installation of such a system. Sonic transducers were applied to both lower limbs with one set of three receivers on both sides

of the walkway. The system's accuracy was given as ±0.5 cm at the centre of the 200 cm long measurement zone and ±1.3 cm at its extremes.

Freeborn (1980) described the development of an ultrasonic tracking system as an alternative to providing triaxial goniometric measurements. The system used is commercially available from Science Accessories Corporation, called the SAC Sonic Digitizer. The sonic microphone set consists of two vertical columns (240 cm apart) with two horizontal columns (60 cm apart) in between. Only one side of the body can be analysed at a time. The system was evaluated and an accuracy of 1.8 mm was claimed.

One advantage with this system is the direct acquisition of three dimensional spatial data free from parallax error. Chao (1978) claimed that this system can provide consistent readings within the range of 10^{o} to 40^{o}C in environmental temperature and an allowable variation of pressure and humidity within laboratory conditions.

For multiple transducers used within the same microphone sensing field, time multiplexing on the sonic waves is necessary in order to differentiate one transducer signal from the others. However, such a time multiplex scheme is restricted by the maximum sampling frequency of the microphone receivers. Chao (1980) quoted the maximum sampling rate to be 140 points per second. Extreme care has to be taken to make sure that the sensing area is free from sound reflecting objects, since reflecting sonic waves can cause substantial interference.

In the application of ultrasonic instrumentation, the data retrieving field is usually restricted to the

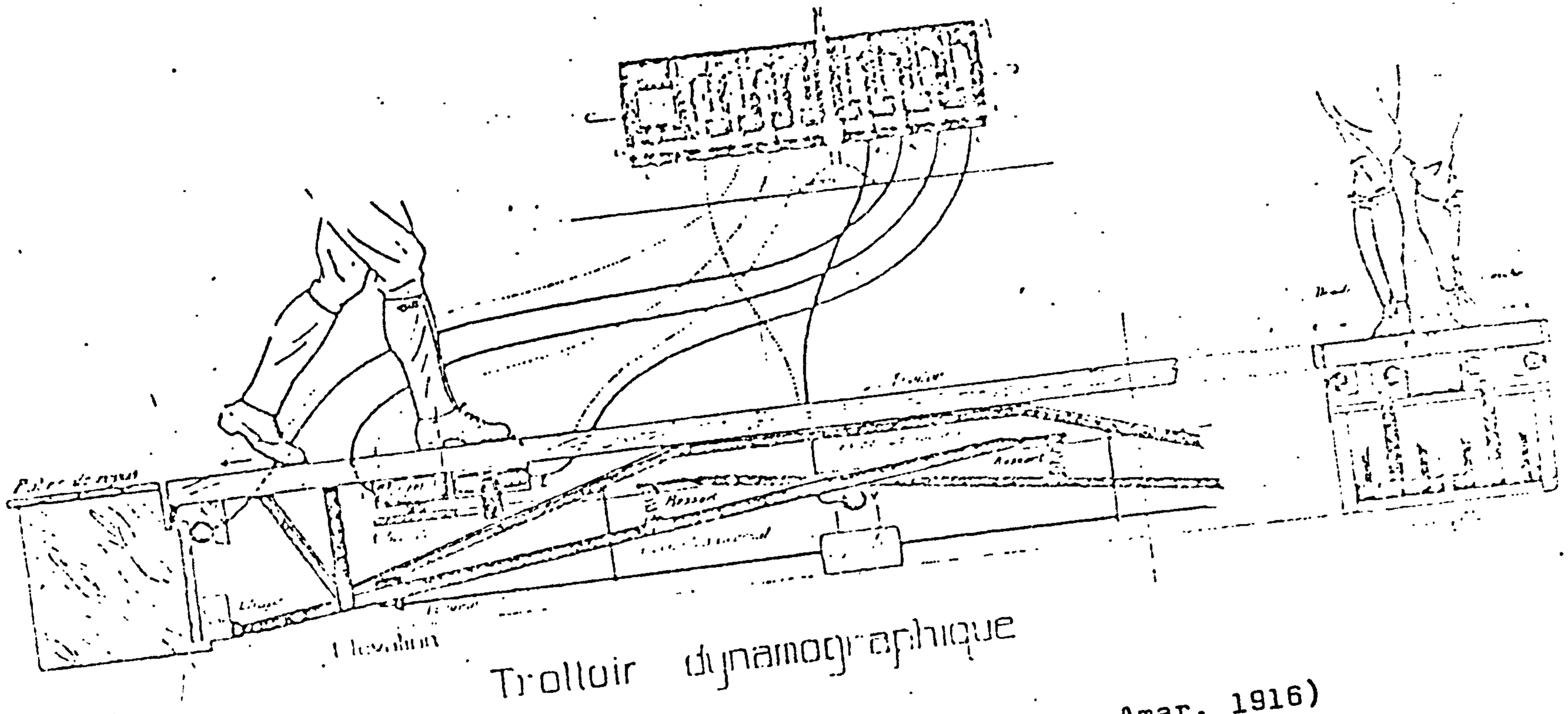

Figure 2.3.1 (a) Amar's Force Platform (from Amar, 1916)

sensing field. For the large sensing area required to accommodate gait analysis, the system is usually very expensive. Small sensing area has been used in the study of small joint movement. Youm and Yoon (1979) in wrist kinematics and Brown (1981) in the study of finger movement.

2.3. Load Measurement Study

For a comprehensive analysis of human gait, a knowledge of the applied forces and their effects is essential. The primary forces acting on the body during gait are the reaction between the foot and the ground. Several types of instrumentation have evolved to measure or deduce these quantities. The following briefly describes the development of the various types of devices that have been applied to human gait studies.

2.3.1 Force Platform

According to Milner (1977), the force platform is the most widely used ground-foot reaction measuring device. Typically, the platform is set in a walkway, with its surface flush with the surrounding floor. As a subject walks along the walkway onto the load-sensitive platform, a record of the forces exerted is made.

Historically, Amar (1916) was perhaps the first to have successfully constructed a force platform. This device was capable of recording the vertical, medio-lateral and backward force components. It consists of a platform supported by a lever arrangement of compression springs. See Figure 2.3.1(a). Deflection of the springs activates a hydraulic system which operates a rotating drum chart recorder. The device was principally used to study lower limb amputee locomotion, with a view to improving the design of artificial limbs.

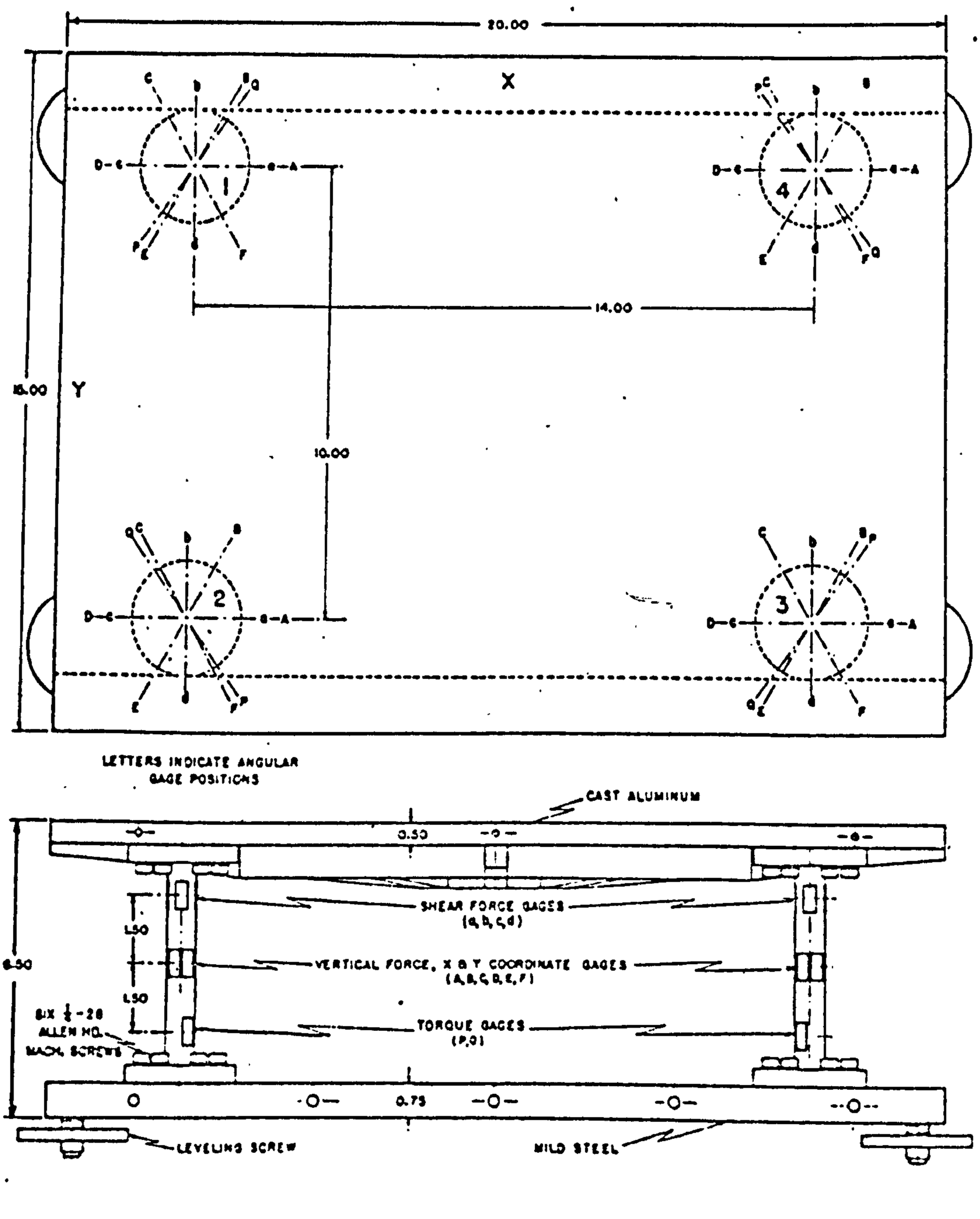

Figure 2.3.1(b). Force platform from Cunningham and Brown(1952).

Elftman (1938) designed a mechanical force platform that could measure the three mutually orthogonal force components. The device consists of a top plate separated from the bottom plate by ball bearings and restrained from side movements by springs. The deflection of these springs measures the horizontal force components. The bottom plate was supported by compression springs and the deflection of these measures the vertical force component. A mechanical lever system amplified the displacements which were recorded on high speed cine films.

These early force platforms however undergo significant displacement during application. This dynamic behaviour would undoubtedly distort the normal gait pattern.

Cunningham and Brown (1952) described a force platform that was developed at the University of California in connection with fundamental research in human locomotion (1947). It consists of a cast aluminium rectangular top plate supported at each corner by tubular aluminium columns on a steel rectangular base plate. The columns were strain gauged to give outputs capable of generating the three mutually orthogonal forces and moments about the three perpendicular axes through the centre of the top plate, see Figure 2.3.1(b). This was the first electronic force platform and one that could produce satisfactorily all the six ground reaction components judged by present day standards. The natural frequency of the device was given as 105Hz for shear and 140 Hz for torsion. The excessive horizontal plane vibrations were reduced by a viscous damping system. No information was given on the amount of "cross-talk" between channels, which is inherent in this type of measuring system.

Paul (1967) developed a similar force platform to

that of Cunningham and Brown, modifying the physical dimensions and strain gauging circuity. This force platform had a transverse natural frequency of 56 Hz and the vertical natural frequency was claimed to occur at 260 Hz. Small "cross-talk" was found during calibration of the force plate. This was corrected in subsequent calculations.

Kirkpatrick et al (1969) also presented a force platform with top and bottom plates separated by strain gauged columns at each corner. However, the top plate was not rigidly fixed to the columns, ball-vee-groove joints being used for the connection instead. Natural frequencies for the vertical and horizontal vibrations were quoted as 1610Hz and 38 Hz respectively. No damping system was incorporated in the device, instead an analogue low pass filter was used to eliminate the noise. No information on the "cross-talk" effect was given.

An alternative to strain gauging is the use of piezoelectric effects. There are many advantages in adopting this alternative, the most important of these being the high rigidity, high sensitivity, high natural frequency and low cross-sensitivity of piezoelectric crystals.

Lauru (1957) developed a triangular force platform using piezoelectric transducers. The device could only measure the three orthogonal force components. The force platform was principally used in the physiological study of industrial workers, cited in Brouha (1960). Details of constructions and technical information of the platform were not discussed.

More recently, a commercially available force platform, with piezoelectric transducers, was marketed by Kistler Instrument AG of Switzerland (1975). It consists

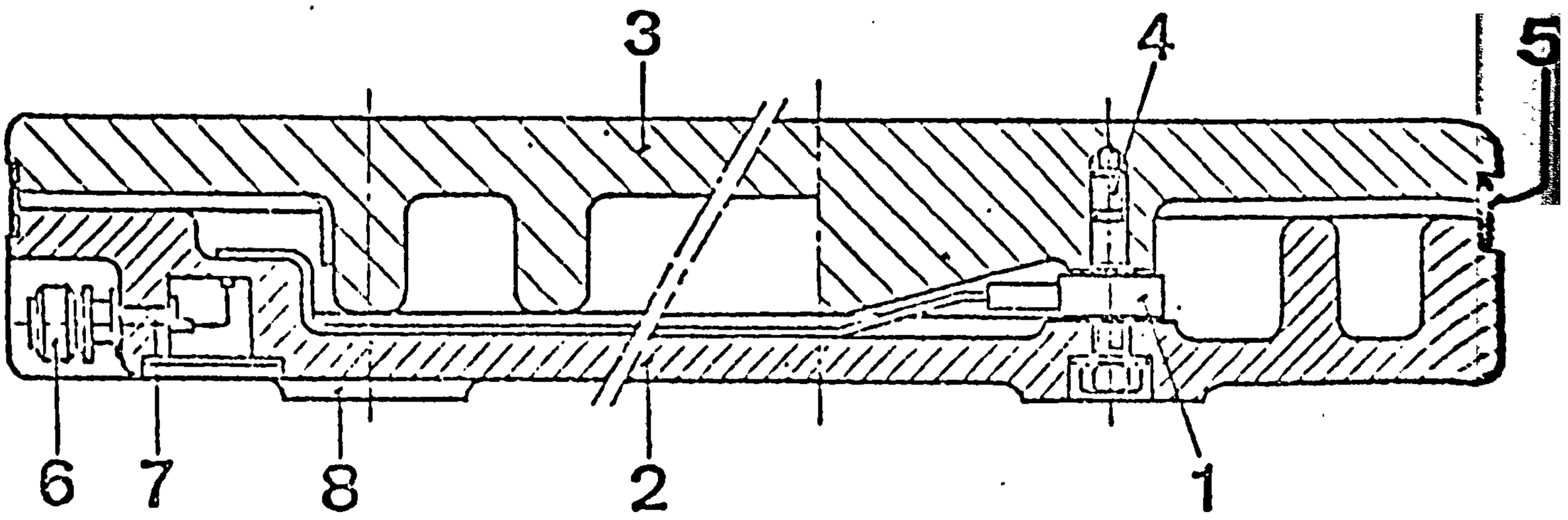

1. 3-component piezo-electric force transducer
2. Base plate
3. Top plate
4. Prestressing bolt
5. Special rubber seal strip
6. TNC connector
7. Switch for selecting measurand combination
8. Supporting surface concentric with the force transducer

Figure 2.3.1(c). Cross section of Kistler's force platform (type 9261A).

of four 3-component force quartz transducers sandwiched between a cast aluminium rectangular top plate and a base plate, see Figure 2.3.1(c). The device together with associated change and summing amplifiers, can produce all the six ground reaction components. The manufacturer claims that the force plate platform (type 9261A) has an all round minimum natural frequency of greater than 200 Hz with maximum "cross-talk" of less than 3%.

McLeish and Arnold (1972) and Cohen et al (1980) developed force plates of the suspended type. Cohen and his associates employed seven strain gauged steel strips pre-tensioned to suspend an inner plate from an outer support frame. Three of these transducers were used to measure the vertical load, while the remaining four were used to measure the horizontal forces. These seven outputs, together with the associated electronics, generate the three orthogonal forces, the two coordinates of the centre of pressure and the moment about the axis normal to the plate. The natural frequency was given as approximately 70 Hz and very low "cross-talk" was claimed, although no values were given. The force plate has to be continually calibrated prior to any measurement and the calibration procedure assumes that there is no "cross-talk" between each of the seven channels. No mention was made of the possible errors of this assumption.

Single-step force platforms i.e. all of those described so far, have the disadvantage that only one foot-ground contact can be studied at a time. Although several of these placed in succession would be a possibility in studying several steps, however making contacts with all of them would be difficult.

Skorecki (1966) described a two-track force platform of 3.3 metres long. Each platform was supported

by two tubular columns near each end. Associated with each column was the elastic element and damping system. The small displacement of the elastic element was amplified by an optical system. Only the vertical component of force exerted by the feet was recorded. The natural frequency of the force platform was claimed to be 85 Hz. Rydell (1966) also described a similar device, however the measurement was done electrically by 'Bofors' force cells. The force platform was also capable of measuring the longitudinal shear force.

Wirta et al (1970) presented a much shorter two-track force platform (0.3 x 1.5 m). It could measure the three orthogonal force components. The strain gauge suspension type of concept was used in recording these parameters. No information was given with regard to calibration, alignment of the transducers, minimum natural frequency and "cross talk" effects.

Although two track force platforms have the advantage of accommodating several successive strides during testing, they are limited to measuring, at the most, only the three force components, which is not sufficient for comprehensive kinetic analysis. Moreover, the subject is constrained to walk with feet astride to avoid landing on the contralateral side, and this may cause the subject to adopt an unnatural gait pattern.

An essential criterion in force platform design is the frequency response of the system. For accurate measurement, the force platform must have a minimum natural frequency higher than all the applied frequencies. Skorecki (1966) suggested that only low frequency components of below 15 to 20 Hz are present in walking, although,Crowninshield and Brand (1978) claimed that significant components of the floor reaction force are in the frequency range of 0 - 50 Hz, while minor components

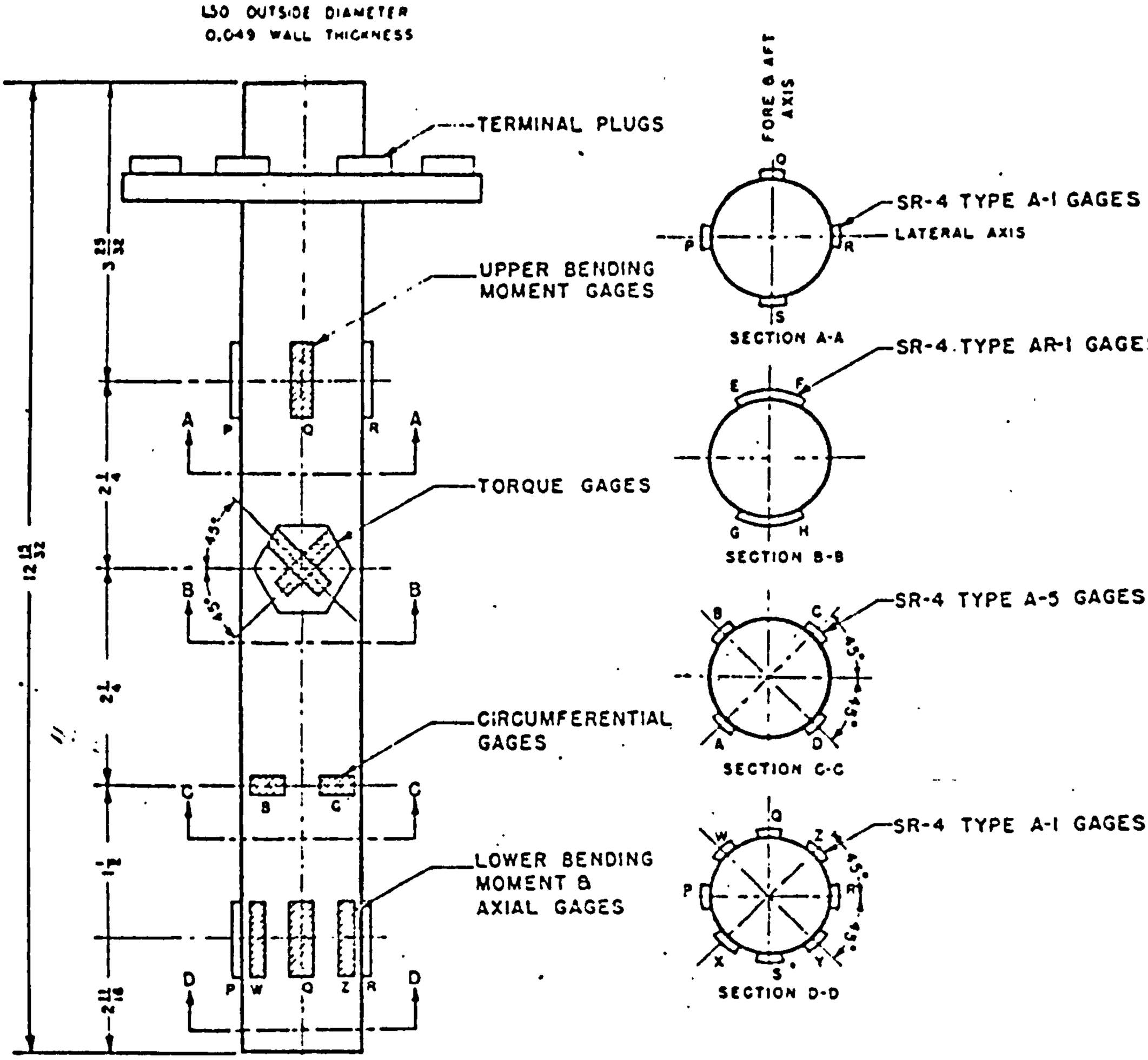

FRONT VIEW OF PYLON

CIRCUMFERENTIAL POSITIONS OF GAGES

Figure 2.3.2(a). Pylon force transducer from Cunningham and Brown(1952).

may be recorded up to 100 Hz or more. Simon et al (1981) reported the existence of high frequency impulsive loads at heel strike - 75 Hz without shoes. The remainder of the force trace had frequency components of 1 - 10 Hz. Force platforms with resonant frequency of 100 - 200 Hz were regarded to be adequate for providing accurate measurement.

2.3.2 Pylon Force Transducer

This is a load-measuring device incorporated in the shank of an artificial leg, to provide direct measurement of the loadings within the leg.

Cunningham and Brown (1952) designed and constructed the first pylon force transducer. It consisted of an aluminium tube 316 mm long, 38 mm outside diameter with a wall thickness of 1.24 mm. It was strain-gauged to measure the axial load, medio-lateral and fore-aft shear, medio-lateral and fore-aft bending moments and torque about the shank axis, see Figure 2.3.2(a).

Transverse shear was obtained from the difference in bending moments measured at two levels on the pylon. For higher shear force sensitivity, the two levels of gauges had to be as far apart as possible. The axial load was measured by four gauges positioned 90^{o} apart around the circumference of the tube. Two torque gauges were located diametrically opposite each other, both orientated at 45^{o} to the principal axis of the pylon, in order to measure the principal strain due to torsion. No mention was made of the amount of "cross-talk" present in the transducer and whether this effect was considered during calibration.

This particular device was not used widely because it was too long. It could only be fitted onto the shank

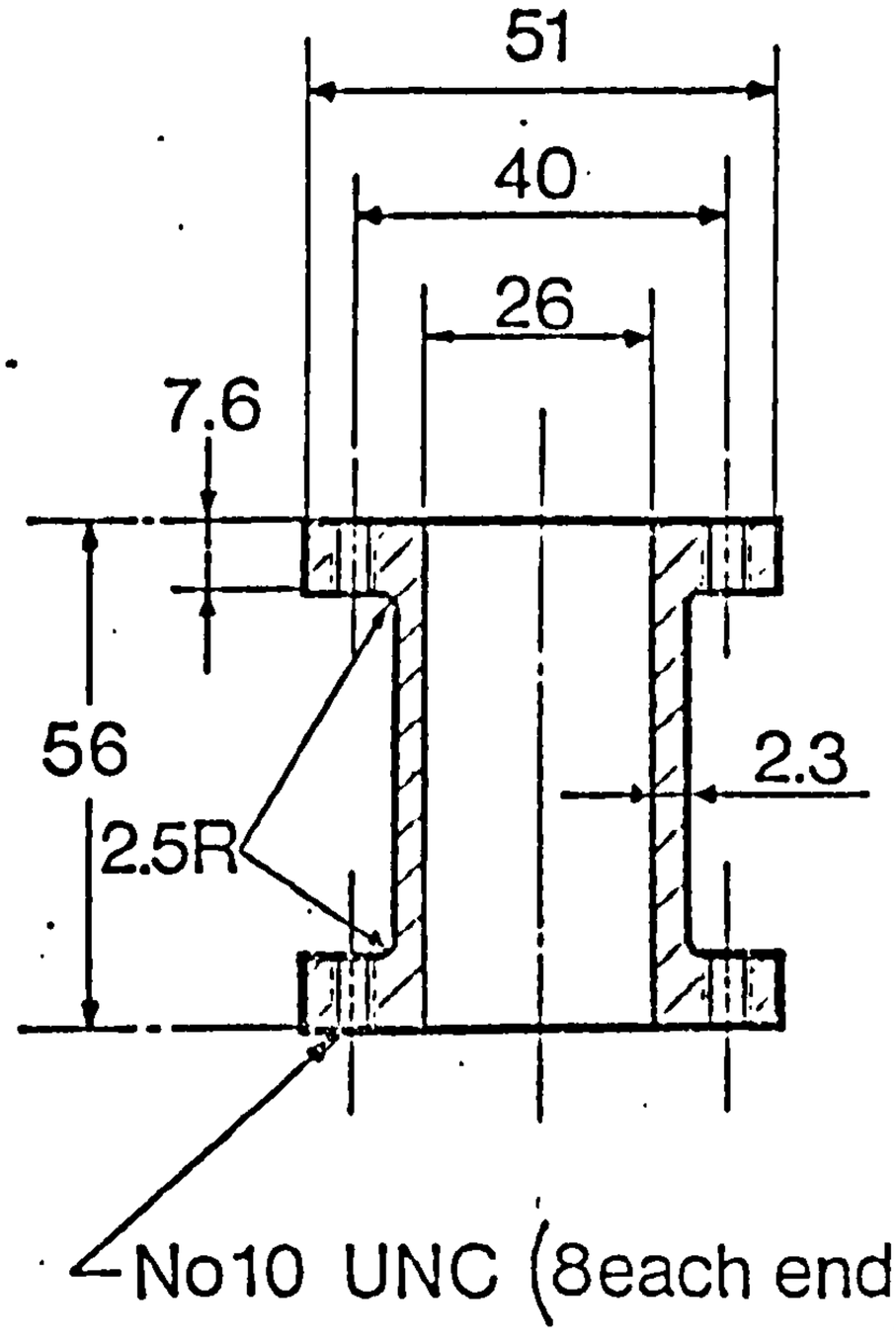

Figure 2.3.2b. Basic dimensions of pylon transducer designed by Berme et al(1976).

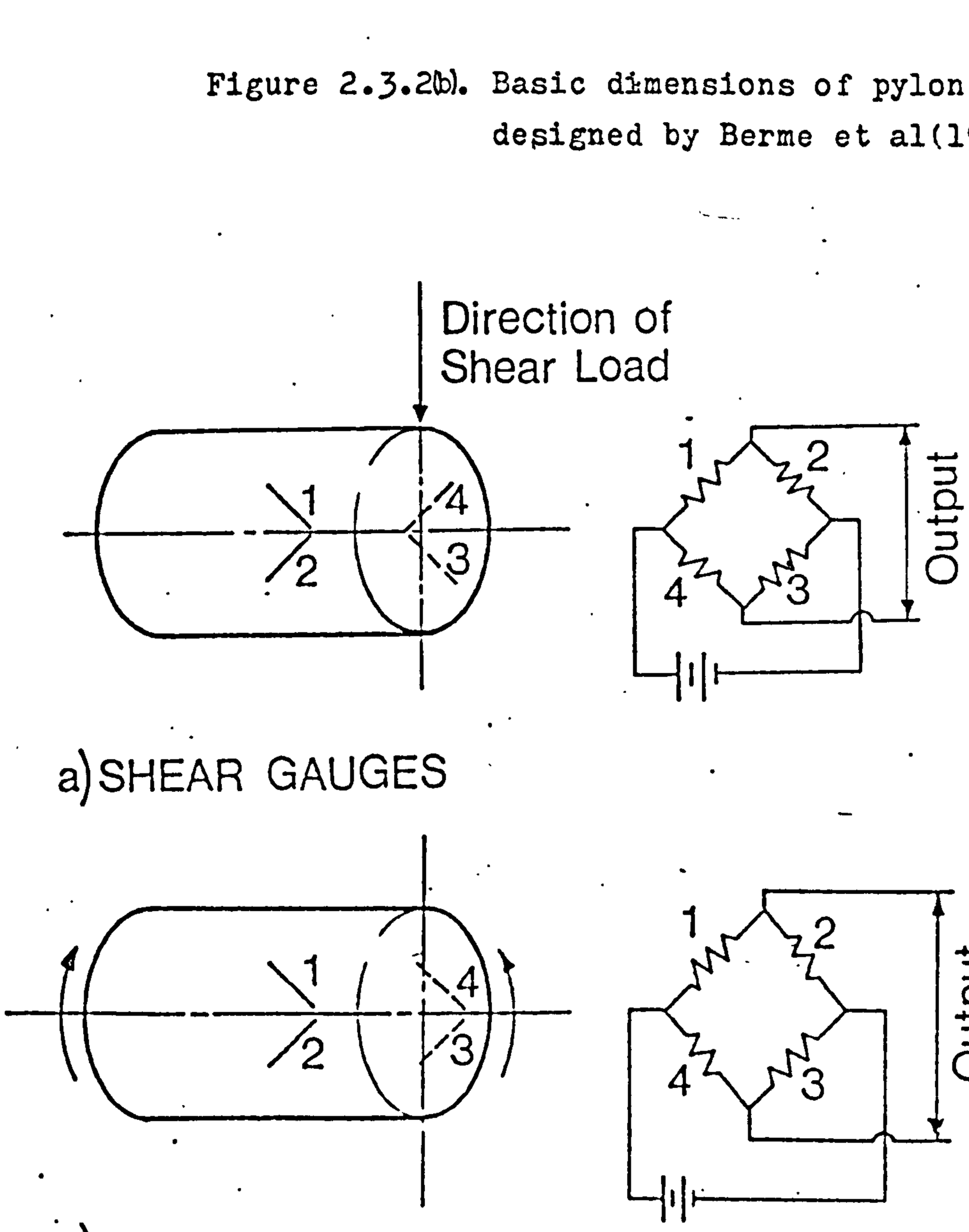

Figure 2.3.2 (c). Strain gauge design for shear and torque measurement (from Berme et al, 1976)

of some above-knee and higher level prostheses with a fairly small knee mechanism.

Lowe (1969) built a similar strain gauged pylon to that of Cunningham and Brown. The only modification was in the length, decreasing from 316 mm to 114 mm. This reduction was made at the expense of lowering the shear force accuracy. However, the compromise was necessary to enable the transducer to be applied to most above-knee prostheses, including some of the below-knee types. "Cross-talk" between channels was accounted for in the calibration calculations.

Berme et al (1976) reported on an even shorter pylon transducer. The basic feature of the device is as shown in Figure 2.3.2(b). The reduction in length was made possible by measuring the shear force directly from two shear strain gauges. These two gauges were positioned in a similar fashion to that of the torque gauges (described previously) but the circuitry is different, see Figure 2.3.2(c). All other parameters were measured using the same design as Cunningham and Brown. Small "cross-talk" between channels was observed when calibrating the pylon, but this was accounted for in subsequent calculations. This pylon transducer has been used successfully in all prostheses fitted to below-knee amputee and to higher levels of amputation.

One inherent limitation is that the transducer can only be applied to the prosthetic leg. For simultaneous contralateral recording, an alternative recording device has to be offered to the sound leg. The major advantages of the pylon transducer are the ability to measure loadings directly and that the recording of parameters is not restricted to the walkway. Lovely (1981) developed a portable recording device capable of registering all the six components of loading continuously

Figure 2.3.3 (a). Pneumatic foot-force measuring device. (from Carlet, 1872)

for one hour. This development eliminates the cumbersome trailing cables and allows outdoor recording to be carried out.

2.3.3 Footwear with Force Transducers

Footwear mounted with force transducers is an alternative method in measuring the forces exerted by the foot on the ground. It has the advantage of measuring the foot forces continuously, without the subject being restricted to a walkpath.

Carlet (1872) reported one of the very first efforts to record the ground foot reaction during gait. Air chambers attached to the sole of the shoe were utilised for the purpose. The pneumatic pressure generated by the compressed air during stance was registered on a hand held recorder, see Figure 2.3.3(a).

Schwartz and Heath (1947) were among the first to attach pressure transducers to the sole of the foot, in order to measure the forces exerted inside the shoe. The pressure transducers were positioned on the first, third and fifth metatarsal heads, medial and lateral heel and the big toe.

Holden and Muncey (1953) modified a shoe to hold a capacitance pressure transducer in the heel and also used transducers 3 mm thick for pressure recordings at other sites, between the foot and shoe (viz the ball of the foot and big toe).

Pressure transducers are useful for measuring pressure on those areas of the sole which are of particular interest. However, it is possible that the presence of the transducers on the sole may change the pressure they are trying to measure. Furthermore, these

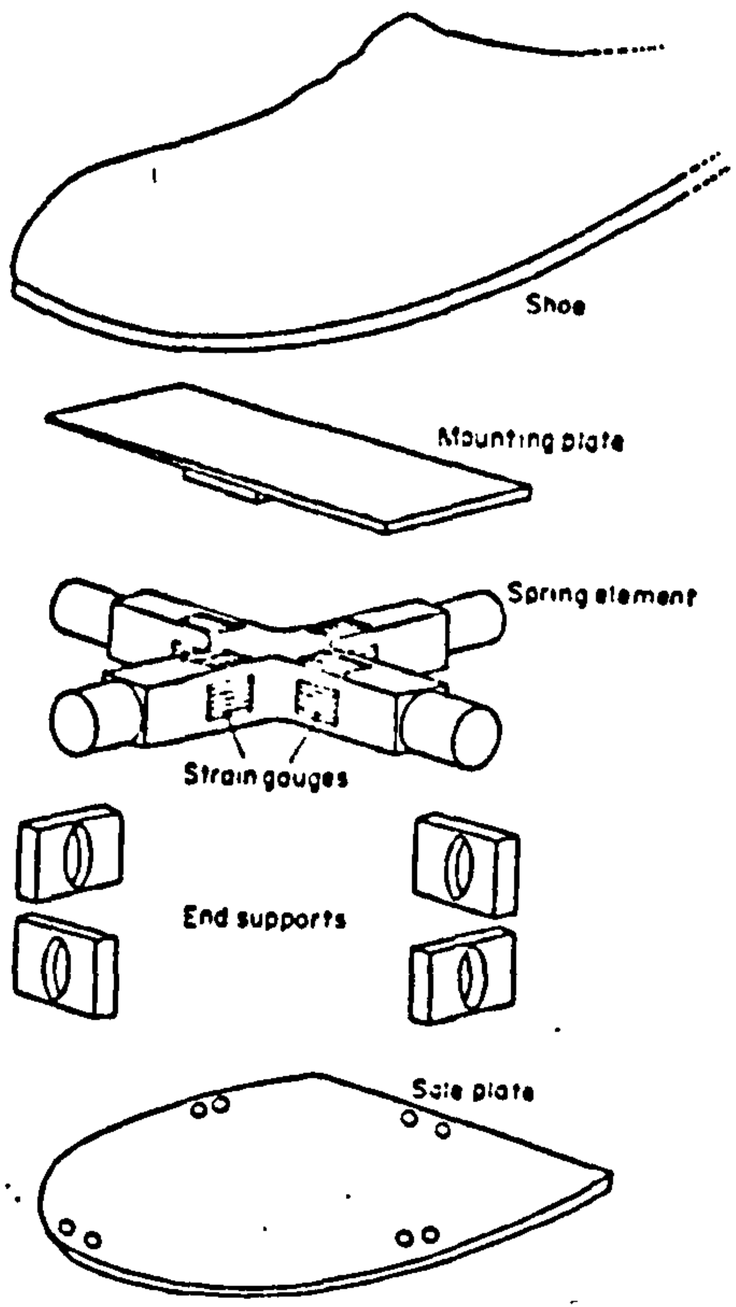

Figure 2.3.3(b). Force transducer design from Spolek and Lippert(1976).

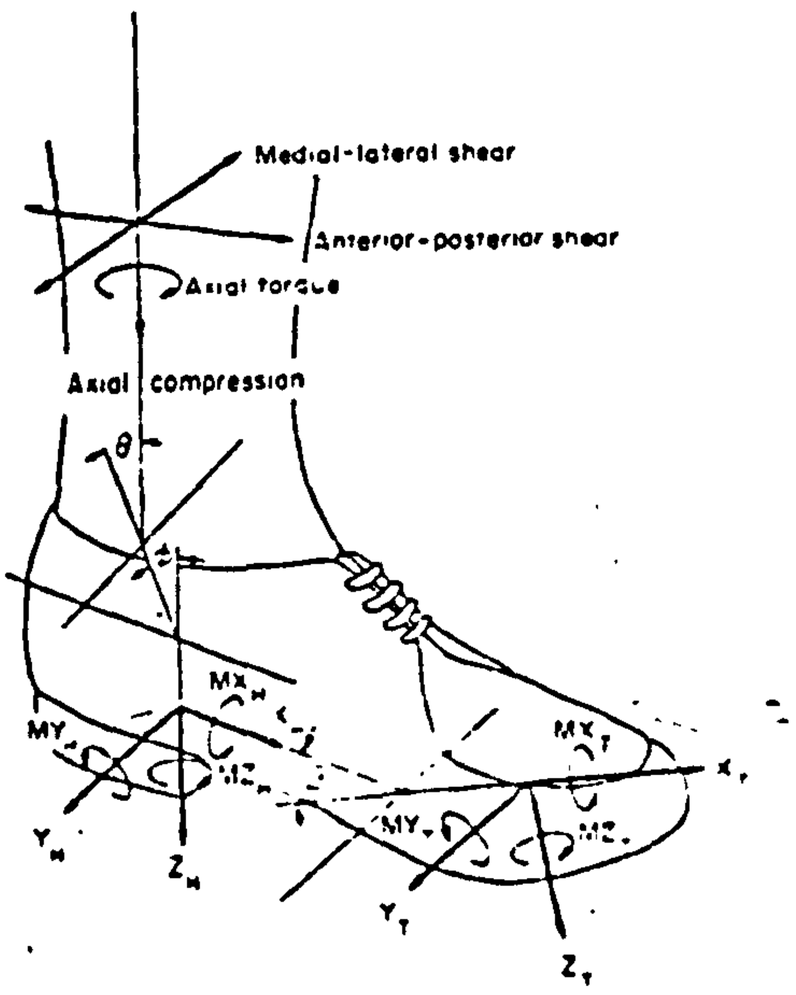

Figure 2.3.3(c). Parameters obtainable from the instrumented shoe of Spolek and Lippert(1976).

transducers are not designed to record the total foot force.

Hargreaves and Scales (1975) reported on a load measuring sandal with a force transducer in the heel. They found that the device was electronically unbalance and that its flat sole led to unnatural gait patterns, hence, a completely new transducer was developed. It replaced the insole of a sports shoe. Detailed construction of the device was not given. The telemetric transmitter and battery unit were housed in pockets on the side of the shoe. Only the vertical force component was measured.

Spolek et al (1975) designed an instrumented shoe with force transducers attached to the heel and fore-foot. This device was also reported by Spolek and Lippert(1976). Each transducer consisted of a strain-gauged "cross" beam supported at its four ends to the base plate, see Figure 2.3.3(b). Loads are applied to the centre of the cross, causing the beam to bend, thereby producing strains which are proportional to the loading. The device measures all the orthogonal components of force and moment acting at the heel and fore-foot, as shown in Figure 2.3.3(c). Incorporated in the instrument was an electrogoniometric system which measures the relative angles between the heel, forefoot and the shank. From this information, the forces and moments acting on the shank were calculated. The authors claimed that the "cross-talk" between channels is negligible.

Another design of a force measuring shoe was presented by Kljajic and Trnkoczy (1977). It consisted of eight strain-gauged cantilever transducers built into the sole of a specially made leather shoe, see Figure 2.3.3(d). The transducers however can only measure the vertical and horizontal forces. It was reported that a

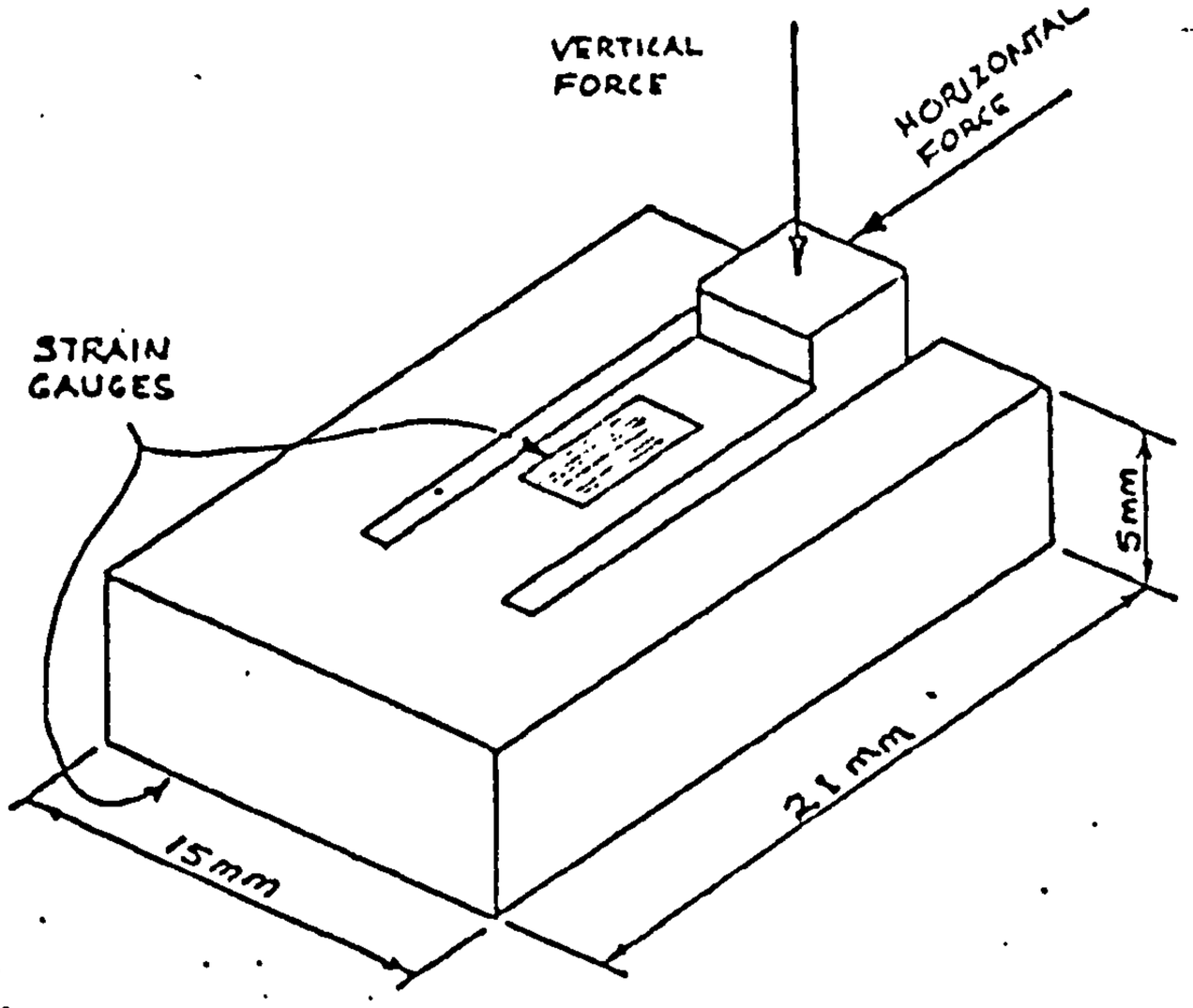

Transducer

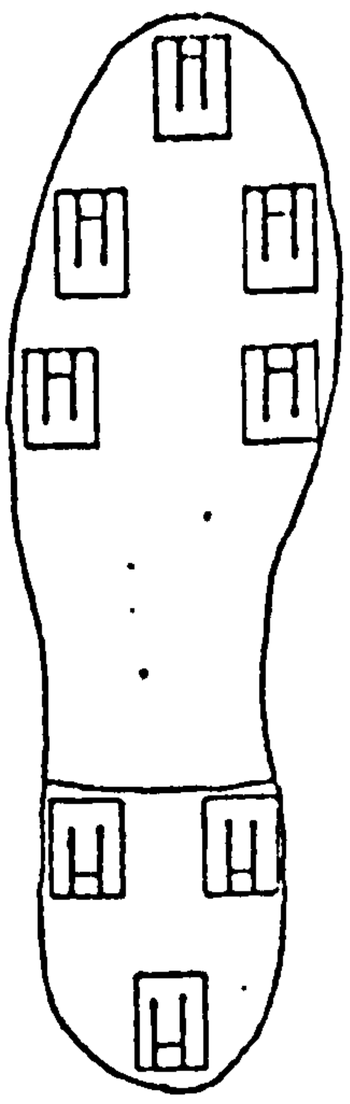

Transducer positions on the shoe

Figure 2.3.3(d). Force measuring shoe.
(from Kljajic and Trnkoczy,1977)

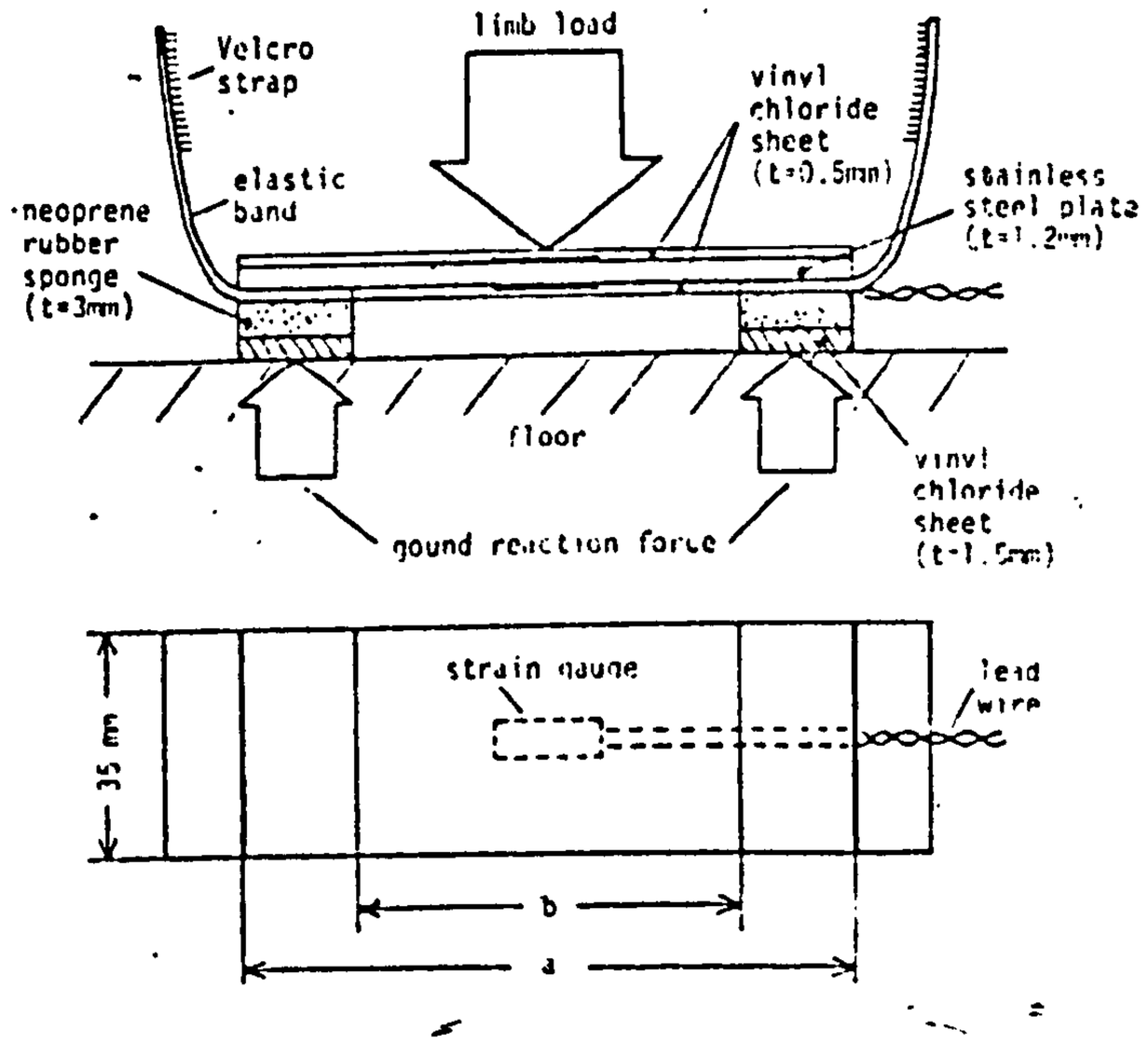

Structure of force transducer
a = 85 mm, b = 55 mm for the front transducer
a = 65 mm, b = 35 mm for the rear transducer

Figure 2.3.3(e). Force transducer design.
(from Miyazaki and Iwakura,1976)

linearity of 2% can be achieved when measuring vertical forces of up to 1000N and that "cross-talk" with the horizontal force was at the most 6%. From the output signals, it was possible to obtain the position of the centre of pressure.

Miyazaki and Iwakura (1978) designed and constructed a transducer which can be strapped to any shoe. It consisted of a stainless-steel rectangular plate with two supports attached to the lower surface of the plate at each end, see Figure 2.3.3(e). Strain gauges were positioned at the centre of the plate to measure the vertical forces during loading. Two such transducer units were fitted to each shoe; one fastened to the sole at the metatarsal region and the other to the heel. It was claimed that the error in measurement is well within 10% of full scale for cadence under 110 steps/min.

Although this type of instrumentation has the advantage of being a portable load measuring device, current designs are still not satisfactory. Those that can record all the six components of ground reaction are too bulky and heavy while others that are relatively thin and light can only measure two force components.

2.3.4 Foot-Force Distribution Recorder

This type of device does not measure the forces and moments exerted on the floor by the foot. However, it does produce foot force distribution pattern either with the subject standing still on the device, or dynamically as the subject walks over it. The primary purpose of the device is to examine barefoot weight bearing patterns. Numerous devices have been developed over the years to perform such recordings. The following is a review of some of these devices.

Elftman (1934) carried out a survey of the earlier methods used in recording foot-force distribution. It included the use of plaster of Paris by Beely (1882) and soil by Momburg (1908), these methods were very unsatisfactory. More accurate methods were also cited, such as that of Abramson (1926), who used a lead plate over steel shot , Forstell's (1925) suspended wire net over an ink pad and Basler's (1926) harp-like machine that produced vibrations when set in motion by a walking subject. He also described a Kinetograph, which was developed by Morton (1930). It consists of a rubber mat with corrugated top surfaces. The mat was covered with an inked fabric and a sheet of paper. As the subject walked on the device, it caused the corrugations to deform and widen the ink impression, thus giving a measure of the degree of pressure exerted by the foot during walking. Elftman presented a similar type of device; in place of the ink fabric and paper, a heavy glass plate was used. By means of cinephotography, a permanent record of the foot-force distribution was possible.

Miura et al (1974) modified the barograph described by Elftman. Light was introduced into the glass plate from the side by fluorescent lamps. A colour densitometer was incorporated into the system to produce the foot pressure distribution contours in colour. A 35 mm cine-camera operating at 50 frames per second was used to photograph the event.

Chodera and Lord (1978) described the pedobarograph which was developed by Chodera in the late 1950s. It consists of a transparent plate capable of conducting light by internal reflection and is covered by an elastic foil with fine surface texture. When load is applied to the foil, contact is made with the surface of the plate, which produces a series of light reflections to map out

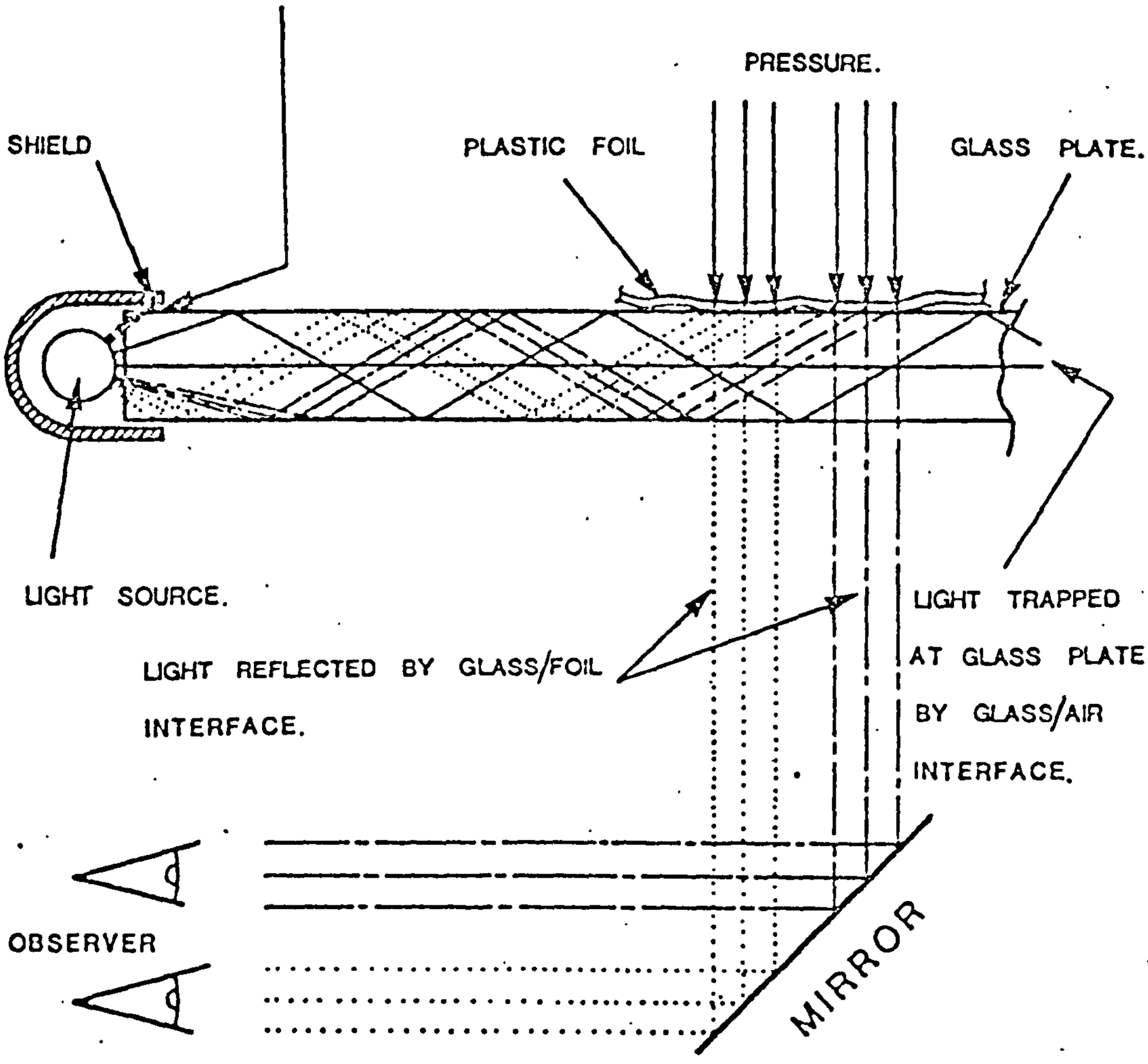

Figure 2.3.4 (a). Pedobarograph
(from Chodera and Lord; 1978)

the contours of the foot pressure distribution, see Figure 2.3.4(a). Currently, they are using an on-line television system equipped with a colour monitor to record the pressure distribution. Their latest version also includes four vertical load cells mounted onto the plate to provide further on-line information, such as (1) the body weight and both A/P and M/L balance, and (2) the vertical projection of the centre of gravity. The authors claimed that this device could be used for studying the alignment of prostheses on lower limb amputees amongst other applications.

Foot-force distribution patterns can give useful information regarding the concentration of loads on various part of the sole. In order,to relate high pressure experienced by the sole during locomotion to other parts of the body, both kinematic and kinetic information is required. Therefore, a combination of multicomponent force plate and a foot-force distribution recorder is highly desirable.

Grundy et al (1975) presented a strain-gauged force plate with a glass surface on which grid wires were marked for simultaneous filming of the foot-floor interface and subsequent contact area determination. Cohen et al (1980) and Kistler (Type 9863) have in their force plate design, the capacity to interchange the contacting surface from metal to glass. These glass top force plates enable the position of the contacting foot on the plate to be recorded. The recording can either be made by photography or T.V. camera and then superimposed onto the calculated centre of pressure pathway.

An electronic foot-floor contact area transducer was developed by Draganich et al (1980). The area transducer consists of a matrix of switches, defined by the intersection of strips of berythium copper (X-lines)

Figure 2.4.1 (a). Stick Diagram
(from Winter, 1980)

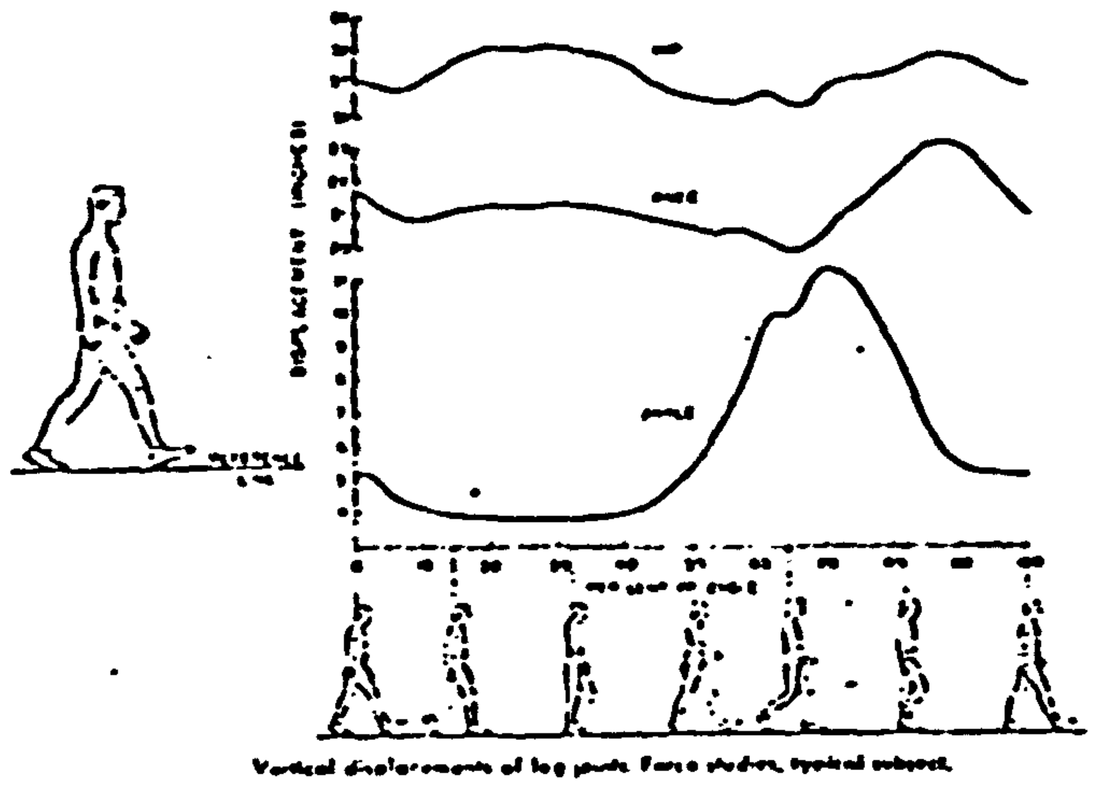

Figure 2.4.1(b). Vertical Displacement of leg joints
(from Eberhart et al, 1954)

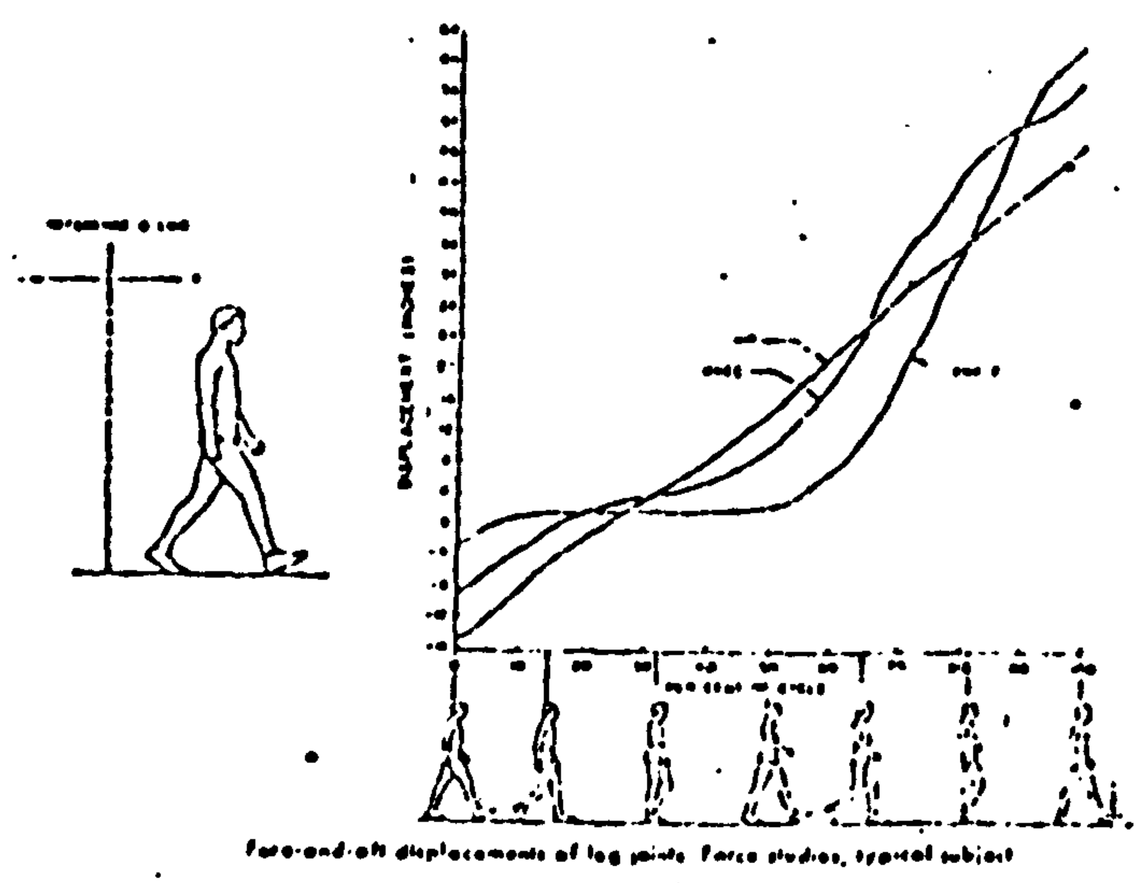

Figure 2.4.1 (c). Fore-and-aft displacement of leg joints
(from Eberhart et al, 1954)

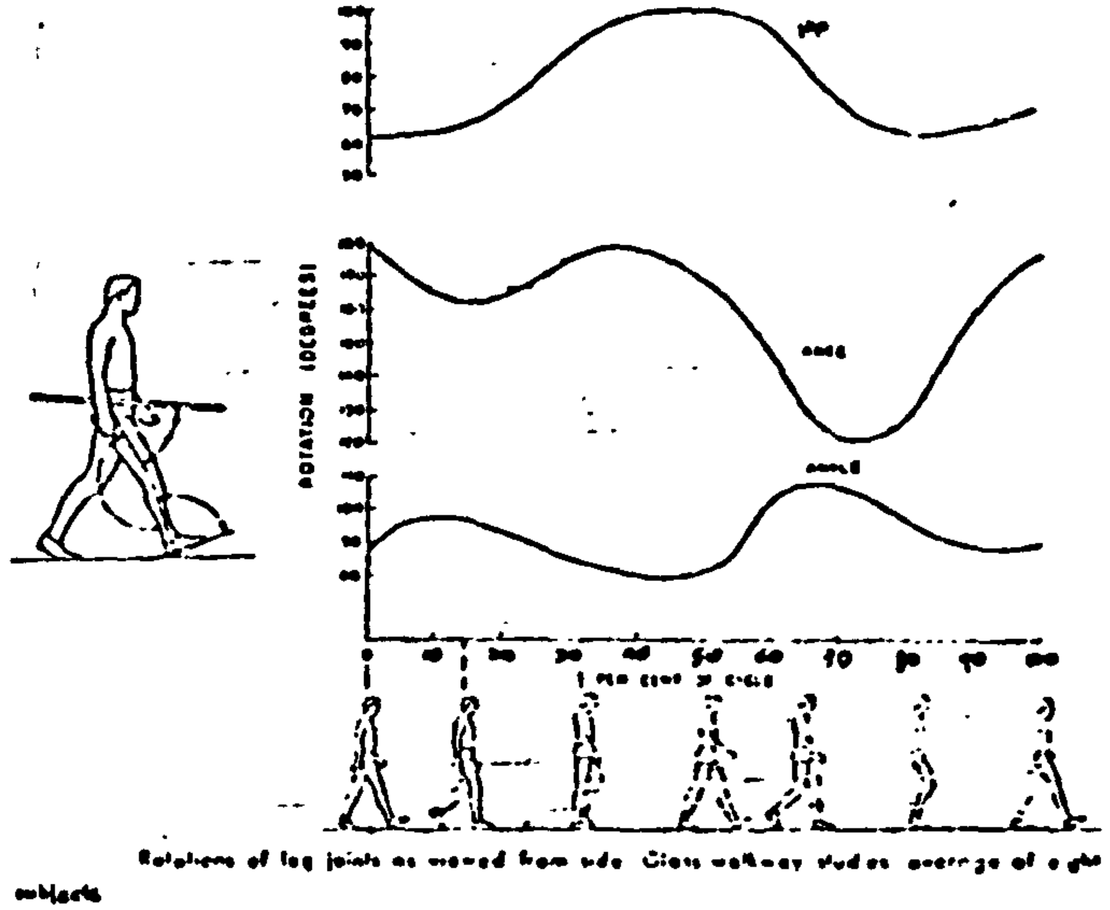

Figure 2.4.1 (d). Rotations of leg joints
(from Eberhart et al, 1954)

and rows of aluminium rivets(Y-lines). Force applied at the intersection of an X and Y line element caused them to make contact. The device was placed over a Kistler force platform and connected to a mini-computer. The system was capable of measuring foot-floor contact areas, average contact pressure, speed of the centre of pressure and the resultant force. The transducer was found to be reliable for applied pressure above 14N/cm^2, this being possible due to the stiffness of the silicon rubber rods that separate the X-line copper strips. The stiffness has to be carefully selected, so that it does not provide a "spongy" contact which may alter the subject's natural gait. There was no mention made of the overall thickness of the contact area transducer or whether its top surface was flush with the surrounding floor.

2.4 Normal Gait Studies

This section attempts to review human locomotion data pertaining to normal male subjects. It is by no means a comprehensive survey, nevertheless it intends to cover the majority of the gait parameters obtainable through the analytical emethods already described.

2.4.1 Kinematic Data

The earliest form of presentation of kinematic data was the "stick diagram", see Figure 2.3.1(a). This can be produced directly using the interrupted light photographic technique. Other methods of data acquisition require the coordinates of the hip, knee and ankle joints in the saggittal plane to be obtained. Any one of the optoelectric techniques coupled with a high speed mini-computer can give an on-line "animated" reproduction of the "stick diagram". This method of presentation is particularly useful in providing a quick and simple

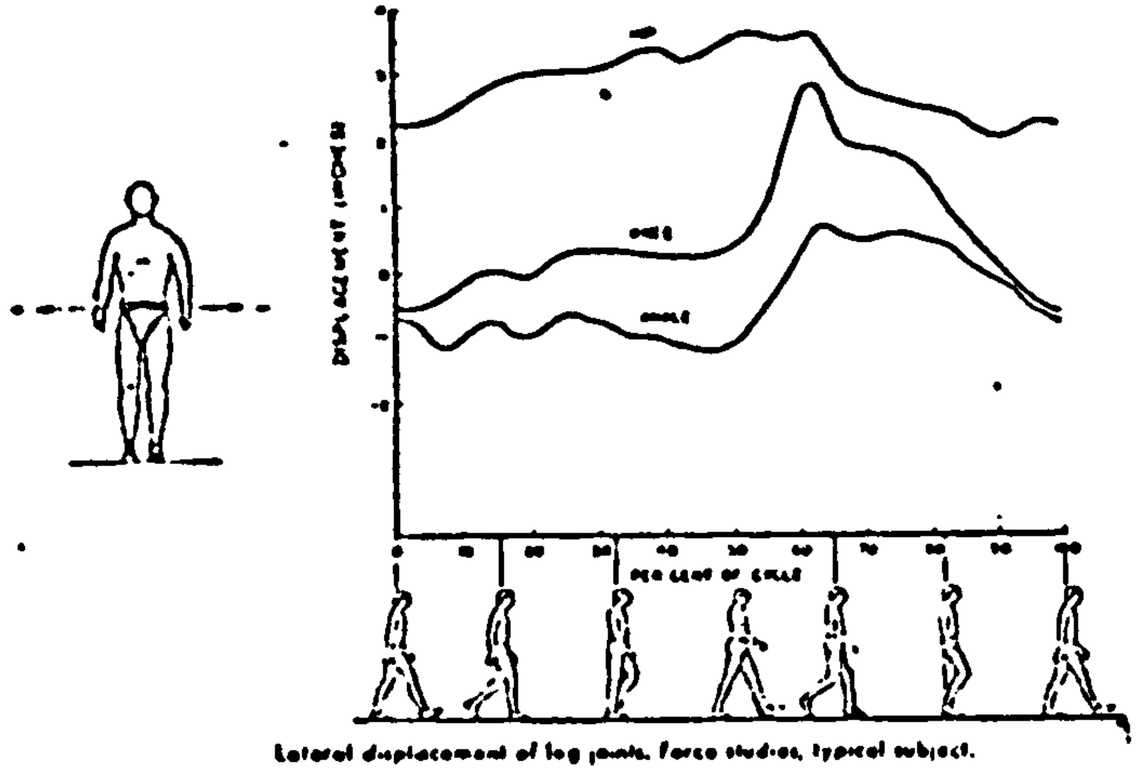

Figure 2.4.1 (e). Lateral displacement of leg joints
(from Eberhart et al, 1954)

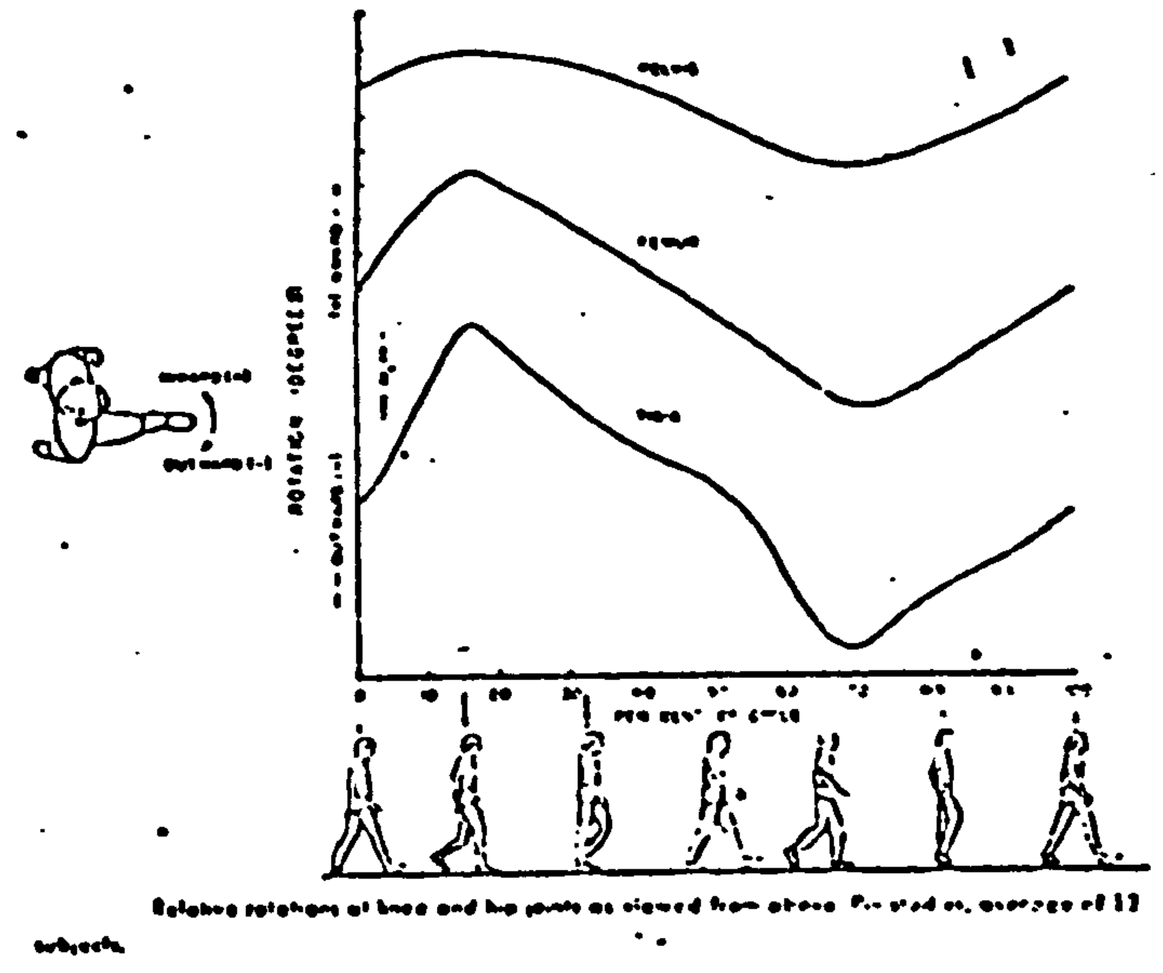

Figure 2.4.1 (h). Relation Rotations at knee and hip joints
(from Eberhart et al, 1954)

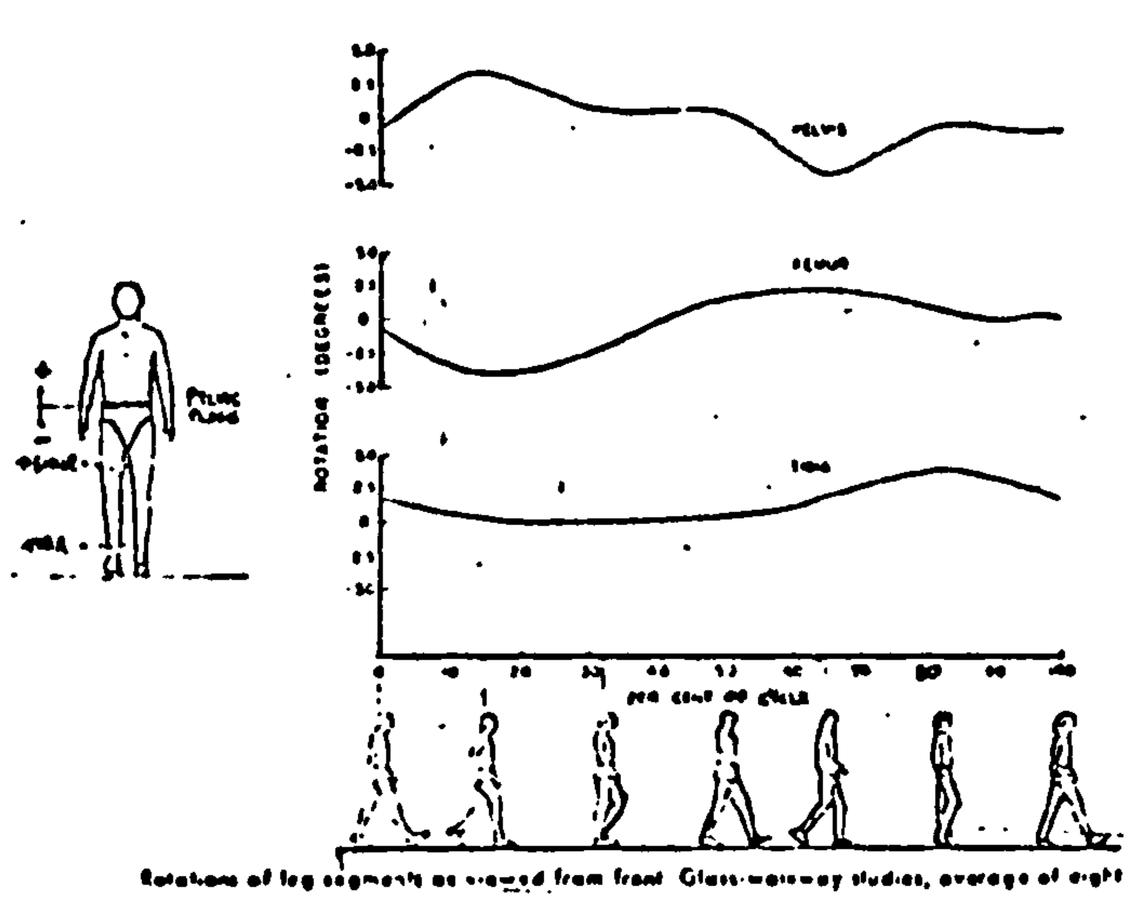

Figure 2.4.1 (f). Rotations of leg segments
(from Eberhart et al, 1954)

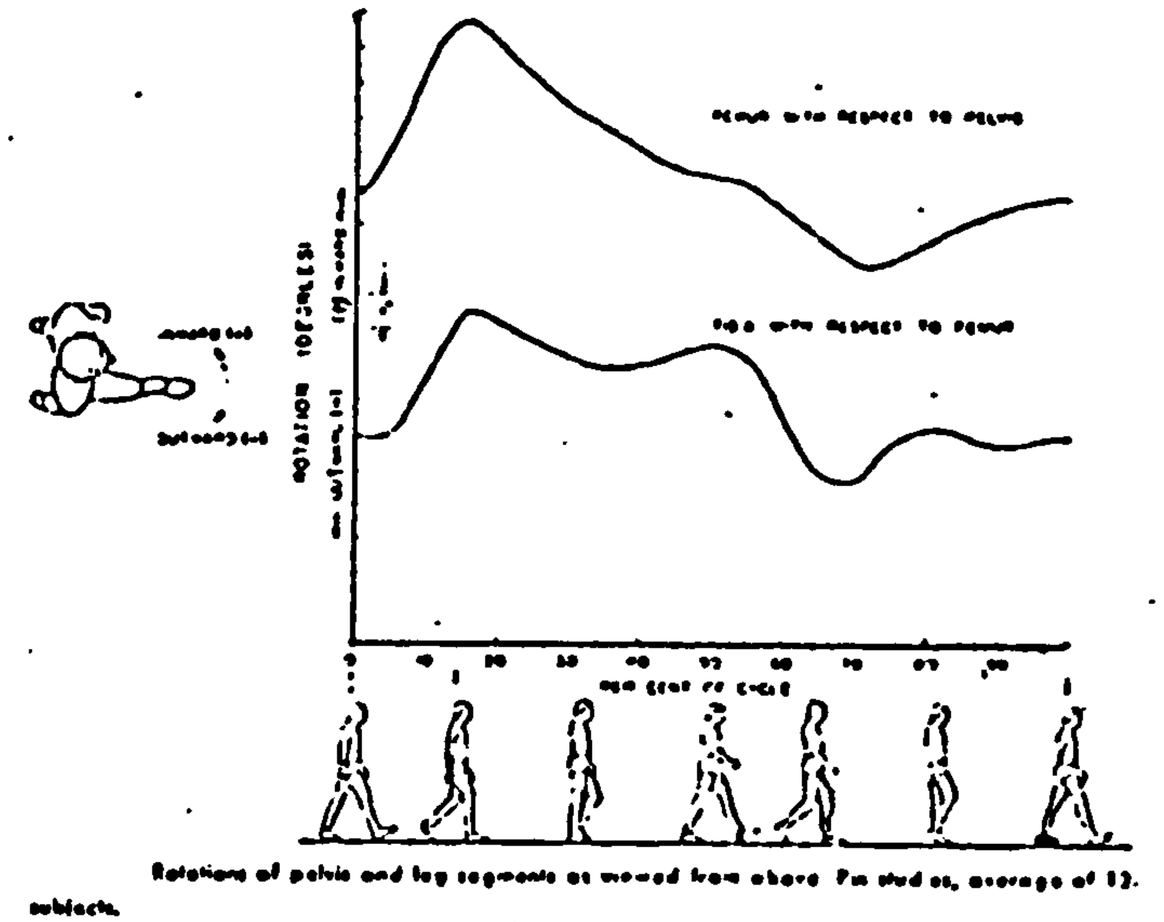

Figure 2.4.1. (g). Rotations of pelvis and leg segments
(from Eberhart et al, 1954)

assessment on the "smoothness" of the gait. The superimposition of force vectors on a stick diagram can also provide a useful technique for gait analysis. Further discussion of this can be found in the next section.

The extensive research carried out during the period 1945-1947 at the University of California, Berkeley (UC-BL) produced important information regarding human locomotion. A summary of their findings was reported by Eberhart et al (1954).

Figures 2.4.1(b) and (c) show the vertical and fore-aft displacements of the joints in the lower extremity respectively. Time derivatives of these data were obtained by a grapho-numerical differentiation technique reported by Felkel (1951). It was found that the acceleration and deceleration of the foot was very large at the beginning and end of swing phase respectively; approximately four times the gravitational acceleration (g). Figure 2.4.1(d) shows the angular displacements of the joints in the saggittal plane. It was observed that the rapid flexion of the hip and knee at the beginning of swing was to give adequate toe clearance. It was suggested that the knee flexion immediately after heel strike was to absorb the shock of the body-weight passing onto the leg.

Linear medio-lateral displacement of the joints is as shown in Figure 2.4.1(e). The magnitude of these displacements is very small but they play an important part in adjusting the body to the line of weight bearing and the maintenance on balance. Figure 2.4.1(f) shows the angular displacement of the lower extremity body segments in the frontal plane. The pelvic rotation (or tilt) in this plane is an important factor in maintaining a "smooth" progression. Since the pelvis tilts down to

MEAN CYCLE DURATION FOR SIXTY NORMAL MEN

Groups	No. of Observations*	Mean Cycle Duration (*Seconds*)†	Equivalent Cadence (*Steps per Minute*)
Total	120	1.03 (.10)	117
Age			
20 to 25 yrs.	21	1.01 (.10)	115
30 to 35 yrs.	21	1.08 (.10)	111
40 to 45 yrs.	21	.98 (.17)	122
50 to 55 yrs.	21	1.02 (.10)	118
60 to 65 yrs.	21	1.01 (.11)	115
Height			
Tall	40	1.01 (.11)	119
Medium	40	1.07 (.10)	112
Short	40	1.02 (.09)	118

THE MEAN DURATIONS OF STANCE, SWING, AND DOUBLE-LIMB SUPPORT FOR SIXTY NORMAL MEN

Groups	No. of Observations*	Duration of Stance (Both Limbs) Seconds†	Duration of Stance (Both Limbs) Per cent of Walking Cycle	Duration of Swing (Both Limbs) Seconds†	Duration of Swing (Both Limbs) Per cent of Walking Cycle	Duration of Double-Limb Support (First and Second Periods) Seconds†	Duration of Double-Limb Support (First and Second Periods) Per cent of Walking Cycle
Total	240	.63 (.07)	61	.40 (.01)	39	.11 (.03)	11
Age							
20 to 25 yrs.	48	.63 (.07)	60	.42 (.01)	41	.10 (.03)	9
30 to 35 yrs.	48	.67 (.08)	61	.42 (.01)	39	.12 (.03)	11
40 to 45 yrs.	48	.59 (.05)	61	.38 (.03)	39	.11 (.03)	11
50 to 55 yrs.	48	.62 (.07)	60	.40 (.01)	40	.11 (.03)	10
60 to 65 yrs.	48	.61 (.08)	61	.40 (.01)	39	.12 (.03)	11
Height							
Tall	80	.61 (.07)	60	.40 (.01)	39	.11 (.03)	10
Medium	80	.65 (.07)	61	.41 (.01)	39	.12 (.03)	11
Short	80	.63 (.07)	61	.40 (.03)	40	.11 (.04)	10

* These numbers represent two trials for each subject and two measurements for each trial.
† The numbers in parentheses represent one standard deviation.

Figure 2.4.1. (i). Temporal Parameters of Sixty Normal Men
(from Murray et al, 1964)

the swing side, this motion has to be opposed to avoid stubbing the toe of the swinging foot. This is normally done by the abductor muscles of the stance leg.

Axial rotations of the leg segments were determined by the technique of inserting pins into the bones. Figure 2.4.1(g) shows the axial rotations occurring in the pelvis, femur and tibia while Figure 2.4.1(h) gives the relative rotation of adjacent segments. It was observed that the directions of rotation and their phase of occurrence are the same for all the three limb segmen segments. The summation of these rotations gives an overall limb rotation of an average of 23^{o}. During foot-ground contact, these rotations are absorbed in the joints of the foot and are related in a very complex way to the function of its arches.

They concluded from these data that locomotion in its essential features is a series of displacements in the saggittal plane accompanied by displacements in the frontal plane, as well as axial rotations of the leg segments.

Murray et al (1964) investigated the walking patterns of normal men; altogether sixty subjects in five age groups (between 20 and 65 years) were selected. Each age group consists of four tall subjects, four short and four of medium height. The test was performed with subjects walking at their own natural speed or cadence.

Temporal/distance factors obtained from the study did not relate systematically with age. However, older subjects (60 to 65 years) took shorter steps and strides and showed a greater degree of toe-out than younger subjects. The only parameters that related systematically with height were the step and stride lengths, viz tall subjects took the longest steps and strides, while short

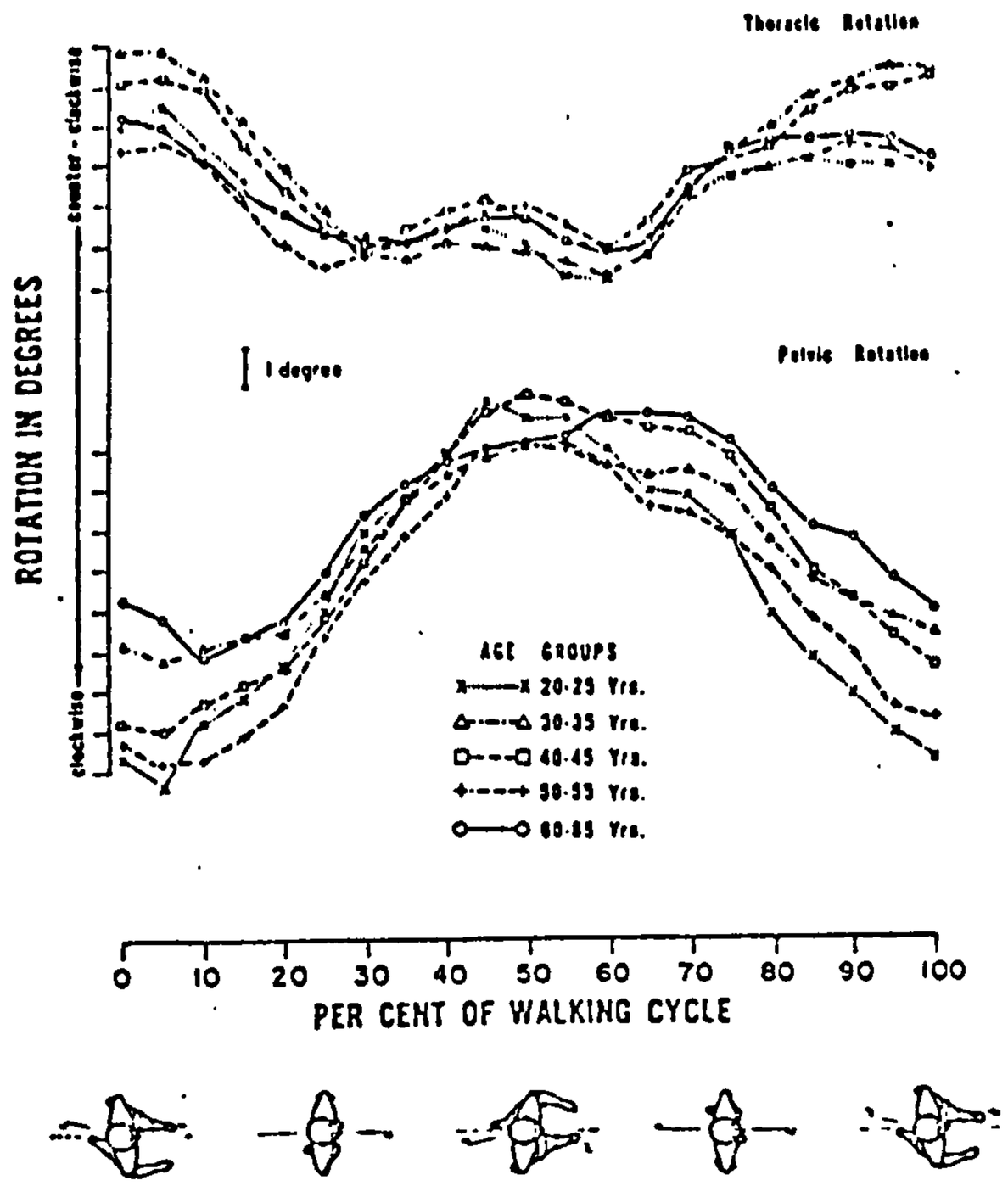

FIG. 10

Mean patterns of transverse rotation of the thorax and pelvis for the five age groups, twelve men in each group, two trials for each man.

Figure 2.4.1. (j). Thoracic and Pelvic Rotations relative to age (from Murray et al, 1964)

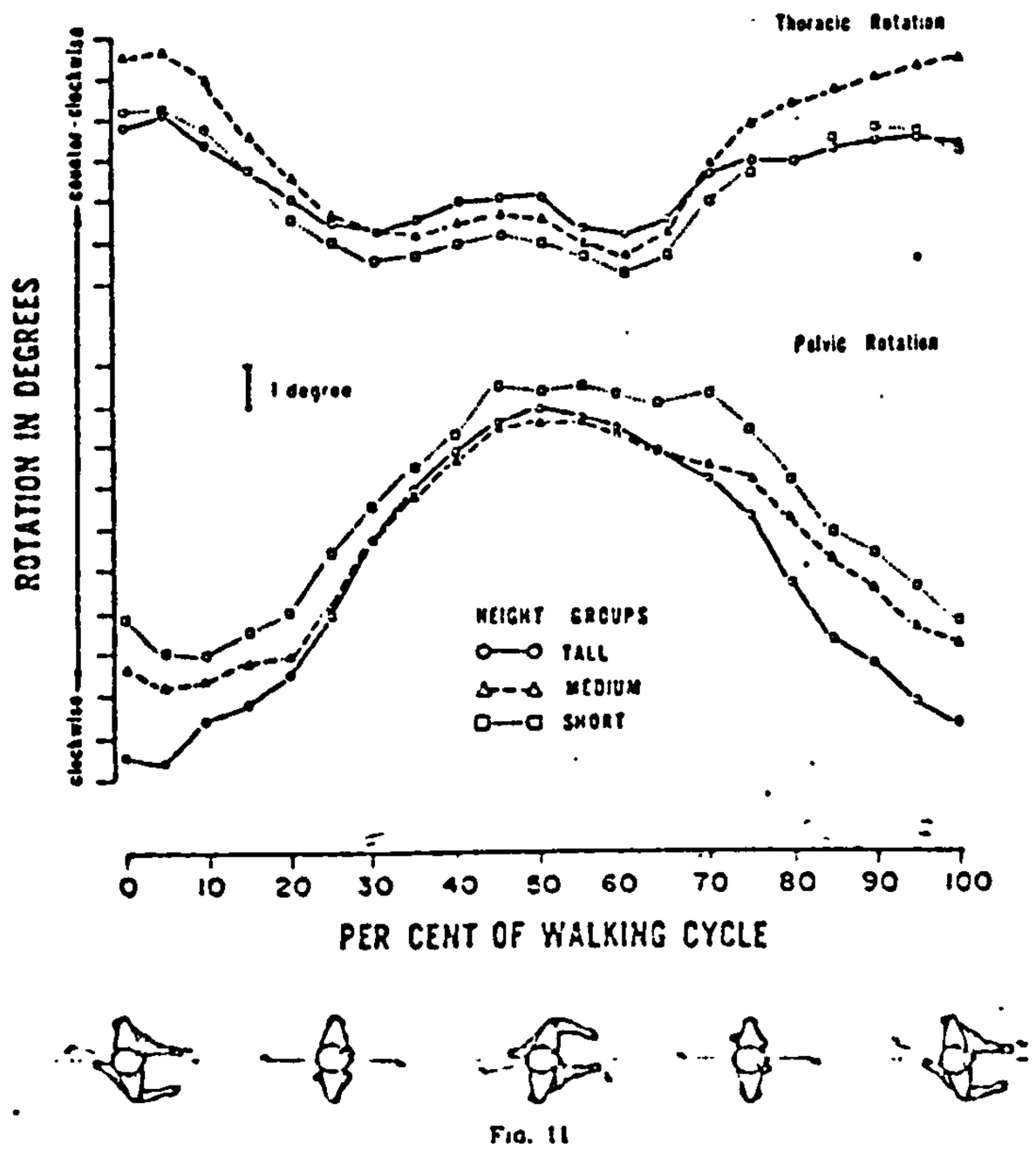

FIG. 11

Mean patterns of transverse rotation of the thorax and pelvis for the three height groups, twenty men in each group, two trials for each man.

Figure 2.4.1. (k). Thoracic and Pelvic rotations relative to height (from Murray et al, 1964)

subjects took the shortest. Mean values of all the parameters obtained are presented in figure 2.4.1(i).

The angular displacements of the pelvis, hip, knee and ankle in the saggittal plane were obtained. These excursions did not vary systematically with height or age. It was observed that hip extension during walking appears to approach the limit of motion anatomically available. The mean values of all the parameters obtained were similar to those of Eberhart and his associates (1954).

Transverse rotations of the pelvis and thorax were also analysed. Figures 2.4.1(j) and (k) show the rotations with respect to age and height, respectively. Differences in the pattern of rotations do not vary systematically with age or height. Pronounced individual differences in the relationship between pelvic and thoracic rotations were observed. Furthermore, in some of the subjects there was an absence of pelvic rotation. It was suggested that these variations meant that pelvic and thoracic rotation are optional movements in normal gait, which are dependent on the speed of walking and the type of footwear.

When pelvic rotation occurs it is always accompanied by the concurrent and opposite rotation of the thorax, which is supposed to provide a damping effect to reduce the magnitude of the overall rotation of the body and also to give a smoother walking pattern. The rotation of the thorax was observed to be closely related to the arm swing which typically finds the right arm advancing with the left lower extremity and vice versa.

Grieve and Gear (1966) reported that the time-distance parameters in gait are dependent on the speed of walking. This fact has been substantiated by other

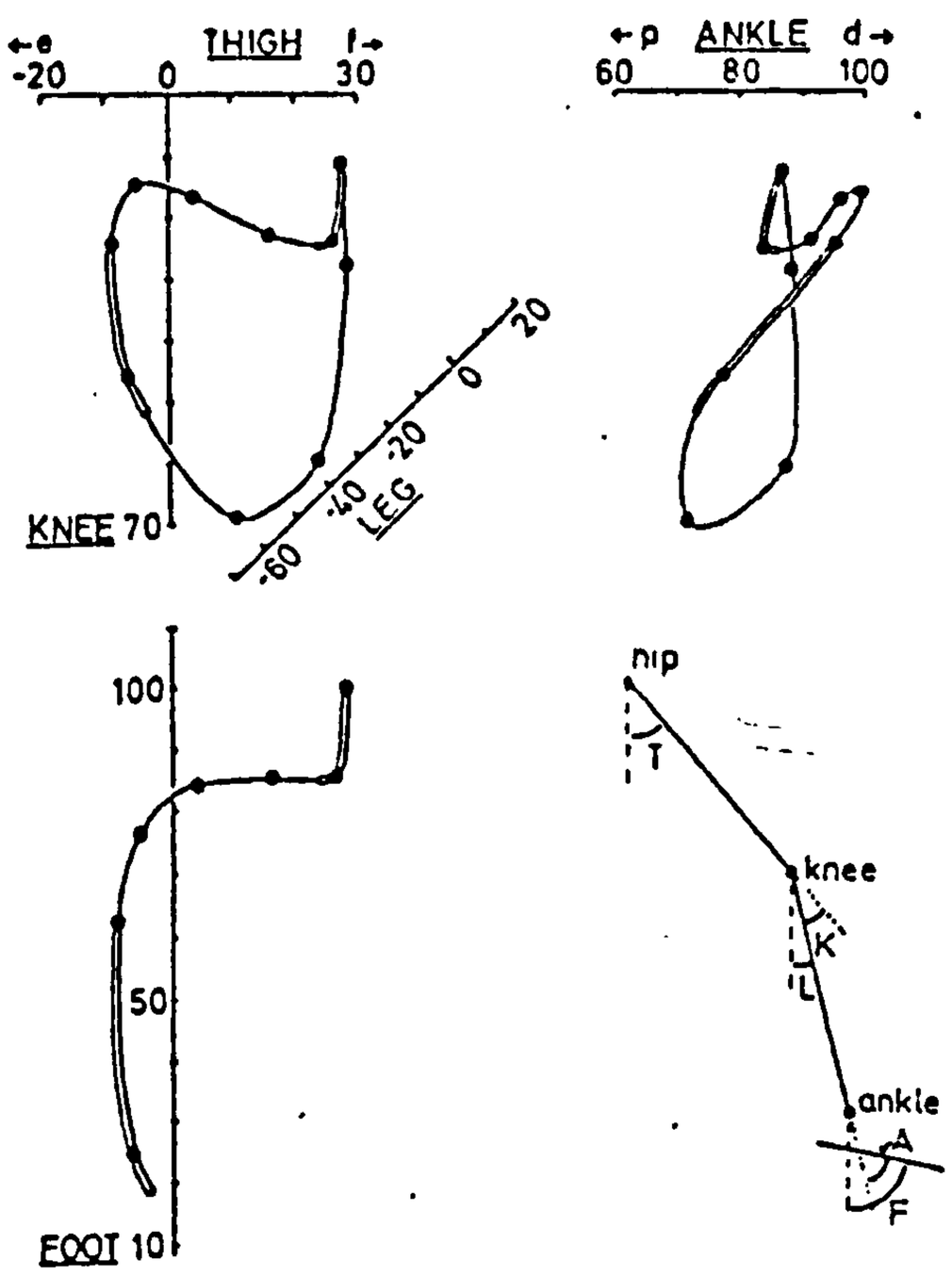

Mean data for the male group computed from angles at 10% stages of the individual's cycles at a relative stride of 0.87. Thigh-knee, knee-ankle and thigh-foot diagrams are shown, the latter during the support phase only. Periods of double support are shown by double lines.

Figure 2.4.1. (1). Angle-angle diagrams (from Grieve, 1968)

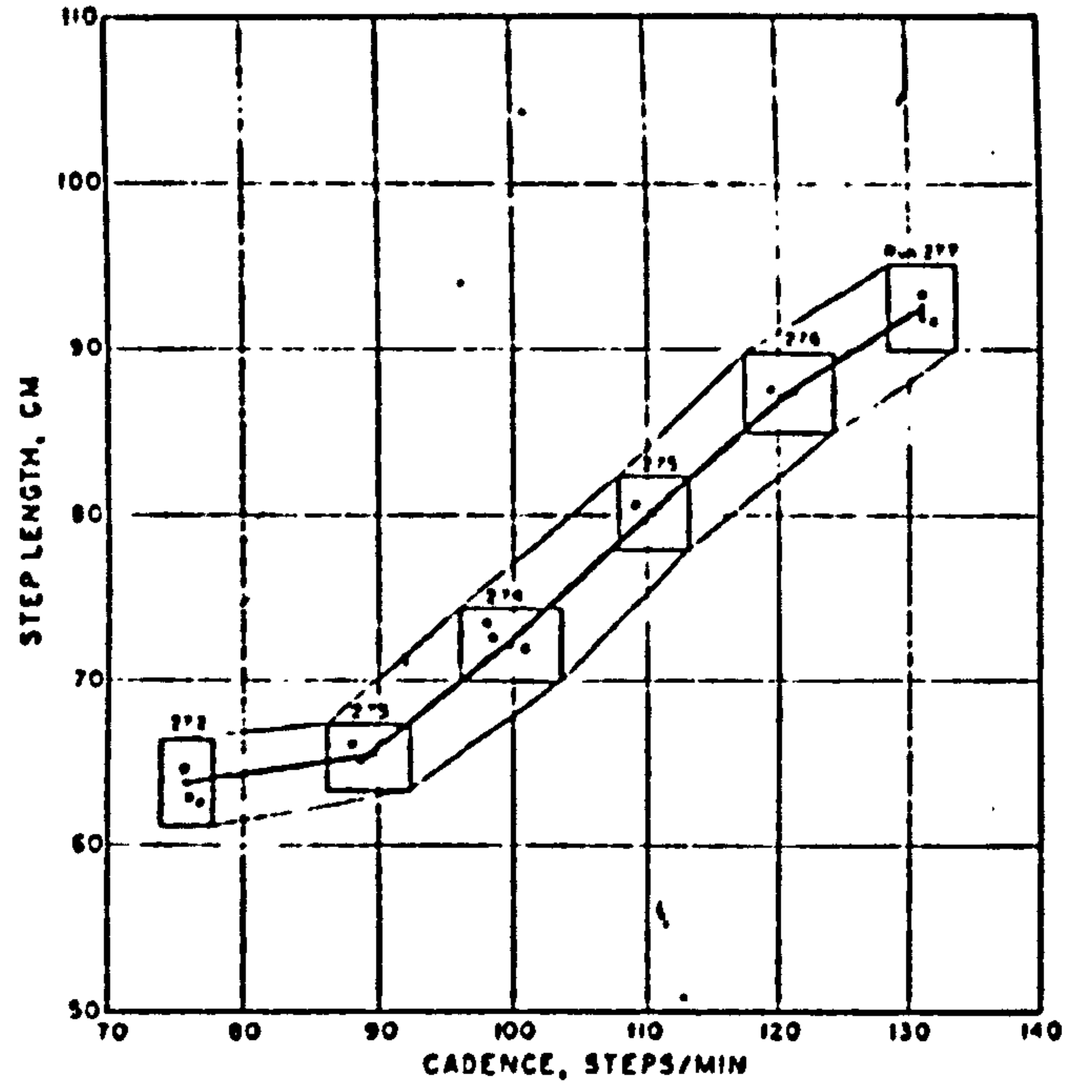

Step length and cadence for runs 272-277

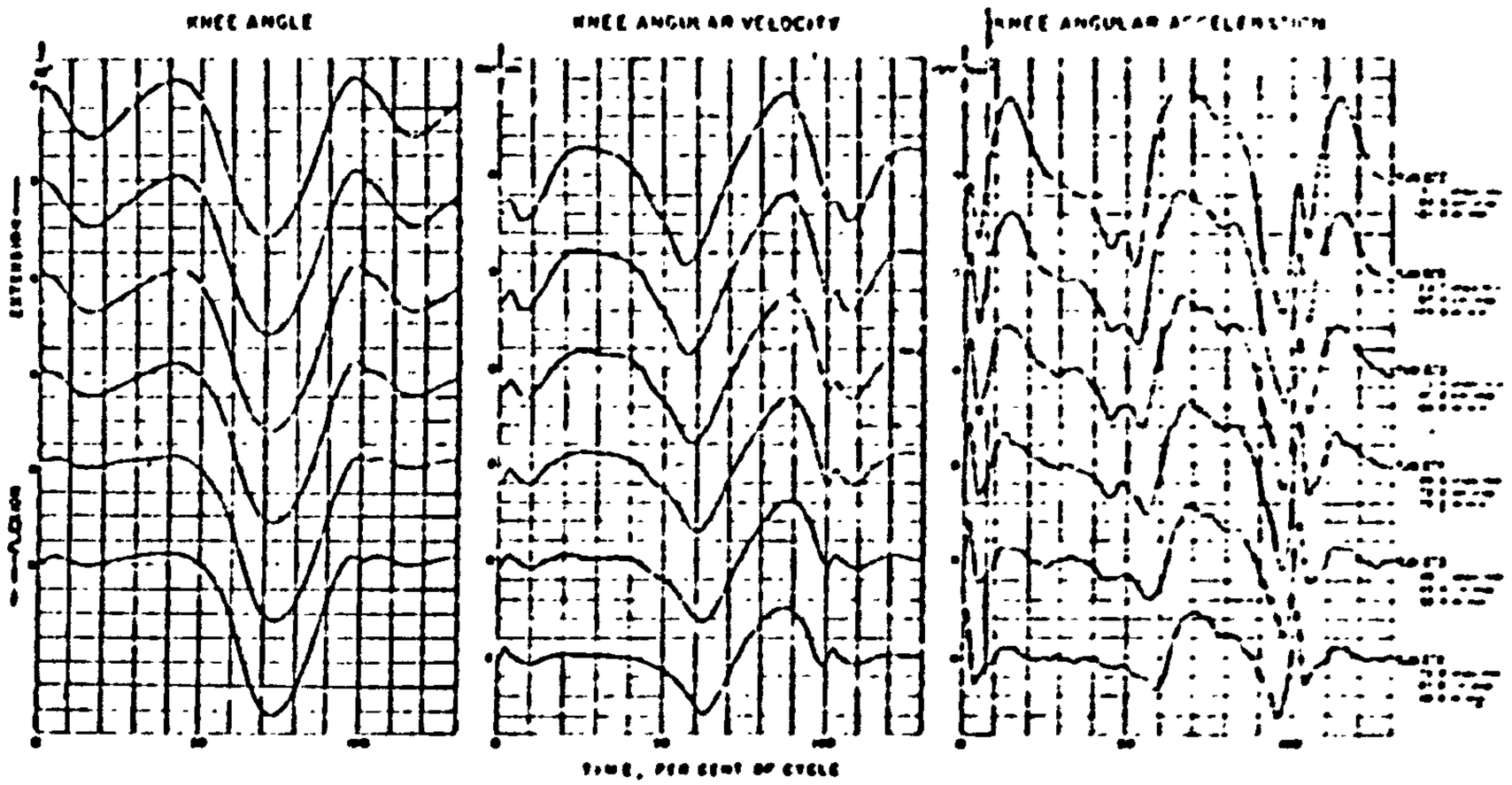

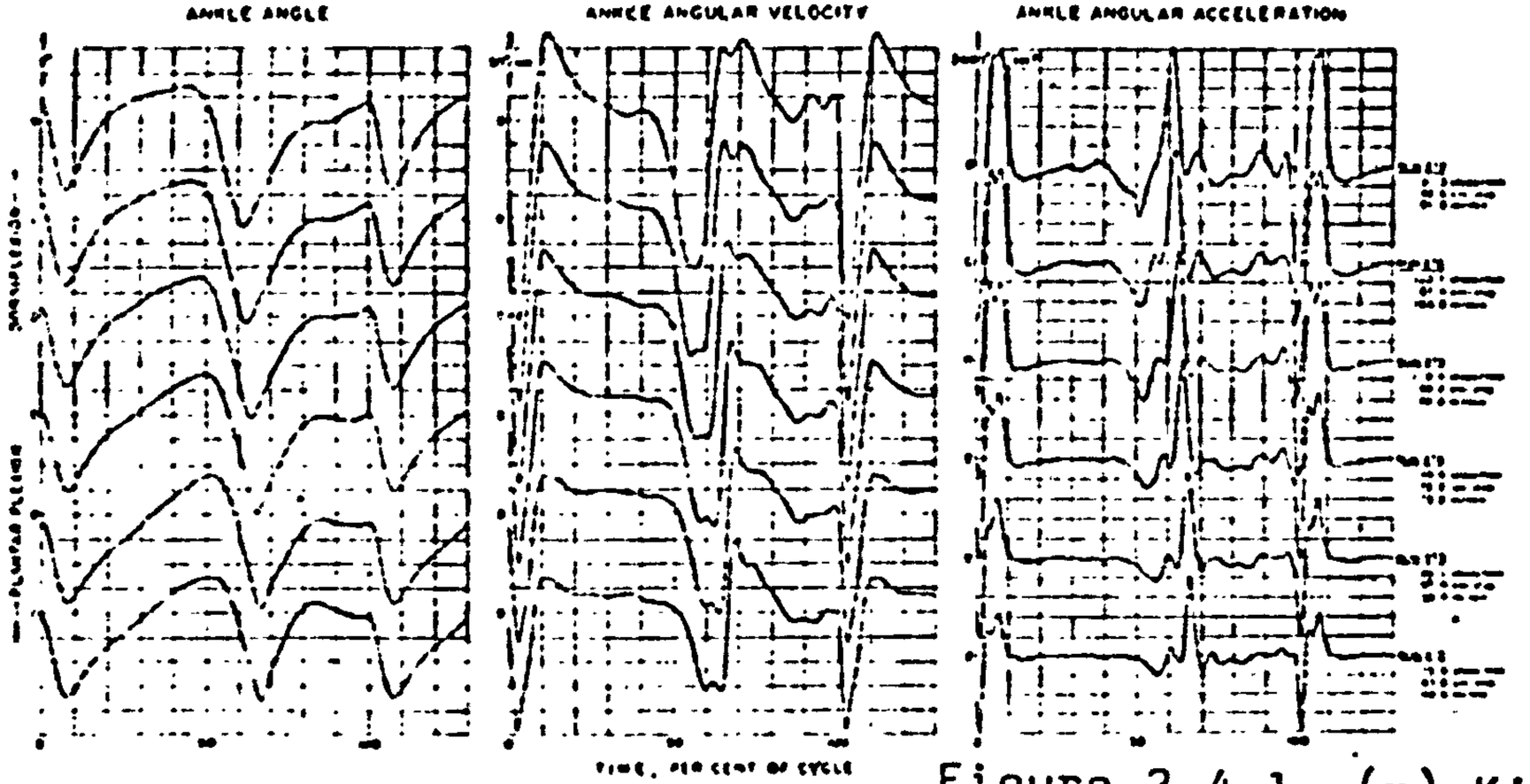

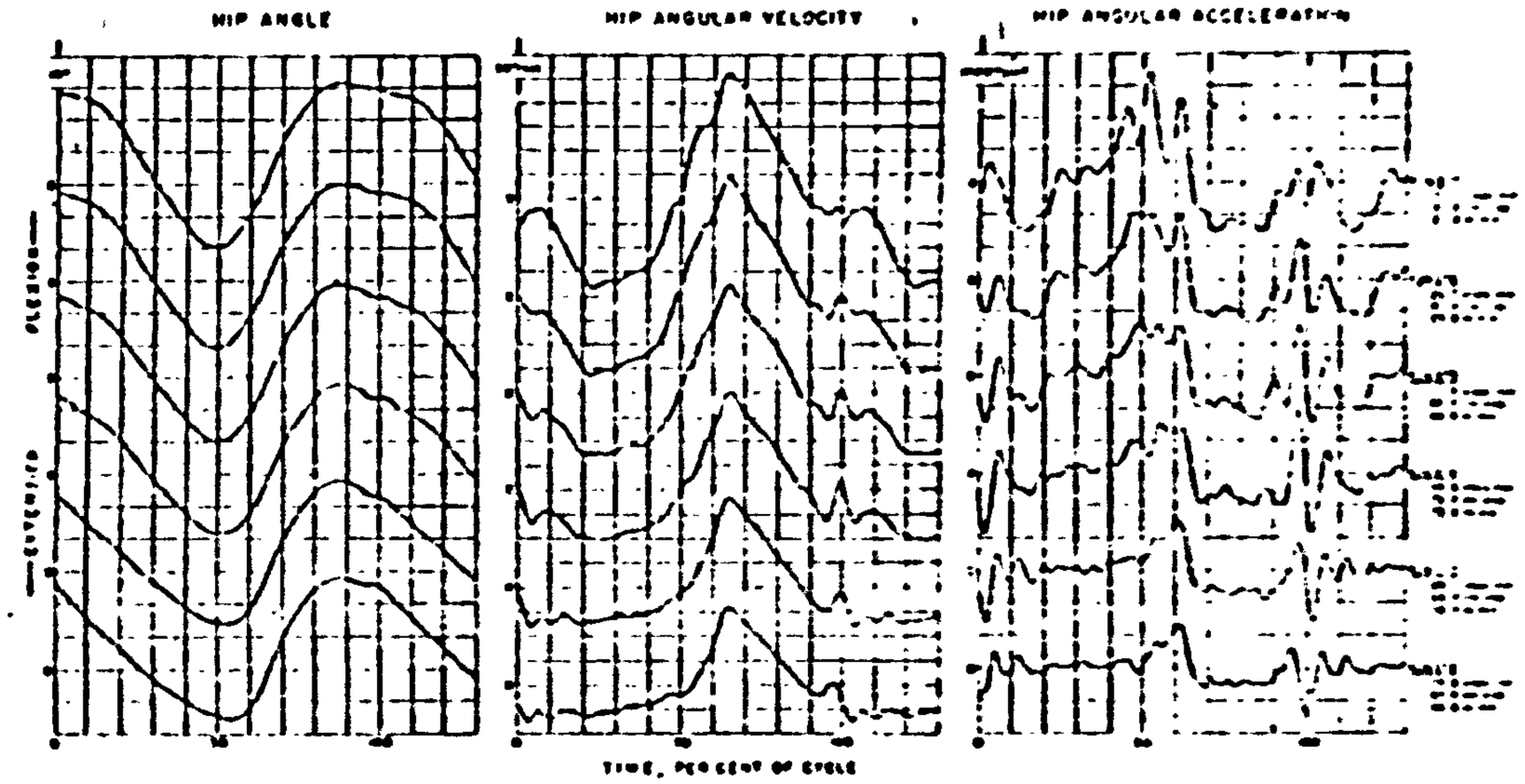

Figure 2.4.1. (m) Kinematic data of leg joints (from Lamoreux, 1971)

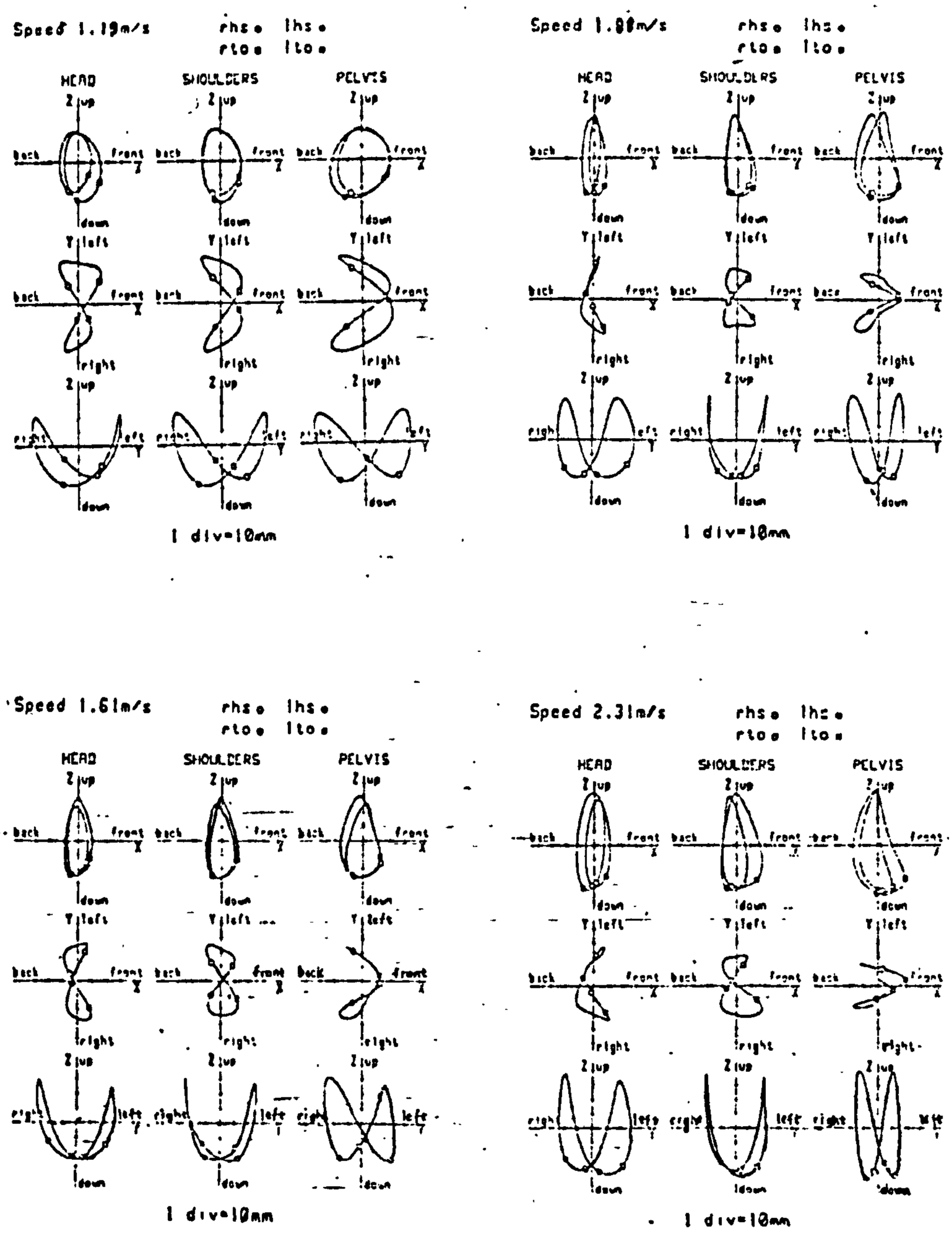

Figure 2.4.1. (n). "Lissajous" figures of Head, Shoulder and Pelvis (from Cappozzo, 1981)

researchers, like Chantinier et al (1970) Lamoreux (1971) and Rosenrot et al (1980). Grieve (1968) presented two equations, one relating the number of complete cycles per second to the relative speed and the other relating swing time to cycle time and stature. Each individual can be characterised by the value of three constants from these two equations. Grieve also presented a method of plotting joint angles, known as "angle-angle" diagram, see Figure 2.4.1(l). In this, the angle at one joint is plotted against the corresponding angle of another.

The speed of walking has also been shown to influence the angular displacement of limb segments, Murray et al(1966). This inevitably affects the corresponding angular velocities and accelerations, Lamoreux (1971). Figure 2.4.1(m) shows the angular displacements, velocities and accelerations of the hip, knee and ankle in the saggittal plane obtained from six different speeds of walking (from 0.8 to 2.0 m/s). The associated step length/cadence relationship is also presented.

Other kinematic data that have been shown to be dependent on the speed of walking are the linear displacements of the head, shoulder and pelvis. A recent study by Cappozzo (1981) demonstrated these variations, see Figure 2.4.1(n). It was observed that along the antero-posterior axis, the excursions about the mean position of the head and shoulder are smaller than those of the pelvis point. Along the medio-lateral axis, the contrary applies, the more so the higher the speed of progression. The vertical excursions at the three considered levels were almost identical. They increase as speed augments to about 2.4 m/s. At higher speeds, these excursions decrease considerably.

This method of presentation of linear displacements of the head and trunk was first used by Braune and

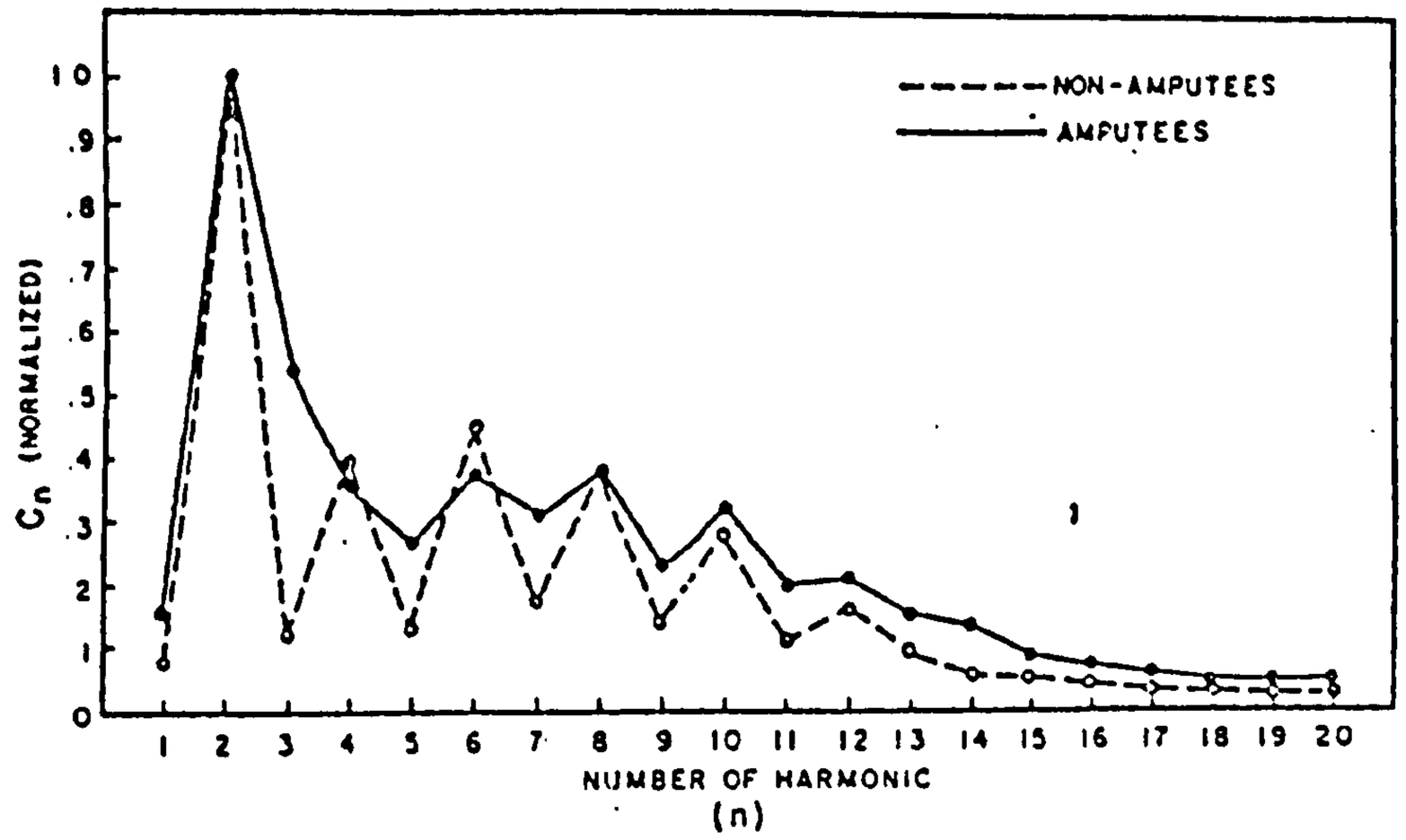

Harmonic analysis of vertical accelerations, level walking. Curves represent mean values

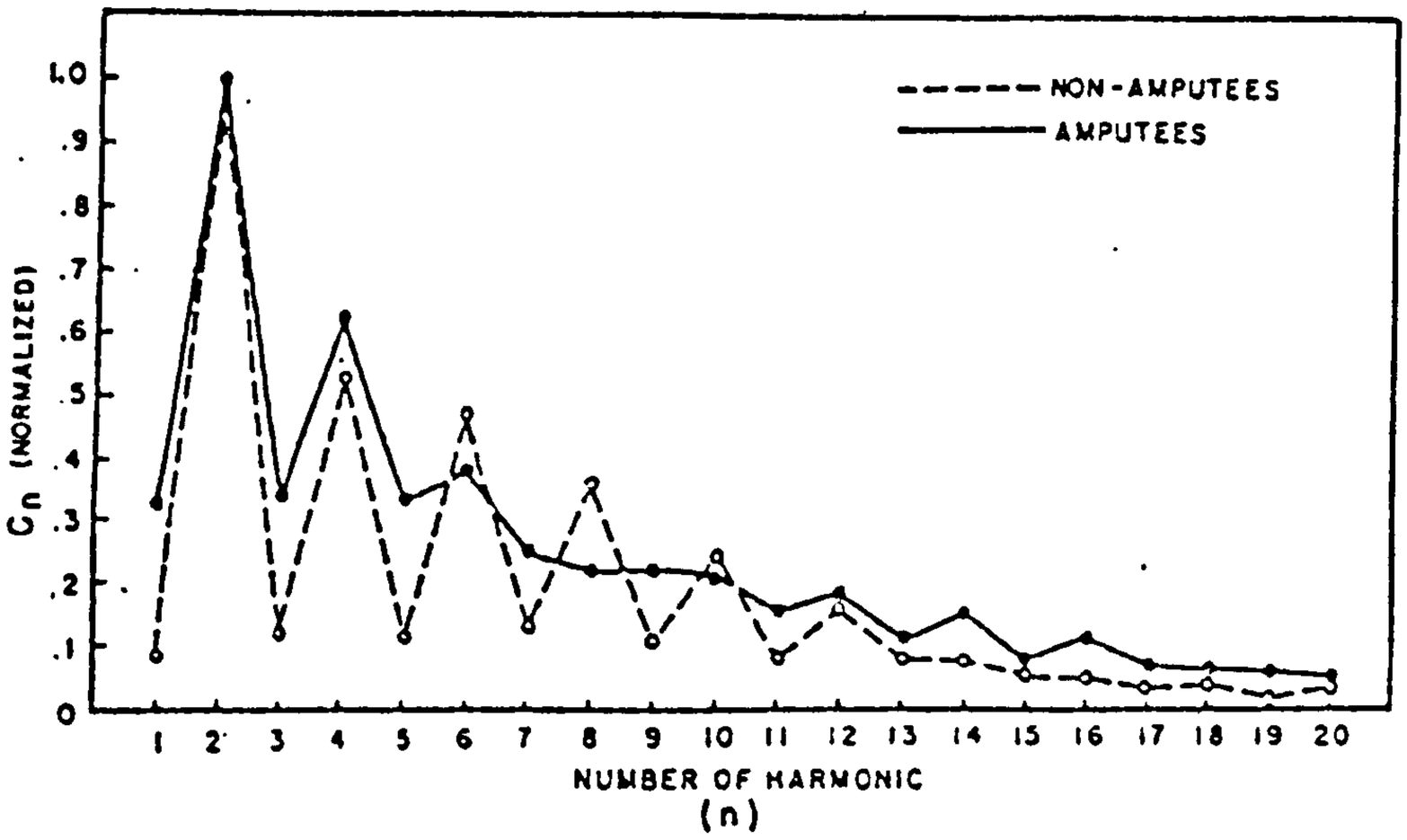

Harmonic analysis of fore and aft accelerations, level walking. Curves represent mean values

Figure 2.4.1. (o). Harmonic Analysis of Kinematic data.
(from Gage, 1964)

Fischer (1895). Lamoreux (1971) also used this method of presentation for the linear displacements of the pelvis from six fdifferent speeds of walking; the results were similar to those obtained by Cappozzo. This graphical display of the linear displacement was termed as "Lissajous" figures by Cappozzo (1981).

Harmonic analysis has also been used in the analysis of kinematic data. Gage (1964) presented harmonic analysis of the vertical and fore-aft acceleration of the trunk during level walking of six normals and nine amputees. It was found that the mean frequency spectra in the vertical and fore-aft directions were similar for both test groups and that they were dependent only on the walking pattern of the subjects. Reproducability of the spectra from subject to subject on several runs for the same mode of walking was claimed to be possible. It was also concluded that the higher even-harmonic values in normal subjects indicated a greater degree of symmetry of gait. The rapid convergence of the spectra provided a measure of smoothness of walking pattern, thus indicating the lack of smoothness in the walking pattern of the amputee, see Figure 2.4.1(o).

Cappozzo (1981) performed harmonic analysis on the linear displacements of the head and trunk along its three directions. It was found that vertical and fore-aft displacements demonstrated significantly higher even-harmonic values, whereas the medio-lateral displacement exhibited odd-order harmonics. No reason was given for the difference.

2.4.2 Foot-Ground Reaction Data

The foot-ground reaction data considered in this section will only be those measured from force platforms.

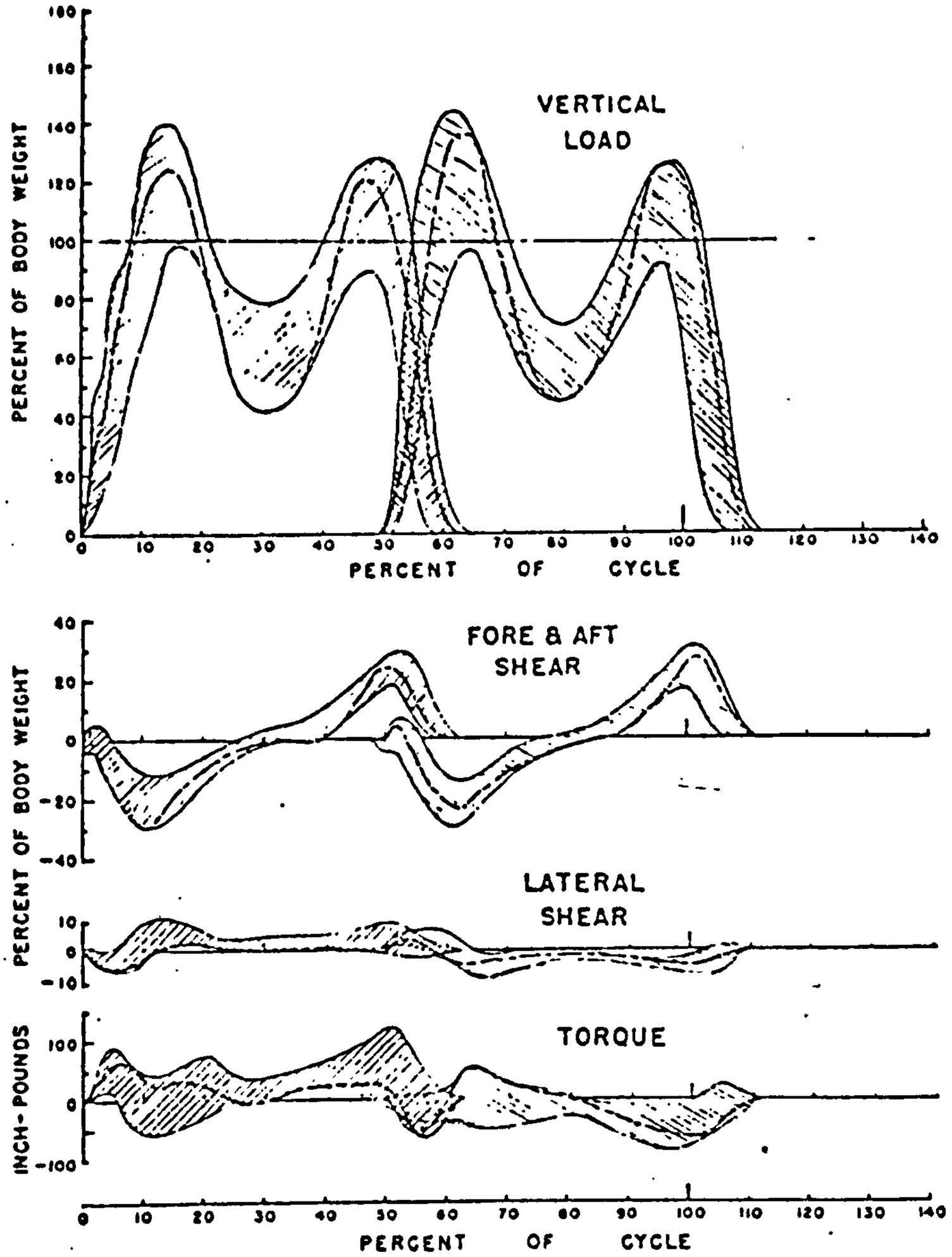

FIG. FLOOR REACTIONS ON THE FOOT

TEN NORMAL SUBJECTS WALKING LEVEL

	SUBJECT NUMBER	RUN NUMBER	STEPS PER MINUTE
TYPICAL	151	3333	120
	190	3525	138
	188	3528	128
	182	2907	115
	19	1814	102
	201	2744	111
	24	2793	115
	3	3530	125
	20	1819	109
	21	2421	107

UNIVERSITY OF CALIFORNIA
PROSTHETIC DEVICES RESEARCH

Figure 2.4.2. (a). Ground reactions of ten normal subjects.
(from Cunningham, 1950)

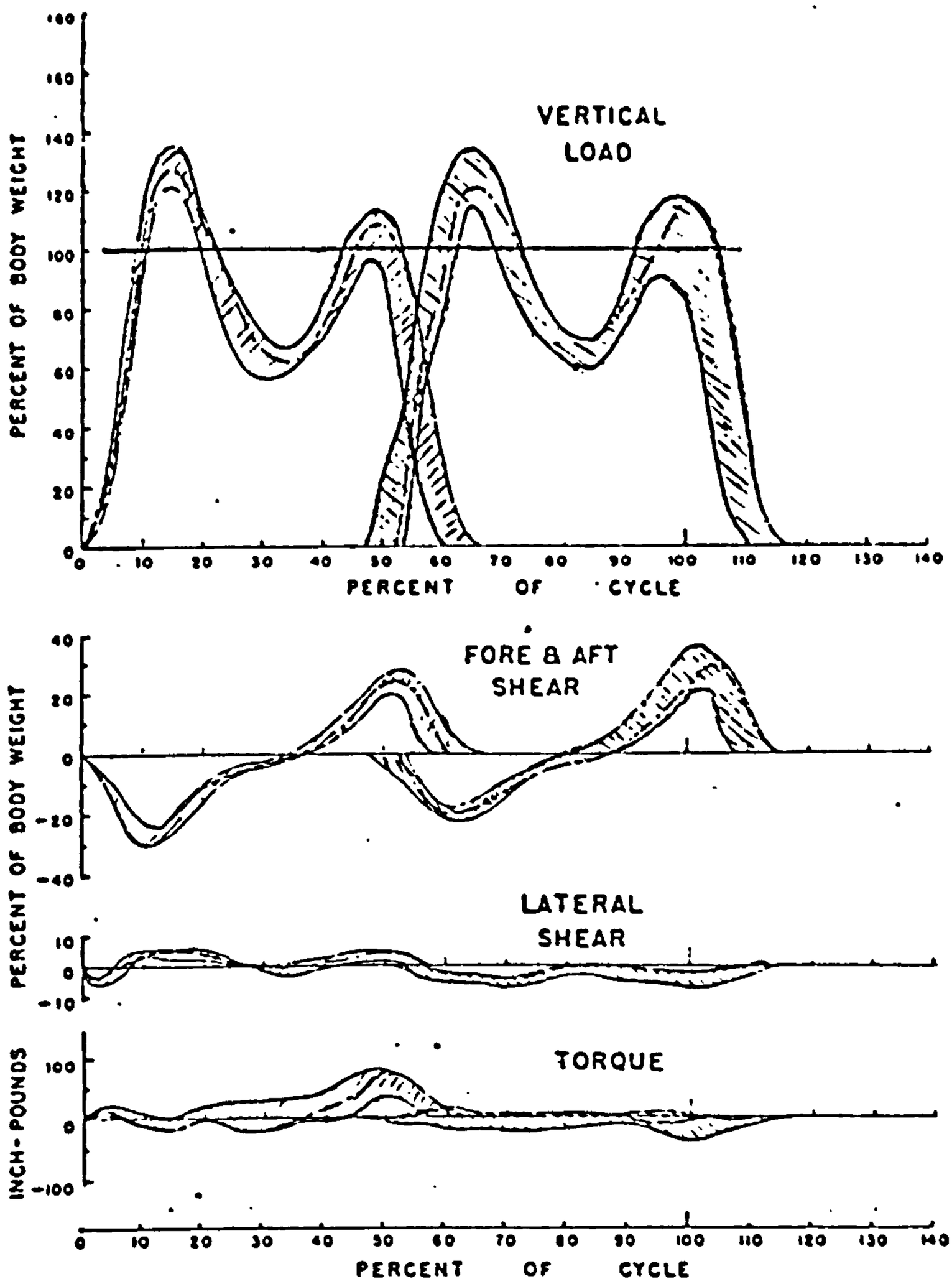

FIG. FLOOR REACTIONS ON THE FOOT

ONE NORMAL SUBJECT WALKING LEVEL SIX TIMES

SUBJECT NUMBER	RUN NUMBER	STEPS PER MINUTE	
M6	2048	109	
M6	2049	114	
M6	2050	111	TYPICAL
M6	2051	107	
M6	2053	108	
M6	2055	114	

UNIVERSITY OF CALIFORNIA
PROSTHETIC DEVICES RESEARCH

Figure 2.4.2. (b). Ground reactions of one normal subject.
(from Cunningham, 1950)

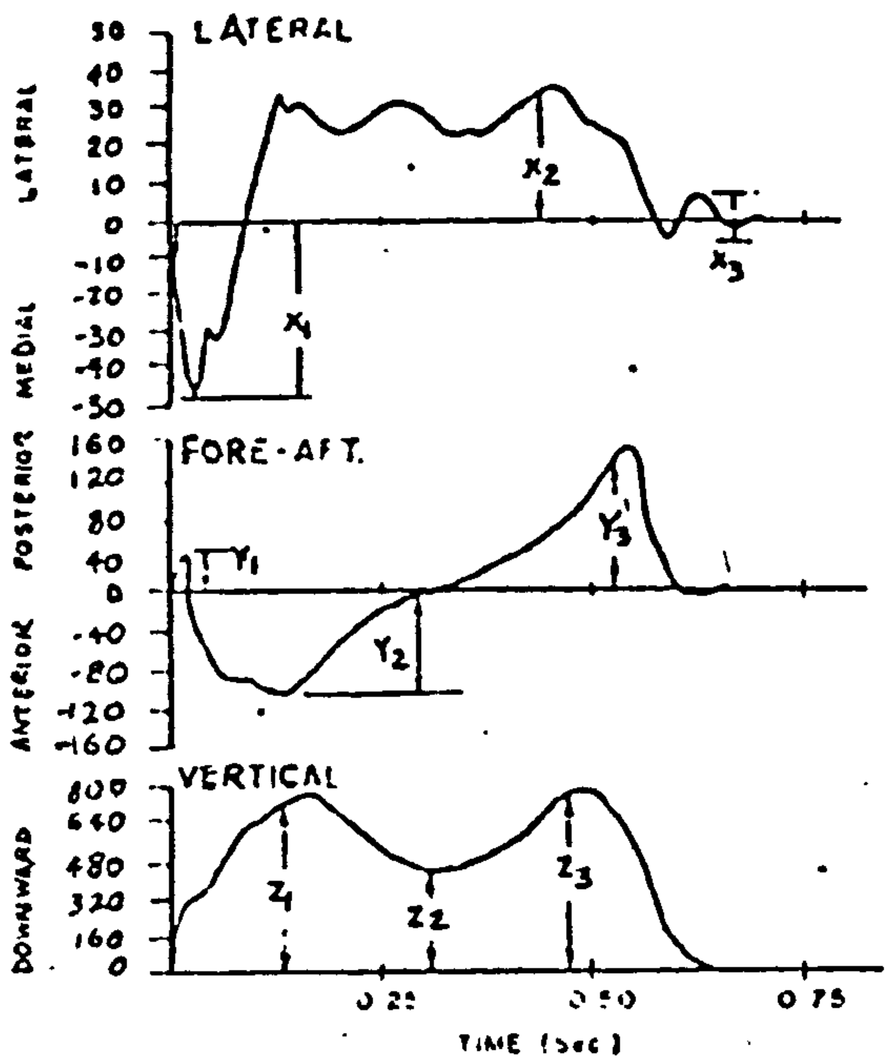

An illustration of the waveforms depicting the three components of foot ground reaction force.

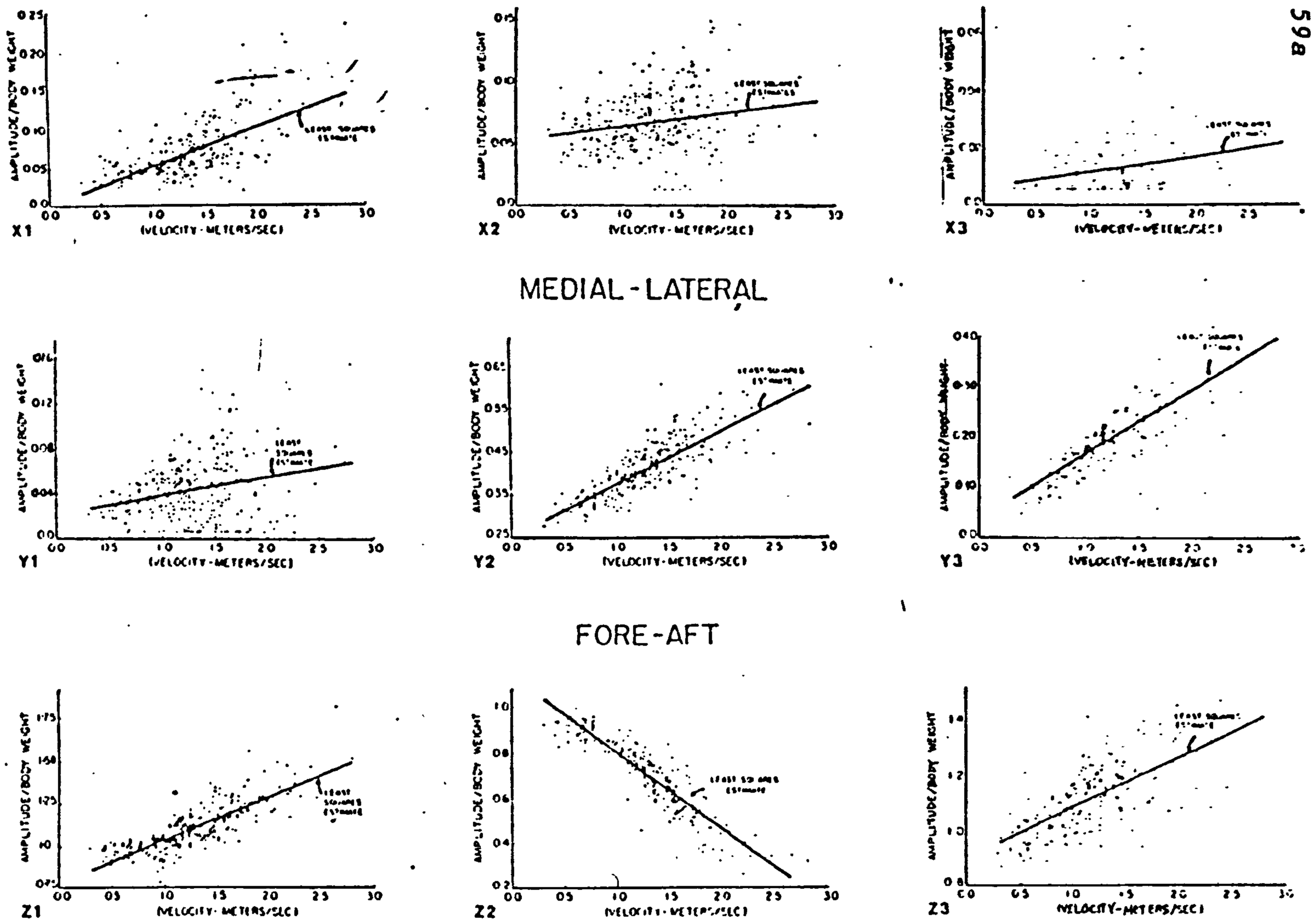

. The composite force amplitude and velocity relationships for the normal observations.

Figure 2.4.2. (c). Relationship between ground reactions and walking speeds. (from Andriacchi et al, 1977)

Cunningham (1950) presented ground reaction data of normal subjects and below- and above-knee amputees performing activities such as level walking, up and down stairs, up and down ramp. Figure 2.4.2(a) shows an envelope of ground reactions on the foot of ten normal subjects during level walking. This "subject to subject". variation was also present in other groups of subjects. Another variation, which is important to note, is the "step to step" variation that exists even within a particular subject, see Figure 2.4.2(b). The envelope of this variation and the width of the band is constant. These variations were attributed to the cadence and the ratio of the leg length to stride length. It was emphasised that these parameters have to be eliminated before any comparison and/or averaging of the force curves can be performed. It must be noted that positive lateral shear is from right to left and that positive torque is in the direction of medial rotation.

Jacobs et al (1972) analysed the vertical component of the ground-foot reactions in normal and pathological gait using the force platform system described by Skorecki (1966). Harmonic analysis was performed on the vertical force waveform. For normal subjects, the authors found that it was possible to generalise the waveform and its harmonic spectrum. However, it was also noticed that there were changes in the frequency content due to the differences in the inertial contribution at different walking speeds.

Andriacchi et al (1977) investigated the relationship between ground reaction forces and walking speed. The waveforms of the lateral, fore-aft and vertical force were characterised by 9 amplitudes, see Figure 2.4.2(c). The figure also shows all the normalised force amplitude-velocity relationships obtained from 17 normal subjects. A linear polynomial regression method was used to

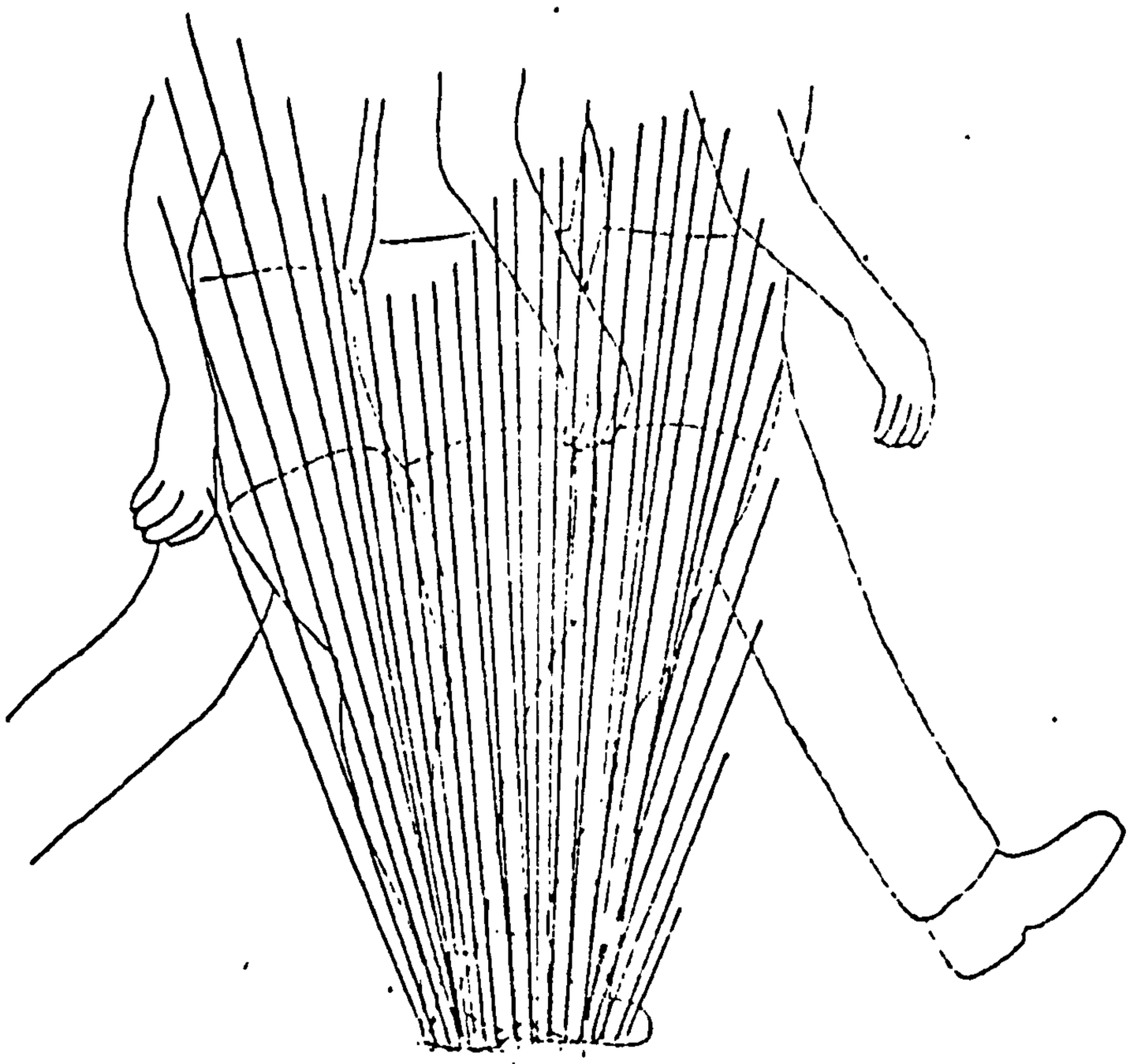

Figure 2.4.2. (d). Superimposing of force vectors.
(from Cook et al, 1979)

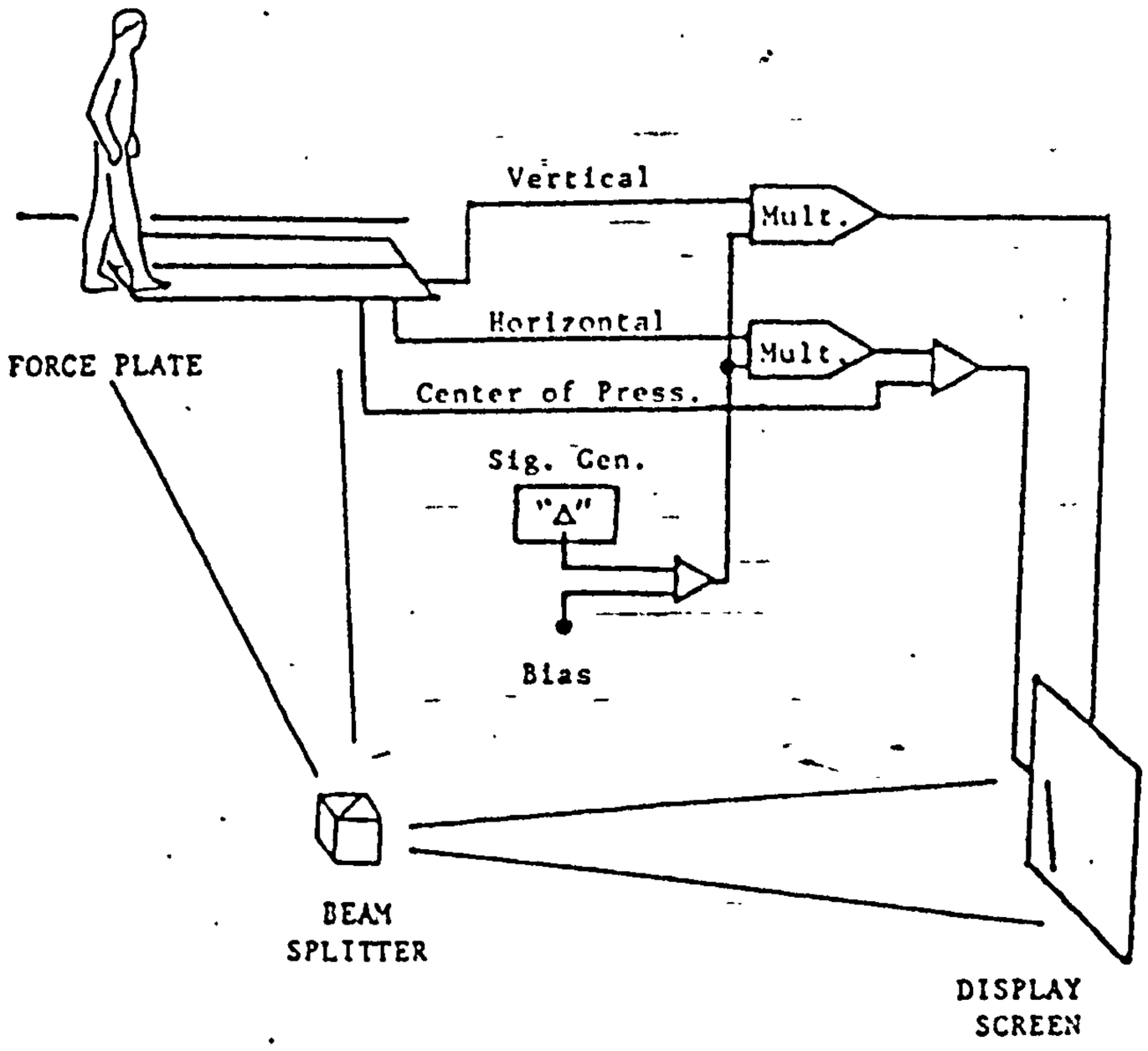

Schematic of the weightline visualization equipment.

Figure 2.4.2. (e). Force Vector Visualisation System.
(from Cook et al, 1979)

describe the relationship. It was observed that the force-amplitudes Z_1, Z_2, Z_3, Y_2, Y_3 and X_1 vary linearly with velocity. In conclusion, the authors stressed the need for characterisation of gait measurements in relation to walking speed and that the method they used was adequate to provide accurate and reproducible normal gait data.

Vector representation of the ground reaction forces was first introduced by Elftman (1939). The method involves the generation of a force vector from two components, often the vertical and fore-aft ground reaction forces at the point of application (viz the centre of pressure). Cappozzo et al (1974), Boccardi et al (1977) and Pedotti (1977) used this method of presentation of ground reactions as a gait analysis procedure. The force vector (or "Butterfly") diagram was obtained in real time at relatively low instrumentation cost, and it was claimed that the method provided an efficient description of human gait.

An extension of force vector representation would be to superimpose the position of the ankle, knee and hip joint centres in relation to the force vector, see Figure 2.4.2(d). Cook et al (1979) developed a system which could produce a real-time visualisation of the ground reaction force vector superimposed onto an image of the subject. Figure 2.4.2(e) shows a schematic diagram of the system. The force platforms system was similar to that described by Wirta et al (1970). The resonant frequencies in the vertical and horizontal directions were given as 55 Hz and 75 Hz respectively. The "cross-talk" effects on the horizontal forces measured was claimed to be 0.4%. The resolution was quoted as 1:700 for the vertical and 1:50 for the horizontal forces. The force vector display signal from the force platform output was generated by an

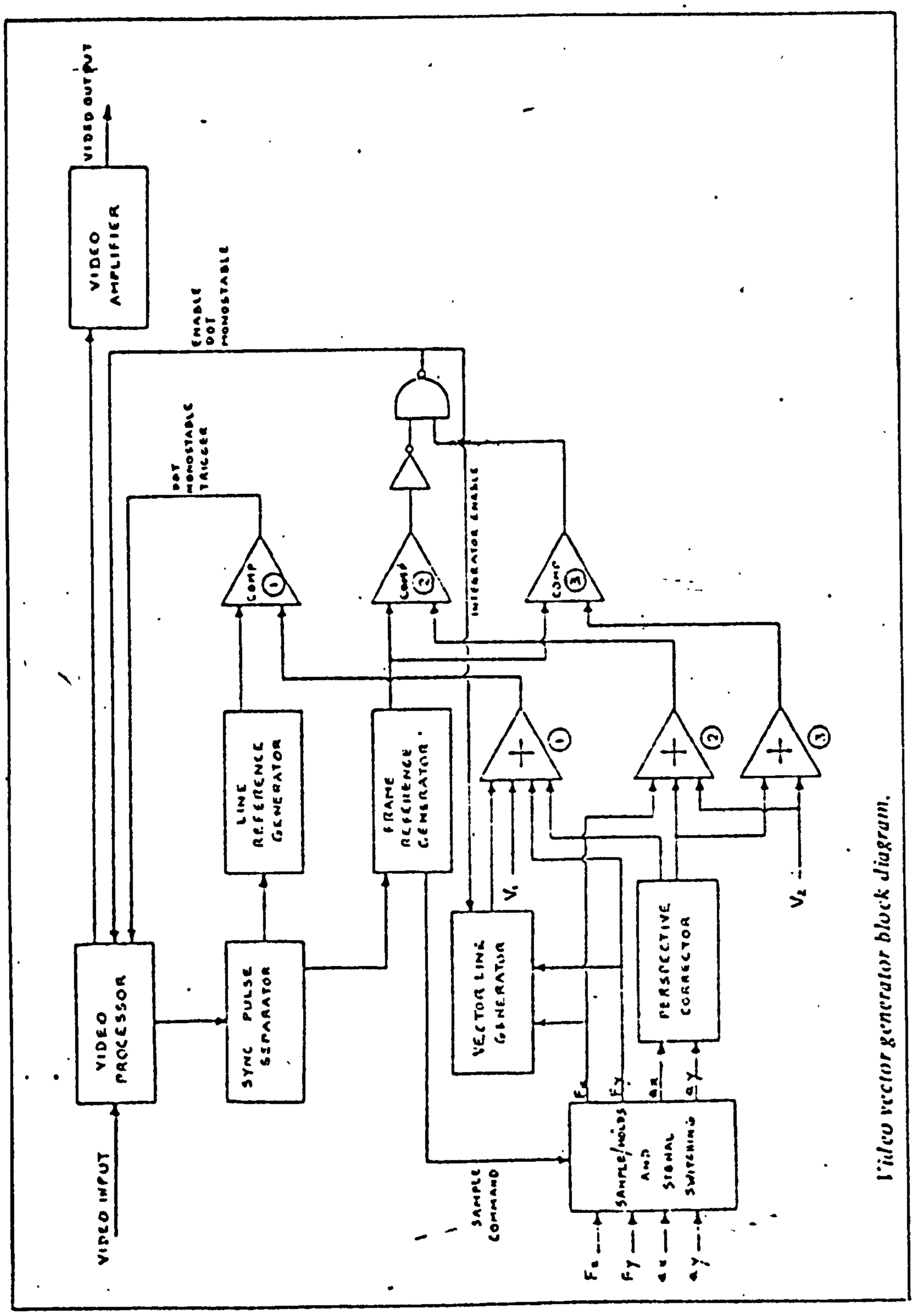

Video vector generator block diagram.

Figure 2.4.2. (f). Video force vector generator block diagram.. (from Tait & Rose, 1979)

analogue signal processor. A laser beam was made to represent the force vector, it was deflected by an X-Y mirror scanning system and projected onto a screen. A beam splitter was used to view simultaneously the walking subject and the force vector display. Direct viewing through the beam splitter allows on line assessment of gait in real time. However, a permanent record of the display is only possible by the use of a photographic method.

Tait and Rose (1979) presented a system which could produce a force vector superimposed instantaneously on a television picture of the subject by electronically processing the video signal. A Kistler force platform (type 9621-A) was used to provide the ground reaction forces and the centre of pressure in analogue form, which were synthesised to give a "line" on the television screen. This "line" correspond to the force vector and was generated by dots on each successive television line. The position of the dot was computed by analogue arithmetic sequences which were controlled digitally. Figure 2.4.2(f) shows the block diagram of the video vector generator.

2.4.3 Intersegmental Joint Forces and Moments

For a complete understanding and description of the behaviour of the human leg in walking, a knowledge of the forces and moments at the joints is essential. To determine these quantities, a physical model of gait has to be set up. In it, the human leg is modelled as three "rigid" body segments (viz foot, shank and thigh) moving in space in accordance with Newtonian Laws of motion. Three fundamental quantities are required to solve the model, they are (1) kinematic information on the leg, (2) the physical properties of the body segments and (3) the foot-ground reaction forces.

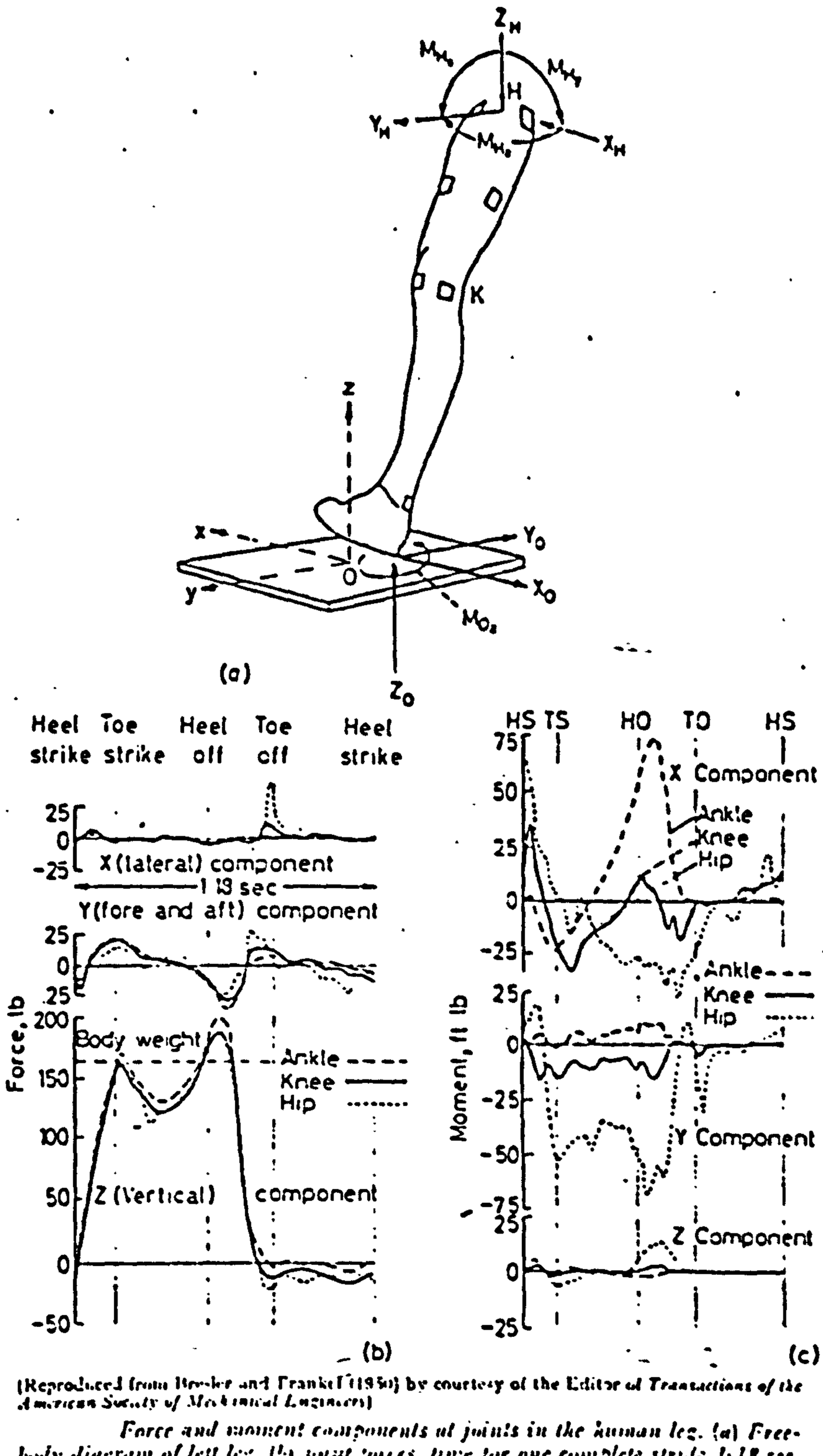

(Reproduced from Brooker and Frankel (1950) by courtesy of the Editor of *Transactions of the American Society of Mechanical Engineers*)

Force and moment components at joints in the human leg. (a) Free-body diagram of left leg. (b) joint forces, time for one complete stride 1·18 sec. (c) joint moments

Figure 2.4.3. (a). Force and Moment Components at leg joints. (from Paul et al, 1975)

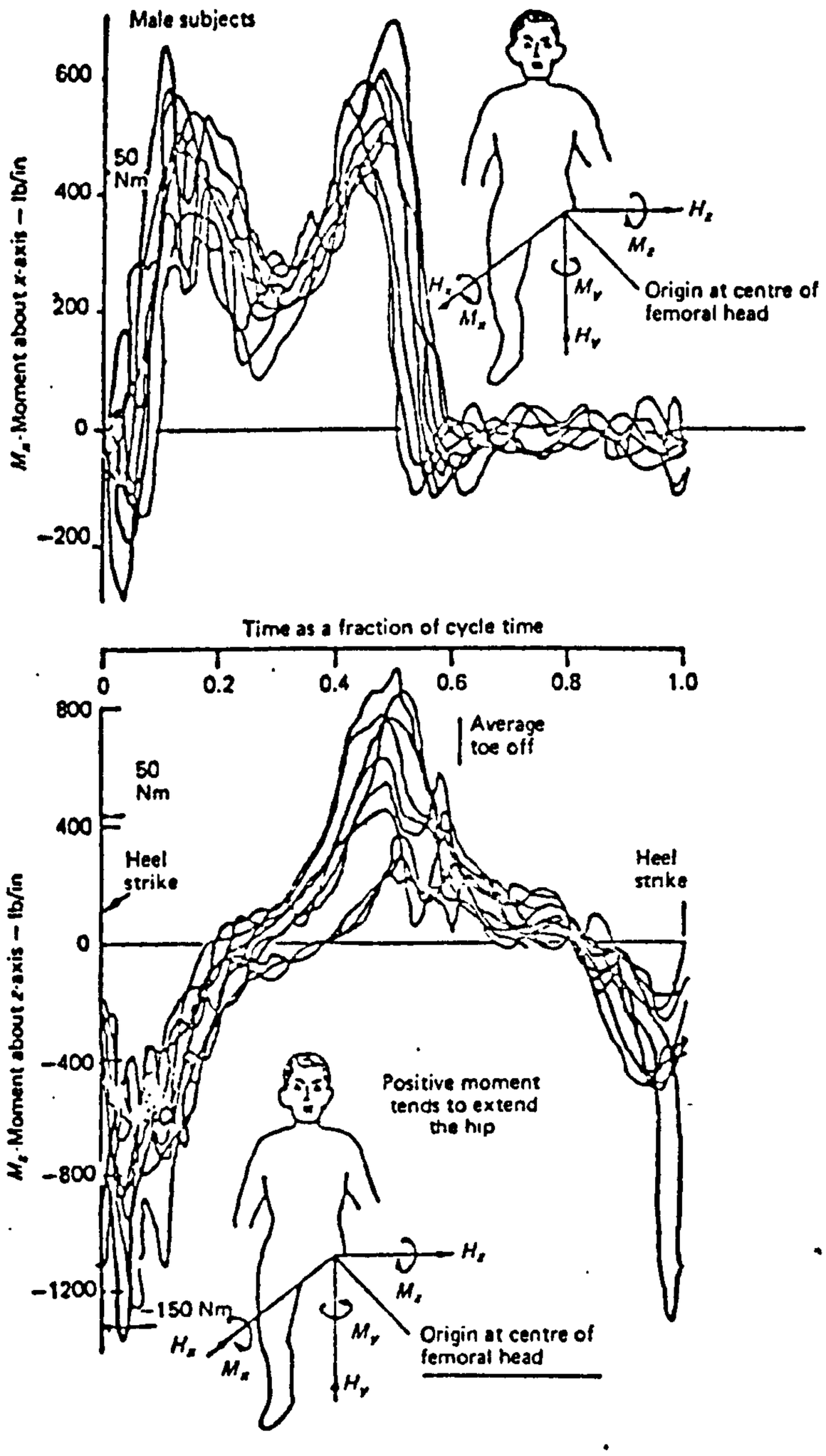

Moments transmitted to trunk by one leg

Figure 2.4.3. (b). Hip moments of ten normal subjects.
(from Paul, 1971)

Bresler and Frankel (1950) were perhaps the first to perform a three-dimensional analysis of the leg by calculating the joint forces and moments of the hip, knee and ankle in their three principal axes. Kinematic data were obtained through cinematography and the physical properties of the body segments were calculated from Braune and Fisher's coefficients of body segment parameters. Foot-ground reaction forces were measured by using the force platform developed by Cunningham and Brown (1952). Analysis was conducted on the left leg of the subject only, altogether four normal male subjects were used. Figure 2.4.3(a) shows the free body diagram of the left leg and also the joint forces and moments at the hip, knee and ankle of one subject. It was noted that the differences between forces at the hip, knee and ankle joints indicate the effect of gravity and mass inertia of the segment distal to these joints.

Paul (1967) and Morrison (1967) used a similar method of data acquisition to that of Bresler and Frankel, to obtain the forces and moments acting at the hip and knee joint respectively. Results were presented from analyses performed on 18 test runs of three female and ten male normal subjects. Figure 2.4.3(b) shows the summary curves for the hip moments about two orthogonal axes obtained from ten normal male subjects. The curves correspond to walking speeds between 5 and 7.5 km/hr. Results from Bresler and Frankel for four male subjects compare fairly well as far as the pattern of the curves was concerned. However, the magnitude of the data was significantly different. This was attributed to the difference in walking speed and the body weight. Paul (1971) presented summary curves of the knee and ankle moments in the saggittal plane calculated by Morrison and Paul respectively. Data from Bresler and Frankel were also superimposed onto the curves, as shown in Figure 2.4.3 (c). Similar differences were also observed

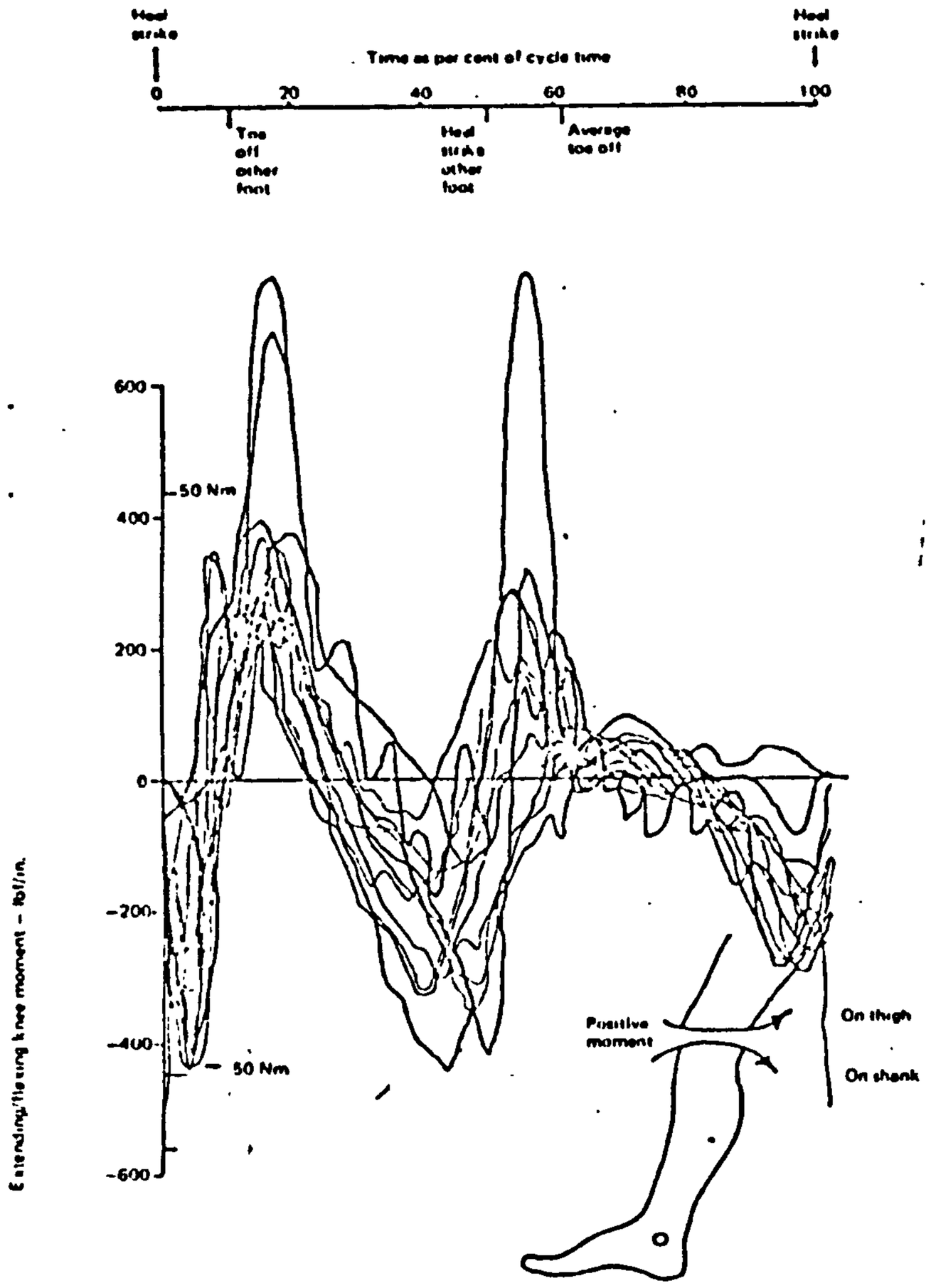

-Knee moment variation with time. Summary curves from Bresler and Frankel (four subjects), Morrison (ten subjects)

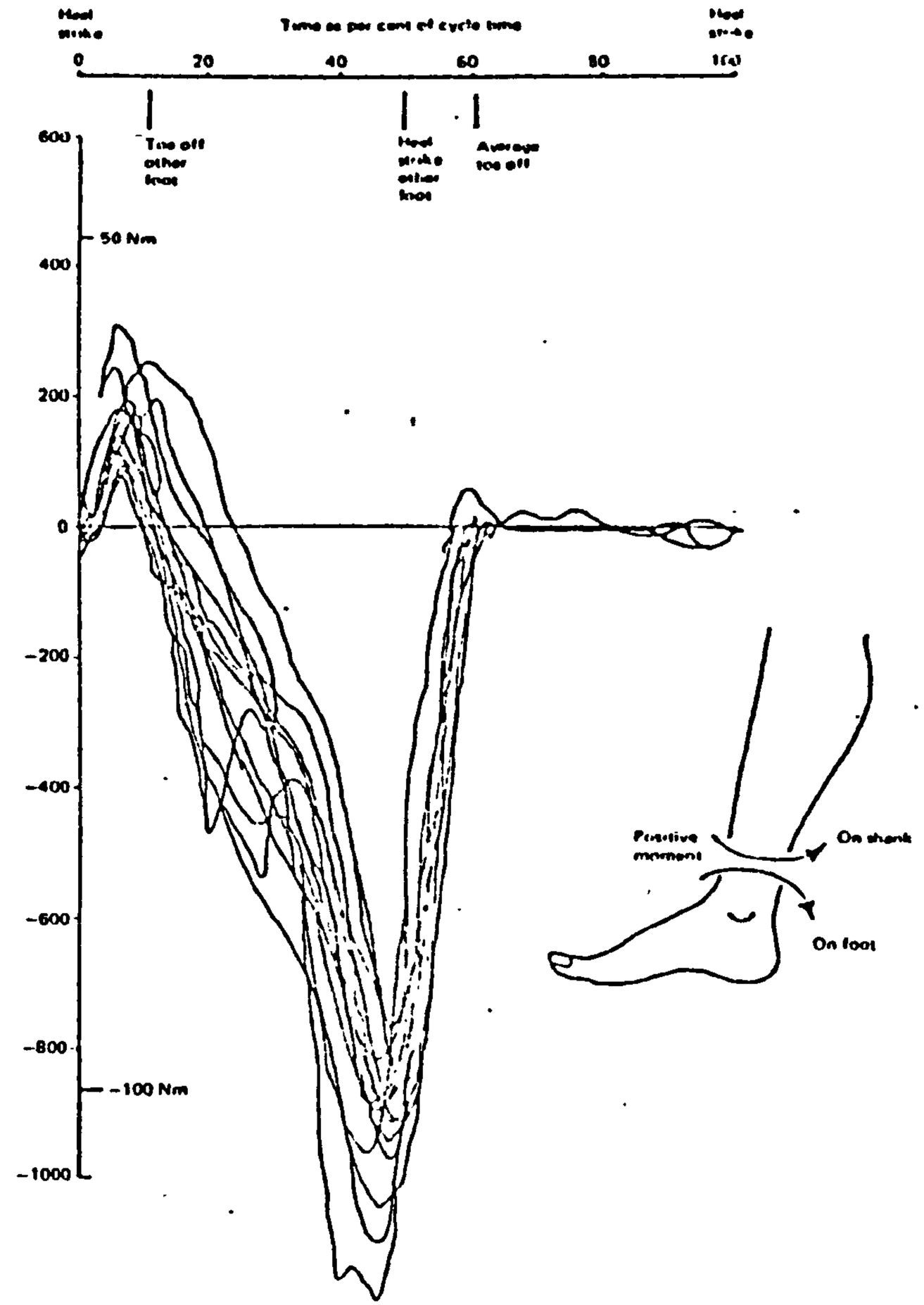

-Ankle moment variation with time. Summary curves from Bresler and Frankel (four subjects) and Paul (ten subjects)

Figure 2.4.3.(c). Summary curves of ankle and knee moments. (from Paul, 1971)

in these curves obtained by the two investigations.

Paul (1970) reported the effect of walking speed on the force actions transmitted at the hip and knee joints. It was concluded that for normal subjects the loading of body components and the amount of muscular effort required corresponds to the body weight and stride length (walking speed) of the individual.

2.5 Energy Measurement

Two different methods have been considered for determining energy expenditure during walking. One method considers the total energy cost of walking by relating it to the net metabolic energy expended by the body. This method will be referred to as the metabolic rate method. The other method considers only the mechanical work during the process of walking, that is the mechanical energy level produced in kinematics and the mechanical work done due to kinetics during locomotion. This method will be referred to as the mechanical work method.

2.5.1 Metabolic Rate Method

There is no direct method available to measure the net metabolic energy expended by the body during locomotion or any other activities. Several types of physiological measurements have been utilised to measure this quantity indirectly.

A literature survey of these measurement techniques, the control of experimental protocol and the up-to-date measuring equipment available was presented by Garton (1979). This survey included findings of research work in this area over the last forty years with the aim of determining the best measurement techniques for use with

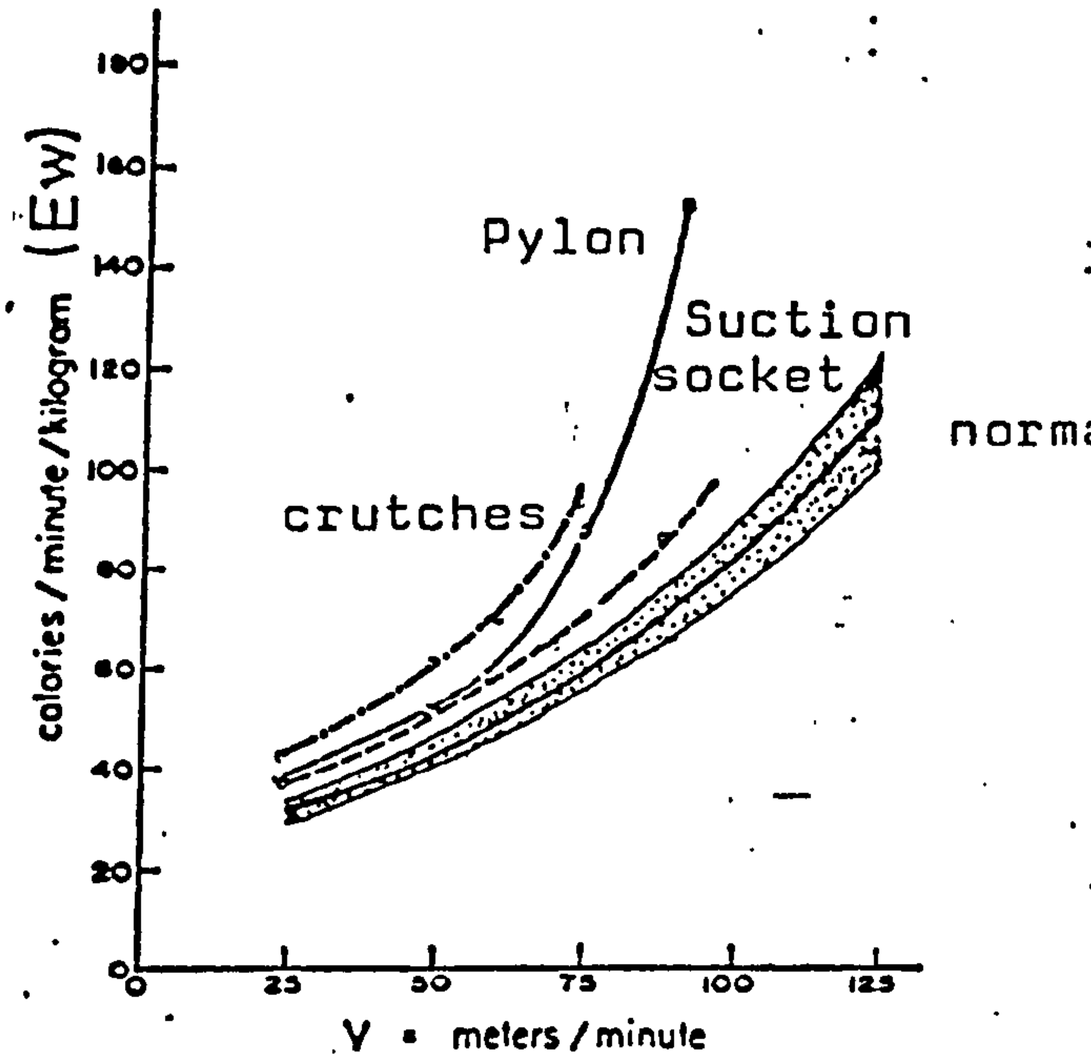

Heavy curve: average energy expenditure in cal./min./kg. of normal subjects walking at various speeds. Stippled area, approximately one standard deviation. Broken line: amputee walking with suction-socket prosthesis. Dotted line: same, using pylon. x—x—x: same, using forearm crutches.

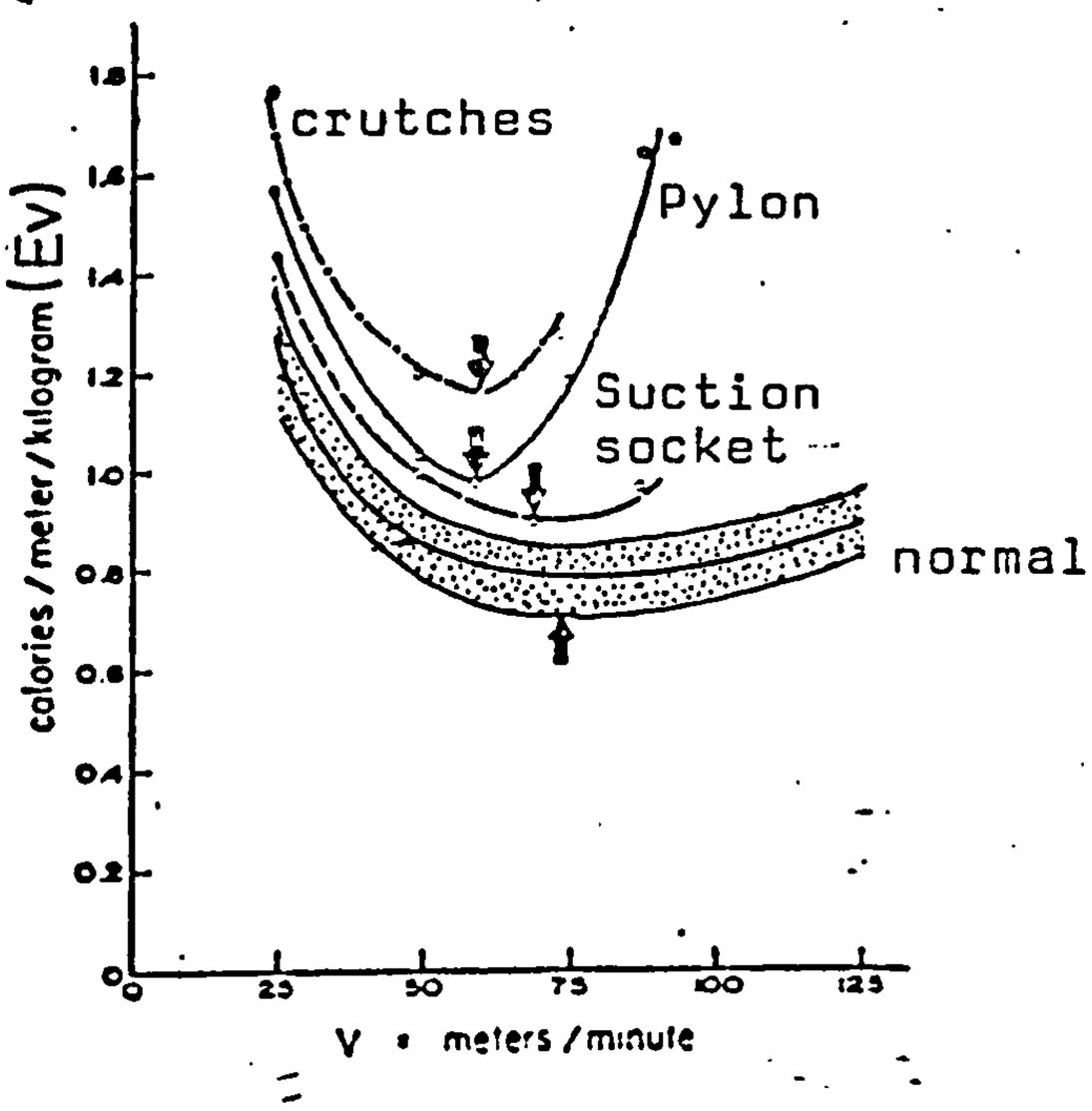

Heavy curve: average energy expenditure in cal/meter/kg. of normal subjects walking at various speeds. Stippled area: approximately one standard deviation. The broken, dotted, and x—x—x lines have the significance described in the legend to figure. Arrows represent natural walking speeds.

Figure 2.5.1. (a). Average energy expenditure during walking (from Bard & Ralston, 1959)

disabled people. It was found that parameters involving respiratory function and heart rate have correlations with energy expenditure. However, they are not necessary linear, they vary between individuals and are also effected by extraneous and sometimes uncontrollable influences.

Analysis of expired gas was regarded to be the most reliable technique in the survey, one that is least affected by extraneous and uncontrollable influences, although stringent control of the experimental protocol is essential to avoid inconsistent and unmeaningful results. Other problems associated with this technique are the cumbersome facial attachments together with the analysis machine or carrying pack on the subject's back and the need for long experimental durations in order to obtain "good" average values over the sampling period. This technique can only measure the overall metabolic energy level the state of metabolism at sites of muscular activity involved in locomotion is still indeterminate.

Several authors using the respired gas analysis method have measured the metabolic energy expenditure during ambulation of normal subjects in relation to the variables influencing it.

McDonald (1961) did a literature review from 1912 to 1958 on the measurement of metabolic cost of walking by normal subjects. He found that there was no significant correlation between age or height and energy expenditure per unit distance but weight, sex and speed of walking were important factors. -It was observed that the energy cost of walking appears to be approximately 10% less for women than for men. The energy expenditure per unit distance was least at a speed of about 80 m/min., however there is little variation for walking speeds of

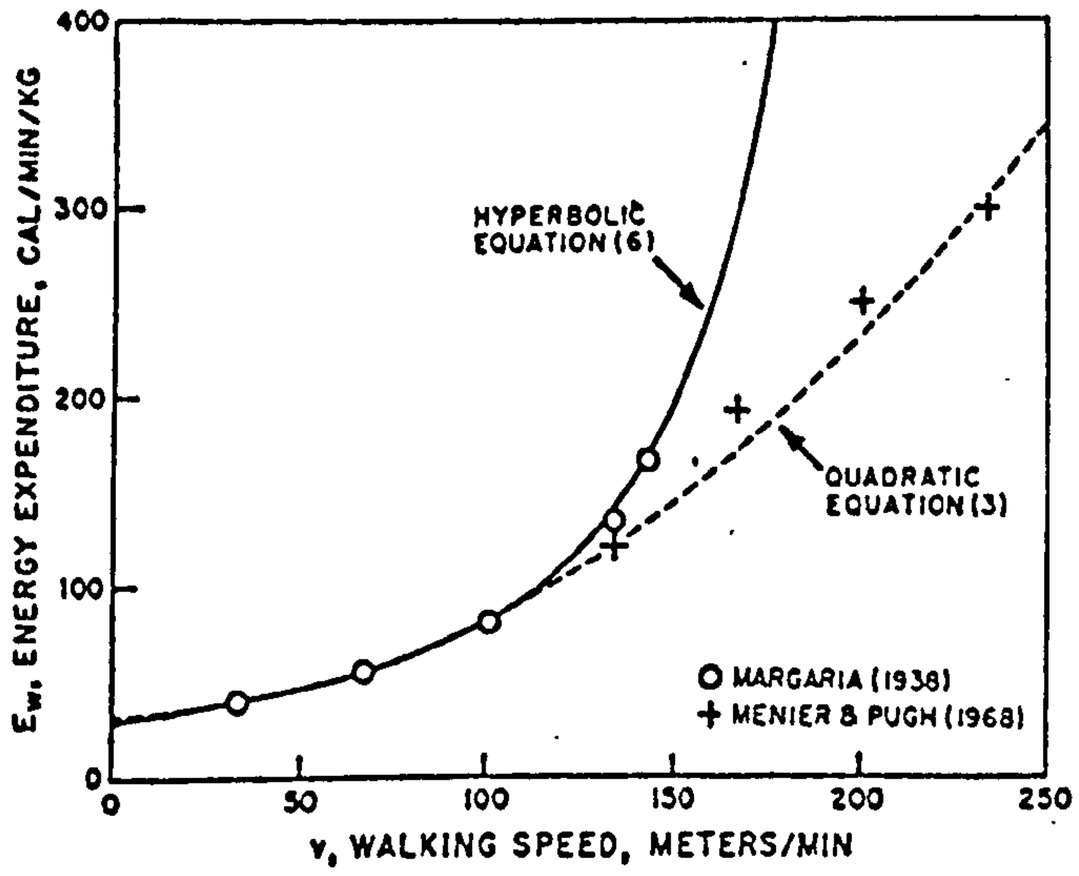

Relation between E_w and v, calculated from the hyperbolic Eq. (6), using $E_o = 28.3$ and $v_o = 242$, solid line, and the quadratic Eq. (3), dashed line

Figure 2.5.1. (b). Comparison between the hyperbolic and quadratic equations.
(from Zarrugh et al, 1974)

60-80 m/min.

Ralston (1958) established the first useful energy-speed relation for level walking. An empirical quadratic equation relating energy expenditure per unit of body weight (E_w) to the square of the speed of walking (V), over a range of speeds of about 25 to 100 m/min, was given as :

$$E_w = 29.0 + 0.0053V^2 \quad \ldots\ldots\ldots (1)$$

This equation indicates that the energy expenditure rises parabolically as walking speed increases and the metabolic energy level at standing is 29 (cal/min)/kg of body weight. Dividing the equation by speed, gives a hyperbolic relationship with a minimum energy expenditure of 0.78 (cal/m)/kg of body weight at a speed of 74 m/min, see Figure 2.5.1(a). No significant difference was found between male and female subjects.

Waters et al (1976) reported on their study of 87 normal male and 74 normal female subjects. It was found that the average speed of walking was 83 m/min and the average energy expenditure was given as 0.77 (cal/m)/kg of body weight. They also noted that female subjects expended significantly more energy per unit distance than males. This contradicts the finding of Ralston and McDonald.

Walt et al (1973) reported a study relating oxygen consumption and step length. Six subjects were tested at 4 different walking speeds between 53 and 133 m/min. A low correlation was found between oxygen consumption and step length. It was regarded that step length was not an important factor for predicting energy expenditure at least for walking speed of up to about 100 m/min.

Zarrugh et al (1974) collated all the results of investigations (including both male and female subjects)

since 1958 that have been represented by similar quadratic expressions and arrived at an average equation based upon 57 normal male and 29 normal female adults :

$$E_w = 32.0 + 0.0050\ V^2 \quad \ldots\ldots\ldots (2)$$

They also derived an empirical equation, based on 10 normal males and 10 normal female adults relating energy expenditure, with step rate and step length :

$$E_w = E_o/(1 - V/V_u) \quad \ldots\ldots\ldots\ldots (3)$$

where V = walking speed (step length x step rate, m/min)

V_u = walking speed when E_w becomes infinite

E_o = energy rate when step length = step rate = 0

This equation was then compared with equation (2) for one subject, with E_o = 28.3 (cal/min)/kg and V_u = 242 m/min, see Figure 2.5.1(b). It was observed that the two curves are almost identical upto about 100 m/min. Therefore, it can be concluded that prediction of energy expenditure for walking speeds up to about 100 m/min is not dependent on step length. This finding is similar to that of Walt et al (1973).

Fisher and Gullickson (1978) in their literature review of the energy cost of ambulation in health and disability over the last forty years concluded that the average natural speed of the normal person is 83 m/min and the average energy expenditure is 63 (cal/min)/kg of body weight or 0.764 (cal/m)/kg of body weight.

2.5.2. Mechanical Energy Method

In the analysis of mechanical energy requirements by the body during locomotion, two aspects have to be considered, viz the instantaneous mechanical energy level of the body segments, which is the summation of the potential and kinetic (translational and rotational) energies, and the mechanical work done by/on each body segment, this being calculated by multiplying the force

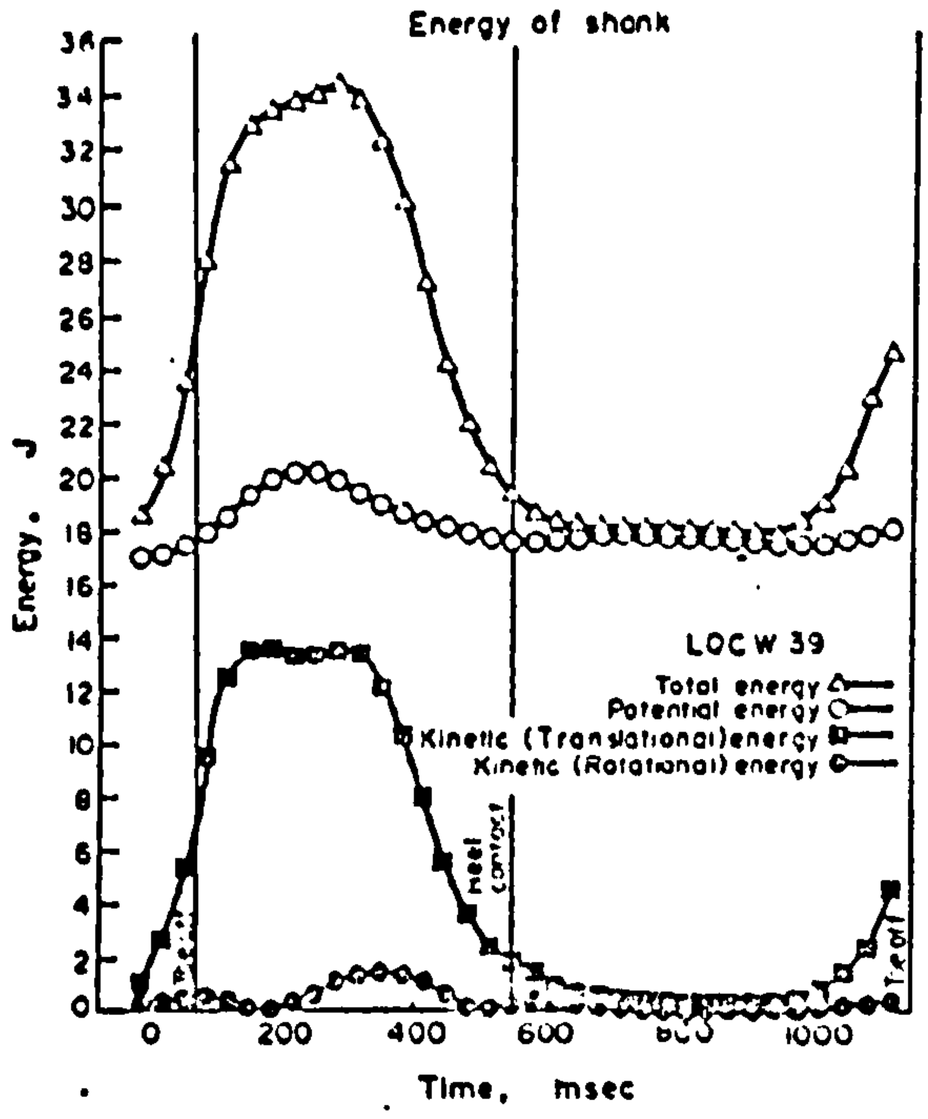

. Instantaneous energy of the shank, as calculated from its two kinetic (rotational and translational) and potential components. Subject is a 20 yr old female, weighing 56 kg and walking 98 steps min.

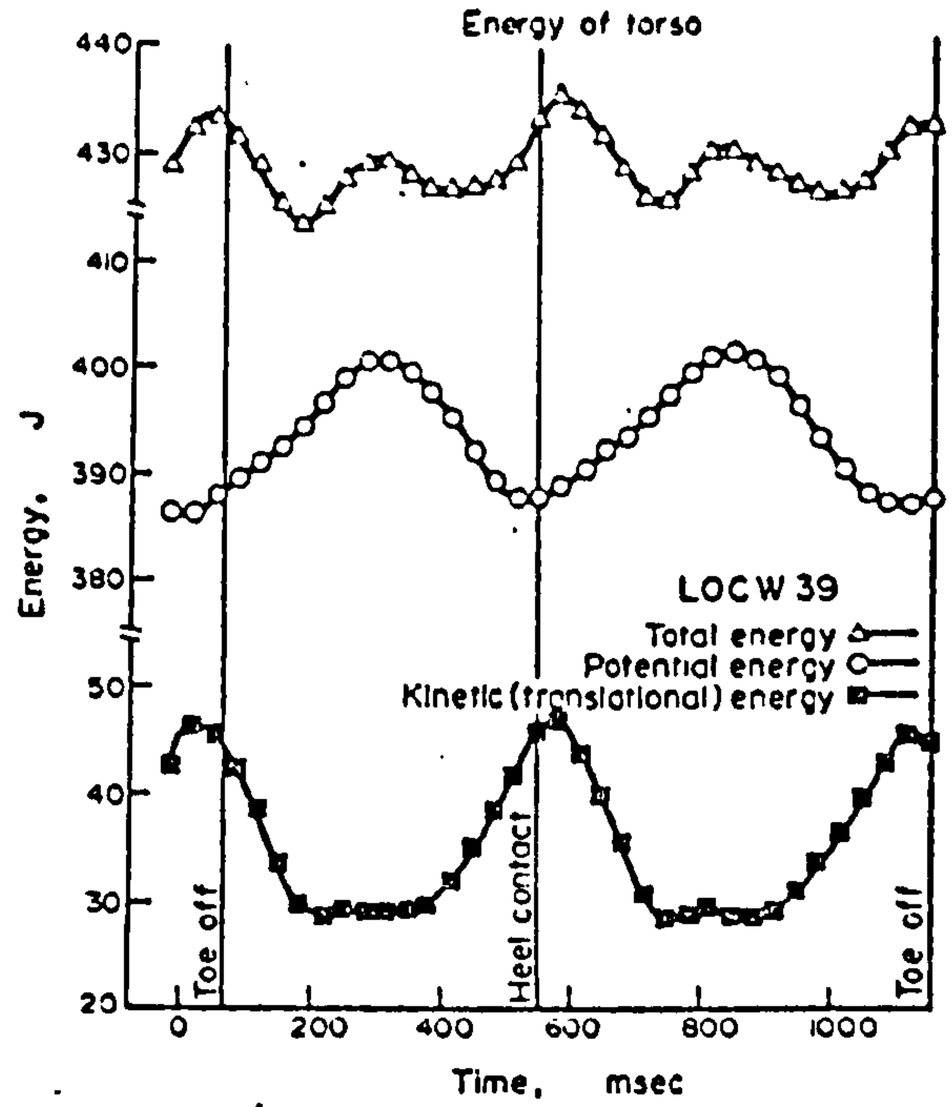

Instantaneous energy of trunk as calculated from its kinetic and potential components. Translational component is the only kinetic component considered.

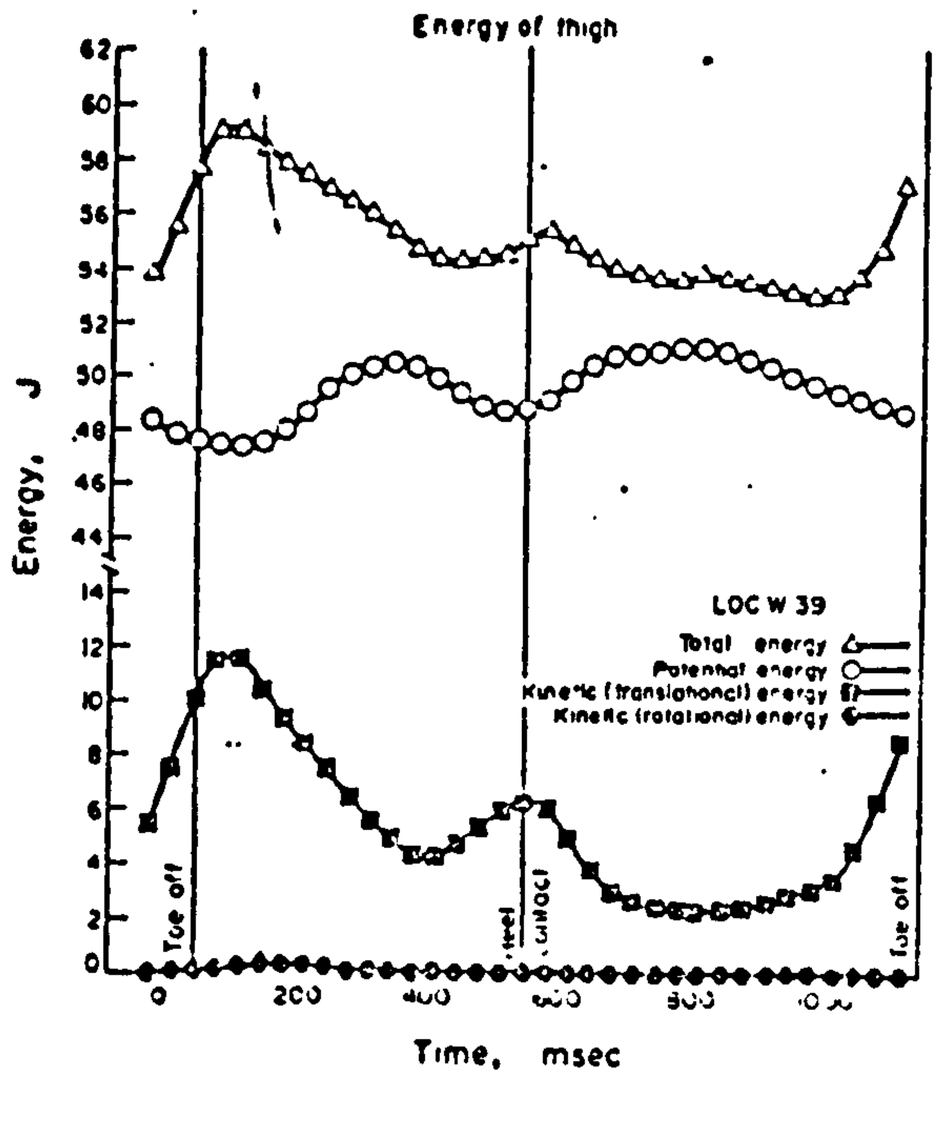

Instantaneous energy of the thigh as calculated from its potential and kinetic components.

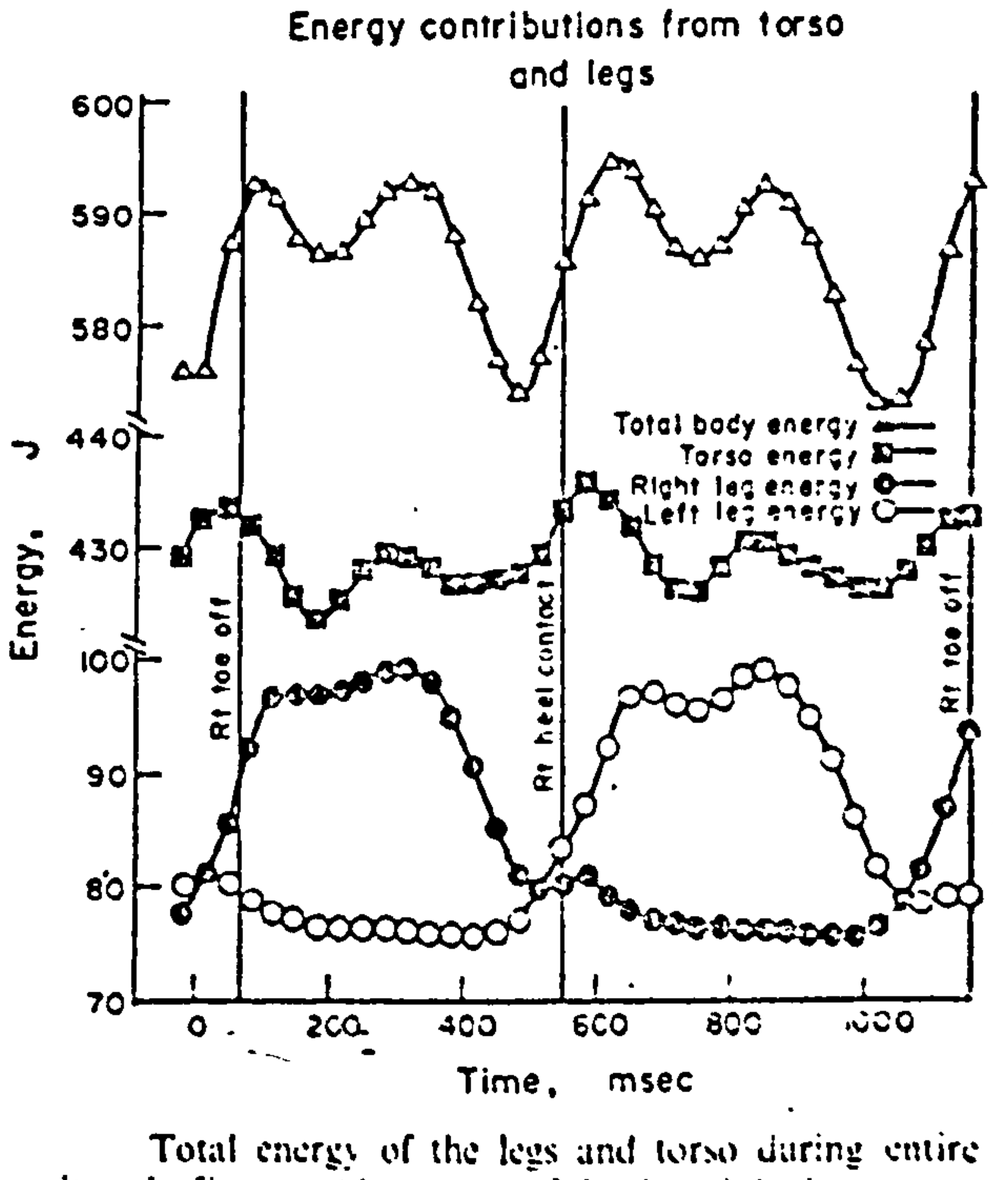

Total energy of the legs and torso during entire gait cycle. Energy of leg is sum of shank and thigh energies. Data used for calculation of left leg energy was same as that used for right leg, but shifted in time by one gait cycle. The energy changes in the legs are considerably larger than those changes in the torso, representing about 80% of the total body energy change.

Figure 2.5.2 (a). Summary results of instantaneous energy of leg segments. (from Winter et al, 1976)

and distance moved.

Earlier researchers like Fenn (1929) and Elftman (1939) had previously considered this method of assessing the energy of human movement. Bresler and Berry (1951) developed a comprehensive model based on Newtonian laws of motion for the energy of normal gait in three dimensions. The basic concept used was that the mechanical work is transferred into a segment when the moment applied on the segment below the joint acts in the same direction as the relative angular displacement at the joint. Mechanical energy levels of the thigh, shank and foot were determined for four normal subjects.

Cavagna et al (1963) computed the "external" work required in walking from three directional accelerometer records of the trunk and cine films records of the limbs in the saggital plane. This method neglected the effect of the lateral translational kinetic energy and the medio-lateral and axial rotational kinetic energies. In 1975, Cavagna utilised data from force plates to calculate directly the energy of the body's centre of mass. The analysis does not take into account the reciprocal movements of the limb segments. This would then underestimate the total energy of the body. Winter (1979) had showed in his analysis that it would be lowered by 16.2%.

Zarrugh (1981) pointed out that in walking, work done is derived from internal sources and does not involve the exchange of mechanical energy between body and environment - if air resistance and friction losses at feet are neglected. It is therefore confusing to refer to work done in locomotion as purely external work.

Winter (1979) provided a rigorous and rational definition of work done for human activities. He

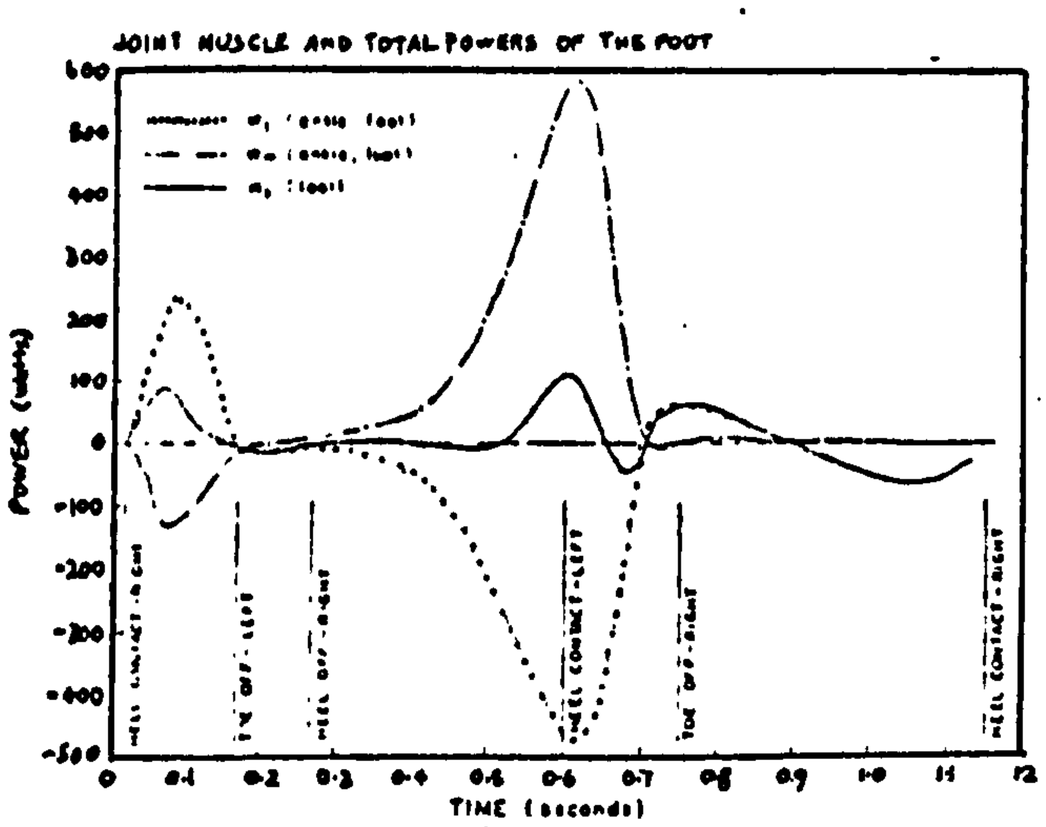

Muscle and joint powers and the total power supplied to the foot.

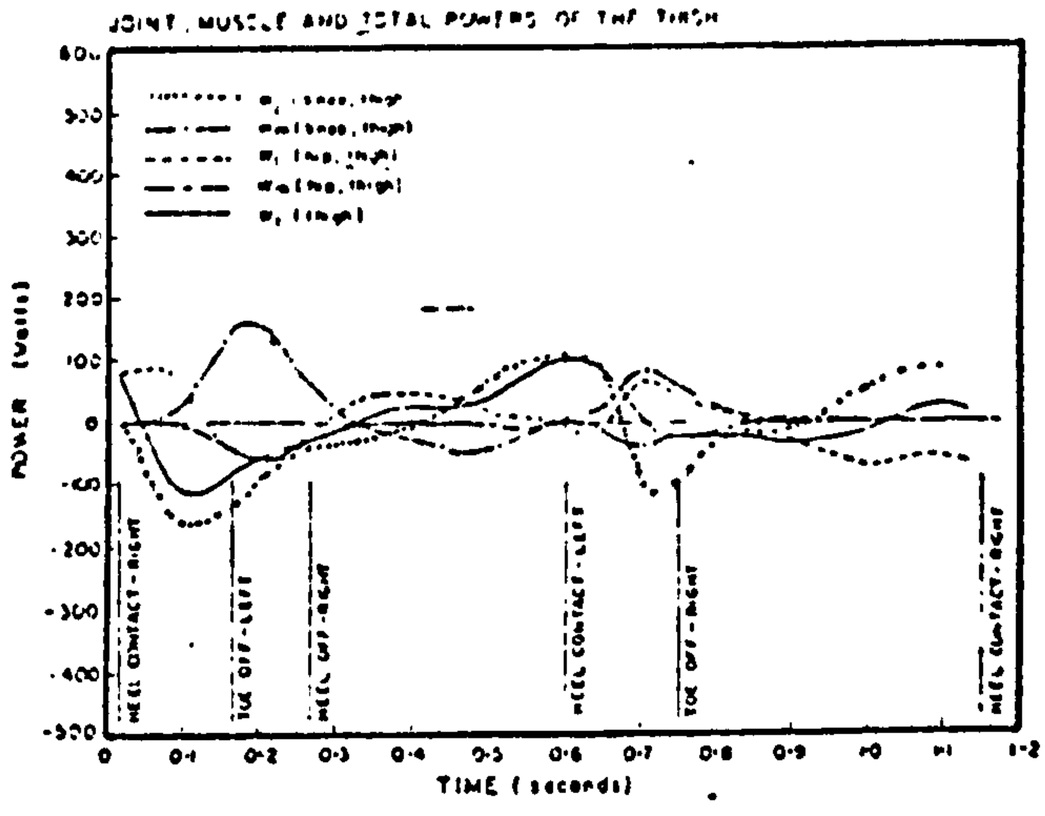

Muscle and joint powers and the total power supplied to the thigh

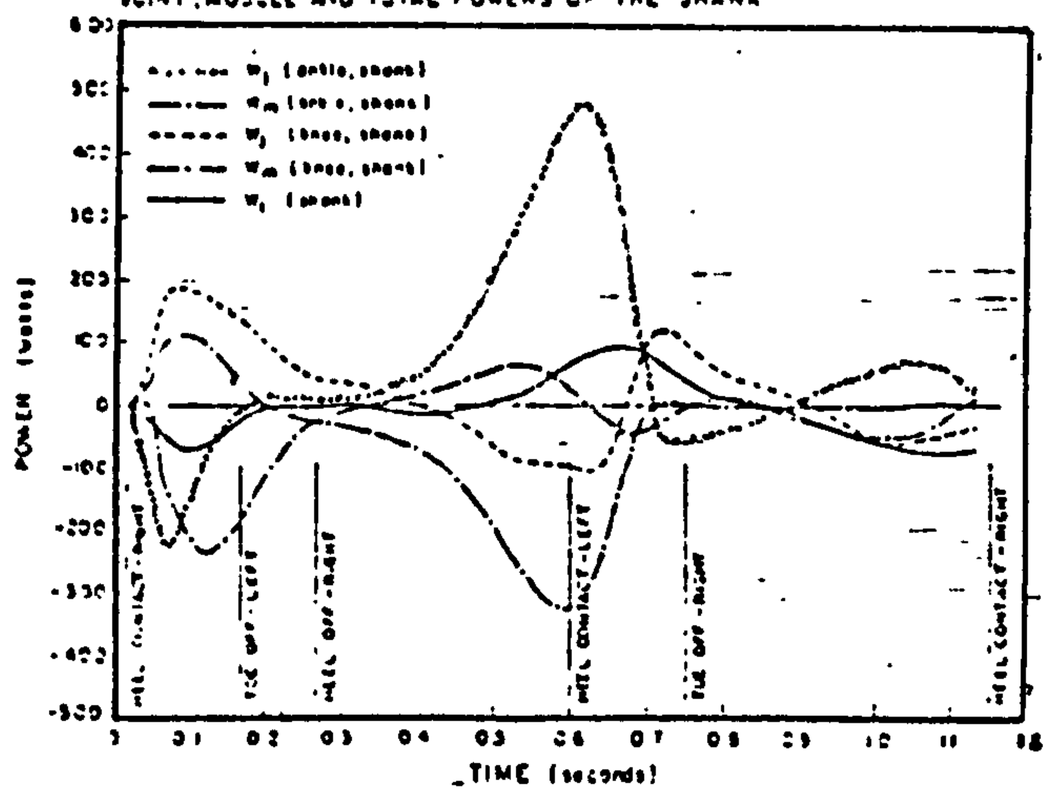

Muscle and joint powers and the total power supplied to the shank

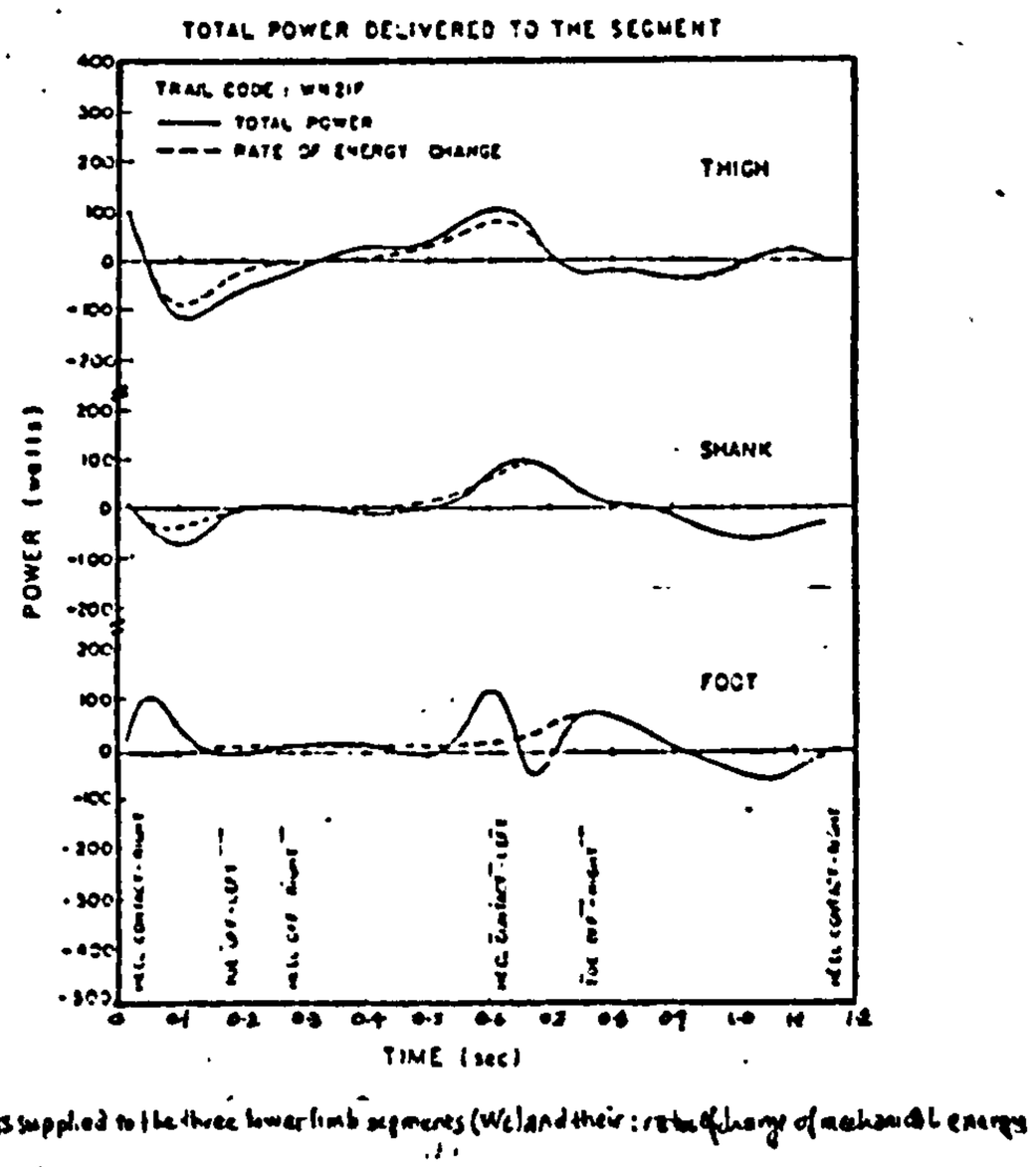

Powers supplied to the three lower limb segments (W_t) and their rate of change of mechanical energy

Figure 2.5.2. (b). Total power delivered to or taken from each segment. (from Robertson & Winter, 1980)

suggested that work can be divided into internal work done, which is required to accelerate body segments and external work done, which is used against an external force such as lifting, pushing or pulling a load.

Winter et al (1976) presented a detailed analysis of the instantaneous mechanical energy requirements of a normal subject during walking at one speed. Their segment by segment analysis was two-dimensional in nature, being based on displacement data recorded by a television-computer system. Therefore, energy changes in the transverse plane(mediol-lateral), are not included in the analysis; these values have been shown to be very small. Figure 2.5.2(a) shows the summary results of an analysis.

Elftman (1939) commented that when rate of change of energy of a segment is positive, i.e. its energy level is increasing, the increase is due to a net flow of energy from work done by forces acting at the segment's joints or by muscle moments. This prompted Robertson and Winter (1980) to formulate equations relating to the rate of work done by the joint forces, viz joint power and the rate of work done by muscle moments, viz muscle power. The total power required at each limb segment is the summation of the joint and muscle power. Figure 2.5.2(b) shows the total power of each limb segment. A comparison between the total power delivered to or taken from each segment and the corresponding segmental rates of change of the instantaneous mechanical energy, indicated that the work-energy principle holds in their analysis. This they claimed validated their assumption that the joints act as ideal hinge connections.

Ralston and Lukin (1969) analysed the energy requirement of treadmill gait using string displacement transducers attached to the approximate location of the

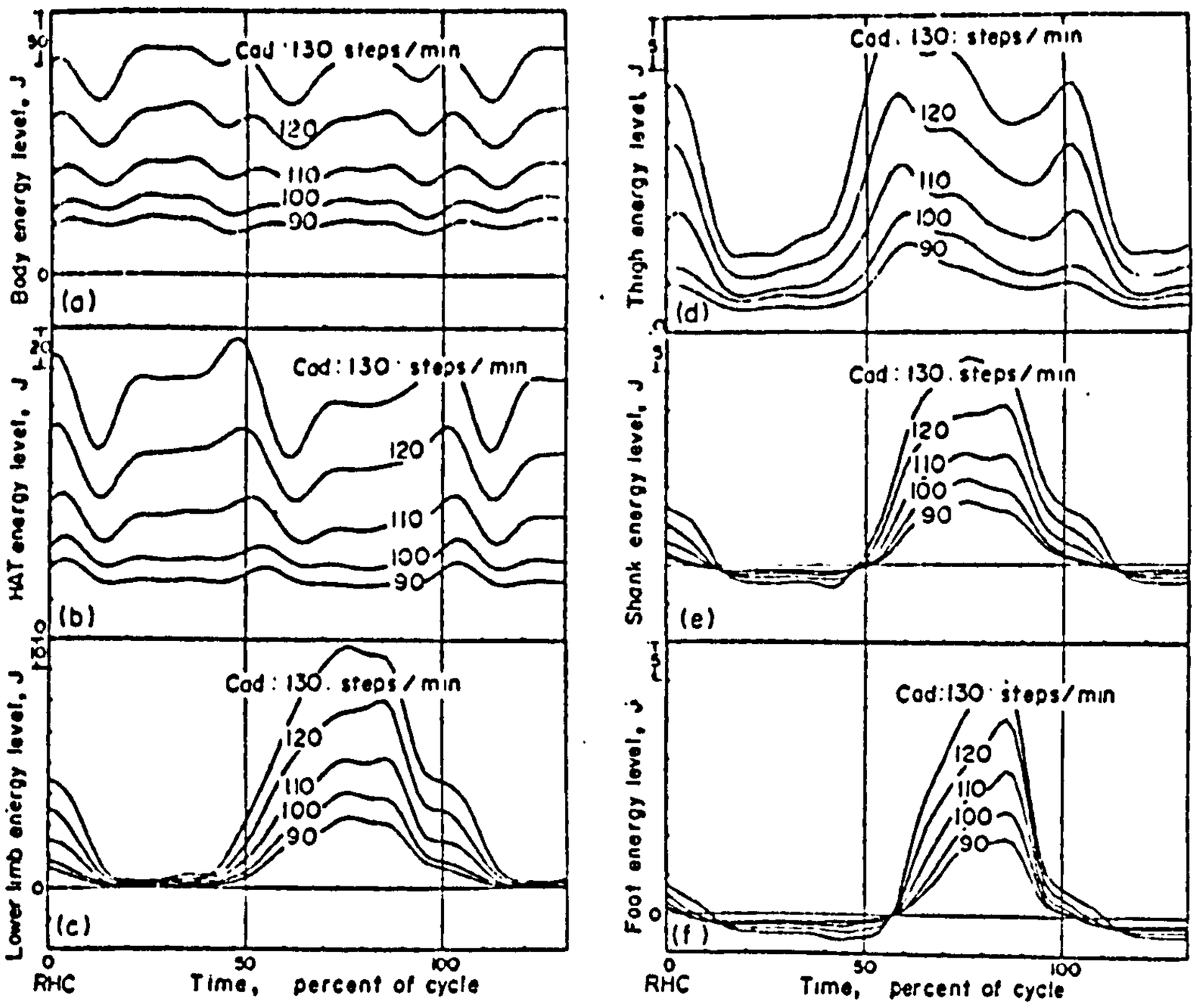

Instantaneous energy levels of the body and its divisions in free walking. For this subject, the walking speed in m/sec can be obtained by dividing the cadence squared in (steps/min)^2 by 8000, e.g. (110 steps/min)^2/8000 = 1.51 m/sec.

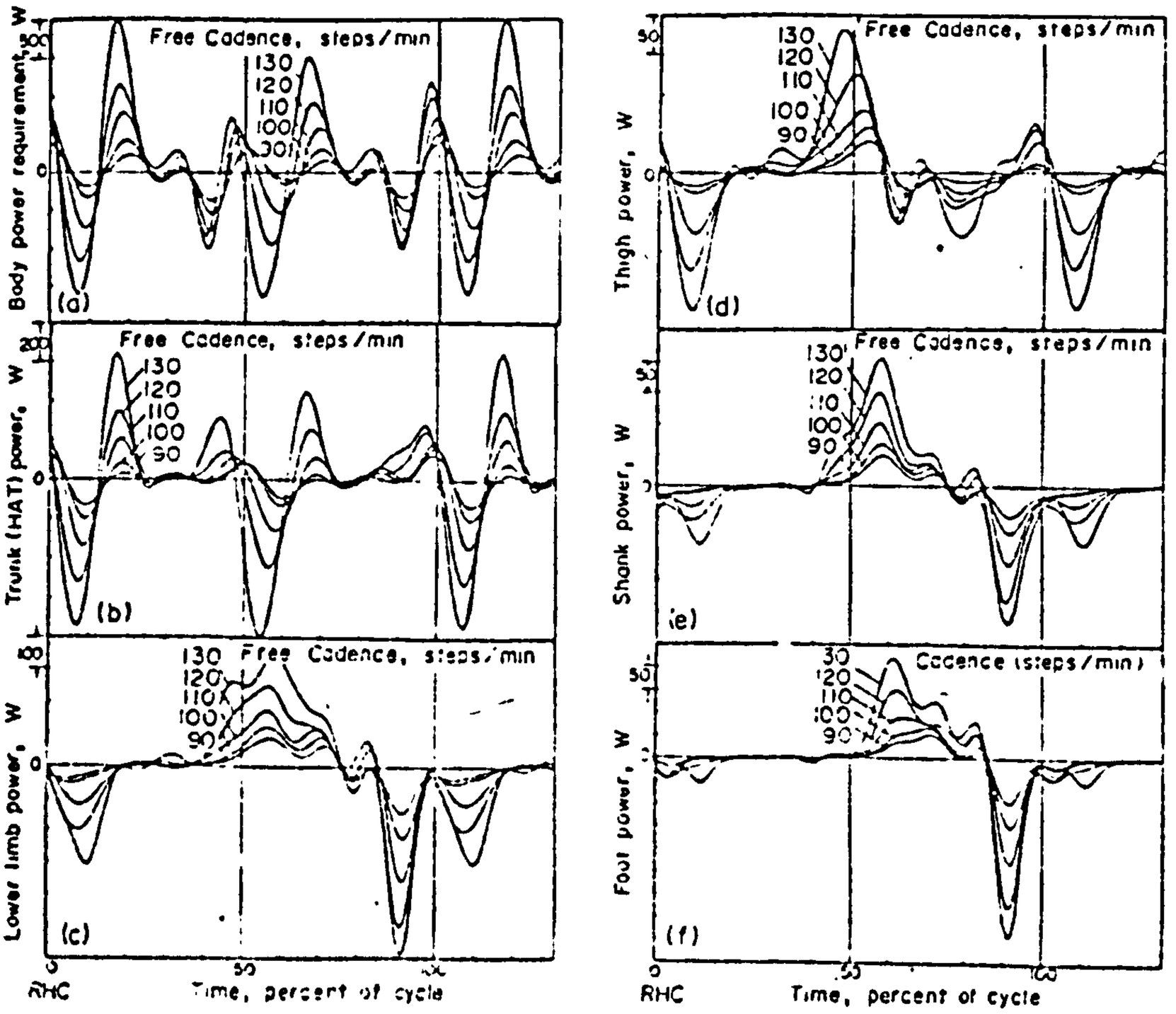

Instantaneous power requirements of the body and its various divisions at different walking speeds.

Figure 2.5.2. (c). Relating Walking Speeds with instantaneous energy and power requirements of the body. (from Zarrugh, 1981)

centre of mass of the foot, shank, thigh and trunk. The potential, vertical kinetic and rotational kinetic energies of all lower limb segments were not taken into account in their analysis. Zarrugh (1981) adopted a similar technique to that of Ralston and Lukin, except that triaxial, self-aligning electrogoniometers were used to determine the limb segment angles. Analysis was performed on subjects walking at different speeds, ranging from 45 to 132 m/min. The results for one subject are as shown in Figure 2.5.2(c), both the instantaneous energy levels and power requirements of the body being presented. The energy level of the body as a whole, as well as its power requirements, were computed using the assumption of symmetry between the two lower limbs. This assumption was also made in the analysis presented by Winter et al (1976). Although this may be valid when considering normal subjects, it cannot be used for pathological subjects. The results reported were similar to those presented by Bresler and Berry (1951), Ralston and Lukin (1967) and Winter et al (1976). The kinetic energy was found to be the largest contributor to the total energy of the body. The rotational kinetic energy was shown to be very small for all segments, the largest being 6% of the maximum total mechanical energy.

CHAPTER 3

Lower Limb Prosthetics

3.1. Amputation Surgery

Archaeological findings of knives and saws, of bone and skeletal remains with amputated bone stumps, dating back to the Neolithic period show some evidence of amputations being practised by early man. These "ancient" amputations were generally performed to remove gangrenous or severely damaged limbs. However, it is believed that amputations were also used for ritual sacrifise, exorcism, appeasement to gods or idols, punishment and in some cases, beautification. Readers who are interested in amputations and prostheses in primitive cultures are recommended to read Friedmann's (1972) article on this topic.

The history of medical amputation follows closely the development of surgery itself, especially orthopaedic surgery. Only a brief account of the development of surgical techniques vital in amputation surgery, is discussed. For a comprehensive history of amputation surgery please refer to Garrison (1963), or Slocum (1949).

Hippocrates described the use of ligatures to control major arterial bleeding during amputations but this technique was lost during the Dark Ages (200 A.D. to 1500 A.D.). It was reintroduced by Ambroise Paré in 1529. As a result the rate of survival became much higher. Another haemorrhage controlling technique, the tourniquet, was introduced by Morel in 1674. These, plus the introduction of techniques in the appropriate handling of soft tissues, secondary wound closure to prevent infection and the recognition of the importance of cleanliness, were major contributions to surgery made by amputation surgery.

The developments of anaesthesia and antiseptic

techniques are the hallmark of modern surgery. They contributed greatly to the overall success of amputation surgery. The speed of performing an operation which used to be a vital factor for success became secondary to surgical technique with these developments. Furthermore, surgeons could focus their attention on improving methods and the selection of appropriate sites.

Amputation surgery has two purposes : ablation and reconstruction. The operation must remove all of or that part of the limb necessary to eliminate the pathological state and provide primary or secondary wound healing. The reconstruction must create the optimum motor and sensory stump for prosthetic substitution and restoration of function. The success of every amputation depends on adherence to these two principles. To be effective, the surgeon must understand the functional limb physiology and the nature of prosthetic substitutes.

3.1.1. Indications, Levels and Limiting Factors

The removal of a part of the body can be a profoundly shocking experience for any human being; the loss is irretrievable. Therefore, amputation surgery must not be treated lightly or undertaken in ignorance, even though the procedure may have validity in one's own field of specialty. The surgeon's first concern should be to make a decision on whether amputation is the correct form of treatment and secondly, to define the correct level of amputation and indeed define the objects of the operation itself.

The event of amputation should be seen as the beginning of a rehabilitation process rather than an end of a story, for amputation does not represent the failure of a physical entity but merely another level of successful treatment. Its success however is dependent

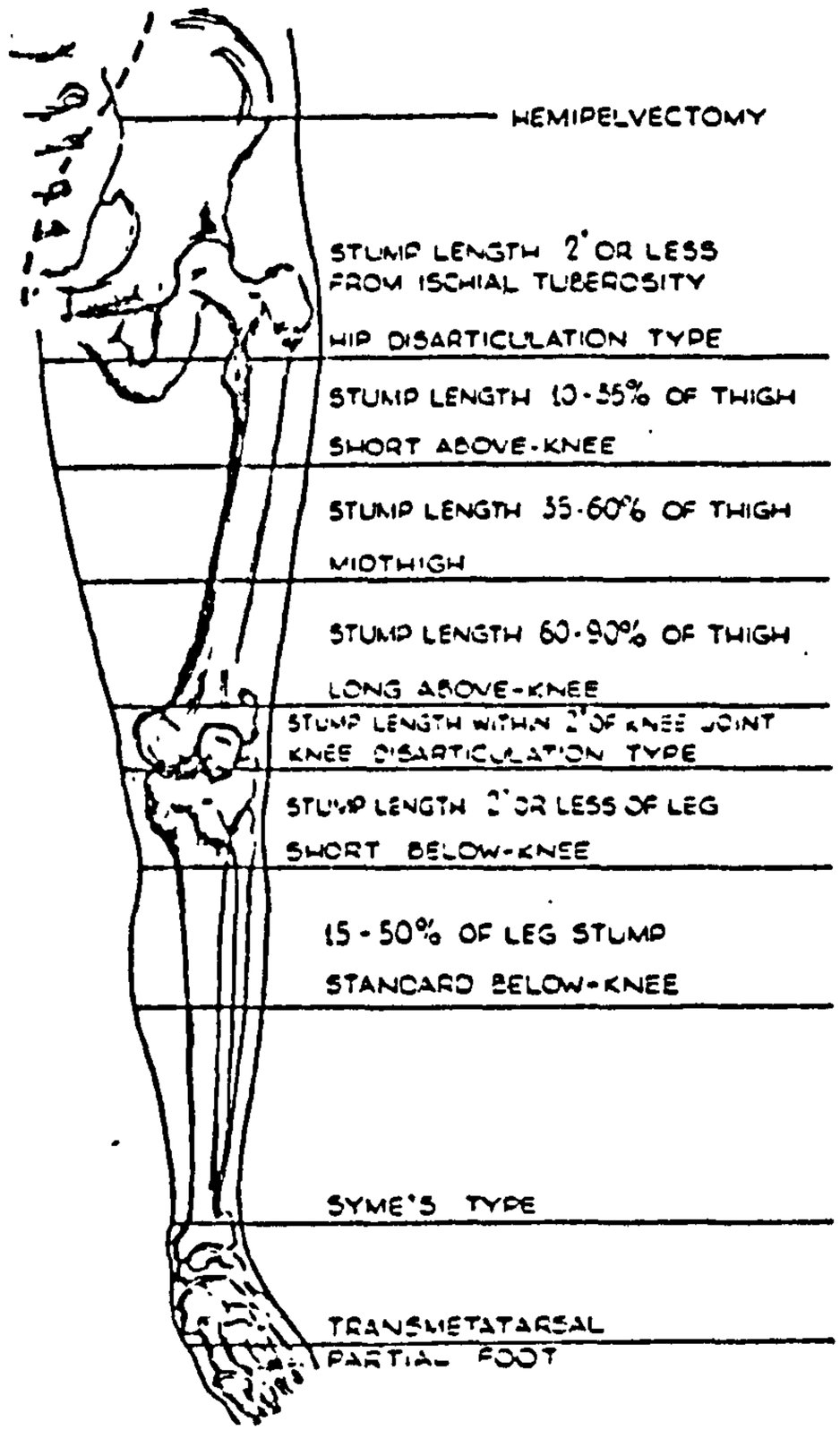

Figure 3.1.1 Major Sites of Amputation in lower extremity
(from Mital & Pierce, 1971)

on the accomplishment of some or all the objectives for which it was performed.

In order to achieve a satisfactory solution, all the following factors require careful consideration : (a) pathological, (b) anatomical, (c) surgical, (d) prosthetic and (e) personal (viz sex, age and occupation). Each of these factors will play some part in the decision and each will have varying emphasis in the light of the clinical situation.

Figure 3.1.1. illustrates the major sites of amputation in the lower extremity. The level of an amputation is determined primarily by the level of vascular sufficiency in the extremity, as determined by careful clinical tests and finally by assessment of the local circulation as seen at operation.

Vascular disease is by far the most common reason for amputation in North Amercia and Northern Europe. Moreover, as developing countries acquire higher standards of living and populations survive longer, amputation for vascular disease increases as a percentage of all amputations. Other indications for amputation include tumors, trauma, chronic infection, paralysis, deformity and limb discrepancy, and congenital limb deficiency.

With the advancement of prosthetic systems and fitting techniques, the level of amputation has become less important; a broad, well-healed and properly constructed amputation stump can now be fitted satisfactorily with a prosthesis. Hence, surgical considerations are the primary determinant of the level of amputation. The principle rule is to conserve joints and preserve all possible length (for optimal prosthetic fitting) consistent with good surgical judgement.

Hindquarter amputation and hip disarticulation are largely determined by pathology. The main indication for these procedures is tumor; however, hip disarticulation is also frequently done in severe vascular disease, particularly where previous reconstructive surgery has been done.

The above-knee amputation stump should be as long as possible, subject to pathology and to the need for providing adequate space for the functional knee mechanism in the prosthesis. Amputation at the supra-condylar level, such as is done in the Gritti-Stokes or Slocum procedures, is not to be recommended as they are not truly end-bearing and furthermore they fail to provide sufficient space for the prosthetic knee mechanism.

The knee disarticulation or through-knee amputation has proved to be an excellent procedure. It is easy to perform and relatively bloodless, and the resulting stump (long and strong) provides a large area for end-bearing. In the past, there have been prosthetic cosmetic disadvantages in amputations performed at such a level but these have been largely overcome.

Below-knee amputation has become increasingly important and with the advent of new surgical techniques it is the amputation most preferred in most cases; it is successful in up to 85 percent of vascular cases (Kostuik, 1981). The main inhibiting factors are knee-flexion deformities and pathology.

In Syme's amputation, the stump has attributes similar to those of the knee disarticulation. However, the prosthesis fitted has cosmetic disadvantages. Many amputational procedures distal to the ankle joint are available. Their main virtue lies in the distal nature

of the procedures but only a few of these procedures give good functional results and careful consideration of the end results of the operation is required.

3.1.2. Statistical Survey

In 1973, LeBlanc reported that a Public Health survey conducted between 1953 and 1965 in the United States reveals that there are 1.35 amputees per 1,000 persons not living in institutions; in the United Kingdom there are 1.58 amputees per 1,000 persons including those in institutions.

Glattly (1964) conducted one of the most extensive statistical survey on amputations in the United States, during the period October 1, 1961 to January 31, 1963. Data were obtained on 12,000 new amputees who presented themselves for fitting of an artificial limb for the first time. These findings were updated in 1975 by Kay and Newman. They used the same method of data collection devised by Glattly, to obtain information from 6,000 new amputees.

Kay and Newman (1975) presented a comparison of the new readings with Glattly's final report. It revealed some apparently significant changes in amputation statistics, as well as some situations where very little change seems to have occurred. The ratio of males to females undergoing amputation dropped from 3.35:1 to 2.57:1. This meant a higher percentage of females amputees now exists. Another significant change was in the site of amputation. There is shown to be a decrease to 32.6 percent from Glattly's 44.1 percent in above-knee amputations and a proportionate increase in below-knee amputations from 36.8 percent to 53.8 percent. However, in both studies, the above and below-knee amputations represent the highest percentage of amputation performed.

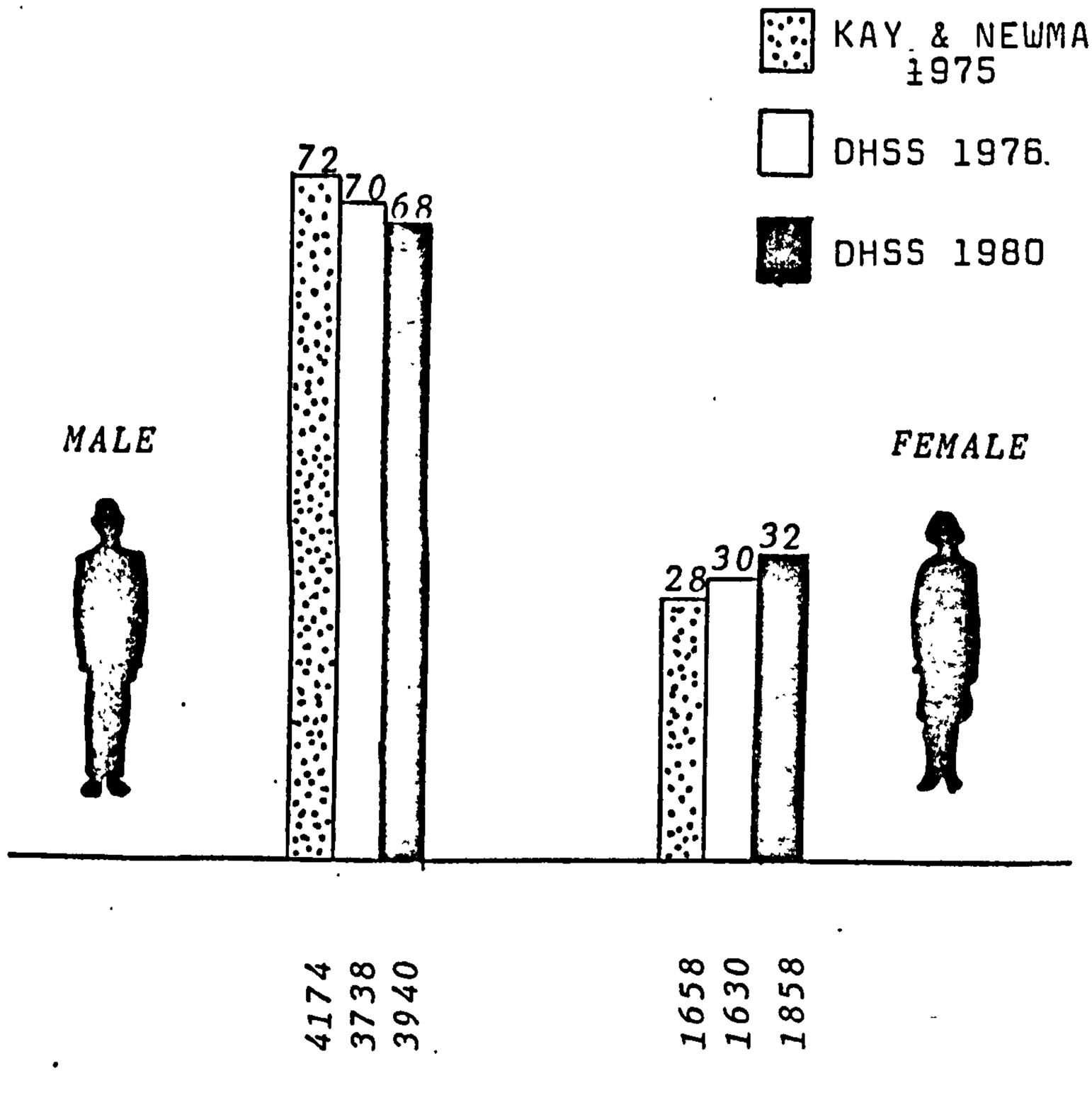

Figure 3.1.2(a) Distribution of Amputation by Sex

RATIO OF "MALE:FEMALE" AMPUTEES

	KAY & NEWMAN 1975	*DHSS 1976*	*DHSS 1980*
TRAUMA	*7.2:1*	*5.0:1*	*5.3:1*
DISEASE	*2.1:1*	*2.2:1*	*2.0:1*
TUMOR	*1.3:1*	*1.1:1*	*1.1:1*
CONGENTAL	*1.4:1*	*2.7:1*	*1.0:1*

Table 3.1.2(a) Ratio of Male to Female Amputees in relation to cause of amputation

It was also found that there were significant changes in the causes of amputation. Amputations due to disease increased from 58 percent to 70.3 percent, while those due to trauma decreased from 33.2 percent to 22.4 percent. Amputations due to tumour or congenital reasons remained at similar levels.

Both studies revealed that the largest number of new amputees fitted with prostheses were in the 61-70 age group. There was an increase in the number of amputees over 70 years of age who were being fitted with prostheses. Kay and Newman reported 22 percent against Glattly's 15.4 percent.

In the United Kingdom, the Department of Health and Social Security (DHSS), Statistics and Research Division published annual reports on amputation statistics for England, Wales and Northern Ireland. Data collected in 1976 and 1980 on 'new' amputations are extracted and used in the following discussions. They are compared with those reported by Kay and Newman. Although the D.H.S.S. publication does not include Scotland, for simplicity's sake, the data obtained from the report will be referred to as that of the United Kingdom.

Figure 3.1.2(a) shows the distribution of amputation by sex. In the United Kingdom, there seems to be a trend towards a higher percentage of female amputees and a corresponding drop in the percentage of male amputees. However, the number of males undergoing amputation is still predominantly higher. The ratios of male to female amputees in relation to the cause of amputation is given in Table 3.1.2(a). In the United Kingdom, the proportion of males to females going through amputation because of trauma is significantly lower than that reported by Kay and Newman for the United States. Furthermore, there was no significant change in this ratio in the United

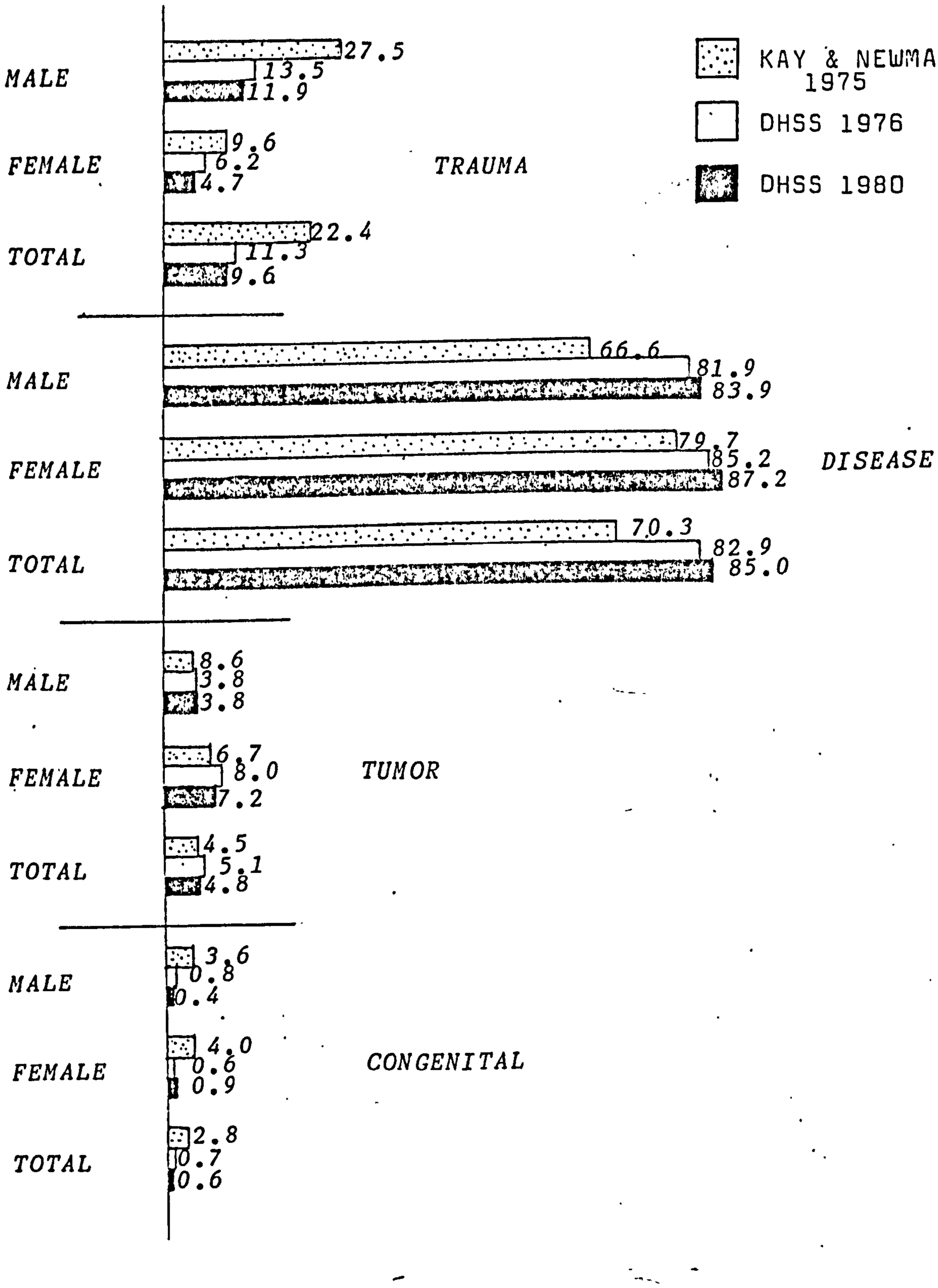

Figure 3.1.2(b) Distribution of Amputation by Cause and Sex

Kingdom between 1976 and 1980.

The distribution of amputations by cause and sex is considered in somewhat more detail in Figure 3.1.2(b). In the total population (male and female) the percentage of amputations derived from trauma dropped from Kay and Newman's 22.4 percent to 11.3 percent in the DHSS (1976) report and down to 9.4 percent in the 1980 report. Substantial decreases in trauma-related amputations in both males and females are apparent. The similar situation is evident in figures for congenital-related amputations. However, the reverse situation is clearly shown in disease-related amputations. In the total sample, the percentage increased from Kay and Newman's 70.3 percent to 82.9 and 85.0 percent in the 1976 and 1980 reports respectively. The percentage increase occurred in both male and female populations. Disease-related amputation remained the prime cause of amputation and the percentage calculated shows an increasing trend both in the United States and United Kingdom. Tumour-related amputation did not appear to show significant changes.

Figure 3.1.2(c) shows the distribution of amputation by cause and age. Note the difference in the class interval used by Kay and Newman and the DHSS. In order to provide a much clearer discussion, a common grouping is used to represent both class intervals. That is (0-9) or (0-10) age group will be termed as the first decade of life and (20-39) or (21-40) age group will be the third and fourth decade of life and so on.

In all the three studies, the largest number of amputations due to trauma occurred in the third and fourth decade of life, while the largest number of disease-related amputations occurred in the seventh and eighth decade of life. In fact, over ninety percent of all the

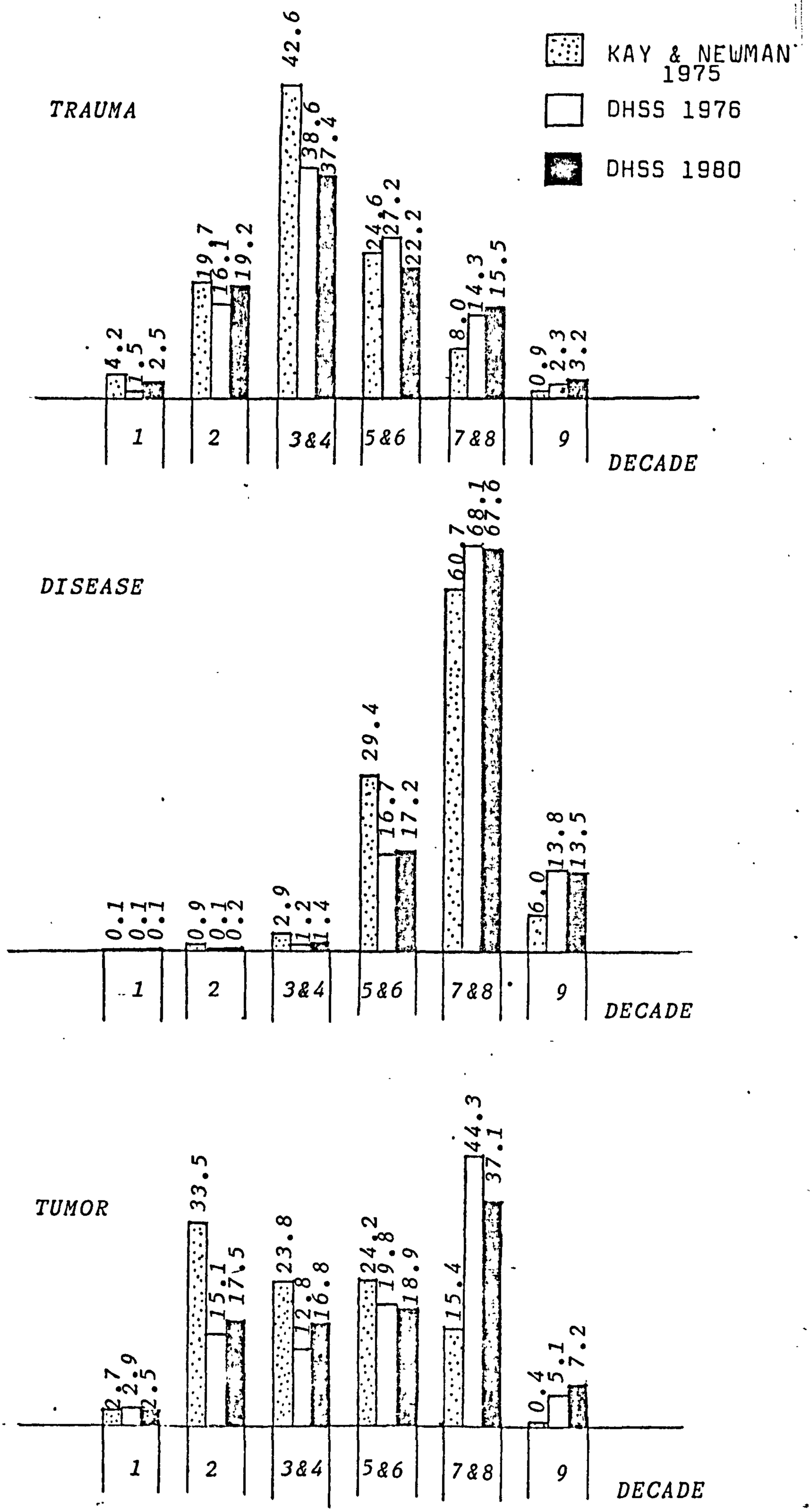

Figure 3.1.2(c) Distribution of amputation by cause & age

amputations in this age group were performed because of disease. Kay and Newman reported the largest number of amputation due to malignancy in the second decade of life. In the DHSS (1976 and 1980) surveys, the largest number of tumour-related amputations occurred in the seventh and eighth decade of life. No detailed information was available to explain the difference.

In the Glattly report, 14.5 percent of all the amputations were performed on the upper extremity. This decreased down to 8.3 percent in the Kay and Newman report. In the DHSS (1976 and 1980) surveys, only 3.6 and 3.0 percent respectively were upper limb amputations. Figure 3.1.2(d) presents a more detailed distribution of amputations by site. In the four studies, between 80 and 90 percent of all the amputations were performed at either the below or above-knee levels.

Glattly (1964) reasoned that the high success in fitting below-knee amputees in recent years should encourage surgeons to reconsider applying the principle that below-knee amputations should be avoided in limbs affected by gangrene due to vascular disease, for fear of the likelihood of a second amputation being subsequently necessary. He urged however for the preservation of the knee joint in the older individuals. Weiss et al (1966) agreed with the view that knee joints could be saved and pointed out that the use of a rigid dressing should improve healing by reducing oedema. Pedersen (1968) also promoted the idea that knee joints in many elderly patients with vascular disease could be saved if proper care were given post-surgically. The increase in below-knee to above-knee ratio reported by Kay and Newman indicated that the suggestion was widely understood and more decisions were being made in favour of below-knee rather than above-knee amputations.

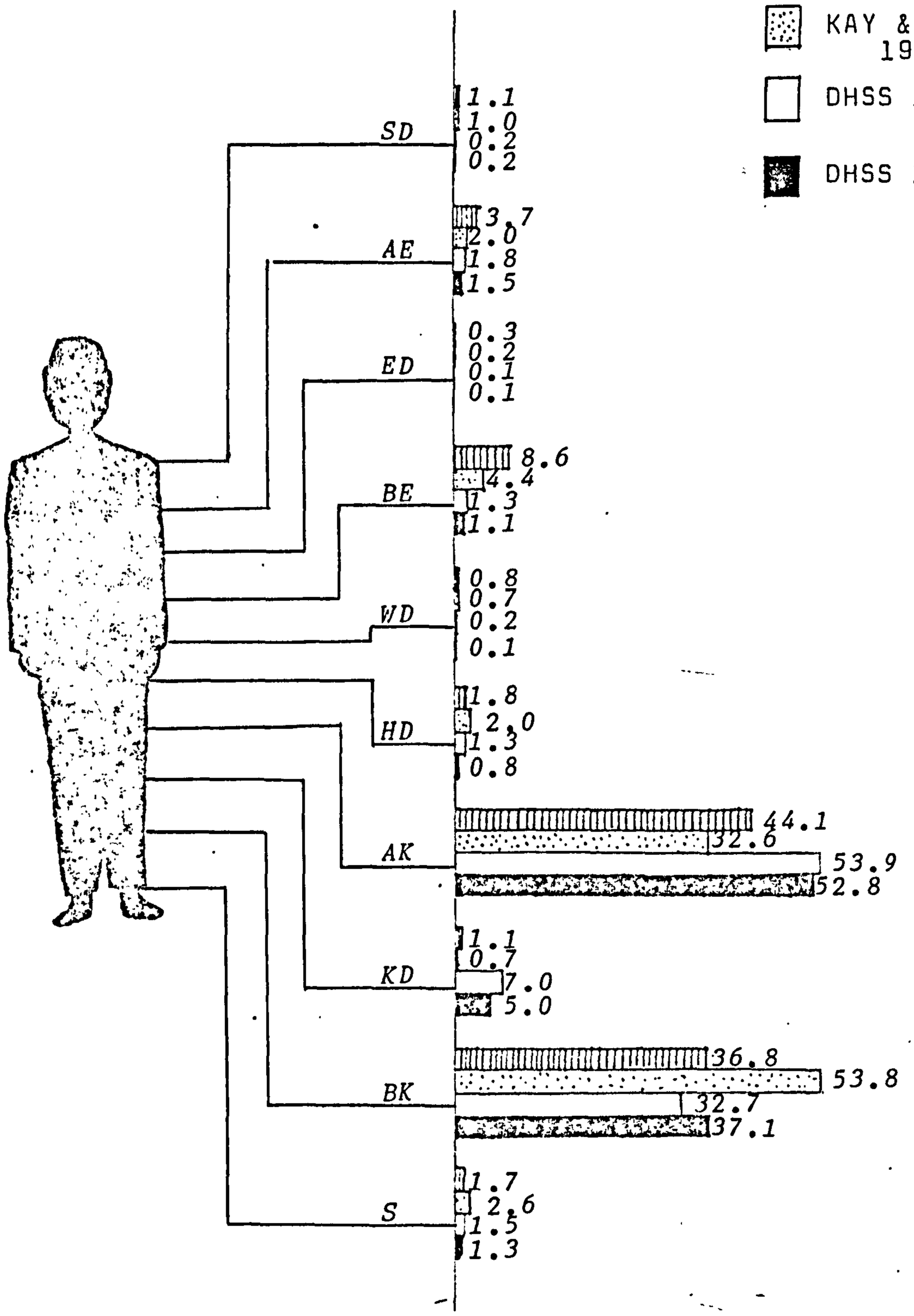

Figure 3.1.2(d) Distribution of Amputation by Site

In the United Kingdom, the reverse situation is true. The percentage of above-knee amputation is approximately one and half times higher than below-knee amputation, although diabetic peripheral vascular disease is only approximately 10 percent of the total vascular disease cases. This may be a reflection of current practice in the United Kingdom, that surgeons are still abiding by the classic instruction of amputating above the knee when vascular circulation has been impaired so that healing can be ensured.

The factors determining the ideal level of amputation in a patient with peripheral vascular disease are many and complex. In selecting the level of amputation, the surgeon must balance the need for retaining optimum limb length against the necessity for obtaining optimum primary wound-healing. Burgess and Matsen (1981) urged surgeons to assess accurately the viability of the limb through the use of precise techniques of testing local healing potential. They concluded that by integrating these data with overall clinical assessment, surgeons would be increasingly able to select the ideal amputation site for their patient. This could result in amputation being performed at the lowest reasonable level and should lead to an increased number of below-knee amputations.

The statistics presented by Kay and Newman representing the American experience of preserving the knee joint should encourage similar practice in the United Kingdom.

From these statistical surveys, the below- and above-knee amputations represent a large majority (approximately 80 percent) of the total amputation population. Therefore, it seems justifiable in this project to concentrate on these two levels of amputation

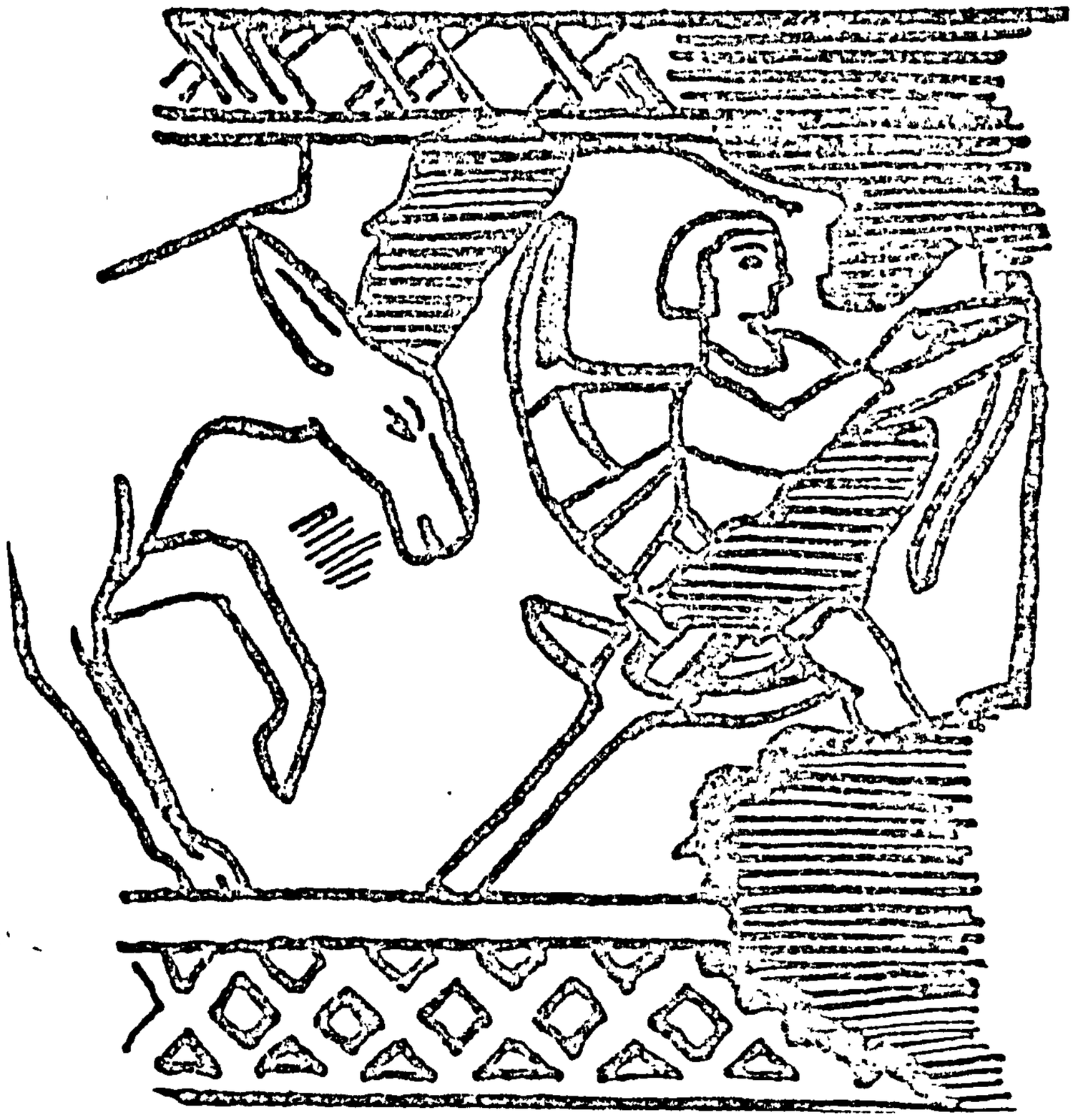

FIGURE —Mosaic from the Cathedral of Lescar, France, depicts an amputee supported at the knee by a wooden pylon. Some authorities place this in the Gallo-Roman era. (From Putti, V., Historic Artificial Limbs, Paul Hoeber, Inc., New York, 1930.)

Figure 3.2(a)

with respect to the type of prosthetic feet that would be prescribed to them.

3.2. Lower-Extremity Prostheses

There is no exact record of when prostheses were first used, but some form of replacement was undoubtedly attempted following the very first surgical or traumatic amputations. Ancient remains and archaeological evidence suggest that crude devices such as peg legs/pylon, wooden props/splints and crutches were used, see Figure 3.2(a).

Ancient history recorded the earliest example of prosthesis being used at the beginning of the fifth century B.C.; the Greek historian Herodotus (484 B.C.) reported the escape of Hegesistratus, a native seer of Ellis sentenced to death. He escaped by cutting off his foot from its chain, and later replacing it with a wooden one. The oldest known artificial limb in existence was constructed of wood and reinforced with bronze and iron. It was unearthed in Capua, Italy in 1858 and dated back to the Samnite Wars of 300 B.C. Unfortunately, it was destroyed during the bombing of London in World War II.

From the pre-Christian era to the fifteenth century, there are few records concerning artificial limbs or prostheses. This corresponds to the dark period of the development of amputation surgery. Most lower-extremity prostheses of the Middle Ages were simple peg legs, with little consideration given to function or cosmesis. It was not until the 16th century that armourers and metal craftsman, skilled in fashioning body armour began to use sections of armour modified for weight-bearing, leading to some improvement in cosmesis.

Ambroise Paré (1510 - 1590) produced the first known jointed leg prosthesis, see Figure 3.2(b). The leg

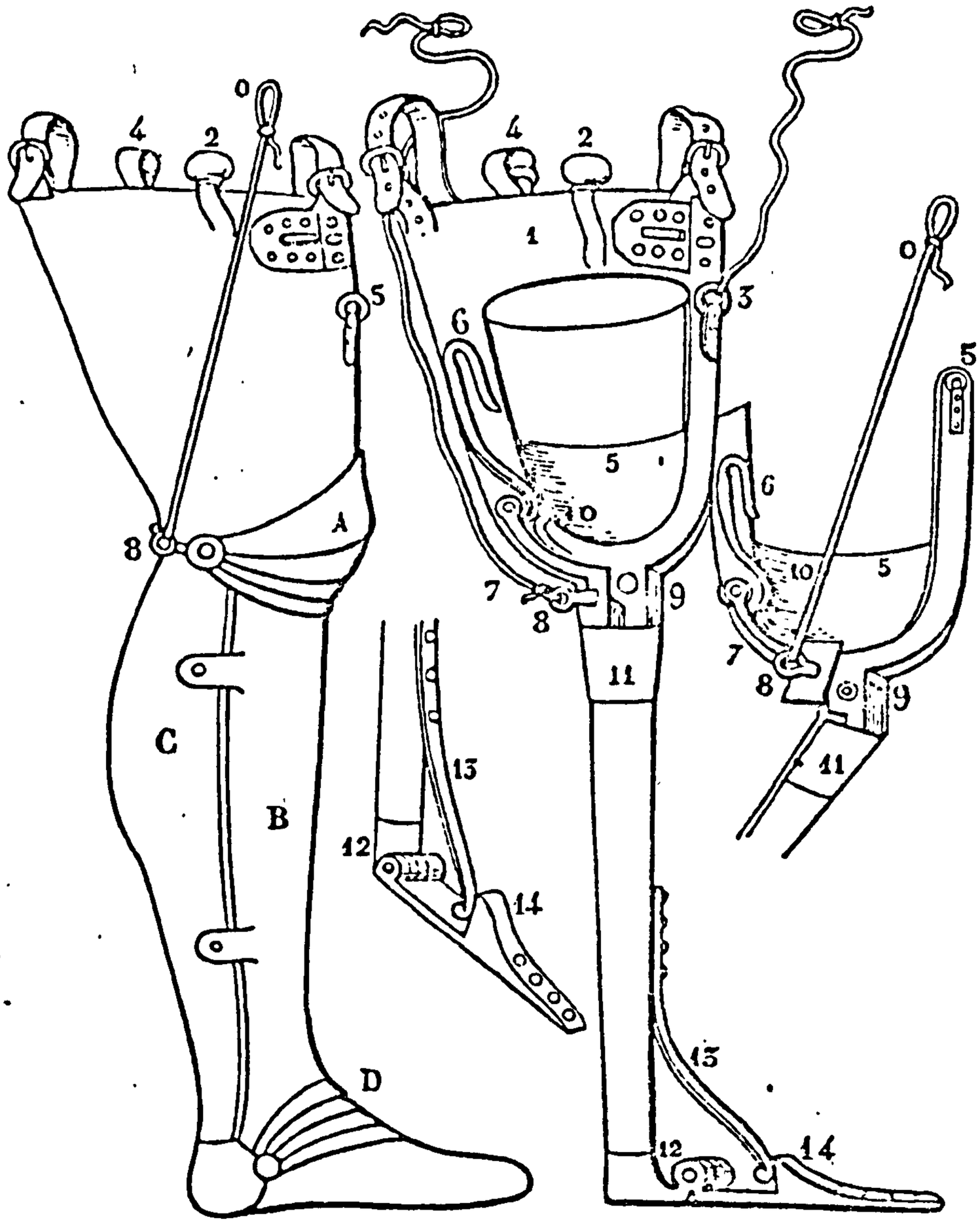

FIGURE -This is the first known jointed leg prosthesis from the 16th century. (From Paré, A., Oeuvres Completes, Edition Malgaigne, Paris, 1840, from the copy in the Armed Forces Medical Library.)

Figure 3.2(b)

incorporates a semi-automatic knee lock and an articulated foot, however, it appears that the prosthesis was far too heavy to be of any practical use. Towards the end of the Seventh Century, attempts were begun to improve prostheses. This period corresponds with the dawning of modern surgical procedures, which led to a higher rate of survival. The increasing number of amputee survivors prompted the search for a better functionally designed prosthesis that was aesthetically acceptable. The historical developments of artificial limbs are well documented in "Orthopaedic Appliance Atlas, Volume 2 - Artificial limbs", (1960) and Lowe (1969). A brief discussion of the important development is presented in the following.

In 1696, the Dutch surgeon Verduin devised a below-knee prosthesis, which was composed of a wooden foot joined to a stump socket of copper lined with leather. A thigh cuff was used to suspend the device and also assist in weight-bearing, and was connected to the leg-piece with external hinges, see Figure 3.2(c). This was the fore-runner of the thigh corset type "conventional" below-knee prosthesis. Yet, for reasons unknown, the Verduin prosthesis attracted very little interest, it was not until the Nineteenth Century that its principles were recognised and applied in prosthetic practice.

James Pott of London in 1800 introduced an above-knee prosthesis, which consisted of a wooden socket, a steel knee joint and an articulated foot. Cord from the knee joint controlled the ankle/foot motion, for example toe lift was coordinated with knee flexion. Because the Marquis of Anglesea wore it after losing his leg at the battle of Waterlóo, this leg became known as the "Anglesea leg", Figure 3.2.(d) shows the above-knee, as well as the below-knee version of the Anglesea leg. With few modifications, this prosthesis was introduced into

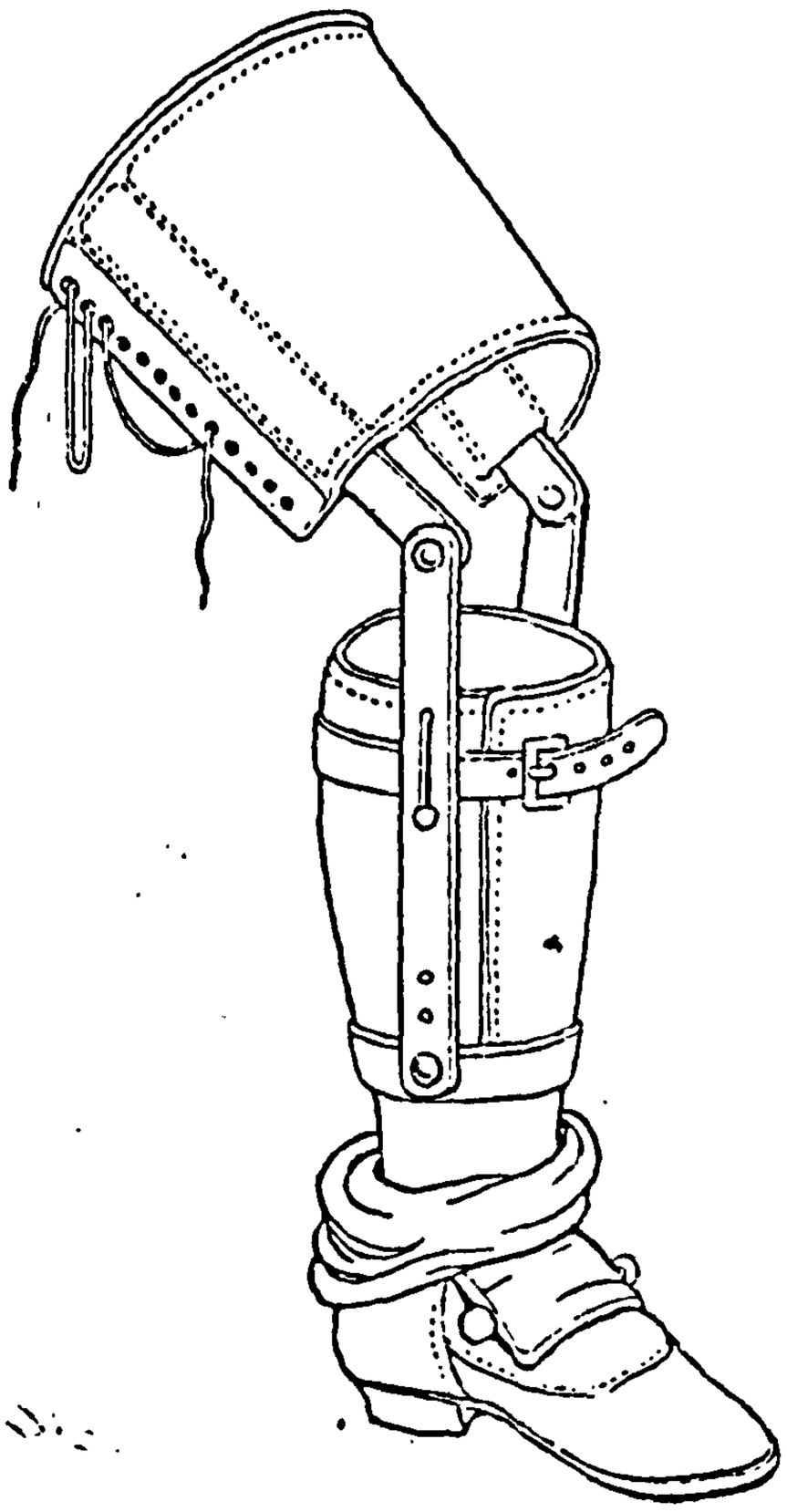

Fig. Verduin Leg (1696). From MacDonald, J., *Amer. J. Surg.*, 1905.

Figure 3.2(c)

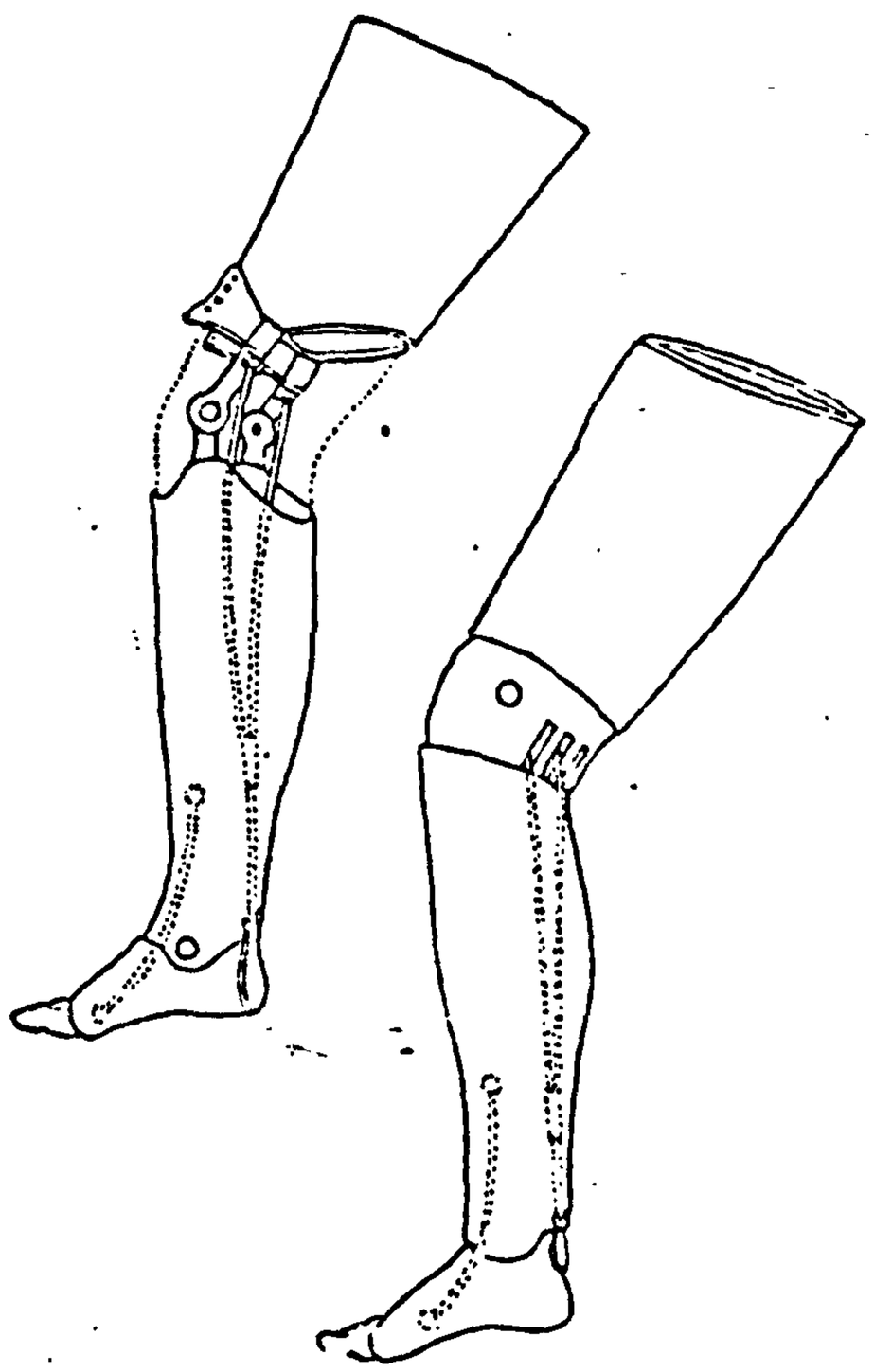

Fig. Anglesea Leg (1800). Below knee at left, above knee at right. Knee, ankle, and foot are articulated. From Bigg, H., *Orthopraxy*, 1877.

Figure 3.2(d)

the United States in 1839. Many refinements were made since then, and eventually Benjamin F. Palmer patented the leg in 1846 and it became known as the American leg.

Other major contributions to the principle of modern day prosthetics were also made in the Nineteenth Century, Goyrand in 1831, developed the ischial weight-bearing concept in above-knee prostheses. In 1842, Martin and Charriere introduced automatic passive control of knee extension by placing the knee centre posterior to the centre axis of the prosthesis.

A.A. Marks in 1860 modified the American leg by replacing the wooden foot with a hard rubber type. This rubber foot had a wooden keel which was fastened directly to the prosthetic leg. The whole prosthesis was covered with a sheath of leather to increase its durability and appearance, and decrease noise. In 1861, J.E. Hanger replaced the cords in the American leg with rubber bumpers about the ankle joint. This design is still widely used in the present day. He also introduced the wooden socket and popularised the technique.

The next major invention was that of the suction socket by Durbois D. Parmelee in 1863. However, it was not accepted until after the second World War, when the Germans introduced its concept. The socket had a long and variable development before it reached its present form. The original design of Parmelee is illustrated in Figure 3.2. (e).

Each major war seems to have been the stimulus not only for improvement of amputation surgical techniques but also for the development of improved prostheses. World War II was no exception, - with great numbers of veteran amputees returning, an organised attempt was undertaken to produce functional, inexpensive prostheses.

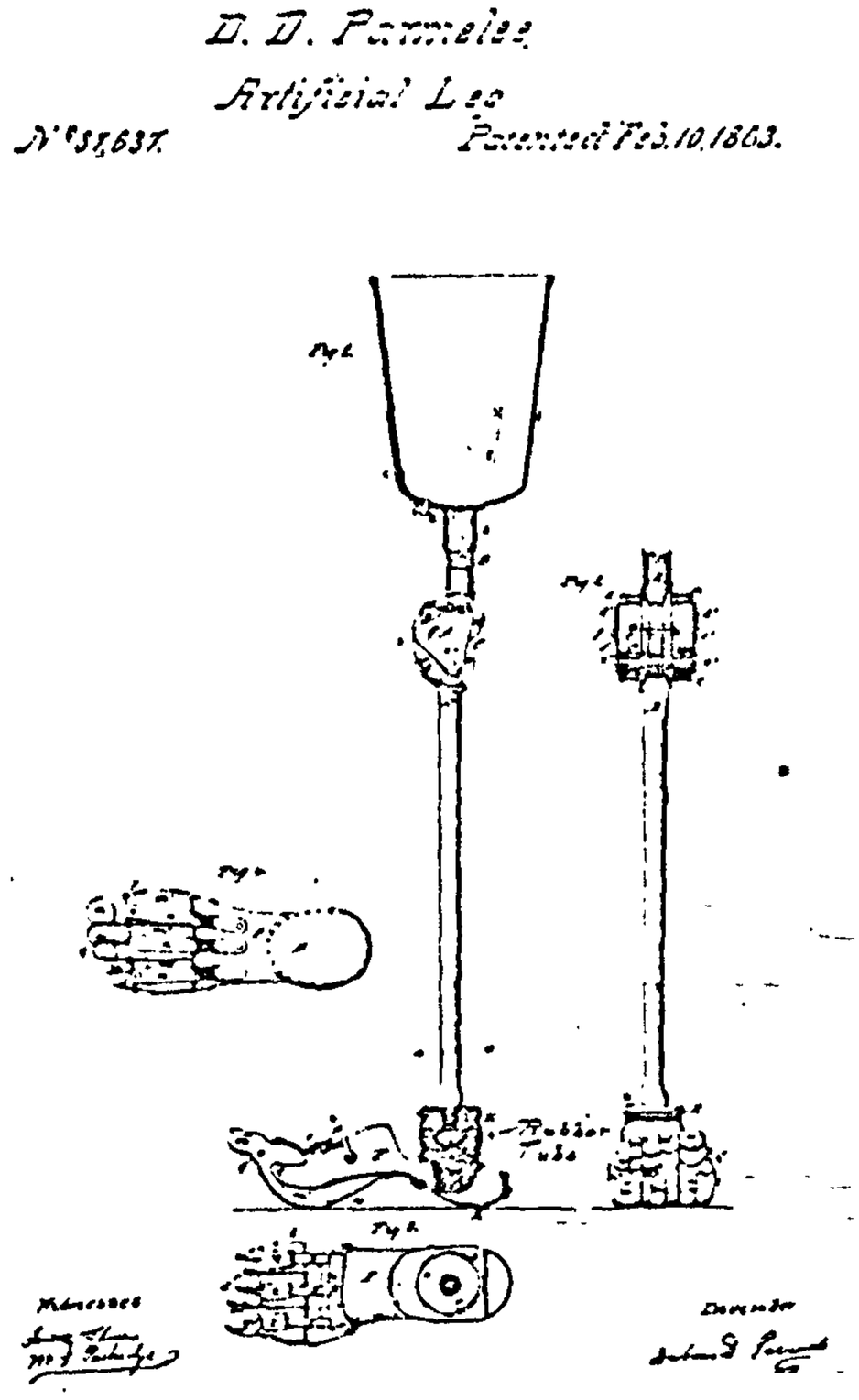

Figure 3.2(e) Parmelee's Suction Socket above-knee prosthesis (from Murphy, 1960)

Both in North America and Northern Europe, amputee research programmes were started to accomplish these goals. Most of the modern, scientifically designed prostheses available nowadays are the direct result of these research programmes. Among these developments, those that are of prime interest in this project are : (i) the total-contact, quadilateral, suction socket for the above-knee amputation, (ii) the patellar-tendon-bearing prosthesis for the below-knee amputation and (iii) the solid-ankle cushion-heel (SACH) foot. These devices will be considered in detail in the subsequent sections.

The modern trend in prosthesis is towards a "Modular" approach. That entails having a prosthesis made up of easily assembled and dismantled components, sometimes interchangeable with other components providing slightly different function. The aims are to reduce time in supplying a functional prosthesis to the patient and also to cut the cost required in producing the prosthesis. This topic will be taken up in detail in Section 3.2.6.

3.2.1. Materials used in Prosthetics

There is a wide variety of natural as well as artificial materials being used in prosthetics today. These materials have to be biocompatible, durable, strong, lightweight and easy for fabrication. The most common materials used are wood, plastic, leather, metal and cloth.

Wood is often used to provide shape and structural strength. Basswood, willow, poplar and linden wood are most commonly used for prosthetic knees and shins. These woods are comparatively lightweight, strong and free from

defects like knotholes and warping. These woods can be shaped easily using standard wood working tools. When finishing a prosthesis, the thigh and/or shin is hollowed out until the wood is approximately 0.8 cm thick. This is to reduce unnecessary weight but still provide adequate structural strength. Traditionally, above-knee prosthetic sockets were carved out from wood in such a fashion that a "plug fit" results, where the stump itself takes a large portion of the load and the ischial seat is of secondary importance. Radcliffe (1955) described a 3-stage technique in constructing a wooden quadrilateral socket. Murphy (1954) in describing the construction of wooden below-knee prosthetic sockets, commented that the fitting and construction of a wooden socket is purely a trial and error process, thus, rendering it unsatisfactory. Hardwoods such as maple and hickory are used for keels in SACH feet and also to reinforce high stress areas of prosthetic knee units.

Aluminium alloys are generally used in the manufacture of metal limbs. They have the properties of being strong and yet light in weight. To form a lower limb prosthetic segment, a cylinder of sheet aluminium alloy (either a drawn-tube or a sheet formed into a cylinder and welded or riveted) is cold-worked into the desired final shape. A cast aluminium knee-strengthening bracket and ankle block are then welded or riveted to the structure at the appropriate end to maintain the shape of the leg. This method of construction is still widely practised in the United Kingdom. Fitting and construction of a metal socket is also a process that is one of purely trial and error, thus it is not satisfactory. Most prosthetic knee and ankle joint units (or components of them) are made from cast aluminium. Pylons used in the modular system are drawn metal tubes.

Leather is a commonly used material in prosthetics.

It is used for making suspension belts, waist belts, soft inserts on PTB prosthesis sockets, socket linings and as fairings to provide cosmesis over knee and hip joints. It is easy to work with, has a soft natural feel, is able to stretch in one direction and is biocompatible. Cloth is primarily used for making prosthetic socks. They are commonly made of wool or cotton, or more recently a blend of these natural fibres with nylon, orlon, acrylics or other synthetic materials.

There is a wide range of plastics being used in prosthetics today. Most of them have now replaced the traditional materials in their application. Nylon is now used for prosthetic sheaths, bushings, suction valves, stockinette and stockings to cover prostheses. The advantages of this material are its strength, elasticity and low coefficient of friction. Acrylic fibres are frequently used in prosthetic socks, since they are soft, durable and machine washable. They provide an alternative to wool and cotton. Liquid polyester or acrylic resin is used in the lamination of prosthetic sockets. Acrylic resins are finding increased use because of their high strength which allows a thinner, lighter weight lamination and the thermoplastic properties allow easier adjustments of the prosthesis by reheating the plastic and remoulding it. Acrylic resins tend to have a softer feel than polyester resins. However, they are much more difficult to use during fabrication. Polypropylene is currently being used in the production of a lightweight prosthesis, (Wilson and Stills, 1976). Polypropylene sheets are heated and vacuum formed over the mould of a socket or complete limb. The material is relatively inexpensive, strong, durable and easy to mould. It can be welded using hot air or nitrogen welding guns to bond seams or add reinforcement. High-density polyethylene is used to make bushings in joints. Polyurethane foams are available in three broad groups : flexible foam,

rigid foam and elastomers. Flexible polyurethane foams are generally used as cosmetic covers for endoskeletal-type prostheses and also for making SACH feet. Rigid polyurethane foams are used as an alternative to wood in providing structural stability to knee units and ankle blocks. This foam is also used to provide strength and shape to exoskeletal-type prostheses.

Fibre-glass is commonly used to reinforce polyester resin laminations where mechanical attachments such as bolts and screws are required. It is also used to stiffen areas of prostheses and to prevent breakage in vulnerable areas. However, it causes skin irritation when in contact with the skin and it is difficult to finish smoothly. One very promising material that can be used in prosthetics is carbon fibre set in epoxy. It has a stiffness twice that of steel at one-fifth the weight. In addition, it also has a fatigue resistance twice that of steel, aluminium and fibre-glass. Therefore, the use of pre-fabricated carbon fibre prosthetic components, such as pylon tubes, knee joints and connectors could drastically reduce the weight of prostheses while increasing the strength.

3.2.2. Prosthetic Socket Design Considerations

There are four major interrelated prosthetic socket design considerations : support, control, suspension and alignment.

Support in a socket is provided through the distribution of pressures on stump tissues in relation to those tissues which are pressure sensitive or pressure tolerant. Pressure distribution for sensitive areas must be based on socket contouring that distributes limb contact pressures evenly and as far as possible putting the maximum loads in areas which can tolerate them.

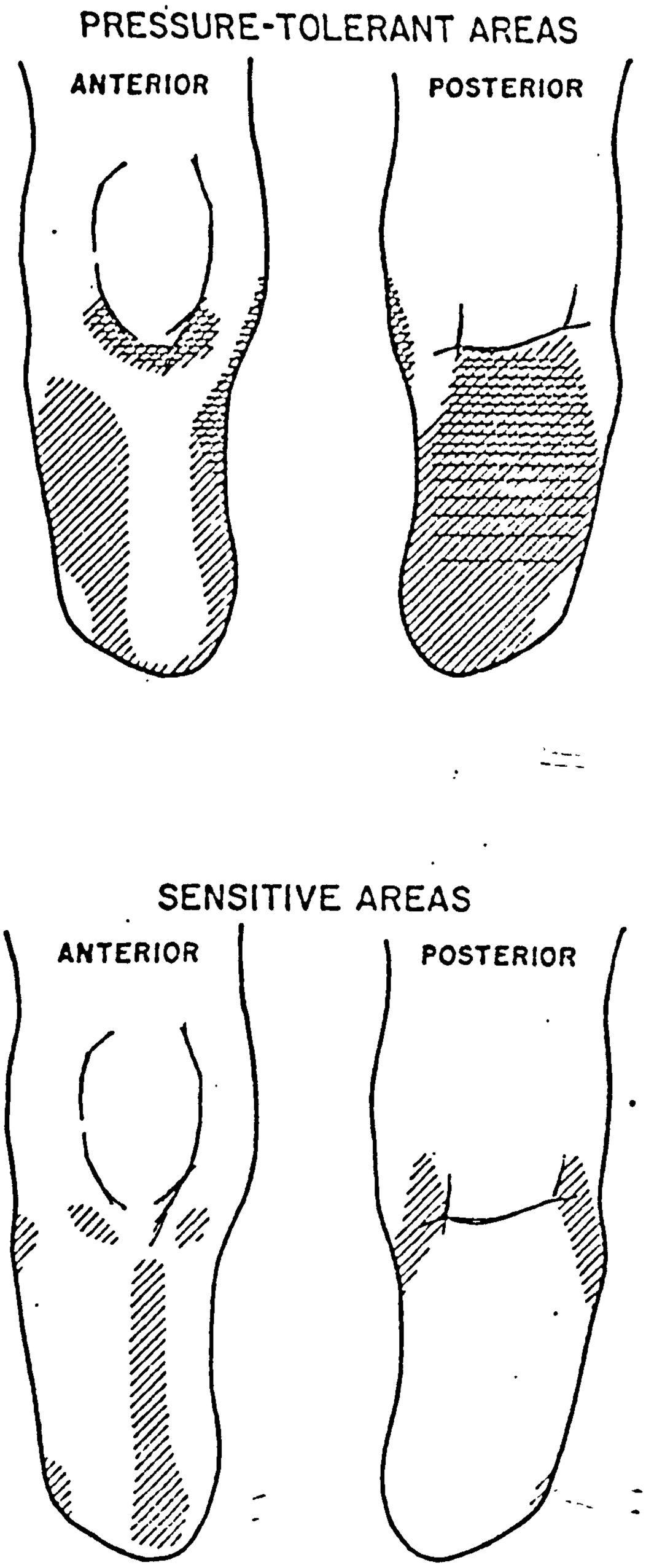

Figure 3.2.2(a) Below-knee Stump (from Radcliffe & Foort, 1960)

Pressure sensitive areas can also be accommodated by the use of soft materials.

Control depends on the pressures generated between the stump and the socket interface. During the stance phase the body must be stabilised over the prosthesis by forces applied by the stump to the socket. Therefore, the socket must be designed to accommodate these forces comfortably and provide stability with a minimum of lateral motion. During the swing phase, full stump to socket contact is required to provide control over the prosthesis, when it is elevated off the ground. The total-contact socket is most suited for these situations.

Suspension can be provided in anyone, (or in combination), of these basic types : (a) mechanical joints with corset, (b) suspension belt, (c) suction socket and (d) socket contouring. These suspension systems will be discussed in the subsequent sections.

Alignment refers to the angular and linear position of the socket relative to the knee and foot. Particularly important in angular alignment is that the socket is in a position where the amputee can gain the best control with the remaining musculature. The socket must be positioned over the prosthetic knee in such a way as to achieve proper balance and/or to obtain the maximum function from the prosthetic components. This is achieved by linear alignment.

The following is a brief description of the below- and above-knee sockets used in the project :

Below-knee Amputation. Currently, the patellar-tendon-bearing (PTB) socket is a widely accepted routine fitting for below-knee amputation. The socket is designed such that the force action is transmitted comfortably and

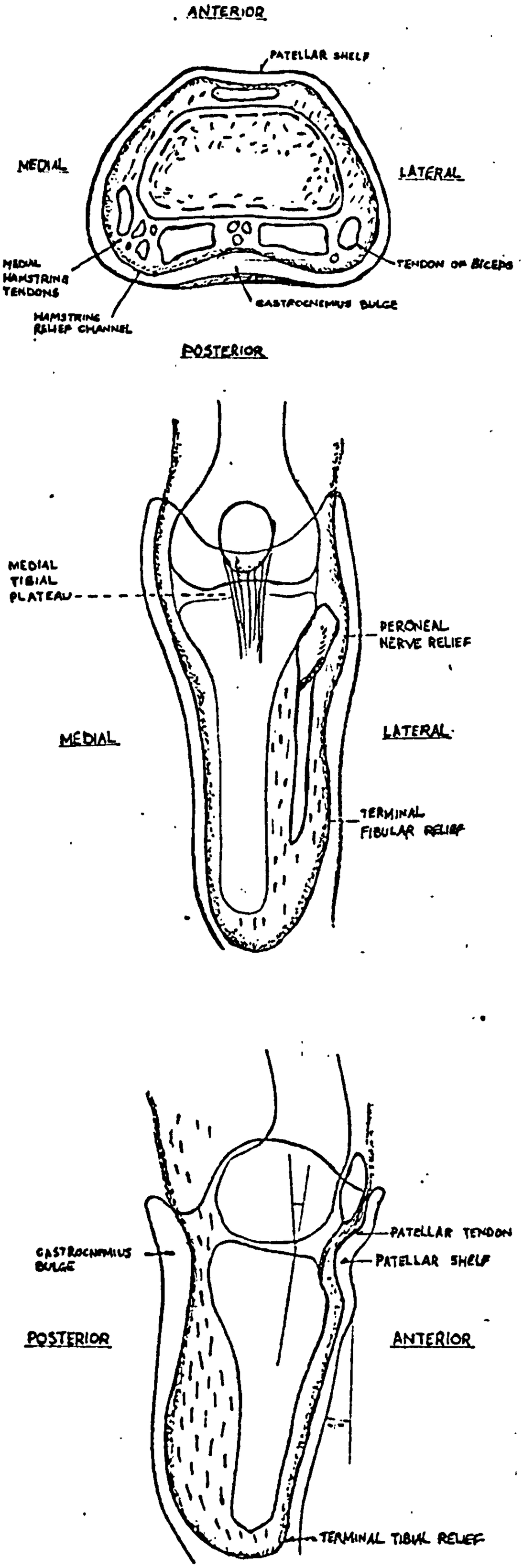

Figure 3.2.2. (b): BK Stump in PTB Socket
(redrawn from Mital & Pierce, 1971)

without excessive movement of the prosthesis relative to the skeletal structures. The detailed biomechanical analysis of force actions on below-knee prostheses in normal, level bipedal walking was very well presented by Radcliffe (1962). The basic concepts in the design of the socket are : The compression of soft tissues to obtain good socket fit which is essential to provide a degree of feedback of the foot position in the absence of tolerant areas and to protect sensitive areas. Figure 3.2.2(a) shows the pressure tolerant and sensitive areas of a below-knee stump.

The socket is shaped so that a substantial amount of weight is borne on the patellar tendon and the medial flare of the tibial condyles. The crest of the tibia, the head of the fibula, the distal cut end of the tibia and fibula and sometimes a prominent lateral condyle are pressure sensitive areas and are thus relieved, see Figure 3.2.2(b). Most of the sockets are used with a soft insert which is contoured exactly to the shape of the socket and is made of a soft synthetic material.

Above-knee Amputation. A number of socket designs are available for the above-knee amputee, but one that has proved to provide the most support and stability is the quadrilateral design. Hall(1964) described five basic principles of this design : (i) The socket must be properly contoured and relieved for functioning muscles, (ii) stabilizing pressure should be applied on the skeletal structures as much as possible, avoiding areas where functioning muscles exist, (iii) functioning muscles, where possible should be stretched to slightly greater than rest length for maximum power, (iv) properly applied pressure is well tolerated by neurovascular structures and (v) force is tolerated best if it is distributed over the largest available area.

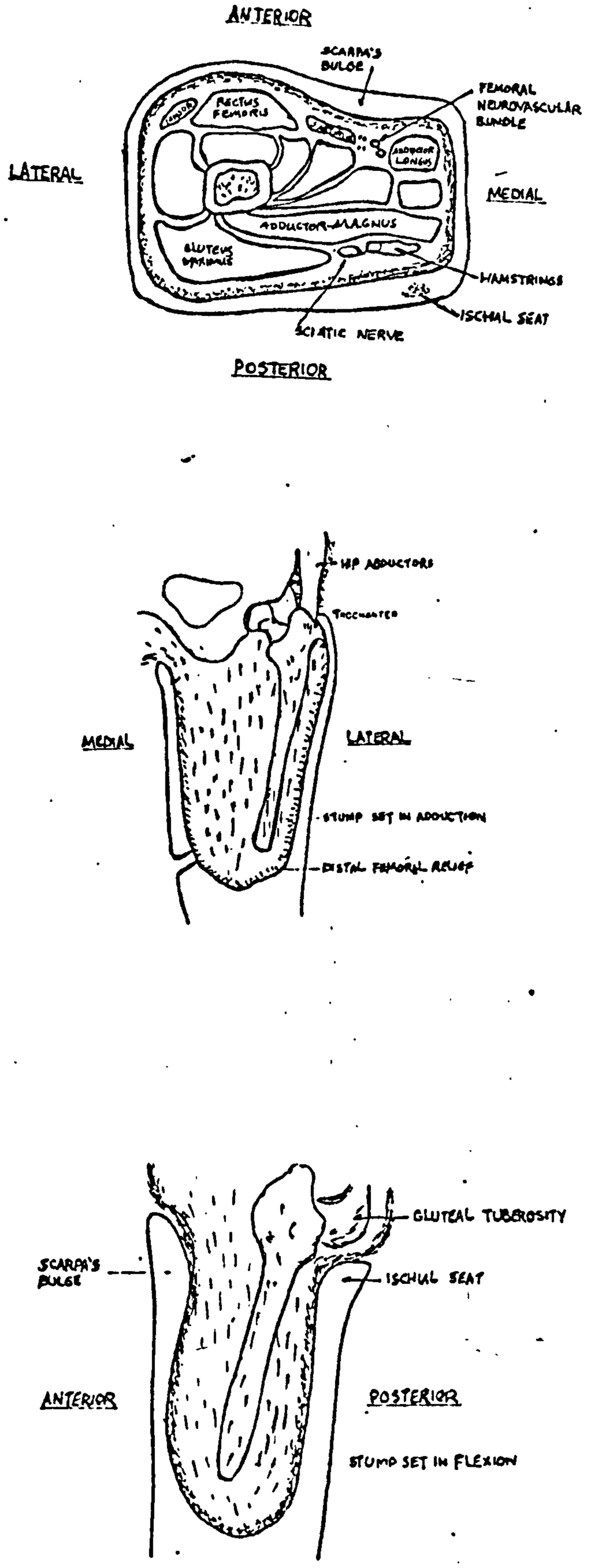

Figure 3.2.2. (c). AK Stump in Quadrilateral Socket
(redrawn from Mital & Pierce, 1971)

The quadrilateral socket is as shown in Figure 3.2.2(c). The inner contour of the socket has reliefs and bulges. Reliefs are hollowed-out areas to reduce pressure on relatively firm tissues, such as tendons, contracting muscles and bony prominences. Bulges are inward directed contours of the socket wall to press soft, pressure-tolerant areas of the stump so that these areas will take higher pressure and thereby their appropriate share of the load. Extending from the posterior wall of the socket is a widely flared area to provide support through the ischial tuberosity and gluteal muscles. The anterior wall is concavely contoured and is higher than the posterior wall in order to provide a counterforce that will hold the ischium back onto the ischial seat. The lateral wall is adducted and relatively flat to evenly distribte the high forces resulting from hip abduction during mid-stance to provide support, see Figure 3.2.2(d). The lateral wall is also high and curved in over the greater trochanter to provide increased lateral stability. The detailed biomechanics of above-knee prostheses were presented by Radcliffe (1969).

The entire socket is statically aligned to give an initial flexion with respect to the hip-ankle line. This will provide a greater range of hip extension and thus allow the patient to take a normal stride length on the sound side. One advantage of the quadrilateral shaped socket is that it provides good rotation stability without restricting muscle function.

3.2.3. Prosthetic Methods

The team approach is a much favoured concept in the field of prosthetics. The aim of rehabilitation of an amputee is not to merely fit him with an artificial limb but to ensure that he is reinstated in society and can take his rightful place within the limits of his own

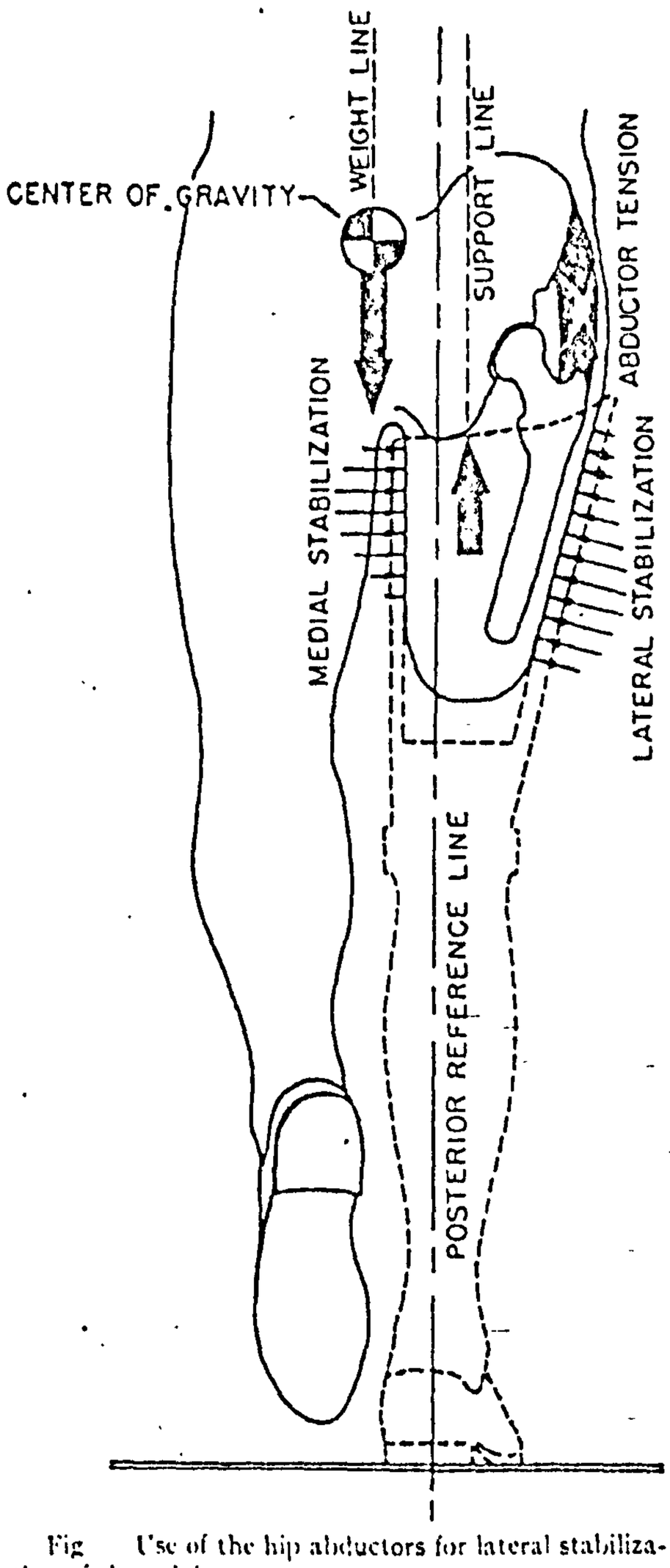

Fig Use of the hip abductors for lateral stabilization of the pelvis.

Figure 3.2.2(d) (from Radcliffe, 1954)

disability and state of health. The clinic team should therefore consist of a physician, prosthetist, therapist, nurse, social worker and possibly a clinic coordinator to achieve this aim. Vitali (1969) advocated that an integrated rehabilitation programme is possible with co-operation, understanding, communication and the goodwill of all concerned. He proposed that each team member should acquire an understanding of biomechanics and the elements of prosthetics in his education.

The patient is the most important member in the clinic team, for it is the patient who is directly affected by all the decisions made. Therefore, it is essential to instill confidence in the patient and encouragement to participate as an active member of the team. Hopefully, in this way, a thorough examination and evaluation of the patient can be achieved. Ultimately, a prescription for the prosthesis will be formulated based on the input of information from all members of the team.

After the initial orientation, the prosthetist's task is to make a detailed evaluation, measurement and casting of the stump. Special forms are used by the prosthetist in his evaluation and measurement, see Figure 3.2.3(a & b).

The socket is made over a modified positive mould of the stump from a lamination process. The most common commonly used material is polyester resins in its liquid form. It can be pigmented to match the patient's natural skin tone. The completed socket is test-fitted to make sure that it fits the stump properly. Then, the rest of the prosthetic components plus the socket are assembled together. Included in the assembly is an alignment device such as the Staros-Gardner coupling or the University of California, Berkeley alignment unit etc. This firstly, allows the whole artificial limb to

PROSTHETIC INFORMATION – BELOW-KNEE PROSTHESIS

Name _____ Date _____

Weight _____ Weight _____ Age _____ Sex _____ Prosthetist _____

Date of Amputation _____ Cause _____ Right or Left _____

Present Type of Prosthesis _____ Date Fitted _____

STUMP DESCRIPTION

Draw stump, indicating levels of tibia and fibula. Show location of stump details. Identify with letter code.

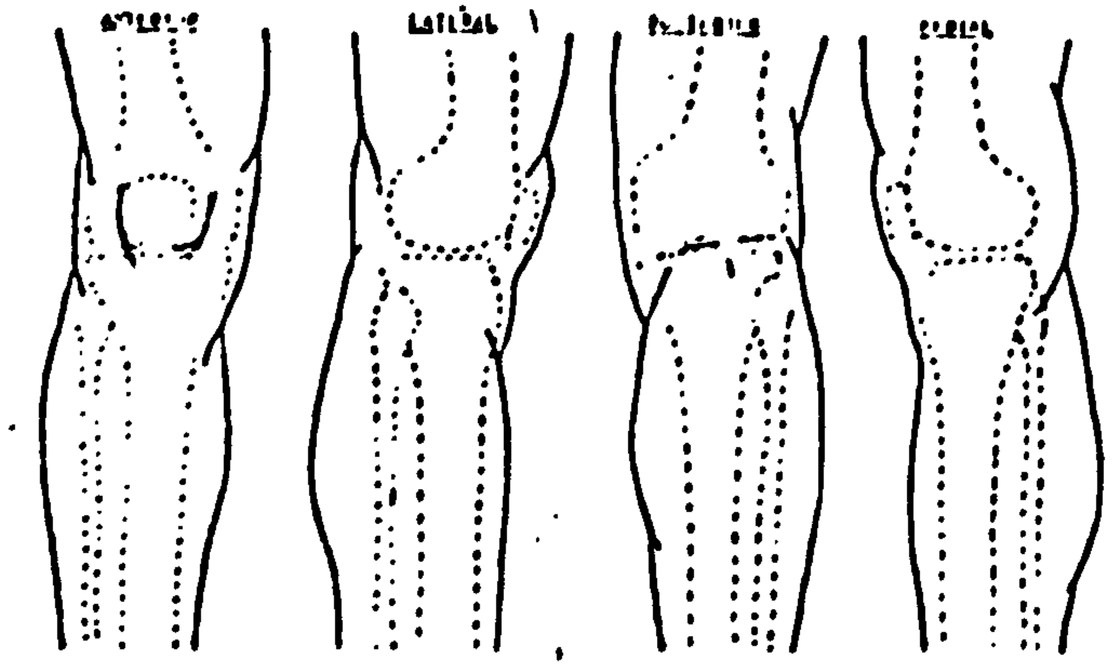

A abrasion
B boil or other skin infection
BS bone spur
Bu bursa
D discoloration
E eczema
P pressure point
S scar
T trigger point

Stump shape _____ Distal padding _____

Condition of subcutaneous tissue _____

Type of skin _____

Condition of thigh musculature _____

Condition of stump musculature _____

Condition of knee joint (a) stability _____ (b) range _____

(c) patella _____ (d) contracture _____

Condition of the cut bones (a) tibia _____

(b) fibula _____

Condition of the femur _____

Pain _____

Type of prosthesis recommended _____

_____

PROSTHETIC MEASUREMENTS

Fitting Aids: Plaster cast of stump ☐

Tracings of normal shank ☐ anterior and lateral views with circumferences at 2" intervals

Stump Measurements: Circumference ☐ Distance above tibial plateau ☐

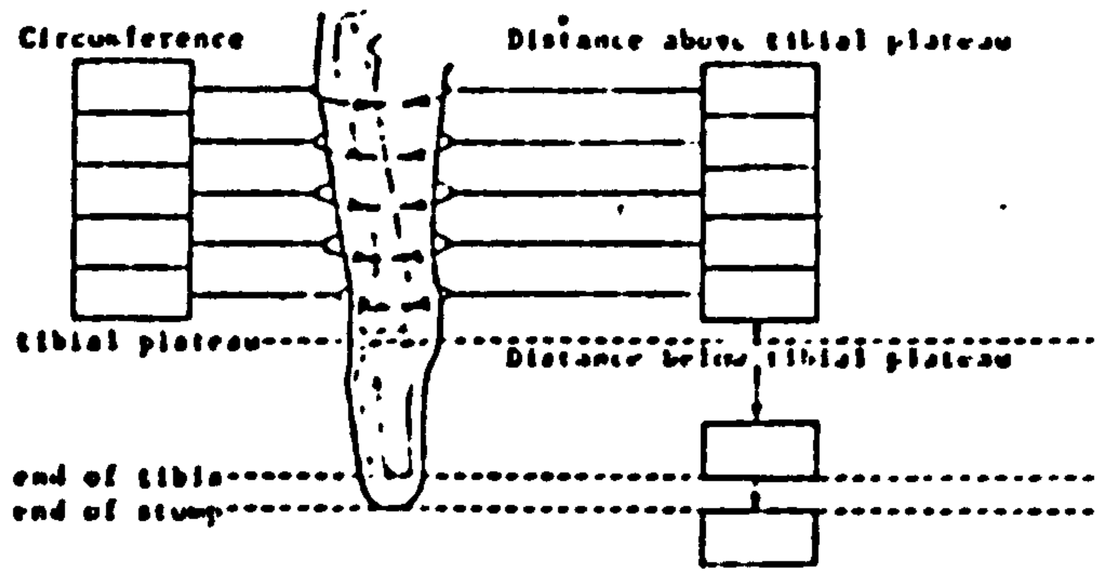

Stump diameters at level of patellar tendon { mediolateral ☐ anteroposterior ☐

Stump sock size ☐

Normal leg Measurements: Height above floor ☐

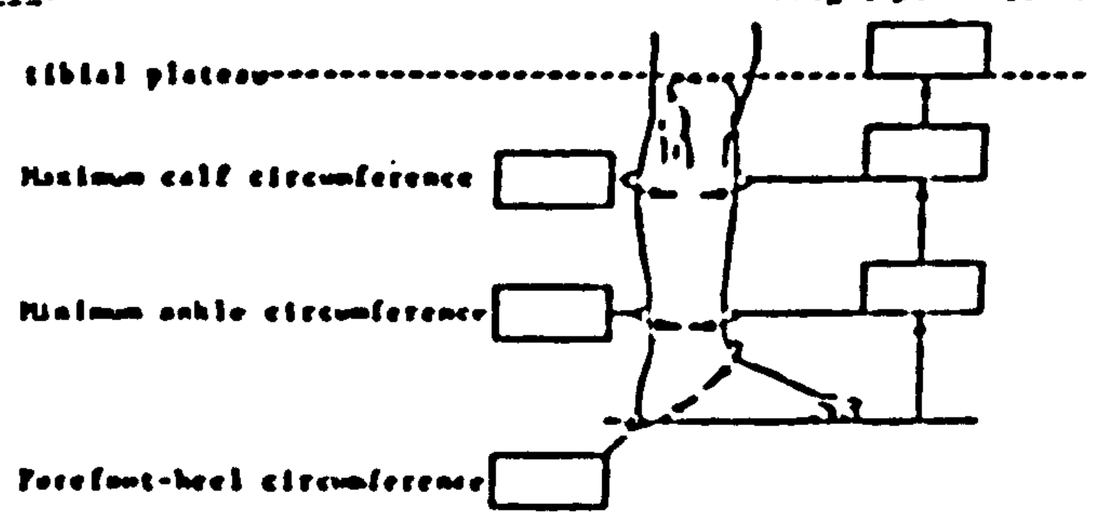

Shoe size ☐ Heel height ☐

Figure 3.2.3. (a). BK evaluation form (from Radcliffe & Foort, 1960)

PROSTHETIC INFORMATION — ABOVE-KNEE PROSTHESIS
A. STUMP DESCRIPTION

Amputee_____ Date_____
Height_____ Prosthetist_____
Weight_____
Age_____
Sex_____

Show location of stump details, identifying with letter code:

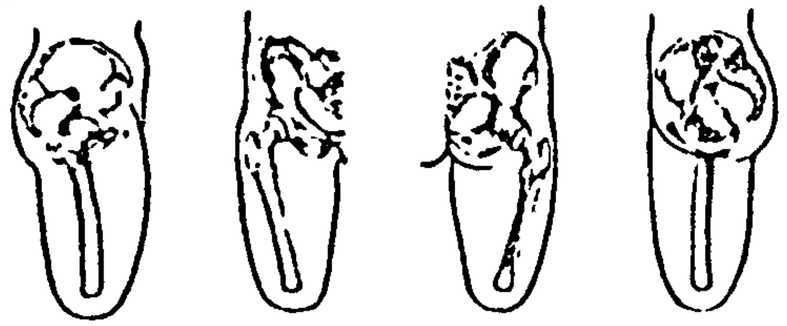

A. Abrasion
B. Boil
BS. Bone Spur
D. Discoloration
E. Edema
I. Irritation
M. Muscle Bunching
P. Pressure Point
R Redundant Tissue
S. Scar
T. Trigger Point

Ischium. Toughened ( ) Pressure sensitive ( )
Muscle padding ( ) Prominent ( )
Previous ischial bearing? yes( ) no( )

Subcutaneous tissue: Heavy ( ) Light ( ) Skin condition: Tough ( ) Thin ( )

Stump lateral contour: Convex outward ( ) Flat ( ) Concave inward ( )

Stump Musculature	Soft	Average	Hard	
General				
Hamstring Group				Prominent with stump extension?
Gluteal Group				Prominent with stump extension?
Rectus Femoris				Prominent with stump flexion?
Adductor Longus				

Stump flexion contracture: _____degrees; abduction contracture:_____degrees

Show modification of basic socket shape, if required:

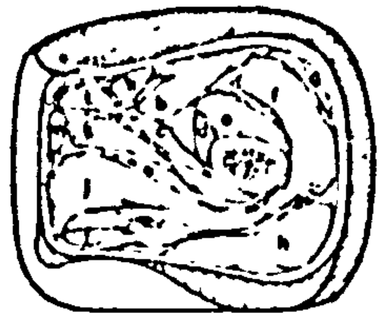

Muscle code
a Sartorius
b Rectus femoris
c Pectineus
d Vastus medialis
e Vastus intermedius
f Vastus lateralis
g Tensor fasciae latae
h Gluteus maximus
i Hamstrings
j Adductor magnus
k Adductor brevis
l Adductor longus
m Gracilis

UNIVERSITY OF CALIFORNIA
PROSTHETIC DEVICES RESEARCH

FORM 7A

PROSTHETIC INFORMATION — ABOVE-KNEE PROSTHESIS
B. PROSTHETIC MEASUREMENTS

Amputee_____ Date_____
Right or Left Amputation_____ Prosthetist_____

☐ Distance from Ischial Tuberosity to Tendon of Adductor Longus

Distance below Perineum	Stump Circumference
0	
	0

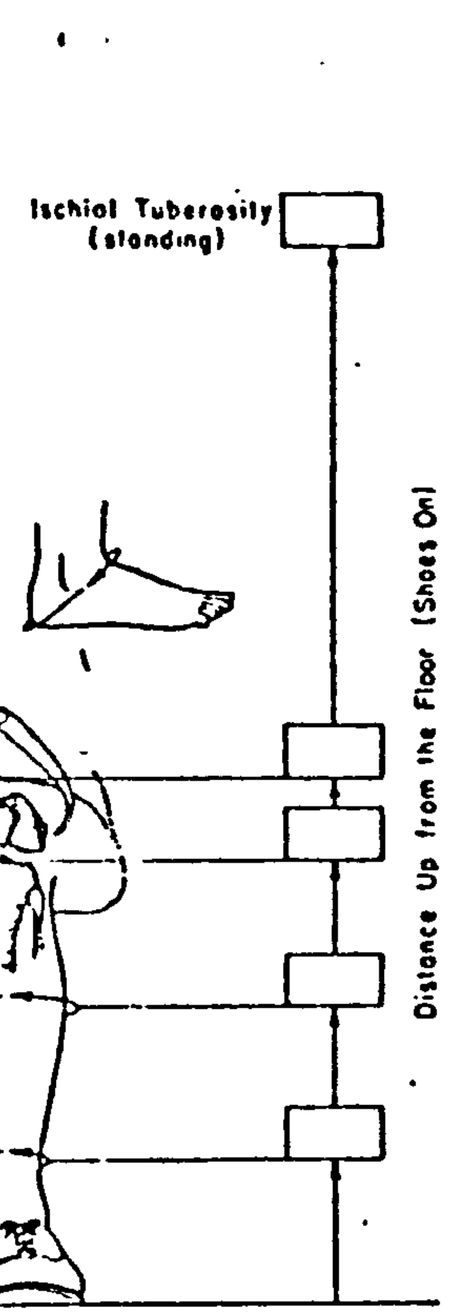

☐ Forefoot-Heel Circumference

☐ Knee Width (sitting)
☐ Top of Knee (sitting)
☐ Tibial Plateau
☐ Calf Circumference
☐ Ankle Circumference
☐ Shoe Size

UNIVERSITY OF CALIFORNIA
PROSTHETIC DEVICES RESEARCH

FORM 7B

Form used at the University of California for recording stump characteristics and measurements in above knee fitting

Figure 3.2.3(b) Above-knee evaluation form (from Radcliffe, 1954)

be statically aligned during assembly and then dynamically aligned during test walking. The purpose of aligning the prosthesis is to provide maximum comfort, efficient function and cosmesis by adjusting the relative position of the components. The different alignment adjustments that can be made are :

1) Anterior or posterior displacement of the socket with respect to the foot.
2) Medial or lateral displacement of the socket with respect to the foot.
3) Tilt of the socket in the sagittal plane: the amount of built-in flexion of the socket.
4) Tilt of the socket in the coronal plane.
5) Stability of the knee joint.
6) Rotation of the foot.

Fitting and alignment of the prosthesis are completed when the patient and prosthetist are convinced and satisfied that the prosthesis is functioning as well as possible. The alignment device is then transferred out of the assembly on to a transfer rig, while keeping the relative position of the components the same. Either rigid polyurethane foam or wood is used to fill up the spaces between the prosthetic components. They are then shaped to match the patient's other leg and it is covered with plastic lamination, providing additional cosmesis and strength.

With some modular assembled prostheses, the alignment device is usually built into the system. Therefore, no transferring is required in the process. Once the optimum alignment is reached, the adjusting screws are locked in place by a strong bonding glue. Flexible polyurethene foam covering shaped to give the desired cosmesis is then assembled onto the endoskeletal structure. A prosthetic stocking is put on to complete the construction.

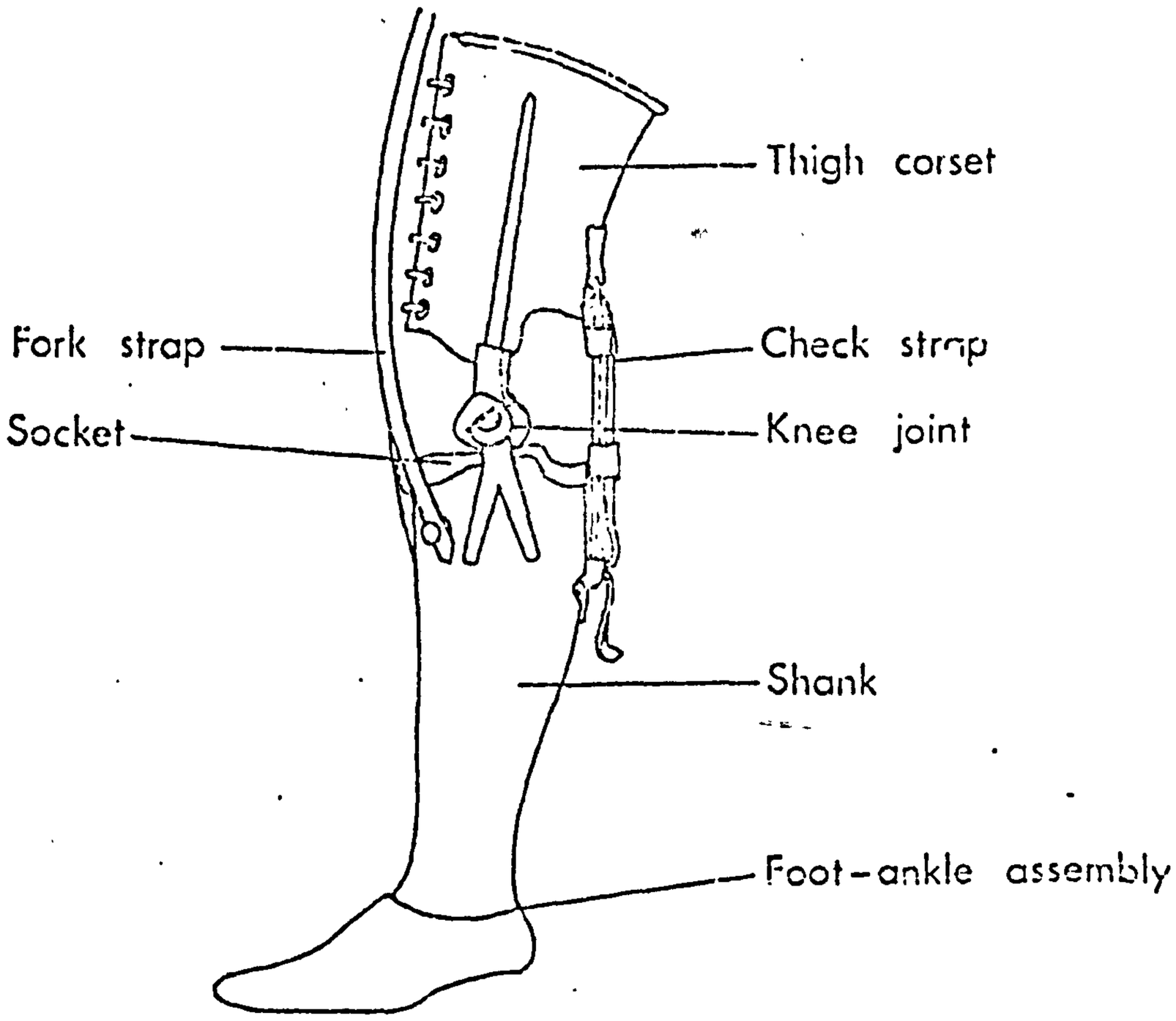

Figure 3.2.4(a) The "Conventional" below-knee prosthesis

3.2.4. Below-knee Prosthetic System

Prior to the introduction of the patellar-tendon-bearing (PTB) prostheses, the thigh-corset and knee joint type of artificial limb was the "conventional" below-knee prosthesis, see Fgiure 3.2.4(a). The thigh corset is contoured proximally to the adductor tubercle of the knee to provide suspension as well as weight bearing and stabilisation against anterior-posterior and medial-lateral forces. The socket and shank were either constructed from wood, metal, fibre or moulded leather, although the basic principle of construction was the same. The distal end of the socket was usually left open. This type of prosthesis has several disadvantages : The human knee joint is not a simple,single-axis hinge joint, therefore relative motion would occur between the prosthesis and the stump and thigh during knee motion when single-jointed side hinges are used. This would result in some chafing and irritation. Oedema was often present at the lower end of the stump, when the open-ended socket was used. This type of prosthesis also discouraged the use of thigh musculatures, therefore causing them to grow weak.

Since the introduction of the PTB below-knee prosthesis in 1959, (Radcliffe and Foort, 1961) the prosthetic field has been besieged with variations of its basic features. Figure 3.2.4(b) shows a chart of the variations.

The variants are of two kinds: (1) socket designs to improve distal pressure and weight-bearing control or to improve the environment around the residual limb and (2) mechanisms for improvement in suspension and knee stabilisation. These variants however do not affect the fundamental principles of PTB fitting, especially the provision for total-contact.

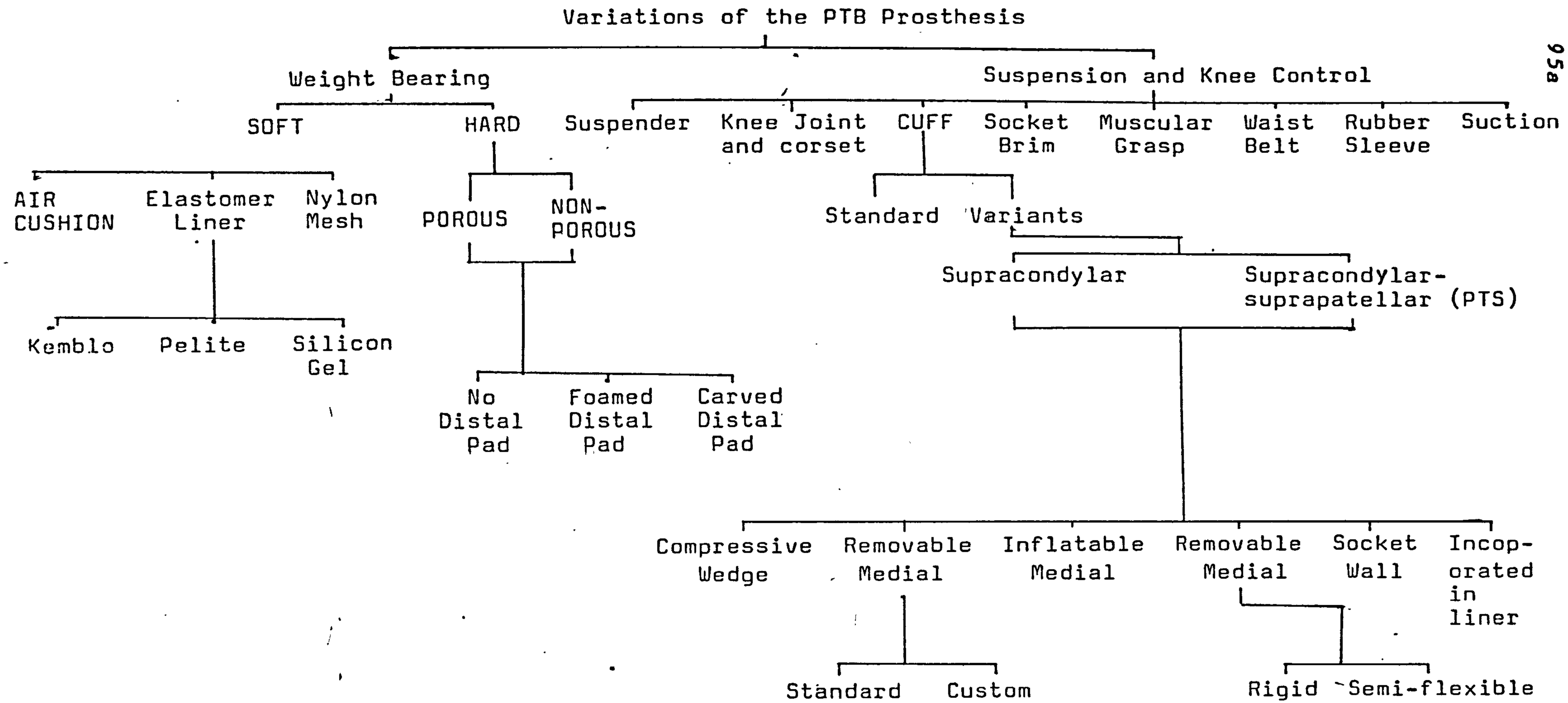

Figure 3.2.4. (b). Variations of PTB prosthesis
(from Pritham, 1979)

The original designed PTB prosthesis has a soft insert/liner and a cuff suspension, see Figure 3.2.4(c). The soft liner tends to deteriorate quite rapidly due to perspiration and will become compressed and take on a permanent set which may require constant replacement. PTB with a hard socket and soft-end will be advantageous to the patient in that retention of fit will probably be maintained much longer, although modification to the distal pad will be more difficult with a hard socket than with a liner. Soft-ends are best done by foaming them in place to assure total-contact. Carving the distal pad is usually not recommended because the technique involved is not as error-proof as the foaming-in-place process.

The PTB air cushion (AC) socket described by Wilson et al (1968), see Figure 3.2.4(d), provides increased distal stump-socket pressure while decreasing the constrictive proximal loading and thus benefits circulation. The adequate pressure distributed over the entire distal area would minimize abrasive skin damage, which might occur with the stump in contact with a rigid socket wall.

Excessive perspiration inside the socket can lead to the stump being immersed in a pool of fluid, which not only causes discomfort but also constitutes a potential cause of skin maceration and breakdown. One solution is to use a hard porous socket (Faulkner and Pritham, 1973) which requires considerable skill to construct. Alternatively, a porous, flexible insert (Rubin and Byer, 1973) can be used instead and some form of drainage is designed into the socket to allow the fluid to escape but still maintain total contact.

From Figure 3.2.4(b) one can realise the enormous range of suspension and knee control methods available. Pritham (1979) presented an overview of all the

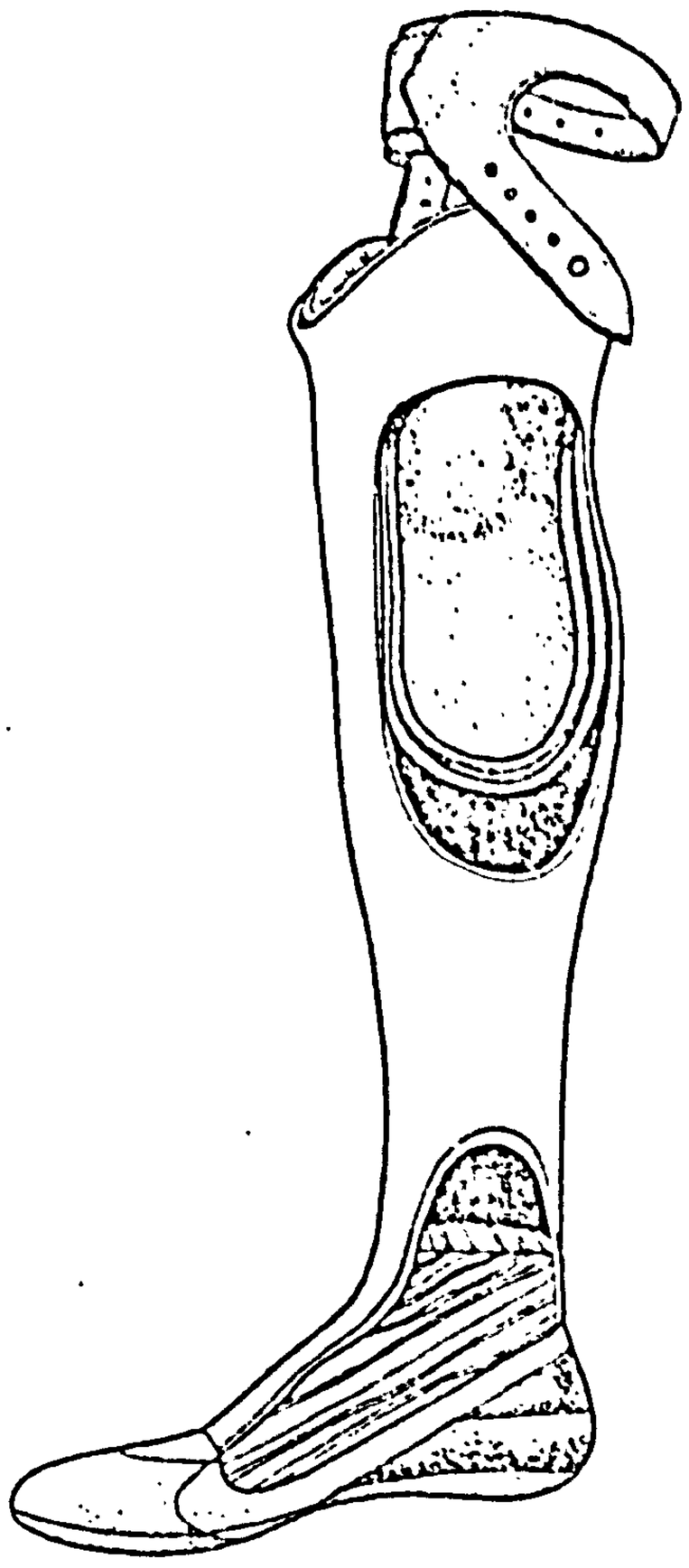

Fig. Cutaway view of the patellar-tendon-bearing leg for below-knee amputees.

Figure 3.2.4(c) Standard PTB prosthesis
(from Wilson, 1970)

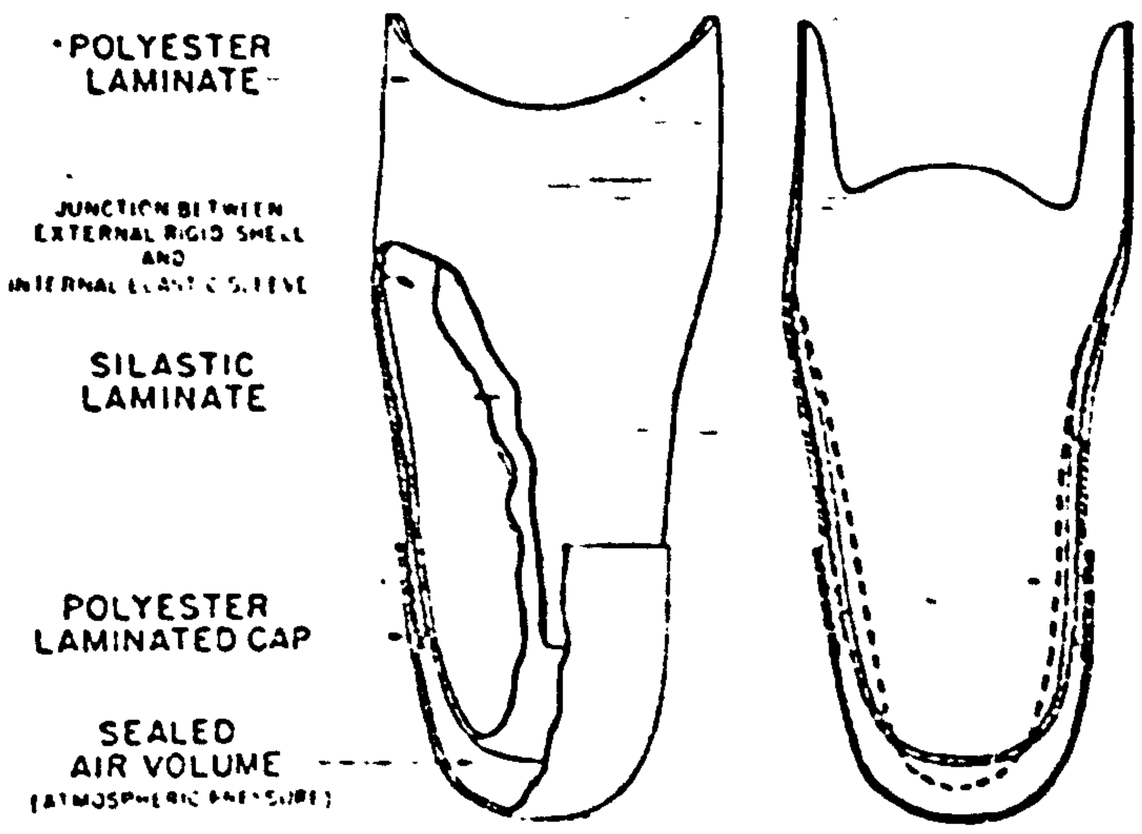

Fig. The basic structure of the PTB air-cushion socket is shown to the left. The function of the silicone laminated sleever is indicated (exaggerated) to the right.

Figure 3.2.4(d) PTB air-cushion Socket
(from Wilson et al, 1968)

suspension systems ever used for the below-knee prosthesis. The following is a brief discussion on the two major suspension systems : the cuff suspension and the socket brim suspension techniques.

The cuff suspension is an integral part of the original PTB prosthesis design, see Figure 3.2.4(c). If it is fitted properly, it would provide an adequate suspension system. However, the strap over the patella may cause difficulty either in not reducing the piston action sufficiently or in restricting circulation. It may also limit knee flexion and give a poor cosmesis around the knee, especially when sitting. This method of suspension will not be suitable for a knee with medio-lateral instability. Nevertheless, it is probably the easiest system to make and fit.

The supracondylar (SC) suspension system utilises the high medial and lateral socket walls to encompass fully the medial and lateral aspects of the femoral condyles, so as to secure a proper grip immediately proximal to the adductor tubercle. There are several designs available to fulfill this condition. One of them is to have high mediolateral socket walls flexible enough to permit the prosthesis to be donned by expanding the high socket walls and then allowing them to retract over the condyles. However, most laminated socket walls are generally not that flexible and therefore, another method would be required to prefabricate a wedge of flexible material which can be inserted between the socket and the medial condyles to obtain a locking fit over the condyle, see Figure 3.2.4(e). The supracondylar suspension system is less restrictive to knee flexion than the cuff suspension type. It also provides mediolateral stability to the knee. However, it is more difficult to fit than the cuff suspension. Fitting of this device requires careful measurement of the mediolateral dimension over the

condyles.

Another variant of the socket brim suspension technique is the supracondylar/suprapatellar (SC/SP) suspension system. It employs high mediolateral walls to encompass the condyles as well as a high anterior wall coming up and over the patella. This design was first described by Pierquin et al (1964) who referred to it as PTS (prosthe'se tibiale Supra-condylienne). The anterior fitting provides the main support function and stabilises the knee in the sagittal plane, especially at pushoff. Consequently, it will reduce any tendency of the knee to go into hyperextension. This suspension system also provides mediolateral stability of the knee. Cosmetically, the proximal brim appears somewhat bulky and in some cases may restrict the extreme flexion that would be required for example in kneeling. Fitting of this system is very difficult, extreme care must be taken with its anterior brim.

In 1977, a workshop on "Limb prosthetics and Orthotics" recommended that comprehensive evaluation on variants on PTB prosthesis should be carried out. However, no literature has been found to date that meets the recommendation, although Staros and Goralnik (1981) presented guidelines for clinical employment of PTB variants as compared to PTB conventional suspension with liner and cuff, see Table 3.2.4.

There are two method for the construction of the shin: exoskeletal and endoskeletal. The exoskeletal type was part of the original PTB design, usually being made of wood, although nowadays, rigid foam and even poly-propylene are also used. The endoskeletal type consists of a metal tube between the socket and the prosthetic foot. Flexible foam provides the cosmetic covering. The endoskeletal type construction has been adopted by most

manufacturers for their modular system.

The Solid-Ankle Cushion-Heel (SACH) foot was an integral part of the original PTB prosthesis, although, the single-axis foot and the multi-axis foot can also be used. Further discussion on prosthetic feet can be found in Chapter 4.

An important factor in the design of prostheses is that of weight. Many attempts have been made to reduce the weight of the below-knee prosthesis, especially those being prescribed to elderly patients. Recently, Wilson and Stills (1976) described the development of an ultra-light below-knee prosthesis made by vacuum forming sheet polypropylene, see Figure 3.2.4(f). It was claimed that the prosthesis weighs one-third of the conventional PTB prosthesis. Reed et al (1979) carried out an evaluation of this prosthesis on a subjective basis. Data on fourteen patients were presented and general conclusions were drawn from these data. All the patients sampled liked the lightness of the prosthesis and felt that they required less energy to walk than with their own prostheses. This, however, was not substantiated by any objective measurement of energy expenditure. Half of them complained about the function provided by the rigid foot; the investigators however felt that this might be simply a matter of "getting used to it". The most inherent problem encountered with the prosthesis, is that it is not structurally strong. It was suggested that the model evaluated is probably best suited for patients who do not subject the prosthesis to extreme stress.

3.2.5. Above-knee Prosthetic System

There have been many different shapes of socket brim designed for the above-knee socket. They vary from circular or oval to triangular or quadrilateral. The

traditional "plug-fit" socket is conical in shape. Its inclined socket wall subjects the stump to very high pressure in order to provide weight-bearing. This proved to be too uncomfortable and painful for many patients.

One of the most popular socket used nowadays is of the quadrilateral design. The origin of this socket is attributed to Striede of Austria. This design was introduced to the United States by Eberhart et al (1949). At the University of California Biomechanics Laboratory in Berkeley, extensive studies were conducted to produce the biomechanical rationale for the shape of this socket design. The relationship between the socket design and the alignment of the knee joint shank and foot under the socket, was also established. This has been discussed in Section 3.2.2.

Kuhn (1956) was able to distinguish six different shapes of brim, as illustrated in Figure 3.2.5(a). It ranges from the total absence of muscle relief (viz flabby stump) to the athletic or muscular stump with strongly marked contours. It was reported that the shape of the muscular stump (picture 'e' in the figure) is most generally used, Naeff and Pijkeren (1980). This shape corresponds to the quadrilateral design.

Another very different socket brim shape presented in Figure 3.2.5(b), is the U.S. Navy Socket developed in 1959. The shape gave laterally more room for the gluteus maximus. No further literature was available for comment on the rationale of this design.

In England, McKenzie developed a triangular brim socket, see Figure 3.2.5(c). The posterior brim, just under the ischial tuberosity is flared to provide some ischial support during weight-bearing. This relieves the stump from being subjected to high pressure.

Redhead (1979) reported on the development of an

above-knee socket desinged to provide total surface support and to dispense with ischial bearing as the primary weight bearing area. The socket is based upon the hypothesis that if the soft tissues of an above-knee stump are adequately supported in a suitably shaped container, they will behave under load as an elastic solid with low stiffness. This design will allow forces to be transmitted through the hip joint rather than the ischial tuberosity. The method of socket casting was also described. Using an elastic sleeve donned over the stump, it provides a grip to stretch the stump distally by traction weight. With the stump tissues deformed in this manner, the cast is allowed to set, see Figure 3.2.5 (d). Results obtained from their measurements of stump/ socket interface pressures under axial loading correlated well with their theoretical calculations on total surface bearing. The socket is now claimed to be routinely fitted at a number of limb fitting centres in England. Follow-up reports showed no evidence of progressive wasting of soft tissues of the stump. An independent research body is required to further evaluate this socket design, if it is to be widely accepted.

Internationally, there is no agreement about the shape of the brim of the above-knee socket. Fulford and Hall (1968) believed that the difference of opinion will only be settled by further experimental work on the pressures within the socket during standing and walking.

Figure 3.2.5(e) shows a classification system for the above-knee quadrilateral socket prosthesis proposed by the Veterans Administration.

There are essentially no special contra-indications to using total-contact sockets other than those which apply to other types of lower limb prostheses, such as a draining osteomyelitis for example. However, total

contact might not be suitable for an amputee with flabby stump and little muscle strength. Limbs with painful neuromas, particularly those caught in scars, might not be suitable for total contact or at least would require special local relief.

Hard sockets are generally used for the softer bulkier stump, where there is room for the femur to move with minimal resistance, while a firm stump requires a soft-end socket to prevent the painful impingement of the cut end of the femur against the socket.

There are three separate types of suspension used on the above-knee prosthesis : suction, Silesian belt and pelvic band with hip joint, although suction suspension can also be combined with the other two systems.

Suction suspension refers to the technique of maintaining the prosthesis by negative air pressure in the socket during swing phase. This is done by using an air expulsion valve at the distal end of the socket and a very well-contoured socket that fits around the stump directly against the skin to form a seal. No prosthetic socks are used with this design because air would tend to leak out through the weave of the sock, resulting in a loss of suspension. Donning a suction socket requires a certain amount of effort and skill from the patient. He has to literally pull himself into the socket, using a sockinette through the valve hole at the distal end. Therefore, suction sockets are contra-indicated for patients with heart disease or other physical problems that will not allow the exertion required to don the prosthesis. It is also contra-indicated for those having significant stump volume fluctuations, balance problems and upper limb disabilities that would make donning the prosthesis difficult.

The Silesian belt (or Silesian bandage) consists of a flexible belt usually made of cloth or leather. The belt is attached at a pivot point at the lateral aspect of the socket at the approximate location of the greater trochanter and extends around the back over the iliac crest to the mid-line of the anterior socket approximately at the ischial level. This form of suspension is reputed to provide a comfortable positive suspension (of the prosthesis) and to control undesirable rotation of the prosthesis and also aid in adducting the prosthesis. The Silesian belt is primary indicated for those patients in whom suction is not adequate as the sole means of suspension. Prosthetic socks are prescribed together with this method of suspension.

The advantages of the Silesian belt are that it is light-weight and comfortable, it is easy to use and not as restrictive as the hip joint with pelvic band suspension, it is more cosmetic under clothes and can provide a definite control of rotation and adduction of the prosthesis. The disadvantages of the Silesian belt are that it is more cumbersome and less cosmetic than the suction suspension. It also does not provide the same degree of control of movement as does the hip joint and pelvic band suspension.

The hip joint and pelvic band also provides a positive suspension and control to an above-knee prosthesis. The hip joint is positioned anterior and proximal to the greater trochanter to approximate the location of the anatomical hip joint centre. The pelvic band is attached proximally to the hip joint, located between the greater trochanter and the iliac crest and contoured to fit snugly on the patient. It extends from the anterosuperior iliac spine to approximately the posterosuperior iliac spine. The pelvic band is attached to a wide cloth or leather waist belt that wraps around

FUNCTIONAL FEATURES OF KNEE MECHANISMS

VA CODE 66

CLASS	TYPE	SWING-PHASE CONTROL						STANCE-PHASE CONTROL				
		NON-ADJUSTABLE	CONSTANT ADJUSTABLE	VARIABLE ADJUSTABLE	VARIABLE ADJUSTABLE AND CADENCE RESPONSIVE	INTERNAL EXTENSION AID		LOCKS	LOCUS SHIFT	MECHANICAL FRICTION	HYDRAULIC RESIST.	
						ADJUST SPRING	NON-ADJ SPRING	MANUAL	POSITION CONTROL	WEIGHT	WEIGHT	GRAVITY
1 FREE KNEE	0	BOCK 3P4 > POLYMATIC >										
2 SWING PHASE CONTROL	1		VARI-GAIT V300A BOCK 3P25 WAGNER 320 VARI-GAIT V300 WAGNER 98 B WAGNER 319									
	2			NW DISC FRICTION VARI-GAIT V200 >								
	3				DUPACO HYDRA-CADENCE > DYNA-PLEX > HOSMER PNEUMATIC >		AIR					
3 SWING AND STANCE PHASE CONTROL	1		WAGNER 205 BOCK 3P23 BOCK 3P24 KOLMAN SAFETY WAGNER 200 > POLYCADENCE >									
	2			VARI-GAIT V100 > LANG POLYCENTRIC > LAURENCE POLYCENTRIC >								
	3				OHC WITH DYNA-PLEX > MAUCH SNS >							GLENRAVEN
4 HYBRID(TWO UNIT) SWING AND STANCE CONTROL	3				BLATCHFORD BSK WITH PNEUMATIC > KOLMAN SAFETY WITH DYNA-PLEX >							

Figure 3.2.5(f) (from V.A. Program Guide G7, 1976)

the patient's waist and buckles anteriorly. The hip joint is aligned to allow for a normal plane of motion in flexion and extension and ease of sitting, without pinching the flesh between the anterior brim of the socket and the pelvic band.

This method of suspension is usually indicated for patients who have poor ability to control their prosthesis and need a very positive suspension. Geriatric patients and some obese patients are in this category. Hip joint and pelvic band suspension is also very easy to learn to use for patients with cognitive disabilities, since it functions in a similar way as a normal waist belt. The hip joint is also indicated for patients with short amputations or weak hip abductors because the additional lever arm will help absorb lateral forces.

Another basic component to the above-knee prosthesis is the prosthetic knee joint. Its functions are to ensure stance phase stability and provide swing phase control. There are a wide variety of designs for the prosthetic knee mechanisms. They range from the very simple single-axis knees to increasingly complex components that control the characteristic of flexion/ extension in various ways.

There are many ways in which prosthetic knee joints could be grouped together for purposes of description and classification. Veterans Administration offered a classification scheme which was published as Program Guide G-7 for the selection and application of knee mechanisms (1976).

Figure 3.2.5(f) illustrates the VA classification scheme being applied to commercially available prosthetic knee joints. Class 1 includes knee mechanisms which provide "free knee rotation", that is knee flexion/

CLASSIFICATION SYSTEM FOR PROSTHETIC KNEE MECHANISMS

	CODE	DESCRIPTION
Kinematic Type	S	Single Axis
	PC	Polycentric "condylar"(Sliding)
	PDA	Polycentric, dual axis
	PLC	Polycentric,"linked condylar (rolling, no sliding)
	PL	Polycentric, multi-bar linkage
Swing Control	N	None
	MC	Mechanical, constant friction
	MV	Mechanical, variable friction
	P	Pneumatic
	H	Hydraulic
	C	Cineplastic muscle control
Stance Control	N	None
	ML	Mechanical lock
	MC	Mechanical, constant friction
	MV	Mechanical, variable friction
	H	Hydraulic
	HY	Hydraulic with controlled yield under load
	HVC	Hydraulic with voluntary control
Other features	E	Extension bias (swing or stance)
	KF	Knee-Foot linkage for toe life in swing
	e	EMG control

Figure 3.2.5.(g). Classification system of prosthetic knee units. (from Judge, 1980)

extension is resisted solely by the friction inherent in the bolt and bushing assembly. There is no adjustment to the magnitude or phase of resistance. Class 2 includes knees whose rotation is controlled by special mechanical or fluid (viz hydraulic or pneumatic) resistance mechanisms which permit adjustment of resistance to knee rotation. Class 3 includes mechanisms which control knee rotation by mechanical friction or by shifting the effective centre of knee rotation, or by fluid resistance devices during both swing and stance phases. Class 4 are "hybrid" knee systems which consist of two separate components - one to control swing phase and another to control stance phase. These units usually permit adjustment to the magnitude of resistance to knee rotation, provide variable resistance and are also cadence responsive.

Judge (1980) in his extensive survey of knee mechanisms for artificial legs, regarded the V.A. classification scheme as inadequate in providing a description of the separate functional groupings. He adopted and extended Radcliffe's (1969) scheme of categorisation, see Figure 3.2.5(g). As an example of this scheme, a single-axis knee with mechanical constant-friction swing control and mechanical-friction stance control is classified as (S-MC-M). If an extension bias device is incorporated in the swing control then it would be classified as (S-MCE-M).

Prescription of a prosthetic knee mechanism is by no means an easy task. There are many factors that have to be considered closely before any decision is made. The Veterans Administration also presented a proposed guideline to the selection of prosthetic knee mechanisms in their Program Guide G-7. Prescription is related to stump and activity level. The prescription chart, as shown in Figure 3.2.5(h), not only deals with prosthetic

Table Prescription related to stump and activity level

	Activity level		
	High, versatile	*Fairly active*	*Relatively inactive*
	Fast walker Walks long distances Uses stairs Walks on hills and uneven ground Alignment stability is insufficient for uneven terrain and other activities	Fast walker Mostly level ground Walks long distances Minimum alignment stability is adequate for level walking	Slow hesitant walker Short distances Needs stability rather than fine swing control
Stump			
Long (50% of femur remaining)	Prescription No. 1: quadrilateral total-contact suction socket; classes 3 and 4 knees; SACH foot for general use; multiaxis foot for special activities and sports	Prescription No. 2: quadrilateral total-contact suction socket; class 2 knees; SACH foot for general use; multiaxis foot for special activities and sports	Prescription No. 3: quadrilateral total-contact; nonsuction suspension; Class 1 knees; single-axis foot for maximum stability
Medium (between 30% and 50% of femur remaining, of stump is strong, consider it long)	Prescription No. 1	Prescription No. 2	Prescription No. 3
Short (less than 30% of femur remaining)	Prescription No. 1: nonsuction suspension	Prescription No. 2	Prescription No. 3
Bilateral and/or others involvements affecting balance	Prescription No. 1:	Not indicated	Prescription No. 3
Prescription advantages	Knee mechanisms provide best adjustable variable cadence response and extension aid and best nonweight dependent stance control Socket provides best control of knee mechanism, better weight distribution, better feedback Foot provides lightweight is prefabricated standardized, and has minimal maintenance	Knee mechanisms provide good swing control, cadence response, use alignment stability for level walking, and have adjustable extensions aid. Socket provides best control of knee mechanism, better weight distribution, and better feedback Foot provides lightweight is prefabricated standardized, and has minimal maintenance	Knee mechanisms provide positive lock-in stance phase, are light-weight, and low maintenance Socket provides good control of prosthesis, good weight distribution, and feed back Foot provides maximum stability and adjustability of resistance to plantar and dorsiflexion

Figure 3.2.5(h) Above-knee prosthesis prescription chart (from V.A. Program Guide G7, 1976)

knee mechanisms, it also includes socket, suspension and ankle/foot mechanisms.

The ankle/foot mechanisms available to an above-knee prosthesis are similar to those already discussed in the section on below-knee prosthetic systems. However, further discussion on this topic can be found in Chapter 4. Another component which can be incorporated into the above-knee prosthesis is an axial rotator. This too will be discussed in the next chapter.

3.2.6. Modular Assembled Prostheses

The concept of modular system for artificial limbs has been around for several decades. Its introduction arose from the development of pylon type prostheses for immediate post-operative fittings. Therefore in prosthetics, the term modular is almost synonymous with tubular or endoskeletal structures. This however was pointed out by Staros (1979) to be "not fully correct", since the crustacean (wood) exoskeletal array used for many years in above-knee limb construction was modular, at least in the assembly process. Each of the major elements used in the construction was in fact a module.

In 1977, a conference sponsored by the Committee on Prosthetic Research and Development (CPRD) developed and adopted the following basic definitions concerning construction of artificial limbs :

Modular: Having accessible a number of interchangeable components which can be assembled easily and quickly into a prosthesis.

Exoskeletal: Used to describe a prosthesis where the supporting structure is outside of or external to the normal shape of the limb.

Crustacean : Used interchangeably with "exoskeletal" - "crustacean" connotes "shell" whereas "exoskeletal" connotes "external support".

Endoskeletal:Used to describe a prosthesis where the supporting structure is internal to the normal shape of the limb.

Endoprosthesis:A prosthesis lying inside the body. (Note: A prosthesis may be entirely endoskeletal or may be partly endoskeletal and partly exoskeletal).

Within these working definitions, the exoskeletal wooden above-knee prosthesis would lose its value of modularity whenever replacement of individual components was required. It would be difficult to replace a major component in this system without re-making the whole prosthesis. Thus, the modularity of the endoskeletal designed system would be advantageous since replacement of components could be done fairly easily and quickly.

The primary objectives of modular systems are to reduce the time required to provide patients with functional prostheses and also to allow the possibility of trying out various combinations of components on each patient with a minimum expenditure of time and effort. Other objectives are to provide for adjustability of alignment throughout the life of the prosthesis and lighter weight and also easy disassembly of components, permitting rapid replacement of worn or damaged parts. Furthermore, it should provide a better service to the amputee population at a very much reduced cost.

The common approach to modular design is endoskeletal in which feet, knee joints, sockets and other components are attached to a metal tube or pylon with clamps, screws or other devices. Cosmetic appearance is provided by use of a nonstructural, flexible foam cover.

Thus, one could draw up the basic elements of a modular system as follows :

(1) Socket and socket attachment to next module
(2) Knee mechanism
(3) Alignment coupling
(4) Shin tube assembly (including upper and lower adaptors)
(5) Ankle/foot mechanism
(6) Cosmetic fairing
(7) Cosmetic cover
(8) Suspension cuffs, belts etc.

All of these elements (except the socket) are available commercially in the form of pre-fabricated modules. Within some of these elements, there also exists a range of sub-modular systems of standardised parts, for example knee mechanisms and ankle/foot mechanisms. Note that, interchangeability of components only exists within the production of the same manufacturer.

At the Ascot Meeting in 1972 on Lower Limb Modular prostheses, the discussion group on sockets condemned the use of prefabricated sockets. Since no two stumps are the same, each socket must be custom-made or "bespoke".

McDougall and Emmerson (1977) described the use of preformed sockets on both below- and above-knee primary amputees. They selected a suitable preformed socket for a patient and fitted it to the stump. Because the socket material is transparent, they could estimate and apply an appropriate sized foam rubber pad to ensure total-contact. They claimed that this method is safe and a prosthetist can fit the limb within the hour. However, this method has to be viewed with caution. There is no report of a follow up of patients supplied with these sockets. At a

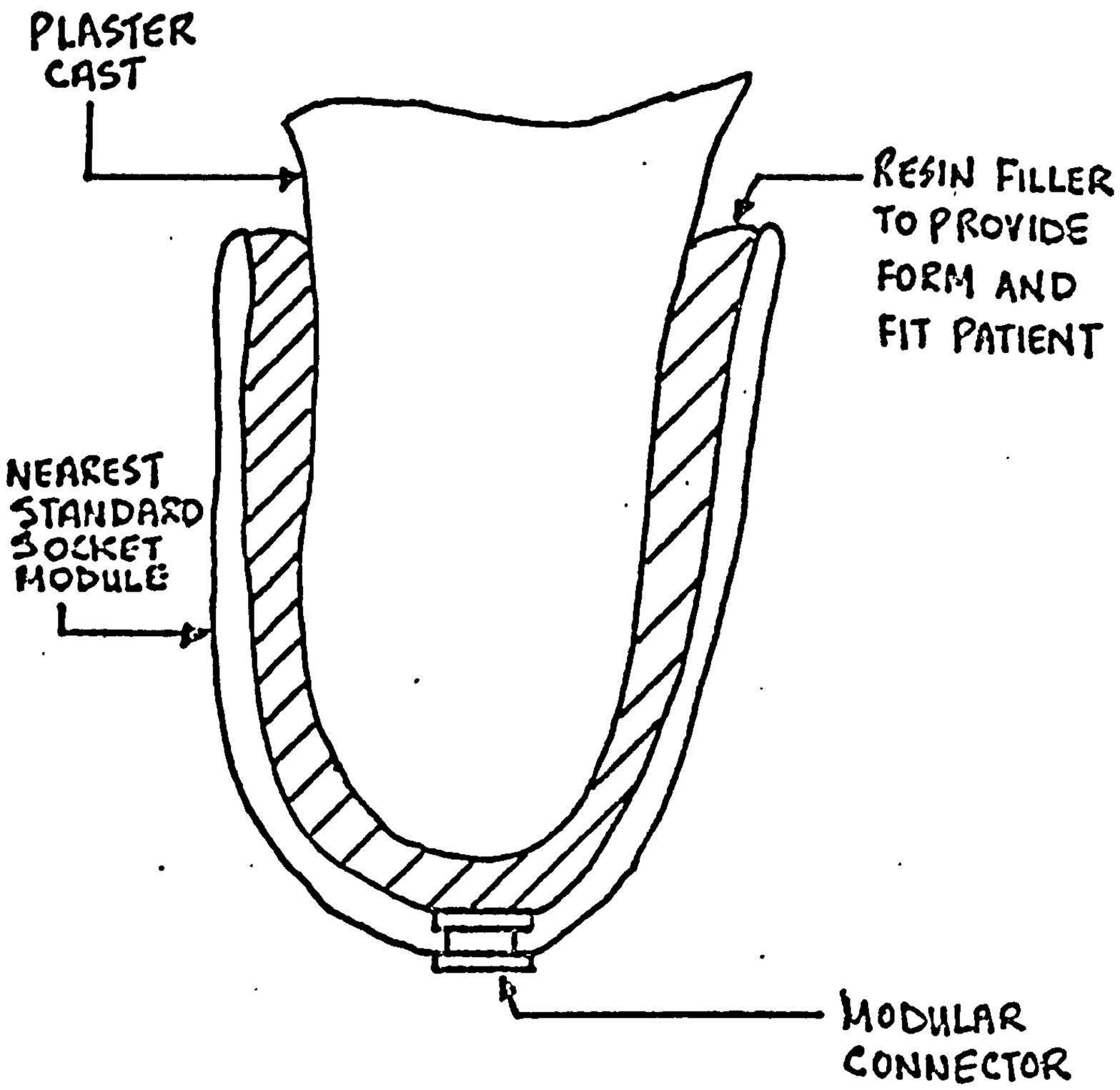

Figure 3.2.6(a) Modular Socket System
(redrawn from Ross, 1969)

glance, this method would not fulfil the basic principles in socket construction, that is, provide accurate relief of pressure sensitive areas and adequate support in tolerant areas.

Therefore, what is required are prefabricated socket modules that could be modified accurately to suit each particular stump. The following are two such suggestions :

Staros et al (1969) reported a method developed at the Veterans Administration Prosthetics Centre (VAPC) for producing accurately fitted below-knee sockets by forming a thermoplastic material directly on stumps. This material can be reheated and reformed to suit a maturing stump. They suggested that prefabricated socket modules based on appropriate fitting principles for all amputation levels can be made and given a refined fit on the patient. One obvious disadvantage of this material is that excessive heat exposure (viz leaving limb in the sun, in the boot of a car on a hot day or leaning against radiator) can cause distortion.

Another method in producing socket modules was put forward by Ross (1969). The outer form of the socket is relatively unimportant in this design, it could be conical or cylindrical in shape. The inner form initially takes after the outer form and would be such as to provide a suitable surface for the retention of a cast in liner to match the plaster cast of the stump. To produce a specific socket for a particular patient would be simply to select the nearest size of standard socket module, insert the modified plaster cast and finally fill the intervening space with a suitable resin which would bond itself to the socket module, see Figure 3.2.6(a). The main difficulty is to find a suitable resin.

Neither of these methods has been evaluated thoroughly to show their suitability in the modular system. Current practice with sockets in the modular system is still to produce them conventionally by plastic lamination processes.

There are two differing opinions in the alignment system of the modular approach. Some manufacturers designed their alignment device, which requires to be removed or transferred out of the assembly after completion of dynamic alignment while others have their alignment component as part of the final structure. It would seem that the latter system is at a distinct advantage in that it provides the possibility of alignment adjustments throughout the effective life of the prosthesis. Moreover, it eliminates the transferring stage in the construction process.

The range of alignment adjustability needed for the fitting process units was specified in the CPRD Report (1971); that is alignment units should possess the following minimum adjustability :

Range of motion in flexion-extension	8 deg
Range of motion in adduction-abduction	8 deg
Horizontal movement in mediolateral plane	20 mm
Horizontal movement in anteroposterior plane	20 mm

These range of alignments were agreed upon at the DHSS Ascot Meeting in 1972, but it was recommended that for above-knee units provision be made for adjusting the relationship of the socket with respect to the axis of the knee about the long axis of the socket or thigh. A range of $\pm$ 10 deg was recommended.

An evaluation programme was carried out at the Bioengineering Unit, University of Strathclyde on

commercially available modular systems. The first report on the evaluation programme was directed towards below-knee systems, Solomonidis(editor)(1975), and the second report was on above-knee systems, Solomondidis (editor) (1980). The evaluation had two principal aims : to provide design information relating to the clinical and constructional requirements of modular assembly systems and to permit comparative judgements to be made about different systems with regard to their clinical suitability and physical features.

In the 1975 report, six systems were included in the evaluation,viz Biomechanical Research and Development Unit (BRADU), Blatchford, Otto Bock, Hanger, Veterans Administration (VA) and Winnipeg. Altogether, 23 patients participated in the evaluation. Each patient was supplied with a conventional PTB , to give the patient a "standard" against which to judge each modular limb. Parameters used in the evaluation included objective measurements of the alignment of the prostheses, the time taken to construct the prostheses, the weight of the prostheses etc. and subjective impressions of patient, surgeon, prosthetist and prosthetic technician.

It is interesting to note that the conventional PTB was found to be signifiantly lighter than the modular systems evaluated. It was stated that none of the systems evaluated was considered as fully developed and that information obtained from the project should be useful in their evolution. Almost 10 years have lapsed since theoriginal below-knee evaluation. Most of the modular systems will now have been updated and improved. It may be worthwhile finding out the effect of the evaluation on the improvement and also the extent to which each system has been improved.

The above-knee systems evaluation reported in 1980

investigated products of four manufacturers, namely Blatchford, Otto Bock, Hosmer and United States manufacturing company (USMC). Twelve patients participated fully in the evaluation program. Each patient was fitted with each of the four modular systems. In an attempt to reduce the variables as much as possible, the socket and prosthetic foot were "standardized". The simplest knee unit available incorporating swing phase control in each of the modular systems, was used. The areas of evaluation were similar to the below-knee systems evaluation except that more parameters were involved. Furthermore, the dynamic loading characteristics were measured by a pylon force transducer.

All the systems evaluated were found to be clinically acceptable. Load analysis on all the systems evaluated showed similar force and moment patterns transmitted by the patient's hip joint during stance phase. No difference was detectable. However, the USMC and Hosmer systems were found to be heavier than the patient's own conventional limb, and their use of a "transferred-out" alignment device bears no advantage over the conventional wood set-ups. The Blatchford and Otto Bock were found to be the preferred systems for limb fitting service in Britain, although it was also pointed out that these systems still have several disadvantages and require further development.

Several recommendations were made in the light of the evaluation results : (i) The design of a new generation modular assembled prostheses using information given in the report was called for; (ii) Evaluation of the various procedures used in bench alignment of prosthesis and also on the understanding of the patient's tolerance in relation to dynamic alignment; (iii) More work is required in the area of cosmetic restoration and evaluation of more sophisticated knee mechanisms.

BELOW-KNEE PROSTHESES

SOCKET	%	SUSPENSION	%
PTB with insert	53	Cuff	58
PTB hard socket	37	SC-SP (PTS)	16
PTB air cushion	1	Corset	14
Wood	6	Supracondylar wedge	9
Other	1	Other	3
TOTAL	100	TOTAL	100

FOOT-ANKLE COMPONENT	%
SACH	81
Single axis	15
Other	4
	100

Table 3.2.7. (a). Prescription of BK Prosthetic Components.
(from Fishman et al, 1975)

At the present moment in the Bioengineering Unit, University of Strathclyde there is an on-going project on the understanding of patients' tolerance towards dynamic alignment and an attempt to quantify "optimum" alignment of modular assembled prostheses.

3.2.7. Survey of Prosthetic Practice

Over the years several studies have been conducted to supply data concerning prescriptions of prosthetic components, notably : Litt and Nattress (1961), Davies et al (1970) and Fishman et al (1975) in the United States and the previously referenced D.H.S.S. amputation statistics for England, Wales and N. Ireland (1976 and 1980).

The terminology used in the D.H.S.S. reports is somewhat different from that used by researchers in the U.S.A., thereby restricting comparison of the practice adopted in both countries. The following discussion will be limited to prosthetic practice exercised on the below- and above-knee amputations only.

Fishman et al (1975) reported an overwhelming prescription choice of the PTB design prosthetic sockets for the below-knee amputees; 91 percent of all sockets compared to 58 percent reported in the Davies et al (1970) survey. A breakdown of the prescribed below-knee prosthetic components presented by Fishman et al is as shown in Table 3.2.7(a). A great majority of the PTB sockets utilized a soft insert, although it was found that a number of prosthetists regularly fitted hard-socket PTB prostheses. The traditional carved wood socket was used in only 6 percent of the below-knee prostheses as compared to 38 percent reported by Litt and Nattress (1961).

ABOVE-KNEE PROSTHESES

KNEE UNITS	%
Single axis no lock	42
Friction lock	23
Hydraulic or pneumatic	22
Manual lock	8
Polycentric	2
Other	3
TOTAL	100

SUSPENSION	
Pelvic band	34
Suction only	32
Suction and Silesian bandage	20
Suction and pelvic band	9
Other	5
TOTAL	100

PROXIMAL SOCKET DESIGN	%
Quadrilateral	97
Peripheral bearing	3
TOTAL	100

DISTAL SOCKET DESIGN	
Total contact	80
Open end	18
Other	2
TOTAL	100

FOOT-ANKLE COMPONENT	
SACH	74
Single Axis	23
Other	3
	100

MATERIALS	%
Plastic	86
Wood	14
	100

Table 3.2.7. (b). Prescription of AK Prosthetic Components. (from Fishman et al, 1975)

Cuff suspension was found to be most frequently prescribed: 58 percent of all the below-knee prostheses. Side joints and thigh corsets were utilised for 14 per percent of the patients. The SACH foot was prescribed for 81 percent of the below-knee amputees, which reflected greater use than the 73 percent reported by Davies et al.

Table 3.2.7.(b) illustrates the breakdown of the prescribed above-knee prosthetic components presented by Fishman et al. Eighty-six percent of all sockets were made of plastic, 80 percent were designed for total contact and 97 percent are quadrilateral shaped. The remaining small percentage of sockets that did not display these characteristics was attributed to long-time amputees who were reluctant to change. This was claimed by Fishman et al.

The single most widely prescribed suspension method was the pelvic belt (34%). This was attributed to the significant numbers of elderly people in the lower limb amputee population, although this figure did represent a decrease when compared to 56 percent reported by Davies et al. The suction technique, either used alone or in combination with a silesian or pelvic belt accounts for 61 percent of the total suspension prescription. This indiciated a wide acceptance of the pressure-differential principle and the recognition of its advantages.

The simple single-axis knee with friction was reported to be the most extensively used knee component (42%), although, when compared to Davies et al (56%) it represents a decrease. The two other major knee components used were the friction-locking knees (23%) and hydraulic or pneumatic units (22%). Polycentric Units accounted for only 2 percent of the knees prescribed. Fishman et al were not clear if this sparse use of

At the present moment in the Bioengineering Unit, University of Strathclyde there is an on-going project on the understanding of patients' tolerance towards dynamic alignment and an attempt to quantify "optimum" alignment of modular assembled prostheses.

3.2.7. Survey of Prosthetic Practice

Over the years several studies have been conducted to supply data concerning prescriptions of prosthetic components, notably : Litt and Nattress (1961), Davies et al (1970) and Fishman et al (1975) in the United States and the previously referenced D.H.S.S. amputation statistics for England, Wales and N. Ireland (1976 and 1980).

The terminology used in the D.H.S.S. reports is somewhat different from that used by researchers in the U.S.A., thereby restricting comparison of the practice adopted in both countries. The following discussion will be limited to prosthetic practice exercised on the below- and above-knee amputations only.

Fishman et al (1975) reported an overwhelming prescription choice of the PTB design prosthetic sockets for the below-knee amputees; 91 percent of all sockets compared to 58 percent reported in the Davies et al (1970) survey. A breakdown of the prescribed below-knee prosthetic components presented by Fishman et al is as shown in Table 3.2.7(a). A great majority of the PTB sockets utilized a soft insert, although it was found that a number of prosthetists regularly fitted hard-socket PTB prostheses. The traditional carved wood socket was used in only 6 percent of the below-knee prostheses as compared to 38 percent reported by Litt and Nattress (1961).

Cuff suspension was found to be most frequently prescribed: 58 percent of all the below-knee prostheses. Side joints and thigh corsets were utilised for 14 per percent of the patients. The SACH foot was prescribed for 81 percent of the below-knee amputees, which reflected greater use than the 73 percent reported by Davies et al.

Table 3.2.7.(b) illustrates the breakdown of the prescribed above-knee prosthetic components presented by Fishman et al. Eighty-six percent of all sockets were made of plastic, 80 percent were designed for total contact and 97 percent are quadrilateral shaped. The remaining small percentage of sockets that did not display these characteristics was attributed to long-time amputees who were reluctant to change. This was claimed by Fishman et al.

The single most widely prescribed suspension method was the pelvic belt (34%). This was attributed to the significant numbers of elderly people in the lower limb amputee population, although this figure did represent a decrease when compared to 56 percent reported by Davies et al. The suction technique, either used alone or in combination with a silesian or pelvic belt accounts for 61 percent of the total suspension prescription. This indiciated a wide acceptance of the pressure-differential principle and the recognition of its advantages.

The simple single-axis knee with friction was reported to be the most extensively used knee component (42%), although, when compared to Davies et al (56%) it represents a decrease. The two other major knee components used were the friction-locking knees (23%) and hydraulic or pneumatic units (22%). Polycentric Units accounted for only 2 percent of the knees prescribed. Fishman et al were not clear if this sparse use of

polycentric components is the result of dissatisfaction with their function or through lack of information, availability of components and experience with these units. The SACH foot accounted for 74 percent of the total foot-ankle components prescribed to above-knee amputees. This is a significant increase from the 55 percent reported by Davies et al.

The modular assembled prostheses (MAP) were not widely prescribed. Only seven percent of above-knee amputees and 9 percent of below-knee amputees were prescribed with the modular system. Fishman et al suggested that these components will become increasingly popular as clinical experience brings further design improvements and wider availability with lower unit cost.

Fishman et al concluded that a relatively small number of components make up the prescriptions for a relatively large number of the patients in each of the categories discussed. For the below-knee amputation, the usual prosthesis prescribed consists of a PTB socket with a soft insert (53%), cuff suspension (58%) and a SACH foot (81%); for the above-knee amputation, the usual prosthesis prescribed consists of a quadrilateral socket (97%), one designed for total contact (80%) with suction suspension (either alone (32%) or in combination with other suspension means (29%)),a single-axis knee unit with adjustable friction (42%) and a SACH foot (74%). This they suggested, could be an indication to propose the concept of a "standard" prescription for the two levels of amputation and supplementary information regarding circumstances requiring modification of the standard prescription could be presented.

From the DHSS annual amputation statistics report, data collected in 1976 and 1980 are used in the following to trace the trend of prescription practice in the

BELOW-KNEE PROSTHESES

1) Type of Prostheses fitted

	1976	1980
Metal leg	28.7%	28.1%
Wooden leg	0.6%	0.4%
Plastic leg	13.0%	12.4%
Peg/pylon Permanent issue	10.1%	11.7%
Modular Prostheses	47.0%	46.4%
Others	0.6%	1.0%
TOTAL	100.0%	100.0%

2) Socket Design

	1976	1980
None	3.4%	0.6%
Conventional	19.5%	10.5%
Proximal Bearing	50.9%	64.1%
End Bearing	1.0%	0.7%
Total Contact	11.1%	3.4%
Total Bearing	3.3%	7.5%
Suction	0.1%	0.0%
Others	10.6%	13.2%
TOTAL	100.0%	100.0%

3) Prosthetic feet

	1976	1980
None	6.2%	6.0%
Uniaxial	88.7%	88.5%
Poliaxial	0.3%	0.1%
SACH	0.5%	0.6%
Others	4.3%	4.8%
	100.0%	100.0%

Table 3.2.7. (c). Prescription pattern of BK prostheses (extracted from DHSS, 1976 & 1980)

United Kingdom.

Table 3.2.7(c) shows the prescription pattern of the below-knee prostheses. As far as the type of prosthesis fitted was concerned, there is no significant difference between data collected in 1976 and 1980. The modular prostheses accounted for 46.4 percent whereas the metal leg was 28.1 percent in 1980. An astonishing fact is that the peg or pylon issued on a permanent basis accounted for 11.7 percent. The description of socket designs used by the report makes it difficult to relate them to their more popular names. Single-axis foot was most extensively prescribed, accounting for 88.5 percent and SACH foot was only used for 0.6 percent of the total below-knee prostheses.

Table 3.2.7(d) shows the prescription pattern of the above-knee prostheses. There is a significant decrease in the use of modular assembled prostheses from 31.6 percent in 1976 down to 26.2 percent in 1980. The most widely fitted prosthesis is the metal type leg, accounting for 44.3 percent. Peg or pylon on permanent issue accounted for a surprising 25.9 percent of the total above-knee prostheses-fitted. The quadrilateral shape socket is only prescribed for 5.3 percent of the total, although this represents a significant increase since 1976 (0.8%). 75.8 percent of the sockets fitted are of the proximal bearing type. Only one percent of the total was fitted with a suction socket. The majority of the knee mechanisms prescribed have no knee control whatsoever (82.2%), and only 11.2 percent had adjustable constant friction swing control mechanisms. 63.9 percent of the knee mechanisms fitted have semi-automatic knee lock, while 13.9 percent were the hand operated type and 12.9 percent had no knee-lock device. The single-axis foot was extensively prescribed for the above-knee prosthesis as well, accounting for 72.7 percent. There

United Kingdom.

Table 3.2.7(c) shows the prescription pattern of the below-knee prostheses. As far as the type of prosthesis fitted was concerned, there is no significant difference between data collected in 1976 and 1980. The modular prostheses accounted for 46.4 percent whereas the metal leg was 28.1 percent in 1980. An astonishing fact is that the peg or pylon issued on a permanent basis accounted for 11.7 percent. The description of socket designs used by the report makes it difficult to relate them to their more popular names. Single-axis foot was most extensively prescribed, accounting for 88.5 percent and SACH foot was only used for 0.6 percent of the total below-knee prostheses.

Table 3.2.7(d) shows the prescription pattern of the above-knee prostheses. There is a significant decrease in the use of modular assembled prostheses from 31.6 percent in 1976 down to 26.2 percent in 1980. The most widely fitted prosthesis is the metal type leg, accounting for 44.3 percent. Peg or pylon on permanent issue accounted for a surprising 25.9 percent of the total above-knee prostheses-fitted. The quadrilateral shape socket is only prescribed for 5.3 percent of the total, although this represents a significant increase since 1976 (0.8%). 75.8 percent of the socketsfitted are of the proximal bearing type. Only one percent of the total was fitted with a suction socket. The majority of the knee mechanisms prescribed have no knee control whatsoever (82.2%), and only 11.2 percent had adjustable constant friction swing control mechanisms. 63.9 percent of the knee mechanisms fitted have semi-automatic knee lock, while 13.9 percent were the hand operated type and 12.9 percent had no knee-lock device. The single-axis foot was extensively prescribed for the above-knee prosthesis as well, accounting for 72.7 percent. There

ABOVE-KNEE PROSTHESES

1) Type of leg fitted

	1976	1980
Metal leg	44.1%	44.3%
Wooden leg	0.2%	0.2%
Plastic leg	0.3%	0.5%
Peg/Pylon Permanent		
Issue	22.9%	25.9%
Modular Prostheses	31.6%	26.2%
Others	0.9%	2.9%
	100.0%	100.0%

2) Socket design

	1976	1980
None	0.4%	0.3%
Conventional	18.9%	12.2%
Proximal Bearing	73.4%	75.8%
End Bearing	4.7%	3.7%
Quadrilateral	0.8%	5.3%
Total Bearing	0.2%	0.4%
Suction	0.5%	1.0%
Others	1.1%	1.3%
	100.0%	100.0%

3) Knee Control

	1976	1980
None	79.7%	82.2%
Central knee Control	0.7%	1.2%
Constant Friction	13.8%	11.2%
Interrupted Friction	1.8%	1.0%
Swing Phase Control	3.1%	2.4%
4-Bar Linkage	0%	0%
Others	1.0%	2.0%
	100.0%	100.0%

4) Knee Lock

	1976	1980
None	12.3%	12.9%
Hand Operated	10.6%	13.9%
Semi-Automatic	64.3%	63.9%
Stablised knee	10.0%	6.6%
Others	2.8%	2.7%
	100.0%	100.0%

5) Prosthetic feet

	1976	1980
None	12.6%	11.5%
Uniaxial	78.8%	72.7%
Poliaxial	0.3%	0.1%
SACH	1.6%	6.1%
Others	6.7%	9.7%
	100.0%	100.0%

Figure 3.2.7. (d). Prescription pattern of AK prostheses (extracted from DHSS, 1976 & 1980)

is a significant increase in the prescription of SACH feet (6.1%) in 1980 as compared with only 1.6% in 1976.

From the data presented, it seems that the prosthetic practice in the United Kingdom is very much different from that in the United States. In the United Kingdom, the usual prosthesis fitted for the below-knee amputee was the modular assembled type (46.4%). The socket design most widely used was the proximal bearing type (64.1%). There is no information available on the types of suspension methods that were employed. However, the 28.1% of metal legs would definitely have thigh corset and knee joint. The single-axis foot was overwhelmingly prescribed (88.5%), which is a complete contrast to the Fishman et al (1975) report. For the above-knee amputation, the usual prosthesis fitted was the metal leg type (44.3%). The suspension systems of metal leg used includes either shoulder suspenders, pelvic band with hip joint or Silesian belt. The proximal bearing type of socket design was usually prescribed (75.8%) with no swing phase knee control (82.2%) and semi-automatic knee lock (63.9%). The single-axis foot was again the foot of choice (72.7%).

The contradicting prescription practice on prosthetic feet between both U.K. and U.S.A. presented in the discussion was one of the primary reason for this project.

3.3. Biomechanical Analysis of Prosthetic Gait

The variability of data obtained in prosthetic gait studies is so wide that it makes generalisation of gait pattern for a particular level of amputees very difficult.

The principal factors affecting the variability of data are :

is a significant increase in the prescription of SACH feet (6.1%) in 1980 as compared with only 1.6% in 1976.

From the data presented, it seems that the prosthetic practice in the United Kingdom is very much different from that in the United States. In the United Kingdom, the usual prosthesis fitted for the below-knee amputee was the modular assembled type (46.4%). The socket design most widely used was the proximal bearing type (64.1%). There is no information available on the types of suspension methods that were employed. However, the 28.1% of metal legs would definitely have thigh corset and knee joint. The single-axis foot was overwhelmingly prescribed (88.5%), which is a complete contrast to the Fishman et al (1975) report. For the above-knee amputation, the usual prosthesis fitted was the metal leg type (44.3%). The suspension systems of metal leg used includes either shoulder suspenders, pelvic band with hip joint or Silesian belt. The proximal bearing type of socket design was usually prescribed (75.8%) with no swing phase knee control (82.2%) and semi-automatic knee lock (63.9%). The single-axis foot was again the foot of choice (72.7%).

The contradicting prescription practice on prosthetic feet between both U.K. and U.S.A. presented in the discussion was one of the primary reason for this project.

3.3. Biomechanical Analysis of Prosthetic Gait

The variability of data obtained in prosthetic gait studies is so wide that it makes generalisation of gait pattern for a particular level of amputees very difficult.

The principal factors affecting the variability of data are :

a) comfort and alignment
b) mechanical characteristics of the prosthesis
c) skill and coordination of the subject
d) training effects
e) speed of walking
f) fatigue
g) physical and psychological condition of the subject

In addition to the above factors, variability of data is also affected by the environmental conditions of the experiment.

Therefore, for any realistic assessment of prosthetic gait to be made, as many variables as possible have to be removed. This may mean imposing certain constraints on the selection of patients and the type of prostheses to be worn, thus validating the "control group" assessment concept.

An acceptable prosthetic gait must be that with absolutely minimal gait deviation. In addition, the patient should feel secure and comfortable with it and furthermore, minimal energy should be required to operate the prosthetic leg. For a thorough evaluation of this gait, not only a subjective examination is required but an objective recording and assessment are also essential.

Most of the instrumentation and measurement techniques discussed in Chapter 2 are capable of this and have been used in assessing prosthetic gait. The criteria in these assessments fall into three areas : kinematics, kinetics and energy requirement.

3.3.1. Kinematic Assessment

The extensive research program conducted in the University of California, Berkeley (UCB) in 1947, used

the interrupted light photographic technique and a glass-walkaway with cinecamera recordings to analyse and compare gait patterns of normal subjects and amputees. It was concluded that on average, the below-knee amputee takes a longer step with his normal leg than he does with his prosthesis whereas the above-knee amputee takes a longer step with the prosthesis. Normal subjects have a longer stride than the below-knee amputee. Displacement-time data showed no significant difference between a normal subject and a below-knee amputee, except that a greater vertical displacement was recorded for the below-knee amputee. The above-knee amputee demonstrated a much greater vertical displacement of the greater trochanter than the normal subject. It was also observed that the knee pattern of the above-knee amputees indicated the manner in which the amputee threw his prosthesis forward during the swing phase in order to have the leg fully extended when the heel makes contact with the floor.

The maximum and minimum horizontal velocities of the below-knee prosthetic leg were of the same magnitude as those of the normal subject in level walking but the shapes of the curves were different. The knee joints of the above-knee prostheses had a slightly higher horizontal velocity than those of the normal subject whereas the ankle velocities were somewhat lower. There were many differences between the horizontal accelerations of the normal subject and the amputees. Reversals in all the acceleration curves were much more numerous for the above-knee amputee and the maximum acceleration of the knee for the above-knee prosthetic leg was unusually high.

Harmonic analysis was applied to the angular displacements from the vertical of thigh and shank. It was claimed that the characteristic differences between normal subject and amputees stand out much clearer in

harmonic terms. However, it was recognised that the small sample of data (viz three normal subject, two below-knee amputees and two above-knee amputees) did not warrant any final conclusions.

The total pelvic tilt in the above-knee amputees was ten degrees while the normal subject's was only six degrees. The higher magnitude of pelvic tilt was to help swing the prosthesis through. During the stance phase, it was noticed that the artificial knee joint of the above-knee prosthesis remained locked for a greater part of stance phase, this showing a difference from the two peak pattern of the normal subject's knee flexion.

The transverse rotation between the shank and foot of the prosthetic leg of the above-knee amputee was zero, while the prosthetic shank rotated a total of 13 degrees with respect to the pelvis. This value was 17.2 degrees for normals (an average taken from 12 subjects), where 9 degrees of rotation took place between the femur and tibia and 8.2 degrees were between the femur and pelvis. Since no transverse rotation is possible between the prosthetic shank and thigh section, some of the rotation must have been taken up by the hip joint, while the remainder occurs between the stump and socket. When an ankle rotator was used, 11 degrees of rotation took place during the stance. The investigators claimed that this would undoubtedly relieve the patient of much discomfort due to the stump twisting in the socket. The magnitude of pelvic rotation of the above-knee amputee was much greater, this being to help in swinging the prosthesis through.

The above-knee amputee's pelvis was observed to list much more to the amputated side during heel contact, placing the stump more directly into the socket and thus preventing too great a pressure upon the lateral side of

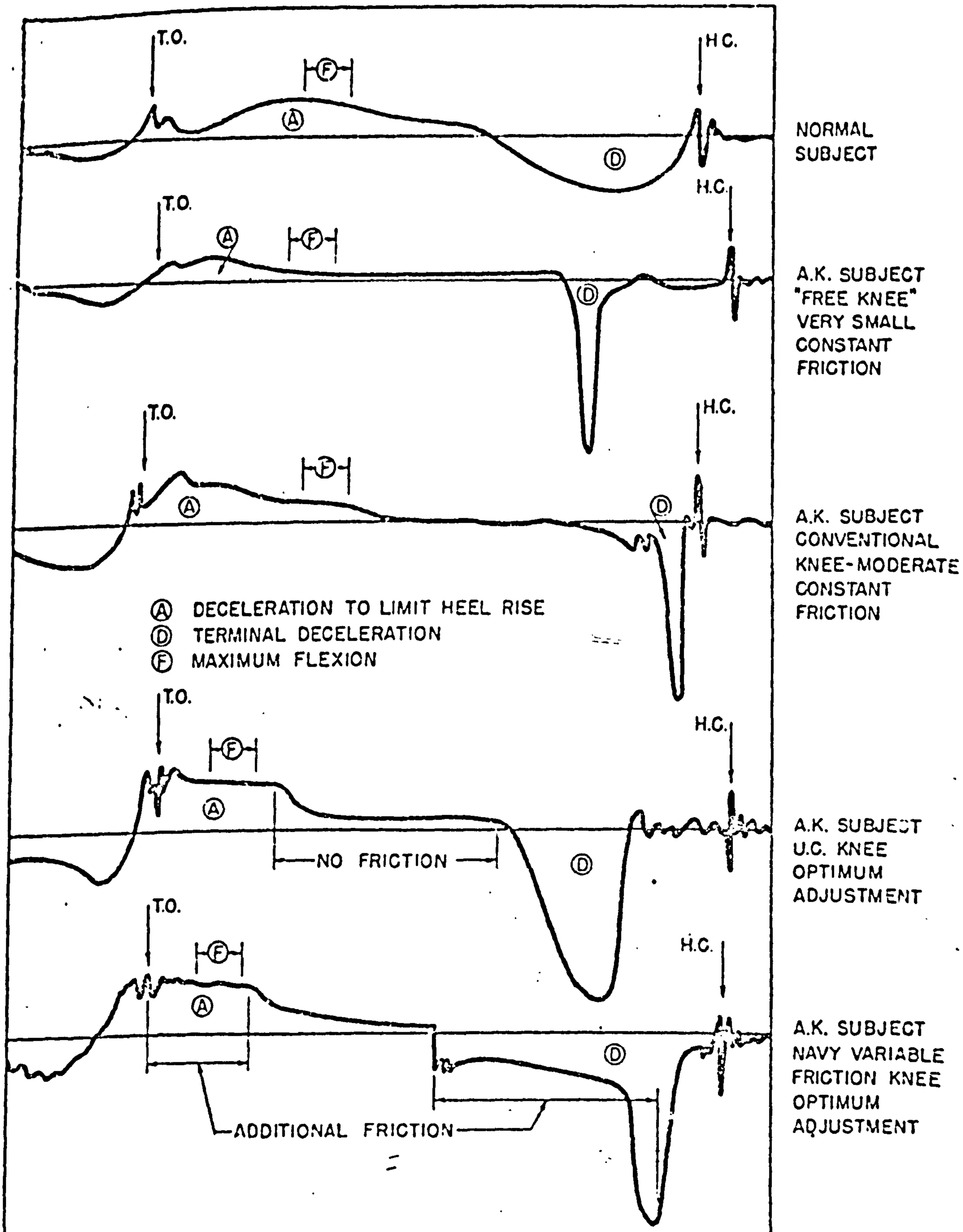

TYPICAL SHANK ANGULAR ACCELERATION RECORDS
FROM ACCELEROMETER RECORDS OF VARIOUS SUBJECTS WITH DIFFERENT KNEE MECHANISMS

Figure 3.3.1(a). Shank angular accelerations
(from Bartholomew, 1952)

the stump end. The investigators affirmed that postural compensations were necessary because of deficiencies inherent in the above-knee stump and that optimum prosthetic alignment, adjusted to resemble the normal is limited by the lack of muscle power to maintain certain positions.

Although, the UCB (1947) report is a classic in its own right, there are a few drawbacks. The investigators were quick to realise that they had only a small amount of data, which could not be used to make concrete generalisation. Furthermore, comparison with data obtained by the investigators would be difficult since no control of variables was made.

Fishman et al (1953) at New York University, conducted a very thorough evaluation on an experimental hydraulic prosthesis for above-knee amputees. In their biomechanical analysis, interrupted light photography, a force plate and tachograph were used. Altogether 10 above-knee amputees participated in the evaluation programme. Analysis was performed on both the amputees' own "conventional" prostheses and the experimental hydraulic legs. Data for normal subjects were also used for comparison.

At free walking speeds, the mean walking cadence increased significantly while wearing the hydraulic leg (viz from 90.4 to 96.1 steps per min). The step time ratio of the good leg to the prosthetic leg while wearing the hydraulic leg, also increased significantly from 0.78 to 0.88. There was a decrease in the time of double support with increasing cadence for the hydraulic leg, which more nearly duplicated the curve for non-amputees. It was concluded that there were strong indications of a more symmetrical gait with the hydraulic leg.

Temporal Components	Murray et al(1980) (10 subjects)	James and Oberg(1973) (34 subjects)	Leavitt et al (1972) (20 subjects)
	Mean (± 1 S.D)		
Stance Phase(sec)			
Sound	0.94(0.12)	0.92(0.10)	0.94(0.13)
Prosthetic	0.80(0.07)	0.80(0.08)	0.83(0.10)
Swing Phase(sec)			
Sound	0.43(0.04)	0.49(0.04)	0.48(0.05)
Prosthetic	0.58(0.06)	0.61(0.03)	0.60(0.06)
Double Support (sec)			
Sound	0.17(0.04)	0.15(0.04)	0.14(0.04)
Prosthetic	0.20(0.06)	0.15(0.04)	0.18(0.04)
Sound-Stance(%)	69	65	66
-Swing(%)	31	35	34
Prosthetic			
-Stance(%)	58	57	58
-Swing(%)	42	43	42
Walking Speed (cm/sec)	100(16)	94(15)	-
Cadence(Steps/min)	87(7)	85(-)	-
Cycle duration(sec)	1.38(0.11)	1.41(0.12)	-
Stride length(cm)			
Sound	64(9)	62(9)	-
Prosthetic	72(8)	68(9)	-
Stride Width(cm)	17.4(3.6)	10.1(3.4)	-

Figure 3.3.1(b) Temporal factors for above-knee Amputees

The speed of amputee gait (level walking) and the total range of velocities increased significantly with the hydraulic leg. The stride length with respect to increasing cadence approached closer to the non-amputee trend when the amputee wore the hydraulic leg. There was generally a much smoother and more symmetrical gait with the hydraulic leg than with the conventional one.

The findings of Fishman et al (1952) indicate that significant changes do occur in the above-knee prosthetic gait pattern when different types of prostheses are used. Bartholomew (1952) showed that different types of knee mechanisms will produce different recordings of the shank angular accelerations, see Figure 3.3.1(a). Bresler et al (1957) presented data obtained from twelve runs made on four above-knee amputees wearing different knee mechanisms. Although the data presented were not large enough to be conclusive, significant differences were observed in the ankle, knee and hip angles when different knee mechanisms were used.

James and Oberg (1973) studied the gait of 34 unilateral above-knee male amputees, all except one being fitted with quadrilateral total-contact suction socket. Most of the prosthetic knee units used had a stability mechanism with swing-phase control and most of the prosthetic feet used had an articulated ankle joint. No description was made of other types of knee unit and prosthetic ankle/foot mechanism used. It was concluded that the above-knee prosthetic gait was characterised by considerable asymmetry with regard to stance and swing phase duration and step length. They found that the subjects took longer steps with the prosthesis than with the intact leg and the stance phase of the prosthesis was shorter than that of the intact leg. They attributed these effects to the prosthetic leg being prevented from having full hip extension, by the pressure of the

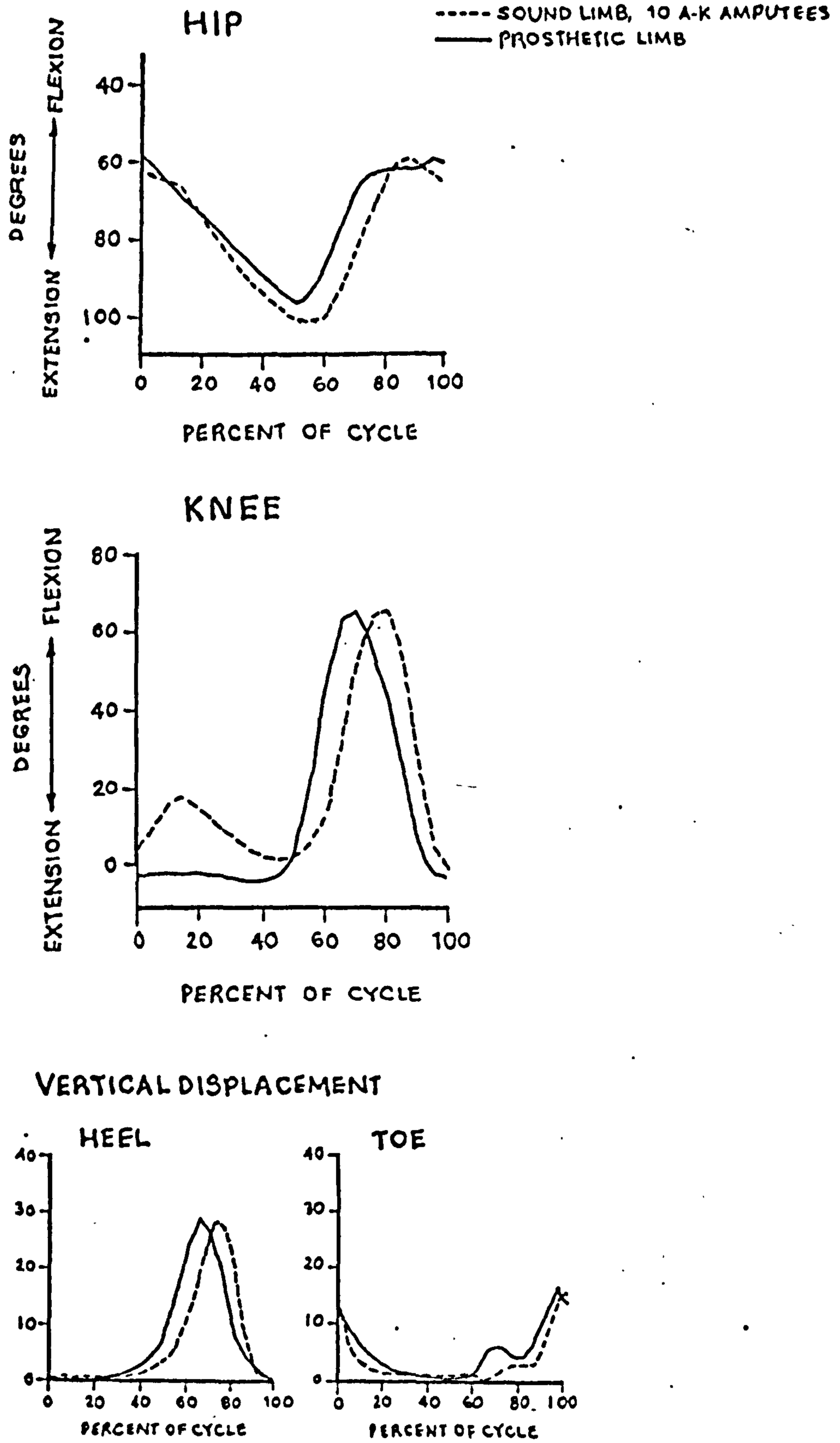

Figure 3.3.1(c) Kinematic Data of Above-Knee Amputees (redrawn from Murray et al, 1980)

prosthetic socket against the ischial tuberosity.

Godfrey et al (1975) investigated the gait characteristics of seven male above-knee amputees; each one was fitted with six different types of knee units in sequence. It was reported that the step length of the intact leg follows closely that of the prosthetic limb. It was suggested that this was most likely due to the close attention paid to alignment and construction of comfortable sockets. It was concluded that each subject walks with a characteristic gait pattern of his own on any stable prosthesis and that complex knee units do not necessarily give a better gait. This however has to be substantiated by further kinematic as well as kinetic evaluation.

Murray et al (1980) studied the gait pattern of 10 above-knee amputees using constant-friction knee components in their prostheses. Half of the sample had suction suspension while the other half had pelvic band suspension. Six had a SACH foot and four had a single-axis ankle, with either a wooden foot or a wooden foot with compressible heel/toe. Six had an extension aid on the prosthetic knee and four did not. Data were presented as an average of the 10 amputees, no distinction was made with regard to the effects of the different prosthetic components on the prosthetic gait.

Figure 3.3.1(b) shows the temporal factors presented by James and Oberg (1973) and Murray et al (1980). The differences in the values may be due to many other factors besides the different prostheses worn by the amputees. Murray et al found that the amputees had an abrupt reversal of the residual hip from flexion to extension just after heel-strike of the sound limb. The prosthetic knee did not yield into flexion in the early stance phase and the maximum knee flexion during swing was similar for

Temporal Components	Molen et al(1973) (13 subjects)	Breakey(1976) (5 subjects)
Stance Phase(%)		
Sound	67	62
Prosthetic	64	60
Swing Phase (%)		
Sound	33	38
Prosthetic	36	40
Double Support Phase(%)		
Sound	17	11
Prosthetic	14	9

Figure 3.3.1(d) Temporal factors for below-knee Amputees

the sound and prosthetic limb, see Figure 3.3.1(c). It was observed that when the prosthetic knee flexion was excessive, the prosthetic heel rise was also excessive.

Kay et al (1957) at New York University, conducted an evaluation on the Navy Celastic Soft Socket for below-knee amputees. Instrumentation methods used in their biomechanical analysis were the same as those used by Fishman et al (1953). Altogether, eleven below-knee amputees participated in the evaluation programme. The main feature in the prosthesis being evaluated was the celastic soft socket insert, otherwise the whole prosthesis was the same as the thigh-corset-with-joint type of wooden socket prosthesis.

No significant difference was found when using the soft socket insert. Although there was a significant increase in the ratio of stride lengths which indicated that the soft socket insert could be providing a slight increase in the feeling of security and stability.

Molen et al (1973) and Breakey (1976) both presented studies conducted to evaluate the gait of unilateral below-knee amputees. Molen et al carried out their work on 13 below-knee subjects but no description was given of the type of prostheses their subjects were wearing. Breakey had 5 below-knee subjects, each wore a PTB prosthesis with supracondylar suspension and a SACH foot. The temporal factors obtained from these two investigations are presented in Figure 3.3.1(d). Although, the differences in the values may be due to the different types of prostheses used, other factors too may have influenced the variation.

Breakey reported that the loss of a normal foot and ankle in the below-knee amputee resulted in a longer stance phase duration in the normal limb and a shorter

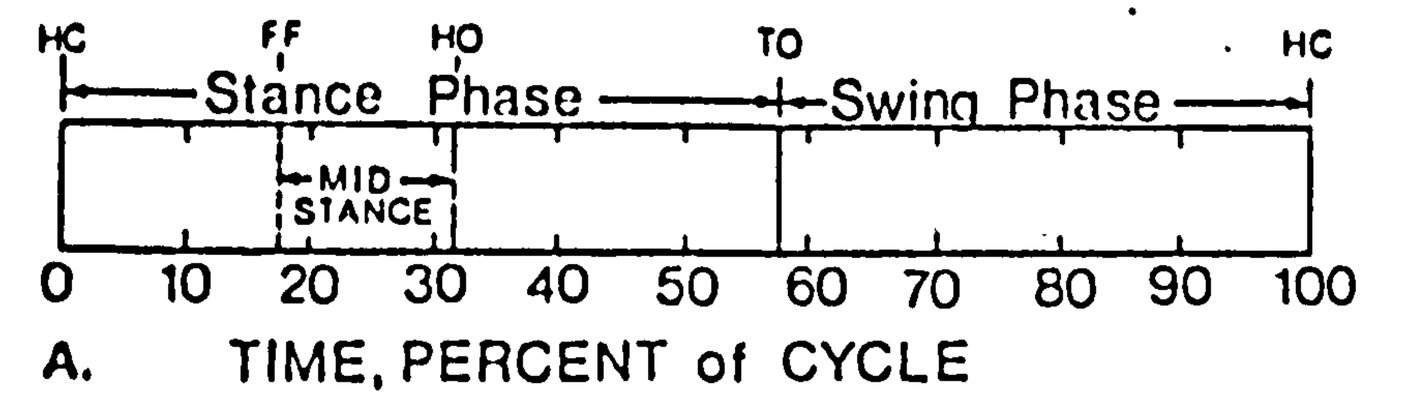

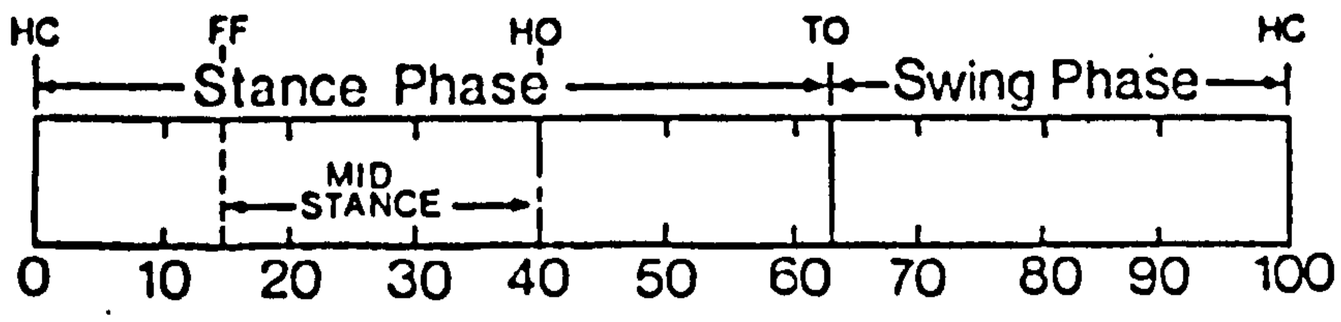

Fig. Foot-timing for the BK amputated subjects.
A. Prosthetic limb B. Normal limb

Figure 3.3.1(e) Temporal Parameters for Below Knee Amputees (from Breakey, 1976)

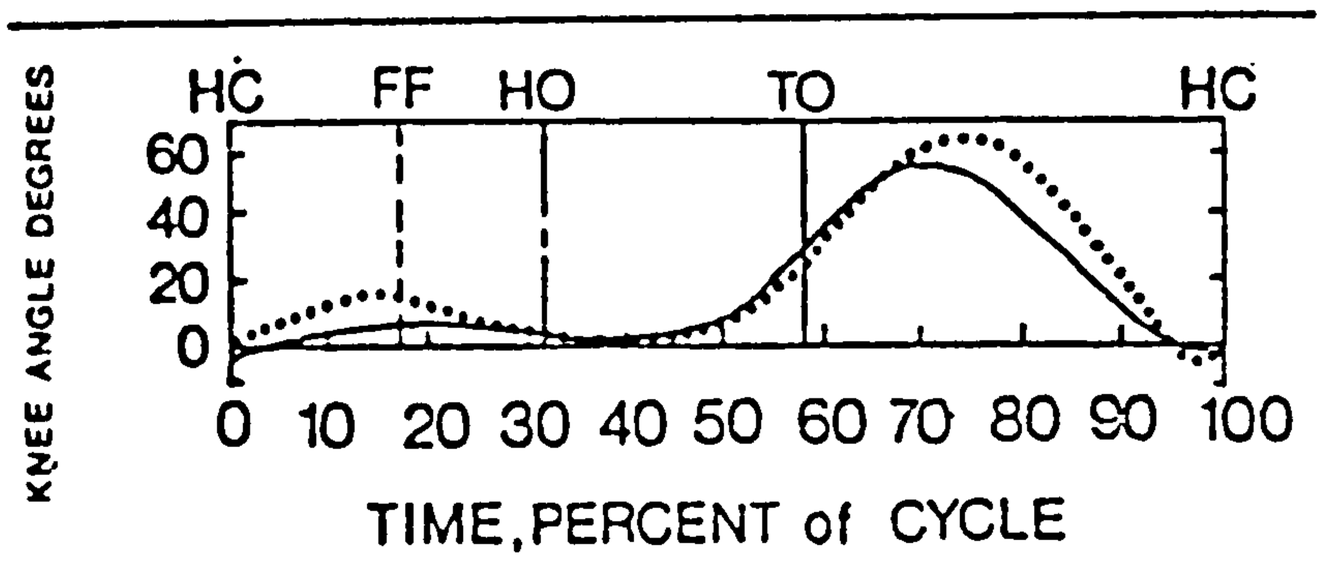

Fig. Knee motion for the prosthetic side. Solid line (_____): Knee motion curve for amputee; Dotted line (. . .): Knee motion curve for normals.

Figure 3.3.1(f) Knee flexion angles for Below Knee Amputees (from Breakey, 1976)

stance phase in the amputated limb. This characteristic was also reported by UCB (1947). The foot-timing during stance phase was found to be different between the sound and prosthetic limbs. Foot-flat on the affected side was longer than the normal side and heel-off on the affected side occurred much earlier than the normal side, see Figure 3.3.1(e). This was attributed to the lack of true ankle function in the prosthetic limb since the prosthetic foot used was a SACH foot. Knee motion in the amputated limb was found to have the same general pattern as seen in normal knee motion. However, the magnitude of knee flexion in the amputated limb was reduced in stance phase, at toe-off and at peak knee flexion during swing phase, see Figure 3.3.1(f).

3.3.2. Kinetic Analysis

The pylon studies conducted at UCB (1947) were directed to the recording of forces and moments on the shank. It was found that the forces acting on the shank were essentially the same for both above- and below-knee amputees. This was suggested to be due to the great number of variables such as type of leg, alignment, wearing time and length of stump, and also partly to the small number of subjects tested. One above-knee amputee was tested to determine the effect on the forces of the changes from the standard pelvic belt type to the suction socket type leg. The results indicated that the amputee was placing more weight on his prosthesis while using the suction socket. It was concluded that the difference in loads due to the type of leg showed that alignment and fit have a great influence on forces on the shank. Furthermore, greater stability was evidenced by the smaller lateral moments in the various walking activities, while using the suction socket. This also resulted in a more symmetrical looking gait.

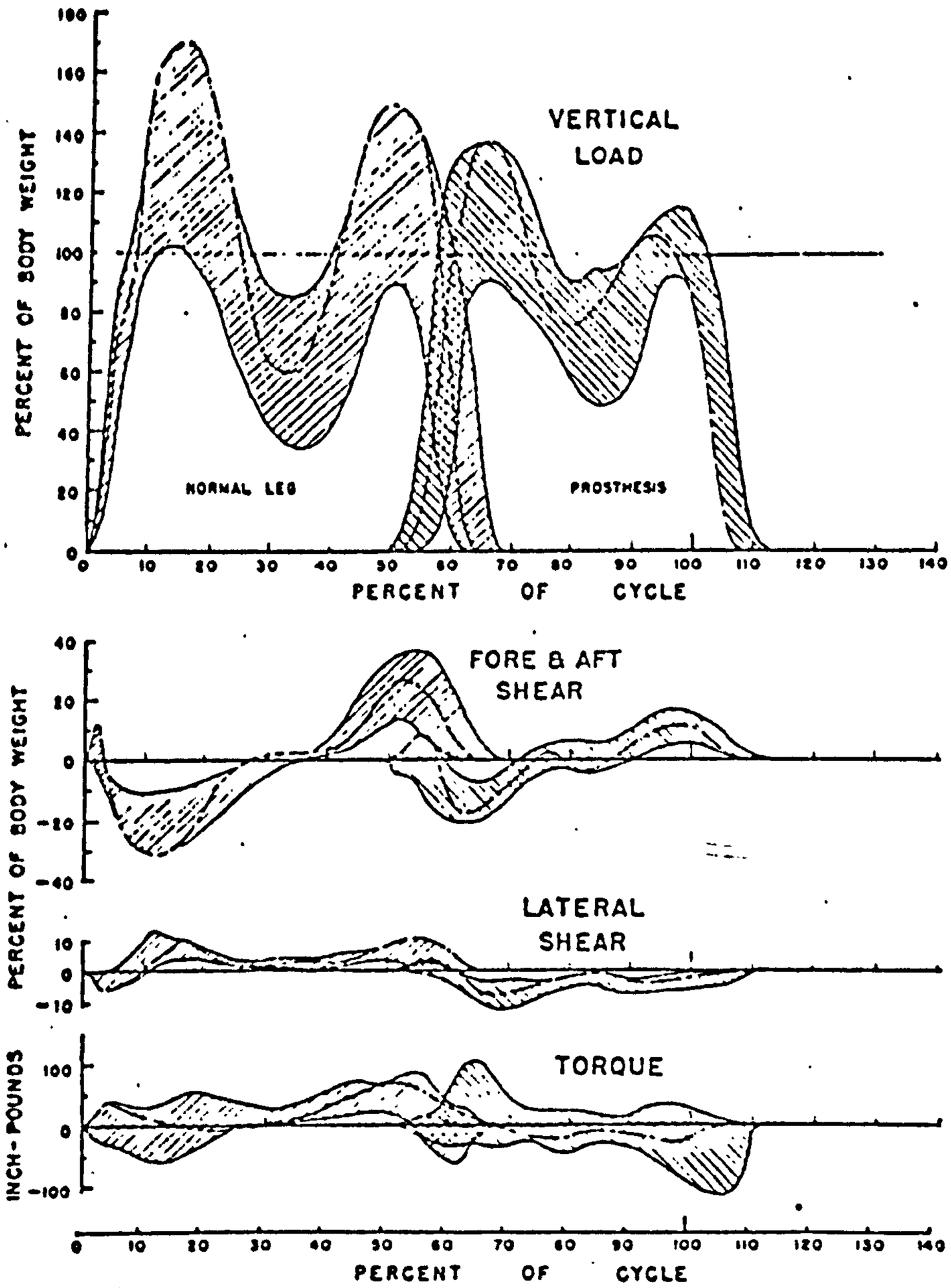

FIG. FLOOR REACTIONS ON THE FOOT

SEVEN B.K. SUBJECTS WALKING LEVEL

	SUBJECT NUMBER	RUN NUMBER	STEPS PER MINUTE
	[illegible]	[illegible]	90
	[illegible]	[illegible]	109
	[illegible]	[illegible]	91
	[illegible]	[illegible]	91
	[illegible]	[illegible]	94
	[illegible]	[illegible]	111
TYPICAL	[illegible]	[illegible]	103

UNIVERSITY OF CALIFORNIA
PROSTHETIC DEVICES RESEARCH

Figure 3.3.2(a) Ground reactions of Below Knee amputees (from Cunningham, 1950)

The UCB group also made extensive studies with the force plates. Further results obtained in this area were reported by Cunningham (1950). Ground-foot reactions of seven below-knee and eleven above-knee amputees during level walking were presented. Each group of results was observed to have a range of variations. The main factors effecting these variations were given as the speed of walking and the ratio of leg length to stride length. Other variables included weight of subject, body build, degree of disarticulation and comfort during walking.

Figure 3.3.2(a) shows the ground-foot reactions of seven below-knee amputees. The vertical force component showed the typical two-peak pattern, although it is evident that more weight was carried by the natural leg than the prosthetic one. This is because the natural leg takes over part of the function of the prosthetic leg in producing the upward movement of the body which allows it to maintain an average elevation. The second peak of the prosthetic side was much lower than that of the normal. This was attributed to the lack of push-off mechanism in the prosthetic foot. The fore and aft shear forces of the prosthetic leg also demonstrated this characteristic . The below-knee amputee. however can be expected to walk as well as non-amputees of comparative health since the knee and hip are intact. With good alignment of a well fitting prosthesis and correct walking training, the below-knee amputee can be regarded as having minimal disability, with a near normal gait, the loading being shared more equally between the sound and prosthetic limb.

The ground-foot reaction data for above-knee amputees are very different from those of non-amputees.Eberhart et al (1947) explained that the middle peak of the vertical load for the sound leg was due to the raising

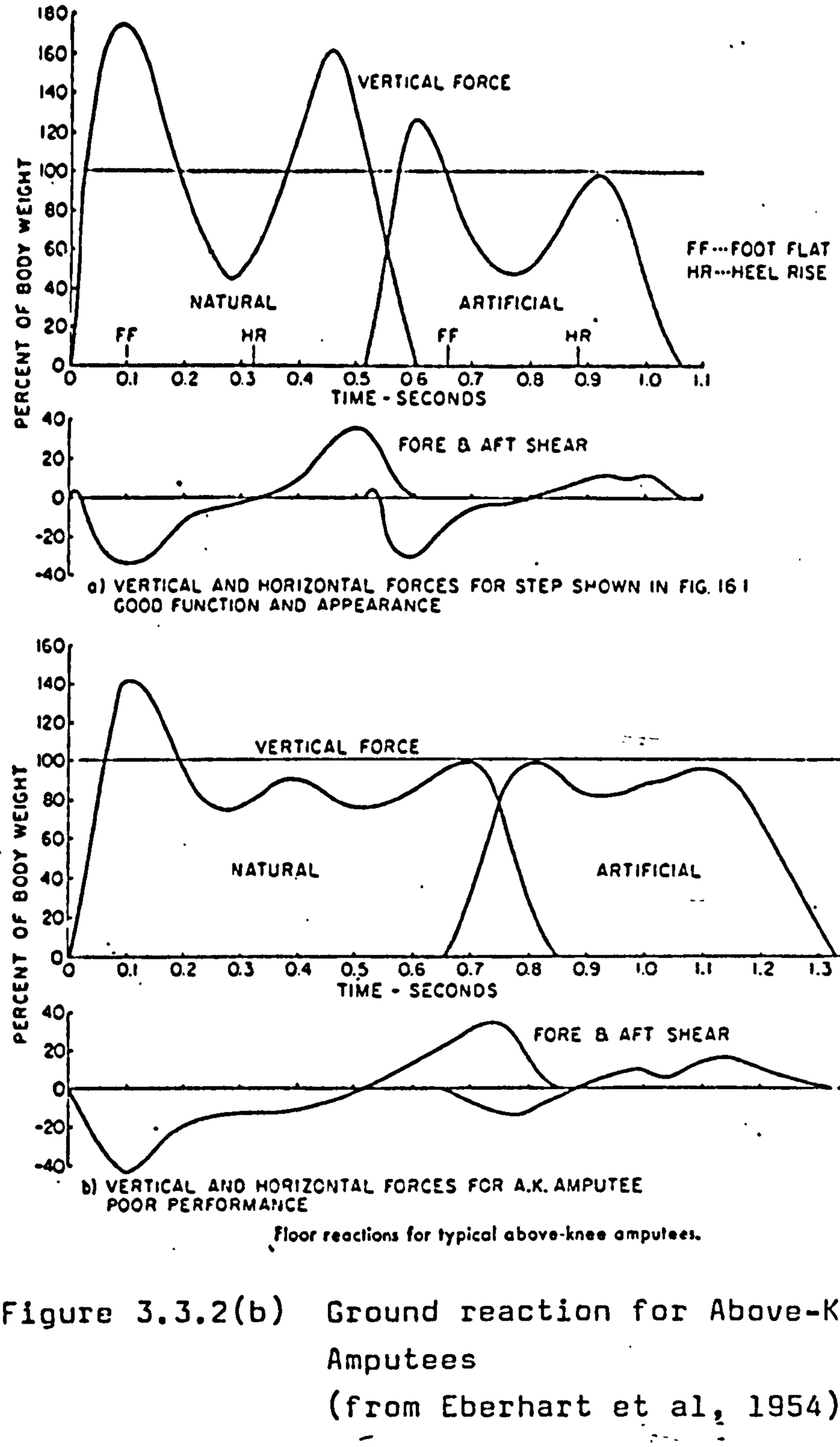

Floor reactions for typical above-knee amputees.

Figure 3.3.2(b) Ground reaction for Above-Knee Amputees

(from Eberhart et al, 1954)

of the hip on the prosthetic side when swinging, thus producing a downward reaction on the weight bearing normal leg which was transmitted to the force plate. Some vertical load curves for the prosthetic side also had three peaks. In these instances, it was due to the attempt made at moving the centre of gravity of the trunk over the prosthesis during weight bearing. This was because the amputees had lost the use of the leg abductor muscles. The prosthetic leg also could not adequately control the downward movement of the hip joint, which resulted in the amputee taking a longer time to move the artificial leg forward than with the sound leg, although the distance moved may be shorter. Eberhart et al (1954) considered these force pattern to be representative of a typical above-knee amputee with poor gait performance. It was stated that with proper attention to prosthetic fit, alignment and training, the performance of an above-knee amputee can be greatly improved, see Figure 3.3.2(b), although, the vertical load is still not carried equally by the sound and the prosthetic leg, the sound leg providing more than its normal share. The time spent on the two legs was more or less the same.

Bresler et al (1957) reported on a kinetic study involving four above-knee amputees wearing different types of knee mechanisms and walking at different speeds. Results on the antero-posterior moment at the ankle, knee and hip of both the natural and prosthetic legs showed varying patterns of curves, which indicated the influence of the knee mechanisms and speed of walking. Variation from subject to subject wearing the same knee unit and walking at the same speed was also clearly illustrated, thus, demonstrating the need to have control over variables that would effect gait pattern in comparative studies.

Cappozzo et al (1975) presented a similar sort of

Table : Ambulation of Below-knee Amputees With Prosthesis

Researcher, date	N	Type of disability and appliances	Speed, m/min	Energy expenditure kcal/min/kg	Energy expenditure kcal x 10^{-3}/m/kg
Waters, 1976	15	Vascular Symes	54[c]	0.055[g]	1.01[f,g]
Reitemeyer, 1955	2	BK	60[d]	0.035[b]	0.58
Ralston, 1971	1	BK	49[d]	0.055[d]	1.12
Molen, 1973	54	Traumatic BK	50[d]	0.060[e]	1.20
Ganguli, 1973	20	BK	50[d]	0.060	1.20
Gonzales, 1974	9	BK	64[c]	0.062[f,g]	0.97[a]
Waters, 1976	13	Vascular BK	45[c]	0.056[g]	1.25[g]
Waters, 1976	14	Traumatic BK	71[c]	0.074[g]	1.04[g]
Gonzales, 1974	?	Bilateral BK	66[c]	0.070[f,g]	1.07[d]

[a]Calculated knowing kcal/min and m/min
[b]Calculated knowing kcal/meter and m/min
[c]Speed chosen by the subjects
[d]Speed chosen by the researcher (the only speed or a representative speed)
[e]Calculated from author's equation and/or percentage figure
[f]Approximated from a graph
[g]Calculated from O_2 consumption

Table 3.3.3(a) Summary of Below Knee Amputees energy expenditure (from Fischer & Gullickson, 1978)

Table : Ambulation of Above-knee Amputees With Prosthetics

Researcher, date	N	Type of disability and appliances	Speed, m/min	Energy expenditure kcal/min/kg	Energy expenditure kcal x 10^{-3}/m/kg
Muller, 1952	2	AK	70[c]	0.053[b]	0.76[b]
Muller, 1952	1	AK	40[c]	0.023[b]	0.60[b]
Inman, 1961	1	AK	62	0.017[b]	1.05[f]
Durnin, 1967	?	AK	60[c]	0.067	1.12[a]
Bard & Ralston, 1959	6	AK	68[c,d,f]	0.061[f]	0.90[f]
Ganguli, 1974	6	AK	50[c]	0.088	1.76[a]
Traugh, 1975	9	AK	39[d]	0.048[f,g]	1.23[a]
Ralston, 1971	1	AK	49[c]	0.049	1.01[a]
Waters, 1976	13	Vascular AK	36[d]	0.061[g]	1.25[g]
Waters, 1976	15	Traumatic AK	52[d]	0.062[g]	1.19[g]
James, 1973	37	Traumatic AK	51[d]	0.061	1.19
Erdman, 1960	9	AK	47[d]	0.035[b]	0.76

[a]Calculated knowing kcal/min and m/min
[b]Calculated knowing kcal/meter and m/min
[c]Most efficient speed of ambulation
[d]Speed chosen by the subjects
[e]Speed chosen by the researcher (the only speed or a representative speed)
[f]Approximated from a graph
[g]Calculated from O_2 consumption
[h]Original data reanalyzed

Table 3.3.3(b) Summary of Above Knee Amputees energy expenditure (from Fischer & Gullickson, 1978)

study; however only two above-knee amputees were tested, each wearing a single-axis knee unit with no swing control and a SACH foot. The analysis was performed with the amputees walking on level ground at their normal cadence. It was found that the high flexing moment at the knee joint of the normal leg during early stance, was due to the prosthetic limb being unable to control the forward falling of the body, resulting in the normal leg striking the ground at a considerable velocity. Furthermore, only a small flexing moment at the hip joint of the prosthetic leg during early swing was found to be sufficient to accelerate the prosthesis. This implied that active plantar flexion of the foot is not essential as far as acceleration of the prosthesis is concerned.

3.3.3. Energy Requirement Studies

Fischer and Gullickson (1978) carried out a literature review on the energy cost of ambulation in health and disability. Table 3.3.3(a) and (b) show summaries of results obtained from various investigations on energy cost of ambulation in below- and above-knee amputees respectively. The general conclusions drawn from averaging the results of those studies in which subjects chose their own speed of walking were:

1) The average below-knee amputee walks at 55 m/min, expends 64.3(cal/min)/kg and 1.077 (cal/m)/kg.
2) The average above-knee amputee walks at 50 m/min, expands 59.8 (cal/min)/kg and 1.444 (cal/m)/kg.

Huang et al (1979), using the Mobile Automatic Metabolic Analyzer (MAMA) obtained the energy costs of ambulation for 66 below- and 65 above-knee amputees. It was found that the average comfortable speed of walking for below-knee amputees was 48 m/min and the average

energy expended was 48 (cal/min)/kg and 0.993(cal/m)/kg. For the above-knee amputees, the average comfortable walking speed was 48 m/min and the average energy expended was 62 (cal/min)/kg and 1.338 (cal/m)/kg. These results were claimed to be within the range reported by other workers as summarised by Fischer and Gullickson.

The results presented show that the below-knee amputees ambulate faster than the above-knee amputees and yet require less energy. This confirmed the statement by Eberhart et al (1954) that the more joints and muscles lost and having prosthetic replacements, the greater the loss of the normal locomotor mechanisms, (major determinants of gait), and therefore the greater the energy cost of ambulation as well as the degree of disability. However, the method of energy expenditure discussed so far can only measure the total energy cost in terms of respiratory gas exchange or metabolic rate. It cannot determine the relative magnitude of the component energy requirements.

Bresler (1951) discussed the use of energy methods for the evaluation of prostheses. He maintained that the energy requirement for walking is one of the important criteria of the performance of a prosthesis. However, he pointed out that the stringent control imposed on persons undergoing metabolic rate studies would be unlikely to be fulfilled with amputee subjects. This would then greatly affect the accuracy of the test and make evaluations based on comparison of metabolic rates very questionable.

He concluded that the use of energy requirement for differential evaluation of prosthetic mechanisms is of doubtful validity since the complicating variables, such as alignment, fit, training, muscular coordination and environmental factors cannot be eliminated. This was

demonstrated by the results obtained from Cummings et al (1979). No clear-cut difference was found between the energy costs of the supracondylar cuff versus sido-joint-thigh corset suspension of below-knee prostheses. Although, the use of energy requirement measurements for the evaluation of prosthesis is not practicable, the measurement of mechanical work is valuable for an understanding of the various operations in walking and for establishing reasonable design criteria.

Bresler et al (1957) presented a study on energy and power in the legs of above-knee amputees during normal level walking. Four subjects using six different types of knee mechanisms and walking at three different speeds were analysed. Although there were a large number of variables and data were not sufficient to provide statistically valid results, the following observations were made :

1) In general, the net energy from the prosthetic leg was adequate to provide for its required movement in space. This was found to be compensated for by the excess of energy provided by the natural leg or body movement.
2) Improvements in the functional characteristics of prostheses which may reduce the energy requirements were initial knee stability, minimising vaulting, push-off compensation, preparation for swing and swing control.
3) Proper design and/or training the amputee could reduce the excessive expenditure of energy recorded.

CHAPTER 4

Prosthetic Feet

4.1. Review of Normal Foot and Ankle Complex

An understanding of the normal is essential for designing prosthetic replacement. Therefore, a brief description of the normal foot and ankle complex is presented to form a basis for further discussions.

4.1.1. Functional Anatomy

The purpose of this section is to correlate some aspects of the anatomy of the foot and ankle complex with function. For further detail of the anatomy of the normal foot and ankle complex, the reader is referred to Warwick and Williams (1973) or Shoji (1977).

The foot basically has two main functions, support and propulsion. Morris (1977) expanded on this and gave a more comprehensive definition. The functions of the foot are to provide :

1) a base of support of sufficient dimensions to give the stability necessary to maintain the upright position without undue muscular effort.
2) a mechanism for the absorption of the rotation of the limb segments above it during stance phase.
3) adequate flexibility for absorption of the shock of the body weight and for accommodation to uneven terrain.
4) propulsion at push-off by becoming a rigid lever.

All these functions are made possible through the complex joints, muscles and ligaments. The following will be a brief description of those structures that contribute most to the functions of the foot.

Since terminology used in the literature to describe the ankle complex of joints has been inconsistent

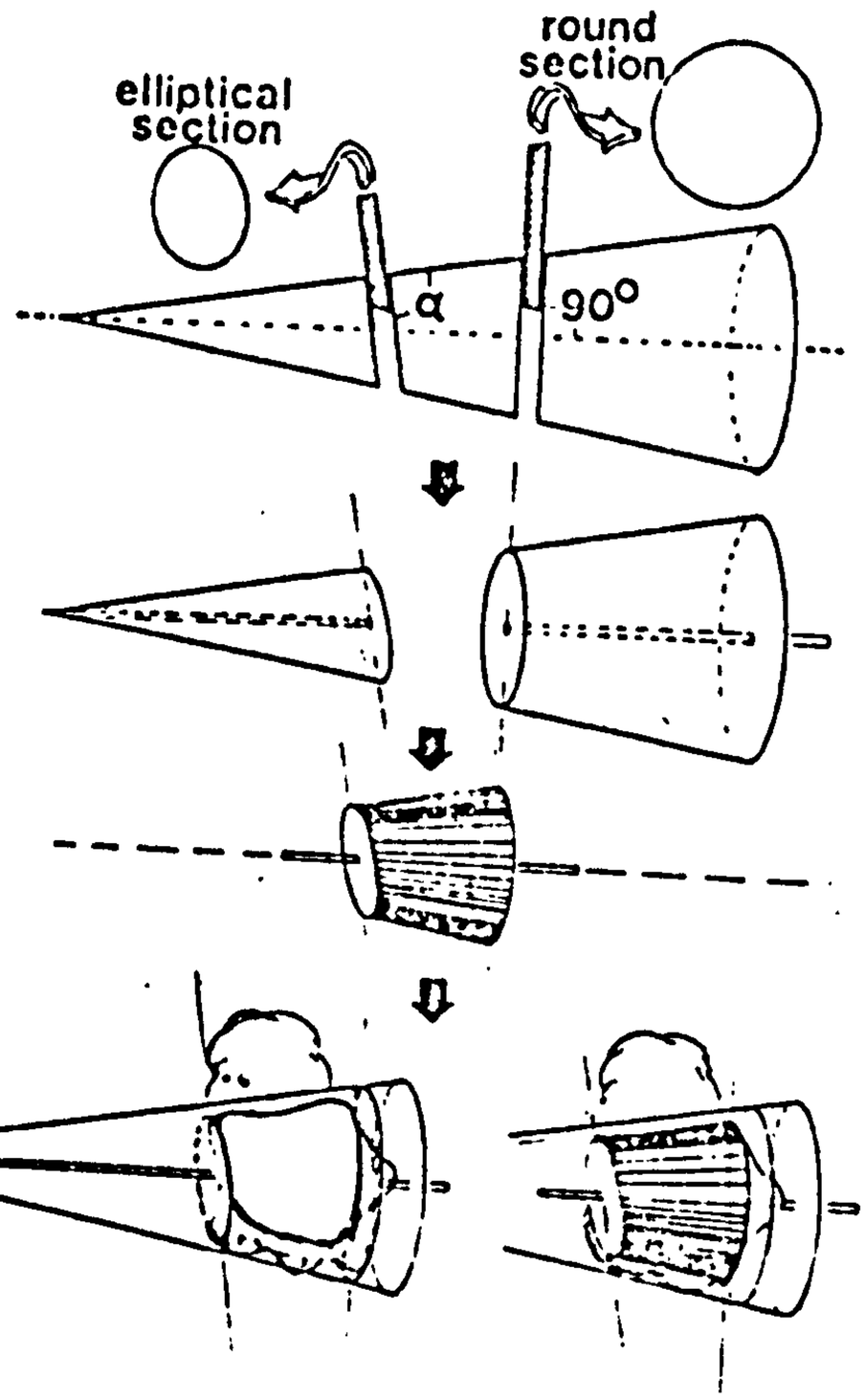

Pictorial representation of present concept of construction of trochlea of talus A frustum is cut from a cone. The section cut at 90° to the axis of the cone is circular when projected onto a transverse plane of the cone (see Barnett and Napier, 1952): this corresponds to the fibular (lateral) facet. The section cut obliquely is elliptical, this corresponds to the tibial (medial) facet. Note that the fibular facet, being farther from the apex of the cone, possesses greater dimensions With minor modifications, a section of the frustum is converted into the trochlea of the talus. The anteroposterior curve of the fibular facet is an ellipse because of the oblique orientation of the conical surface of the trochlea when viewed from above.

Figure 4.1.1(a) Model of Conical trochlea concept
(from Inman, 1976)

and often confusing, an explanation of the terms used here will be given to avoid any misunderstanding.

The ankle joint proper is the articulation between the talar trochlea and the mortise formed by the distal end of the tibia and fibula. The trochlea is slightly wider anteriorly than posteriorly. The malleolar articular surfaces are also wider anteriorly than posteriorly. Close and Inman (1952) demonstrated that the surface of the trochlea is conical in shape, with the base of the cone towards the fibula. Figure 4.1.1(a) illustrates a proposed model of the concept from Inman (1976). The conical surface of the trochlea imposed an external transverse rotation of the talus in the mortise when the foot is dorsiflexed. Furthermore, the lateral malleolus will be displaced by an extremely small amount of between 0.13 - 1.8 mm, as reported by Close and Inman. These displacements are permitted by the anatomical attachments of the three-part lateral collateral ligaments. Plantar flexion will produce internal rotation at the ankle joint and return the lateral malleolus to its original relative position.

The primary movements of the ankle joint are dorsiflexion and plantarflexion. Inman (1976) concluded from his study on the joints of the ankle that for all practical purposes, motion at the ankle joint can be considered to be about a single axis. He stated that the average ankle joint axis is $8\frac{1}{2}^{o}$ to the mid-line of the foot in the transverse plane and 10^{o} to the horizontal in the sagittal plane, see Figure 4.1.1(b). Isman and Inman (1969) were able to relate the ankle joint axis to the most medial point of the medial malleolus and the most lateral point of the lateral malleolus, see Figure 4.1.1(c).

The 'normal' free range of motion in the ankle

(a) Superior view

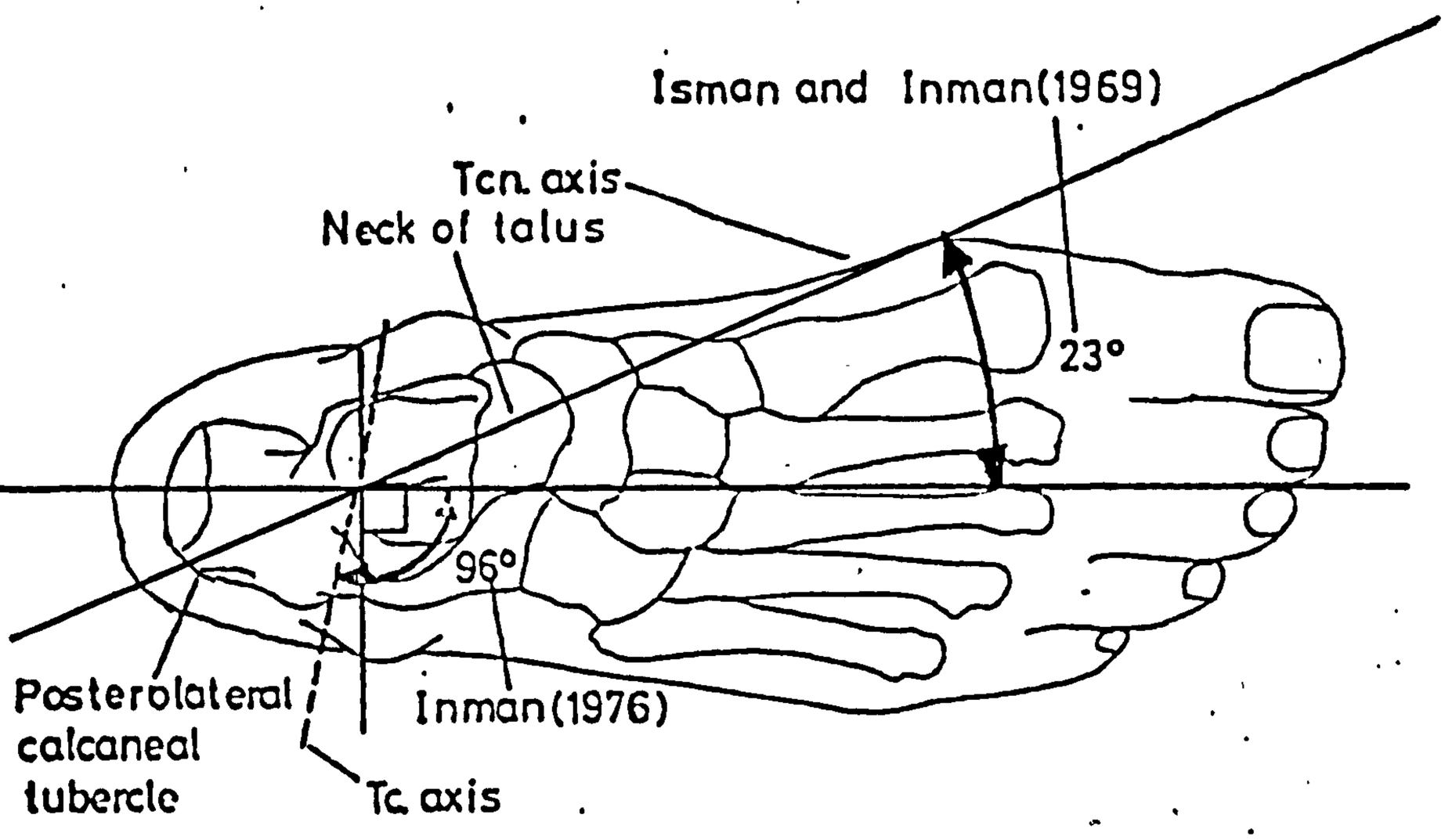

(b) Lateral view

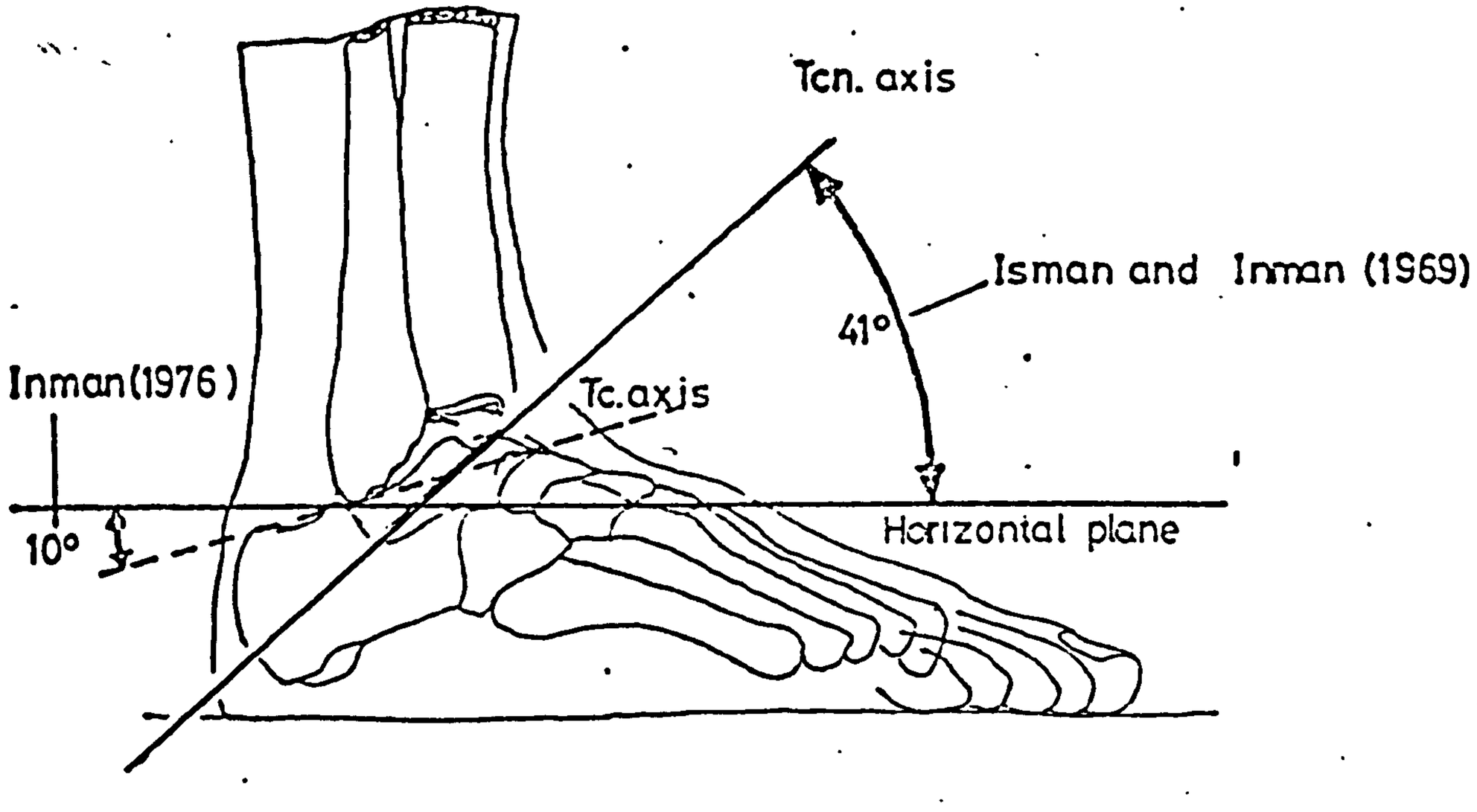

Figure 4.1.1(b) Ankle(Tc) Joint Axes and Subtalar(Tcn) Joint Axes projected on the right foot

joint is 20^{o} of dorsiflexion and 50^{o} of plantar flexion (Mann, 1975). In normal locomotion, the range reported is much less, 10^{o}dorsiflexion and 20^{o} to 30^{o} of plantar flexion. (Close and Inman,1957 ; Wright et al, 1964, Root et al, 1971). During the walking cycle, plantar flexion occurs from heel-strike through approximately the first 10% of the cycle, then dorsiflexion occurs from heel-off to 40% of the cycle at which time plantar flexion again occurs. The ankle is normally in dorsi-flexion during swing phase.

The subtalar joint comprises three articulations between the superior surface of the calcaneus and the inferior surface of the talus. The posterior articula-tion is between the concave facet of the talus and the convex facet of the calcaneus. The middle articulation is between the facet of the undersurface of the talus and that of the sustentaculum tali of the calcaneus. The anterior articulation is between the convex under-surface of the head of the talus and a small concave facet of the calcaneus. Within normal range of motion, these three articulations essentially move in unison about a single common axis. This axis of motion passes through the subtalar joint obliquely, behaving like a mitre hinge (see Figure 4.1.1(d)).

The average subtalar joint axis is 41^{o} to the horizontal in the sagittal plane and 23^{o} to the mid-line of the foot in the transverse plane, see Figure 4.1.1(b). Isman and Inman (1969) stated that there appeared to be no accurate method of determining the axis of the sub-talar joint from prominent anatomical landmarks in the living subject.

Root et al (1977) stated that the subtalar joint moves in the direction of supination and pronation and that in relation to the leg, supination of the subtalar

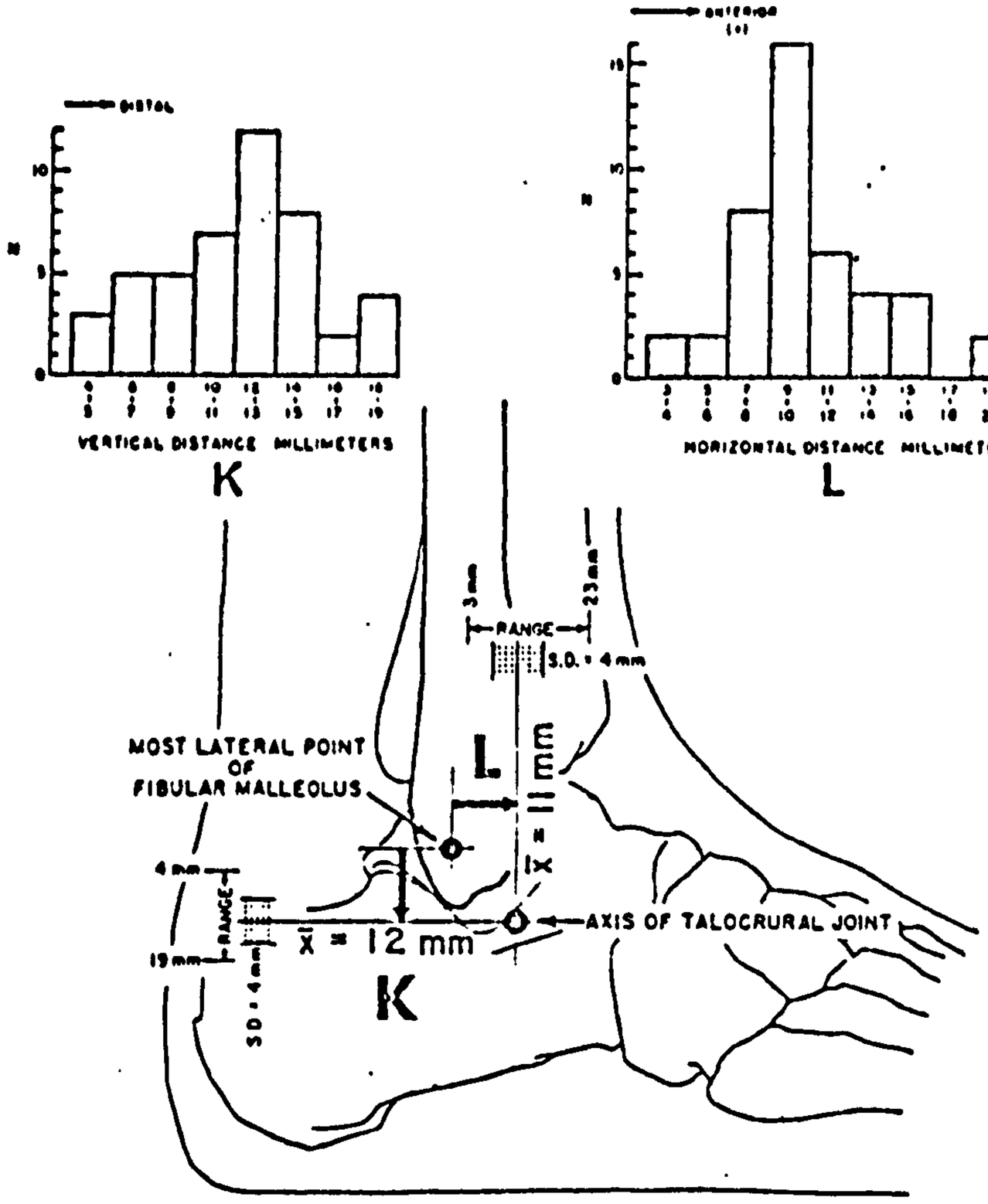

FIGURE .—Location of axis of talocrural joint with respect to most lateral point of lateral malleolus.

Figure 4.1.1(c) (from Isman & Inman, 1969)

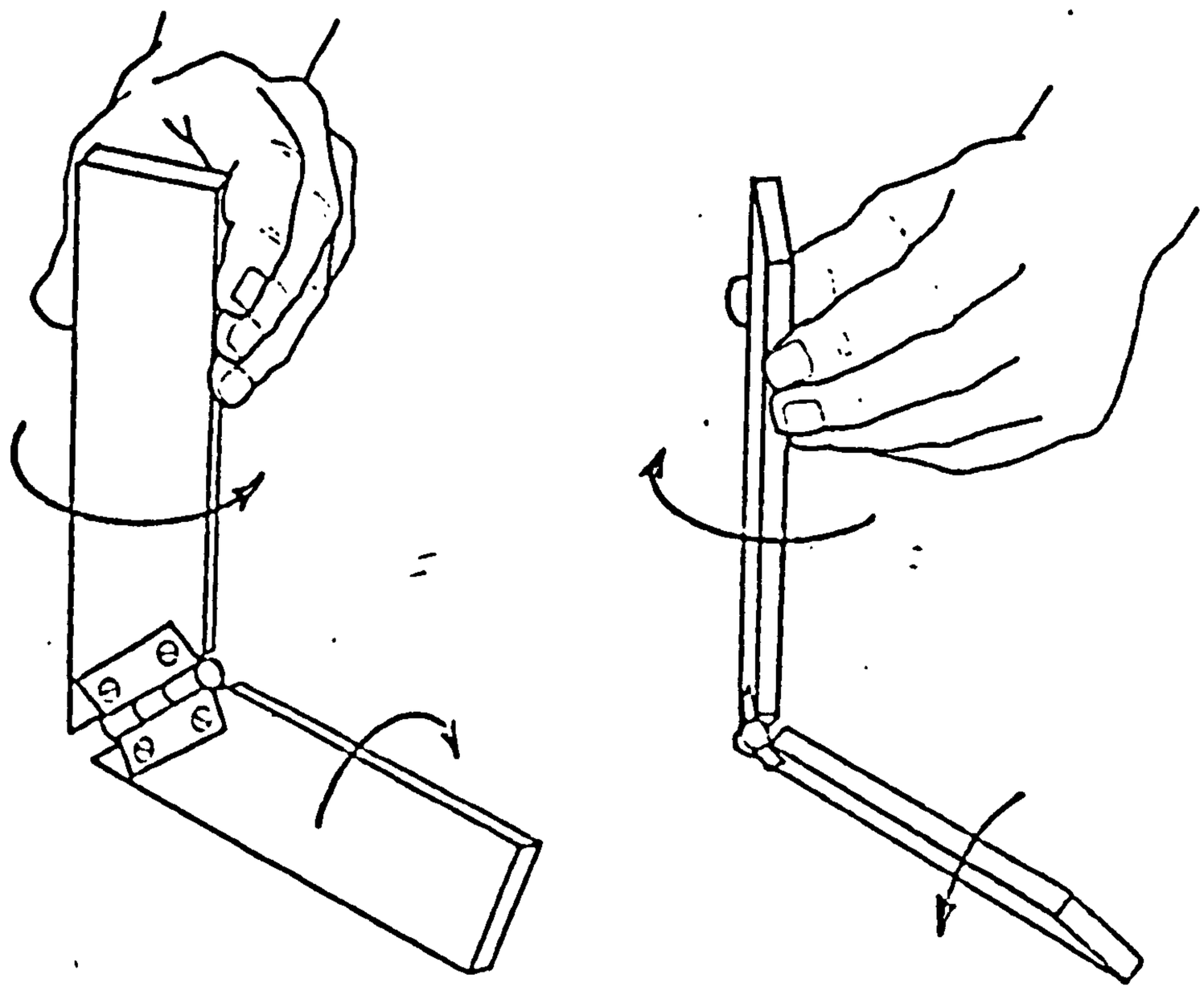

Movements of segments connected by a mitered hinge.

Figure 4.1.1(d) Mitre hinge concept of Subtalar Joint (from Inman, 1976)

joint inverts the calcaneus twice as much as pronation can evert the calcaneus. They stated that measurement of the range of inversion-eversion of the calcaneus is not really a measure of supination-pronation at the subtalar joint; it is in fact only the frontal plane component of subtalar joint supination-pronation. Root et al (1971) reported that in normal locomotion, an average minimum range of 4^{o} to 6^{o} inversion of the calcaneus with supination of the subtalar joint and 4^{o} to 6^{o} eversion with pronation are required.

The mid-tarsal joint consists of the talonavicular and calcaneocuboid joints, which function together about two common axes of motion. Both these axes pass obliquely through the foot in an anterior, medial and dorsal direction but the obliquity of the angle with which each axis passes through the foot is quite different, see Figure 4.1.1(e). The average longitudinal axis is 15^{o} from mid-line of foot in the transverse plane and 9^{o} from the horizontal in the sagittal plane. The average oblique axis angles 52^{o} from the transverse plane and 57^{o} from the sagittal plane (Manter, 1941).

When the hindfoot is everted, these two axes of motion will be parallel and free motion can occur (Elftman, 1961), thus resulting in an increase in flexibility or instability. However, when the rearfoot is inverted, the axes are no longer parallel, restriction of motion is imposed and stability is increased.

The minimum range of mid-tarsal joint motion about the longitudinal axis is given as 4^{o} to 6^{o} by Hicks (1953), while motion about the oblique axis is unknown. The rearfoot normally everts 4^{o} to 6^{o} during normal locomotion and the rearfoot requires to be able to invert to compensate for that amount of calcaneal eversion.

(a) Superior View

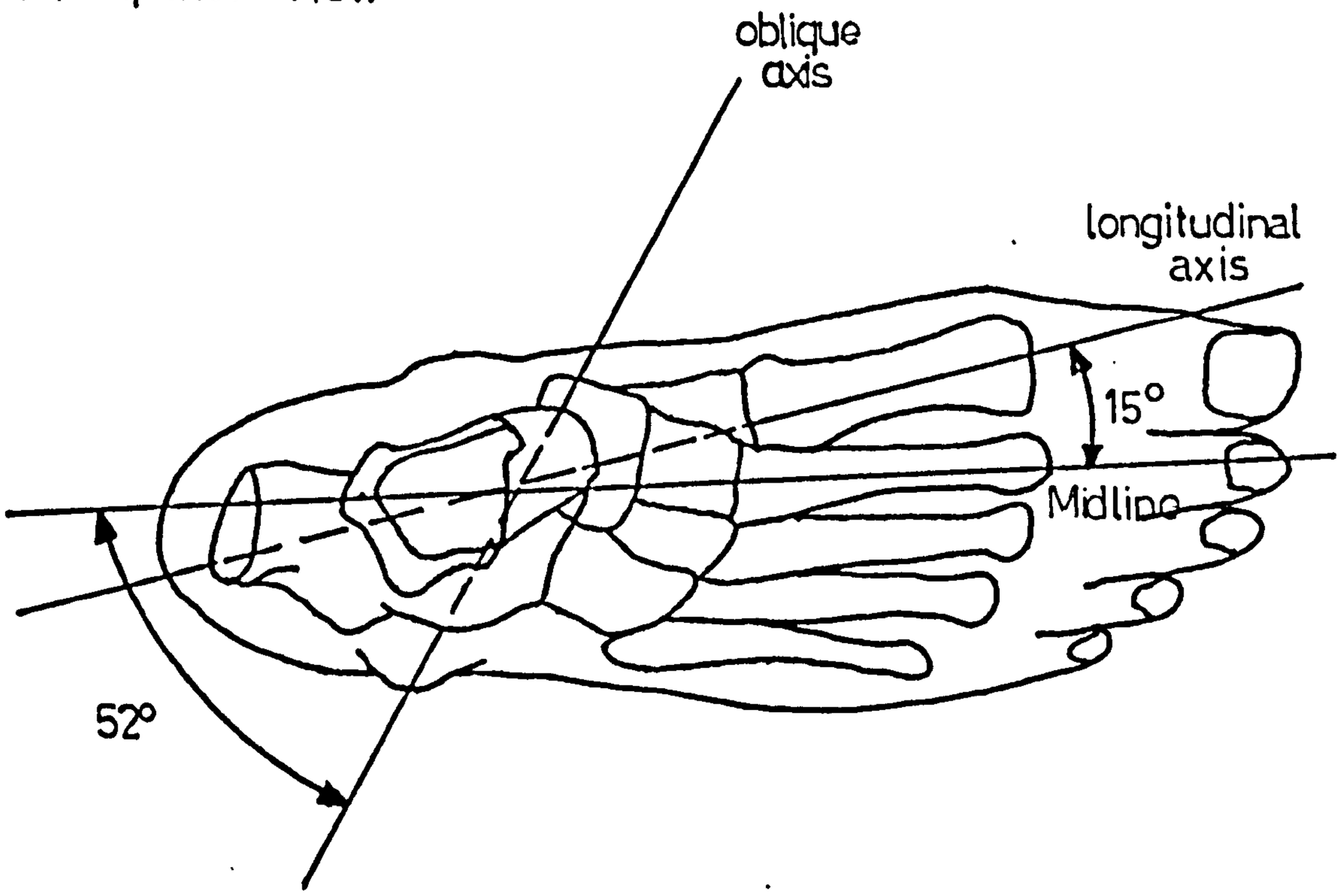

(b) Lateral View

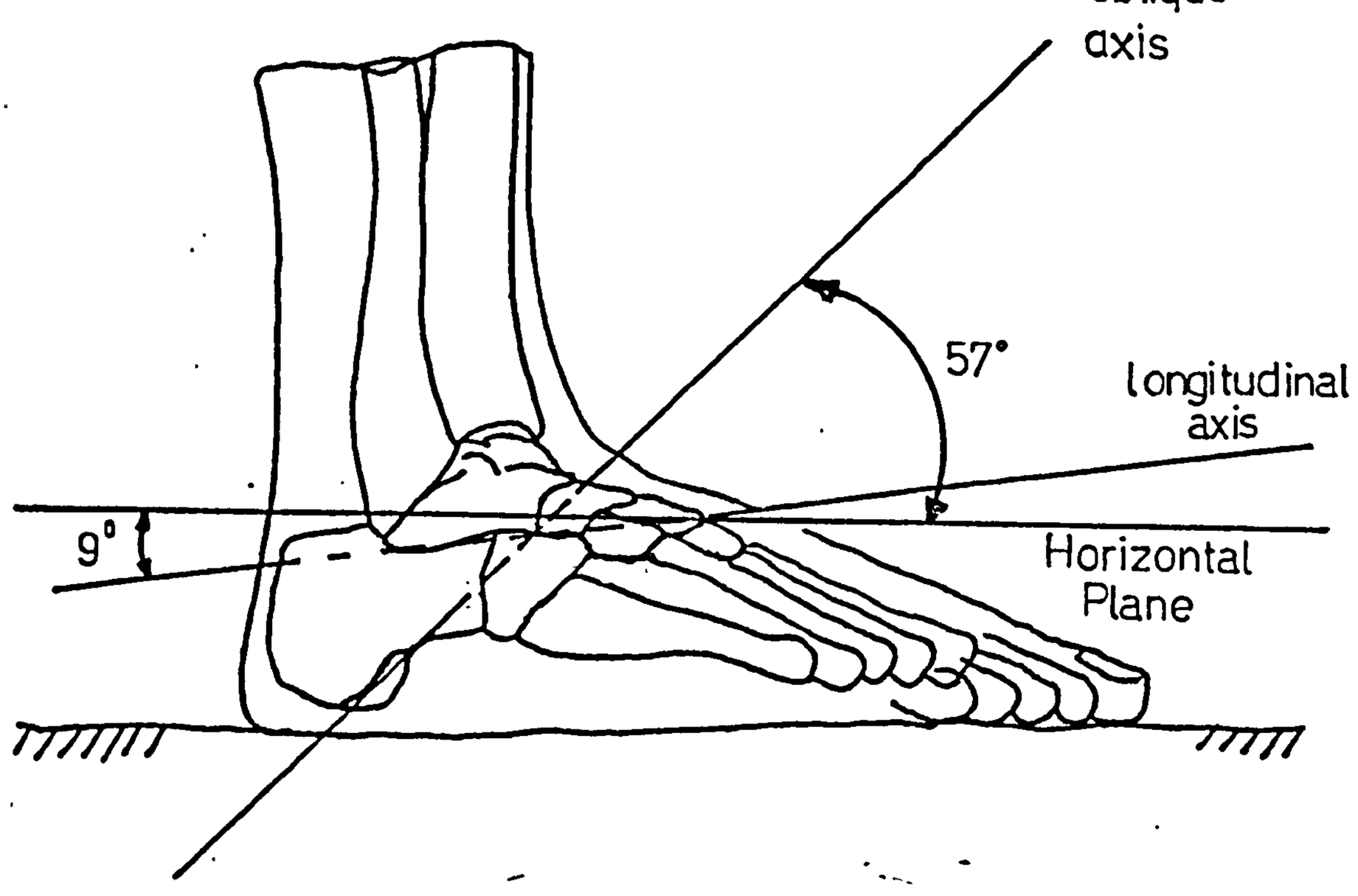

Figure 4.1.1(e) Midtarsal Joint axes projected on the right foot

The metatarsophalangeal break refers to the oblique axis through the second to fifth metatarsophalangeal joints. Isman and Inman (1969) reported that the angle between the break and the mid-line of the foot in the transverse plane varies from 53° to 73°. During push-off, the rearfoot and midfoot are angled outward as the heel is inverted and the metatarsophalangeal break distributes weight on all the metatarsal heads.

Another important feature in the foot, essential to providing successful functions, are the arches. The twenty-six bones of the foot are held together by ligaments, connective tissue and capsules. The seven tarsal bones and the five metatarsal bones are arranged in such a manner as to form a triangular shaped arch having one common base proximally, the calcaneus, and five bases distally, the metatarsal heads. The medial side of the arch is highest while thelateral side is on the ground. This led Jones (1949) to describe the arch as a half-dome, which is geometrically a stable structure. The articulating bones in the half-dome allow the foot to be flexible, while with the long plantar ligament and plantar fascia attached to the ends of the half-dome, the foot can become very strong and stable, capable of resisting the forces of the super-incumbent weight.

The extrinsic muscles in the leg and the intrinsic muscles both play a vital role in the mechanics of the foot. The pretibial muscles dorsiflex the foot during swing phase and early stance. This action enables the foot to clear the ground during swing phase and then allows it to be placed gently on the ground after heel strike. The calf muscles act from midstance to toe-off plantar flexing the foot. During this period the intrinsic muscles of the foot are also active, stabilizing the foot.

WALKING CYCLE

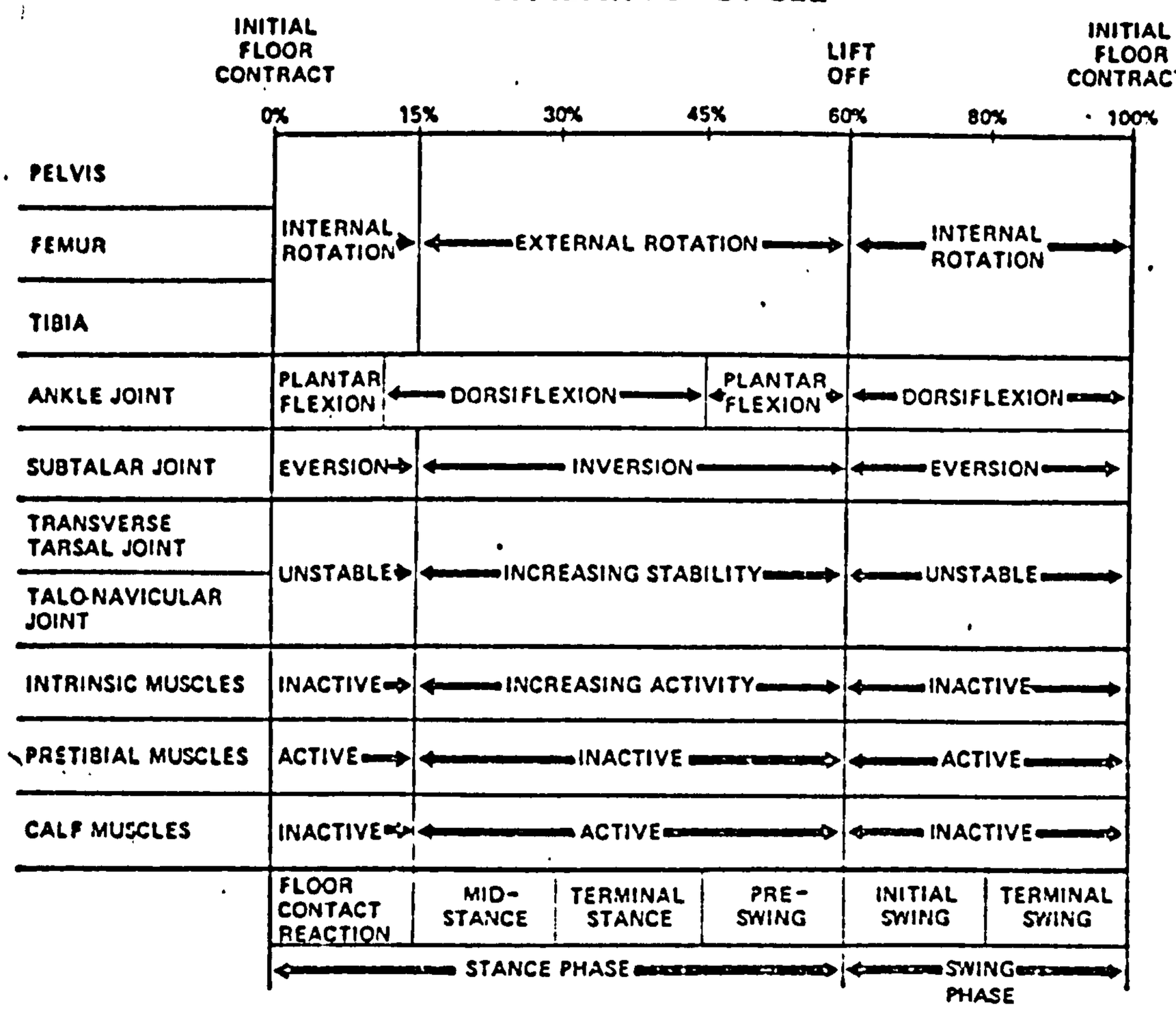

Fig. Schematic diagram of complete walking cycle, showing rotations that occur in the various segments and joints as well as the activity in the foot and leg musculature.

Figure 4.1.1(f) (from Mann, 1975)

Mann and Inman (1964) found that there was very little significant activity of the intrinsic muscles during the first half of stance phase, therefore they concluded that the entire weight of the body must be borne by bones and ligaments. Mann (1975) presented a schematic diagram of the inter-relationship between joints and muscular activities in one walking cycle, see Figure 4.1.1(f).

4.1.2. Biomechanical Studies

Levens et al (1948) reported that there are significant transverse rotations in the lower limb segments during level walking. (Note that this was briefly discussed in Section 2.4.1. also see Figure 2.4.1(g)). These rotations increase from the proximal to distal segments, which means that the thigh and shank do not absorb rotation imposed by the trunk but instead they increase it. Normally, during level walking, the pelvis rotates an average of 6^{o}, the femur 14^{o} and the tibia 18^{o}. Since these rotations also occur during stance phase, when the foot is fixed on the ground and does not slip, some form of mechanism in the foot must be present to permit these rotations and yet be resistant enough to produce a measurable torque (Eberhart et al, 1947).

Wright et al (1964) suggested that the ankle and subtalar joints act together somewhat like a universal joint to convert the transverse rotation of the leg into supination-pronation of the foot. Inman (1976) pointed out that this concept is true only if the two axes of motion intersect and are orientated perpendicular to one another. This however is not the case with the ankle and subtalar joints axes. Jones (1949) and Inman (1976) suggested that the oblique orientation of the ankle and subtalar joints axes together might be a form of mechanism that allows axial rotation of the leg to be transmitted

to the foot. Further discussion on this mechanism is undertaken in relation to the walking cycle.

In normal locomotion, the foot spends about 60% of the walking cycle in contact with the ground (stance phase) and the remaining 40% swinging through to take up its new position ahead of the supporting foot (swing phase) (Murray et al, 1964). The stance phase is of primary importance when considering the biomechanics of the foot. In order to review the events that occur during stance phase clearly and systematically and also to simplify discussion, the stance phase can be divided into three periods.

The first period extends from heel contact to foot-flat. As the heel strikes the floor, the impact and the subsequent loading of the foot results in a floor reaction that exceeds 20% of the body weight. (Eberhart et al, 1947). This sudden impact is partially absorbed by lowering the body through plantar flexion of the ankle and the pronation of the foot, which helps to flex the knee, Saunders et al (1953). The foot at this period is also subjected to a posterior shear due to the moving foot being suddenly stopped by friction from the ground as contact is made. A small amount of lateral shear is also experienced by the foot as the body weight is shifted from one weight bearing foot to the other. During this period, the entire lower limb rotates internally (Levens et al , 1948), a follow-up event from mid-swing. The foot at this time is still free to move and therefore participates in this rotation. In addition, the plantar flexion of the foot further exaggerates this internal rotation. Therefore the ankle joint does not appear to have absorbed this internal rotation but rather increases it, and depending upon the obliquity of the ankle axis, the foot will toe-in to a varying degree (Inman, 1976). The internal rotation of the leg causes the foot to pronate

through the action of the subtalar joint. The pronation of the foot enables the mid-tarsal joint to be mobile and therefore gives the foot the ability to adapt to irregular walking surfaces.

The next period occurs from foot-flat to heel rise. This period is characterised by vigorous muscular activity in the intrinsic foot and calf muscles, see Figure 4.1.1(f). The vertical floor reaction decreases to less than the body weight (i.e. 65%). During this period the leg reverses the direction of its axial rotation to external rotation and thus supinates the foot through the action of the subtalar joint. The supination of the foot causes the talonavicular joint axis to be no longer parallel to that of the calcaneocuboid joint, thereby locking the midtarsal joint (Elftman, 1960) to increase stability. Since the foot is fixed and immobilized, the supination is absorbed by the flexible arch mechanism through twisting along its longitudinal axis and thus elevating the longitudinal arch. This elevation converts the foot from being flexible during the first period into a rigid lever for transferring the body weight to the forefoot and subsequent push off. The intrinsic muscles of the foot add further support to the longitudinal arch to keep it rigid.

The final period stretches from heel rise to toe off. During this period the heel rises rapidly with increased ground reaction which may exceed 20% above the body weight. An anterior shear is also caused by the heel lift as well as the active push off which imparts a linear acceleration to the trunk. As the heel rises, the metatarsophalangeal joints begin to extend and cause the plantar fascia to be in tension, which further raises and stabilizes the longitudinal arch. Hicks (L954) called this the "windlass effect" of the plantar fascia. This period is also characterised by the relative plantar

flexion and the progressive supination of the foot, causing increased external rotation of the leg through the action of the subtalar joint. As the foot tips forward onto the metatarsal heads, the lateral metatarsal heads tend to leave the ground as a result of the oblique axis of the metatarsophalangeal break. However, the supination of the foot diminishes this effect and provides the mechanism to distribute the body weight over the metatarsal heads.

During the swing phase the foot is actively dorsiflexed to provide ground-foot clearance for the leg to swing through, preventing the toe from stubbing the ground.

4.2. Prosthetic ankle/foot mechanisms

From the study in the previous section, it is evident that the normal foot and ankle complex is a unique structure. It is flexible during swing phase and early stance, and then converts into a rigid lever arm prior to toe-off. The flexibility is required for the foot to be adaptable to uneven terrain and by becoming rigid the foot provides support and stability during midstance.

The basic movements of the normal foot and ankle complex are plantar flexion and dorsiflexion, supination and pronation. Transverse rotations of the leg are transmitted to the foot through the action of the subtalar joint and are absorbed by the arch mechanisms. The foot also acts as a shock absorber during heel contact.

To duplicate these functional characteristics of the normal foot and ankle complex reasonably well, the prosthetic ankle/foot mechanisms will have to provide the same freedom of motion with means of restraining and restoring these motions. No prosthetic device designed

to date has approached the complexity of movement of the natural foot and ankle complex. However, a great variety of prosthetic ankle/foot mechanisms have been devised through the years.

This section attempts to lay down the design requirements of prosthetic ankle/foot mechanisms; discuss the validity of the shank axial rotator used to accommodate transverse rotation; present a survey of prosthetic feet and also discuss the "popular" practice of prescribing prosthetic feet.

4.2.1. Design Requirements

It is quite an impossible task to design an artificial ankle and foot that will mimic the natural one exactly. However, certain criteria can be laid down to form a realistic guide in designing a prosthetic ankle/foot mechanism.

The following requirements were basically presented by Vitali et al (1978), they can be discussed initially in terms of the functional aspect of the normal foot and ankle complex. Consider first the stance phase :

1) At heel contact, it should provide some means of shock absorption, and allow plantar flexion without foot slap.
2) Some form of mechanism should be incorporated to absorb the transverse rotation of the whole leg.
3) Some mediolateral movement should be accommodated to adapt the foot to camber on rough ground.
4) It should provide a smooth roll-over when transferring load bearing from the hindfoot to the forefoot.
5) Slight dorsiflexion is desirable before heel rise so as to reduce extending moment on the knee joint.
6) Mechanism for active push-off is desirable.

7) Consideration must be given to stability and support during this phase.

For the swing phase :

1) It must rise at toe-off with knee flexion to clear the ground.
2) Some form of mechanism to actively dorsiflex the foot during this phase is desirable.

The prosthetic foot, being a terminal device, will greatly influence the inertia of the shank. Therefore, to minimise this inertia effect during swing phase the prosthetic ankle/foot mechanism has to be light. The prosthetic device also has to withstand high cyclic loads encountered during walking. This high strength/ weight ratio thus limits the materials that may be used. Hence, functions that can be duplicated will be limited and the mechanism used has to be kept simple.

Besides these functional requirements, the prosthetic ankle/foot mechanism should be aesthetically pleasing. It should simulate the anatomical foot in appearance and the construction of it must be such that the size and shape of the prosthetic one can be matched with the natural foot, so that a normal pair of shoes can be fitted.

The prosthetic device will have to be durable, to avoid high maintenance cost. The materials used will have to be non-toxic and free from any offensive odour. It must also be economcially viable to mass produce to an acceptable standard.

The Veterans Administration Prosthetic Centre has been producing standards and specifications for prosthetic foot/ankle assemblies since 1958. Their latest version,

VAPC-L-7007-2 was published in 1973. The prosthetic foot/ankle assemblies are classified into three classes, according to their functional capabilities. They are :

Class I - foot/ankle assemblies principally designed to provide motion in the anteroposterior plane in simulation of plantar flexion and dorsiflexion of the ankle and extension of the toes.

Class II - foot/ankle assemblies principally designed to provide motions in both anteroposterior and frontal planes simulating plantar flexion and dorsiflexion, inversion and eversion.

Class III - foot/ankle assemblies principally designed to provide motions in three planes simulating plantar flexion, dorsiflexion, inversion/aversion and transverse rotation of the ankle.

The standards and specifications given in the report are supposed to be the minimum levels of function, durability, and acceptable physical dimensions (i.e. weights and shapes) required for proper fitting into a shoe.

Specifications are also given with regards to testing procedures. Each prosthetic foot/ankle assembly is tested by applying graded loads in each of its functional directions. The loads applied and motion required are based on the normal foot and ankle force-motions relations.

Daher (1973) commented that load versus deflection tests should be done with continuous recordings of both loading and unloading. This method would give a hysteresis curve that can be interpreted as a measure of elasticity of the material. Furthermore, he suggested that a "roll-test" method is worth establishing, i.e. a method

of testing resistance to take the foot from heel-contact to toe-off under load. He believed that this would be a more functional test than separate resistance tests of the heel and toe-break, specified by the VAPC.

The VAPC specification also set standards for durability, noise and deformation by cyclic loadings. It specifies that each prosthetic foot/ankle assembly should withstand 500,000 cycles under 150 lb (68 kg) load without failure of any kind. Permanent deformation should not exceed 1/8 inch (0.31 cm).

4.2.2. Axial Rotators

The transverse rotation occurring in the prosthetic leg of the below-knee and above-knee amputees is usually absorbed at the interface between the socket and the stump, generating shear forces on tissues. This shearing action may result in a variety of skin disorders. To solve this problem, the Biomechanics group at the University of California, Berkeley (1947) developed a shank axial rotator.

An axial rotator is a device that permits external and internal rotation to occur when a torque is applied at the prosthesis-floor interface and allows the foot to return to its aligned position gently without altering the gait of the amputee, when the torque is removed.

The original UC-BL shank rotator design was too large and heavy, and it lacked adequate damping of the return spring. A subsequent design was compact but had excessive bearing friction which prevented rotation at the very time it was needed (Mulby and Radcliffe, 1960). Staros and Piezer (1972) and (1973) reported designs that were unable to withstand the severe bending moment which occurs during weight-bearing on the forefoot - others had

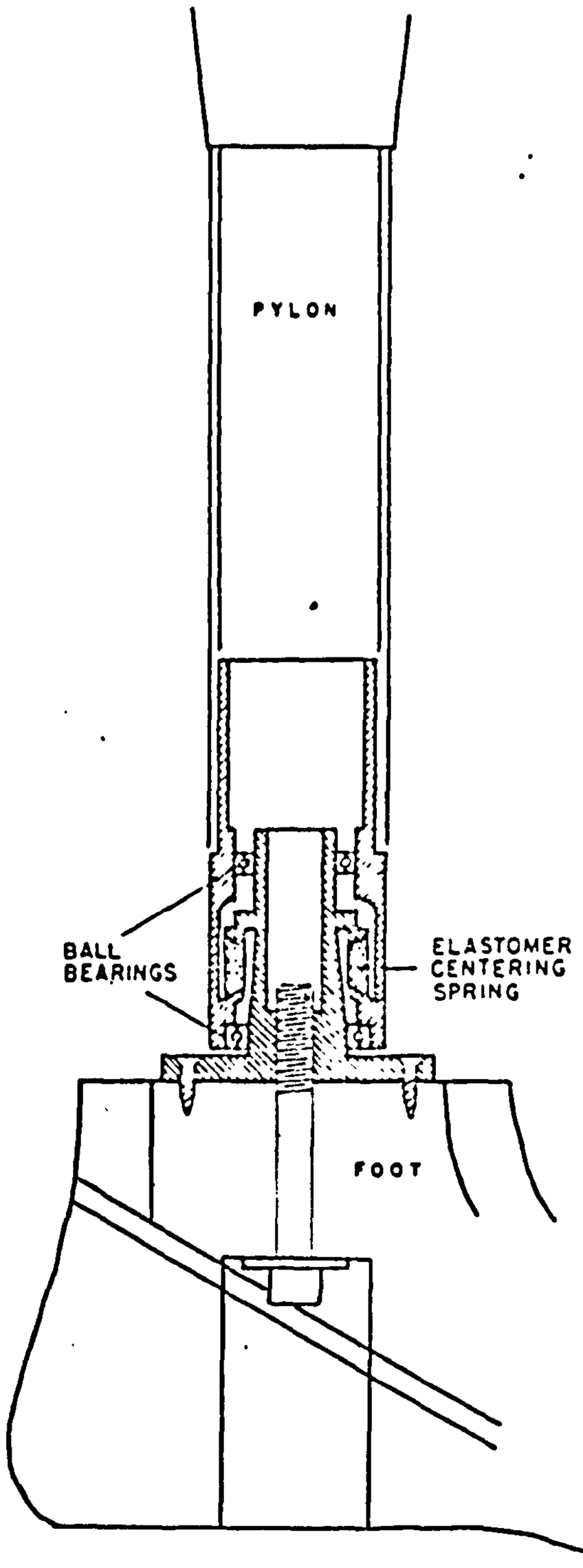

Fig. . The UC-BL shank axial rotation device in cross section. Although the unit is shown mounted on a foot, an alternative and preferred installation would invert the device and mount it as high as possible in the prosthetic shank. This preferred installation moves the mass of the unit proximally and minimizes bulk at the ankle.

Figure 4.2.2(a) UC-BL Shank axial rotator (from Lamoureux & Radcliffe 1977)

excessively stiff return springs or are excessively large and heavy. Therefore, it could be seen that there are a number of difficulties in designing an axial rotator : it has to have high strength and low friction, a soft but well-damped, return spring and be light-weight. Each one of these essential features is vital to the success of the device.

Lamoureux and Radcliffe (1977) established design criteria based on amputee tests of an experimental unit with adjustable stops and variable return spring characteristics. The final recommendation was that a light-weight unit be designed which would permit rotations of up to 20^{o} in either direction about the long axis of a prosthetic limb, with a centralising spring torque of approximate 0.23 Nm per degree of rotation.

The device reported by Lamoreux and Radcliffe consists of a pair of thin-section, "full-ball - complement" ball bearings which support axial loads and bending moments and elastomer torsion spring in a ring configuration as shown in Figure 4.2.2(a). The spring is shaped with conical end plates to allow uniform shear strains throughout the volume of the elastomer. Evaluation was performed by comparing the axial torques occurring in an above-knee prosthesis with and without the axial rotator unit operating.

It was found that approximately 60% of the external torque on the prosthetic shank during late-stance phase was reduced when the axial rotator unit was installed. See Figure 4.2.2(b). It was also found that the relative internal-external rotation between pelvis and above-knee socket increased during stance phase with an axial rotation unit operating. See Figure 4.2.2(c). This increased rotation was attributed to the effects of muscle action within the above-knee socket acting about

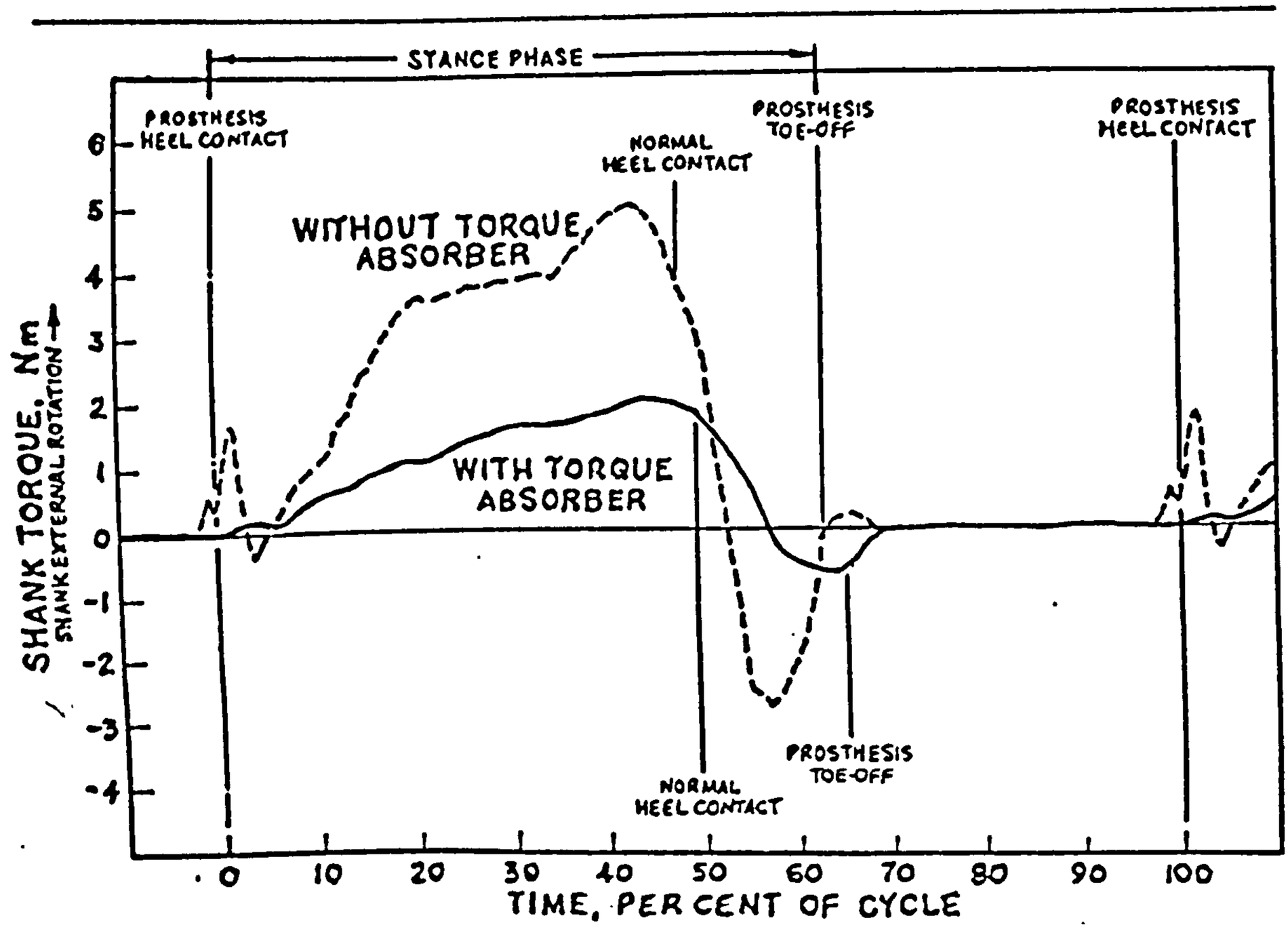

Fig. . A comparison of axial torques occurring in an above-knee prosthesis with and without the Axial Rotation Unit operating. (From Lamoreux and Radcliffe, 1974).

Figure 4.2.2(b)

the long axis of the prosthesis, thus permitting the socket to move freely to relieve the pressures and torques caused by cyclic action ofthe musculature.

Lamoreux and Radcliffe concluded that the use of an axial rotator unit offer the amputee the following advantages :

1) Improved gait symmetry
2) Reduction of axial torques between the stump and the socket.
3) Reduction of the frequency of occurrence or elimination of sebaceous cyst due to skin trauma at the socket brim.
4) Improved freedom of movement when changing direction of motion, working at a bench or counter and in sport activities.

Racette and Breakey (1977) performed a clinical study on the use of axial rotators with 65 below- and 60 above-knee amputees over an 18 month period. Three types of commercially available axial rotators were prescribed. It was found that for below-knee amputees good suspension was required to combat the extra weight of the device. Therefore, many of the 65 below-knee amputees using rotators were fitted with side joints and thigh lacers or PTB with supracondylar/suprapaterllar suspension. All the below-knee amputees reported feeling less shear on the stump and less restriction of motion in performing their varied activities of daily living. This was substantiated by the reduction of previous problem areas seen on the stump of the patients. The Hosmer Modulator was claimed to be the most effective in below-knee prostheses because of its small size and light weight and the most cosmetic for the crustucean type of prosthesis. The weight of the Weber-Watkins design was a contra-indication for its use in below-knee prostheses.

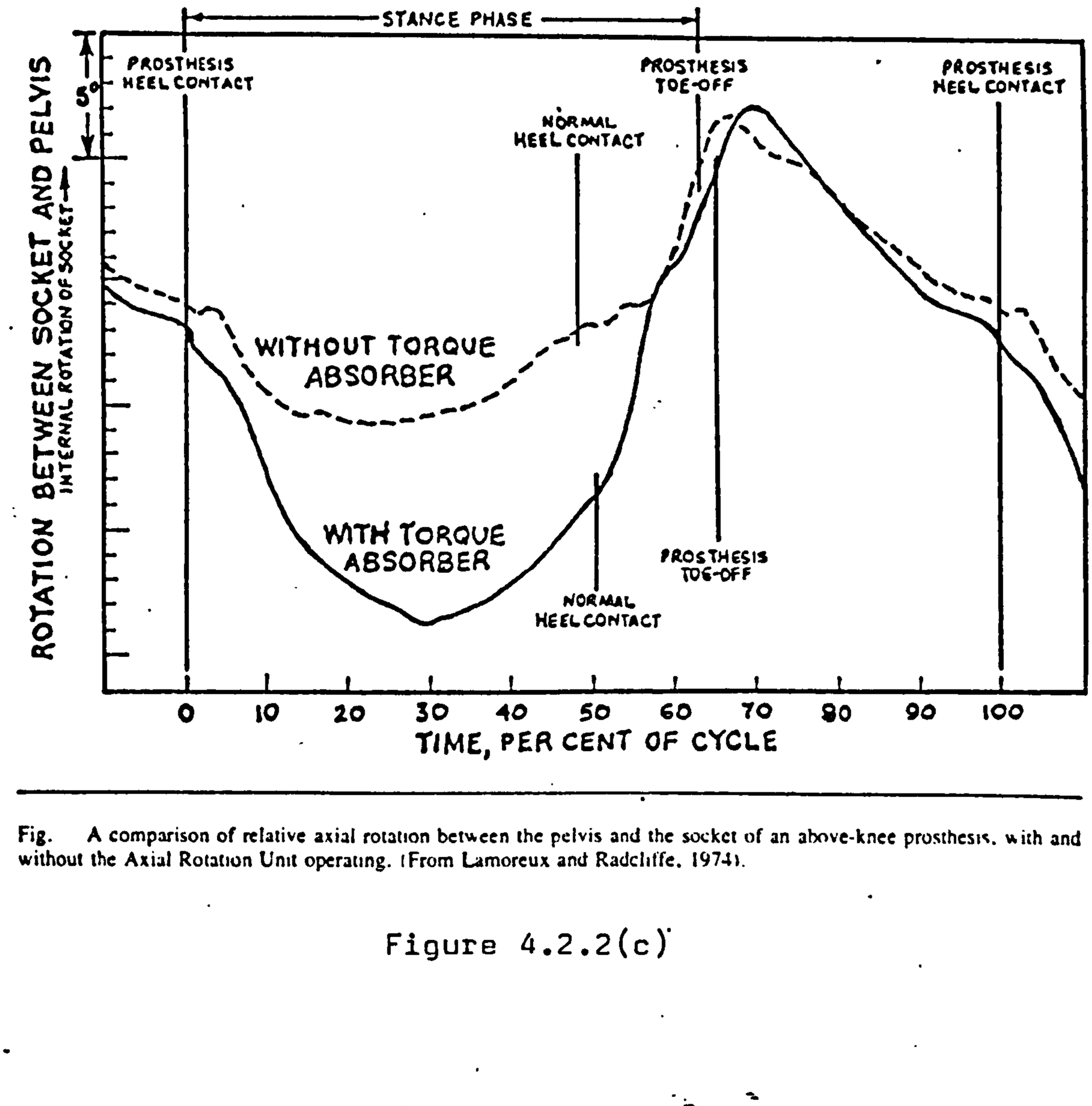

Fig. A comparison of relative axial rotation between the pelvis and the socket of an above-knee prosthesis, with and without the Axial Rotation Unit operating. (From Lamoreux and Radcliffe, 1974).

Figure 4.2.2(c)

Racette and Breakey claimed that the rotator gave most benefit to the above-knee amputees. Most patients with suction socket experienced relief from discomfort in the proximal socket brim area (both medial and posterior). Many reported the clearing up of troublesome skin abrasion in the ischial tuberosity and ischio-pubic ramus regions and generally experienced less soreness. Patients wearing pelvic band and hip joint commented on a much 'freer', less restricted feeling while turning, sitting, getting in and out of cars and many other twisting type of activities. There was generally greater socket comfort with the incorporation of the rotator. Racette and Breakey made the same conclusion as Lamoureux and Radcliffe.

It is probably worth noting that Racette and Breakey reported that extreme care must be taken during the initial period of fitting the rotator. Training to use the rotator is essential to enable the amputee to adapt and appreciate the increased freedom of motion.

Campbell and Childs (1980) pointed out that the transverse rotations absorbed in the prosthetic shank will develop a torque that will externally rotate the prosthetic foot violently and strike the contralateral leg as it swings through. To prevent this, the amputee after the first few steps, will automatically suppress some of these rotations. This could well explain the need to train the amputee to get adapted to the rotator.

While it is clear that during the stance phase, the rotator offers great benefit to the amputee in terms of stump/socket comfort, more research is required to clarify the effects it has during the toe-off/early swing period and also perhaps the amount of damping that may be required to minimise or eliminate these effects.

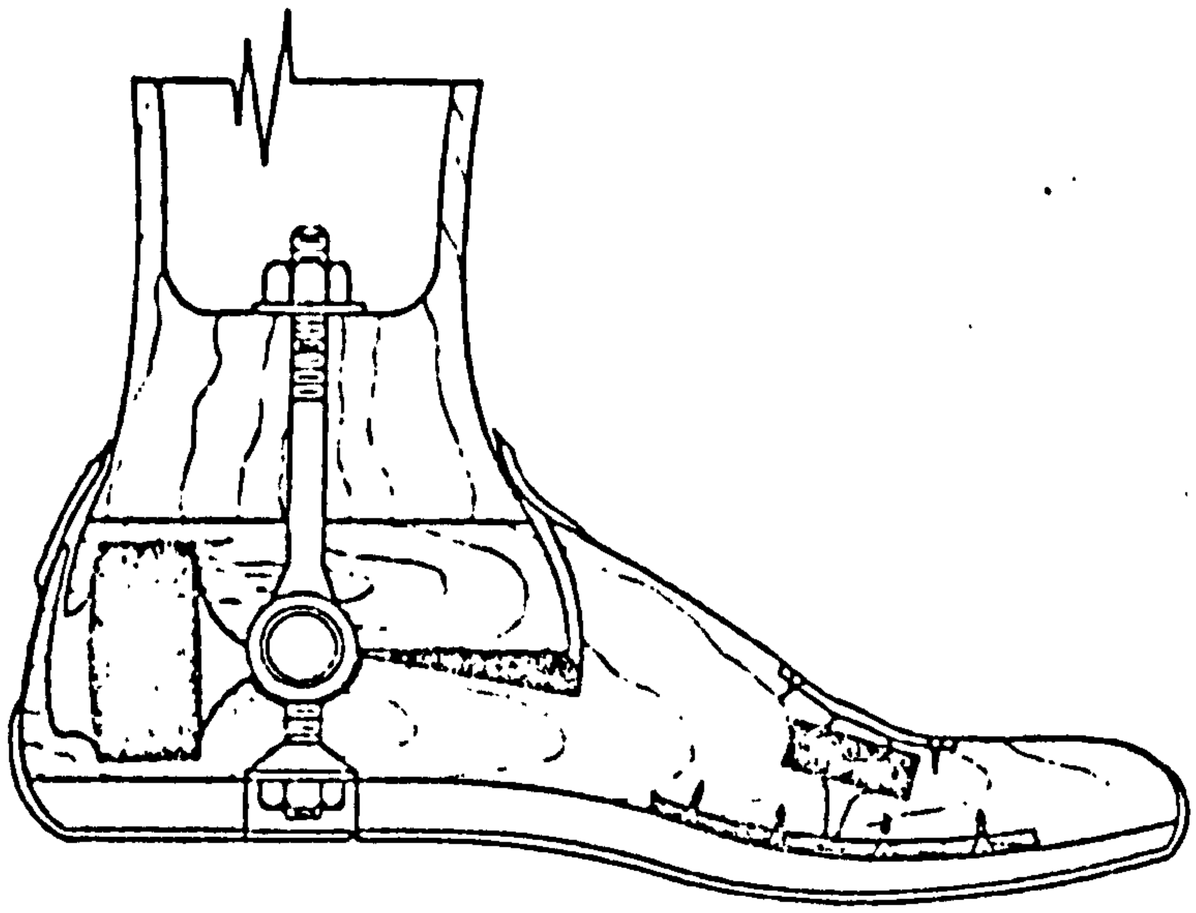

FIG. Conventional ankle/foot assembly.

Figure 4.2.3(a) Single-axis wooden foot with toe-break (from Murphy, 1960)

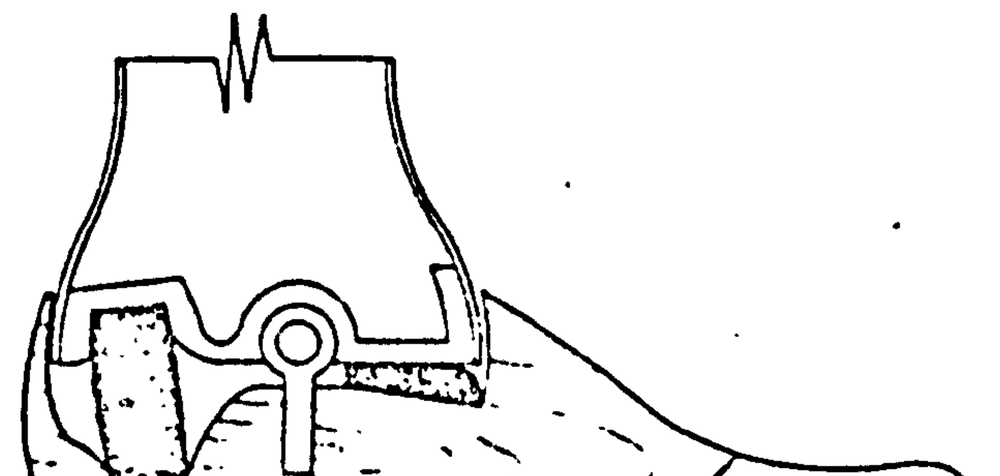

FIG. Conventional wooden foot, felt toe, ankle joint, rubber bumpers, and metal shank.

Figure 4.2.3(b) (from Murphy, 1960)

4.2.3. Review of Some Prosthetic Feet

A large number of prosthetic ankle/foot mechanisms has been designed, some incorporating ingenious mechanisms capable of imitating the functions and movements of the normal foot and ankle complex. However, the complexity of most of the designs, excessive maintenance requirement and their unacceptably high mass have prevented their wide use. References to these prosthetic feet can be found in Gocht et al (1920), Northwestern Technological Institute (1947), Klopsteg and Wilson (1954), and American academy of Orthopaedic Surgeons (1960).

The following discussion will concentrate on some of the popular and commercially available prosthetic feet, as well as some of the experimental designs still undergoing evaluation and development.

By far the most common device has been the Uniaxial (or single-axis) type prosthetic foot. This foot had its origin in 1861, when J.E. Hanger replaced the cords in the American leg by rubber bumpers about the ankle joint. Since then the device has undergone many detail modifications. However, its basic principles of operation still remain the same.

Traditionally, this type of prosthetic foot is made of willow wood, shaped to fit the individual shoe. The wooden foot is then covered with raw-hide. Applied wet, the raw-hide attempts to shrink as it dries, thus subjecting the wood to compression, and thereby reducing the tendency for the wood to split. Plastic laminate however has been regarded as a better alternative, as it has greater water resistance and saves manufacturing time and costs when compared with raw-hide.

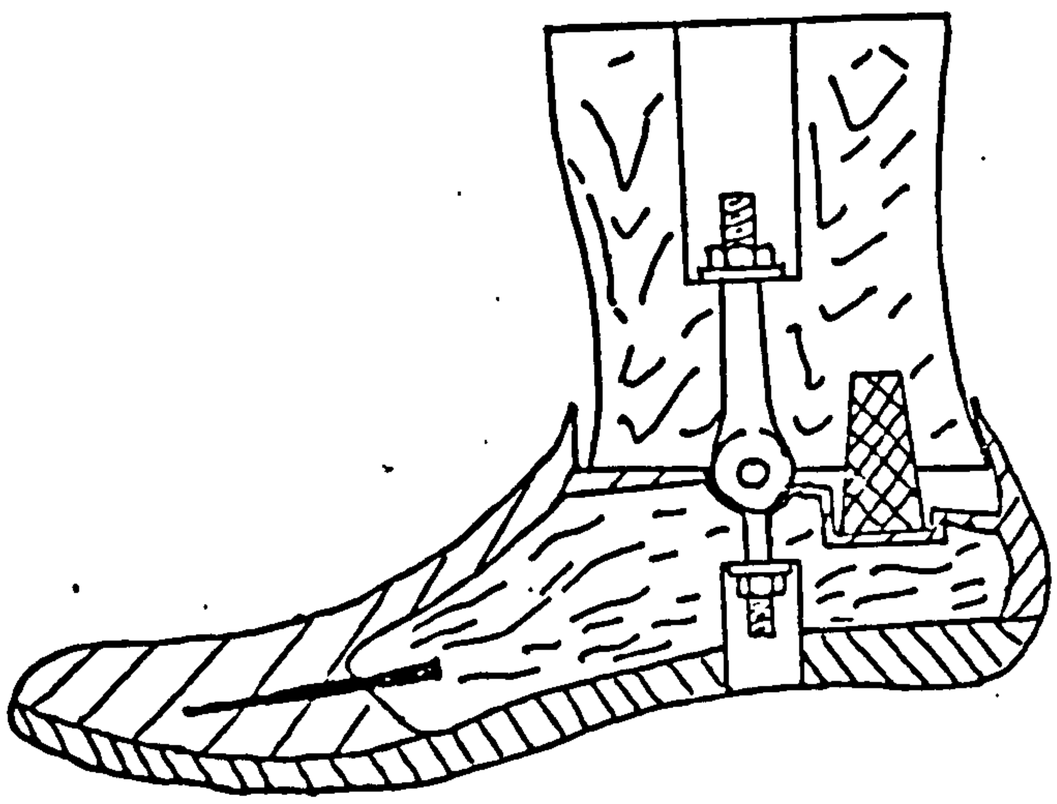

Figure 4.2.3(c) Rubber-moulded Uniaxial foot

Conventionally, the ankle joint provides plantar and dorsiflexion only, with means for restraining and restoring these motions. It consists of a horizontal shaft which is located in plain bushes. The construction of the joint may vary in the choice of bearing material or the means of attachment to the shank, whether by single or double bolts or by the use of U-bolts. The restraining and restoring moments are provided by a compressible plantar flexion (rear) rubber bumper and a relatively stiff dorsiflexion (front) rubber stop. These bumpers are replaceable when worn or permanently compressed. The rear bumper should be relatively soft to provide shock absorption at heel strike and subsequent plantar flexion of the foot, so as to stimulate the action of the pre-tibial muscles. Selection of the correct stiffness of this rubber bumper is important - if it is too hard the knee will buckle and if it is too soft then foot slap will occur. The front bumper has to be fairly hard to provide resistance to compression fulfilling the action of the calf muscles and Achilles' tendon in resisting dorsiflexion and forcing heel rise after mid-stance phase.

A metatarsophalangeal (or toe) break is usually provided by means of a rubber bumper situated in between the forefoot and toe sections, see Figure 4.2.3(a), although in certain designs this toe break is replaced by a felt (or rubber) toe firmly glued to the main wooden foot, see Figure 4.2.3(b).

Most of the commercially available uniaxial feet nowadays are manufactured from a wooden keel embedded in a polyurethane foam rubber moulding, see Figure 4.2.3(c). The distal portion of the wooden keel is carefully shaped to simulate the action of the toe break. A toe-spring, usually made from balata, is included to provide enough resilience to restrain and restore motion during late-

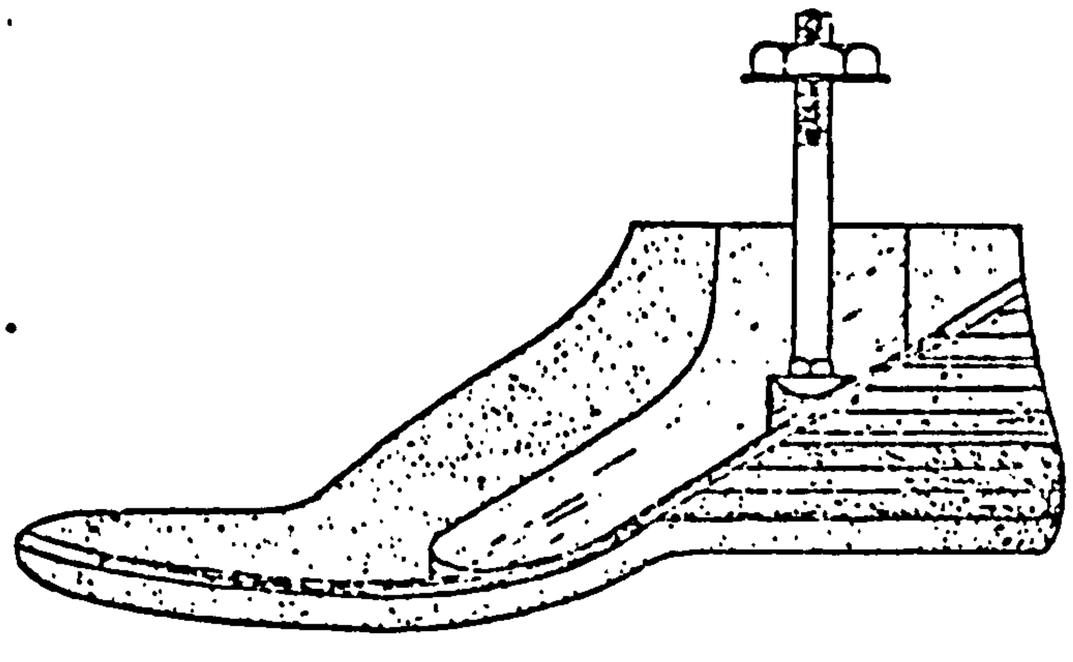

The Solid Ankle Cushion Heel (S.A.C.H.) Foot.
(From *The Patellar Tendon Bearing Below-Knee Prosthesis.* C. W. Radcliffe & J. Foort, Biomechanics Laboratory, University of California, Berkeley & San Francisco.)

Figure 4.2.3(d) The SACH foot

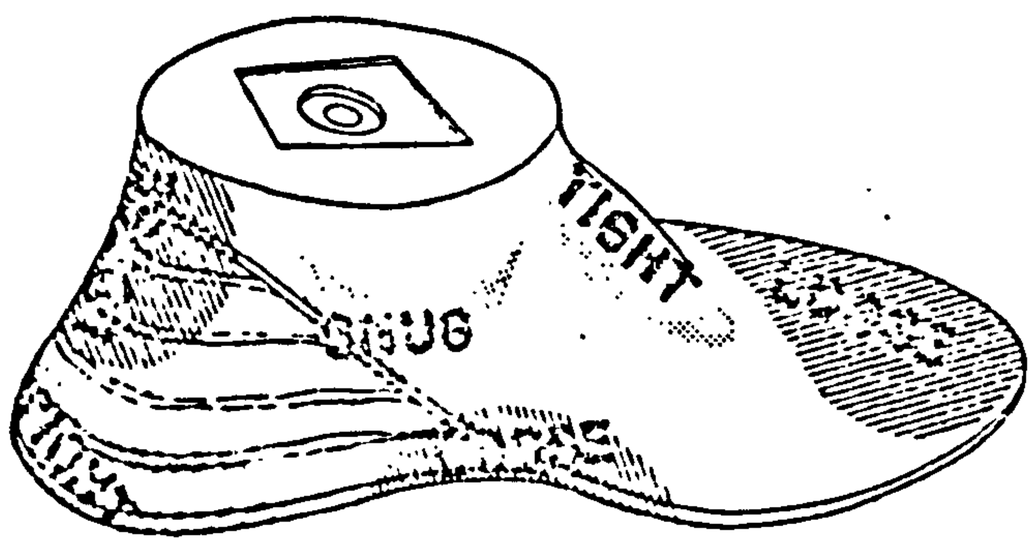

. Shaping of the SACH Foot.
(From *The Patellar Tendon Bearing Below-Knee Prosthesis.* C. W. Radcliffe & J. Foort, Biomechanics Laboratory, University of California, Berkeley & San Francisco.)

Figure 4.2.3(e) Shaping of the SACH foot

stance phase and toe-off. This 'new' generation of Uniaxial foot is designed with the provision of a wooden ankle block for a crustacean type prosthesis as well as a metal foot adaptor for the modular assembled prosthesis.

Compared with most prosthetic feet the Uniaxial foot is not excessively heavy. In certain designs, there is even provision for adjusting the heel height to suit different types of footwear. While the foot itself is fairly durable, the rubber bumper on the other hand requires replacement at intervals, depending on usage. Vitali et al (1978) claimed that on average they last a year or more.

The Uniaxial foot has obvious limitations, there is no provision for mediolateral movement and axial rotation. Although,modification to the basic design, like the Teufel's Telasto foot/ankle assembly, can incorporate a slight degree of inversion/eversion. Other disadvantages included the moving parts of the ankle mechanism which could cause noise and wear. The appearance of the junction line between the prosthetic foot and shank could be objectionable, although the ability to control plantar flexion of the foot does give a better cosmesis during locomotion. It has also been reported that sudden changes in resistance that can arise at the ankle joint during locomotion have caused problems for some amputees.

In order to overcome some of these problems, the Solid Ankle Cushion Heel (SACH) foot was developed in the 1950s in order to provide function without the use of an articulated ankle joint, see Figure 4.2.3(d). The basic functional principles of the SACH foot are not new to the prosthetic technology. Many foot designs of similar types have existed for some time. In 1880, A.A. Marks patented an artificial foot for direct attachment to a prosthetic shank, with no ankle joint. The patent

describes layers of rubber used to provide sufficient elasticity for toe action, particularly at toe-off. Although not specifically claimed in the patent, the heel position of the foot had rubber of sufficient thickness to provide some degree of plantar flexion during walking. A core made from wood, or any other suitable material was shaped in a manner rather similar to the SACH foot, to provide a smooth roll-over at the end of the stance phase.

In another patent in 1895, G.E. and W.L. Marks described a similar artificial foot having an internal, inelastic core, but also specifying a rubber heel portion which contained a spring which is free to yield with the rubber. They also described the foot as having "actions when under heel or toe pressure as during the act of walking, which greatly enhance the value of the foot and facilitate its use and add comfort to the wearer ..... The foot may be made of sponge rubber for softness, noiselessness and comfort .... to insure the desired resiliency under heel and toe pressure."

Following these patents, there was evidence of limb-shops in the United States, Germany and Austria (Eberhart et al, 1949) fitting artificial feet similar to the basic SACH foot design. In Canada, the design of a lightweight but durable Syme's prosthesis with necessary foot-ankle function was facilitated by the use of SACH foot principles.

Experience gained from studying these preceding designs combined with the locomotion studies by the University of California, Berkeley enabled J. Foort and C.W. Radcliffe to develop the first prototypes of the current version SACH foot. With reference to Figure 4.2.3(d), the SACH foot consists of a wedge of cushioning material built in to the heel and an internal wooden core or keel, shaped at the ball of the foot, in order to

provide a rolling action. Extending from the wooden keel is a toe-spring to reinforce the simulated rubber toe-piece and also to assist in providing the restraining and restoring motion required during late stance-phase and toe-off. The heel material cushions the impact at heel strike and simulates normal plantar flexion closely. The heel also allows a certain degree of movement in the mediolateral direction. The cushion heel is normally available in three different degrees of compressibility; hard, medium and soft, to suit patient requirements.

The SACH foot offers several advantages; it is usually light and in most versions it is durable. It has no articulated moving parts and thus requires little or no maintenance. Furthermore, there is no junction line between the foot and shank, which makes it cosmetically more acceptable. Its main disadvantages are that it has no range of adjustment in plantar- and dorsi-flexion and also replacement of heel wedge is difficult. Moreover, to attain the desired function with the foot, selection and installation of it is of paramount importance. Radcliffe and Foort (1961) presented a detailed description of the fitting procedure. An extremely important feature is the shape of the foot, its fit within the shoe will ultimately govern foot function. There are three areas of particular importance when shaping the foot prior to fitting; the heel cushion, arch of the foot and the toe-section, see Figure 4.2.3(e). The foot should fit into the shoe firmly both in the uncompressed and compressed states.

The SACH foot although permitting a slight degree of mediolateral movement, still lacks in providing transverse rotation. To compensate for this motion, some have tried to incorporate an axial rotator, as discussed previously, while others have resorted to designing a prosthesis that would provide transverse rotation and

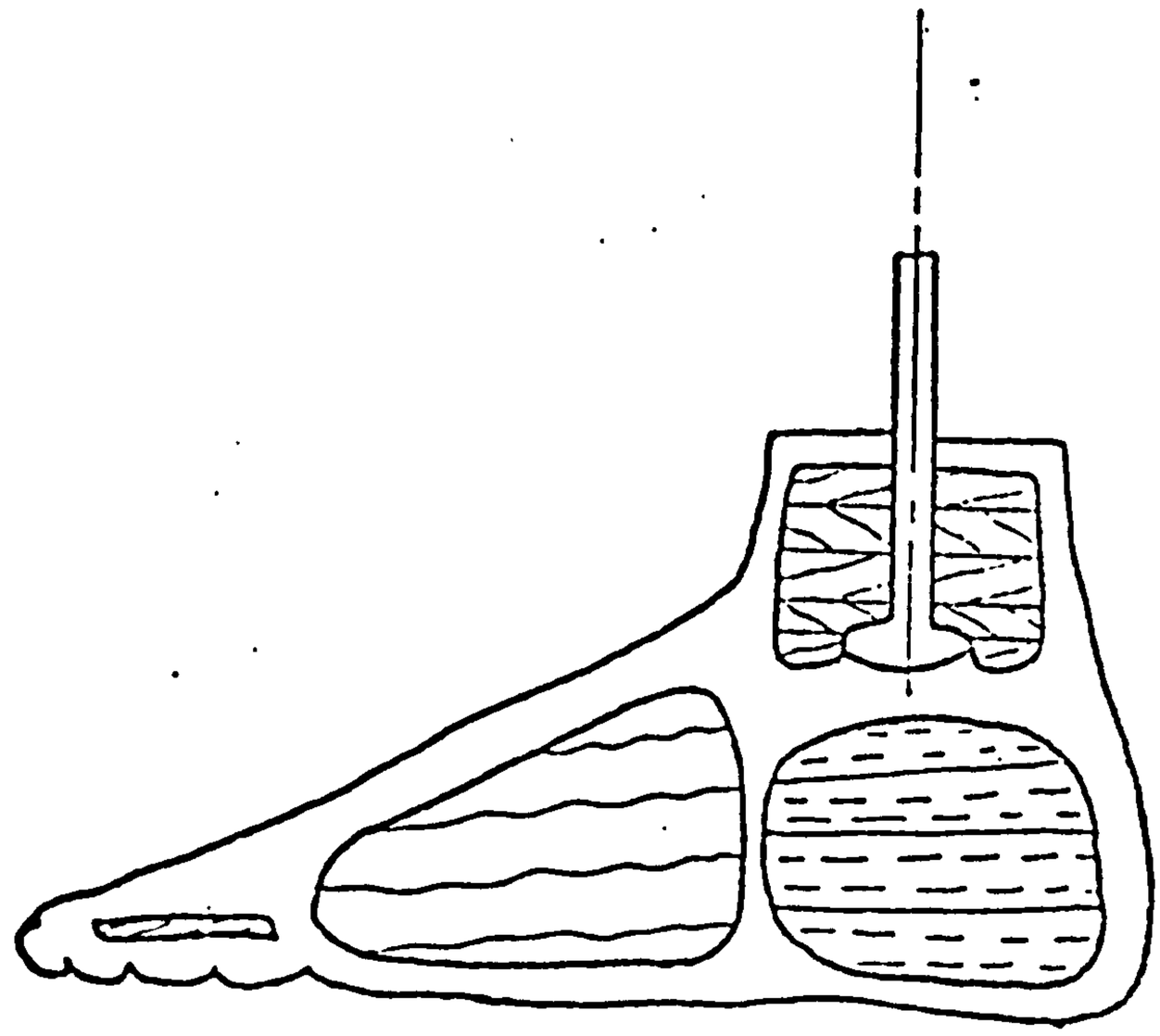

Figure 4.2.3(f) The Jaipur Foot
(from North et al, 1974)

still maintain the solid-ankle cushion-heel principles.

One such design developed recently is the Jaipur Foot, (Sethi et al, 1978). The primary purpose of this development was for amputees living in the rural areas of India. Therefore, certain criteria were imposed on the design :

1) It should not require a shoe and consequently should have a certain degree of cosmesis acceptable to the amputee.
2) The exterior should be made of a waterproof and durable material.
3) It should allow enough dorsiflexion to permit an amputee to squat, at least for short periods.
4) It should permit a certain amount of transverse rotation of the foot on the leg to facilitate the act of walking as well as to allow cross-legged sitting.
5) It should have a sufficient range of inversion and eversion to allow the foot to adapt itself while walking on uneven surfaces.
6) It should be inexpensive.
7) It should be made of materials which are readily available.

The Jaipur foot consists of a proximal wooden block that simulates the lower end of the tibia, which is used for securing the carriage bolt and a distal wooden block that represents the forefoot. The intervening space is filled with layers of sponge rubber glued together and protected by a shell of solid rubber. The whole foot is then enclosed by vulcanized hard rubber reinforced with cord lining giving a strong, durable and waterproof prosthetic foot, see Figure 4.2.3 (f).

The large sponge rubber heel section supposedly allows freedom of movement in all direction, representing

the ankle, subtalar and midtarsal joint complex.

Sethi et al (1978) reported that the foot has been tested in the laboratory as well as in field trials over a period of eight years with more than a thousand amputees. It was found to be very satisfactory and was capable of fulfilling all the objectives. It was claimed that some farmers were using these feet in the environment of Indian villages for as long as 3 years without breakdown. However there was apprehension that the range of dorsiflexion present might lead to a feeling of insecurity, especially in above-knee amputees. They observed that this was not the case because of the physical property of the hard rubber which provides a substantial resistance to dorsiflexion at the initial stage and then yields easily with increased load. This they claimed allows the activity of squatting to be performed smoothly and that during normal walking there is a "fair degree of resistance" to dorsiflexion.

The main disadvantage of the Jaipur foot is its weight. The developers suggested that this drawback can be overcome by rubber technologists, although they commented that the combination of a SACH foot with overlying shoe would weigh more than the Jaipur foot.

Another recent development was aimed at producing an artificial foot that will conform to the shape and mechanism of the normal anatomical foot. The designers termed it the Stationary Attachment Flexible Endoskeleton or SAFE foot, Campbell and Childs (1980).

The foot consists of a flexible keel encased in a soft foam cover and is bolted directly to the shank. It was designed to meet five predetermined criteria : a dome shaped arch and a long plantar ligament band, a flexible endoskeleton, a subtalar joint, a windlass

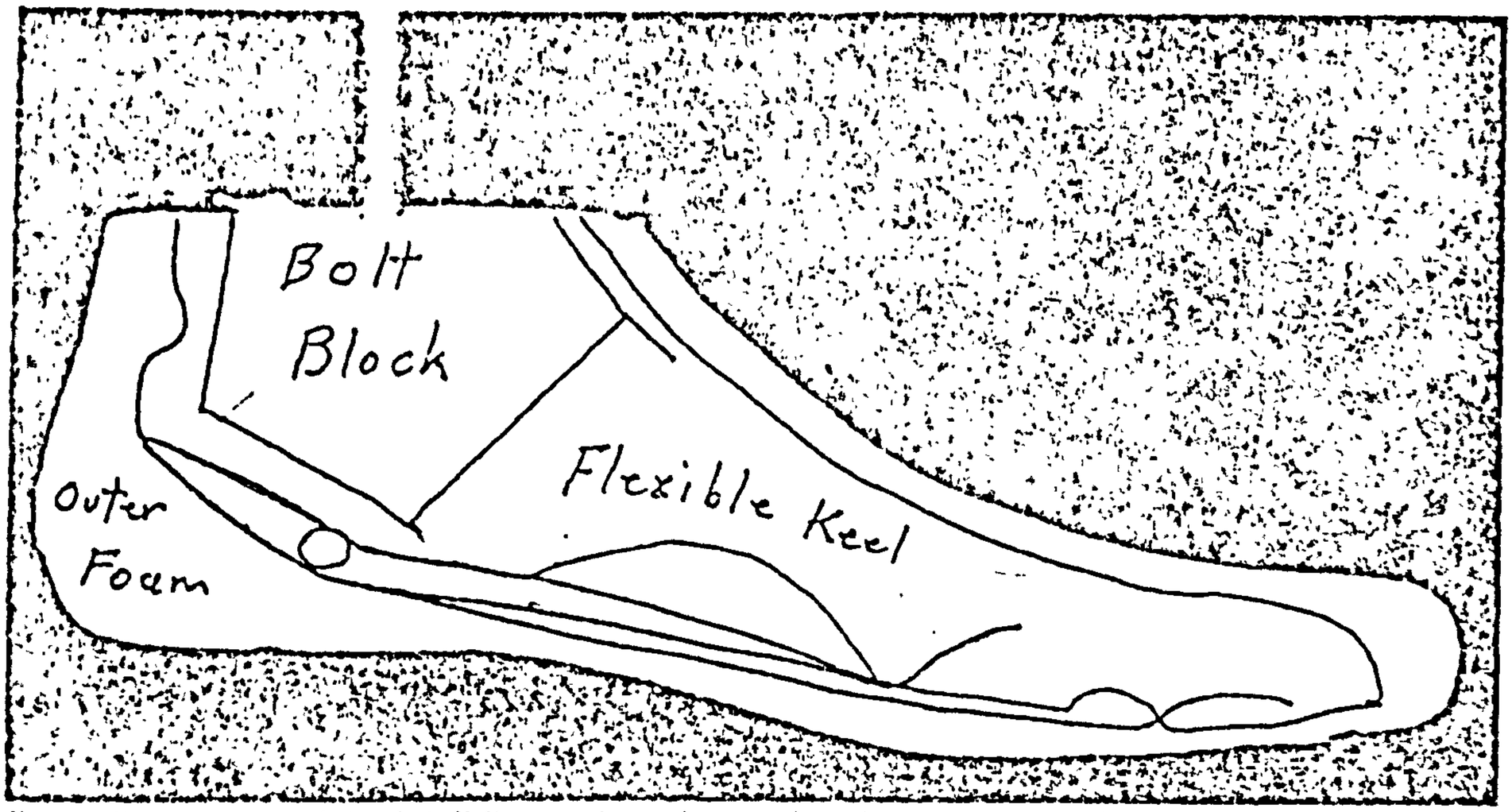

Fig. Cross-section of the S.A.F.E. foot throughout its length in a parasagital plane.

Figure 4.2.3(g) The SAFE foot
(from Campbell & Childs, 1980)

mechanism (toe-break and plantar fascia), and was made entirely from plastic materials with no mechanical joints. The anterior surface of the bolt block was cut at approximately where the average subtalar joint is located, this gave the flexiblity required in providing transverse rotation, see Figure 4.2.3(g).

The foot is claimed to be capable of sustaining the patient's weight due to the dome shape of the arch and its tie, the long plantar ligament band. Inversion and eversion were demonstrated to be possible with the foot. Plantar flexion is being provided by the soft heel and the relative movement of the bolt block and the rest of the foot. Some degree of dorsiflexion can also be achieved through the movement of the bolt block relative to the rest of the foot. It will permit transverse rotations due to the ability of the flexible keel twisting within the shoe. When this twisting occurs from heel-off to toe-off, the plantar ligament band is tightening as the windlass action takes effect, holding the forefoot tightly against the walking surface. The windlass action converts the foot to a semi-rigid lever. The designers claimed that this gradual tightening of the windlass band produces a smooth roll-over to toe-off without the usual snapping of the knee caused by a rigid keel or the toe-break rubber bumper.

Campbell and Childs (1980) reported that field trials have been conducted with 35 patients (including 9 above- and 10 below-knee amputees) for 6 months. Thirty-two subjects favoured the new design while two below-knee amputees rejected it. There was no mention of the weight of the prosthesis and no information was given on the importance of foot shape and shoe fitting,and with only 6 months of trials, maintenance problems will not be clearly identified. Therefore, more long term field trials are required and furthermore cyclic load testing

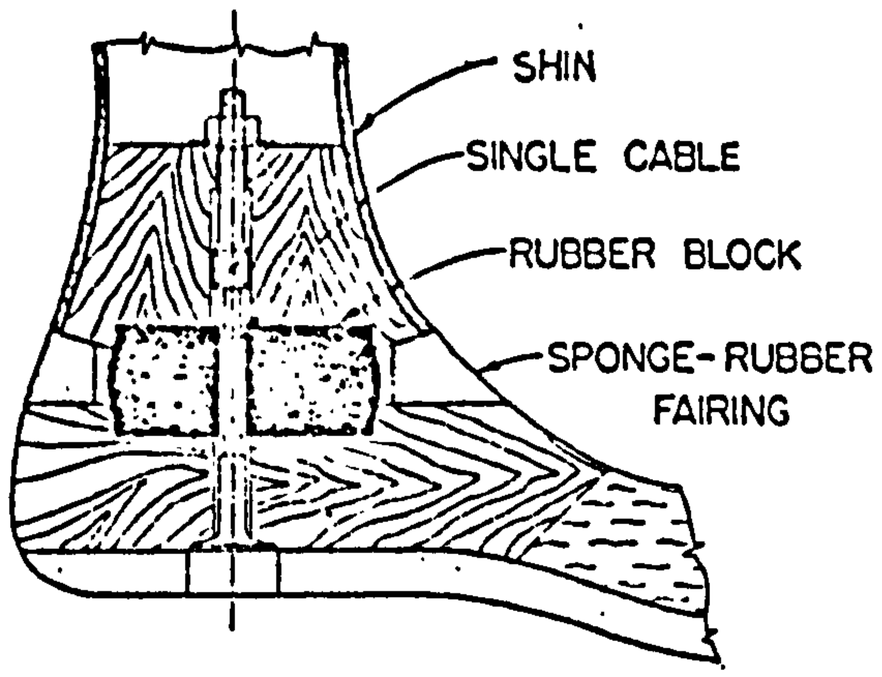

Navy functional ankle with two-durometer rubber block.

Figure 4.2.3(h) The U.S.Navy foot
(from Wagner & Catranis, 1954)

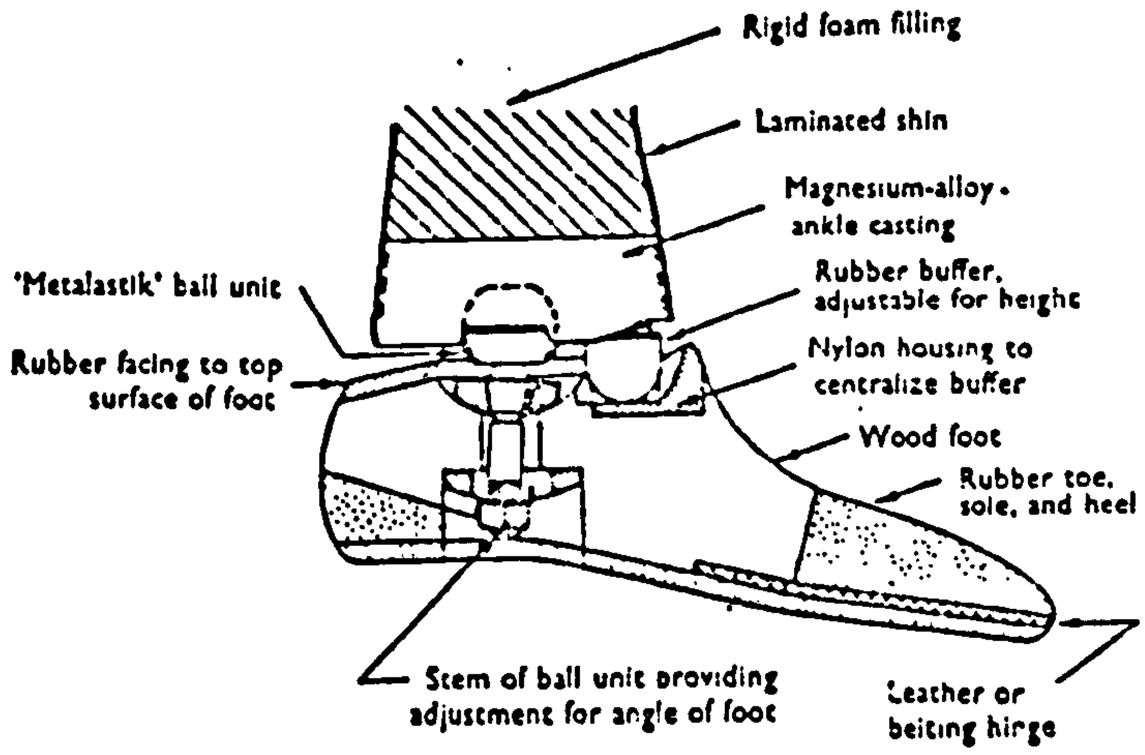

Metalastik foot and ankle unit. (*From Ministry of Health Progress Report*, 1965.)

Figure 4.2.3(i) The Metalastik foot
(from Fulford & Hall, 1960)

would be very helpful to verify design strength.

There have been many attempts made at designing a multi-axis ankle/foot mechanism. Most of them have been too heavy, complex and not durable, therefore are not widely used.

The U.S. Navy Functional Ankle (Asbelle and Canty, 1957) design is an extremely simple ankle assembly consisting of a flexible cable and a special moulded rubber block interposed between the shin and foot, see Figure 4.2.3(h). Deformation of the block provides for plantar- and dorsi-flexion, inversion, eversion and transverse rotation. Forces opposing these motions can be altered by adjusting the cable tension or by the use of rubber blocks with different density. Note that adjustments for individual functions are not entirely independent.

The Metalastik ankle available in the United Kingdom owes its origin to some extent to the U.S. Navy Functional Ankle design. It consists of a rubber ball bonded between the shin and foot at the centre of ankle rotation with an adjustable rubber instep and some adjustment as well for heel height, see Figure 4.2.3(i). This too provides freedom of motion in all three directions. Accurate alignment is essential with this device. Although these designs are simple they lack durability and are rarely used.

One of the most popular multiaxial foot in recent times is the Greissinger foot. Its main components are the shaped ankle part, connecting assembly and shaped foot part. The connecting assembly consists of a resilient rocker rubber block, an upper joint and a lower portion in metal. The shaped foot part consists of the mid-tarsal portion, the flexible toe piece and the

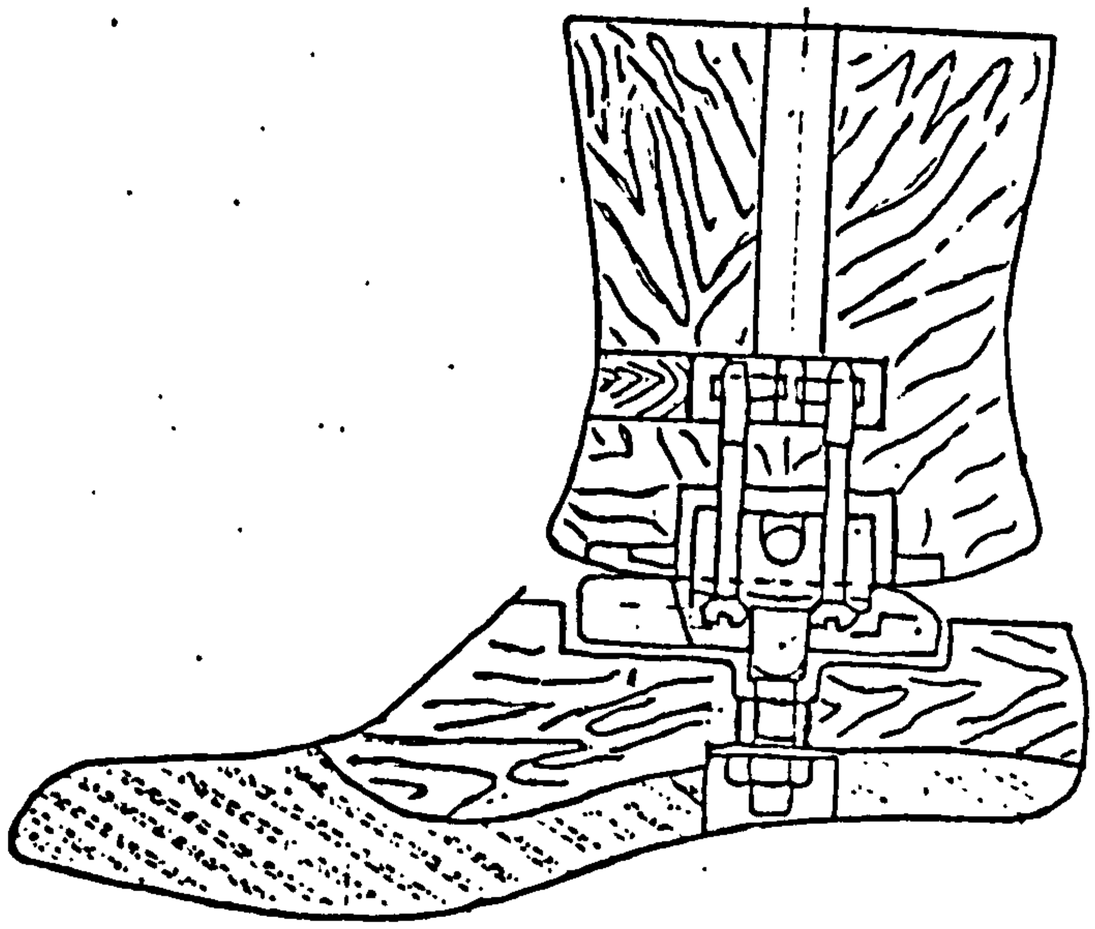

Figure 4.2.3(j) The Greissinger Foot

flexible sole. The mid-tarsal portion has moulded bearings to accommodate the resilient rocker block. The rocker rubber block are available in three grades of density. A slight modification to this design is the inclusion of a sponge heel wedge to provide additional cushioning at heel impact, see Figure 4.2.3(j).

A more revolutionary modification to the Greissinger foot is the introduction of the moulded foot. The wooden mid-tarsal portion is embedded in polyurethane foam. Instead of the original one-piece rocker rubber block, a separate plantar flexion bumper is accommodated and the rocker rubber block is shortened to make way for the rear bumper. The foot can be used in either the more conventional crustacean or the modular endoskeletal prosthesis.

One of the major disadvantages of this foot is that it is very heavy. It is usually prescribed for the more active amputees who are keen on sports and games or work on rough ground daily. Therefore it is not generally prescribed.

All of the prosthetic ankle/foot mechanism described so far are passive in operation. Each prosthetic foot when fitted is usually aligned for level walking. Thus, when an amputee walks uphill or downhill, he will experience some loss of stability. To overcome this, in 1956, Hans Mauch of Dayton, Ohio invented an ankle control with an automatically adaptable dorsiflexion stop, enabling the amputee to walk uphill and downhill without loss of stability.

The Mauch hydraulic foot-ankle system has since been undergoing constant improvement. The latest design includes the variable hydraulic dorsiflexion stop, a mechanical inversion/eversion control, an axial rotator

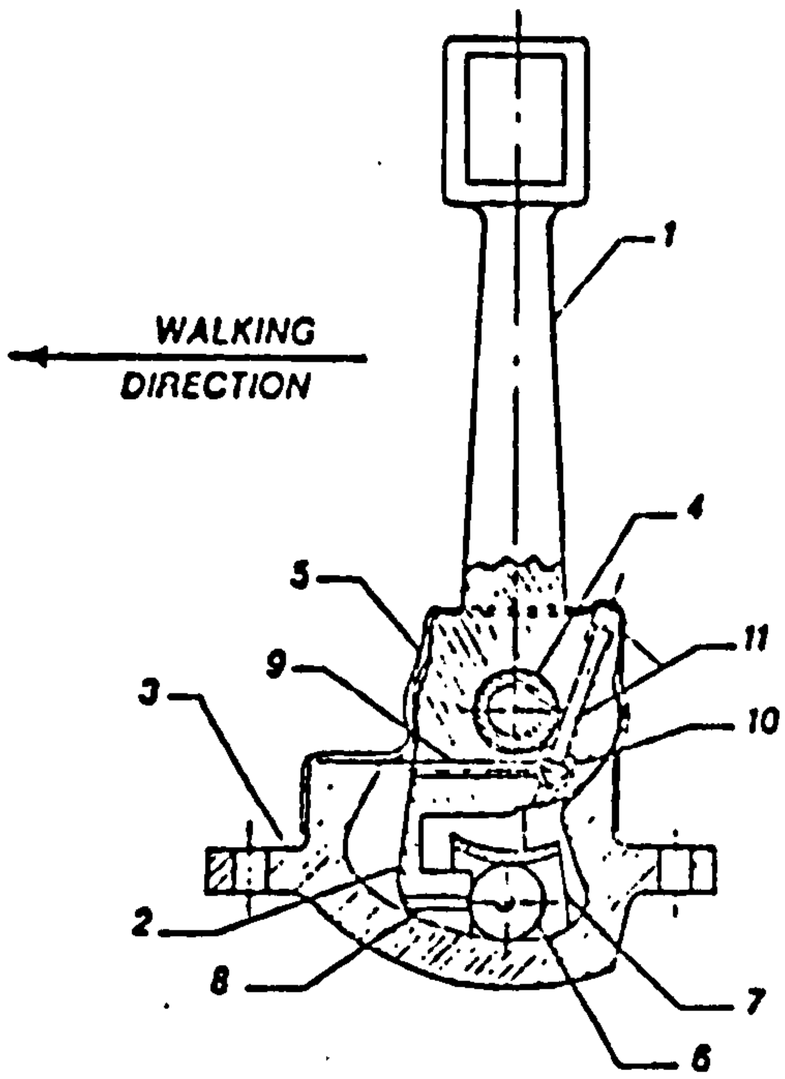

Fig. The hydraulic unit. 1-piston rod. 2-vane type piston. 3-housing. 4-axle. 5-rubber boot. 6-control ball. 7-ball cage. 8-control port. 9-bypass port. 10-bypass valve. 11-valve stem.

Figure 4.2.3(k) The Mauch Hydraulic Ankle Unit
(from Sowell, 1981)

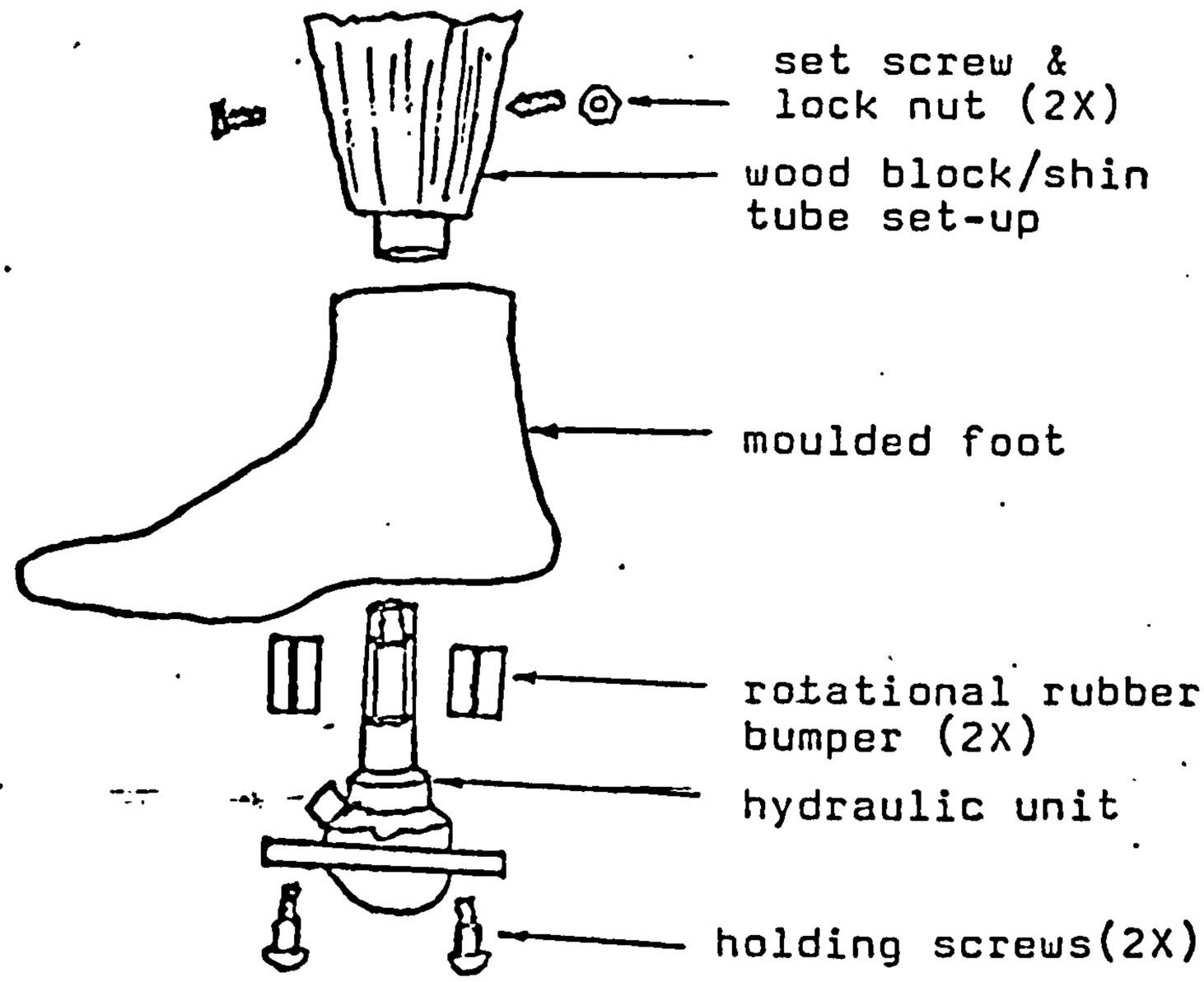

Figure 4.2.3(l) The Hydraulic ankle and foot assembly
(redrawn from Sowell, 1981)

and also hydraulic toe-slap damping and toe pickup.

The hydraulic unit illustrated in Figure 4.2.3(k) contains a gravity controlled element which closes a port in the vane and therefore prevents oil flow from the rear chamber to the front chamber of the housing whenever the piston rod and attached shank are in vertical postition or inclined forward from the vertical. This means that resistance to dosiflexion will occur later in uphill walking and sooner in downhill walking. Furthermore, the ankle automatically compensates for changes in heel height of different footwear.

The design of the hydraulic orifice is such that it produces turbulent flow, which means that the plantar flexion speed upon heel contact will only increase by 40% if the amputee's weight is doubled. This in a way provides controlled toe-slap damping.

A second port through the vane piston enables the foot to assume any position from 10^{o} dorsiflexion to 20^{o} plantar flexion when the foot is unloaded and the port is opened. The port will close whenever the amputee applies weight onto the foot (a minimum load of 13.6 kg). This will permit the amputee to walk downstairs step-over-step without having to aim for the edge of the stairs with his prosthetic foot. Also when he sits on a chair, the prosthetic foot can be manoeuvred to adopt a natural postiion, without the toe sticking up.

A third port in the vane piston is spring-loaded and acts as a pressure relieving valve. It opens when the load on the ball of the foot exceeds 136 kg, this is to prevent the entire structure from being over-stressed.

The housing of the hydraulic unit is attached below to the inside of a hollow keel of the foam foot by two

screws, see Figure 4.2.3(1). The housing pads and four rubber washers are so shaped that 10^{o} inversion of the foot encounters little restriction but eversion is strongly resisted.

Transverse rotation is provided by two profiled rubber bumpers interposed between the two flat surfaces of the paddle and the inside of the shank, where each bumper is kept from rotating with the piston rod. The bumpers are solid on one side of their groove and channelled on the other, providing different torque resistance for piston rotation in opposing directions. The arrangement is such that forward rotation of the pelvis is facilitated but backward rotation is opposed.

Eight prototypes have been evaluated and reported recently by Sowell (1981). One above-knee, three below-knee and one bilateral above-knee/below-knee amputees participated in the evaluation. This preliminary study concluded that the prototype ankle system does simulate the anatomical ankle in activities such as walking on uneven terrain, descending stairs step-over-step, running, ascending and descending inclines and a variety of sports including skiing.

The major complaints were the presence of "a squeaking noise" and hydraulic leakage. However, it was claimed that the noise element has been eliminated from the system but leakage still persists. A nation-wide full-scale clinical application study is reported to be currently underway in the United States. The outcome of this evaluation is being awaited with interest.

Although, there seem to be several ankle/foot mechanisms available for fitting. The choice of a terminal device remains in practice between the Uniaxial foot and the SACH foot.

Prescription criteria for prosthetic ankle/foot units have been derived mainly from experience gained by the clinician and the prosthetist. They tend to vary depending on the country and the particular limb fitting centre. In Britain for instance, the Uniaxial foot is predominantly prescribed whereas in the United States, the SACH foot is preferred, see Section 3.2.7. However, Fulford and Hall (1968) commented that in general the SACH foot should be prescribed for the unilateral below-knee amputee. For the above-knee amputee and the bilateral amputee the uniaxial foot is preferred because it is believed that lateral stability can be obtained sooner after heel strike than with the SACH foot, with which it is not obtained until the body-weight has been transferred to the front of the keel.

Another suggestion with regard to prescription was given by Staros and Goralnik (1981). They stated that for patients without complications, regardless of the level of amputation, the SACH foot is preferred. In cases where no stance-control features in the knee unit are present and patient must depend on alignment ability and the plantar-flexion of the foot and ankle, the Uniaxial foot would be more adequate.

So far, prescription of prosthetic ankle/foot mechanisms is conducted on a broad rule of thumb basis with not enough scientific data to substantiate their practice. Furthermore, the choice of the stiffness of rubber bumpers of the Uniaxial foot or heel wedge of the SACH foot is decided purely in a subjective manner. Therefore more objective information in terms of the characteristics and biomechanical performance of both types of feet is required.

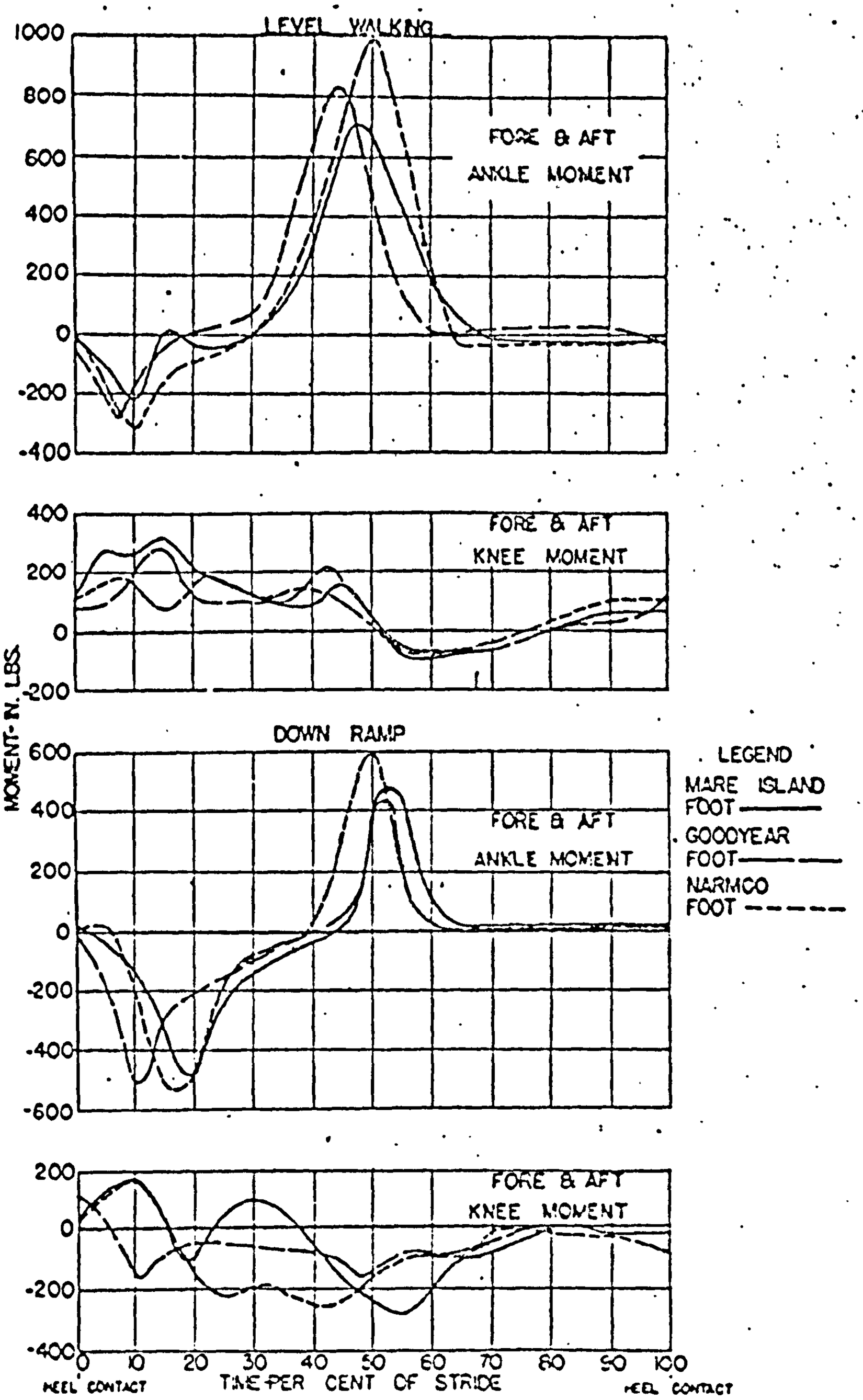

FIG. COMPARISON CURVES FOR SUBJECT NO. 1 WITH THREE TYPES OF FOOT

BASED ON FORCE DATA FROM PYLON TESTS

UNIVERSITY OF CALFORNA PROSTHETIC DEVICES RESEARCH

Figure 4.3.1(a) (from UCB, 1947)

4.3. Evaluation of Prosthetic Feet

The following sections are intended to give an insight into the different aspect of evaluation that have been carried out on prosthetic feet. Some of the studies were aimed at defining the characteristics and biomechanical performance of the device, while others concentrated on clinical evaluation.

4.3.1. Biomechanical Analysis

The fundamental studies of UCB (Eberhart et al, 1947) included a test made with one below-knee amputee so as to determine the effect of three different foot designs on the forces in the shank. This was done with a force transducing pylon. The three types of feet tested were : Mare Island foot (single-axis type); Goodyear and Narmco feet (both multi-axial type).

Differences found in the force curves were attributed to the varying bumper stiffness of the three feet, with the Mare Island foot indicating the least stiffness and the Narmco foot, the most stiffness. Figure 4.3.1(a) shows the effects on the ankle and knee moments of the three types of feet. The difference in lateral moments was suggested to be due to the lateral motion as well as fore and aft motion allowed in both the Goodyear and Narmco feet. It was stated that the amount of flexion and position of toe-break have a large effect on the ankle moments. The Narmco foot produced the greatest ankle moments, since its toe break was well forward.

Bresler and Berry (1950) also from the UCB group, reported on some fundamental aspects of energy characteristics of ankle joints, (normal as well as artificial) and also compared several artificial ankles. They stated

	Energy Input (ft-lb)	Energy Output (ft-lb)	Ratio= Output / Input
Average of four Normal ankles	10.2	24.1	2.3
Average of two Below-knee Amputees (with Single-axis Ankles)	8.43	2.73	0.32
Average of two Above-knee Amputees (with Single-Axis Ankles)	12.8	3.97	0.31

Table 4.3.1. (a) (from Bresler & Berry, 1950)

that when an artificial foot rotates about the ankle joint from the neutral position,work must be done against one of the bumpers and stored in that bumper. This rotation constitutes energy input to the joint. When the foot is returned from the displaced position to the neutral position, the compression is relieved and energy is returned to the system; this constitutes energy output of the joint.

In the normal ankle, however, the muscles are incapable of storing mechanical energy, they could only generate power. Therefore it is more difficult to define the input (or output) energy of a normal ankle. In order to compare normal ankles with artificial ankle mechanisms, Bresler and Berry generalised the definition of the output and input energy as follows :

a) the work done while the forces on the foot act in the same direction as the rotation of the foot is defined as input to the ankle joint.

b) the work done while the forces on the foot act in the direction opposite to that of the foot rotation is defined as output of the ankle joint.

The values of the input and output energy as well as the ratio of output for normal ankles and the single-axis ankles are as shown in Table 4.3.1(a).

For the normal ankles, the excess of 13.9 ft-lb of energy output was regarded as the net amount of energy supplied to the body by the muscles of the ankle joint for each step. The investigators commented that if an amputee is to walk at the same speed and cadence as a normal person he must compensate for the lack of muscles in his prosthetic leg by doing more work with his normal leg.

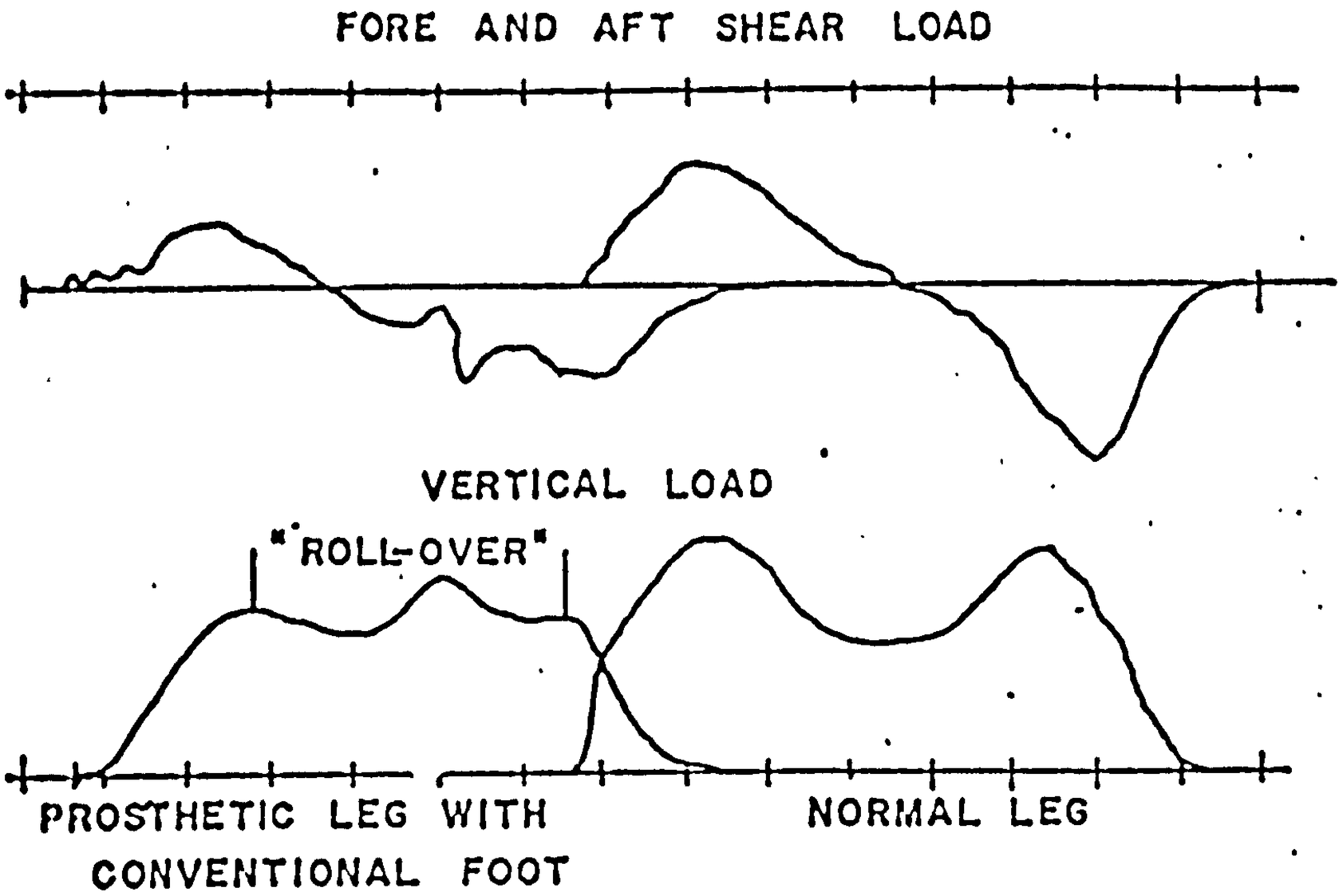

FORCE PLATE CURVES — SUBJECT VI-A/K
NORMAL SPEED

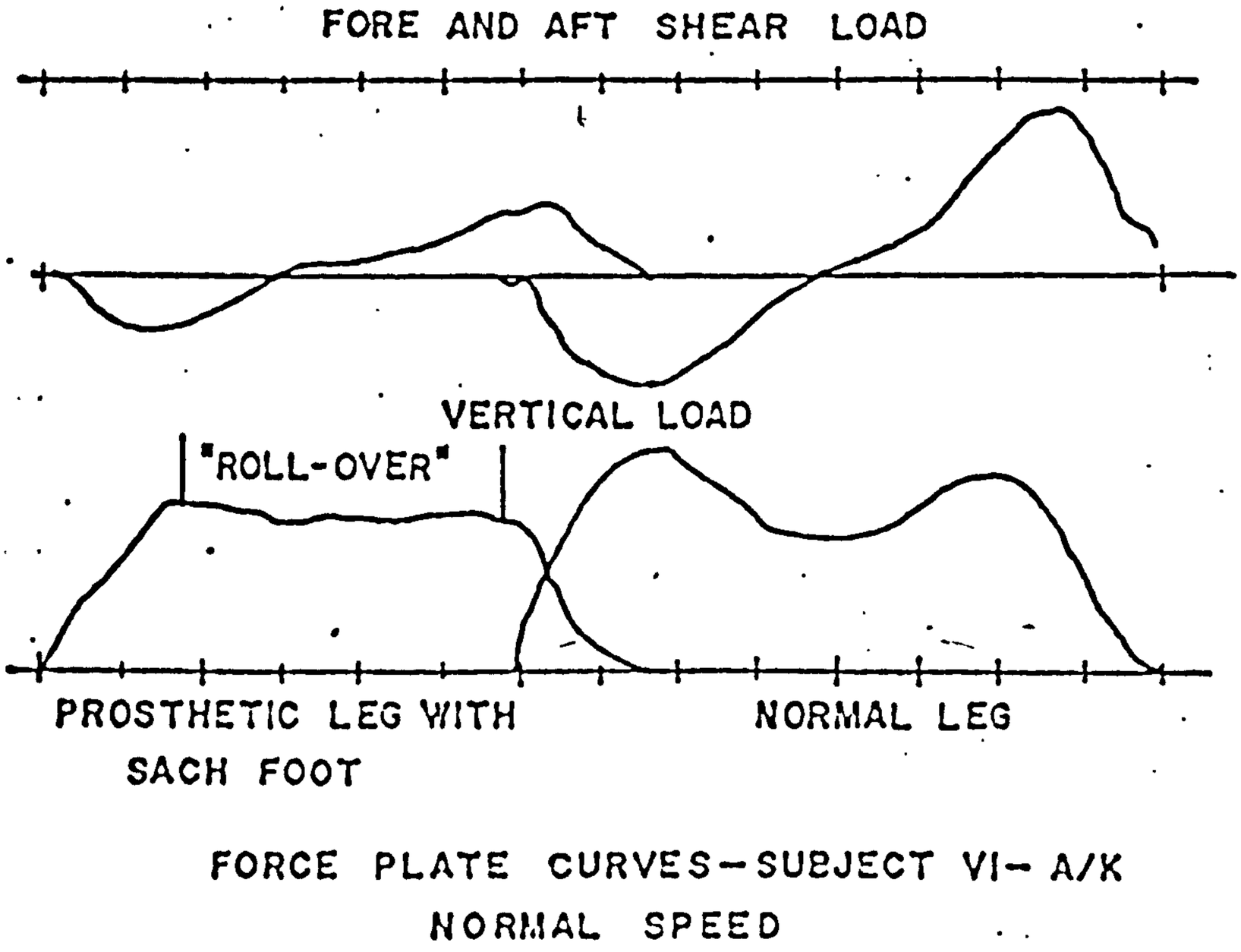

FORCE PLATE CURVES — SUBJECT VI-A/K
NORMAL SPEED

Figure 4.3.1(b) (from Fishman et al, 1955)

It is apparent that the value of the ratio of output to input can never exceed one for an artificial ankle joint, as this ratio indicates the efficiency with which the joint stores and releases energy.

For the single-axis ankle, the excess of 8.83 ft lb input registered for the above-knee amputees and 5.7 ft lb input for below-knee amputees represented the net amount of energy lost in friction by the ankle joint. Both groups of amputees indicated a loss of nearly 70% of the energy. The investigators stated that the loss is excessive and suggested that through proper design of bumper seats, better materials and workmanship, these losses can be minimised.

When the SACH foot was being developed at UCB in the early 1950s, six prototypes were submitted to New York University for an independent evaluation, (Fishman et al, 1955). Three below-knee and three above-knee(male) amputees participated in the evaluation programme. All were accustomed to wearing conventional wooden (single-axis with toe-break) prosthetic feet and were rather active prostheses users.

The evaluation programme involved four separate independent analyses. The "Medical group" studied the effects of the SACH foot on amputee performance; the "psychological group" was looking at the effects of the 'new' foot on the psychological aspects of prosthetic use; the "Engineering Group" was interested in establishing objective identification of effects on gait and an analysis of the design of the SACH foot and the "prosthetic Section" considered the fitting aspects of the foot.

The protocol was that each subject was studied first by wearing his own prosthesis with the conventional foot.

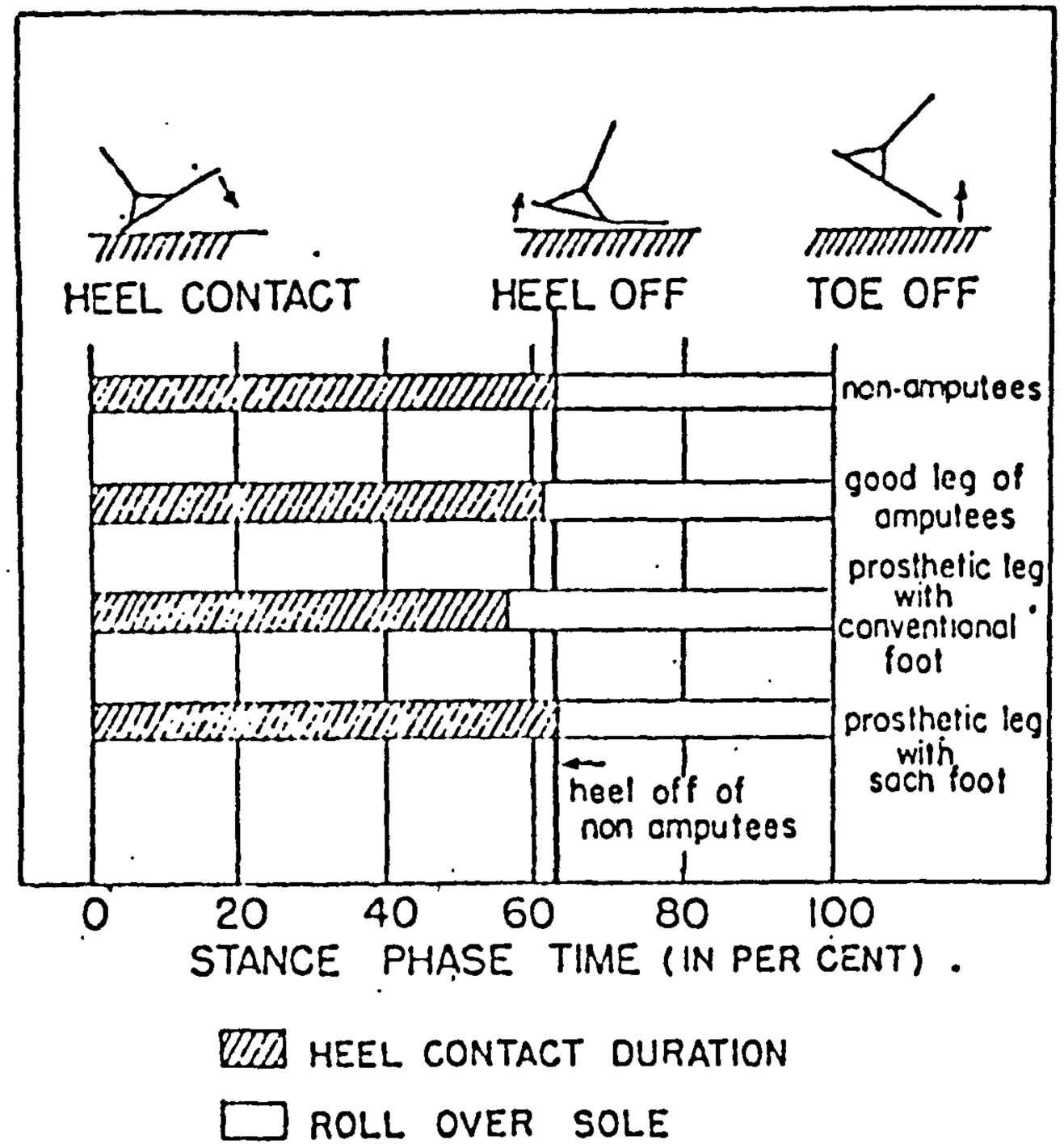

STRUCTURE OF STANCE PHASE TIME

Figure 4.3.1(c) Temporal Structure of stance phase (from NYU, Nov. 1955)

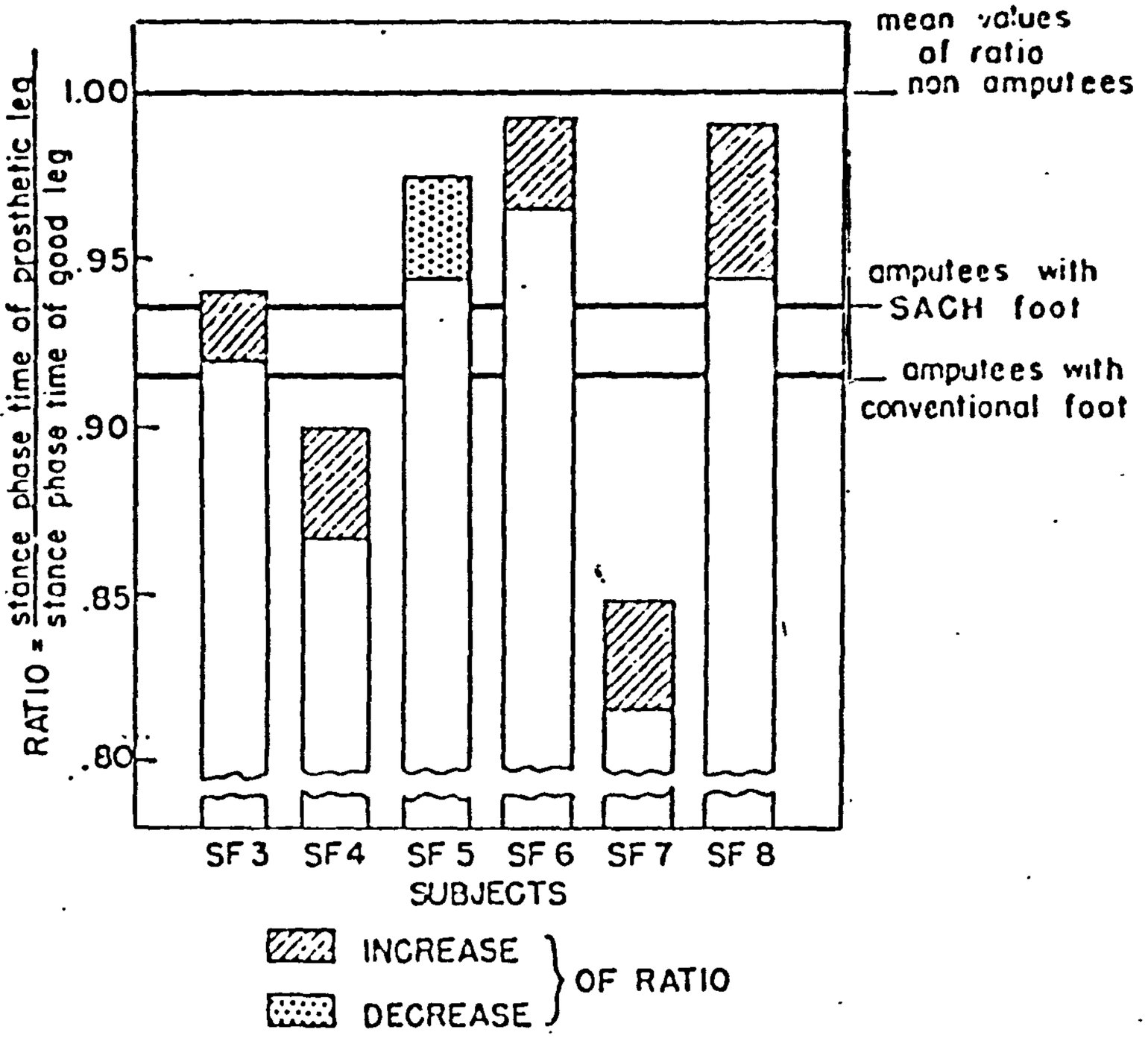

CHANGE IN RATIO OF STANCE PHASE TIME

Figure 4.3.1(d) Ratio of Stance phase time (from NYU, Nov. 1955)

Then the ankle and foot assembly was removed and the SACH foot was installed in its place. After four weeks of wearing the 'new' foot, the studies were repeated and comparisons between pre- and post- data were made.

The "Medical group" reported no observable difference in ambulation with the conventional and SACH foot. However, subjective reactions of the amputees to the 'new' foot were extremely favourable. The major advantages were in relation to the cushioning effect of the foot at heel contact and the smooth transition of weight from heel to toe during stance phase. The amputees, to a lesser degree, also liked the security and improved socket comfort afforded by the new foot, especially for walking on uneven ground.

There was unanimous acceptance of the SACH foot by all subjects from the psychological point of view. The psychological experiences were positive towards an increase feeling of balance, simulated proprioceptive sensations and improved cosmesis. Negative reactions were claimed to be insignificant.

The engineering analysis revealed only one major functional difference with the SACH foot. There was a tendency for a smoother transition from heel to toe for above-knee amputees, see Figure 4.3.1(b). Although, no such difference was observed for the below-knee amputee, the investigators believed that it was obscured by certain characteristics of below-knee amputee gait. It was observed that the direction of the fore and aft shear for the SACH and "conventional" foot, presented in Figure 4.3.1(b), was different. No explanation was given by the investigators for the change in direction.

The structural analysis found that the probability of foot laminations separating with continued use was

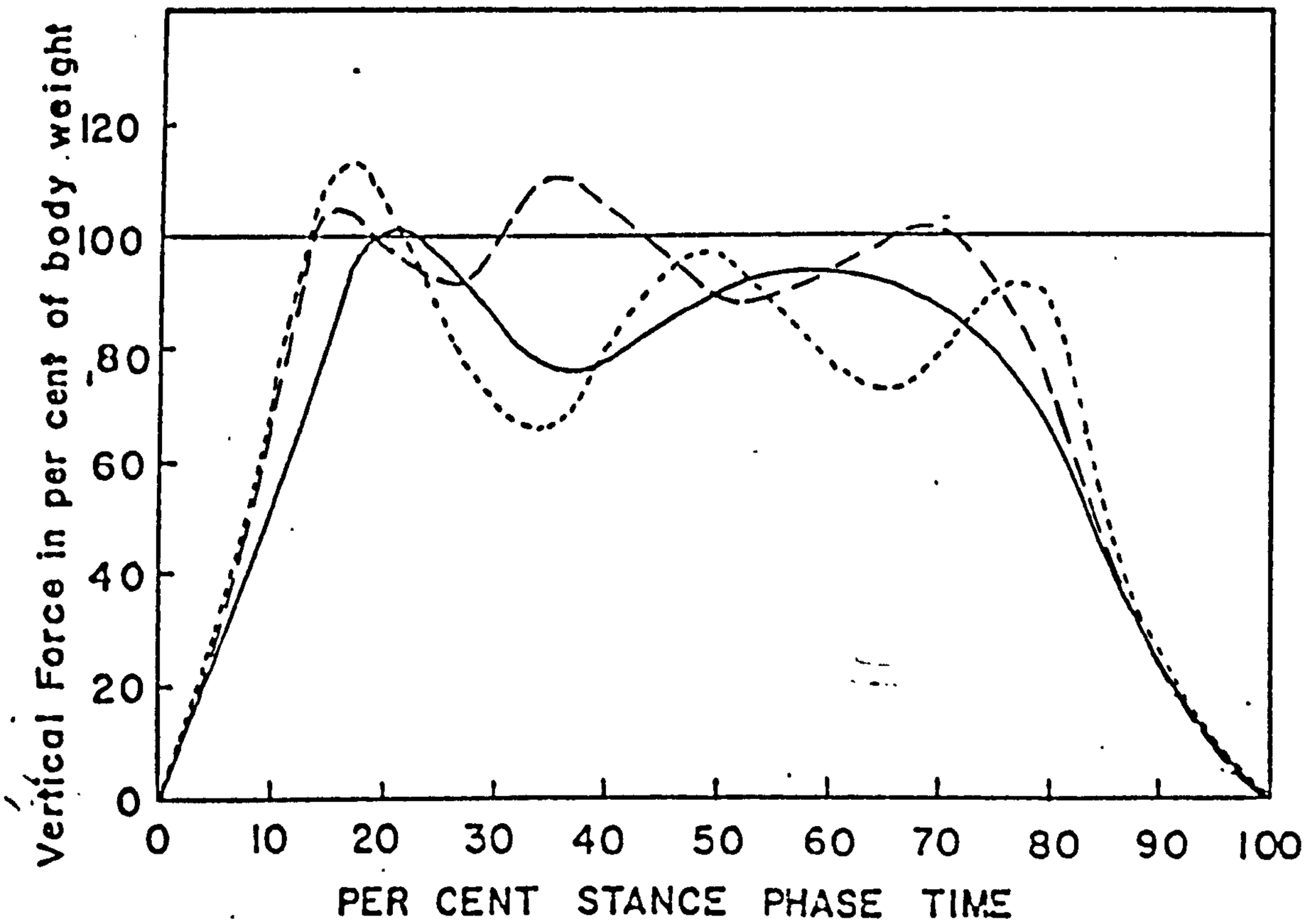

Figure 4.3.1(e) Force Plate patterns of Prosthetic feet

(from Kay et al, 1957)

high. This was confirmed by the prosthetic fitting assessment section. Apart from this defect, the conclusion from the evaluation was that the SACH foot has desirable functional characteristics.

A supplementary report (NYU, Nov. 1955) took a closer analysis of the stance phase characteristics of the SACH foot, particularly the heel stance time. The indicator chosen to represent heel compresion was not satisfactory. While it is valid to use the variation of distance between a defined ankle position and the heel line for the SACH foot, it is not a true measure of heel compression for the Uniaxial wooden foot, since this distance does not vary with heel compression. Therefore, comparison made between the two measures has to be viewed with caution.

The report claimed that the SACH foot is almost identical to non-amputee characteristics and closely approximates that of the amputee's good leg when considering the temporal structural of stance phase, see Figure 4.3.1(c). Furthermore, comparison of the ratio of prosthetic to unaffected leg stance phase showed that with the SACH foot there was a slight improvement over the conventional wood foot, see Figure 4.3.1(d). This was regarded as an indication for better comfort and stability. In this report the investigators were quick to realise the limited sample that they had and therefore stated that the findings reported were not conclusive but serve merely as indicative of trends.

From the encouraging results of the evaluation, subsequent revisions were made to improve the prototype SACH foot, according to the recommendation. Investigation on this revised SACH foot (NYU, April 1956) indicated that the foot had overcome the maintenance problems of the earlier model without sacrificing its

Type of Amputation	Body Weight	Recommended Heels Stiffness
Above-knee	Over 180 lbs (82 Kg)	Firm
	Under 180 lbs	Medium
Below-knee	Over 140 lbs (64 Kg)	Firm
	Under 140 lbs	Medium

Table 4.3.1. (b) (from Kay et al, 1957)

functional characteristics. As a result of this study, the SACH foot was placed in production and the first batch of satisfactory production models was again subjected to evaluation, Kay et al (1957).

The production models SACH feet were compared with the previously tested prototypes. Structural functional comparisons under static conditions, (i.e. not involving amputee use) and the more dynamic conditions of amputee wear were undertaken. Static compression and heel compressibility during walking revealed that the production model feet were softer than the prototypes and that there was little difference in compressibility between "firm" and "medium" heel stiffness of the production models. Data from force plate studies showed that the vertical load curves for the prototypes and production model SACH foot and the conventional wood foot were all completely different, see Figure 4.3.1(e). The cause of these differences was not known by the investigators.

Tests for stability and gait pattern produced no significant differences between the production model SACH foot and the prototypes. Another aspect evaluated was the developer's guides for selecting the proper heel stiffness for male adult above-knee and below-knee amputees, see Table 4.3.1(b). The analysis revealed that the two categories of heel stiffness tested tended to overlap in their compressibility qualities. In terms of function there was no measurable differences in the two classes of heel stiffness. Furthermore, the amputees were not able to discriminate accurately between "firm" and "medium" heels.

In general the evaluation team recommended the acceptance of the production model SACH foot and its installation manuals with the condition that strict

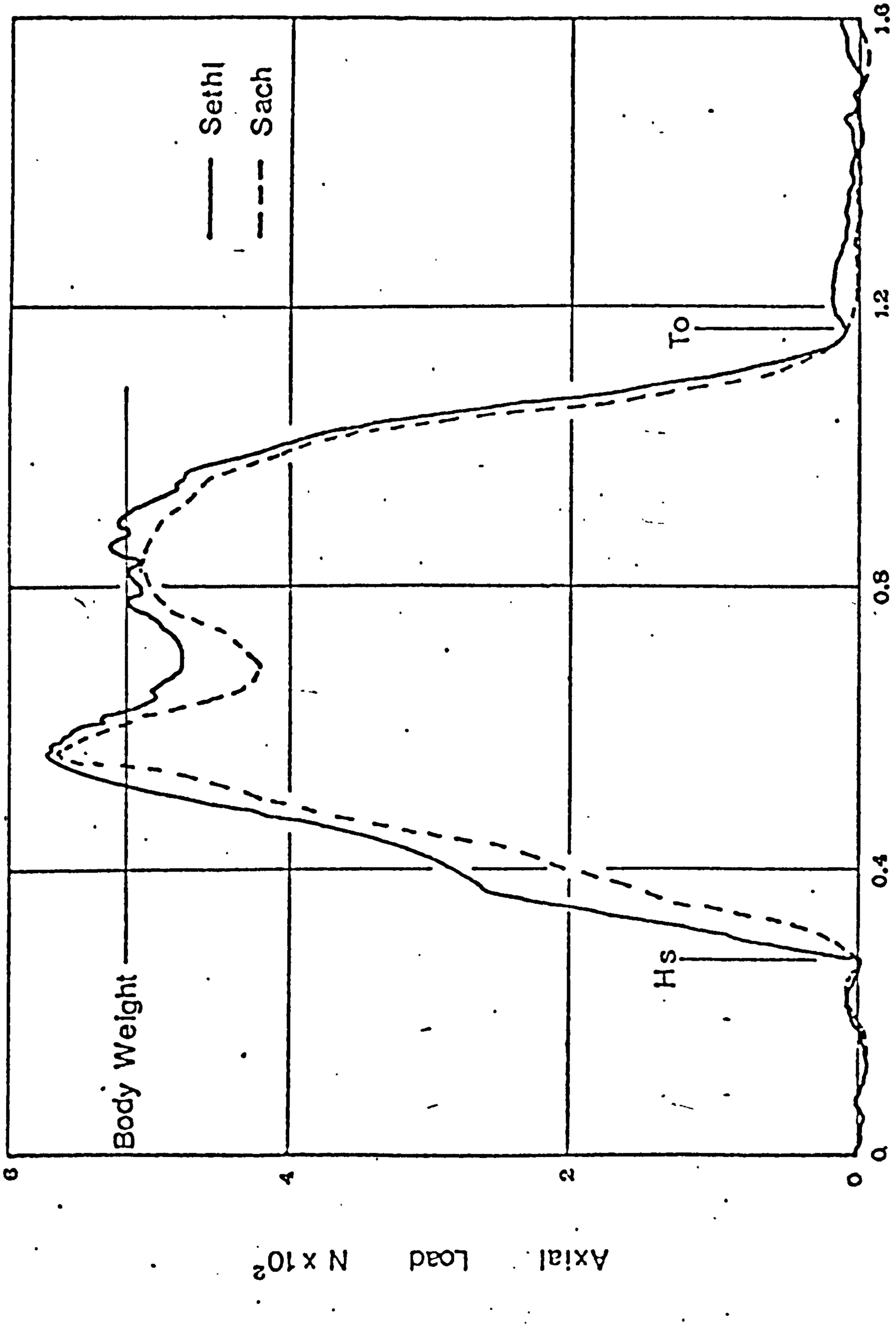

Figure 4.3.1(f) Comparison of SACH and Jaipur feet
(from North et al, 1974)

quality control should be exercised in the manufacturing process.

North et al (1974) reported on the performance of the Jaipur Foot. Using an instrumented force transducing pylon attached to a PTB prosthesis, they compared the biomechanical performance of the Jaipur foot with the SACH foot. The analysis was not able to significantly evaluate the difference in the kinetic data. It was recognised that a large number of patients tests is required to investigate the significance of the variations. However, from the axial force curves, Figure 4.3.1(f) it would appear that the SACH foot has a smoother heel to toe transition than the Jaipur foot, although North et al claimed that the amputee subject preferred the Jaipur foot and adapted to the less compliant heel section quickly.

Mass is one of the important criteria in the design of prosthetic ankle/foot assemblies, see Section 4.2.1. Godfrey et al (1977) studied the effect of additional prosthetic foot mass on gait pattern. Six above-knee amputees each with a different knee unit were observed while walking with two different weights 113.4 and 226.8 gm added to their prosthetic foot. Gait characteristics were determined by direct measurement of the knee angle, heel strike interval, stride length, stance time and knee angle at heel strike. Average horizontal velocity and heel rise velocity were calculated as well for analysis.

No significant change in the gait pattern was observed in the study. One subject was then loaded with an extra 0.45 kg mass on his leg. This also made no difference to the gait parameters. The possibility of patients tiring sooner due to the extra load was not taken into account in the study. Even so, more studies

DATA ON DISTRIBUTION OF S.A.C.H. FEET TO 123 AMPUTEES

Type of Prosthesis	No. of S.A.C.H. Feet Issued	No. of S.A.C.H. Feet Unsatisfactory	No. of S.A.C.H. Feet Repaired	No. of S.A.C.H. Feet Replaced with Conventional Feet	No. of Amputees Satisfied	No. of Amputees Noticing No Difference
Canadian-hip-disarticulation prosthesis	3	0	0	0	2	1
Above-the-knee prosthesis (conventional and suction socket)	46	0	2	0	45	1
Below-the-knee prosthesis (slip socket, conventional, all types) unilateral	68	1	10	1	67	1
bilateral (3)	6	2	2	2	2	0
Syme's type prosthesis	3	0	1	0	3	0

Table 4.3.2(a) Distribution of SACH feet to Amputee population
(from Gordon & Ardizzone, 1960)

in this area is perhaps required to establish the optimum range of prosthetic foot mass for future design and development.

4.3.2. Clinical Evaluation

Most of the clinical experiences with prosthetic feet reported in the literature have been concerned with the prescription of SACH foot.

Gordon and Ardizzone (1960) reported their experiences of prescribing SACH feet and following-up 123 amputees. Table 4.3.2(a) illustrates the distribution of SACH feet amongst the various levels of amputation and its success rate. Three amputees found no significant differences between the SACH foot and the conventional wood foot. Another three (one unilateral and two bilateral) below-knee amputees preferred the conventional wood foot. Altogether about 5% did not enthusiastically approve the SACH foot. Of the remaining amputees who constantly used the SACH foot, four had their devices replaced, while those requiring repair and maintenance were reported to have minor problems.

The two principal advantages of the SACH foot noted by amputees of all levels were the shock absorption at heel strike with resultant minimum jarring and irritation of the amputation stump, and the reduced amount of maintenance and repairs as compared with previous wooden feet. The major disadvantage reported was that of instability resulting from the compressible heel. This they stated could cause impaired balance during standing and during the stance phase of walking, especially in bilateral above-knee amputees.

Wilson (1962) reported on a survey of the extent to which the SACH foot had been used and the problems

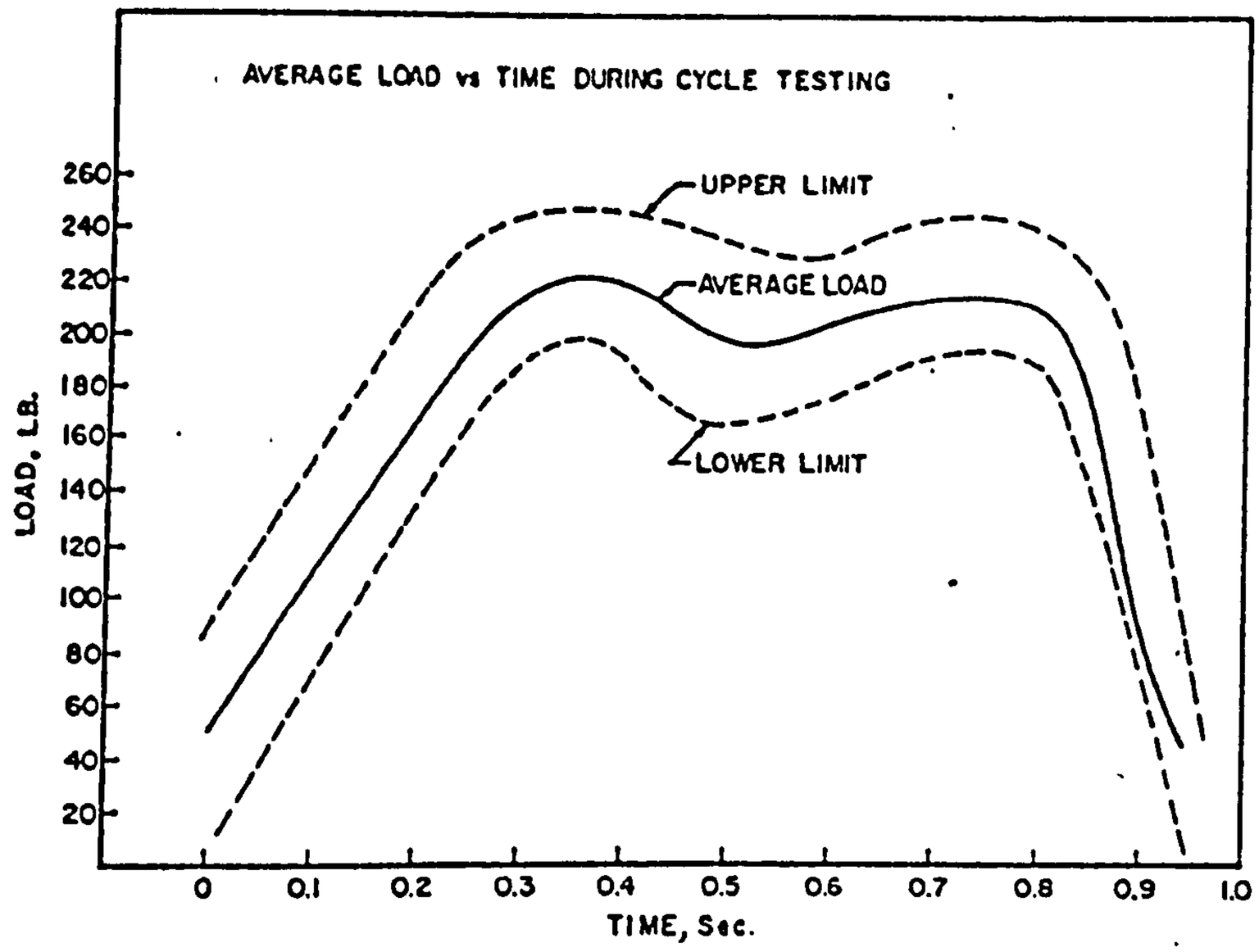

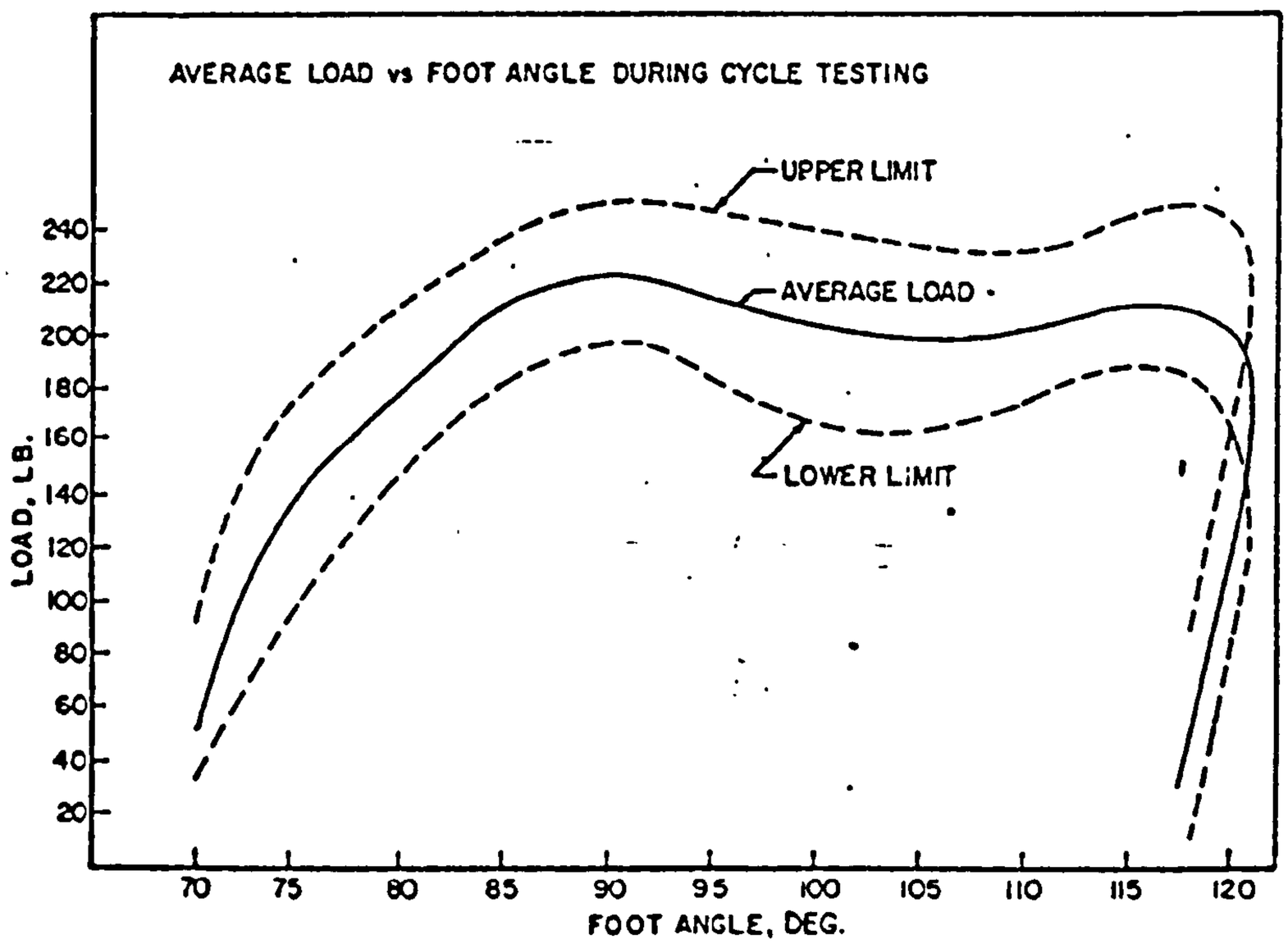

Figure 4.3.3(a) Artificial loading of SACH foot
(from Daher, 1975)

encountered in using SACH foot. Ninety-nine limb fitting centres in the United States participated in the survey.

The SACH foot was found to be in widespread use. Although 61% of the centres found that maintenance problems were significant, 75% reported that less maintenance was required for the SACH foot than for any other types in general use. All levels of amputation were claimed to have had successful fittings with the SACH foot.

These data were discussed amongst manufacturers of SACH foot, who all agreed that less than one percent of the feet produced had total troubles. They stated that the problem of heel collapsing had been rectified by using another type of rubber in the heel cushion. The "noisy" feet due to unsaturated belting has been corrected by substituting a high grade rubber belting for the previously used balata belting.

Taylor (DHSS, 1973) commented that 24 below-knee amputees, who participated in an evaluation programme on the below-knee modular system, were users of Uniaxial wooden feet. However, when they were introduced to the SACH foot in the evaluation programme, 20 expressed a preference for the SACH foot while the remainder were satisfied with it. The amputees' comments were mostly on the lively feel of the foot and the nice cushion effect at heel strike compared to the Uniaxial wooden foot.

4.3.3. Mechanical Testing

Durability is an important feature in prosthetic ankle/foot mechanisms. The only known research towards this area was reported by Daher (1975). This study was

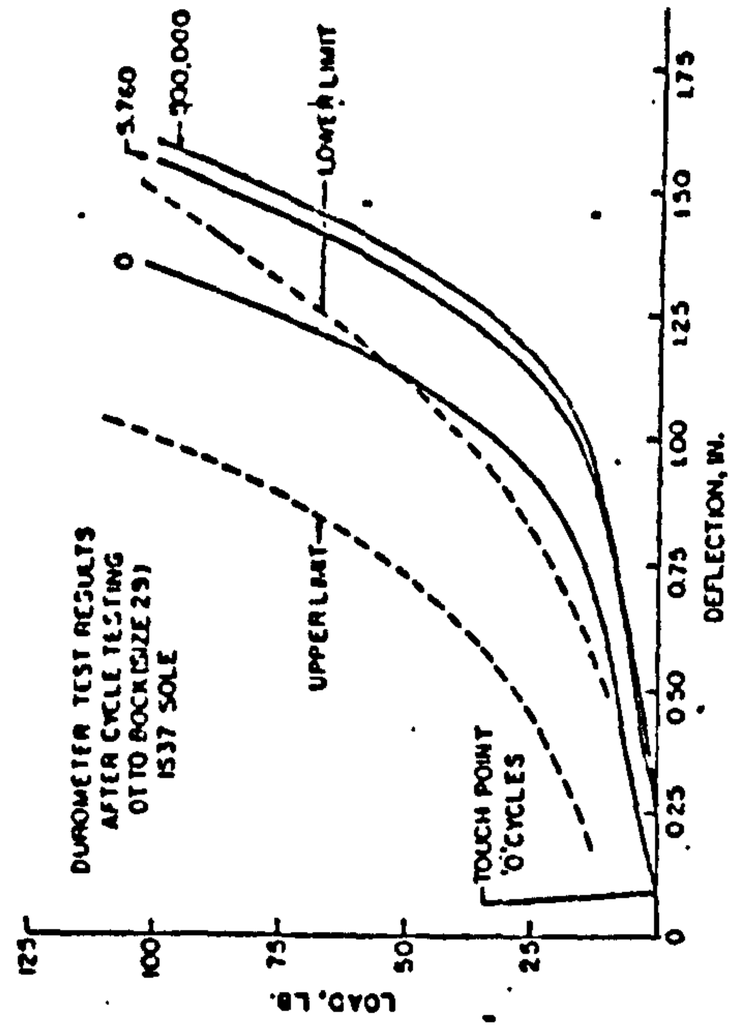

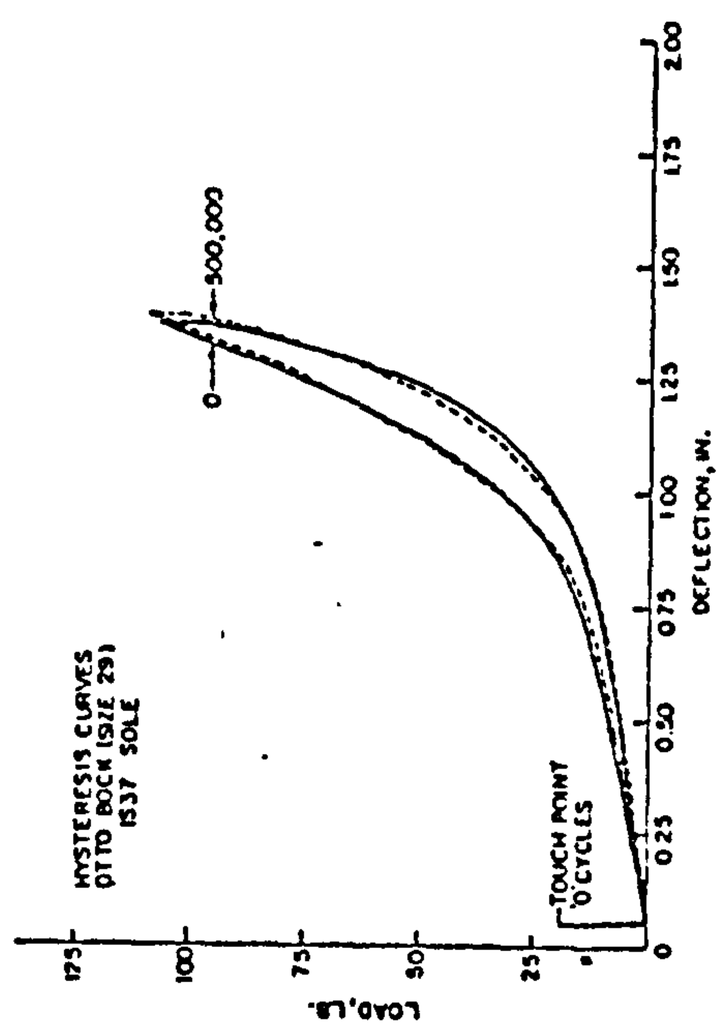

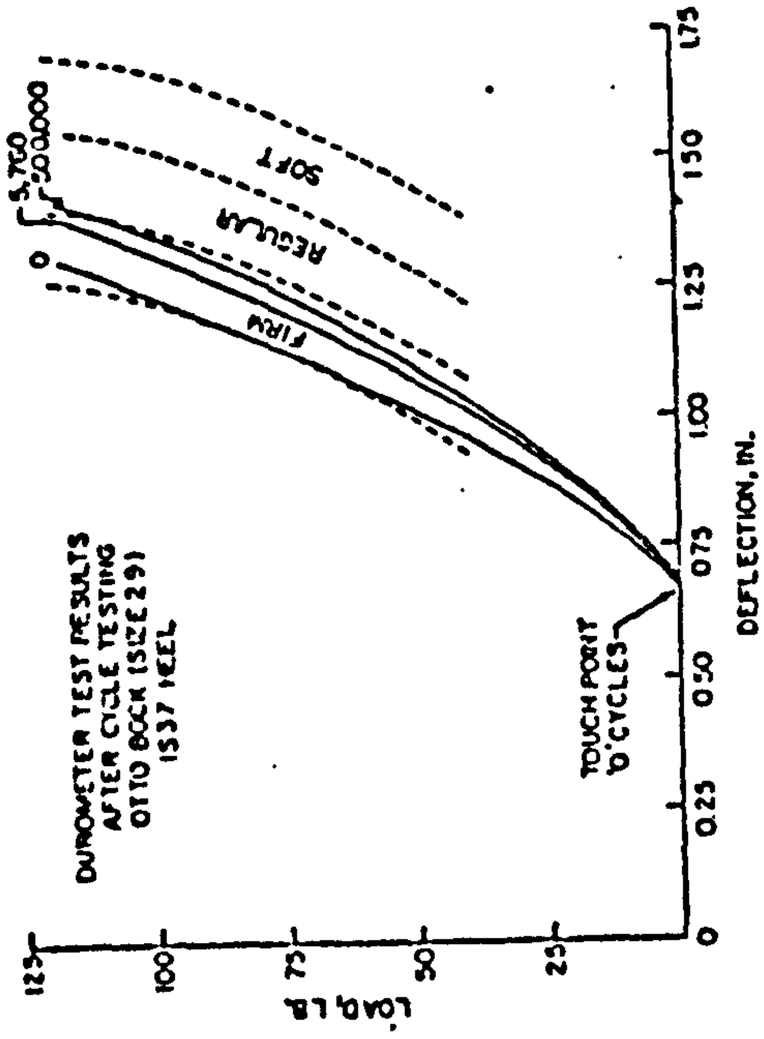

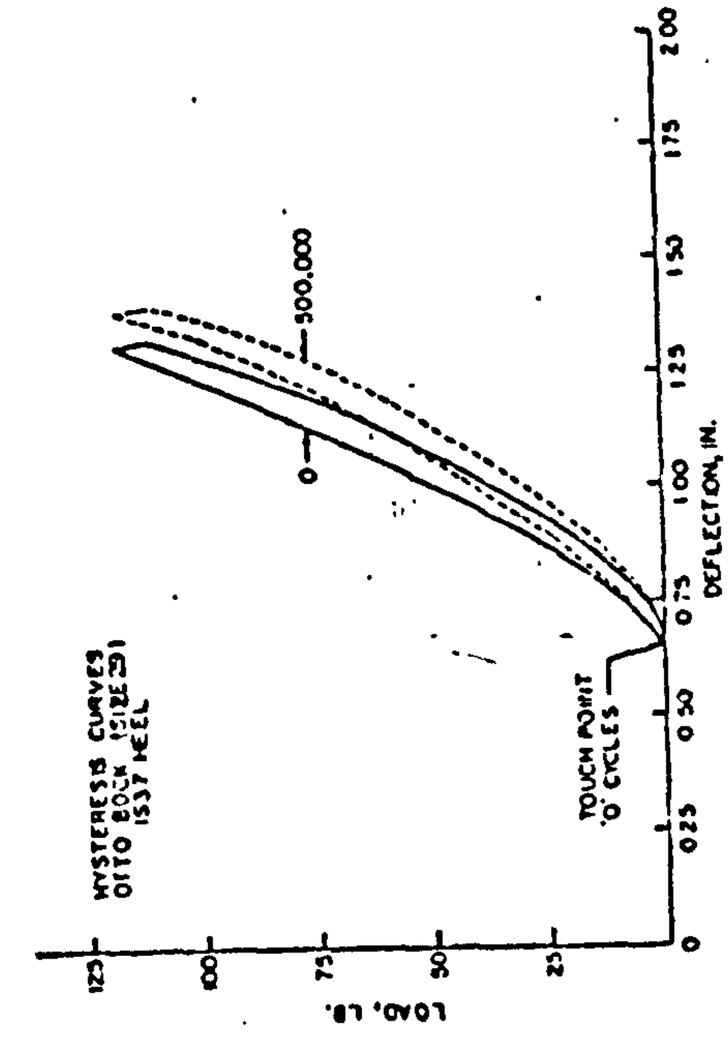

4.3.3(b) Hysteris curves for heel and sole resistance (from Daher, 1975)

Figure 4

aimed at evaluating the durability of nine different commercially available SACH feet. The test procedure was based on the criteria outlined by the Veterans Administration Prosthetic Centre, New York in its "Standards ans Specifications for prosthetic foot/ankle assemblies". A brief description of the protocol used is as follows :

An X-ray was taken of each foot before testing. Hardness tests on the heel and sole of the foot were conducted using a "Durometer" machine, which is capable of recording the loading and unloading phases. This apparatus was described in Daher et al (1974). The foot was then mounted onto a cyclic load testing machine, which simulates the walking cycle. Details of the machine were given in Daher and Heath (1974). The cyclic load applied to the prosthetic foot was such that it simulated the vigorous walking of an active amputee weighing approximately 100 kg. Figure 4.3.3(a) shows the average loading on the foot in one cycle.

During the cycling process, hardness testing was conducted at 5,000; 10,000; 20,000; 50,000 and 100,000 cycles. Subsequent hardness testing was also carried out at every 100,000 cycles. After testing, an X-ray was again taken of each foot.

Figure 4.3.3(b) shows the hysteresis curves for heel and sole resistance of one of the specimens being tested; the hardness test taken at '0' cycles is superimposed onto the test taken at 500,000 cycles. The permanent deformations experienced by each of the nine SACH feet at cycling intervals of 5,000 and 500,000 for the heel and sole is as shown in Figure 4.3.3(c). Feet that registered high permanent deformation values show up visibly in the comparison of X-ray films prior to and subsequent to testing.

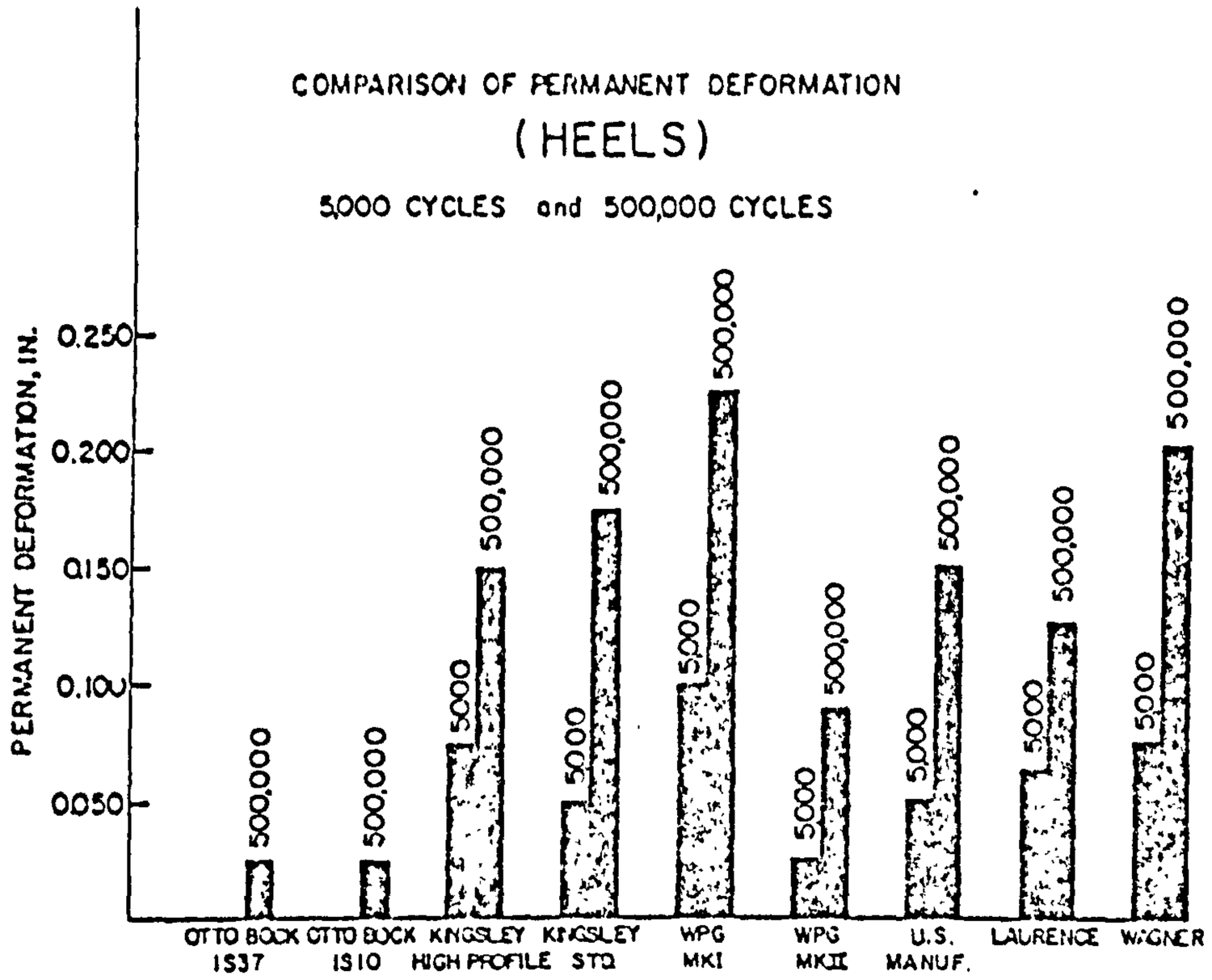

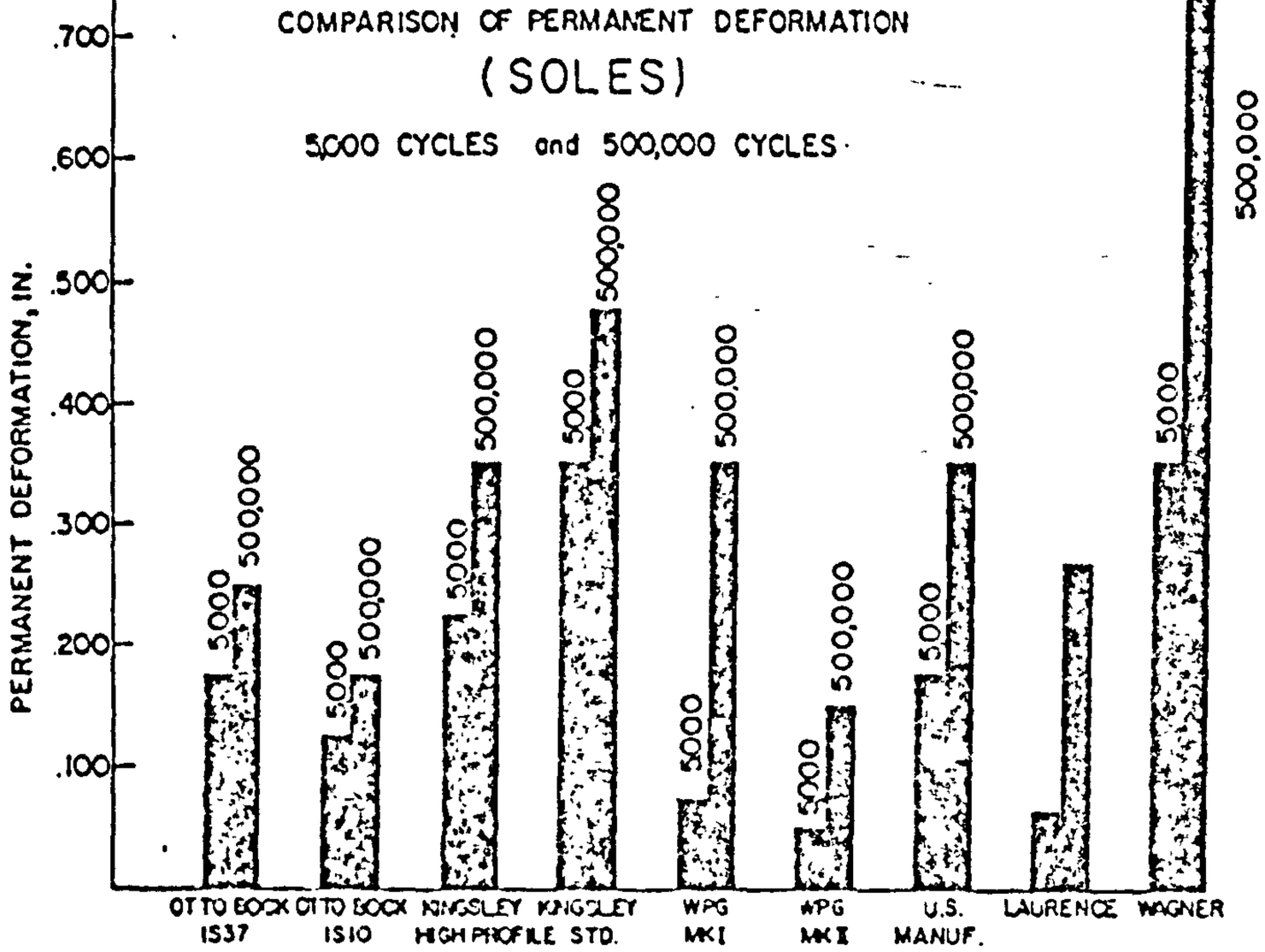

Figure 4.3.3(c) Permanent deformation of SACH feet
(from Daher, 1975)

From all the results gathered, Daher concluded that if the initial hardness test on sole resistance falls below the minimal Veterans Administration specified resistance, regardless of resilient response indicated by the initial hysteresis curve, unacceptable permanent deformation and resistance changes may be anticipated. As for the heel section, significant reduction of the encompassed area of the hysteresis curve within 5,000 cycles would give rise to unacceptable permanent deformation and/or resistance change. In general, a large response of the materials to load changes would lead to premature breakdown of the foam or foam and belting used.

Several recommendations were made with regard to the design of the SACH foot: a more resilient foam is required in the toe break area, single belting to maintain the bond of the toe section to the heel is desirable, cross-sectional dimensions at toe-break should be increased to the limit, hardwood keel should be used in all SACH feet and a good bond between the foam and rigid members of the structure must be insured.

For quality control in setting standards, it was recommended that cyclic testing of all SACH feet may be determined at 5,000 cycles or less, since, major deformation and changes in resistance occur prior to 5,000 cycles. It was highly emphasized that durability is only one criterion of a functional SACH foot and therefore results obtained as such must be interpreted with a degree of caution. It was stated that further studies were required to adequately define and correlate functions of artificial feet as related to levels of amputation and levels of activity, to provide the ultimate in amputee comfort and gait.

CHAPTER 5

Methodology and Instrumentation

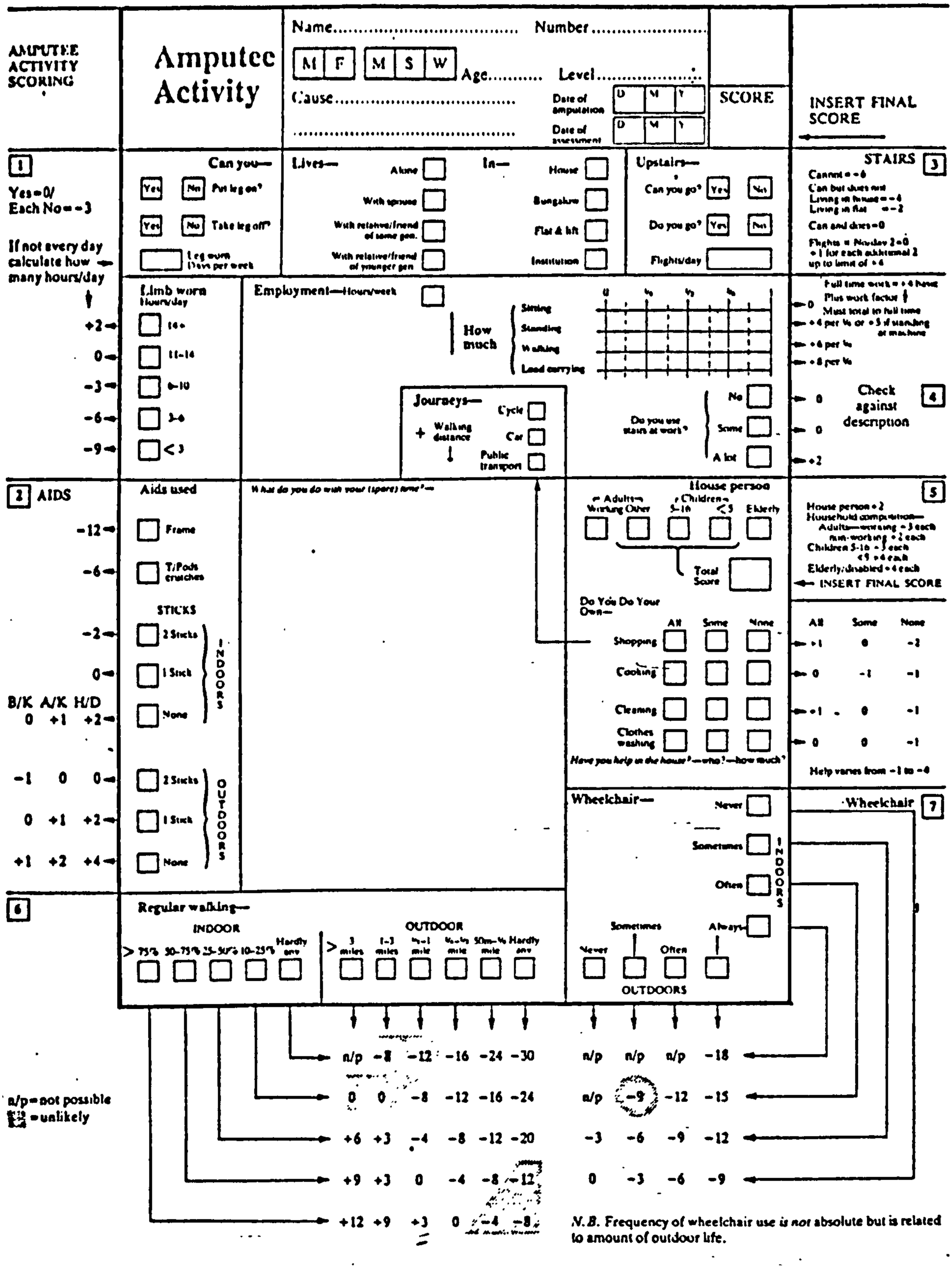

N.B. Frequency of wheelchair use *is not* absolute but is related to amount of outdoor life.

Marking aid with report sheet inserted

Figure 5.1(a) Amputee activity assessment form and marking aid

5.1. Patient Profiles

This section gives a brief description of the profiles of patients who participated in this evaluation programme. To quantify the activity level of each patient, the assessment method defined by Day (1981) was used. Figure 5.1(a) illustrates the assessment report sheet (i.e. within the darker border lines) together with the scoring aid.

All patients are male and will be identified by the assigned subject code as defined in Appendix D1.1. A description of the patient's prescribed prosthesis is also given.

5.1.1. Below-knee Amputees

Figure 5.1.1(a) shows the general particulars of the six below-knee amputees involved in the project.

Patient Code : BRØØ2 (activity level - 21)

This patient, 67 years of age, is a retired foundryman. He spends most of his spare time in gardening and motoring. He does all the shopping, cooking, cleaning and clothes-washing in the house.

His stump is conical and rather bony, although there are some soft tissues present on the anterior half of the stump. The distal ends of both the tibia and fibula are rounded but no bony bridge exists between them. The knee joint has a full range of motion and is well powered.

The prosthesis issued to him is an Otto Bock modular PTB with supracondylar suspension and a medium grade heel SACH foot. The patient tends to walk with a long stride although the step length is fairly even.

Patients	Year of Birth	Year of Amputation	Course of Amputation	Side of Amputation	Condition of Stump
BRØØ2	1915	1964	R.T.A.	Right	Good
BRØØ3	1947	1967	R.T.A.	Right	Good
BRØØ4	1926	1967	Trauma	Left	Good
BRØØ5	1927	1952	Trauma	Right	V.Good
BRØØ7	1922	1944	Trauma	Right	Good
BLØ12	1939	1974	Osteomyel-itis	Left	V.Good

Figure 5.1.1(a)Particulars of Below-Knee Amputees

He has a relatively good gait except for a tendency to linger on the ball of the prosthetic foot and then drop onto the sound side abruptly. This was considered to be habitual.

Patient Code : BRØØ3 (activity level - 26)

This patient, 35 years of age, is a taxi driver. He also holds a driving licence for every road vehicle, which indicates that his amputation has had little limiting effect. He spends most of his spare time in gardening as well as various sporting activities.

His stump is in good condition with a full range of motion available and a powerful knee joint. The cut bones are rounded with the fibular being approximately 25 mm shorter than the tibia.

The prosthesis prescribed is a standard PTB with cuff suspension and a SACH foot of medium grade level. The patient walks with a relatively good gait except for the narrow base.

Patient Code : BLØØ4 (activity level - 42)

This patient, 56 years of age is employed as a factory worker. This job requires him to do a fair amount of walking. He spends his spare time bowling, fishing and dancing.

His stump is in good condition; stable and well-matured with a full range of motion available. It is of medium length and conical in shape.

The contractor's limb issued is a standard PTB with cuff suspension and a wooden Uniaxial foot.

Patient Code : BRØØ5 (activity level - 21)

This patient, 55 years of age is unemployed. He spends most of his spare time in gardening and decorating the house, as well as doing odd jobs.

His stump is in good condition with a full range of motion available. It is of medium length and possesses good muscular strength.

The contractor's limb prescribed is a standard PTB with supracondylar suspension and a SACH foot with a firm grade heel.

Patient Code : BRØØ7 (activity level - 44)

This patient, 60 years of age, is employed as a caretaker of a shopping centre. His job includes sweeping, cleaning and general maintenance of the centre. He spends his spare time fishing, model making, dancing and cycling (both pedal and motor).

His stump is long and is in good condition with a full range of motion available. The knee joint is well powered and good muscular strength is available.

The prescribed prosthesis is a standard Kellie No.8 with a thigh corset, side steels with knee joint and leather socket metal leg, and a wooden Uniaxial foot. The patient walks with an exceptionally good gait.

Patient Code : BLØ12 (activity level - 44)

This patient, 43 years of age is employed full-time as an engineer with Rolls Royce. On top of this, he spends another 40 hours per week as a farmer, working on his own farm. His spare time, if any, is spent in

Patients	Year of Birth	Year of Amputation	Course of Amputation	Side of Amputation	Condition of stump
ARØØ1	1925	1944	Trauma	Right	V. Good
ALØØ6	1934	1957	Trauma	Left	Good
ARØ1Ø	1920	1953	R.T.A.	Right	Good
ARØ11	1936	1962	R.T.A.	Right	V. Good
ALØ13	1949	1968	Elective (Deformity)	Left	V. Good

Figure 5.1.2(a) Particulars of Above-knee Amputees

playing golf and dancing.

His stump is in good condition with a full range of motion available and the knee joint is well powered.

The prescribed limb is a standard PTB with cuff suspension and a moulded-type Uniaxial foot. The patient walks with a relatively good gait.

5.1.2. Above-knee Amputees

Figure 5.1.2 (a) shows the general particulars of the five above-knee amputees participating in the evaluation programme.

Patient Code : AR00l (activity level - 19)

The patient, 57 years of age, is unemployed. He does his own shopping, cooking, cleaning and clothes washing. He spends his spare time socialising, reading and watching television.

His stump is in good condition with a full range of motion available. It is of medium length and has very good muscular strength.

The prescribed contractor's limb is an Otto Bock modular quadrilateral, total-contact suction socket with a single-axis knee unit and a SACH foot with medium grade heel. The patient uses a stick when walking outdoors.

Patient Code : AL006 (activity level - 30)

The patient, 48 years of age is employed as a telephone operator. He spends his spare time bowling and socialising.

His stump is in good condition with a full range of motion available. The muscle strength in the stump is fair.

The prosthesis issued is an Otto Bock modular, quadrilateral, total-contact suction socket with a single-axis knee unit and a moulded-type Uniaxial foot.

Patient Code : ARØ1Ø (activity level - 49)

This patient, 62 years of age, is employed as a technical officer with the RAF. In his spare time he coaches trampoline, plays golf and does quite a bit of walking.

His stump is in good condition with a full range of motion available. It is fairly short in length but possesses very good muscular strength.

The prosthesis issued is a Kellie Metal leg with a plastic quadrilateral total contact suction socket. The knee unit is the single-axis type and the prosthetic foot is SACH with medium grade heel.

Patient Code : ARØ11 (activity level - 45)

This patient, 46 years of age, works as a carpenter in fitting out ships. He spends his spare time in gardening, reading, socialising and watching television.

He has a long and powerful stump. It is also in very good condition with a full range of motion available.

The contractor's limb supplied is a Kellie Metal leg with a "H" type metal suction socket. It has a

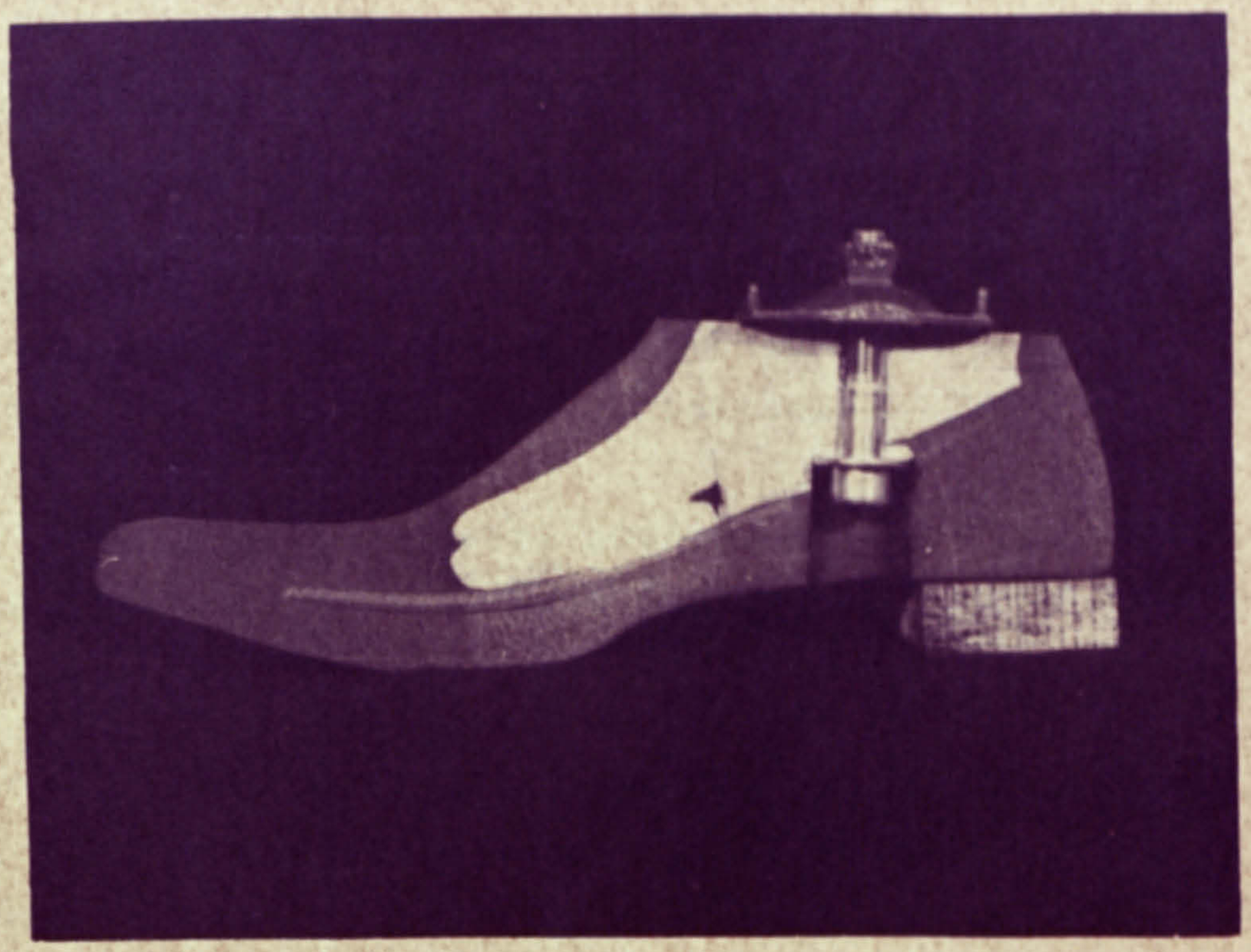

Figure 5.2(a) Cross-section of Otto Bock SACH Foot

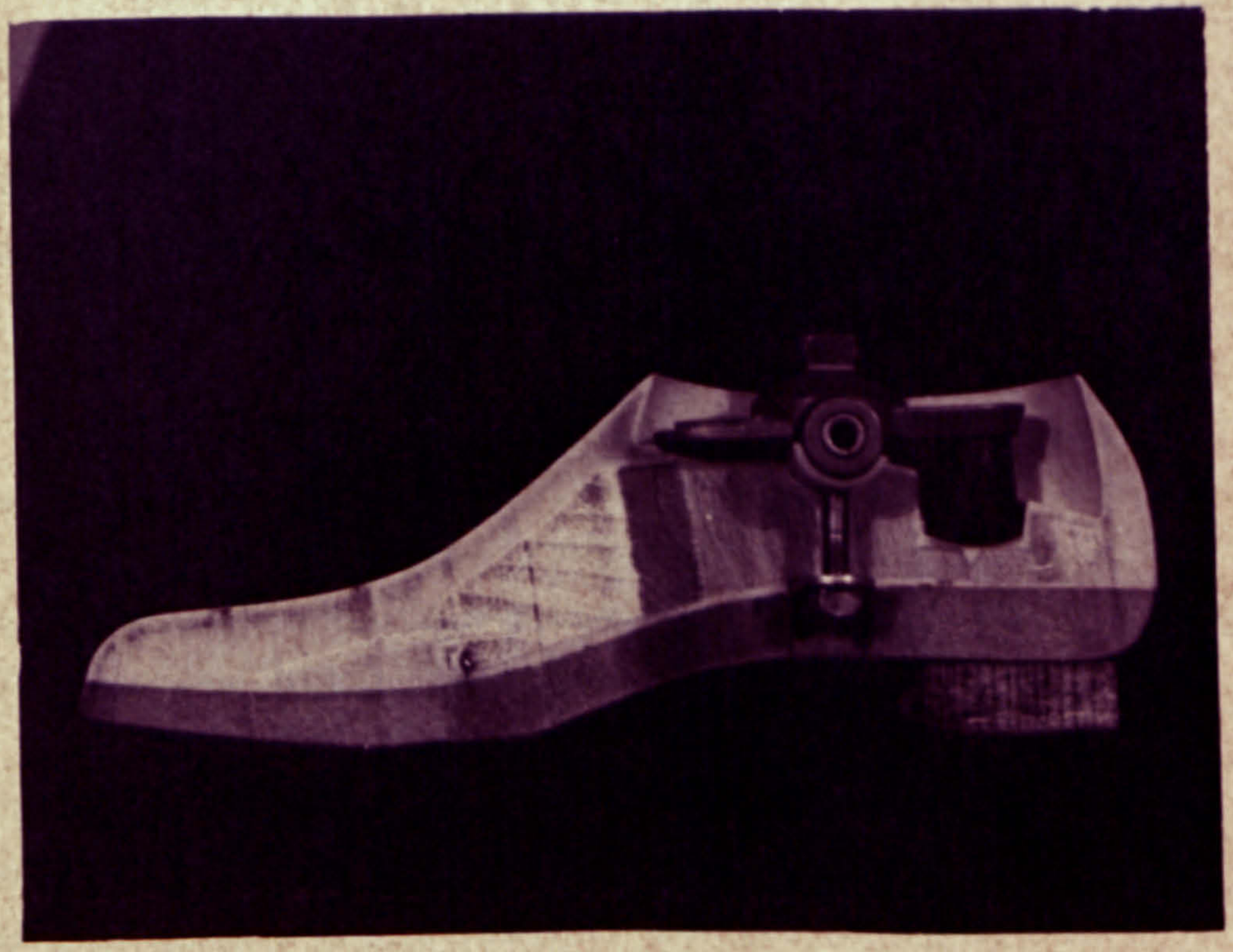

Figure 5.2(b) Cross-section of Otto Bock "moulded-type" Uniaxial Foot

single-axis knee unit and a wooden Uniaxial foot.

Patient Code : ALØ13 (activity level - 42)

This patient is 33 years of age, is employed as a prosthetist. He helps in some of the household chores like shopping, cooking and cleaning. In his spare time he plays golf, snooker and socialises.

His stump is in very good condition with a full range of motion. It is long and has very good muscular power.

The prosthesis prescribed is a Kellie Metal leg with a plastic quadrilateral total-contact suction socket. It has a single-axis knee unit and a SACH foot with a firm grade heel.

5.2. Selection of Prosthetic Feet

The two types of prosthetic feet being evaluated in this project are : the SACH foot and the "moulded-type" Uniaxial foot (hereafter referred to as Uniaxial foot). Both these feet were manufactured by Otto Bock Orthopadische Industrie KG. Figure 5.2(a) and (b) show the cross-section of the SACH and Uniaxial feet, respectively. The construction of the internal wooden keel of both prosthetic feet was found to be very different. The distal section of the keel of the SACH foot and the belting are somewhat concave in shape. This tends to give a smooth rolling action over the ball of the foot. The distal section of the keel of the Uniaxial foot and the belting are slightly convex in shape. Furthermore, the keel of the Uniaxial foot was observed to be made up of wood of different hardness. The rationale behind these designs is not clear.

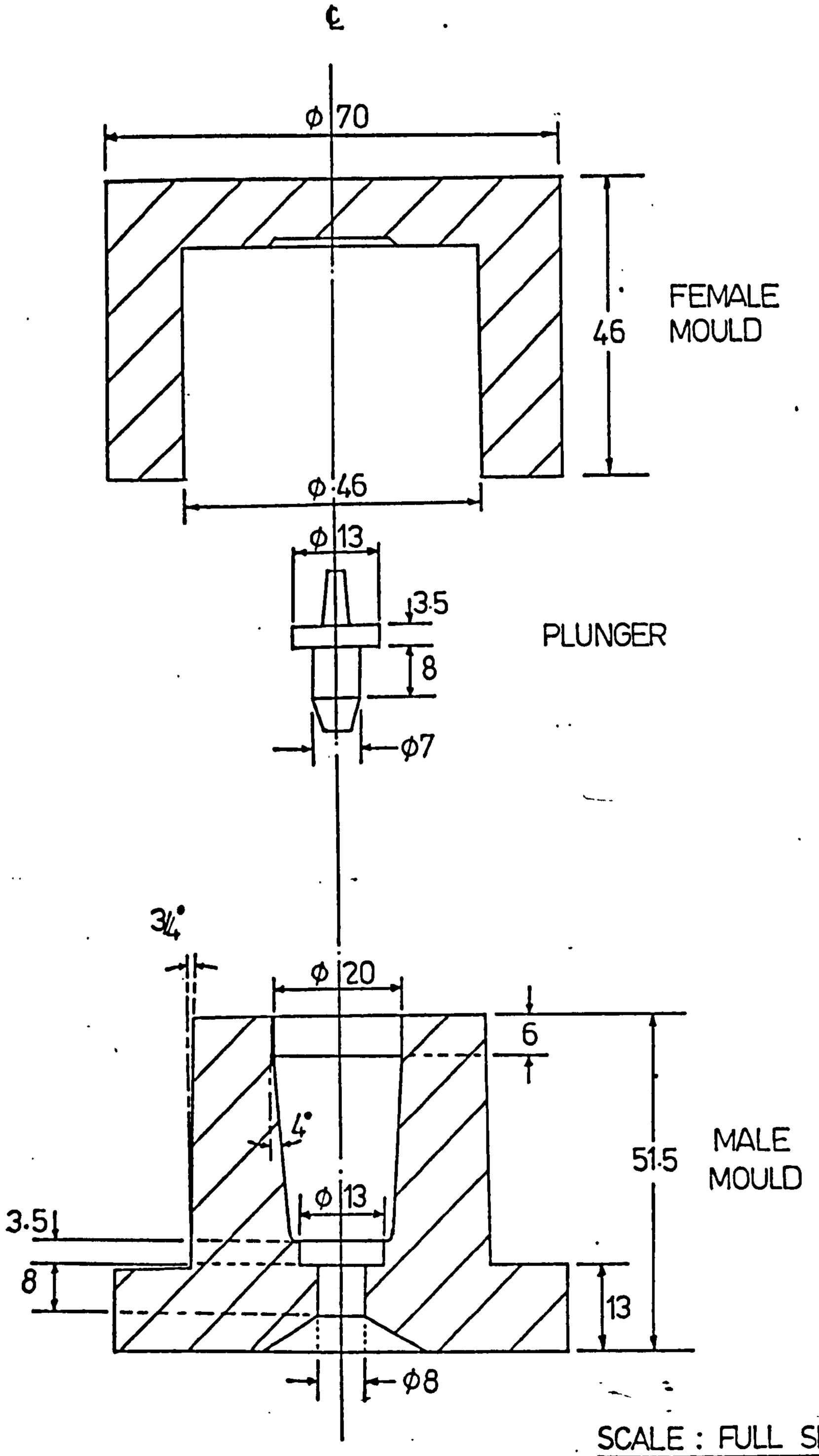

Figure 5.2.1(a) Plantar Rubber Bumper Compression mould

The SACH foot is available in three different grades of heel stiffness : soft, medium and firm. This range of choices was found to be sufficient for all the patients tested. The Uniaxial foot has only one plantar rubber bumper of standard stiffness supplied together with the modular type foot-shank attachment unit. This proved to be inadequate during fitting. The solution adopted to solve this problem is presented in the following section.

Load-deflection tests as specified by the Veterans Administration were carried out to check if the foot used complied with the specification. Furthermore, they allowed comparisons to be made between the heel stiffness of the SACH and Uniaxial feet preferred by a particular amputee.

5.2.1. Plantar Rubber Bumpers

Traditionally, most manufacturers supply one rubber bumper of a certain stiffness and the correct stiffness is achieved by precompression using suitable packing material or by paring down the rubber. In this investigation, the problem of achieving the appropriate rubber stiffness is being solved by providing a selection of bumpers of varying stiffness. It was envisaged that this will make fitting easier and make the achievement of the desired characteristics of the foot more exact.

Natural rubber compounds designated D42/3, D42/4, D42/5 and D42/6, having vulcanised Shore A hardness values of 56^{o}, 60^{o}, 80^{o} and 85^{o} respectively, were provided by the Malaysian Rubber Producers' Research Association. A simple three part compression mould, including an ejector, was designed and manufactured, see Figure 5.2.1(a). The shape of the mould was designed to

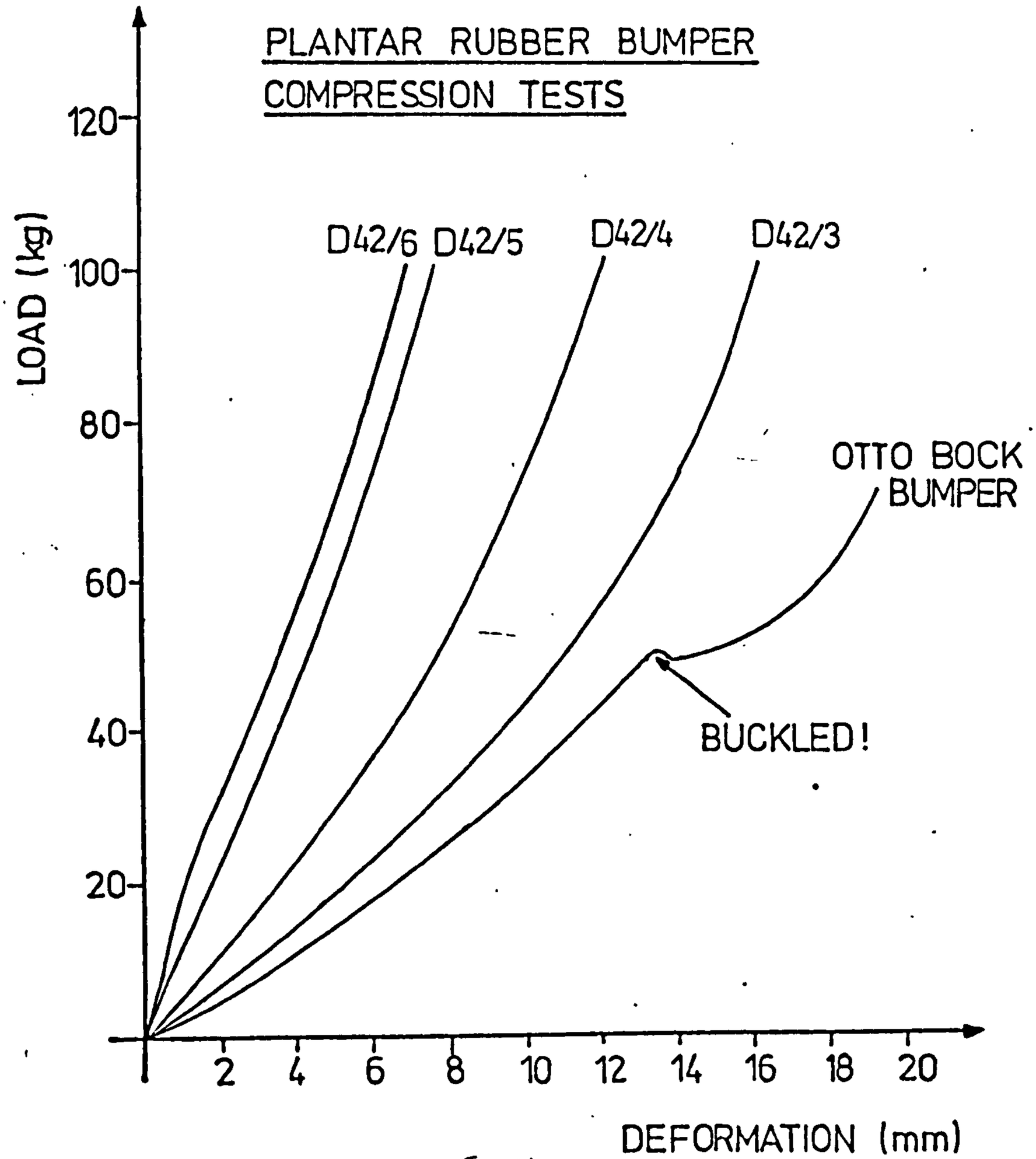

Figure 5.2.1. (b). Load Vs Deformation Curves of Plantar rubber bumpers

be exactly the same as the Otto Bock rubber bumper.

By weighing the Otto Bock rubber bumper, an estimate of the required amount of material to form the 'new' bumper could be obtained. It was then packed into the mould which by now was already warmed up in the hot plates of the moulding press. The loaded mould was then compressed between the hot plates at a pressure of 5 tonf/sq. ft. The curing time was set for 20 minutes at 155^{o}C.

The four rubber bumpers made in the Bioengineering Unit (hereafter called "Strathclyde" bumpers), as well as the Otto Bock rubber bumper were subjected to compression tests on an Instron Mechanical testing machine. Figure 5.2.1(b) shows the load versus deflection curves of each of the bumpers. The original rubber bumper tends to buckle at a load of about 50 kg., even with extreme care taken in ensuring pure compressive loading. All the "Strathclyde" bumpers proved to be much more stiff than that of the Otto Bock.

5.2.2. Mechanical Testings

Initial fittings and pilot tests were conducted on each of the patients involved in the evaluation programme. On these ocassions, the preferred heel stiffness of the SACH foot and the Uniaxial foot for each patient was noted. Each prosthetic foot recorded was then subjected to mechanical testings according to the standards and specifications proposed by the Veterans Administration Prosthetic Centre (1973).

A brief description of the different types of test is presented in the following, for detail the reader is referred to the article VAPC-L-7007-2, June 1973.

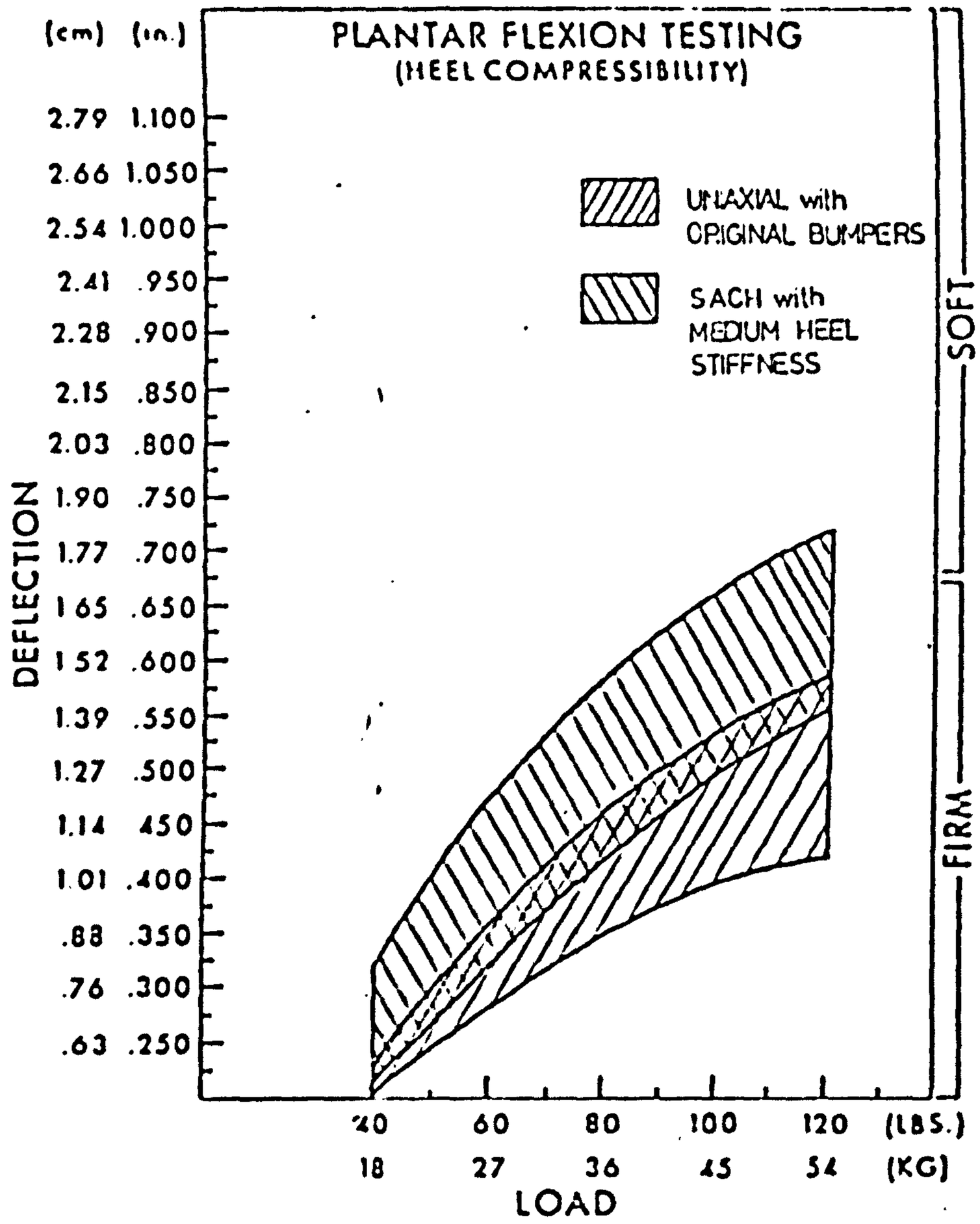

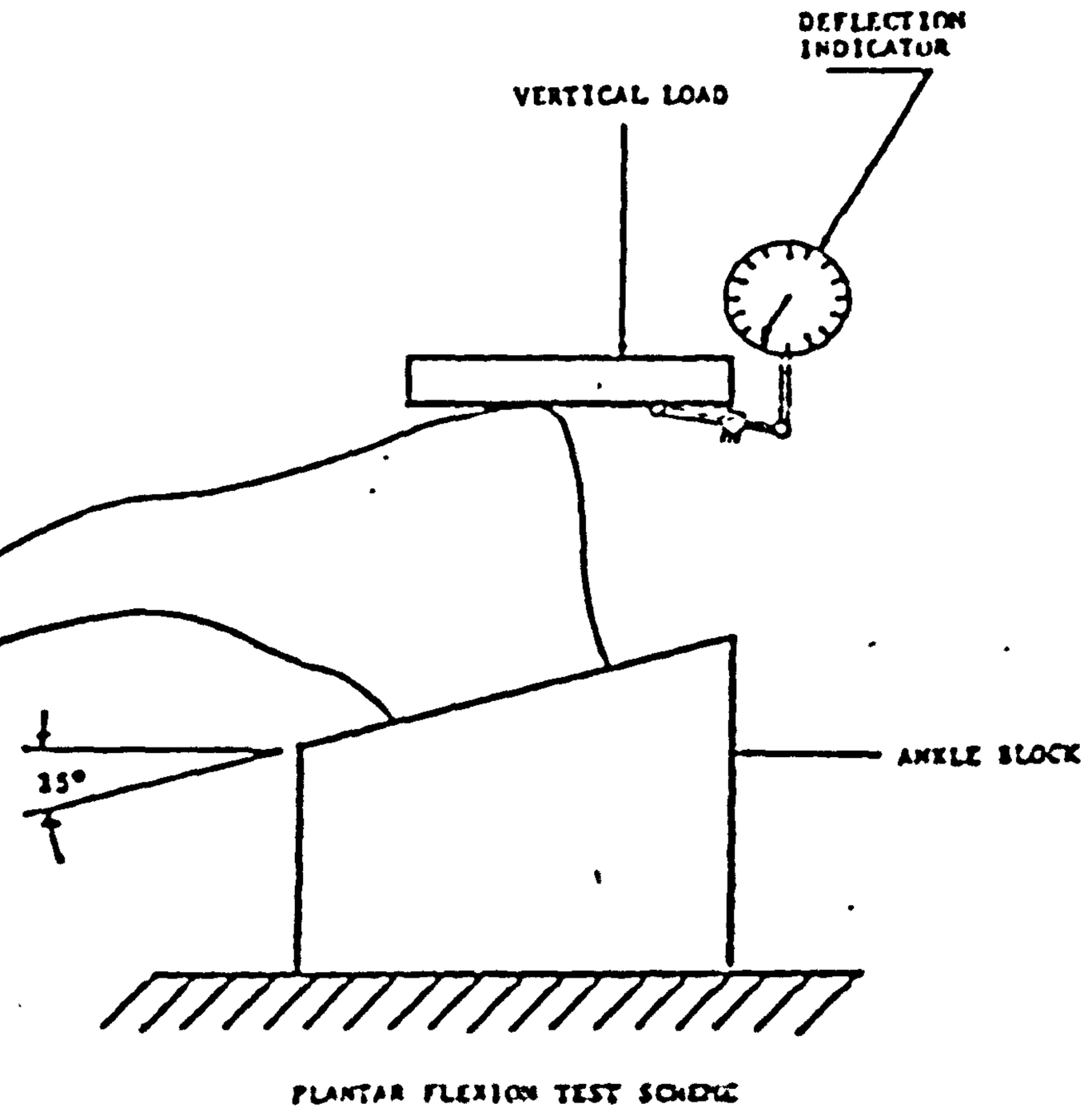

PLANTAR FLEXION TEST SCHEME

Figure 5.2.2(a) Plantar Flexion Testing

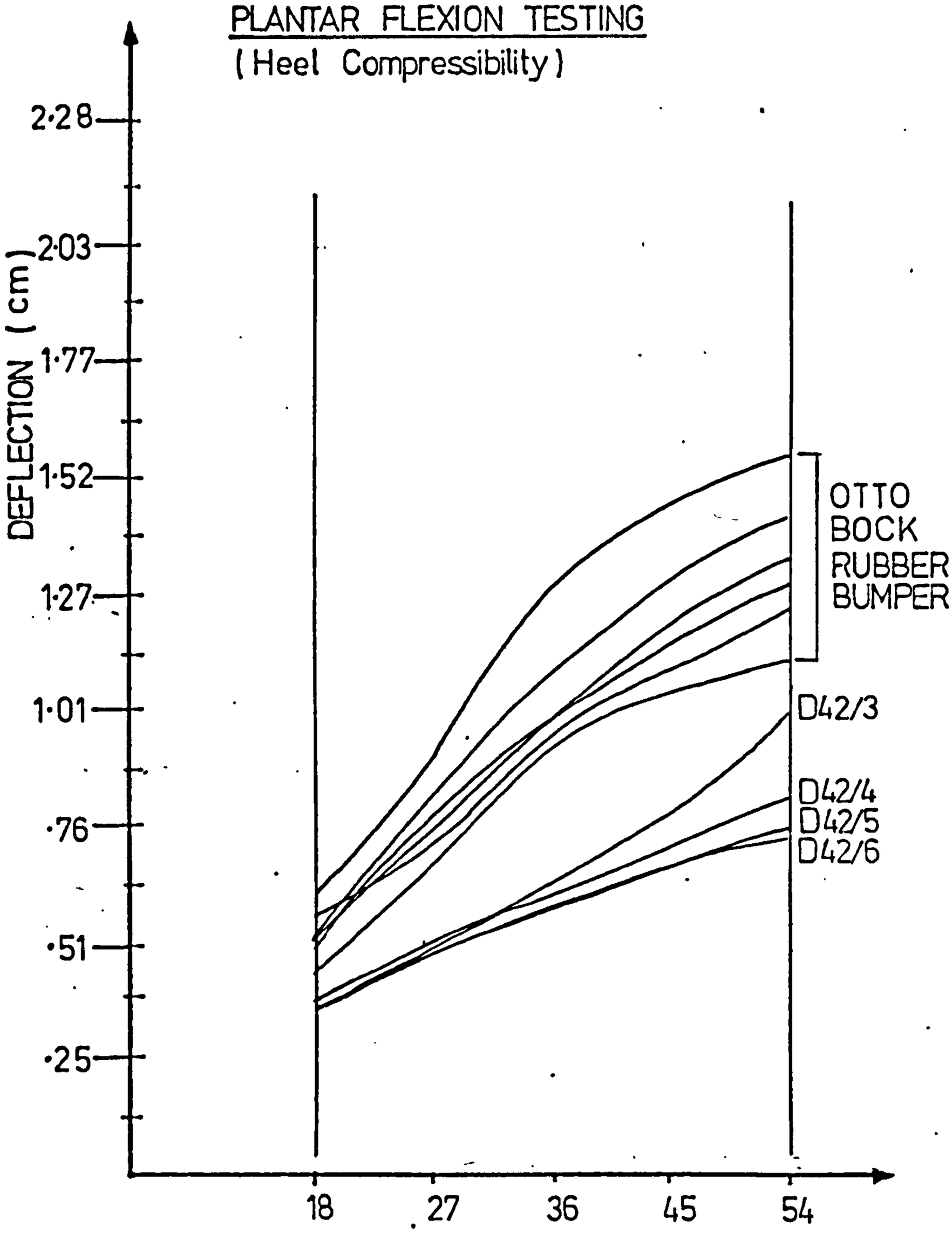

Figure 5.2.2(b) Plantar Flexion Curves of Uniaxial foot with varying plantar rubber bumpers

Plantar flexion of the foot was tested by applying load to the apex of the heel to approximate the forces applied to the foot during the period of heel contact to foot flat. The foot was placed in a plantar flexed position, 15^{o} to the horizontal. This represents the angle of approach for the foot during heel contact in normal level walking. The maximum load applied was 54kg as specified.

Dorsal flexion and toe-extension was tested by applying load to the plantar surface of each foot in the area of the toe. The foot was placed in a dorsiflexion position, 30^{o} to the horizontal. This represented the angle of foot during push-off in normal level walking. Vertical loads up to 45 kg were applied to approximate the forces applied to the foot during the period of mid-stance to push-off.

Although no mechanism was designed in either the SACH foot or Uniaxial foot for eversion and inversion movements, the polyurethane foam moulding does provide medio-lateral cushioning. Therefore, resistance to eversion and inversion forces was also tested. A vertical load of 45 kg was applied to the lateral border of the heel, which was mounted at an angle of 6^{o} to the horizontal in a position of inversion. The linear deflection recorded represents motion in the direction of eversion. The foot was then tested by applying the same load on the medial border of the ball of the foot, held at an angle of 6^{o} to the horizontal, in a position of eversion.

No transverse rotation is incorporated in either of the feet tested, therefore a rotational test procedure was not included.

A rig and fixture was fabricated to permit the

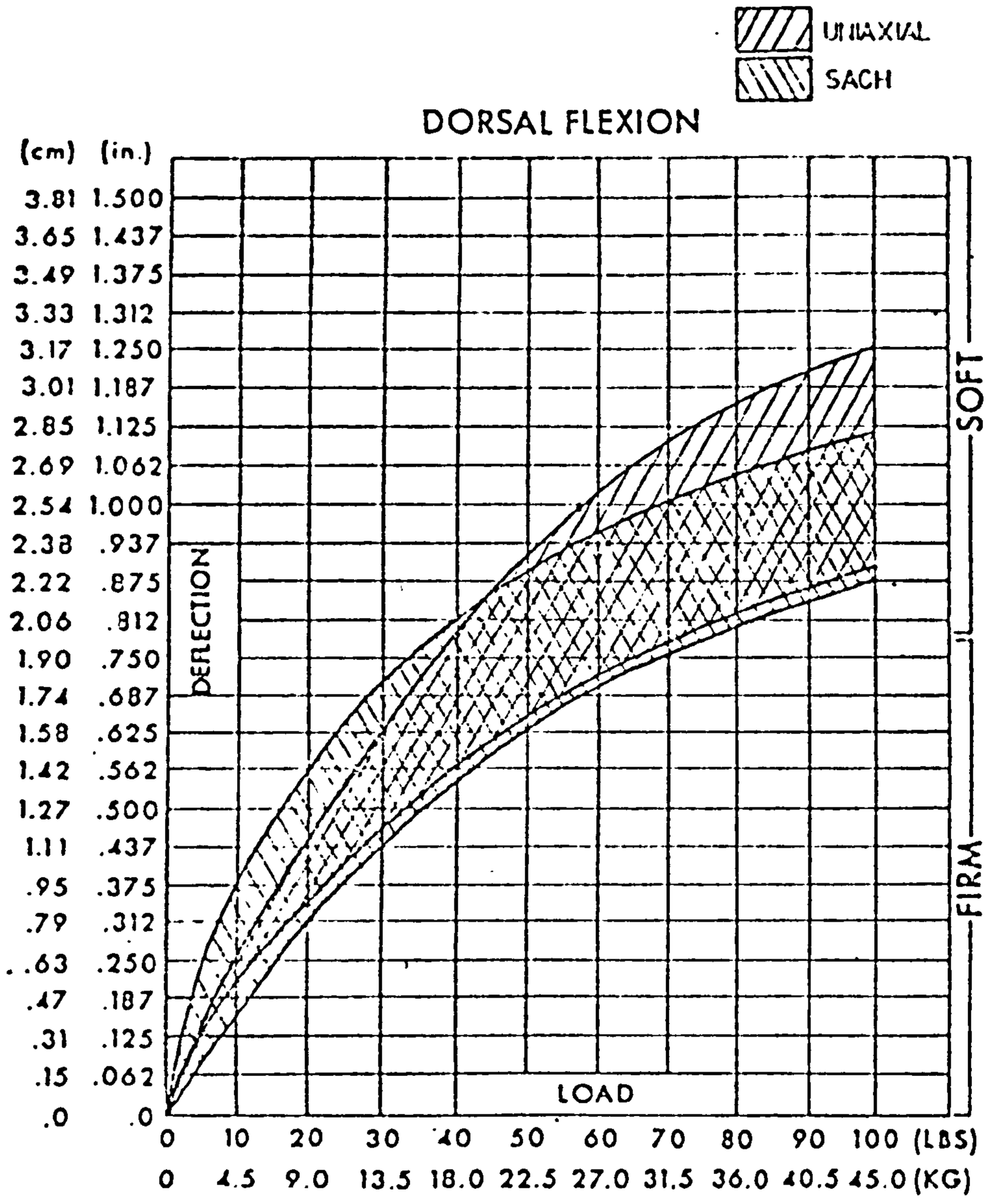

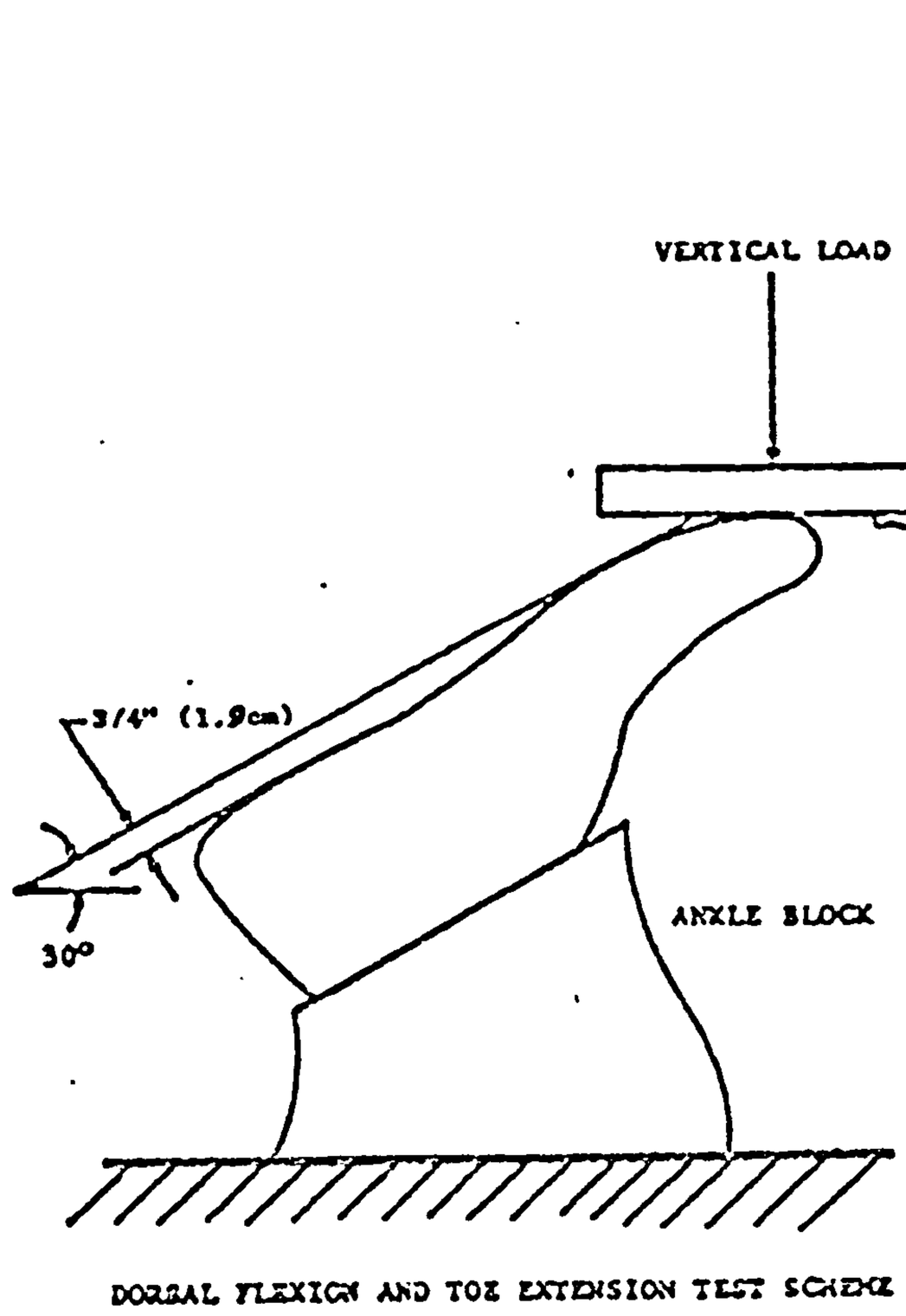

DORSAL FLEXION AND TOE EXTENSION TEST SCHEME

Figure 5.2.2(c) Dorsiflexion Testing

prosthetic foot to be fixed up in the various positions as specified. The foot when set up, was subjected to compression load on the Tinius-Olsen Mechanical Testing Machine.

The plantar flexion tests showed that each of the SACH feet tested complied with the VAPC specification as far as the heel stiffness was concerned. The variation of the data found in the same specified stiffness could be due to the slight quality difference in the foam used as heel cushion. The Uniaxial feet with original heel bumpers were found to be in the firm heel stiffness range. The variation of data present could be due to the quality of the rubber bumper and/or the position of the hinge-axis relative to the bumper, see Figure 5.2.2.(a).

The firm heel stiffness provided by the original rubber bumper was found to be "too soft" by most amputees during the initial fitting period and also during pilot tests. Therefore, "Strathclyde" rubber bumpers with higher stiffness were used. These were tested one at a time on the same foot. The results showed that all the "Strathclyde" rubber bumpers were much more stiff than the original one, see Figure 5.2.2(b).

The curves plotted for the "Dorsal Flexion and toe-extension" tests show very similar characteristics between the SACH and Unixial feet. Figure 5.2.2(c) shows the variations of the data collected from all the feet tested. The band of variations for the SACH feet seems to be fairly constant, whereas the band for the Uniaxial feet tends to spread wider with increasing load. Nevertheless, according to the VAPC specification, all the feet tested are classified as "soft" for dorsal flexion and toe extension.

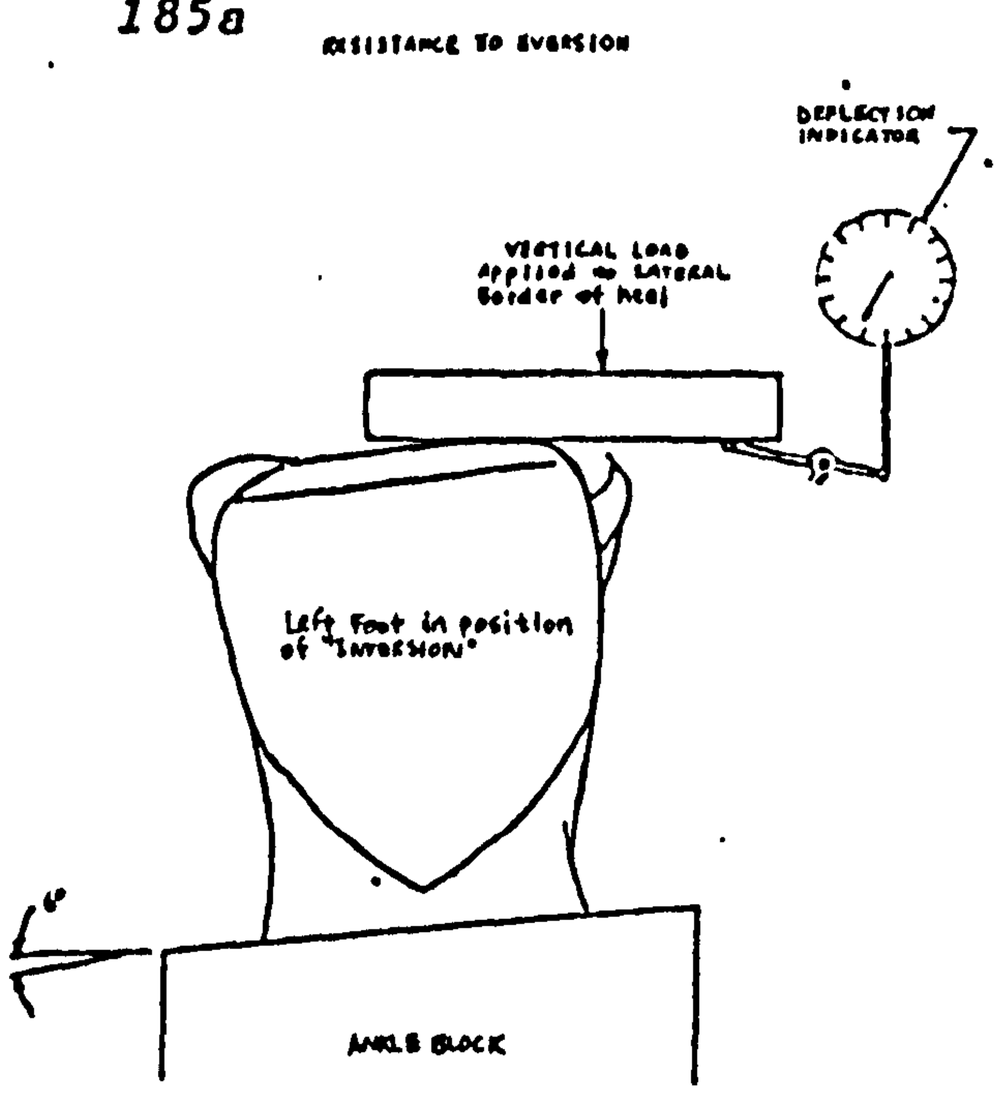

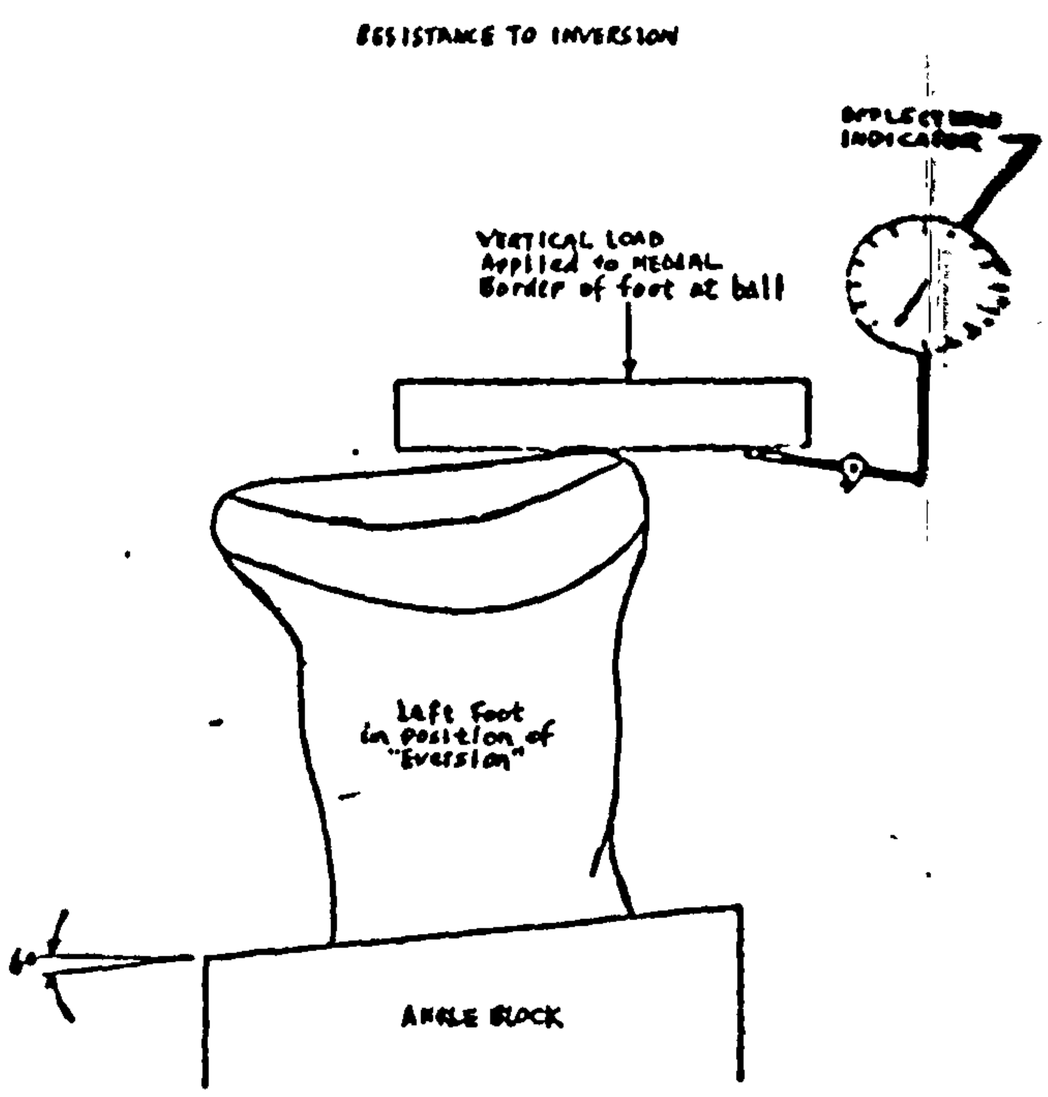

Uniaxial foot

Eversion (cm)	Inversion (cm)
0.9906	0.7874
0.9398	0.6985
0.8382	0.5969
0.8636	0.5334
1.0414	0.7112
1.2446	1.1430
Average= 0.9864	0.7451
(±0.1476)	(±0.2146)

SACH foot

Eversion (cm)	Inversion (cm)
0.7239	1.2319
0.8382	1.6510
0.8255	0.9271
0.9982	1.2319
0.8128	1.7018
0.9906	0.9906
Average= 0.8649	1.2891
(±0.1081)	(±0.3250)

Figure 5.2.2(d) "Eversion/Inversion" Testing

Figure 5.2.2.(d) shows the results of the "eversion-inversion" tests carried out on 6 SACH feet and 6 Uniaxial feet. All the deflection values shown, exceed the minimum deflection specified by the VAPC, viz 0.5cm. The average "eversion" values for both the SACH and Uniaxial feet show very small differences, however the average "inversion" values of the SACH foot are considerably larger than the Uniaxial foot.

5.3. Experimental Set-up

The review of existing recording systems for kinematic data in Chapter 2 provided a basis for the selection of a suitable system for use in this project.

The main options considered were : television system, Selspot, and cinecamera system. In view of the enormous amount of kinematic data that were going to be handled, the first two options seemed highly recommendable. Both have the advantage of recovering kinematic data very rapidly when used with an on-line computer. However, closer examination of these systems revealed several undesirable characteristics.

In the case of the television system, ambiguous signals may arise when markers are physically close to each other and therefore make them undistinguishable. This problem is understood to have been overcome by the Selspot system through the time-multiplexing technique used in sampling. However, the Selspot system has several drawbacks, mainly the unresolved reflection problem, especially when markers are positioned near to the floor. Besides these shortcomings, both the systems require human intervention where marker trajectories are incomplete or confused.

Data recovery from cine film is both tedious and

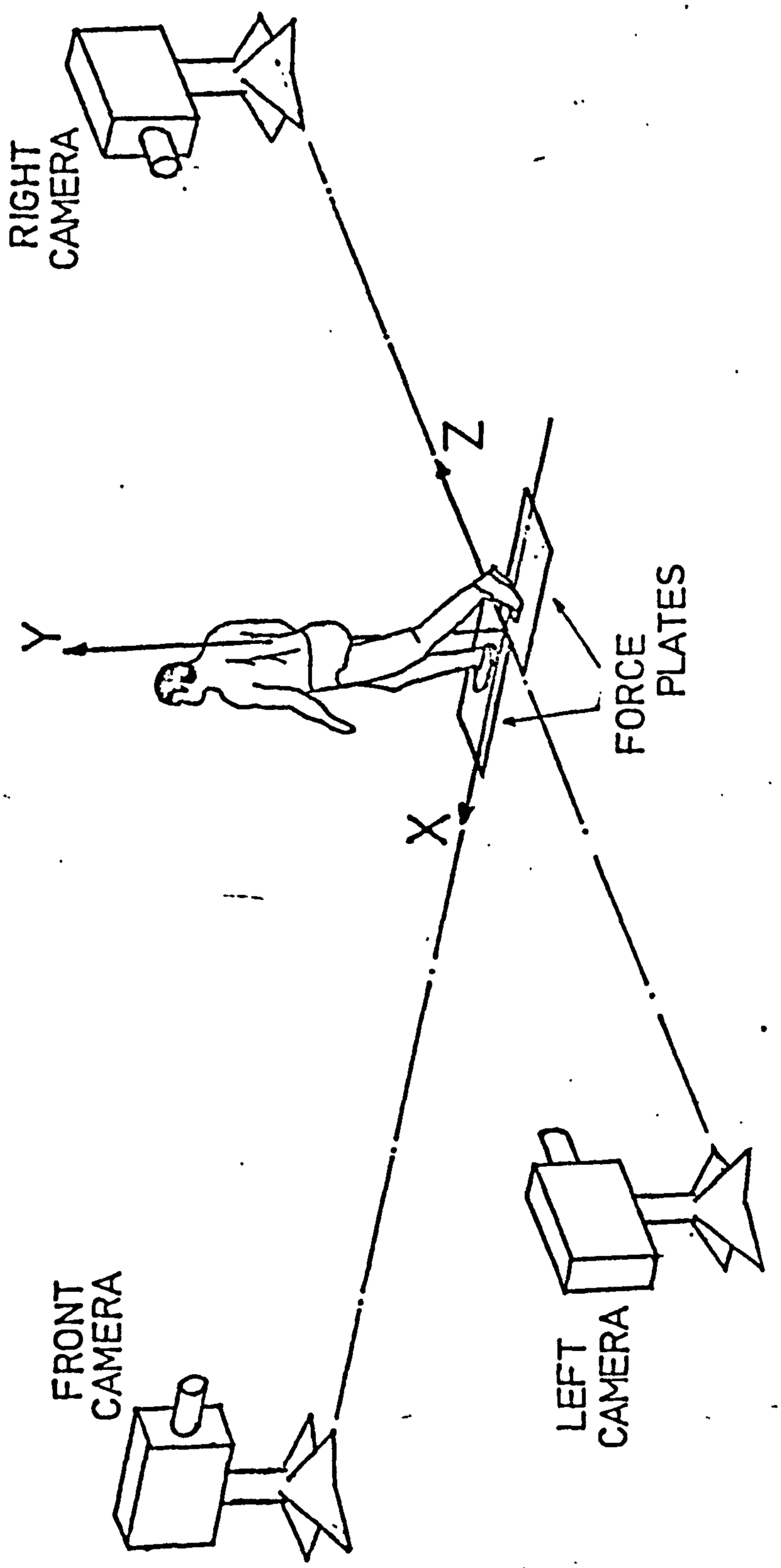

Figure 5.3.1. (a). Diagrammatic illustration of Cinecamera and Force plates arrangement

time-consuming, thus making the cine camera system very undesirable. However, the system does provide a complete visual image and when a marker is completely obscured for a short interval, the human operator can interpolate its position without too much difficulty. Furthermore, the system can be easily designed to allow three-dimensional analysis on the contralateral sides of the human body. It was for these reasons that the cine-camera system was chosen.

Since both the natural and prosthetic legs were going to be investigated in contralateral fashion, it appeared that a force platform measuring system was most suitable.

5.3.1. Kinematic Recording System

The walkpath is approximately 20 metres long. It consists of 2 force measuring platforms, 3 cine-cameras and a set of overhead floodlights above the force platforms. A diagrammatic representation of the overall arrangement is illustrated in Figure 5.3.1(a).

The prime purpose in using this particular set up is that it allows a 3-dimensional analysis on the contralateral sides of the human body.

The frame supporting the lamps can be adjusted to the required height to suit filming condition. Altogether 10 lamps are used, these being spread appropriately over the frame to give an even light distribution over the test area. The overall light intensity can be varied to accommodate the type of films used in the cinecameras. A light meter is used for this purpose.

The three cameras used are trade-named Paillard Bolex H16. The films used were 16 mm "Kodachrome 40"

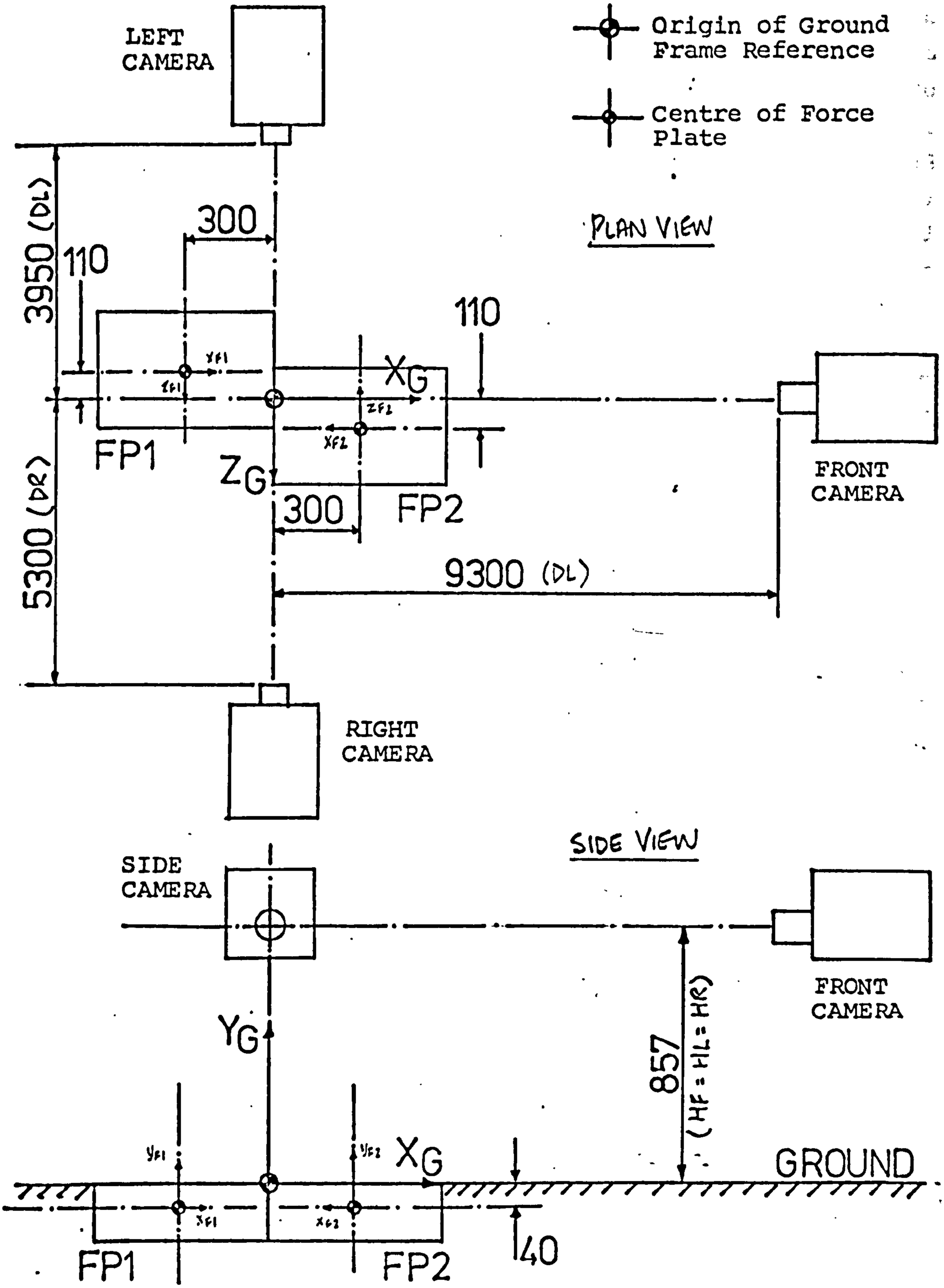

Figure 5.3.1(b) Dimensions of Cine-Cameras and Force Plates Arrangement

colour films. The reason for using colour was that it gives clearer and better definition of the body markers as well as the prominent anatomical features of the body.

Each camera is driven by a synchronous motor at mains frequency (i.e. 50 Hz $\pm$ 0.2 Hz) through a gear ratio of 8:1. The internal gear ratio of the camera is 1:8, therefore a shutter frequency of 50 cps (i.e. 20 ms per frame) is achieved. However, the shutter is set at a speed of 1/125th of a second; i.e. the shutter stays open for 8 ms of the 20 ms duration.

The cameras were aligned and bolted to the ground, such that the relative position was fixed throughout all the experimental tests. The optical axes of the three cameras intersect directly above the centre of the two force plate arrangement, which was the origin of the ground frame reference. All the camera units were equipped with a "Forward/Rewind" switch, which determined the direction of rotation of the motor and a "Local/ Remote" switch, which allowed all the cameras to be operated locally or from the control unit by a single switch.

The relative position of the cameras and the force plates was such that the walking cycle, (i.e. the stride), of both legs could be accommodated within the field of view of all the cameras and both feet were able to hit the force plates sequentially.

The height of the cameras and the distance of each one to the origin of the ground frame reference is as shown in Figure 5.3.1(b). In order to allow the full stature of the subject to be filmed, different lenses had to be used; 10 mm for the left and right, and 15 mm for the front.

5.3.2. Force Measurement System

The two force plates used in the experiment were manufactured by the Kistler Instrument AG of Switzerland. The force plate, according to the manufacturer's description, is a "multi-component measurement platform for biomechanics".

Each of the rectangular force plates has 4 transducers, one mounted on each pillar at each corner. Each transducer consists of three pairs of piezoelectric discs. One pair is used to determine the fore and aft shear (Fx), another is for the vertical force component (Fy) and the third one is for the medio-lateral shear (Fz). Besides measuring these 3 orthogonal components of an applied force on the platform, it is also capable of determining the resulting moment vector in its 3 components (i.e. Mx, My and Mz). Eight charge amplifiers and two summing amplifiers are required to obtain these six variables. Each of the force plates has its origin 40 mm below the top surface, with the direction of its axes similar to that of the ground frame of reference. All the variables are measured or calculated with respect to this axes system.

The two force plate arrangement is as shown in Figure 5.3.1(b). The plates are situated on the ground floor of the building and mounted in a concrete recessed pit, minimising (if not eliminating) any structural vibrations inherent in multi-storey buildings. The top surface of the plates is flush with the surrounding floor. Force plate No. 1 (FP1) was positioned in a reverse order to that of force plate No. 2 (FP2). This was due to the wiring difficulties that exist in this type of arrangement. Since the axes system used in the analysis is the one recommended in the CPRD's "Standardisation of gait analysis parameters and data-reduction

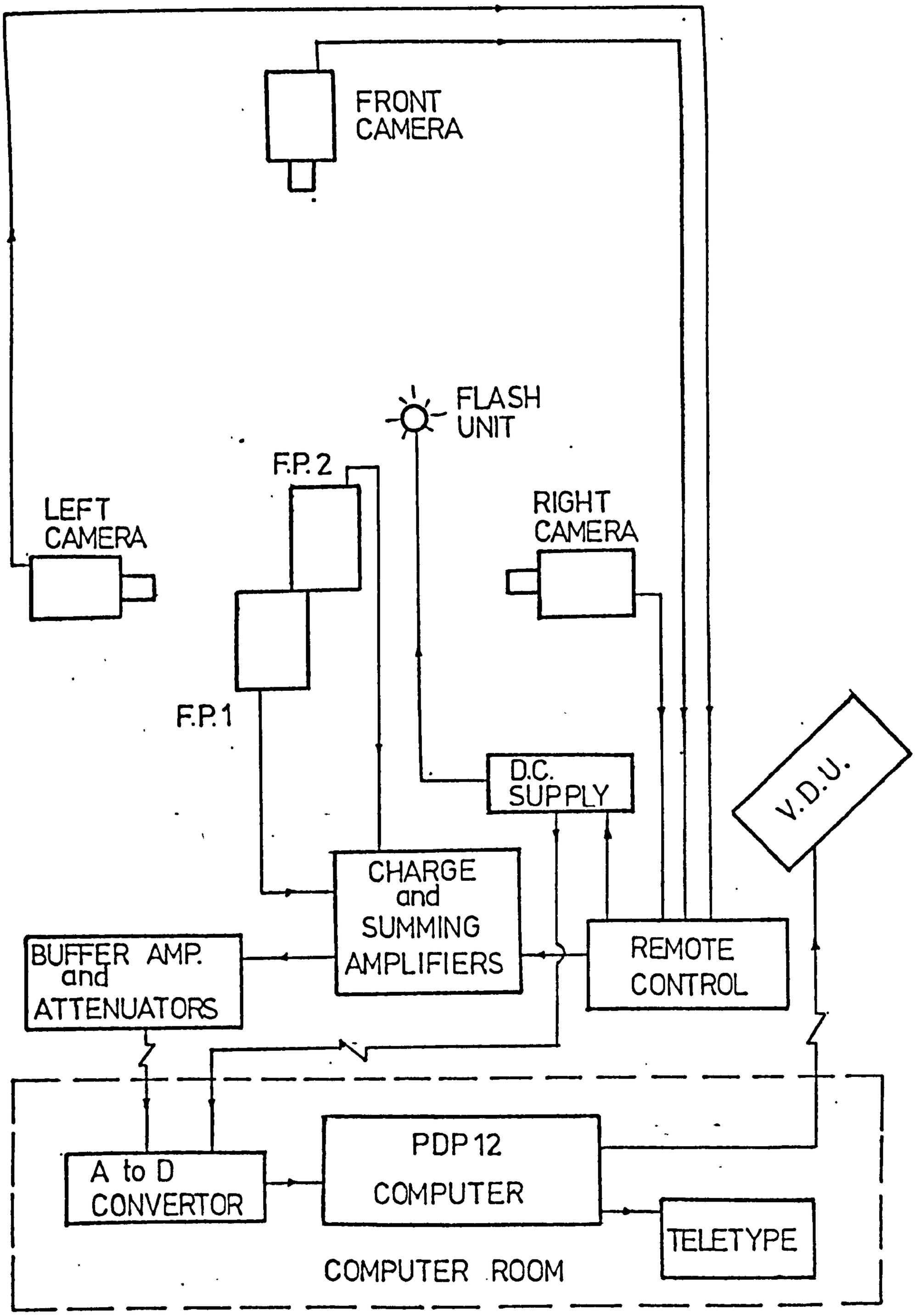

Figure 5.3.4 Schematic view of Walkpath and Computer Room Arrangement

technique" (1975), the "X" and "Y" directions of FP1 are in the opposite direction. This sign difference was remedied in the scaling factor during conversion to real units, (see Section 6.5.1).

5.3.3. Synchronisation of Kinematic and Force Data

A single filament flash bulb was used to synchronise data from both the force plates and the cinecameras. A 12 volt D.C. power supply was used to charge up the bulb to flash when operated, simultaneously sending a pulse to be registered in the starting channel of the PDP12 computer. Since the sampling frequency of both the force plates and cinecameras was chosen to be the same (i.e. 50 Hz), the flash on the cine films marked the same event as the pulse in the starting channel of the force plates data, thus making it possible to relate both these data.

The flash unit was positioned in such a way that it could be viewed by all the three cameras and, at the same time, not obscure, (or be obscured by), the subject walking over the force plates. A shield was put over the bulb to prevent glaring and the sudden effect of flashing on the subject's vision as he performed the test walk. The flash unit also carried the test number display card visible to all the three cameras, so that the particular test could be identified for analysis.

5.3.4. Data Storage System

The computer used in the set-up was a Digital PDP12 mini-computer. Figure 5.3.4 shows a schematic representation of the arrangement of the equipment in the walkpath and the computer room.

The output of the summing amplifiers was twelve

a) Shank & Foot Marker

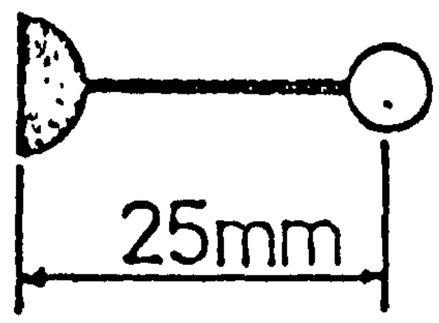

b) Shoulder Marker

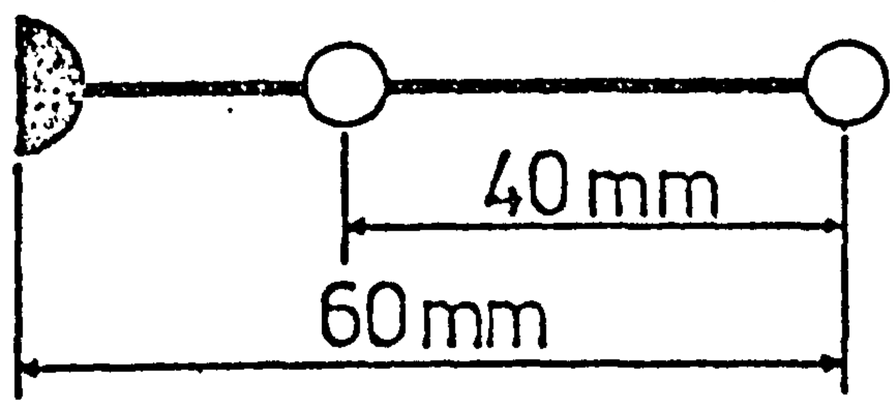

c) A.S.I.S. Marker

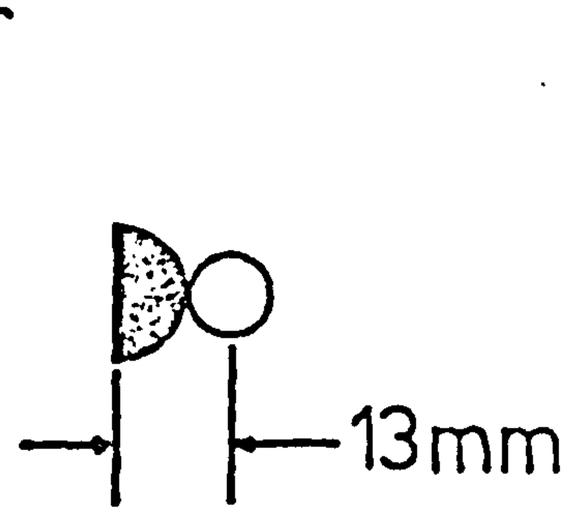

d) Tail Marker

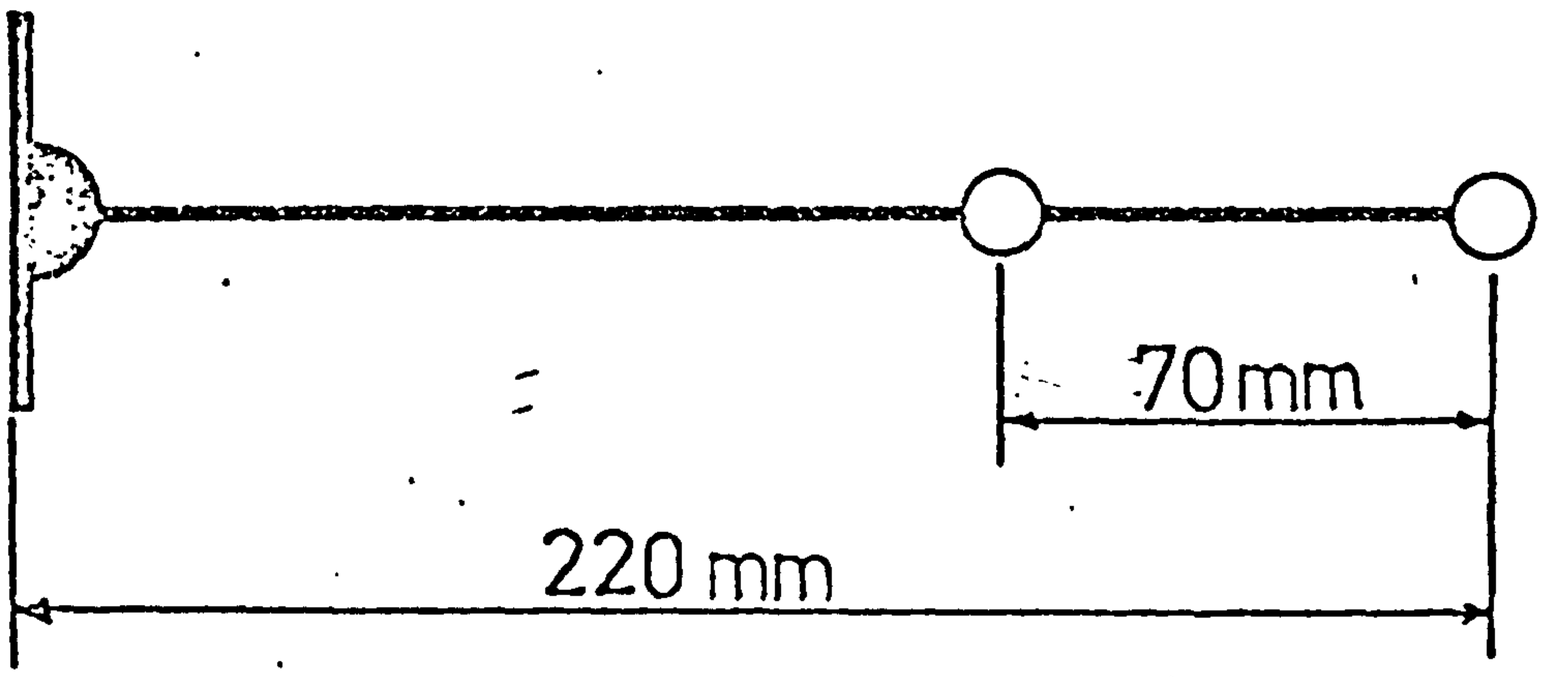

Figure 5.4.1. (a). Different types of body markers used.

variables, (six from each force plate), in the form of electrical signals. These have to be converted into digital data before they can be stored in the computer. However, the analogue to digital (A/D) converter has a limiting range of ±1V, therefore, varying attenuators, (so that each variable can be adjusted independently), were incorporated into the buffer amplifiers being connected to the output of the summing amplifiers. The reduction in value of the variables was accounted for in the scaling factors, see Section 6.5.1.

Thirteen channels were used during the sampling period to store the twelve variables from the force plates and the single pulse from the flash unit. After sampling was completed, all the data were then written on magnetic 'LINC' tape, with each channel occupying three blocks, after which the data were displaced on the Visual Display Unit (V.D.U) for examination. A successful test run and its relevant data can be retrieved and processed at a later date.

5.4. Experimental Approach

The detailed experimental procedure is presented in the following sections.

5.4.1. Body Markers

Markers used in the experiment were made from light weight spherical plastic beads of 10mm diameter. These beads were offset from the skin by wooden sticks with a hemispherical wooden base of 16mm diameter. The beads were painted with luminous yellow paint, so that they could be seen clearly on the cine films. The stalks and bases were painted matt black.

The different types of markers used for identifying

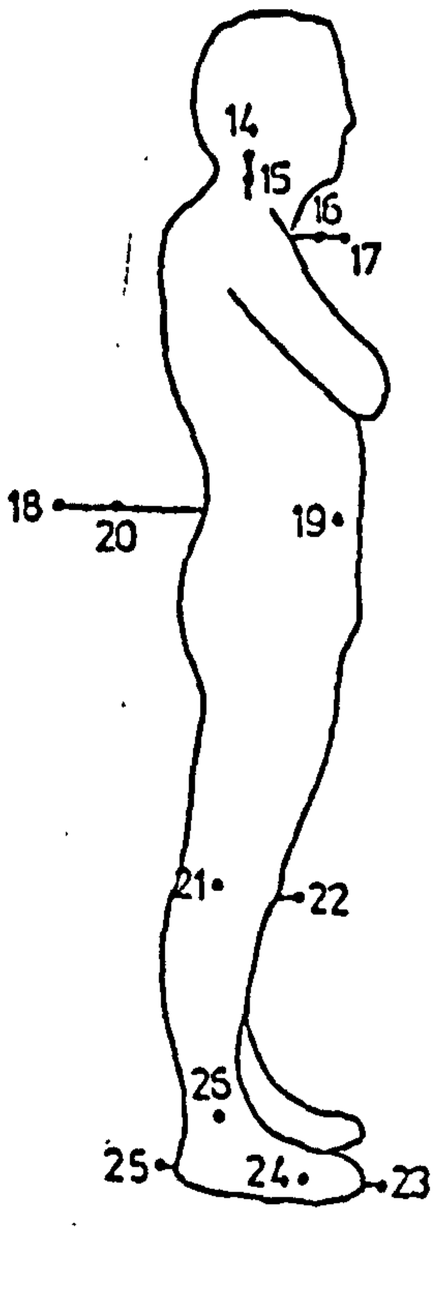

RIGHT VIEW

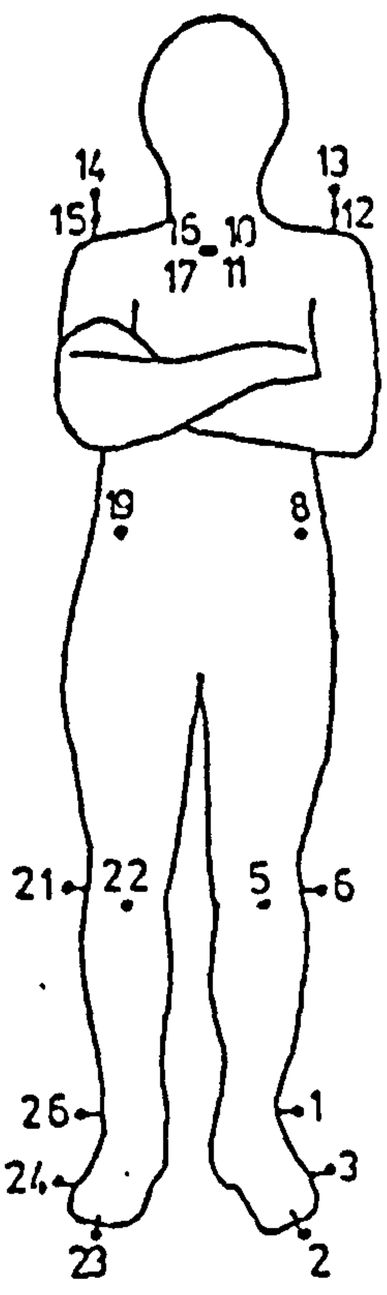

FRONT VIEW

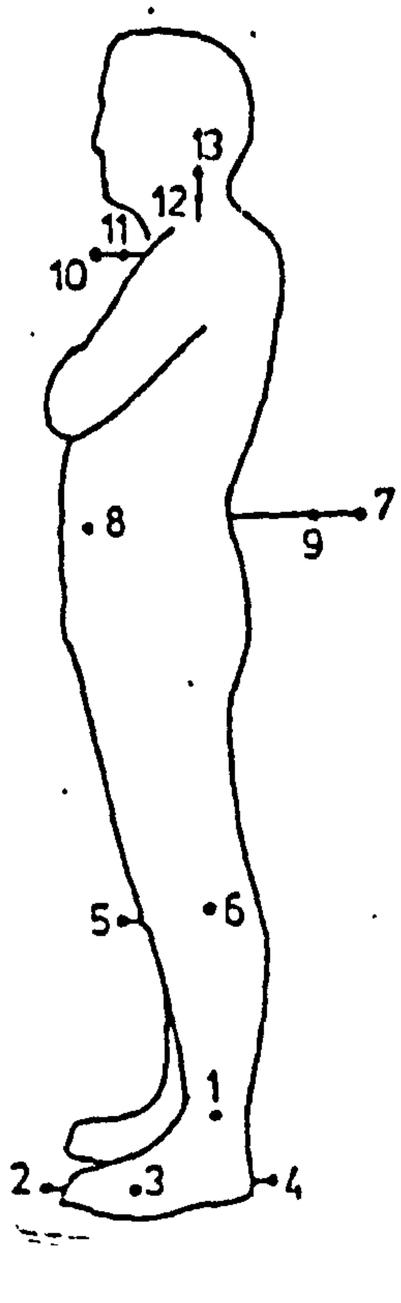

LEFT VIEW

MARKER NUMBERS AND ITS LOCATIONS

RIGHT	DEFINITION	LEFT
14	Acromion Process 1	13
15	Acromion Process 2	12
16	Sternum 2	11
17	Sternum 1	10
18	Pelvic Tail 1	7
19	Anterior Superior Illiac Spine	8
20	Pelvic Tail 2	9
21	Fibula head	6
22	Tibial tuberosity	5
25	Mid-Heel/Calcaneus	4
24	2nd ToeTip	3
23	5th Metarsar Base	2
26	Lateral Malleolus	1

Figure 5.4.1. (b). Locations of body markers.

the different anatomical features on the body are as shown in Figure 5.4.1(a). The reason for using the raised markers was that they can be seen by both front and side cameras, thus resulting in high resolution in the parallax correction involved in determining the true coordinates of the markers. As for the double bead markers, the coordinates of a "hidden" point can be calculated by knowing the coordinates of the two beads.

Positioning of the markers is an important exercise. These markers are used to locate the spatial coordinates of joint centres and also to determine the orientation of each body segment. (See Section 6.3). Therefore, extreme care had to be taken to position these markers accurately on the proper sites to define the joints and segments. Bony prominences were chosen as suitable sites for these markers because they can be easily located by palpation; skin movement about the area was minimal and joint centres can be easily referred to them.

As for the prosthetic leg, the marker arrangements for the shank and foot were slightly different. For the below-knee prosthesis, the tibial tuberosity and fibula head markers were transferred onto their respective position on the socket, whereas for the above-knee prosthesis, the fibula head marker was used to define the lateral aspect of the knee axis and the tibial tuberosity marker defined the frontal aspect of the artificial knee joint centre.

The mid-heel, toe-tip and 5th metatarsar base markers were placed on the prosthetic foot so that they corresponded to the similar positions on the natural foot. When the SACH foot was used, the lateral malleolus marker was positioned on the most lateral point at the top of the foot. However, with the Uniaxial foot, the

marker was positioned on the shin/shank tube directly above the ankle axis.

Double-sided adhesive tapes were used to position and fasten the markers to their locations. Figure 5.4.1(b) shows a diagrammatic representation of a subject with a full set of markers, as well as a list of descriptions of the markers' locations. The numbering system of the markers is important for analysis; it also indicates the flow of data collection (i.e. from the least to the largest number)of each particular film frame.

5.4.2. Experimental Prostheses

With the wealth of experience gained in the evaluation programme on modular assembled prostheses in the Unit; viz Solomonidis(editor)(1975 and 1980), it was decided that the experimental prosthesis would be constructed from the modular assembly system, since it permits the change of the ankle/foot component while keeping the rest of the components the same.

From the two studies cited above, the Otto Bock Modular system emerged as the system of choice for both the below-knee and above-knee prostheses. It was fairly simple to construct and easy to fit. It also provided a wide range of alignment adjustment for the prosthetist to work with. Patients found it just as acceptable as their conventional limbs.

Following is a description of the experimental prostheses used in the patient test.:

a) Below-knee Prosthesis

All below-knee amputees were provided with an Otto

List of Components

	Description	Material
1.	Socket shell	Polyester laminate
2.	Socket Attachment block	Wood and plastic
3.	Socket base plate	Steel
4.	Socket head screw	Steel
5.	Adjustment screws	Steel
6.	Adjustable Clamp adaptor	Steel
7.	Clamp screw	Steel
8.	Shin tube	Aluminium Alloy
9.	Adjustable adaptor	Steel
10.	Connection plate	Plastic
11.	Foot adaptor	Steel
12.	SACH foot	P.U. foam rubber and wood
or	Uniaxial foot with ankle mechanism	P.U. foam rubber, wood, metal and rubber

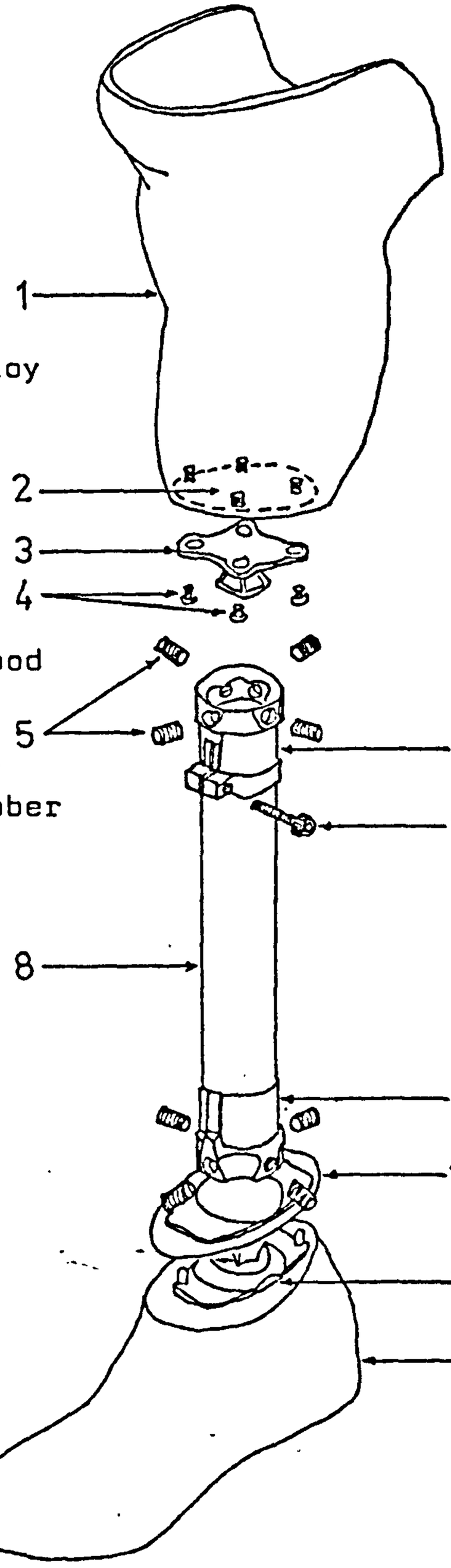

Figure 5.4.2. (a). A Typical BK experimental prosthesis

Bock Modular, Standard PTB with suprapatellar cuff suspension prosthesis. Each socket had an A20 density P.E. Lite (a closed foam polyethylene) liner, 5mm thick. A typical below-knee experimental prosthesis is as shown in Figure 5.4.2(a) with a listing of the components and its material.

Standard bench alignment was carried out when the inner socket was being bonded to the socket attachment block, broadly according to the P.T.B. manual, (Radcliffe and Foort, 1961). Four screws were used to secure the socket base plate to the attachment block. The socket base plate has a pyramid which was inserted into the adjustable adaptor and is held in place by four screws. The shin tube was attached to the adaptor and secured by a clamp screw. A similar pyramid/adjustable adaptor assembly was used to attach the foot to the distal end of the shin tube. The SACH foot was held in place by a single foot bolted onto the attachment plate. As for the Uniaxial foot, a pair of threaded stems on the ankle/foot attachment plate and corresponding nuts were employed. It must also be pointed out that two shin tubes of different lengths were used; one for the SACH foot and the other for the Uniaxial foot.

The prosthesis was then ready for dynamic alignment. Alignment adjustment can be made by rotating the socket and foot relative to the shin tube in the antero-posterior (A/P) and medio-lateral (M/L) planes. This was achieved by successive loosening and tightening of the appropriate screws on the adjustable adaptor at either end of the shin tube. External and internal rotations of the foot were made by loosening the clamp screw of the adaptor and rotating the shin tube to the required angle.

List of components

Description	Material
1.Pedilen ring	Rigid P.U. foam
2.Socket shell	Polyester laminate
3.Suction valve	Metal and plastic
4.Adjustable screws	Steel
5.Socket head screws	Steel
6.Socket base plate	Steel
7.Pyramids	Steel
8.Knee unit	Steel and plastic
9.Adjustable Screws	Steel
10.Adjustable Clamp Adaptor	Steel
11.Clamp Screw	Steel
12.Shank tube	Aluminium alloy
13.Adjustment screws	Steel
14.Connection plate	Plastic
15.Foot Adaptor	Steel
16.SACH foot	P.U. foam rubber and wood
or Uniaxial foot with ankle mechanism	P.U. foam rubber, wood, metal and rubber.

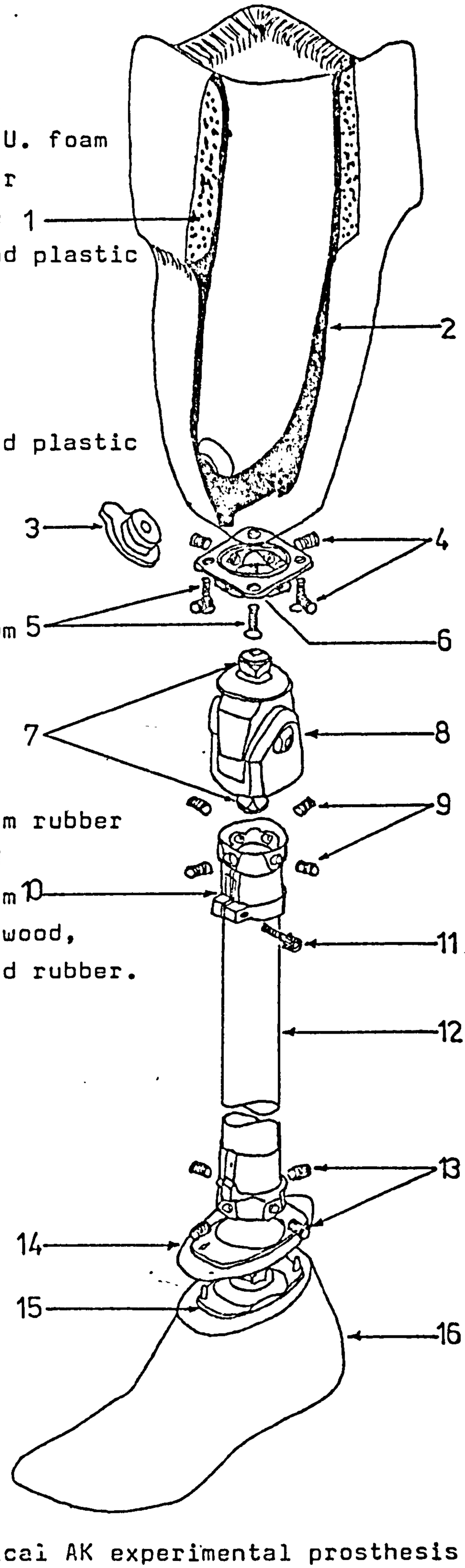

Figure 5.4.2. (b). A Typical AK experimental prosthesis

b) Above-knee Prosthesis

All the above-knee amputees were provided with an Otto Bock modular prosthesis, fitted with a quadrilateral (total contact) suction socket and a Uniaxial knee mechanism. A typical above-knee experimental prosthesis is as shown in Figure 5.4.2(b) with a listing of the components and its materials.

Bench alignment was done during the casting of the stump. The required socket flexion and lateral tilt were incorporated into the cast. The dimensions of these parameters depend on the length and musculature condition of the stump. Values quoted in Radcliffe (1969) were used as guidelines.

The fabricated socket has to be assembled so that the built-in bench alignment is maintained. This was done by setting both the medial and posterior surfaces of the casting brim horizontally. A plumb line was then used to establish the medial and posterior vertical reference lines passing through the mid-point of the respective brims. With the socket held in this position, the socket attachment block was then bonded squarely to the distal built-up end of the socket. The medial and posterior vertical reference lines were used to centralise the attachment block. The build-up of the distal end of the socket with rigid polyurethene foam to approximately the length of the thigh is necessary for the correct positioning of the knee mechanism.

A socket base plate adaptor was secured to the attachment block with four screws. The pyramid/adaptor configuration described in the below-knee prosthesis, was used to assemble the socket, knee unit, shank tube and the foot together. Again two different lengths of shank tubes were required for the two types of feet used (i.e.

SACH and Uniaxial). Attachment of those feet to the foot attachment plate was similar to that described in the below-knee prosthesis.

The prosthesis was then ready for dynamic alignment. Alignment adjustment of the above-knee prosthesis was more complicated than that of the below-knee prosthesis, due to the presence of the prosthetic knee mechanism. All the components in the above knee prosthesis can be rotated relative to each other in both the antero-posterior and medio-lateral planes via the four tilting screws in the adjustment adaptor securing the pyramid. External and internal rotations of the foot can be achieved by loosening the clamp screw on the adaptor distal to the knee mechanism and rotating the shank tube and foot. Rotation of the knee mechanism relative to the socket in the transverse plane was done by loosening the four socket head screws securing the base plate adaptor and rotating the knee mechanism.

All the prostheses (both below-knees and above-knees) were constructed, fitted and aligned by the same prosthetist and prosthetic technician.

5.4.3. Preparation of test equipment

Primarily, two areas were involved during patient test; namely the computer room and the walkpath.

In the computer room, the appropriate sampling program was loaded onto the PDP12 computer together with a magnetic 'LINC' tape for data storing. The program ("SAMPLBM", written by Jordan, 1978) allowed the force plates data to be sampled at a specified frequency (i.e. 50 Hz) and then stored onto the 'LINC' tape. Thirteen channels were required to register all the variables present (see Section 5.3.4). The program

PATIENT CODE: | | | | | |

VISIT NUMBER: | | | |

FORCE PLATE INFORMATION

CHARGE AMPLIFIER	TOP	BOTTOM
FP1		
FP2		

BUFFER AMPLIFIER	FX	FY	FZ	MX	MY	MZ
FP1						
FP2						

TEST WALK RECORDS

RUN NUMBERS	ACTIVITY	REMARKS	STARTING BLOCK NUMBERS
1			
2			
3			
4			
5			
6			
7			
8			
9			
10			
11			
12			
13			
14			
15			

Other Comments:

Figure 5.4.3. Test Information Form

had the advantage of not requiring an operator at the computer terminal, which was two floors above the walk-path. The connections between the computer and the force plates, and the flash unit had to be checked, to ensure continuity.

In the walkpath, the three cinecameras were loaded with films. The floodlights were adjusted and switched on well before the actual patient test, (approximately about 20 mins). The focal lengths of all the cameras were adjusted under these lighting conditions, with the help of a field marker positioned at the centre of the ground frame of reference. The aperture on the front camera was set at f1.5 and the side cameras were set at f2.0. All the cameras were then switched on to 'Remote', ready for operation. The power supply to both force plates was switched on to allow the plates to warm up and stabilise. The settings on the buffer amplifiers were checked and recorded (see Figure 5.4.3). The gains on both charge amplifiers were adjusted to suit the weight of the patient. These too were recorded. The flash unit was set up, with the flash bulb and the pulse going to the computer connected in parallel.

In this way, the recording system was ready for the patient test.

5.4.4. Test Procedure

The following is the test procedure with the patient fitted with the experimental prosthesis, either with the SACH or Uniaxial foot.

Dynamic alignment was performed by an experienced prosthetist. This not only involved the rotating or tilting of the various components, but it also involved the selection of the most suitable density of heel

PATIENT CODE: | | | | | |

VISIT NUMBER: | | | |

GAIT ANALYSIS FORM
==========

SCORING SCALE :

1 - None; 2 - Some but Satisfactory; 3 - Some but Fair;

4 - Excessive and Unsatisfactory

GAIT DEVIATIONS	SACH	Uniaxial
a) Abducted gait		
b) Circumduction		
c) Vaulting		
d) Uneven arm Swing		
e) Uneven Step length		
f) Lateral bending of trunk		
g) Excessive trunk extension		
h) Terminal swing impact		
i) Instability of prosthetic knee		
j) Excessive prosthetic knee flexion		
k) Insufficient knee flexion		
l) Excessive prosthetic lateral thrust		
m) Early knee flexion		
n) Delay knee flexion		
o) Uneven heel rise		
p) Medial whip of foot		
q) Lateral whip of foot		
r) Prosthetic foot rotation at heel strike		
s) Foot-slap		
t) Toe-out		

Other comments :

Figure 5.4.4. (a). Gait Analysis Form

PATIENT CODE: | | | | | |

VISIT NUMBER: | | | |

PATIENT'S PARTICULAR

NAME : | | DATE OF TEST : | |

AGE : | | WEIGHT : | | AMPUTATION HISTORY

SEX : | M | F | HEIGHT : | | DATE : | |

CAUSE: | |

LEVEL: | |

SIDE : | |

BODY MEASUREMENT(All dimensions in mm)

(i) Shoulder

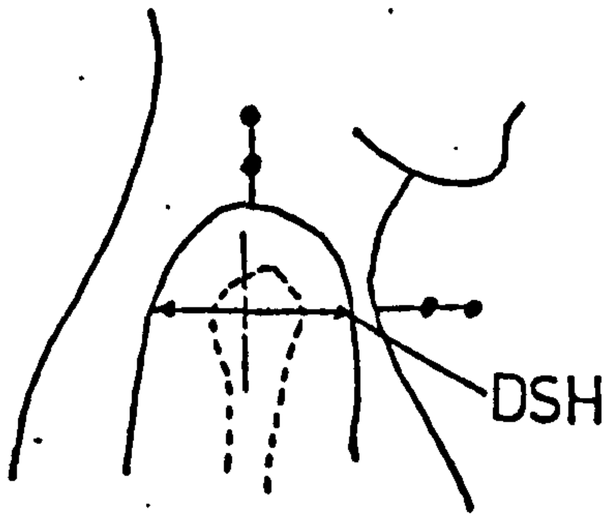

	Left(L)	Right(R)
DSH		

(ii) Pelvis

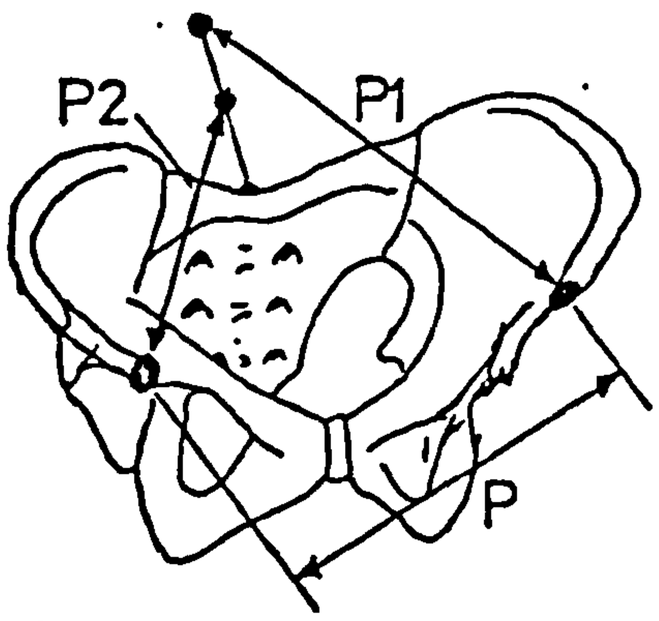

P		
	Left(L)	Right(R)
P1		
P2		
HX		
HY		

Figure 5.4.4(b) Body Measurement Form

to be cont'd

(iii) Shank

	SACH Foot		Uniaxial Foot	
	Left(L)	Right(R)	Left(L)	Right(R)
S1				
S2				
S3				
S4				
S5				

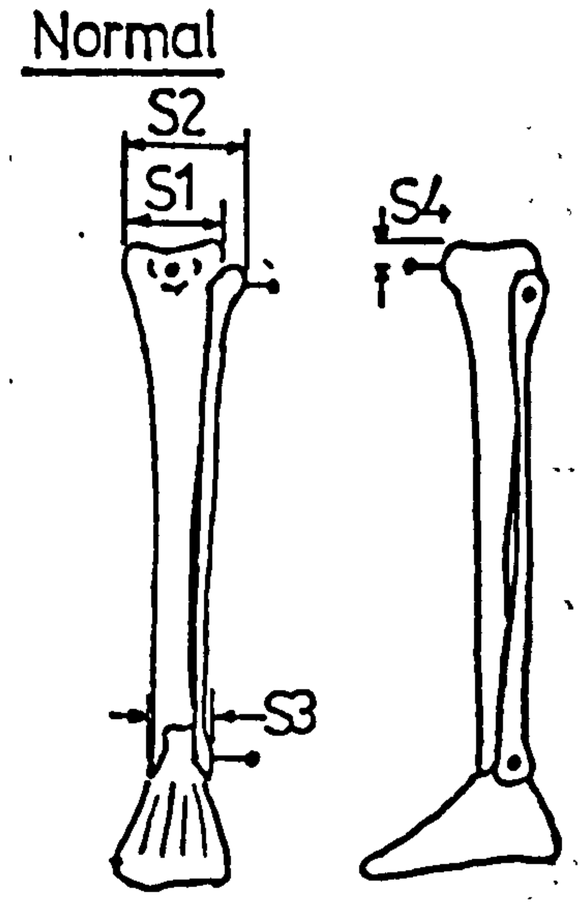

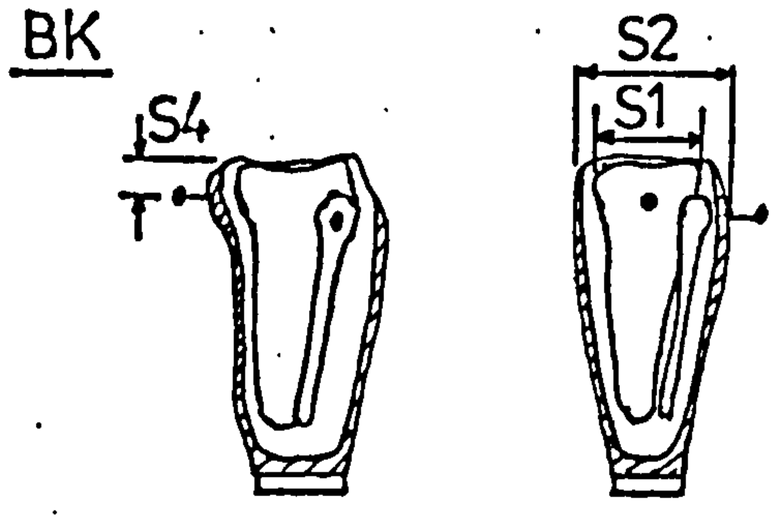

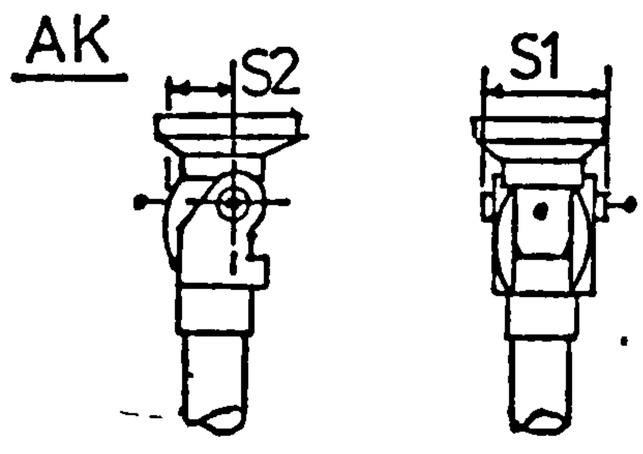

Socket thickness†
ST

†For BK Socket Only

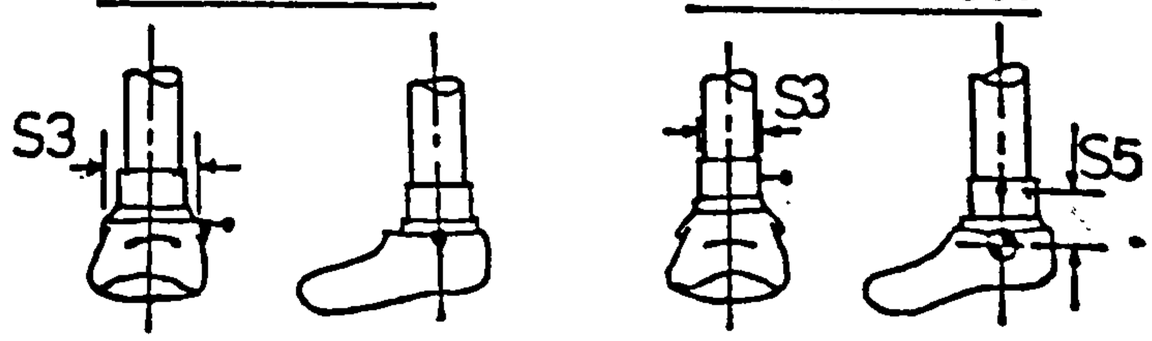

(iv) Foot

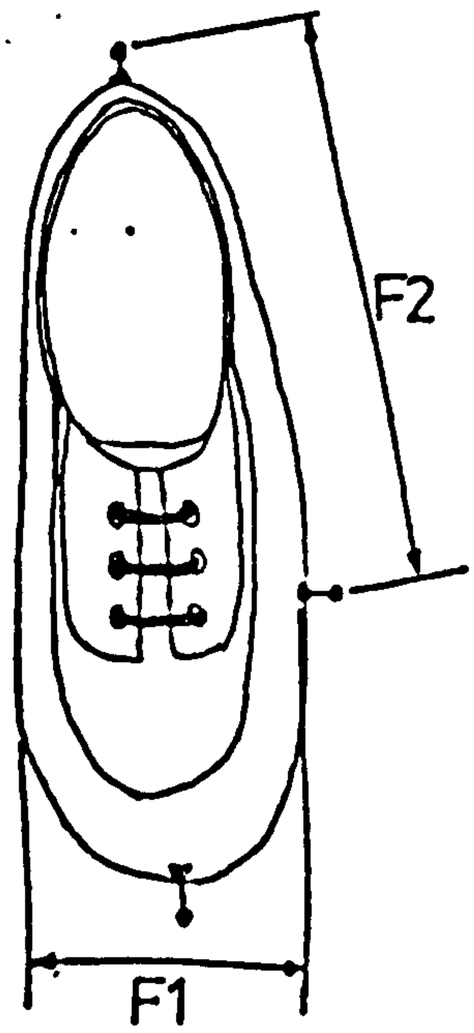

	Left(L)	Right(R)
F1		
F2		

Figure 5.4.4(b) Body Measurement Form (Cont'd)

cushion for the SACH foot or the plantar bumper for the Uniaxial foot. When the "optimum" alignment was achieved, which satisfied both the patient and the prosthetist, the patient was allowed to get accustomed to the experimental prosthesis. Meanwhile, the prosthetist made the final assessment of the patient's gait on a gait analysis form. (See Figure 5.4.4(a)).

Markers were positioned and stuck on to the anatomical landmarks with double-sided adhesive tape. (See Section 5.4.1). The patient was then again permitted to get used to the markers during locomotion. When everything was ready for the test walk, the patient was directed to walk along the walkpath towards the front camera at his own natural walking speed. Several "dummy" walks were required to establish the starting mark for the patient, in order that he would strike both force plates during the test walk. Most patients were aware of the existence of the force plates and had the tendency to alter their walking speed and step length in order to hit both plates. To overcome this, an object/ target was positioned at the patient's eye level above the front camera for the patient to focus on when performing the test walk.

The appropriate test number was displayed and a new bulb inserted into the flash unit. The data sampling sequence is as follows; as the patient approaches the force plates, (approximately two steps before), the cine-cameras are switched on, to allow the cameras to pick up to normal running speed. Immediately, after that the charger to the amplifiers of the force plates is activated and just before the left foot hits force plate No.1, the sampling switch is operated. Immediately after the right foot leaves force plate No. 2, the flash bulb is fired, so that it will not affect any relevant film frame due to the brightness of the flash. After this the

(iii) Shank

	SACH Foot		Uniaxial Foot	
	Left(L)	Right(R)	Left(L)	Right(R)
S1				
S2				
S3				
S4				
S5				

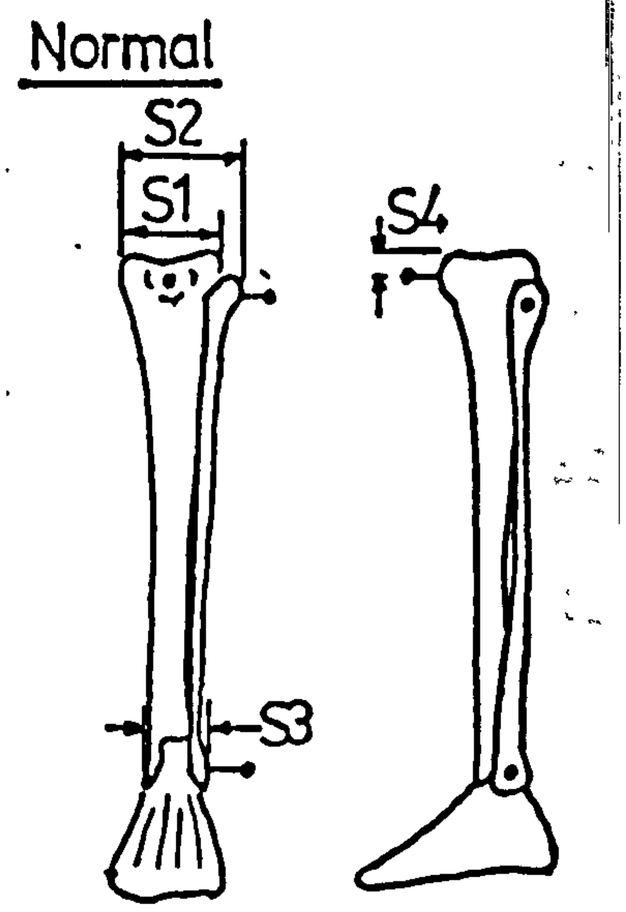

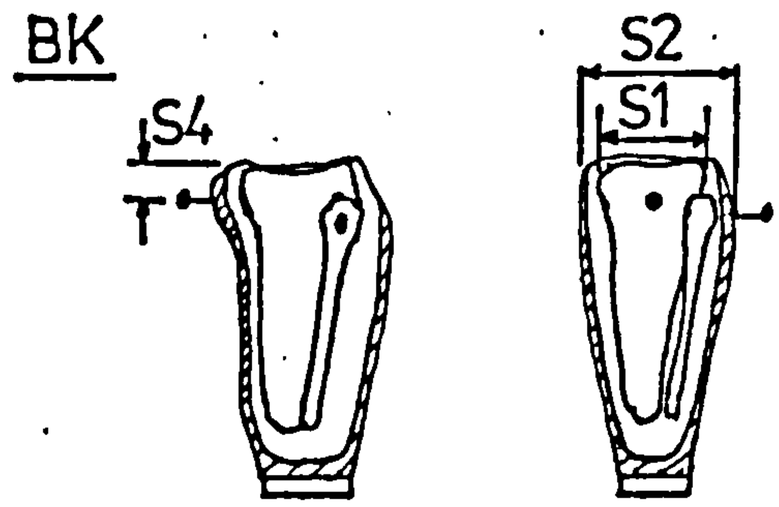

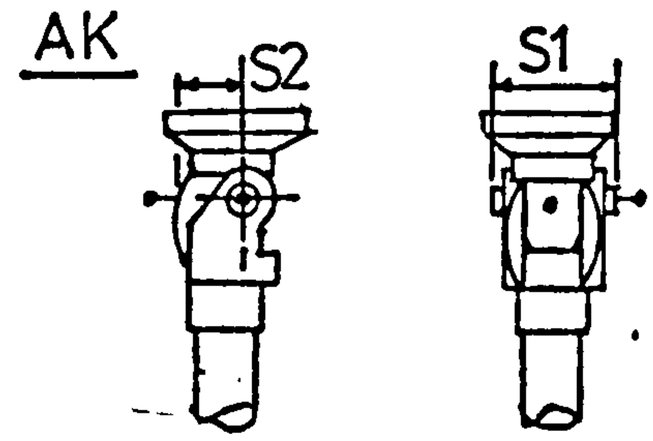

Socket thickness†
ST

†For BK Socket Only

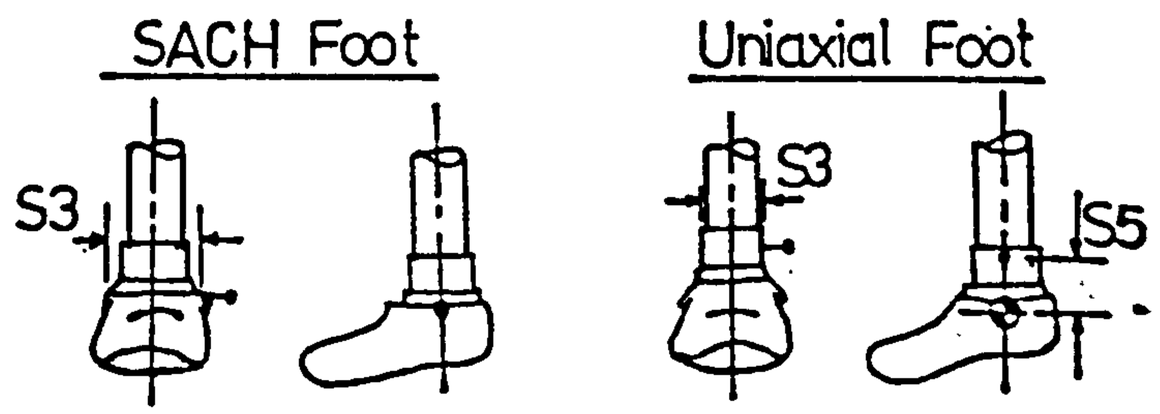

(iv) Foot

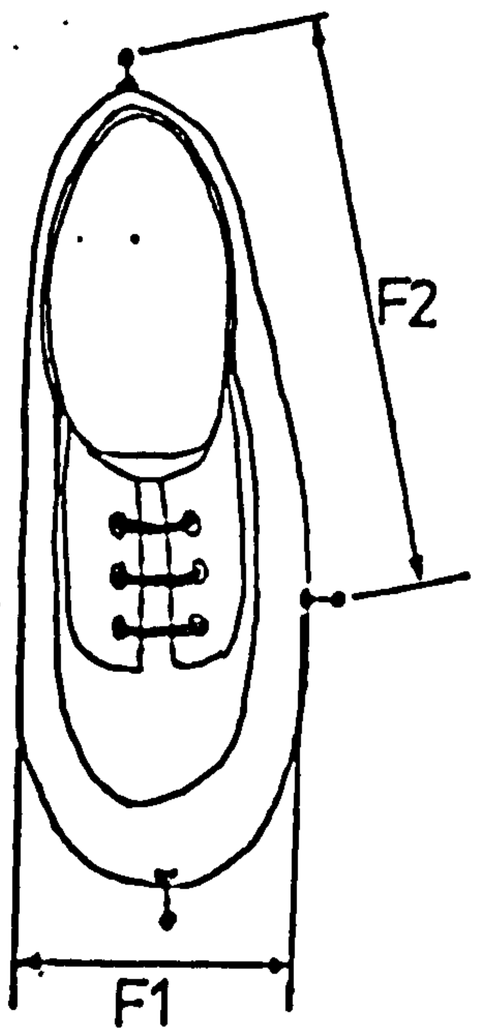

	Left(L)	Right(R)
F1		
F2		

Figure 5.4.4(b) Body Measurement Form (Cont'd)

cushion for the SACH foot or the plantar bumper for the Uniaxial foot. When the "optimum" alignment was achieved, which satisfied both the patient and the prosthetist, the patient was allowed to get accustomed to the experimental prosthesis. Meanwhile, the prosthetist made the final assessment of the patient's gait on a gait analysis form. (See Figure 5.4.4(a)).

Markers were positioned and stuck on to the anatomical landmarks with double-sided adhesive tape. (See Section 5.4.1). The patient was then again permitted to get used to the markers during locomotion. When everything was ready for the test walk, the patient was directed to walk along the walkpath towards the front camera at his own natural walking speed. Several "dummy" walks were required to establish the starting mark for the patient, in order that he would strike both force plates during the test walk. Most patients were aware of the existence of the force plates and had the tendency to alter their walking speed and step length in order to hit both plates. To overcome this, an object/target was positioned at the patient's eye level above the front camera for the patient to focus on when performing the test walk.

The appropriate test number was displayed and a new bulb inserted into the flash unit. The data sampling sequence is as follows; as the patient approaches the force plates, (approximately two steps before), the cine-cameras are switched on, to allow the cameras to pick up to normal running speed. Immediately, after that the charger to the amplifiers of the force plates is activated and just before the left foot hits force plate No.1, the sampling switch is operated. Immediately after the right foot leaves force plate No. 2, the flash bulb is fired, so that it will not affect any relevant film frame due to the brightness of the flash. After this the

PATIENT CODE: | | | | | |

VISIT NUMBER: | | | |

AMPUTEE REACTIONS
==========

SCORING SCALE :

1 - Excellent ; 2 - Satisfactory ; 3 - Fair ; 4 - Poor

	SACH	Uniaxial
a) Cushioning effect at heel impact		
b) Smoothness of "roll-over"		
c) Security of balance		
d) Effects on Socket comfort		
e) Cosmesis		

Overall preference : SACH/Uniaxial

Other Comments :

Figure 5.4.4(c) Amputee Reactions Form

cinecameras are switched off and the charger is reset.

A display of all the forces and moments from the two force plates, as well as the flash pulse,on the on-line V.D.U., will give an indication as to whether the test walk was successful or not. However, for a completely successful test walk, the corresponding cine films of all three cameras has to be good. Approximately five successful test walks were usually taken. Body measurements and measurements of markers distance were recorded, (see Figure 5.4.4(b)). Both the prosthetist and patient were then asked to comment on the performance of the prosthetic foot. (See Figure 5.4.4(c)).

Due to the specific design of the modular system used, which allows the foot and shin (or shank) tube to be dismantled without disturbing the alignment when assembled at a later stage, (see Section 5.4.2), the measurement of alignment and determination of the mass moment of inertia of the prosthesis can be done outwith the patient test period, thus,not making the test last longer than necessary.

The procedure was then repeated, changing the prosthetic foot and shin or shank tube, depending on whether the patient is a below-knee or above-knee amputee.

After the test, when all the test walks had been filmed, all the three cameras were rewound to their respective starting point. A grid board was positioned in front of each camera in turn, perpendicular to the optical axis of the particular camera, with its origin coincident with that of the ground frame of reference. Operating each camera locally forward the films were

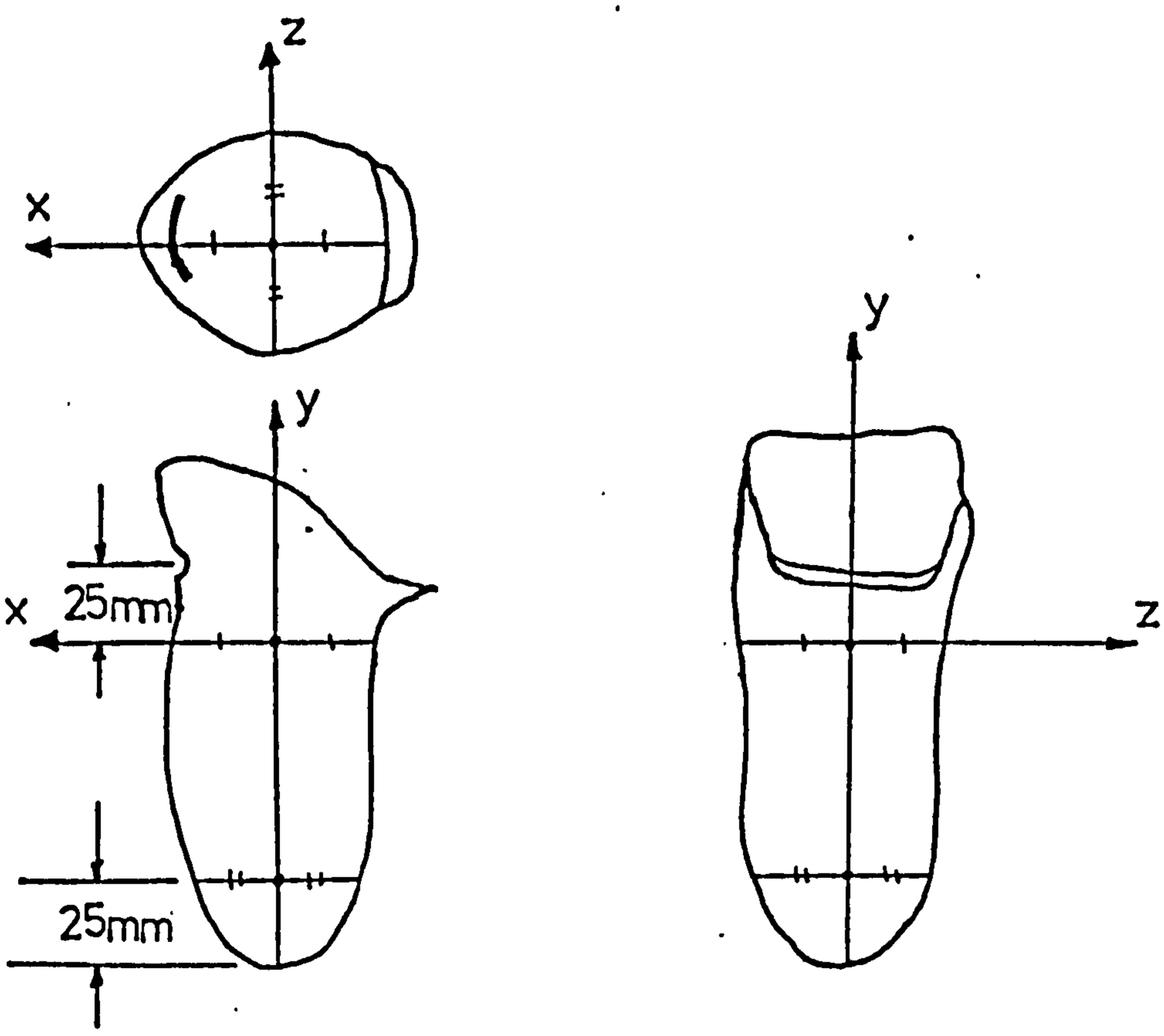

Figure 5.4.5(a) PTB Socket Reference Axes
(redrawn from Purdey, 1977)

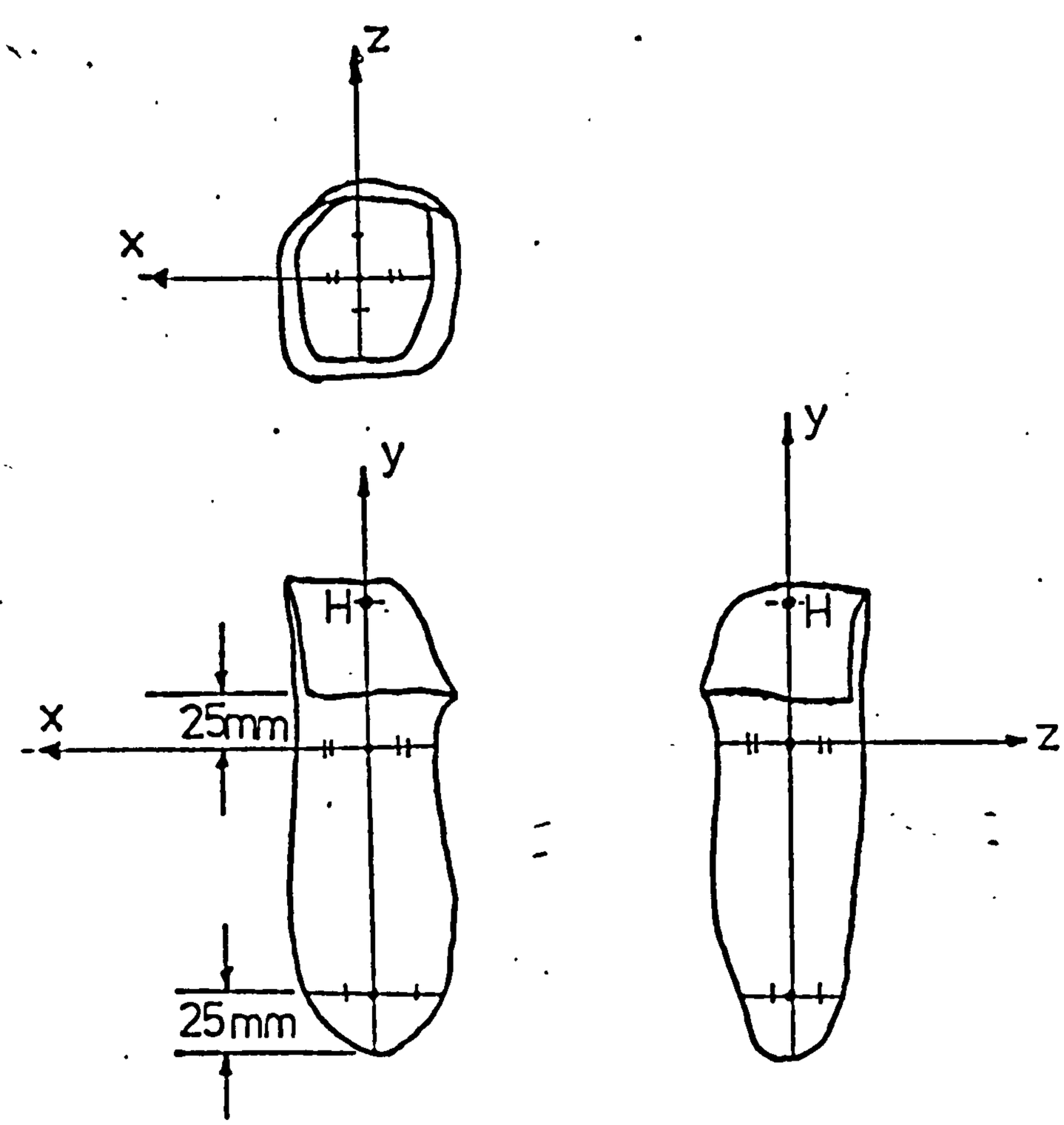

Figure 5.4.5(b) Quadrilateral Socket Reference Axes
(redrawn from Purdey, 1977)

re-exposed to superimpose the grid board onto the test walks for calibration purposes. See Section 6.2.1.

5.2.5. Alignment Measurement

In order to define the position and orientation of the components of a prosthesis in three dimensions, it was necessary to specify a frame of reference to which all measurements may be referred. This reference system was reported by Berme et al (1978).

Briefly, the origin of the orthogonal reference axes is at the prosthetic ankle joint centre or the centre of the bolt hole on the top of the SACH foot. Therefore, the top surface of the foot is taken to form the X-Z plane and the Y-axis is normal to it. The forward direction, (X-axis), for the above-knee prosthesis is normal to the projection of the knee flexion/extension axis onto the X-Z plane. The Z-axis in turn is obtained to form a right-handed orthogonal system. For the below-knee prosthesis, the forward direction is defined using the socket reference axis.

The socket reference axis is defined by locating two parallel planes in the socket. The inferior plane is located 25 mm from the distal end of the socket. For the PTB socket, the superior plane is 25 mm distal to the patellar bar and for the quadrilateral socket, it is 25 mm distal to the ischial seat. The positive Z-axis for the PTB socket is defined to be parallel to the posterior brim in the plan view and, lying in the top plane, it is directed towards the patient's right. The Y-axis is located equidistant from the socket walls both anteroposteriorly and mediolaterally in the two planes; positive direction is directed proximally. The X-axis is chosen to form a right handed orthogonal set. See Figure 5.4.5(a). The positive X-axis for the quadri-

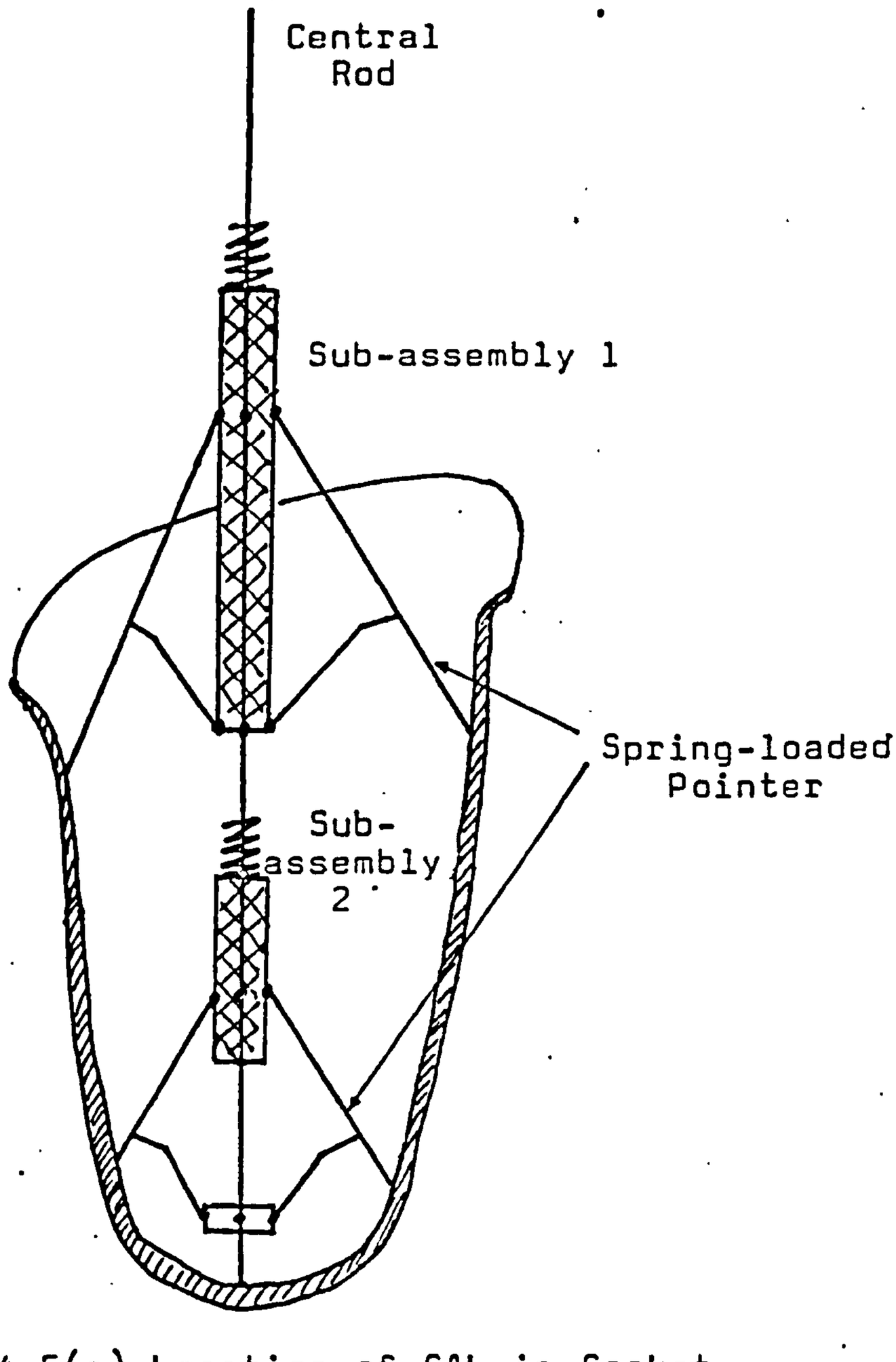

Figure 5.4.5(c) Location of SAL in Socket
(redrawn from Szulc, 1982)

lateral socket is defined to be parallel to the flat medial brim in plan view and anteriorly directed. The Y-axis is established as in the case of PTB sockets and the Z-axis is chosen to form a right handed orthogonal set. See Figure 5.4.5(b).

A socket axes determination device was used to establish the socket reference axes. The reader is referred to Szulc(1982) for a detailed description of the design and application of the device. The Socket Axes Locator (SAL) consists of a central rod upon which are mounted two sub-assemblies. Each sub-assembly comprises 4 spring-loaded pointers that operate like an umbrella. Figure 5.4.5(c) illustrates the manner in which the device locates itself in a socket, and allows the position of all the pointers to be marked onto the inner surface of the socket. The four points produced from each sub-assembly define the required planes.

With the socket marked, the prosthesis to be measured is bolted by the foot fastening bolt, (after the prosthetic foot is removed),to a vertical bracket at one end of the measuring table. The table forms a surface parallel to the Y-Z reference plane and a grid is inscribed on it for ease of measurement. A scribbing block with an adjustable pointer is used on the table top to touch the marked out reference points in turn. By measuring the position of the scribbing block on the grid and the height of the pointer above the surface of the table the three coordinates for each reference point are obtained.

For the above-knee prosthesis, a moment was applied in order to extend the knee when the prosthesis was bolted to the measuring table. The value of the applied knee moment was recorded and subsequently used on the same prosthesis for the measurement of other alignment

Body Segment	Average Density Values (gm/cm^3)
Thigh	1.060
Lower Leg	1.095

Table 5.4.6. Densities of Body Segments (from Drillis & Contini, 1966)

changes. Besides the measurement of the socket reference points, the positions of the knee joint axis on the medial and lateral sides were also measured.

The terminology and definition of alignment parameters used in the description of alignment is presented in Appendix (C).

5.4.6. Physical Properties of Prostheses

The parameters to be determined from each body segment for kinetic calculation are as follows :

1) Mass of segment
2) Distance between proximal joint and centre of mass
3) Mass moment of inertia.

For the normal limb, these parameters are estimated by using coefficients of body segment parameters as presented in Table 2.1, collated by this author. (See Sections 2.1 and 6.6.1(a)). For the prosthetic limb, these parameters have to be obtained experimentally.

The mass of each prosthetic segment was determined by a weighing scale. For the segment that includes the socket, the mass of the stump was also considered. This was done by stuffing the socket with cloths and lead shot making up the mass of the stump. This mass was estimated by taking the volume of the socket to be approximately the same as that of the stump and multiplying it by the average value density (obtained by three principal investigators) given by Drillis and Contini (1966). (See Table 5.4.6).

The method used in determining the centre of mass was to balance the segment lengthwise across a knife edge. The distance between the proximal joint and the

PATIENT CODE : | | | | | |

VISIT NUMBER : | | | |

PHYSICAL PROPERTIES OF BELOW-KNEE PROSTHESIS

	Mass(Kg)
Shoe	
SACH foot	
Uniaxial foot	
Attachment	

Volume of Stump(cm^3): _____

Mass of Stump(kg : _____

TIMES(S) FOR 10 OSCILLATIONS

	Prosthesis, Stump & Shoe	
	SACH	Uniaxial
1		
2		
3		
4		
5		

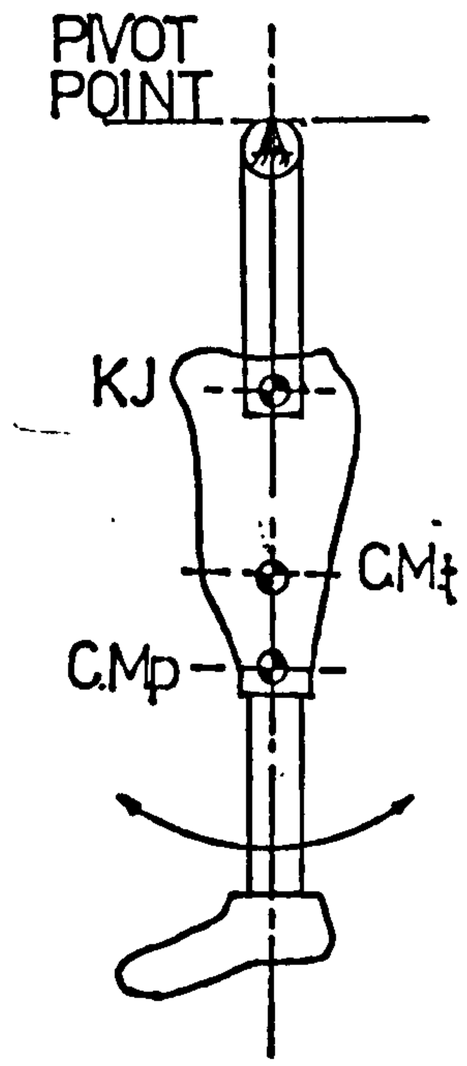

Measurement

	With Attachment		Without Attachment	
	SACH	Uniaxial	SACH	Uniaxial
Total Mass(kg)				
Total Length(m)				
CM to Pivot Point/ Knee Joint				

Figure 5.4.6(a) Physical Properties of Below-knee prosthesis Form

centre of mass could then be measured.

A simple rig was fabricated to enable the prosthesis, either in part or whole, to be oscillated freely. Altogether seven sets of readings were taken of 10 oscillations of a prosthetic segment over a small angulation. From these, the average period of one oscillation was obtained. Due to the different configuration of the prosthetic limb segment, the pivoting point and determination of mass moment of inertia has to be clarified.

a) For the below-knee prosthesis (including the 'stump' and shoe), a pair of attachments (clamps) was used , one end of which grips firmly onto the lateral and medial wall of the socket respectively, directly over the approximate position of the knee joint. The other end of the attachment pivots about a knife edge blade on the rig, so that the whole prosthesis can be made to swing about the A/P axis. The average period per oscillation was obtained. The prosthesis, including the attachments was weighed and the distance between the pivoting point and the centre of mass of the whole structure was measured. The distance between the knee joint and the centre of mass of the whole structure was also measured. By inserting these quantities into the equations in Section 6.6.1(b), the mass moment of inertia about the A/P axis at the knee can be calculated. The whole procedure can then be repeated, changing the shin tube and foot assembly.

b) The above-knee prosthesis was divided into two sections :

1) the prosthetic thigh comprising all components above the knee including the 'stump'.
2) the prosthetic shank comprising all components

PATIENT CODE : | | | | | |

VISIT NUMBER : | | | |

PHYSICAL PROPERTIES OF ABOVE-KNEE PROSTHESIS.

	Mass(Kg)
SHOE	
SACH Foot	
Uniaxial foot	

Volume of Stump(cm^3):_____

Mass of Stump(kg) : _____

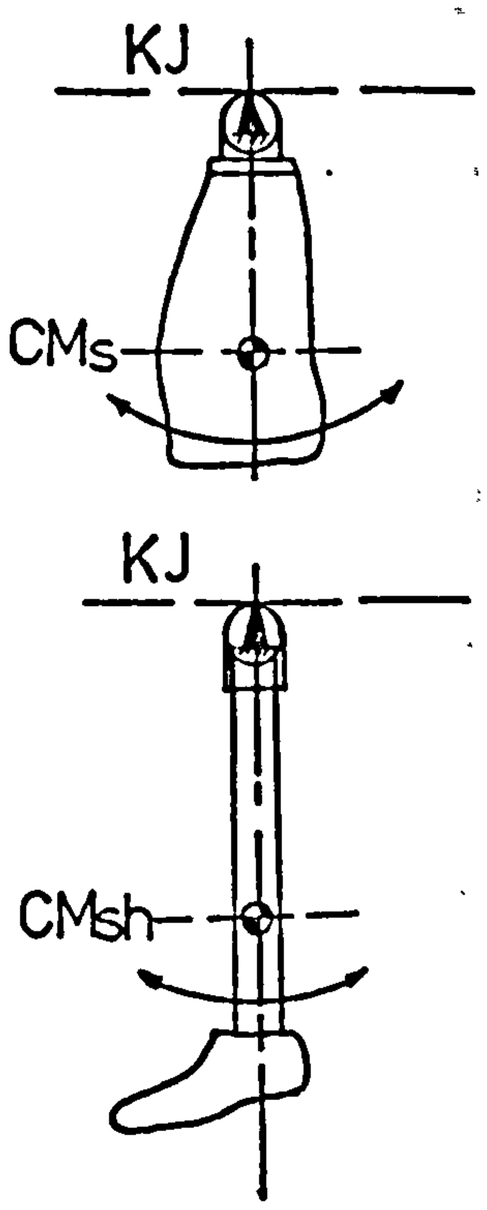

TIME(S) FOR 10 OSCILLATIONS

	Socket & "Stump"	Shank, Foot & Shoe	
		SACH	Uniaxial
1			
2			
3			
4			
5			

Measurement

	Socket & "Stump"	Shank, Foot & Shoe	
		SACH	Uniaxial
Total Mass(kg)			
Total Length(cm)			
C.M. to pivoting Point(cm)			

Figure 5.4.6(b) Physical Properties of Above-knee Prosthesis Form

below the knee including the shoe.

Due to the difficulty in defining the hip joint relative to the socket, the prosthetic thigh was pivoted at the knee joint about the A/P axis. The average period per oscillation was obtained and the distance between the knee joint and the centre of mass was measured. By inserting these numbers in the equation in Section 6.6.1(b), the mass moment of inertia about the A/P axis at the knee can be calculated. Using the parallel axis theorem, the mass moment of inertia at the hip can then be determined. This was incorporated into the computer program 'KINETIC', because by this stage the hip joint position would be known.

The prosthetic shank was pivoted about the A/P axis at the knee joint. From there, the average period per oscillation was obtained. The distance between the knee joint and the centre of mass was measured. Again, by inserting these numbers in the equation in Section 6.6.1(b), the mass moment of inertia at the knee joint could be calculated.

The mass moment of inertia of the foot, at the ankle joint about the A/P axis was small enough to be neglected in the analysis. However, the distance between the ankle joint and the centre of mass was measured. The centre of mass was determined by suspending the foot in three different points and locating the intersection of the corresponding three vertical plumb lines.

Figures 5.4.6(a) and (b) summarise the measurements required for the below-knee and above-knee prosthesis respectively.

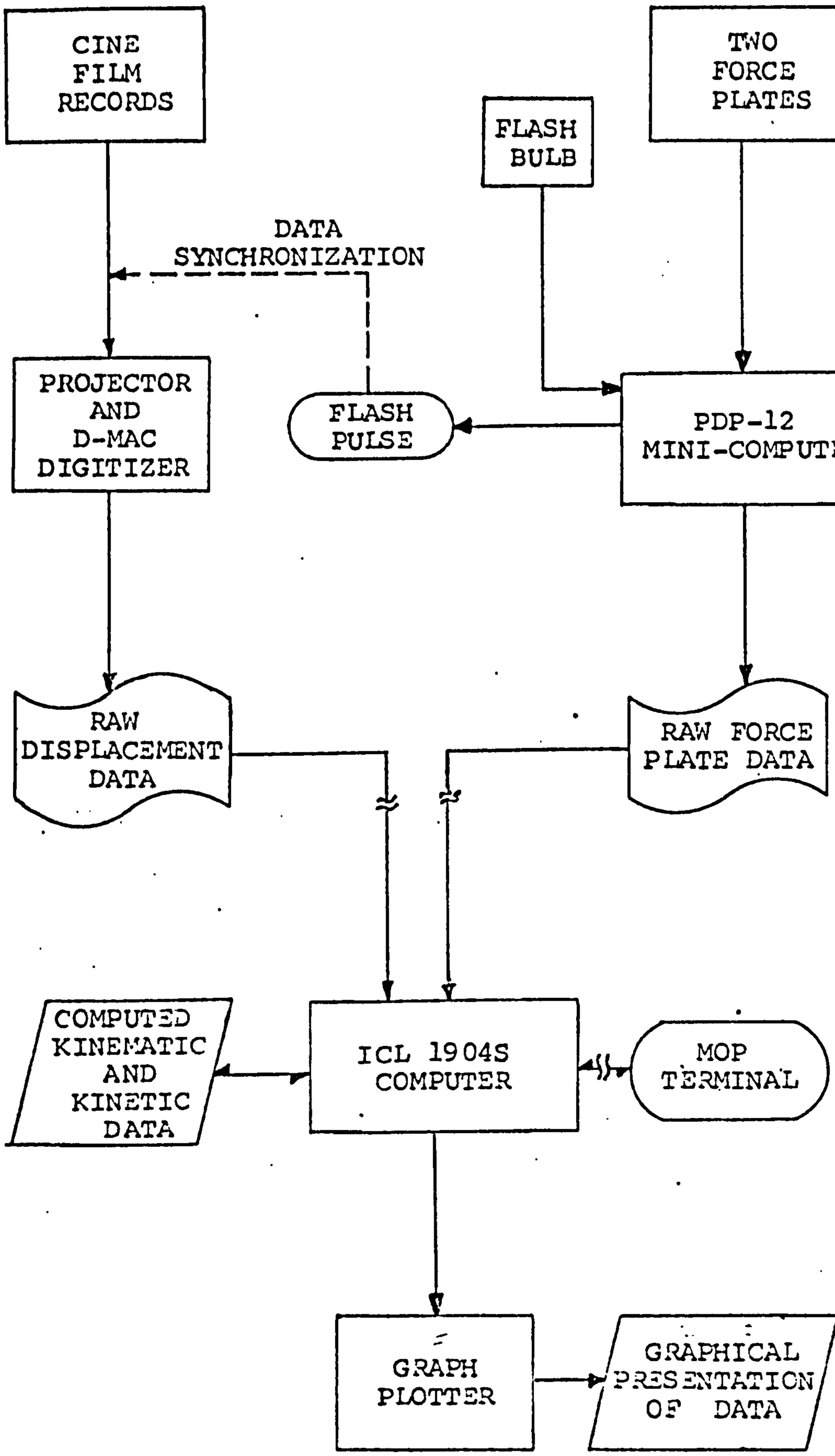

Figure 5.5. Data Acquisition and Reduction Flow Chart

5.5. Data Reduction and Preparation

Data obtained during the patient test have to be retrieved from their store. The force plate data were recorded in the magnetic 'LINC' tape, see Section 5.4.4, while the kinematic data were on cine films. Only those successful test walks, i.e. satisfactory force plate and corresponding cine films records, were retrieved and transferred to the University's ICL 1904S computer for further processing analysis.

A summary of the procedure is as shown in Figure 5.5.

Data processing was transferred from the PDP12 to the ICL 1904S for the following reasons :

a) Large quantities of data can be processed more quickly than on the PDP12.
b) Processing can be requested and then left to the machine (i.e. background jobs) because jobs were principally run in a "batch processing" environment.
c) A considerable amount of filestore was available with relative ease of accessibility of files, except when files were stored offline on magnetic tape.
d) A library of software routine packages was available for use which could accelerate software development.
e) The "George III" operating system enabled the construction of file handling and job control macros. This facilitated the use of single line commands to run jobs and also allowed the development of the job chain concept.
f) Line printers and graph-plotters were accessible through the 1904S.

The main disadvantage of this system was that the operating system was not suitable for interactive

program operation. This made program debugging more difficult and interactive results analysis difficult.

5.5.1. Force Plate Data

The computer program 'EDITOR' (written by Jordan, 1978) and the 'LINC' data tape were loaded onto the PDP12 computer for data sorting.

Of all the ground reaction signals from the F.P., the vertical force component, Fy, gave the clearest indication of the heel strike and toe off event. The first task was to locate the position of the first sampled point of the flash signal in relation to the first effective Fy signal (LHS) on force plate No. 1 and the last effective Fy signal (RTO) on force plate No. 2. This information would then be used in synchronisation with the corresponding cine films.

Ground reaction data from both force plates were sorted separately, since the computer program used to process them can only take in one set of force plate data. Hence, two data files were generated for every test walk, one for signals from force plate No. 1 (left leg) and the other for signals from force plate No. 2 (right leg).

The sorting program had the facility to transfer any data that fall in between two movable cursors onto punch paper tape. The baselines of all the six channels were obtained and transferred onto the paper tape first and were then followed by the ground reaction data. For entry into the ICL 1904S computer, job statements were spliced on at the beginning and end of the data. The format of these "raw" ground reaction input data file is as given in Appendix D 2.1.

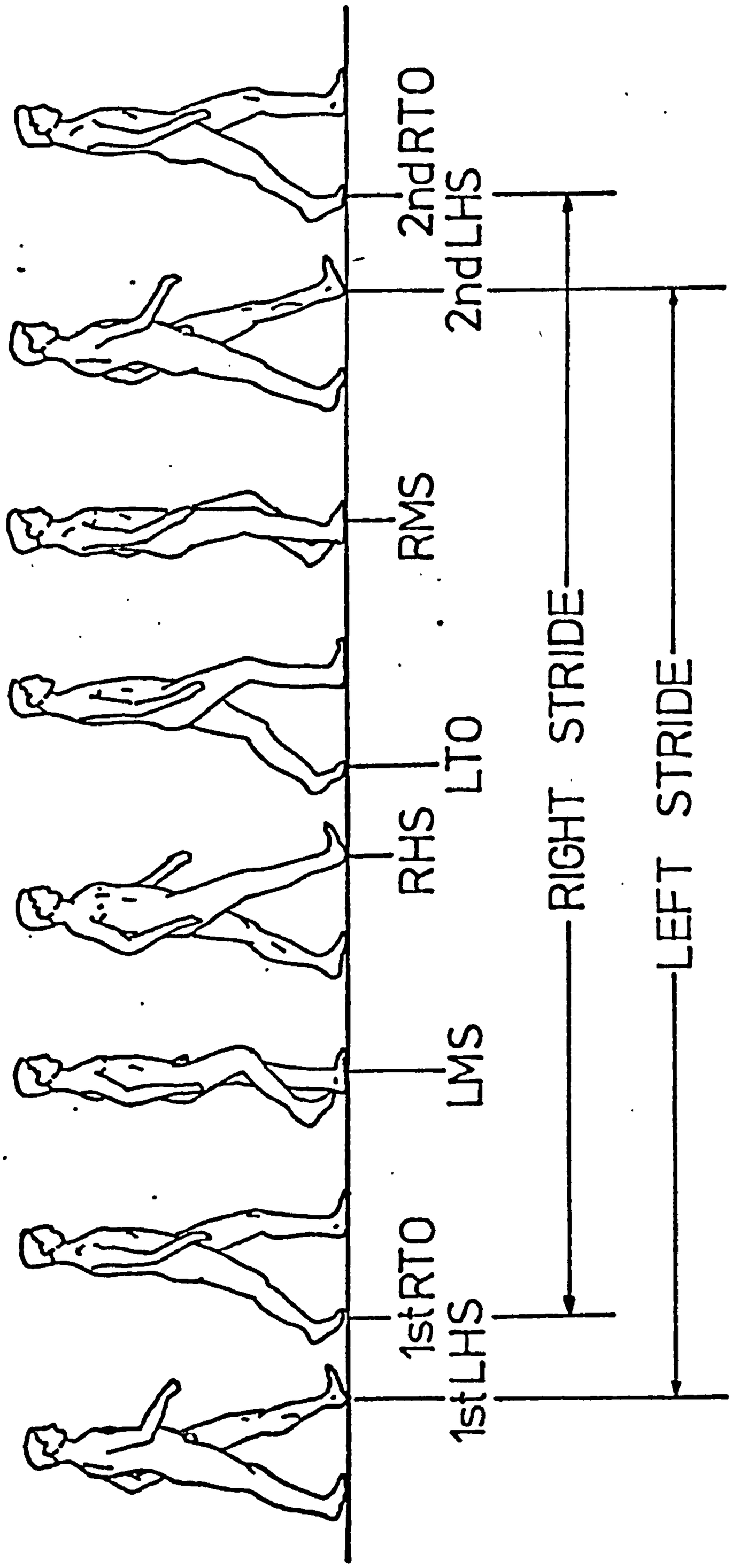

Figure 5.5.2 Events required for Analysis

5.5.2. Kinematic Data

Although each camera was driven by a synchronous motor that records events at 50 frames per second, the shutters of all the cameras were not synchronous, i.e. they do not open at the same time. This became obvious when filming the flash bulb as it was fired. The first flash seen on the cine films from the three cameras varied in intensity, although they were supposedly capturing the same event at an instant of time. By comparing the sequence of flashes and their intensities between films from the three cameras, the time lag between shutters can be estimated. This was at the most one frame, i.e. 20 ms apart. The estimated time lag (T(N)) was recorded to correct for this phase difference, see Section 6.2.2.

By synchronising the first flash seen on the cine films of the three cameras with the first sampled point of the pulse, the relevant frames of cine films required for analysis can be established from the total number of ground reaction data. The events required for analysis are as shown in Figure 5.5.2, i.e. from the first heel-strike of the left foot to the second toe-off of the right foot. The events of the first toe-off of the right foot and the second heel-strike of the left foot were determined from the cine films. Five additional frames were added to the beginning and four to the end of the required length of cine films. The extra frame at the beginning was to allow for phase correction and the remaining eight were used to compensate for the errors introduced in the end data when differentiating for velocities and accelerations. These additional frames were discarded immediately after processing.

Frame numbers were scratched onto the required length of cine films to be analysed. The films were

projected onto a digitising table, trade-name "D-MAC", and were analysed frame by frame. The projector was carefully aligned so that the image was projected squarely onto the table without any apparent distortion due to misalignment.

Digitising was done by placing a cursor over the centre of the marker bead and activating a switch to register the coordinates of the marker onto the paper-tape. The unit used was that of the D-MAC table; one unit being equal to 0.1 mm. The first two points digitised on every frame were calibration markers on the grid board. The sequence with which body markers were digitised, was from the lowest marker number to the highest marker number on a particular frame. See Figure 5.4.1(b). The total number of points digitised per frame from the front camera was 22 and from the side camera was 15.

When markers became completely obscured, their positions were interpolated by the human operator, therefore no marker was left undigitized.

Job statements were spliced to the beginning and end of the data,for entry into the ICL 1904S computer. The format for these "raw" displacement input data is given in Appendix D 3.1

CHAPTER 6

Theoretical Consideration of Analysis

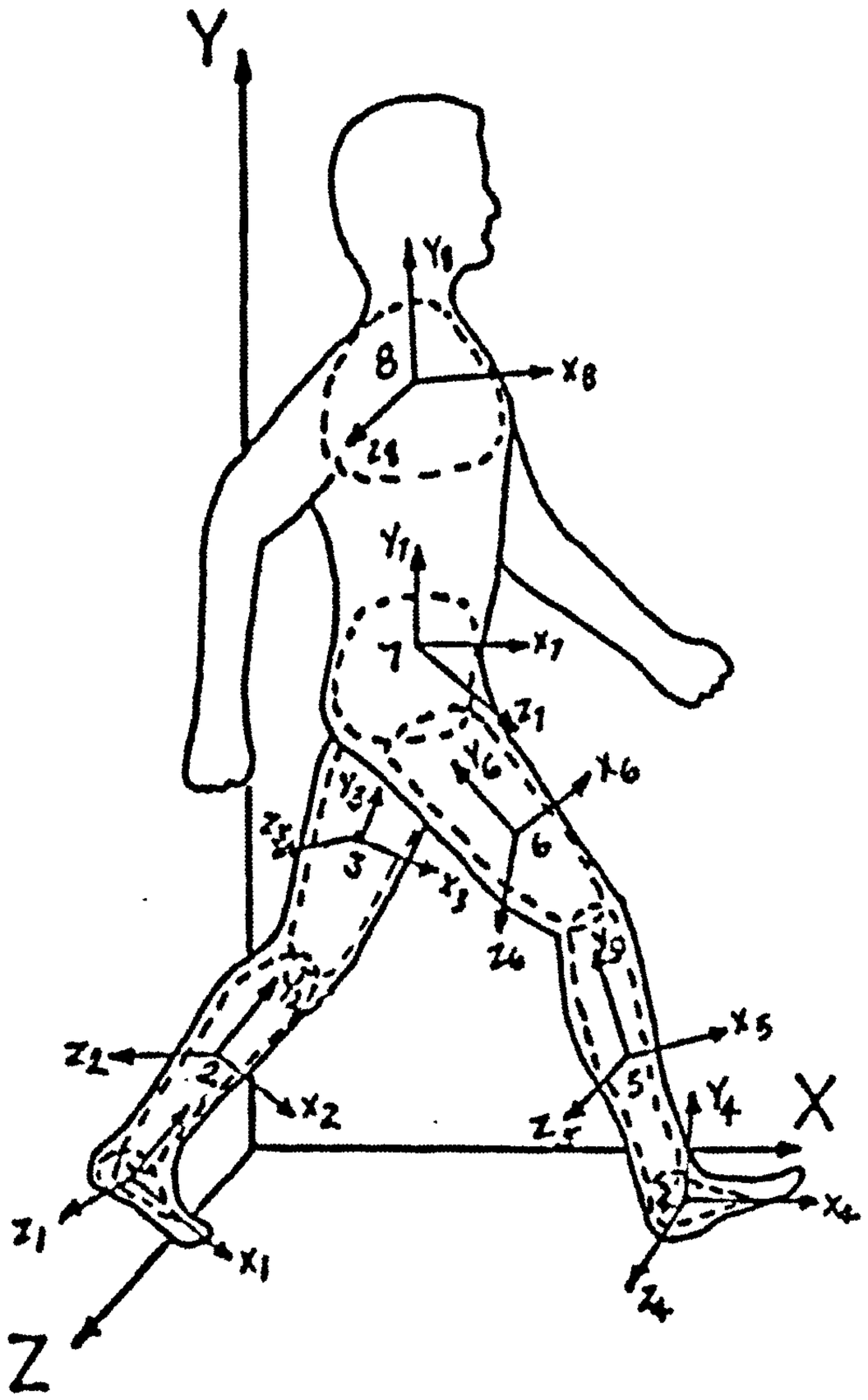

	DEFINITION
1	LEFT FOOT
2	" SHANK
3	" THIGH
4	RIGHT FOOT
5	" SHANK
6	" THIGH
7	PELVIS
8	SHOULDER

Figure 6.1.1(a) Mathematical Model of human body

6.1 Introduction

The experimental system and method presented in Chapter 5 allows a three dimensional analysis of the contralateral sides of the human body during locomotion. This chapter will consider the theoretical approach adopted in the analysis.

6.1.1 Outline of Theoretical Consideration

The human body is mathematically modelled into an eight segmented structure, as shown in Figure 6.1.1(a). Each body segment is regarded kinematically as a rigid body. Therefore, it has six degrees of freedom and requires six independent coordinates to specify its spatial position at any instant of time.

Body markers are placed at various appropriate anatomical features as shown in Figure 5.4.1(b). Each body segment is then defined by a set of axes system generated from these markers. As will be noticed, only the torso and the lower limbs are considered in the analysis. Although arm swing could prove to be a valuable parameter (Elftman, 1939), it is however deemed that any significant changes in gait will also be apparent and can be characterised by the shoulder movement.

Each segment moves in various orientation during locomotion. The axes system attached to it is referred as the moving system. This set of axes is defined in relation to the ground (or fixed)frame of reference by Direction Cosine (D.C.) or Transformation (T) matrix.

The ground frame of reference is taken to be the fixed axes system, defined by the position of the three cinecameras and the force plates arrangement, with its

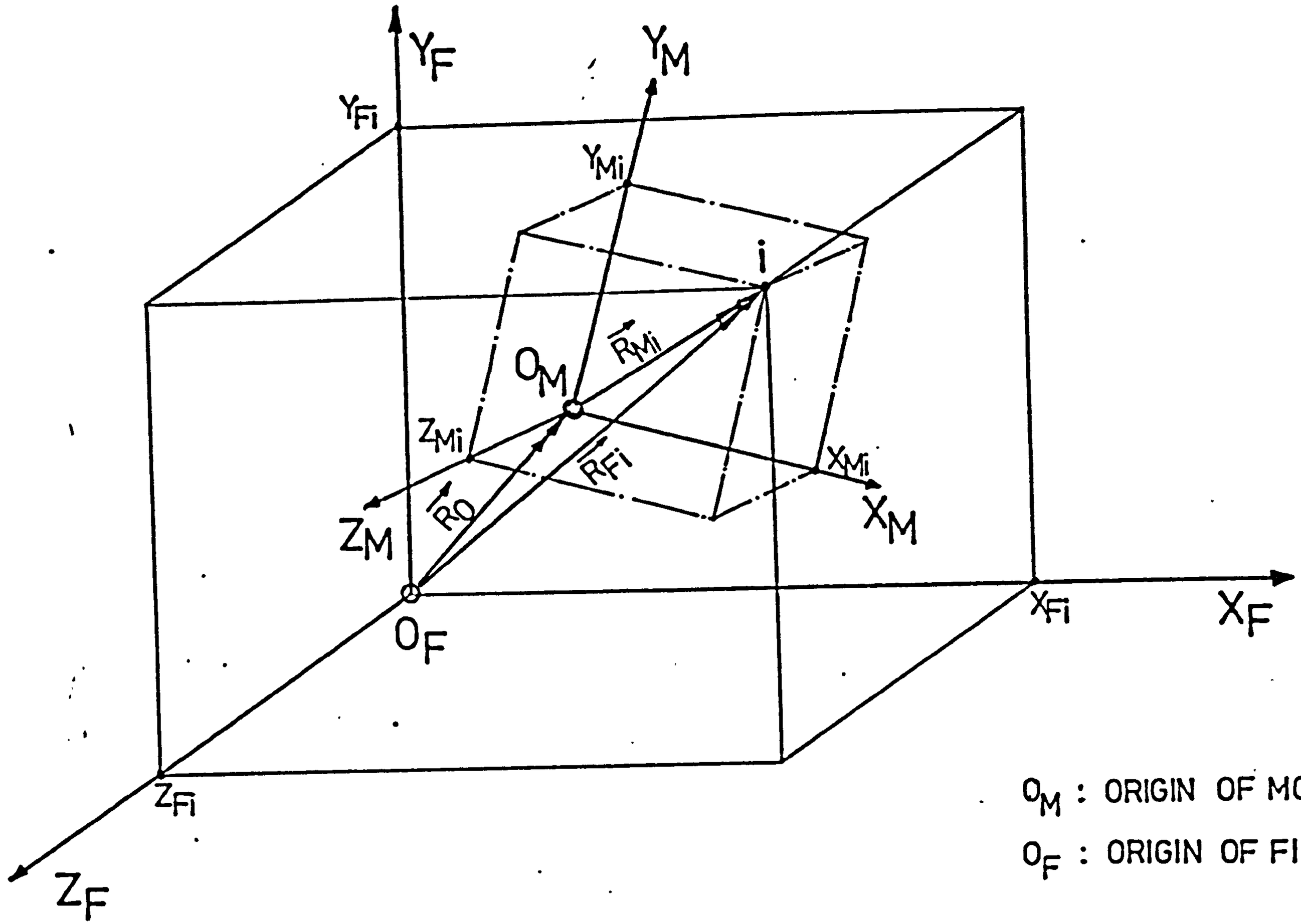

Figure 6.1.2(a) Vector representation of Spatial Object

origin being the centre of the force plates configuration, see Figure 5.3.1(a).

Ground reaction measurements taken from the two force plates are related to the reference axes system. From the synchronisation method described in Section 5.3.3,a relationship between kinematic and force plate data is developed and thus making kinetic calculation possible.

6.1.2. Mathematical Representation

Vector and matrix notations are used to express the theoretical consideration. This is to provide a clearer understanding of the theory in a more compact manner.

The origin of a rigid body, in this case a body segment, can be represented by a vector (see Figure 6.1.2(a)) :-

$$\bar{R}_o = \begin{bmatrix} X_o \\ Y_o \\ Z_o \end{bmatrix}$$

Its orientation in space can be related to the ground (or fixed)frame of reference by a direction cosine (D.C.)·Matrix, (see Figure 6.1.2(b)) :

$$[\bar{B}] = \begin{bmatrix} B_{11} & B_{12} & B_{13} \\ B_{21} & B_{22} & B_{23} \\ B_{31} & B_{32} & B_{33} \end{bmatrix}$$

where the elements (B_{MF})in the matrix are cosine of the angles between the fixed (F) and moving (M) axes.

Although there are 12 scalar quantities in the two expressions, only 6 are independent because there are 6

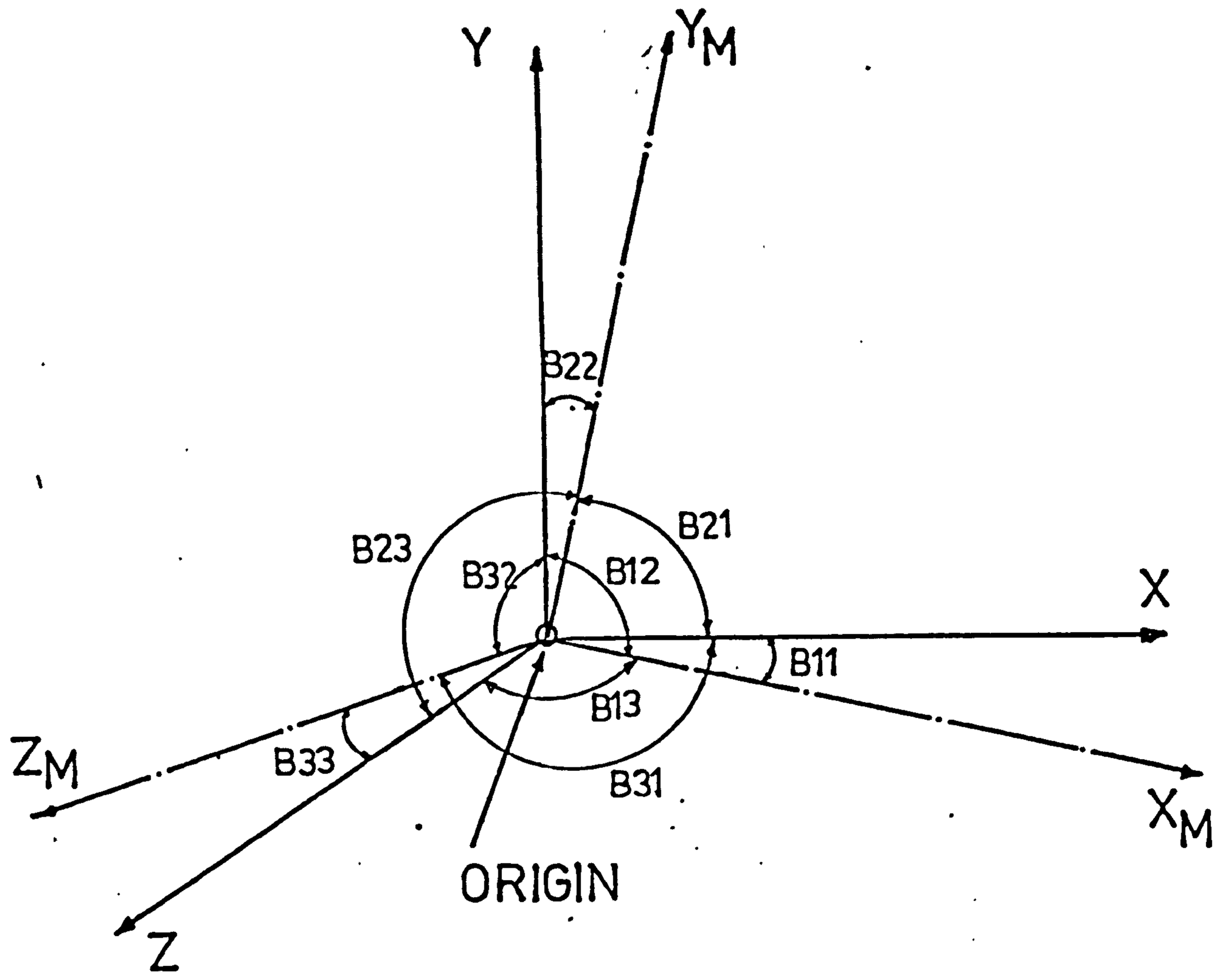

Figure 6.1.2(b) Definition of D.C. Matrix

conditions which are imposed on the rigid body for orthogonal transformation. They are :

$$B_{11}^2 + B_{12}^2 + B_{13}^2 = 1 \quad \ldots\ldots\ldots (1.1)$$

$$B_{21}^2 + B_{22}^2 + B_{23}^2 = 1 \quad \ldots\ldots\ldots (1.2)$$

$$B_{31}^2 + B_{32}^2 + B_{33}^2 = 1 \quad \ldots\ldots\ldots (1.3)$$

$$B_{11}.B_{21} + B_{12}.B_{22} + B_{13}.B_{23} = \emptyset \quad \ldots\ldots\ldots (1.4)$$

$$B_{21}.B_{31} + B_{22}.B_{32} + B_{23}.B_{33} = \emptyset \quad \ldots\ldots\ldots (1.5)$$

$$B_{11}.B_{31} + B_{12}.B_{32} + B_{13}.B_{33} = \emptyset \quad \ldots\ldots\ldots (1.6)$$

Therefore, what it means is that the product of the D.C. matrix and its transposition should be equal to unity, i.e.

$$[B] * [B]^{-1} = [U] = \begin{bmatrix} 1 & 0 & 0 \\ 0 & 1 & 0 \\ 0 & 0 & 1 \end{bmatrix}$$

If it is not so, the D.C. matrix may be corrected to orthogonality by an iterative procedure, described by Jordan (1969),

$$[B]_{n+1} = [B]_n \left\{ [U] - \tfrac{1}{2}([B]_n^{-1} * [B]_n - [U]) \right\}$$

where "n" is a term in the series with an orthogonal D.C. matrix and "$n+1$" is the term under consideration.

The determinant (D) of an orthogonal matrix is one,

$$D = B_{11}\begin{bmatrix} B_{22}B_{23} \\ B_{32}B_{33} \end{bmatrix} + B_{21}\begin{bmatrix} B_{12}B_{13} \\ B_{32}B_{33} \end{bmatrix} + B_{31}\begin{bmatrix} B_{12}B_{13} \\ B_{22}B_{23} \end{bmatrix}$$

$$= 1$$

This is used as a mean of checking the orthogonality

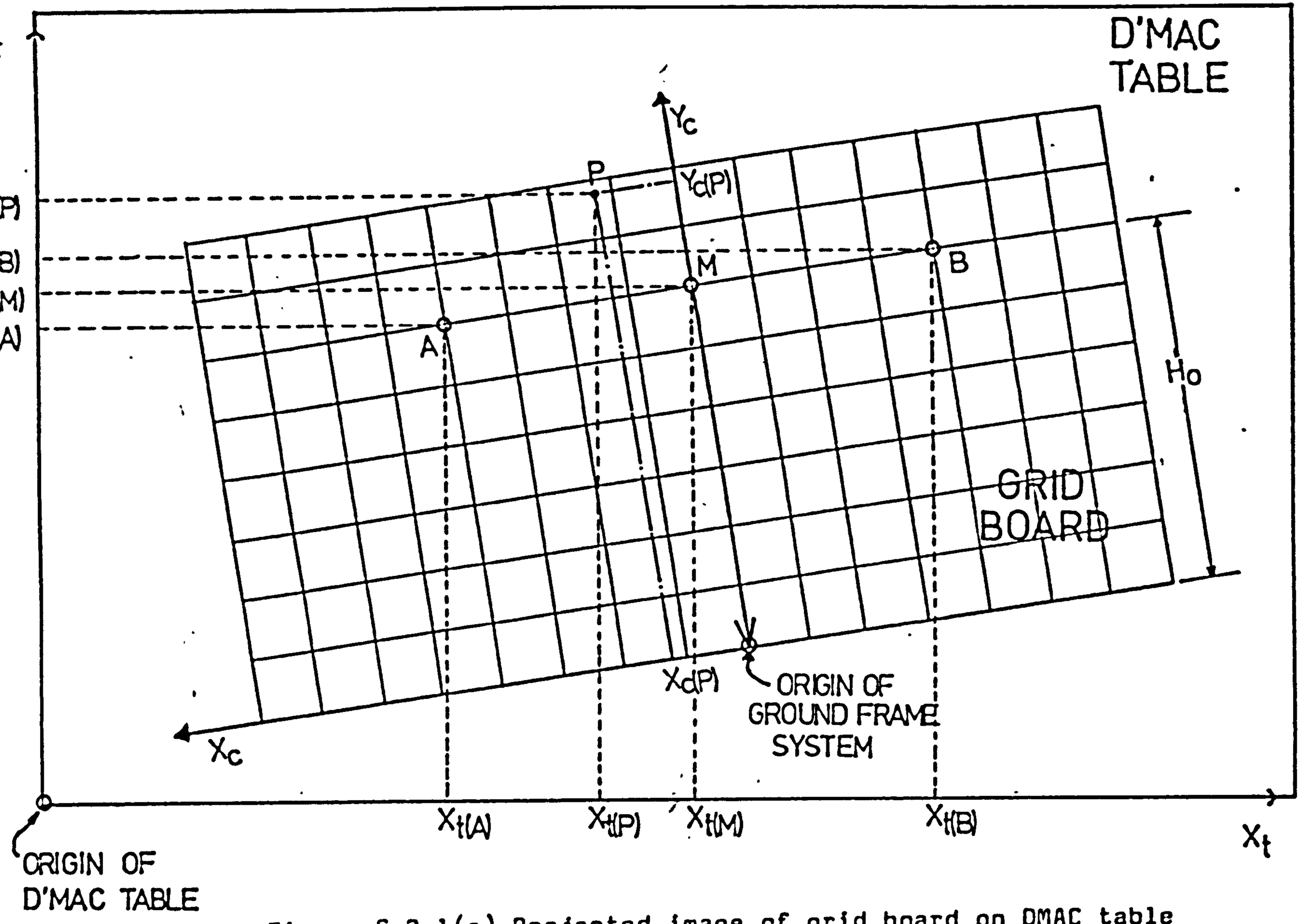

Figure 6.2.1(a) Projected image of grid board on DMAC table

of the D.C. matrix in the analysis. However, it should be noted that not every matrix with a determinant of one is an orthogonal matrix.

To define spatial point (i) on a rigid body, the vector $\bar{R}_{Mi}$ is used. This is in reference to the moving axes system associated with the rigid body. To relate it to the ground frame of reference, we have (see Figure 6.1.2(a)) :

$$\bar{R}_{Fi} = \bar{R}_o + ([B] * \bar{R}_{Mi})$$

To transform from the fixed axes system to the moving system, we have :

$$\bar{R}_{Mi} = [B]^{-1} * (\bar{R}_{Fi} - \bar{R}_o)$$

6.2. Generation and Rationalisation of 3-D Spatial Coordinates

In using cine-photography as a technique in spatial data acquisition, several factors have to be considered. They are : the method of scaling, correction of parallax error, minimising distortion of data either through lens characteristics or digitising, correction of phase difference and eliminating random noise.

6.2.1. Calibration

Transformation of digitised coordinates to the reference axes system and scaling them to real dimensions was done by re-exposing the film to the grid or calibration board. This also serves the purpose of minimising distortion caused by projection of film onto the digitizing table which has been discussed in Section 5.5.2.

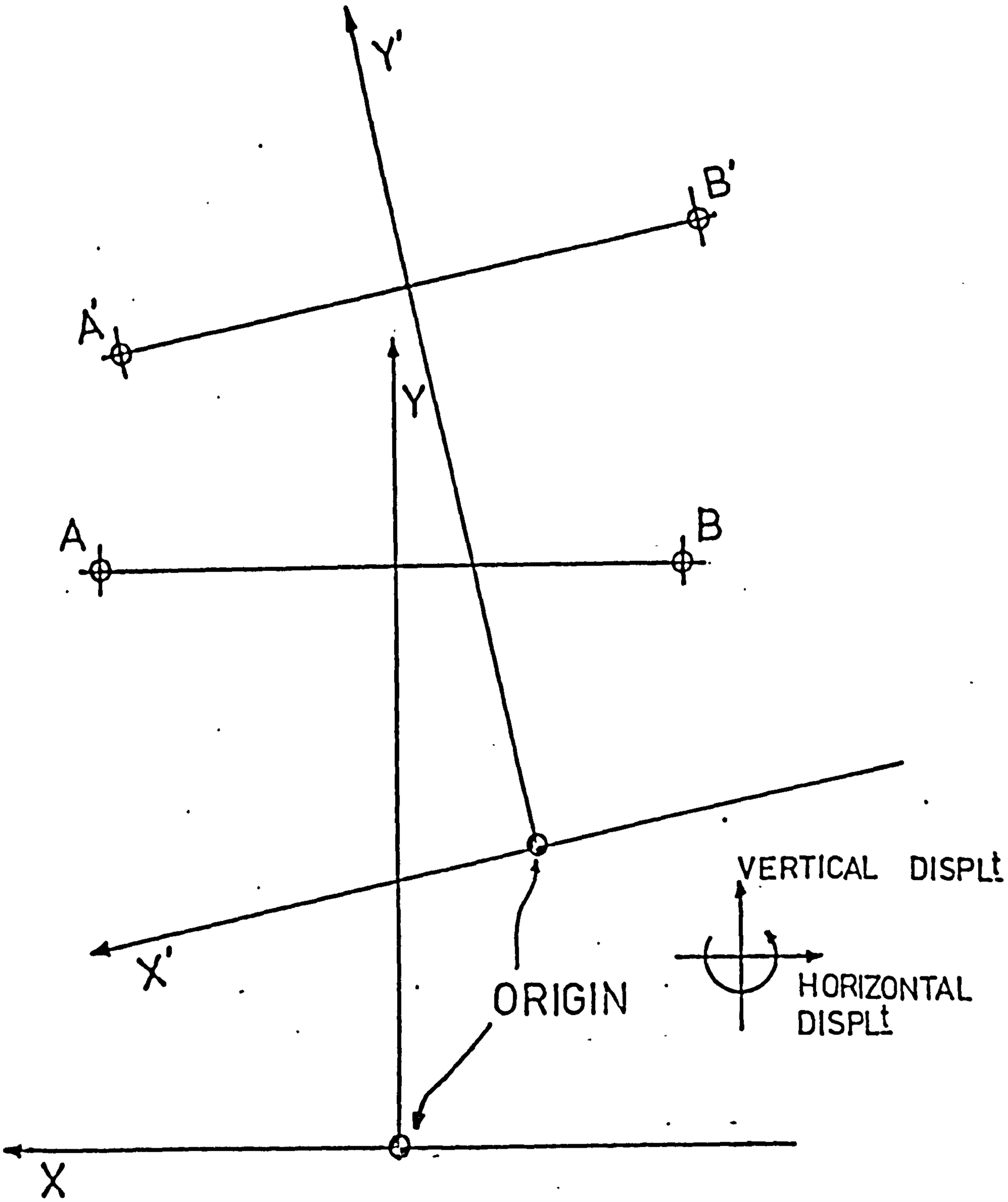

Figure 6.2.1(b) Misplacement of Projected Image

The first 2 points digitised in each film frame are A and B, which are marked on the grid board, see Figure 6.2.1(a). Since the actual physical distance between A and B is known, a scaling factor can then be formulated :

$$F = \frac{L(AB)}{\sqrt{[(Xt(A) - Xt(B))^2 + (Yt(A) - Yt(B))^2]}}$$

where, $L(AB)$ = Actual physical distance between A and B.
X,Y = horizontal and vertical axes respectively
A,B = calibration points on the grid board
t = suffix denoting D-MAC table as reference

Each frame is usually not projected squarely on the digitising table. There exist three misplacements of the projected image; i.e. 2 linear shifts and one rotation, see Figure 6.2.1(b). Since each frame picks up the two calibration points A and B, the 2 linear shifts are eliminated. However, the rotational displacement still presents a problem. To account for this the angle (β) is calculated,

$$\tan\beta = \frac{Yt(B) - Yt(A)}{Xt(B) - Xt(A)}$$

To transform the digitized coordinates to the reference system, scaling it to the actual physical dimension and also to eliminate the rotational displacement, the following procedure is adopted.

Let P be the point to be processed. The mid-point (M) between A and B is at a distance H_o directly above the centre of the force plates arrangement.

First, refer point P to M and then transferring it to the centre of the force plates arrangement, O, we have,

$$Xc(P) = [(Xt(P) - Xt(M))Cos\beta - (Yt(P) - Yt(M))Sin\beta]*F$$

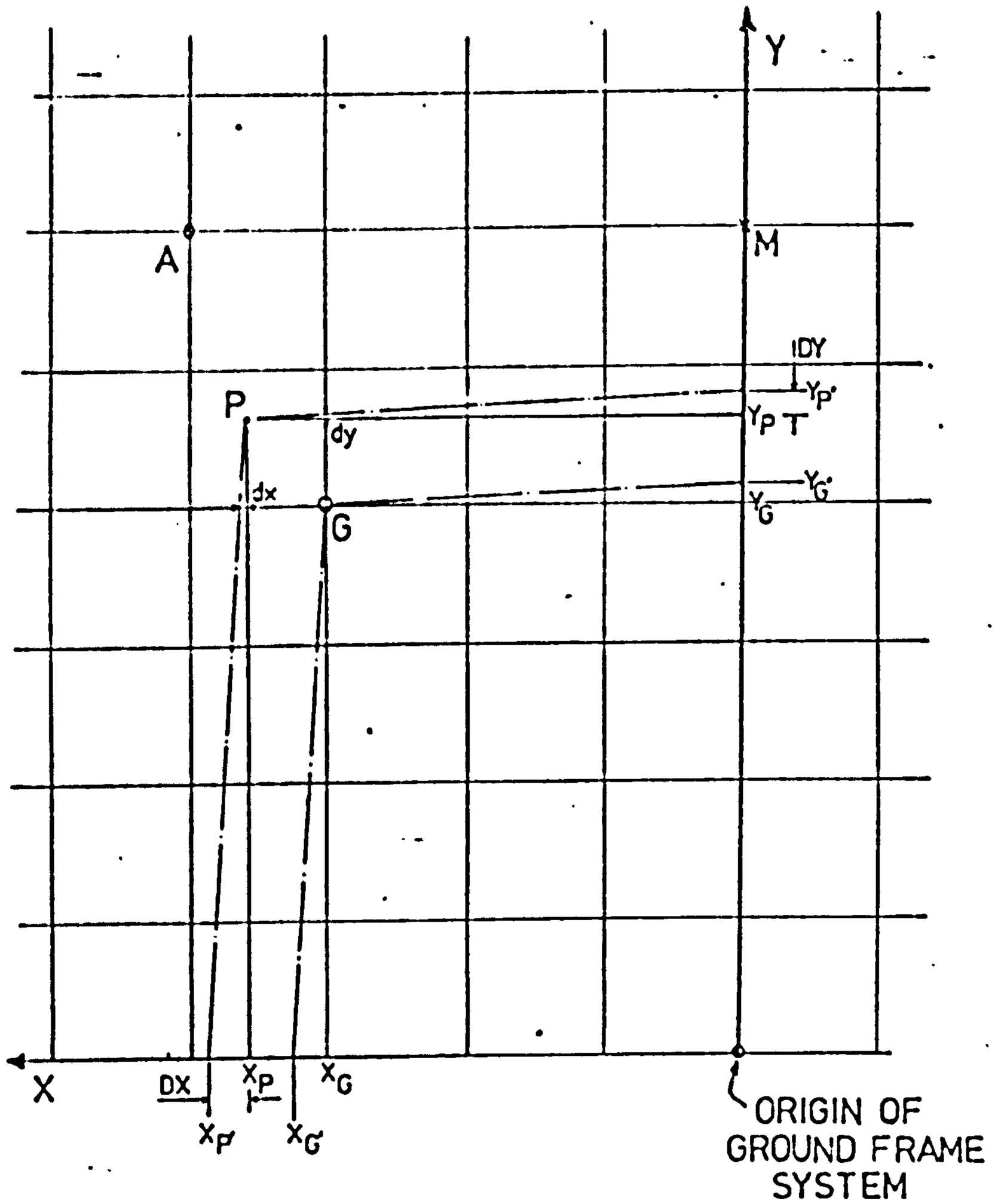

Figure 6.2.1(c) Minimising Lens Distortion

$$Yc(P) = [(Yt(P) - Yt(M))Cos\beta + (Xt(P) - Xt(M))Sin\beta]*F + H_o$$

Note that the procedure developed here is for an axes system as shown in Figure 6.2.1(a), which refers to that of the front and left cameras situation. Hence for the right camera, the ultimate 'sign' direction for the horizontal coordinate has to be changed.

A secondary feature of re-exposing the film to the grid board is that errors due to lens distortion can be minimised. Since, the actual physical dimension of each square on the board is known, i.e. 127 mm square, a point (P) in space can be referred to the nearest grid junction (G) (relative to the origin of the system). The distance from the system origin to (G) can be accurately calculated by considering the number of squares between them. This will minimise the distorted length, limiting it to the distance between the spatial point and the grid junction, i.e. from DX to dx and DY to dy. See Figure 6.2.1(c).

The corrected coordinates are as follows :

$$Xp = \{[Integer(XP'/127)*127] + (XP' - XG')\}$$
$$Yp = \{[Integer(YP'/127)*127] + (YP' - YG')\}$$

6.2.2. Correction for Phase Difference

The shutter opening times of the three cameras are known to be out of phase during operation. In order to synchronise the three cameras, the method of linear interpolation is used.

Ishai (1975) presented a method which requires that the left camera would always be in phase advance and the right camera would be in phase lag. The system used in this project, was found to have variable out-of-phase

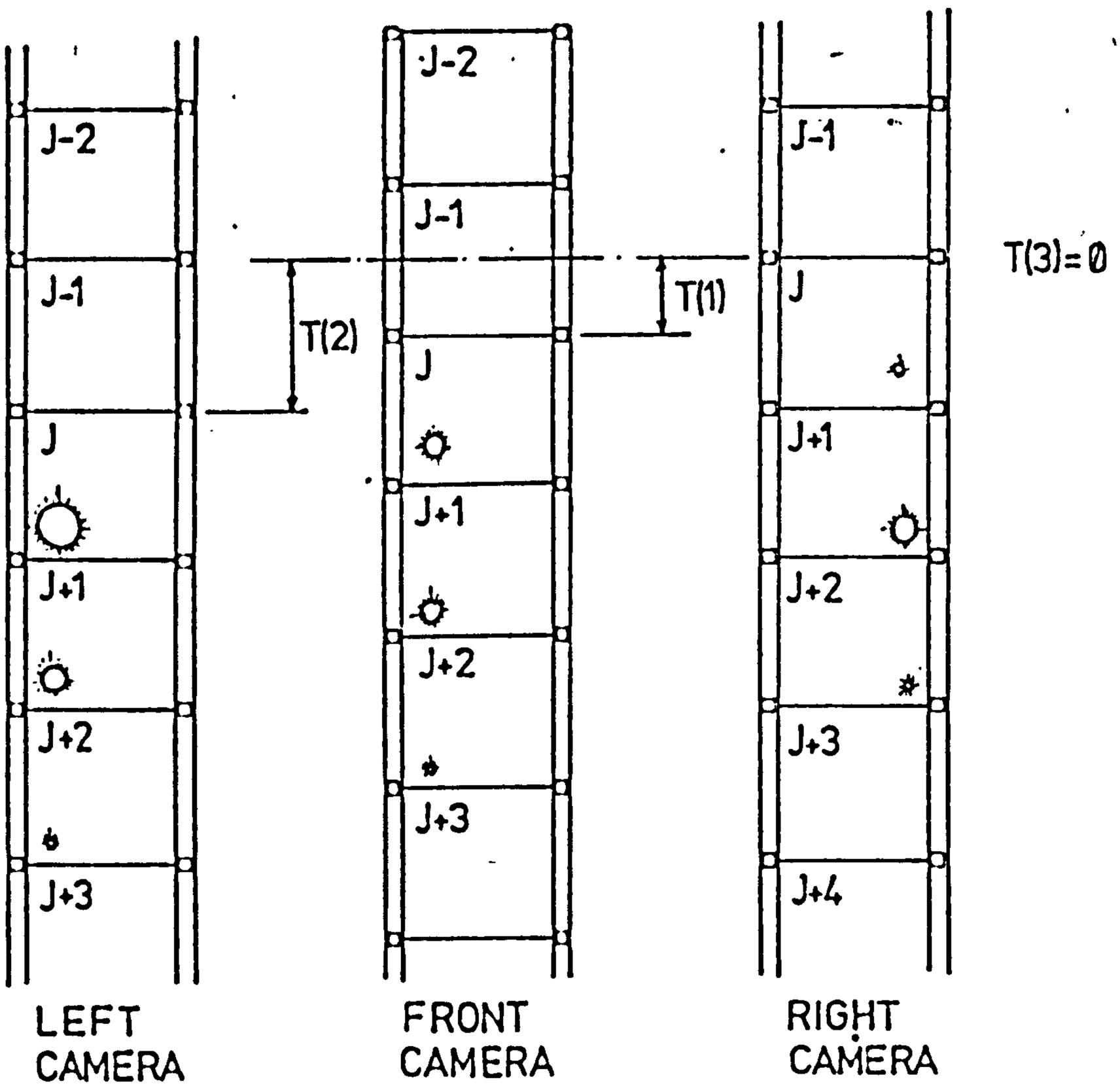

Figure 6.2.2. Phase difference between cameras

situation between each camera. Hence, a modified version is presented here which accounts for this variability.

From the flash bulb intensity, the leading camera can be established and the phase lag timing of the two trailing cameras relative to the leading camera can also be estimated. It was noticed that the phase difference between cameras does not exceed 20 ms, i.e. one frame interval. The following equation is formulated, with reference to Figure 6.2.2.

$$X_J = X_{J'} + (X_{J'-1} - X_{J'}) * \left[\frac{T(N)}{CT}\right]$$

where, CT is the time interval between successive frames (i.e. 20 ms)

$T(N)$ is the phase lag timing for camera (N)

N = 1 for front camera
= 2 for left camera
= 3 for right camera

6.2.3. Parallax Correction

Digitized coordinates of a marker are subject to parallax errors, due to perspective effects in cine-photography.

Referring to Figure 6.2.3., the following parallax equations are generated (using similar triangles) :

$$Za/Zt = DF/(DF - Xt) \quad ..... \quad (2.1)$$
$$Xa/Xt = DS/(DS + E*Zt) \quad ..... \quad (2.2)$$
$$(Ya - HS)/(Yt - HS) = DS/(DS + E*Zt) \quad ... \quad (2.3)$$
$$(Ya - HF)/(Yt - HF) = DF/(DF - Xt) \quad ..... \quad (2.4)$$

where X, Y, Z - coordinates of a marker
HS, HF - height of side and front cameras, respectively

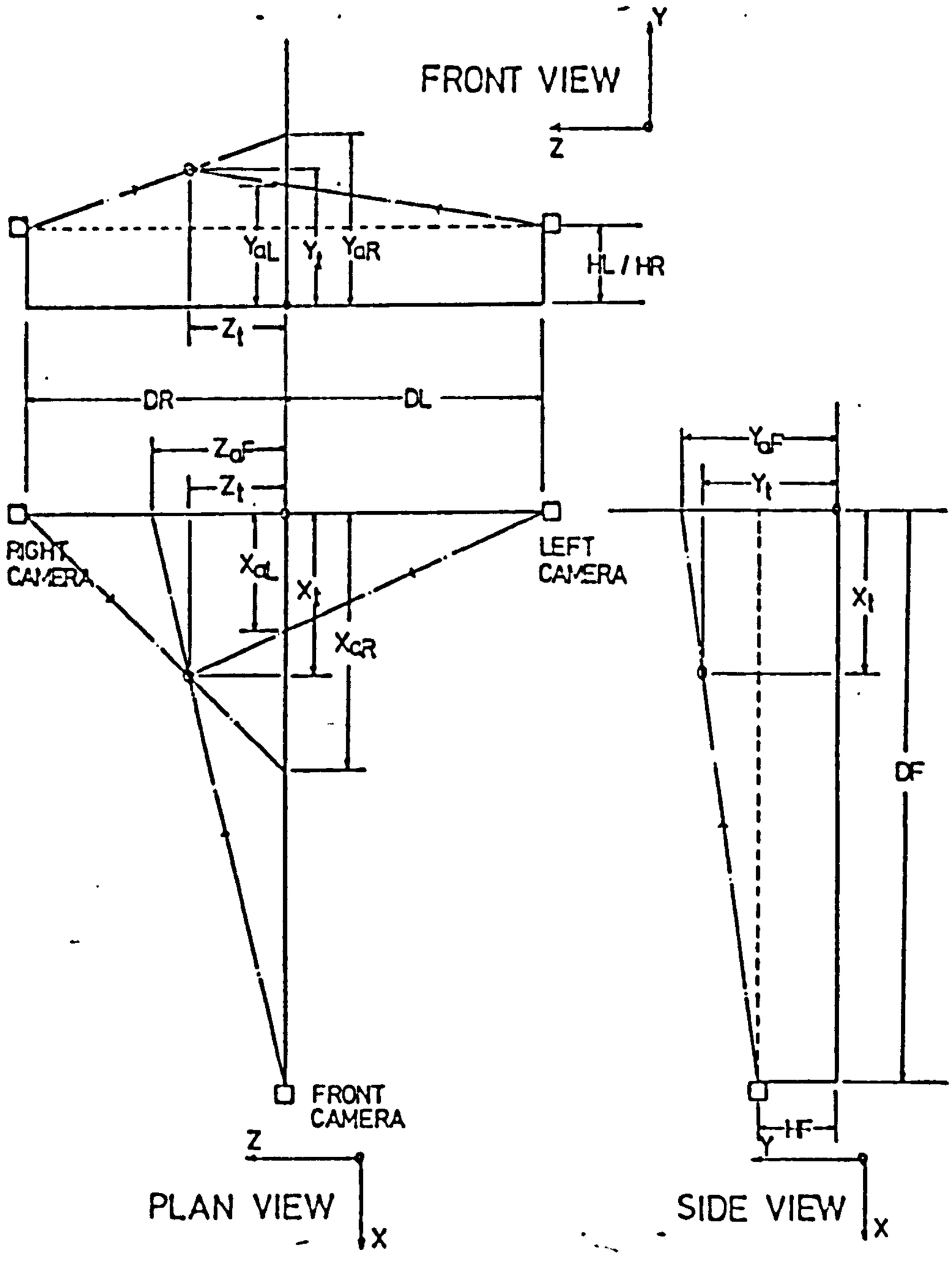

Figure 6.2.3. Parallax Correction

DS, *DF* - distance of side and front cameras, respectively, to the centre of system.

a - suffix denoting apparent coordinate

t - suffix denoting true coordinate

E - qualifier for left or right camera

= +1 - left camera

= -1 - right camera

Before applying these equations to correct for parallax errors, three unique cases associated with the measuring system have to be considered :

(i) "FRONTSIDE" Case - when a marker can be viewed from both the front and side cameras. From equations 2.1, 2.2 & 2.4, the following solution is obtained,

$$Xt = Xa*DF(DS + E*Za)/(DS*DF + E*Za*Xa)$$
$$Yt = Ya - Xt*(Ya - HF)/DF$$
$$Zt = Za*(DF - Xt)/DF$$

(ii) "FRONTONLY" Case - when a marker can only be viewed from the front camera. Solution is possible only when the distance between the marker and an adjacent marker(in the same rigid body) is known. Furthermore, the coordinates of the adjacent marker must be known first.

Using equations (2.1) and (2.4) together with the following equation :

$$D = SQRT\left[(Xt - XK)^2 + (Yt - YK)^2 + (Zt - ZK)^2\right] \quad ..(2.5)$$

where *D* is the known distance from the adjacent marker
and *K* is the suffix denoting the known coordinates of the adjacent marker.

Two solutions are obtained,

$$Xt = (B \pm SQRT(B^2 - A*C)/A$$
$$Yt = Ya - Xt*(Ya - HF)/DF$$
$$Zt = Za*(1 - Xt/DF)$$

where
$$A = 1 + ((Ya - HF)/DF)^2 + (Za/DF)^2$$
$$B = XK + (Ya - HF)(Ya - YK)/DF + Za(Za - ZK)/DF$$
$$C = XK^2 + (Ya - YK)^2 + (Za - ZK)^2 - D^2$$

The relevant solution is determined from the geometrical considerations of the marker being investigated.

(iii) "SIDEONLY" Case - when a marker can only be viewed from one of the side cameras. The same conditions as for "FRONTONLY" case apply here as well. Using equations (2.2), (2.3) and (2.5), two solutions are obtained.

$$Zt = (B \pm SQRT(B^2 - A*C)/A$$
$$Xt = Xa(1 + E*Zt/DS)$$
$$Yt = Ya + Zt(Ya - HS)/DS$$

where
$$A = 1 + ((Ya - HS)/DS)^2 + (Xa/DS)^2$$
$$B = ZK - E*(Ya-HS)(Ya-YK)/DS - E*Xa(Xa-YK)/DS$$
$$C = ZK^2 + (Ya - YK)^2 + (Xa - XK)^2 - D$$

Again, the relevant solution is determined by considering the geometry of the marker configuration.

6.2.4. Data Smoothing

The three dimensional spatial coordinates generated through the measuring system and data reduction process described above, are contaminated by noise. These are random errors which are superimposed onto the actual displacement data. The sources of these errors will be

discussed in Section 7.1.2.

The noise generated in human locomotion data is all in the high frequency level. Winter et al (1974) found that in normal level walking the highest harmonics were in the toe and heel trajectories and that 99.7% of the signal power was contained in the lower seven harmonics (i.e. below 6 Hz). Andrews (1975) reported that the power spectrum of the displacement data of the ankle joints were contained below 10 Hz. Zarrugh and Radcliffe (1979) concluded that 7 to 12 harmonics (i.e. 6 to 10 Hz) represented a good compromise between information retained and noise rejected for most gait variables in normal level walking. The author also performed a spectral analysis on all the displacement data obtained and found that almost all the signal power was contained in the first seven harmonics.

Therefore, some form of technique is required to remove the high frequency noise content. If not, the amplitude of the noise will be amplified through differentiation for velocity and acceleration and consequently affect the accuracy of dynamic calculations. Andrews et al (1981) described several methods that have been used in the removal of noise from kinematic data.

The filter used in this project is a fourth-order Butterworth low pass digital filter developed by Andrews (1975). Due to the non-symmetry of such filters, a phase shift is introduced to the filtered signals. This is eliminated by processing the data in both a forward and backward direction. This will mean that the overall filter will have a cut-off point of 6dB instead of the original 3dB. Therefore from the frequency response curve, a cut off frequency of 8Hz at 6dB correspond to 6Hz at 3dB. Hence, 8 Hz is chosen as a compromise cut-off frequency for the filtering process. For the theory

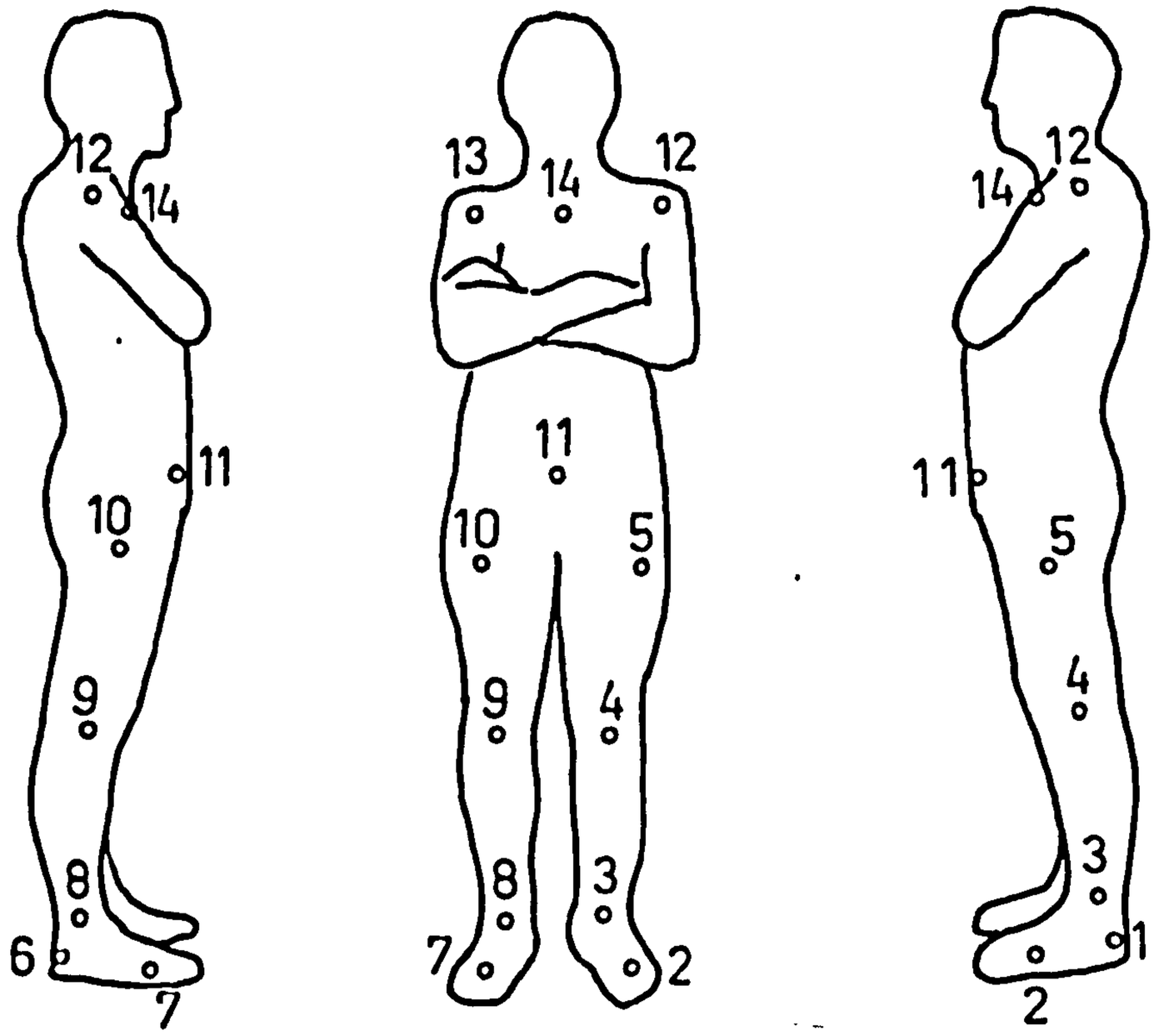

RIGHT VIEW FRONT VIEW LEFT VIEW

DEFINITION OF JOINT CENTRES

	LEFT	RIGHT
Heel	1	6
Metatarsal-phalangeal Joint	2	7
Ankle Joint	3	8
Knee Joint	4	9
Hip Joint	5	10
Shoulder Joint	12	13
Mid-pelvic position	11	
Sternum	14	

Figure 6.3. Definition of Joint Centres

and design of digital filters, the reader is referred to Hamming (1977).

6.3. Definition of Joint Centres and Body Segments

This section deals with the mathematical approach in defining the body segments and joint centres from the body markers. The eight body segments considered in the analysis are the foot, shank and thigh of both legs, the pelvis and the shoulder, see Figure 6.1.1(a). The joint centres analysed are as shown in Figure 6.3. Altogether, twelve joint centres and two other positions on the body are considered.

6.3.1. Shank; Knee and Ankle Joint Centres

This project has the task of looking at 3 different shanks, i.e. the normal, the below-knee and the above knee. The prominent features and physical measurement are therefore somewhat varied. In order to formulate a general solution to suit the three types of shank, a set of standard parameters has to be defined. The following classified initial analysis is aimed at defining these parameters.

a) The 'Normal' Shank

The knee joint in the normal shank is not a simple hinge, (i.e. having a single, fixed axis of rotation) but one where complex motions occur due to interaction between articular cartilage, muscle and joint capsule at various stages of limb movement (Weber and Weber, 1836). This complex joint motion is the result of the rolling and sliding action of the joint during flexion and extension of the knee (Gunston 1971). Hence, the axis of rotation does not remain fixed but moves along a path determined by the geometry of the articulating surfaces and

221a

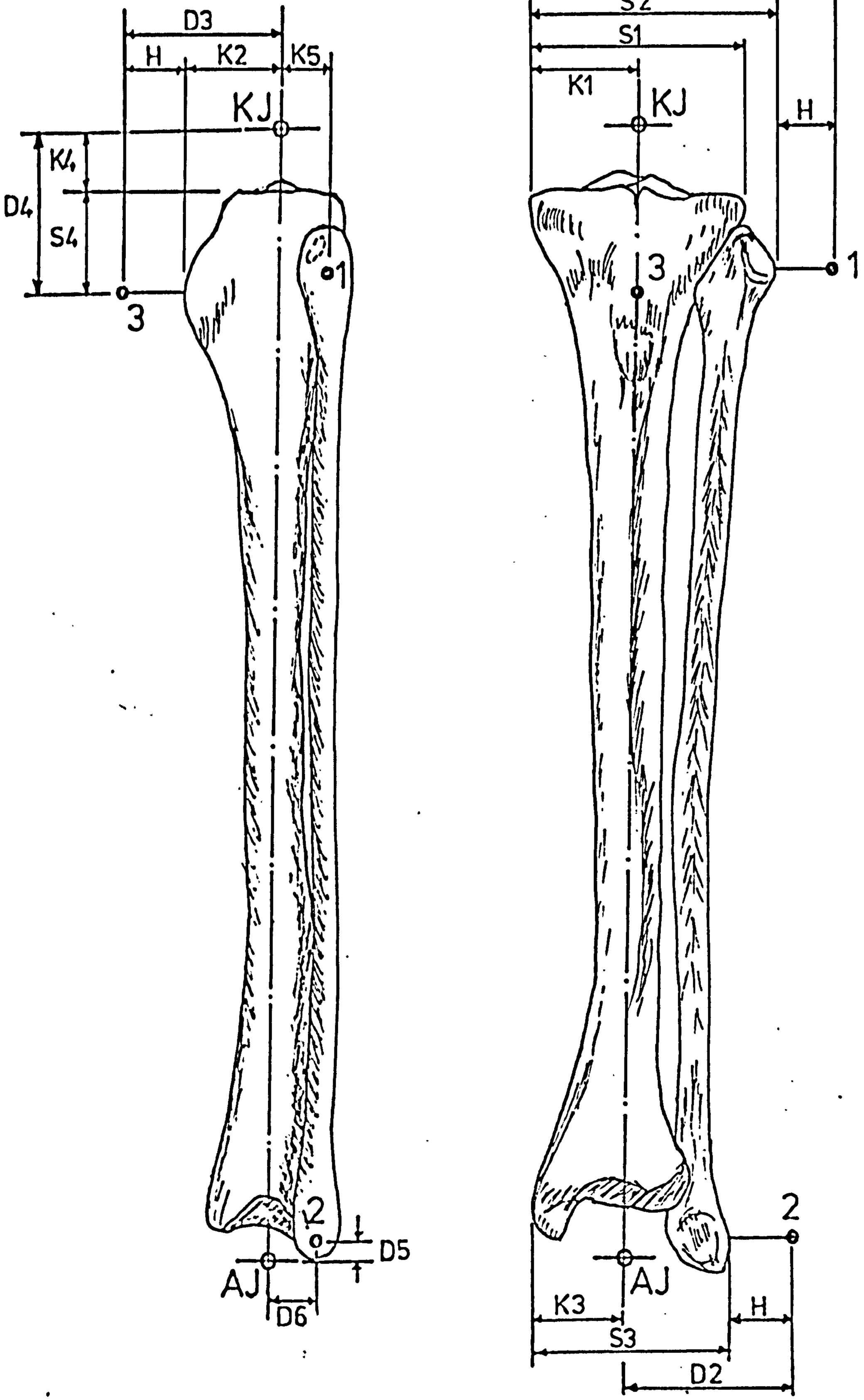

Figure 6.3.1(a) Normal Shank

ligamentous attachments. The exact position, size and shape of this path of instantaneous centres of rotation for any individual is still in considerable dispute, see Mayott et al (1975), Nietert (1977) and Soudan et al (1979). In view of the uncertainty in defining the exact knee joint centre and also to simplify the mathematical analysis, a fixed knee joint centre relative to a suitable anatomical reference is assumed.

Walker et al (1972) and Smidt (1973) presented dimensions of the knee joint from their studies of normal living subjects. The average values of the knee joint centre which can be drawn from their studies are 25 mm above the knee gap, measured along the longitudinal shank axis and 15 mm posterior to that axis. The knee gap was chosen as a reference because it can be easily palpated.

A regression technique was used to locate the knee joint centre from a set of external measurements, i.e. S_1,S_2,S_3,S_4 and S_5.(See Figure 6.3.1(a) and Section 5.4.4) Ishai (1975) presented the following equations, (from a study of 8 cadaveric tibias) to relate the knee joint centre to the external measurements :

$$K_1 = 0.37 * S_1 + 14.0 \text{ mm}$$
$$K_2 = 0.75 * S_1 - 21.6 \text{ mm}$$
$$K_3 = 0.32 * S_1 + 4.4 \text{ mm}$$
$$K_4 = 25 \text{ mm}$$
$$K_5 = 0.14 * S_1 + 2.7 \text{ mm}$$

K_4 being the distance between the knee joint centre and the knee gap, measured along the longitudinal shank axis. It is assumed that the knee joint centre lies along the longitudinal shank axis. Hence, K_5 can be used to evaluate the accuracy of this assumption.

Therefore the relevant dimensions can be calculated

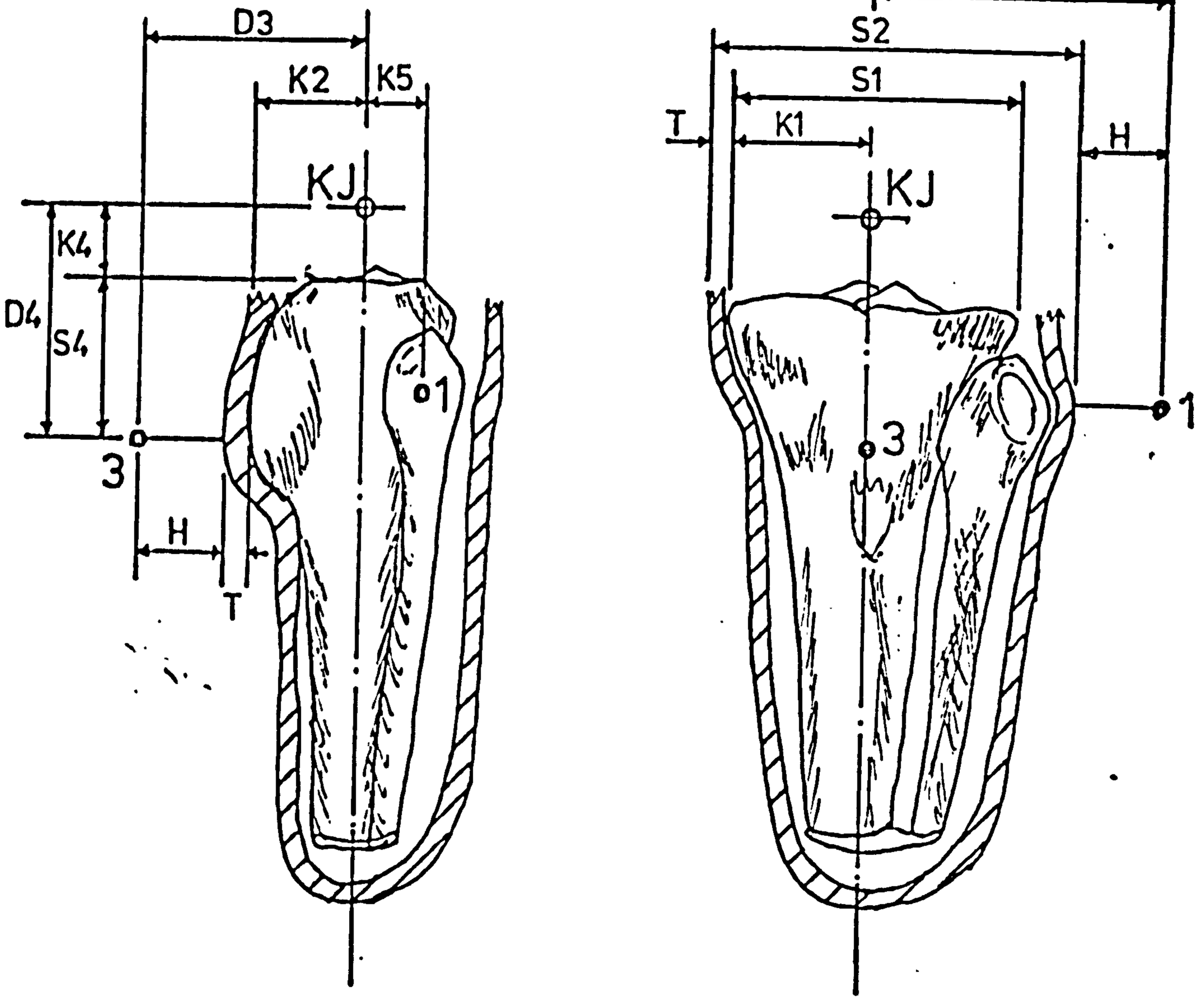

Figure 6.3.1(b) Below-knee Stump and Socket

as follows, see Figure 6.3.1(a) :

$$D_1 = S_2 - K_1 + H$$
$$D_2 = S_3 - K_3 + H$$
$$D_3 = K_2 + H$$
$$D_4 = S_4 + K_4$$

The normal ankle joint has been discussed in some detail in Section 4.1. It has been assumed that the joint centre lies along the longitudinal axis of the shank, therefore the parameter "D_6" can be excluded from the analysis. Marker (2) represents the ankle joint centre from the lateral view, thus D_5 is zero

b) <u>The 'Below-Knee' Stump and Socket</u>

The below-knee stump still has the normal knee joint preserved. Therefore, the regression equations (as for the normal knee) can be used in this analysis. However, the markers on the tibial tubercule and fibula head are transferred outside onto the socket as shown in Figure 6.3.1(b). Furthermore, measurement has to include the thickness of the socket, giving :

$$D_1 = S_2 - K_1 + H - T$$
$$D_2 = (S_3/2) + H$$
$$D_3 = K_2 + H + T$$
$$D_4 = S_4 + K_4$$

With the SACH foot, the ankle joint centre is assumed to be at the interface between the adaptor and the top of the foot, and that it lies along the longitudinal shank axis, see Figure 6.3.1(c). Marker (2) represents its lateral view, therefore D_5 is zero.

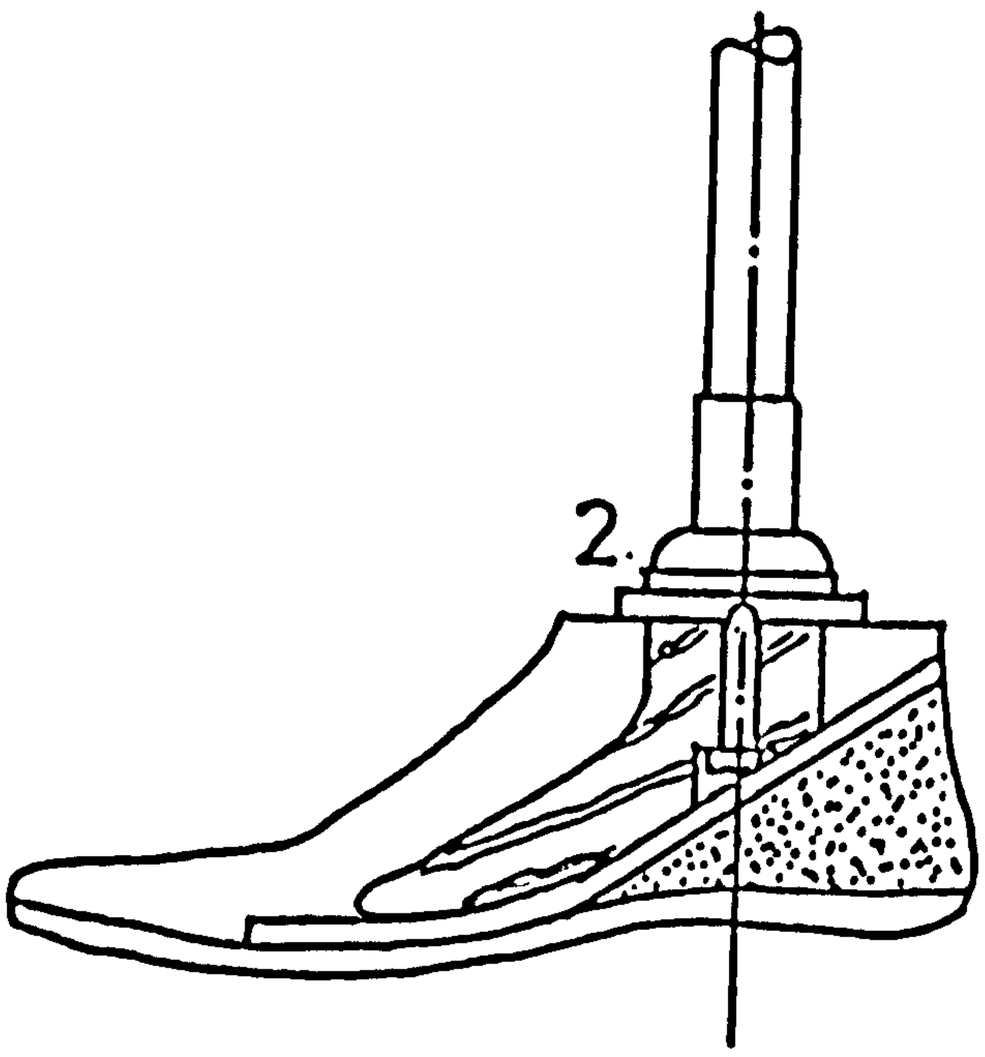

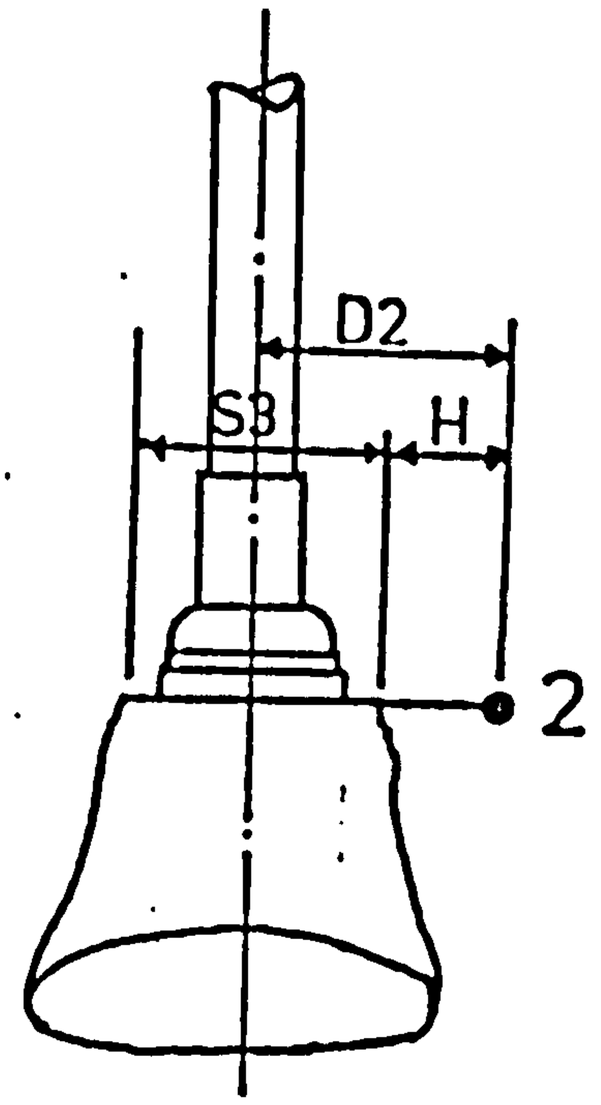

SACH FOOT

Figure 6.3.1(c)

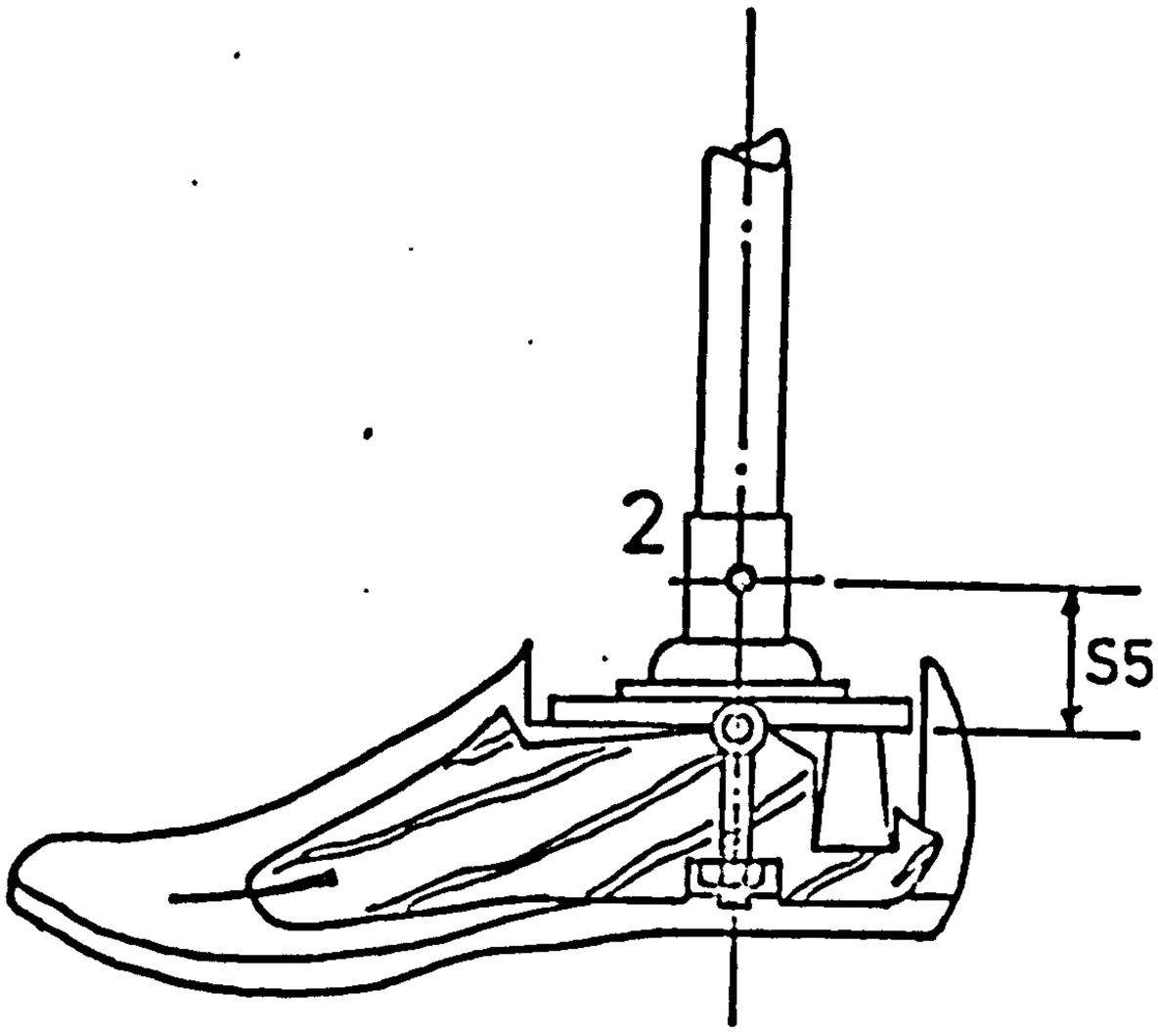

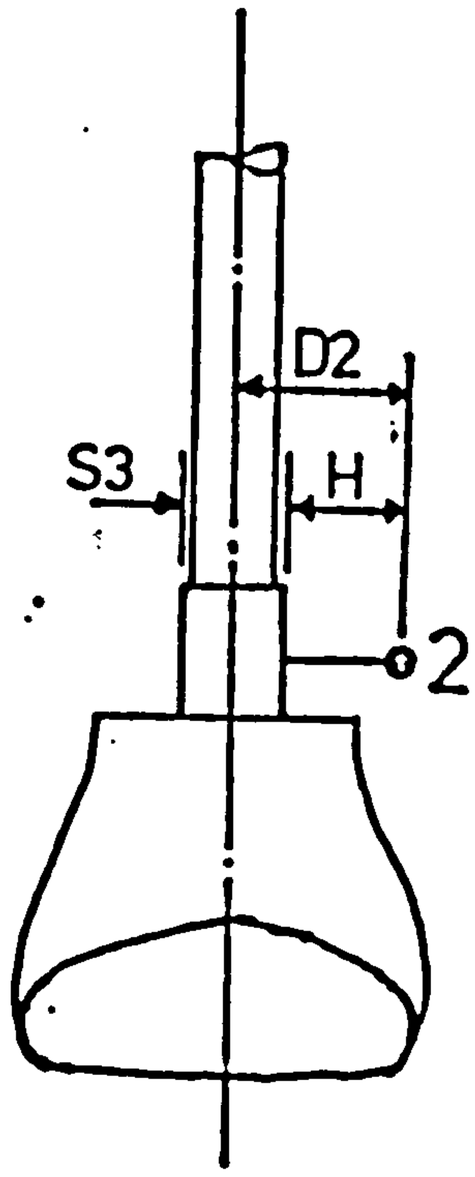

UNIAXIAL FOOT

Figure 6.3.1(d)

With the uniaxial foot, the ankle joint centre is clearly defined by the axis of the rotating shaft as shown in Figure 6.3.1(d). Marker (2) is positioned on the modular tubing above the joint, along the longitudinal shank axis. Therefore, D_5 is the distance between ankle joint centre and marker (2), i.e. $D_5 = S_5$

c) The Above-Knee Shank

The prosthetic knee used was an Otto Bock Single-axis knee mechanism. The knee joint centre is therefore easily and clearly defined. The relevant dimensions are calculated from the measurement taken, see Figure 6.3.1(e) they are as follows :

$$D_1 = (S_1/2) + H$$

$$D_2 = (S_3/2) + H$$

$$D_3 = S_2 + H$$

$$D_4 = \emptyset.\emptyset$$

The ankle joint centres are defined as those in the B/K shank, i.e. with SACH foot, $D_5 = 0$, *and*
with Uniaixial foot, $D_5 = S_5$

Solving for the D.C. Matrix of the Shank

With the relevant dimensions for the 3 cases being defined as a set of standard parameters, a general formulation of the analysis of the shank can be carried out as follows :

Figure 6.3.1(f) shows a schematic representation of the left shank in space relative to the ground frame of references. From it, the following expressions are drawn:

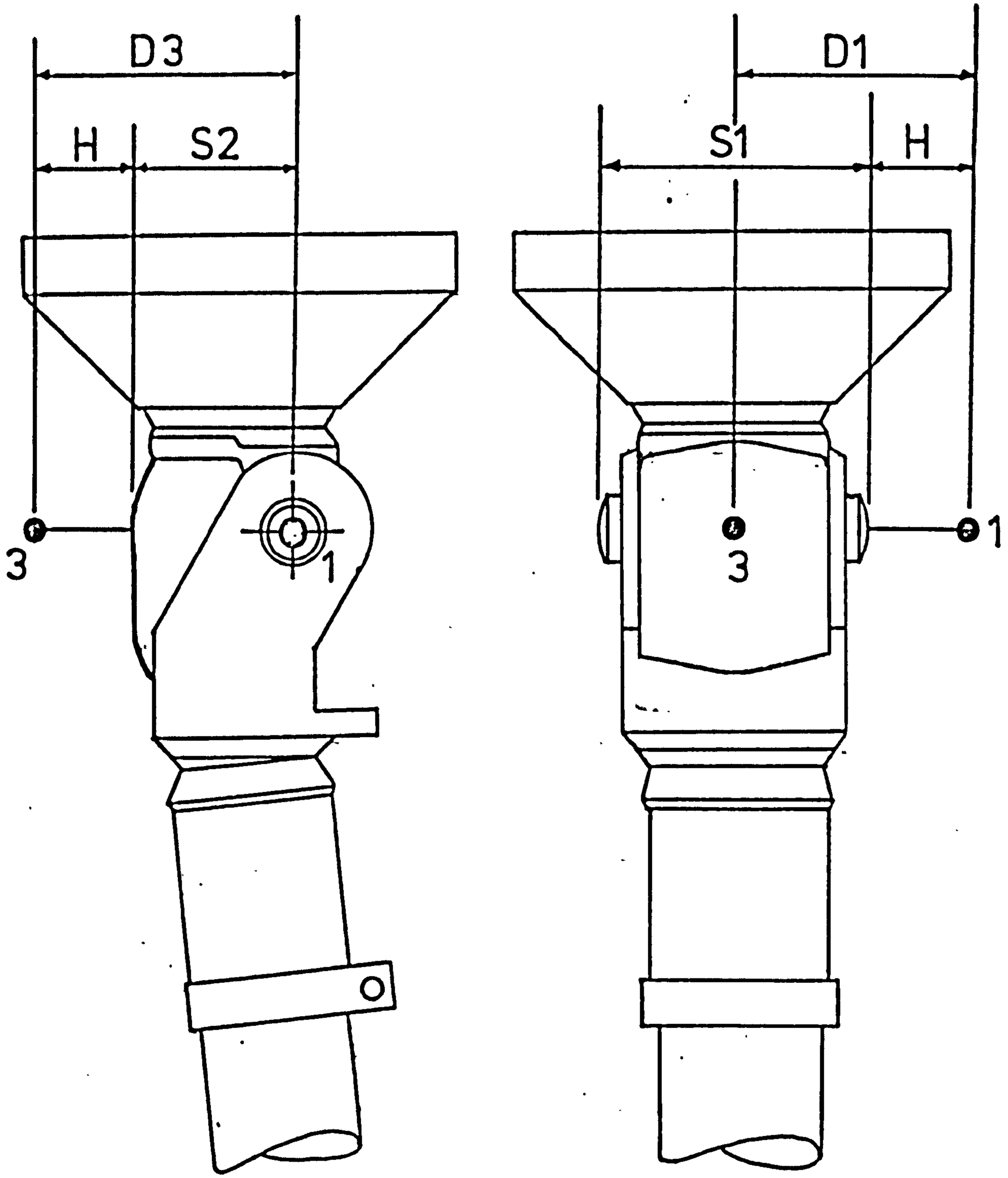

Figure 6.3.1(e) Prosthetic Knee Unit

$$\bar{R}_1 = \bar{R}_o - L_2*\bar{e}_x + L_1*\bar{e}_y - E*D_1*\bar{e}_z \quad \ldots\ldots\ldots (3.1)$$

$$\bar{R}_2 = \bar{R}_o - D_6*\bar{e}_x - E*D_2*\bar{e}_z \quad \ldots\ldots\ldots (3.2)$$

$$\bar{R}_3 = \bar{R}_o + D_3*\bar{e}_x + L_3*\bar{e}_y \quad \ldots\ldots\ldots (3.3)$$

where E = qualifier for left (+1) or right (-1) shank
$\bar{e}_n$ = represents the unit vector associated with axis 'n'.

By using the 'dot-product' theory, in vector analysis, the unknown variables $\bar{R}_o$, L_1, L_2 and L_3 can be eliminated, thus

$$(\bar{R}_3 - \bar{R}_1)*\bar{e}_z = E*D_1 \quad \ldots\ldots (3.4)$$

$$(\bar{R}_3 - \bar{R}_2)*\bar{e}_z = E*D_2 \quad \ldots\ldots (3.5)$$

$$(\bar{R}_3 - \bar{R}_2)*\bar{e}_x = D_3 + D_6 \quad \ldots\ldots (3.6)$$

(Note that from previous consideration, D_6 can be excluded in the analysis). Expanding these expressions in scalar form, we have

$$(X_3 - X_1)*B_{31} + (Y_3-Y_1)*B_{32} + (Z_3-Z_1)*B_{33} = E*D_1 \ldots (3.7)$$

$$(X_3 - X_2)*B_{31} + (Y_3-Y_2)*B_{32} + (Z_3-Z_2)*B_{33} = E*D_2 \ldots (3.8)$$

$$(X_3 - X_2)*B_{11} + (Y_3-Y_2)*B_{12} + (Z_3-Z_2)*B_{13} = D_3 \ldots (3.9)$$

From equations (3.7) and (3.8), we have

$$B_{31} = G_x + H_x*B_{33} \quad \ldots\ldots (3.10)$$

$$B_{32} = G_y + H_y*B_{33} \quad \ldots\ldots (3.11)$$

where

$$G_x = \left[E*D_2(Y_3-Y_1) - E*D_1(Y_3-Y_2)\right]/(-P_n)$$

$$H_x = \left[(Y_3-Y_1)(Z_3-Z_1) - (Y_3-Y_1)(Z_3-Z_2)\right]/(-P_n)$$

$$G_y = \left[E*D_2(X_3-X_1) - E*D_1(X_3-X_2)\right]/P_n$$

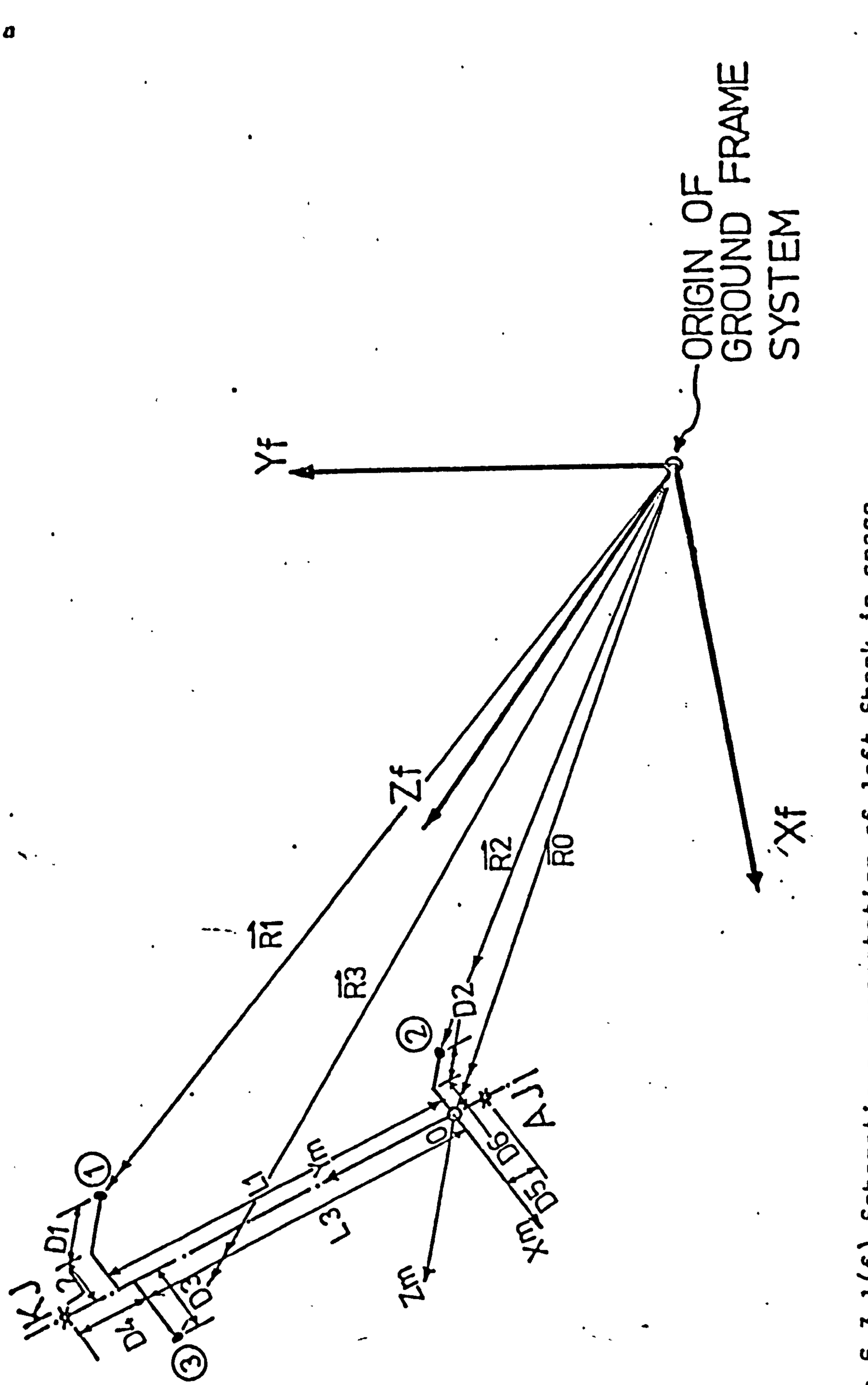

Figure 6.3.1(f) Schematic representation of left Shank in space

$$H_y = [(X_3 - X_2)(Z_3 - Z_1) - (X_3 - X_1)(Z_3 - Z_2)]/P_n$$

$$P_n = [(X_3 - X_1)(Y_3 - Y_2) - (X_3 - X_2)(Y_3 - Y_1)]$$

Substitute B_{31} and B_{32} in the orthogonality condition (1.3) by equations (3.10) and (3.11), respectively, we have

$$(G_x + H_x*B_{33})^2 + (G_y + H_y*B_{33})^2 + B_{33}^2 = 1$$

$$\therefore \quad (1+H_x^2+H_y^2)B_{33}^2 + 2(G_x*H_y + G_y*H_y)B_{33} + (G_x^2+G_y^2-1) = \emptyset$$

let,

$$a_3 = (1 + H_x^2 + H_y^2)$$

$$b_3 = 2(G_x*H_x + G_y*H_y)$$

$$c_3 = (G_x^2 + G_y^2 - 1)$$

Therefore,

$$a_3*B_{33}^2 + b_3*B_{33} + C_3 = \emptyset$$

hence,

$$B_{33} = \frac{-b_3 \pm \sqrt{(b_3^2 - 4a_3*c_3)}}{2a_3}$$

There are two solutions for B_{33}, the correct solution must be positive and its magnitude smaller than and nearest to unity.

Substitute solution into equations (3.10) and (3.11) to solve for B_{31} and B_{32}. Together with these known variables, the orthogonality condition (1.6) and equation (3.9), we get

$$B_{12} = S_y + T_y*B_{11} \quad \ldots . \quad (3.12)$$

$$B_{13} = S_z + T_z*B_{11} \quad \ldots . \quad (3.13)$$

where

$$S_y = -D_3*B_{33}/P_1$$

$$T_y = [(X_3 - X_2)*B_{33} - (Z_3 - Z_2)*B_{31}]/P_1$$

$$S_z = D_3*B_{32}/P_1$$

$$T_z = [(Y_3 - Y_2)*B_{31} - (X_3 - X_2)*B_{32}]/P_1$$

$$P_1 = [(Z_3 - Z_2)*B_{32} - (Y_3 - Y_2)*B_{33}]$$

Substitute B_{12} and B_{13} in the orthogonality condition (1.1) by equations (3.12) and (3.13) respectively, we have

$$B11 = \sqrt{\frac{-b_1 \pm (b_1^2 - 4*a_1*c_1)}{2a_1}}$$

where

$$a_1 = (1 + T_y^2 + T_z^2)$$

$$b_1 = 2(S_y*T_y + S_z*T_z)$$

$$c_1 = (S_y^2 + S_z^2 - 1)$$

Again 2 solutions are derived, the correct solution should be positive and its magnitude smaller than and nearest to unity. Substitute the solution into equations (3.12) and (3.13) to solve for B_{12} and B_{13}. And from the remaining orthogonality conditions (1.2), (1.4) and (1.5), we have

$$B_{21} = (B_{12}*B_{13} - B_{33}*B_{12})$$

$$B_{22} = (B_{33}*B_{11} - B_{31}*B_{13})$$

$$B_{23} = (B_{31}*B_{12} - B_{32}*B_{11})$$

Thus, solving for all the elements in the D.C. Matrix for the moving shank, i.e.

$$[\ B_S\ ] = \begin{bmatrix} B_{11} & B_{12} & B_{13} \\ B_{21} & B_{22} & B_{23} \\ B_{31} & B_{32} & B_{33} \end{bmatrix}$$

Calculating the Ankle Joint Centre Coordinates

From equations (3.4), (3.5) and (3.6), we have

$$\bar{R}_o*\bar{e}_x = \bar{R}_3*\bar{e}_x - D_3$$

$$\bar{R}_o * \bar{e}_y = \bar{R}_2 * \bar{e}_y$$
$$\bar{R}_o * \bar{e}_z = \bar{R}_1 * \bar{e}_z + E * D_1$$

or

$$\bar{R}_o * [B_S] = [Q]$$
$$\therefore \quad \bar{R}_o = [Q] * [B_S]^{-1}$$

where

$$[Q] = \begin{bmatrix} X_3 * B_{11} + Y_3 * B_{12} + Z_3 * B_{13} - D_3 \\ X_2 * B_{21} + Y_2 * B_{22} + Z_3 * B_{23} \\ X_1 * B_{31} + Y_1 * B_{32} + Z_1 * B_{33} + E * D_1 \end{bmatrix}$$

The ankle joint centre is $\bar{r}_A$ away from the origin of the moving axes system. To relate it to the ground frame of reference, we have,

$$\bar{R}_A = \bar{R}_o + [B_S] * \bar{r}_A$$

where

$$\bar{r}_A = \begin{bmatrix} \emptyset.\emptyset \\ -D_5 \\ \emptyset.\emptyset \end{bmatrix}$$

To solve for the unknown variables L_1, L_2 and L_3 we require equations (3.1) and (3.3), which gives

$$L_1 = (\bar{R}_1 - \bar{R}_o) * \bar{e}_y$$
$$L_2 = (\bar{R}_o - \bar{R}_1) * \bar{e}_x$$
$$L_3 = (\bar{R}_3 - \bar{R}_o) * \bar{e}_y$$

<u>Calculating the Knee Joint Centre Coordinates</u>

The knee joint centre is $\bar{r}_K$ away from the origin of the moving axes system, to relate it to ground frame of reference, we have :

$$\bar{R}_K = \bar{R}_o + [B_S] * \bar{r}_K$$

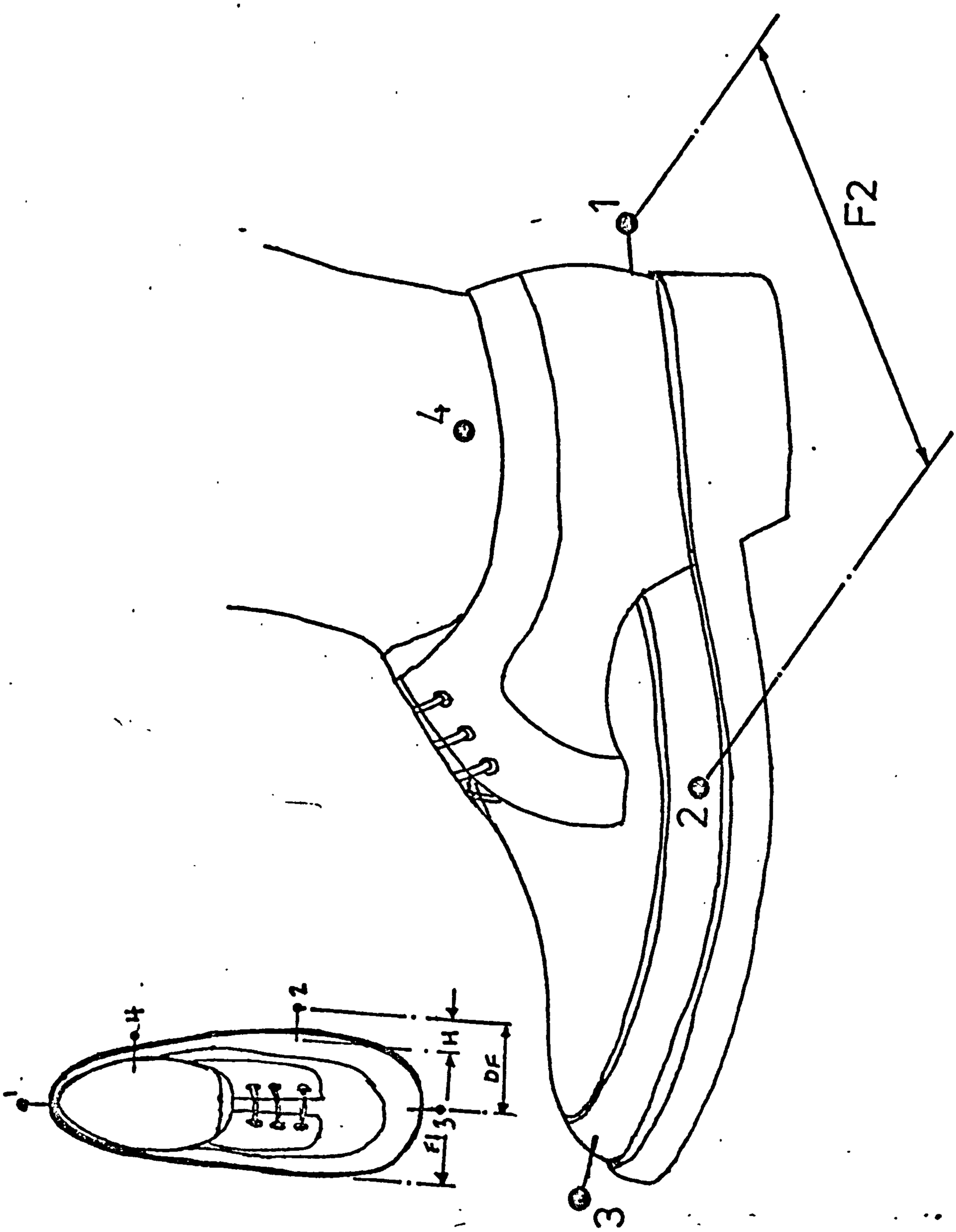

Figure 6.3.2(a) Foot Markers

where, $$\bar{r}_K = \begin{bmatrix} \emptyset.\emptyset \\ L_3 + D_4 \\ \emptyset.\emptyset \end{bmatrix}$$

6.3.2. Foot

Markers are positioned on the foot-wear as shown in Figure 6.3.2(a). For the normal foot, marker (3) is positioned between the 2nd and 3rd toe, marker (1) is on mid-heel and marker (2) is on the 5th metatarsal base. For the prosthetic feet (both the SACH and Uniaxial), the marker (3) is positioned on the tip of the foot, marker (1) is on mid-heel and marker (2) is on a similar position, corresponding to that of the normal foot.

With the spatial coordinates of the ankle joint centre known, (calculated from the previous analysis in Section 6.3.1) the orientation of the foot can be formulated as follows :

From the coordinates of the 3 markers and ankle joint centre,we have (see Figure 6.3.2(b)) :

$$\bar{e}_{xa} = (\bar{R}_3 - \bar{R}_1)/ABS(\bar{R}_3 - \bar{R}_1)$$
$$\bar{e}_{ya} = (\bar{R}_A - \bar{R}_2)/ABS(\bar{R}_A - \bar{R}_2)$$

and by cross-product theory,

$$\bar{e}_z = (\bar{e}_{xa} * \bar{e}_{ya}).$$

Now, $\bar{e}_{xa}$ and $\bar{e}_{ya}$ are only the apparent orientations of the foot, because of the action of the metatarsalphalangeal joint during locomotion (see Figure 6.3.2(c)). Therefore, these direction cosines have to be re-defined, firstly by determining the metatarsalphalangeal joint centre,

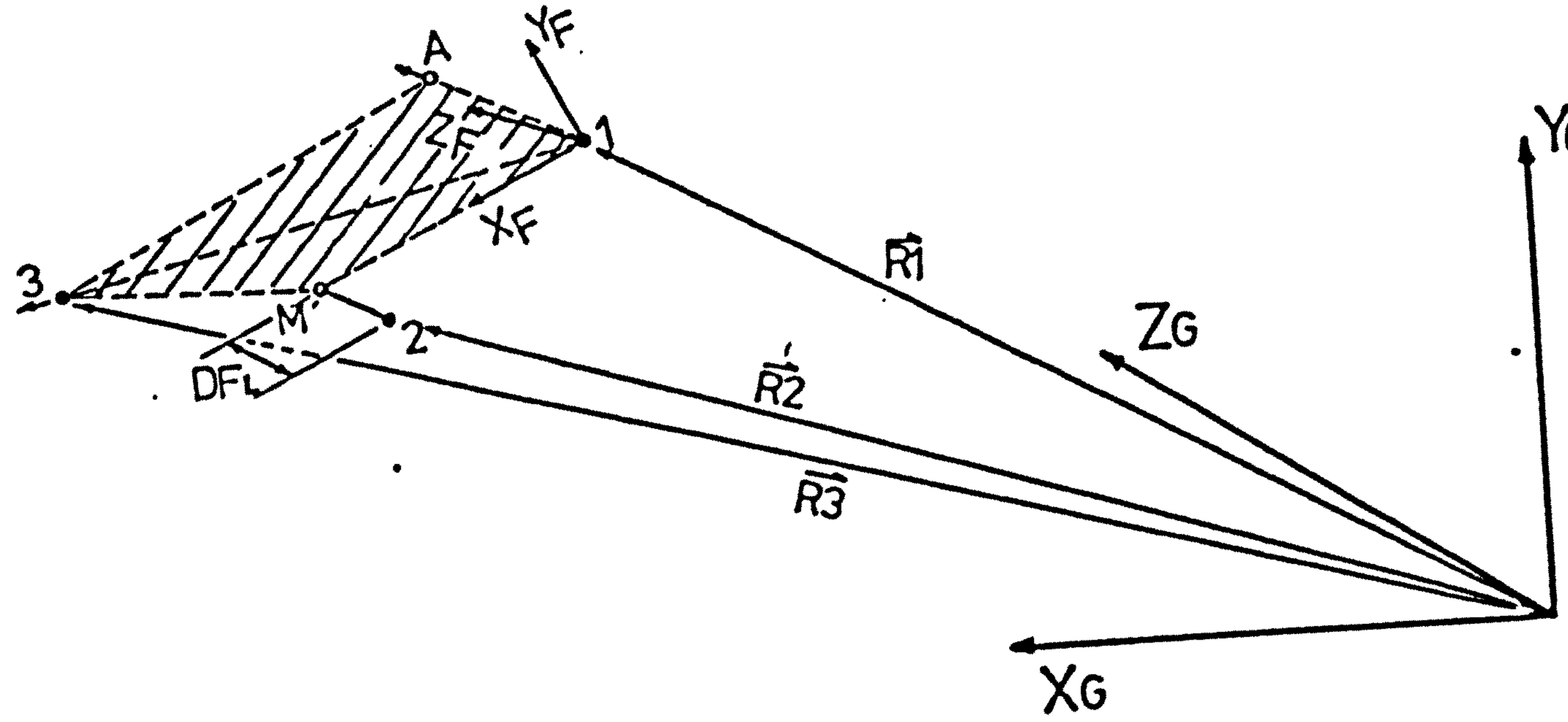

Figure 6.3.2(b) Schematic representation of left foot in space

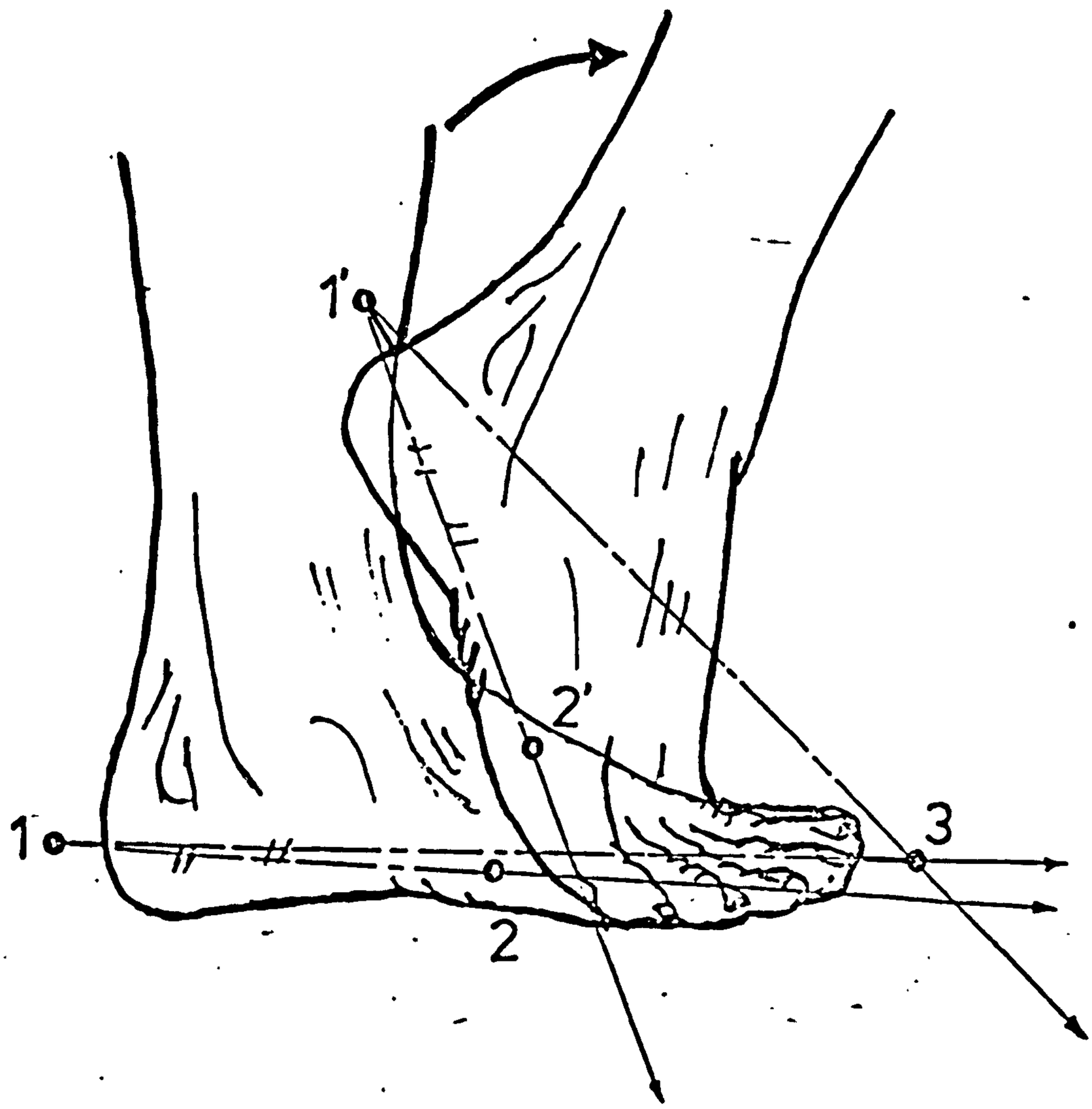

Figure 6.3.2(c) Flexion of metatarsal phalangeal joint during push off

$$\bar{R}_M = \bar{R}_2 + E*(\bar{e}_z*D_F)$$

where E is the qualifying code for the side under consideration, i.e. +1 for left side and -1 for right side.

D_F is the distance from marker (2) to the joint centre.

Hence,

$$\bar{e}_x = (\bar{R}_M - \bar{R}_1)/ABS(\bar{R}_M - \bar{R}_1)$$
$$\bar{e}_y = (\bar{e}_x*\bar{e}_z)$$

Calculating the position of the heel, we have

$$\bar{R}_H = \bar{R}_2 + (\bar{e}_x*H)$$

where H is the length of the marker stalk.

Therefore, the direction cosine of the foot is as follows:

$$[B_F] = \begin{bmatrix} \bar{e}_x \\ \bar{e}_y \\ \bar{e}_z \end{bmatrix}$$

6.3.3. Pelvis and Hip Joint Centres

The markers are positioned as shown in Figure 6.3.3. There are two sets of coordinates obtained for the tail markers, $\bar{R}_{T1L}$ and $\bar{R}_{T2L}$ from the left camera and $\bar{R}_{T1R}$ and $\bar{R}_{T2R}$ from the right camera. These values are averaged to give,

$$\bar{R}_{T1} = (\bar{R}_{T1L} + \bar{R}_{T1R})/2$$
$$\bar{R}_{T2} = (\bar{R}_{T2L} + \bar{R}_{T2R})/2$$

From these known coordinates, position (3) on the sacrum can be obtained by extrapolation,

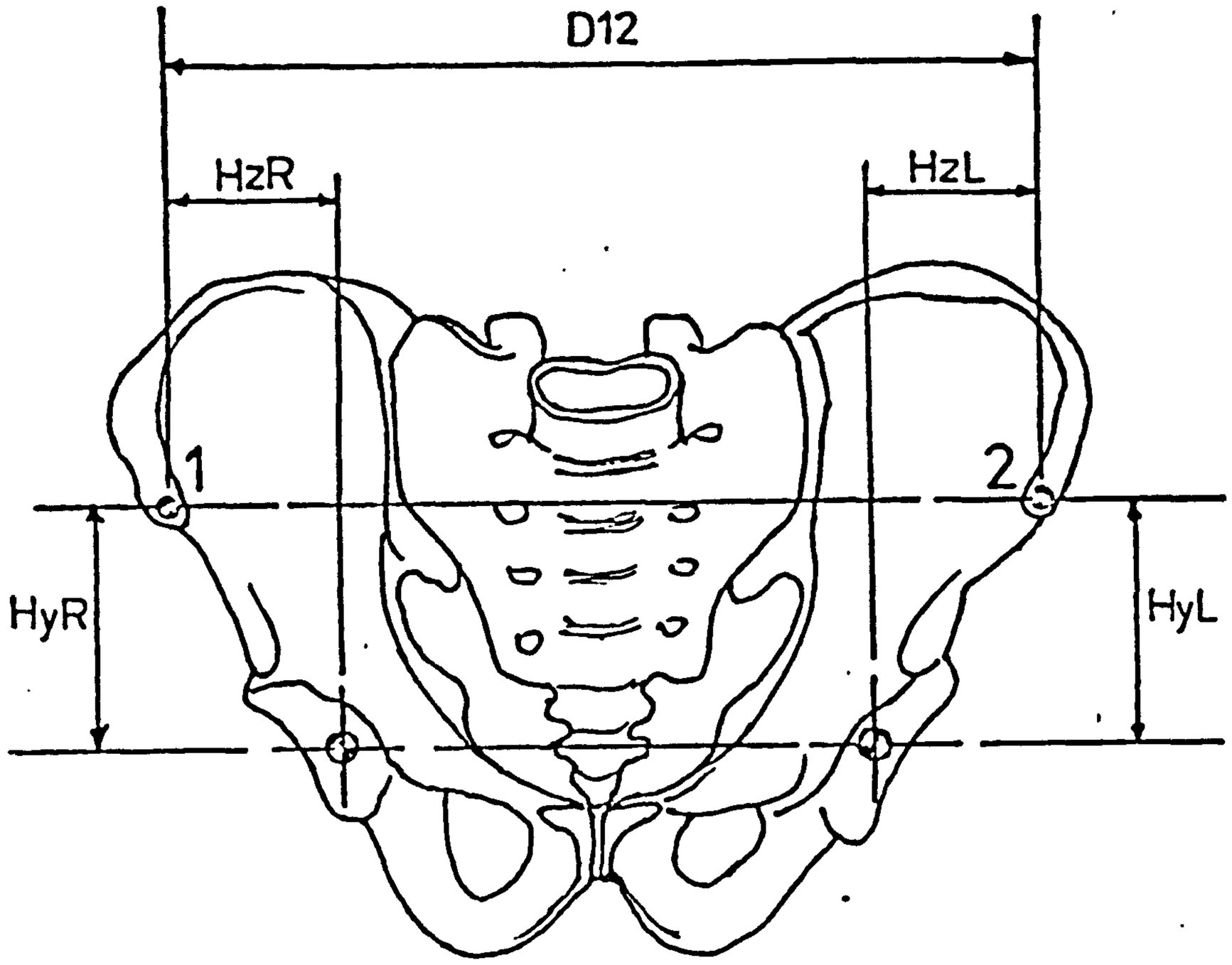

Figure 6.3.3 Relation of pelvis markers to hip joint centres

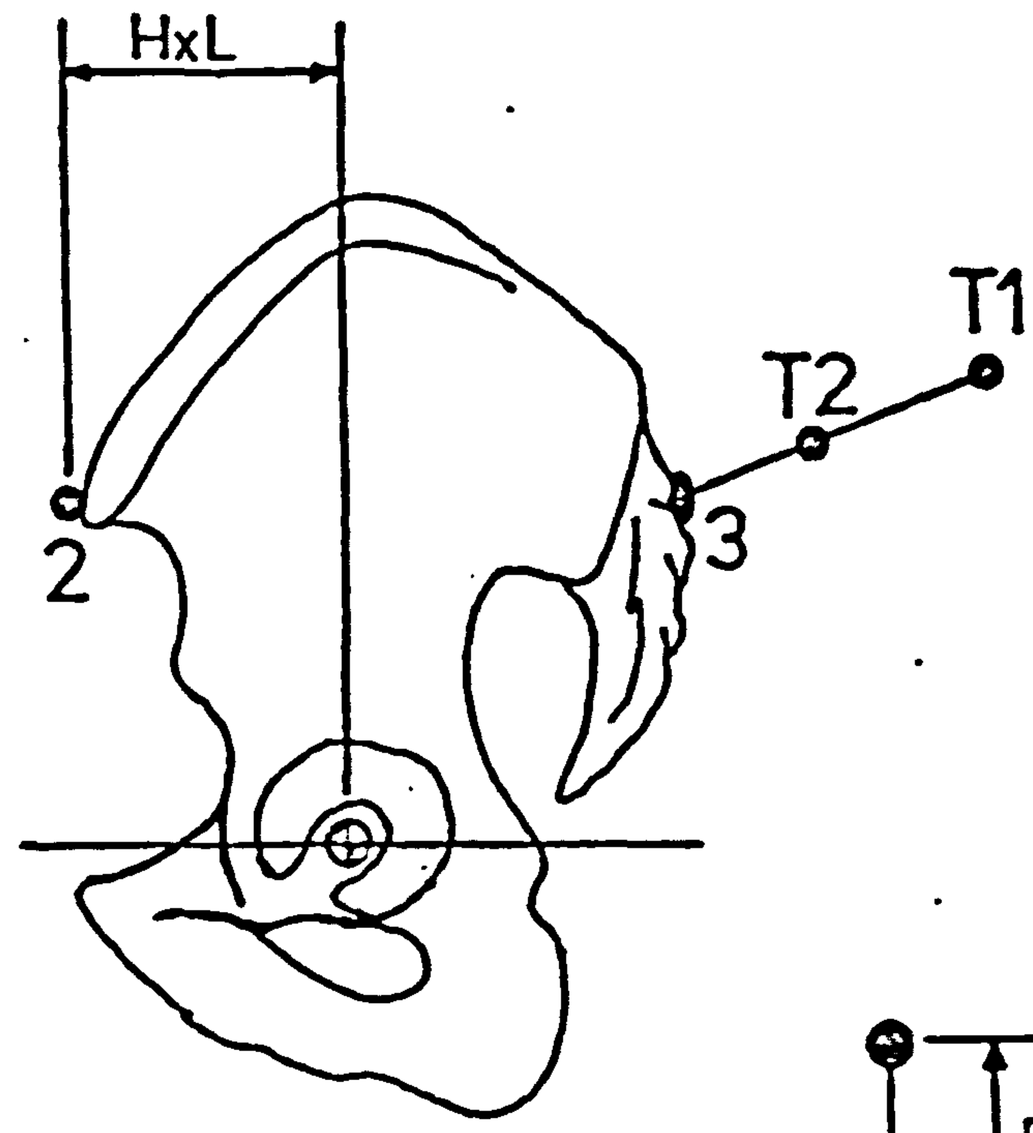

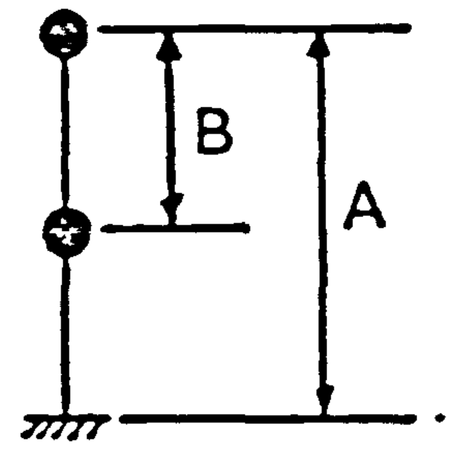

MARKER RATIO.

$r_p = [A/B]$

$$\bar{R}_3 = (\bar{R}_{T1} - (\bar{R}_{T1} - \bar{R}_{T2})*r_p)$$

where r_p is the ratio of the length between the 2 tail markers (see Figure 6.3.3).

The orientation of the pelvis in space can be determined as follows :

$$\bar{e}_z = (\bar{R}_1 - \bar{R}_2)/ABS(\bar{R}_1 - \bar{R}_2)$$

$$\bar{e}_{xa} = (\bar{R}_3 - \bar{R}_2)/ABS(\bar{R}_3 - \bar{R}_2)$$

and by using 'cross-product' theory,

$$\bar{e}_y = \bar{e}_z * \bar{e}_{xa}$$

$$\bar{e}_x = \bar{e}_y * \bar{e}_z$$

Thus, the direction cosine of the pelvis is,

$$[B_P] = \begin{bmatrix} \bar{e}_x \\ \bar{e}_y \\ \bar{e}_z \end{bmatrix}$$

A mid-pelvic position is defined as the origin of the pelvic axes system,

$$\bar{R}_P = (\bar{R}_2 + \bar{R}_1)/2$$

Note : An approximate position of the centre of gravity of the whole body can be calculated as follows :

$$\bar{R}_{cg} = (\bar{R}_3 + \bar{R}_P)/2$$

To determine the hip joint centres, an anthropometric scaling technique is usually used, Ishai (1975), Harrington (1974) and Trappitt (1981). The scaling factors presented by these investigators are as follows

$$Hx = 0.183\ D12$$
$$Hy = 0.305\ D12$$
$$Hz = 0.122\ D12$$

Initial tests using these factors showed that they were grossly inaccurate in that high knee hyper-extension angles were obtained on normal subject during locomotion. Dorstal and Andrews (1981) presented anthropometric data of a cadaveric pelvis. From these data, another set of scaling factors was obtained, they are as follows :

$$Hx = 0.221\ D12$$
$$Hy = 0.327\ D12$$
$$Hz = 0.175\ D12$$

Although these "new" scaling factors are larger than those mentioned earlier, tests with these factors still gave fairly high knee hyper-extension angles. It was then decided to measure Hx and Hy directly from the subject, while Hz could be determined from the "new" scaling factor.

From tests using interrupted light photography, the normal leg was found to swing about the tip of the greater trochanter in the sagittal plane. Therefore, Hx and Hy are measured along their respective axes from the anterior superior iliac spine to the tip of the greater trochanter, while the subject is standing. Measurements from the contralateral side were taken.

To locate the hip joint centres, from these measurements, all coordinates have to be transformed to the pelvic axes system :

$$\bar{R}_{1P} = [B_P] * [\bar{R}_1 - \bar{R}_P]$$
$$\bar{R}_{2P} = [B_P] * [\bar{R}_2 - \bar{R}_P]$$

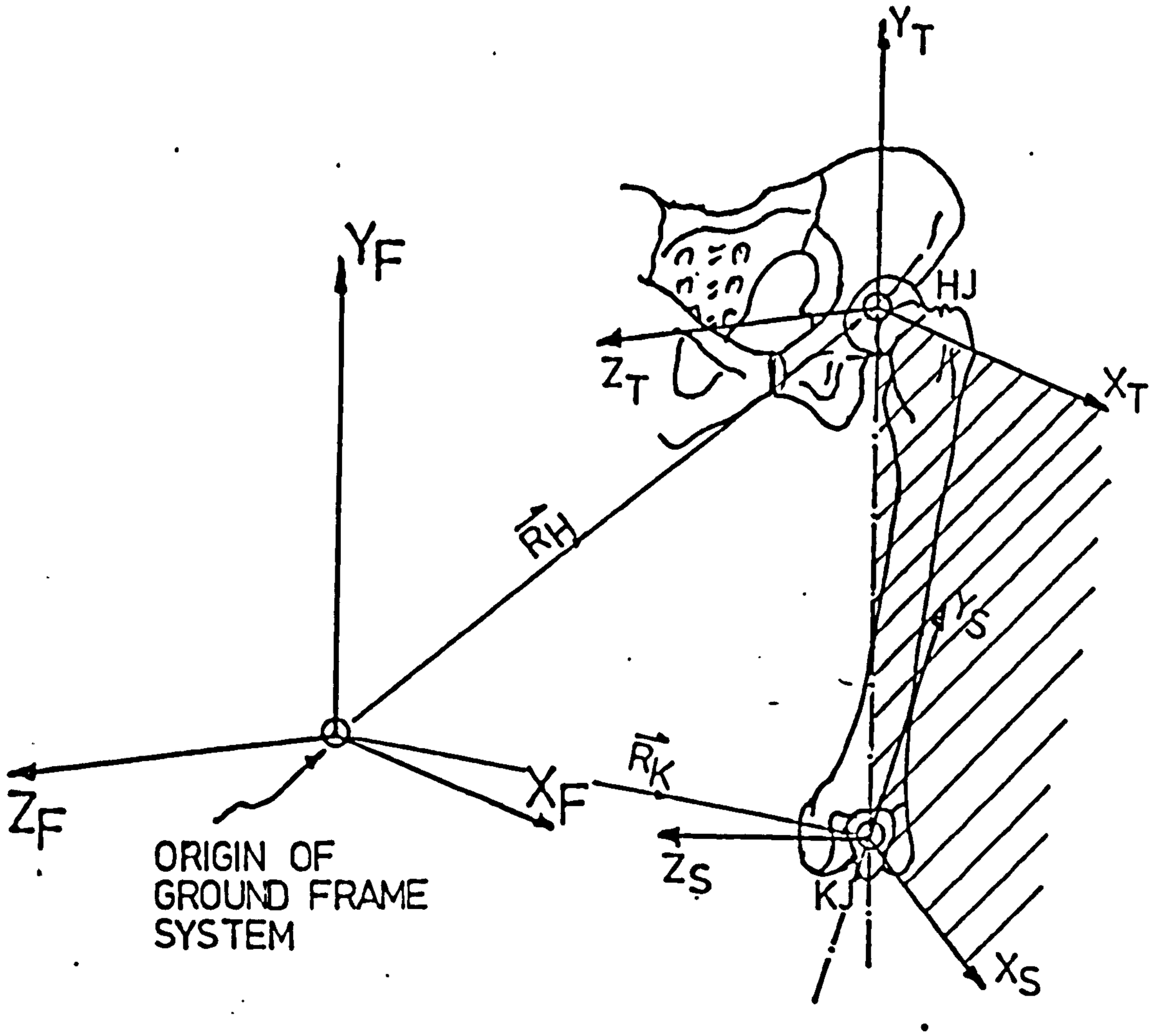

Figure 6.3.4. Spatial orientation of left thigh

Therefore, the hip joint centres in the pelvis axes system are as follows :

$$\bar{R}_{LP} = \bar{R}_{1P} + [B_P] * \begin{bmatrix} -H_{xL} \\ -H_{yL} \\ H_{zL} \end{bmatrix}$$

and,

$$\bar{R}_{RP} = \bar{R}_{1P} + [B_P] * \begin{bmatrix} -H_{xR} \\ -H_{yR} \\ -H_{zR} \end{bmatrix}$$

Transforming back to the ground frame of reference, we have :

$$\bar{R}_{LH} = \bar{R}_P + \{[B_P]^{-1} * \bar{R}_{LP}\}$$

and

$$\bar{R}_{RH} = \bar{R}_P + \{[B_P]^{-1} * \bar{R}_{RP}\}$$

6.3.4. Thigh

It is assumed that the knee joint is a single-axis hinge joint, therefore the direction of progression is common to both the shank and thigh axes systems.

Hence, by making use of the direction cosines($\bar{e}_{xS}$) associated with the x-axis in the shank axes system, the D.C. Matrix of the thigh can be solved.

Coordinates of the hip and knee joint centres have already been determined from the previous calculations. Therefore, the orientation of the thigh can be determined as follows : (refer to Figure 6.3.4)

$$\bar{e}_y = [\bar{R}_H - \bar{R}_K] / ABS(\bar{R}_H - \bar{R}_K)$$
$$\bar{e}_z = [\bar{e}_y * \bar{e}_{xS}]$$
$$\bar{e}_x = [\bar{e}_y * \bar{e}_z]$$

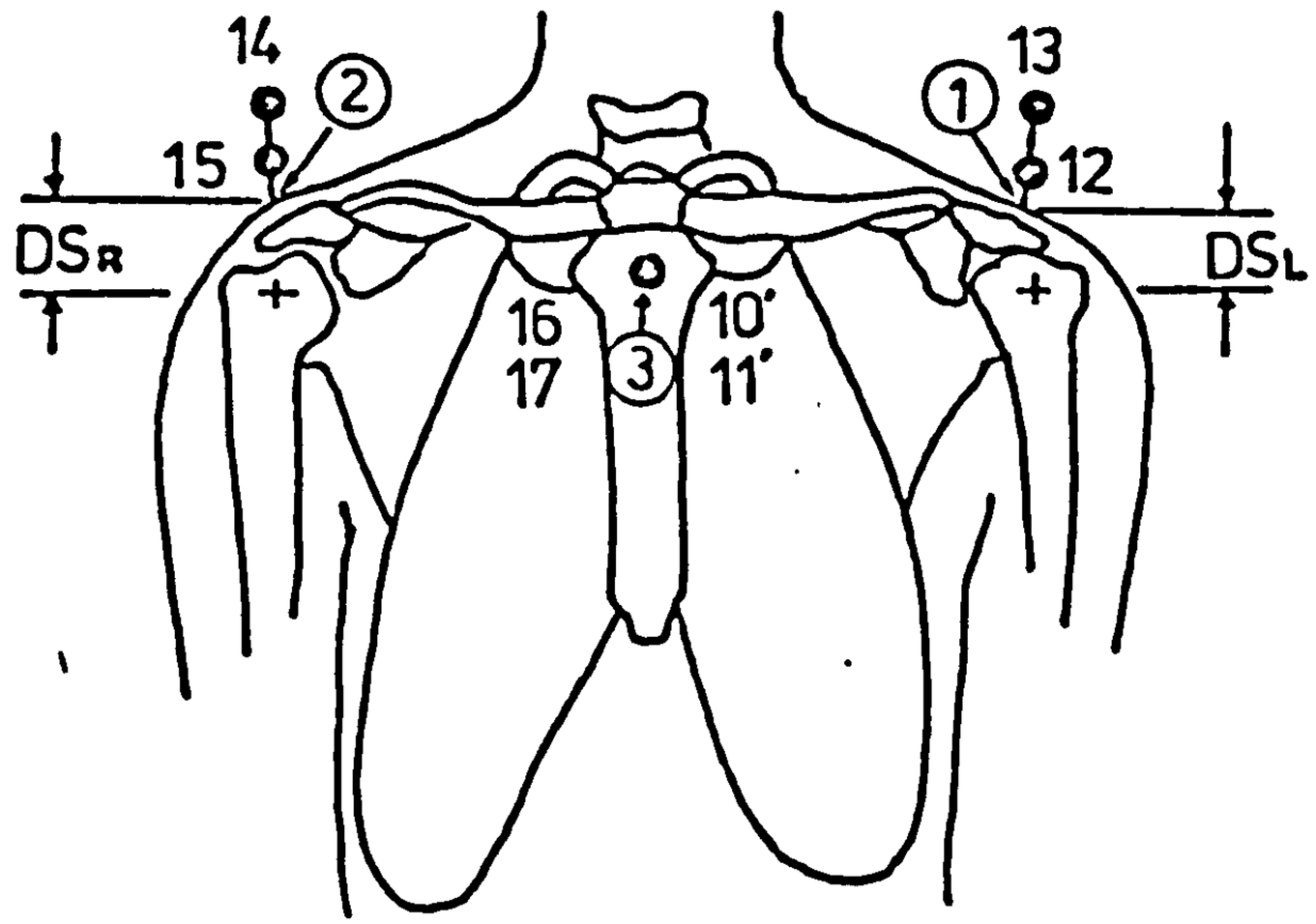

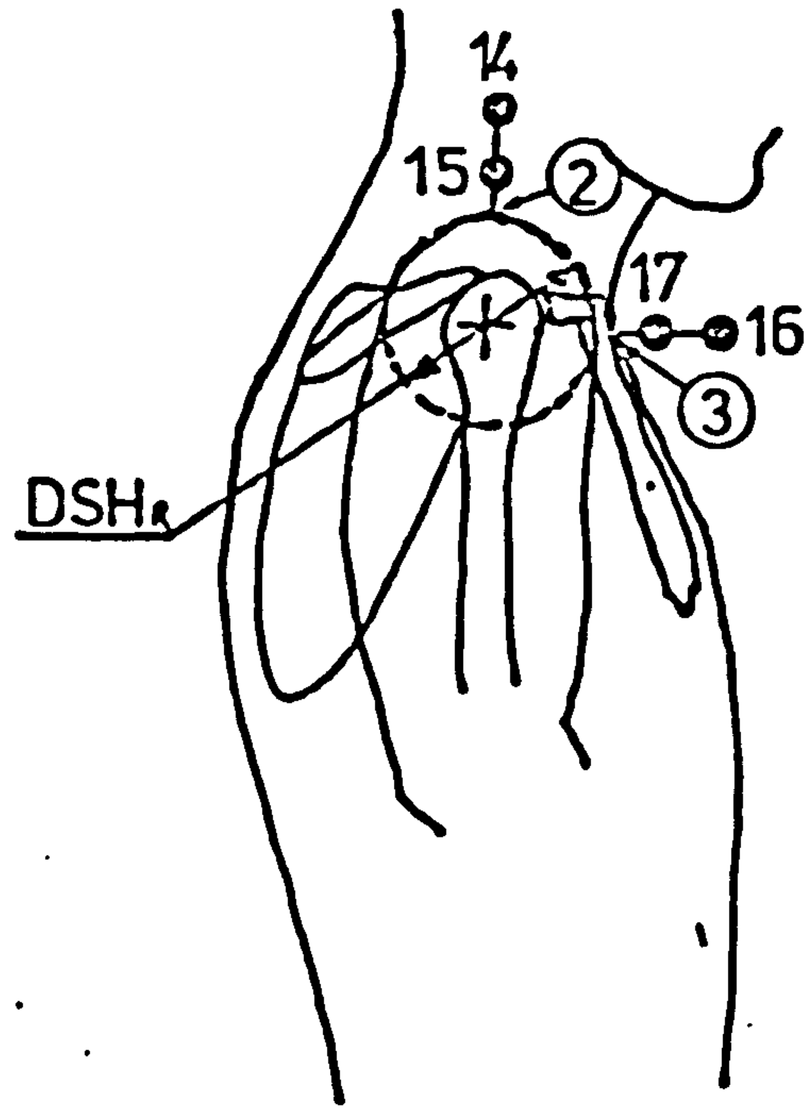

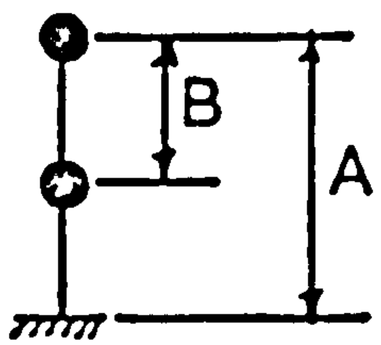

MARKER RATIO , $r_S = [A/B]$

Figure 6.3.5. Shoulder markers

Thus, the direction cosine matrix of the thigh is

$$[B_T] = \begin{bmatrix} \bar{e}_x \\ \bar{e}_y \\ \bar{e}_z \end{bmatrix}$$

6.3.5. Shoulder

Markers are positioned as shown in Figure 6.3.5. Two sets of sternum markers are obtained from the measuring system. They are averaged out as follows :

$$\bar{R}_{10} = (\bar{R}_{10'} + \bar{R}_{16})/2$$
$$\bar{R}_{11} = (\bar{R}_{11'} + \bar{R}_{17})/2$$

Position (1), (2) and (3) are determined by extrapolation,

$$\bar{R}_1 = [\bar{R}_{13} - (\bar{R}_{13} - \bar{R}_{12})*r_S]$$
$$\bar{R}_2 = [\bar{R}_{14} - (\bar{R}_{14} - \bar{R}_{15})*r_S]$$
$$\bar{R}_3 = [\bar{R}_{10} - (\bar{R}_{10} - \bar{R}_{11})*r_S]$$

where r_S is the ratio of the length between markers (see Figure 6.3.5).

A mid-position between (1) and (2) is defined,

$$\bar{R}_4 = (\bar{R}_2 + \bar{R}_1)/2$$

It can be assumed that there is no rotation about the z-axis and that the mid-position is at the same level as point (3) i.e.

$$R_4(y) = R_3(y)$$

The orientation of the shoulder in space can be

determined as follows :

$$\bar{e}_z = (\bar{R}_2 - \bar{R}_1)/ABS(\bar{R}_2 - \bar{R}_1)$$
$$\bar{e}_x = (\bar{R}_3 - \bar{R}_4)/ABS(\bar{R}_3 - \bar{R}_4)$$
$$\bar{e}_y = (\bar{e}_z * \bar{e}_x)$$

Thus, the D.C. matrix of the shoulder is

$$[B_{SH}] = \begin{bmatrix} \bar{e}_x \\ \bar{e}_y \\ \bar{e}_z \end{bmatrix}$$

The shoulder can be approximated as being circular from the lateral view, (Nicol, 1977),see Figure 6.3.5., therefore the shoulder joint centres can be calculated as follows :

$$\bar{R}_{LS} = \bar{R}_1 - (\bar{e}_y * D_{SL})$$
$$\bar{R}_{RS} = \bar{R}_2 - (\bar{e}_y * D_{SR})$$

where D_{SL}, D_{SR} are half the left and right Anterior/ Posterior width of the shoulder respectively.

6.4. Kinematic Analysis

Felkel (1951) evaluated three methods of determing acceleration from displacement-time data and concluded that the grapho-numerical technique was the best, with an estimated error of 20%. This procedure is however tedious and time-consuming. With the advent of high speed, large core computers, numerical techniques have become very popular in biomechanical analysis.

Paul (1967) evaluated the performance of a numerical technique described by Lanczos (1959). In this method a quadratic curve is fitted to 'n' number of points using

least squares. Comparisons were made between n=3, 5, 7 and 9 point double differentiation equations. The conclusion was that the 7 and 9 point equations tend to over-damp, while the 3 and 5 point equations introduced a large amount of noise. Note that this technique incorporated a 'smoothing' function in the equation.

Plagenhoef (1968) used a Chebyshev least squares polynomial curve fitting technique presented by Kuo(1965) to smooth the displacement data before applying the polynomial differentiation to determine the acceleration. Winter et al (1974) introduced a 2nd order Butterworth digital filter with a first order difference differentiation technique. Tooth (1976) used a similar technique, a 4th order Butterworth digital filter presented by Andrews (1975) and a Newtonian numerical differentiator described by Dorn and McCracken (1972). Zernicke et al (1976) suggested fitting biomechanical data with cubic spline functions and differentiating the function for the derivatives.

Pezzack et al (1977) compared film generated acceleration curves with the analogue signal (obtained from an accelerometer) of a single segment movement. Three techniques were considered, (a) a second order finite difference equation cited by Miller and Nelson (1973) (b) Chebyshev least squares polynomials followed by differentiation and (c) the second order recursive Butterworth digital filter followed by first order finite difference differentiation. They concluded that digital filtering combined with a first order finite difference technique produced acceleration data very closely approximating the analogue signals. Soudan and Dierckx (1979) using raw displacement data from Pezzack et al (1977), computed acceleration data while using spline functions. They reported that similar accuracy can be obtained to that of the digital filtering/finite

difference technique. This author also used the same raw displacement data from Pezzack et al (1977) to test the Lanczos 5-point differentiator used by Paul (1967) and also the digital filtering (with different cut-off frequency)/Newtonian differentiator used by Tooth (1976). The Lanczos 5-point differentiator and digital filtering (5Hz cut-off frequency)/Newtonian differentiator, both overdamp the data in its 2nd derivatives, Digital filtering (8Hz cut-off frequency)/Newtonian differentiator method gave similar accuracy to that obtained by Pezzack et al (1977) and Soudan and Dierckz (1979).

It can be concluded that both the digital filtering coupled with an appropriate differentiator and the spline function techniques are both acceptable and reliable to be used in determining the derivatives of human motion data. However, care should be taken in choosing the right cut-off frequency for the digital filter and an appropriate smoothing factor for the spline function is required. Another problem associated with both methods is the end point conditions. For the spline function technique, the derivative has zero value endpoints, so unless endpoint conditions are known, this can present serious errors. For the digital filtering/finite difference differentiator method, the endpoints of the derivative are erroneous. One solution for this method is to have dummy values at endpoints and discard them after processing.

6.4.1. Numerical Differentiator

As discussed in Section 6.2.4, all the data used in this project are filtered by a 4th order Butterworth digital filter. The differentiator used is the one cited in Dorn and McCracken (1972) and used by Tooth(1976). The equation is as follows :

$$f'(X_o) = \frac{1}{12h}\left[f(X_o-2h) - 8f(X_o-h) + 8f(X_o+h) - f(X_o+2h)\right] \quad \ldots\ (4.1)$$

where h is the interval between points(which must be greater than zero)

X_o is the point under consideration.

The linear velocities of the joint centres in the three planes can be calculated by using equation (4.1) on the displacement data. As for the linear accelerations of the joint centres, the equation (4.1) is used on the calculated linear velocities.

The angular velocities and accelerations of the body segments can be calculated as follows :

Transformation between a fixed system (S_F) and a moving system (S_M) can be represented by

$$\bar{S}_F = [B].\bar{S}_M \quad \ldots\ (4.2)$$

where $[B]$ is the direction cosine matrix.

Let P be a fixed point in the S_M system. When the S_M system moves(rotates and translates with respect to the fixed system S_F, the velocity of point P relative to fixed system is

$$\dot{\bar{S}}_F = [\dot{B}].\bar{S}_M \quad \ldots\ (4.3)$$

It is assumed that the moving system is kinematically rigid and that the coordinates of P in the moving system remain constant. Equation (4.2) can be rewritten as :

$$\bar{S}_M = [B]^{-1}.\bar{S}_F \quad \ldots\ (4.4)$$

Substituting equation (4.4) into (4.3), we have

$$\bar{S}_F = [\dot{B}][B]^{-1}.\bar{S}_F \quad \ldots\ldots (4.5)$$

Now, expression $[\dot{B}][B]^{-1}$ is known as the angular velocity matrix of the moving system relative to the fixed system and is always a skew symmetric matrix. See Pipes (1963). Hence,

$$[\dot{B}][B]^{-1} = \begin{bmatrix} 0 & -W_{zF} & W_{yF} \\ W_{zF} & 0 & -W_{xF} \\ -W_{yF} & W_{xF} & 0 \end{bmatrix}$$

where W_{xF}, W_{yF} and W_{zF} are the absolute angular velocities of the moving system with respect to the fixed system. Note that, the first derivative of the D.C. Matrix is obtained by using equation (4.1). Therefore,

$$\bar{W}_F = \begin{bmatrix} W_{xF} \\ W_{yF} \\ W_{zF} \end{bmatrix}$$

To relate it back to the moving system, the transpose D.C. matrix is used,

$$\bar{W}_M = [B]^{-1}.\bar{W}_F$$

The angular acceleration relative to the moving system, is obtained by applying the numerical differentiator, equation (4.1), to the angular velocities, thus

$$\bar{W}_M = \bar{\alpha}_M = \begin{bmatrix} \alpha_{xM} \\ \alpha_{yM} \\ \alpha_{zM} \end{bmatrix}$$

Direction Correction Factors :

(Force action on body)

FP1	$-_{*}Fx$	$+_{*}Fy$	$+_{*}Fz$	$-_{*}Mx$	$+_{*}My$	$+_{*}Mz$
FP2	$+_{*}Fx$	$+_{*}Fy$	$-_{*}Fz$	$+_{*}Mx$	$+_{*}My$	$-_{*}Mz$

Charge Amplifiers

(for both force plates)

Top Amp.	Fx		Fz		My	
Bottom Amp.		Fy		Mx		Mz

Buffer Amplifier Settings

(for both force plates)

Fx	Fy	Fz	Mx	My	Mz
1	1	2	1.25	2	1.25

Table 6.5.1(a) Force Plate Calibration Information

6.5. Force Plate Data

The analogue signals of the ground reactions obtained from the force plates are converted into digital form by the PDP12 computer. These digital data are however in "PDP12 Computer" units, which have to be calibrated and scaled to the real mechanical values. With the knowledge of these ground reactions, the centre of pressure can be calculated and force vectors can be produced.

6.5.1. Calibration

The scaling factors required depend on the values of the setting of both the charge and buffer amplifiers. Referring to Section 5.3.1, the top charge amplifiers are used to set up suitable limits for Fx, Fz and My channels, while the bottom amplifiers are for Fy, Mx and Mz, see Table 6.5.1(a).

The sign convention adopted in this analysis is taken from the CPRD task force's recommendation in "Standardization of gait analysis parameters and data-reduction technique" (1975). Therefore, the direction of the forces and moments has to be corrected for consistency. For forces acting on the body, the correct direction factors are presented in Table 6.5.1(a). These are to be included in the scaling factors.

Therefore, the force plate data are calibrated as follow :

$$\text{Forces (in Newtons)} = S_F * \text{Forces (in "PDP units)}$$

$$\text{where } S_F = \frac{\text{Charge}}{\text{Buffer}} * \frac{1}{51.2} * \text{SIGN}$$

$$\text{Moments (in Newton-Metre)} = S_M * \text{Moments (in "PDP" Units)}$$

Buffer Settings	Amp. Settings	Scaling factors for Forces (S_F)	Scaling factors for Moments(S_M)
1	1:10	0.1953	0.0516
	2:10	0.3906	0.1031
	5:10	0.9766	0.2578
	$1:10^2$	1.9531	0.5156
	$2:10^2$	3.9063	1.0313
	$5:10^2$	3.9063	1.0313
	$1:10^3$	19.5313	5.1563
1.25	1:10	0.1563	0.0413
	2:10	0.3125	0.0825
	5:10	0.7813	0.2063
	$1:10^2$	1.5626	0.4125
	$2:10^2$	3.1250	0.8250
	$5:10^2$	7.8125	2.0625
	$1:10^3$	15.6250	4.1250
2	1:10	0.0977	0.0257
	2:10	0.1953	0.0516
	5:10	0.4883	0.1289
	$1:10^2$	0.9766	0.2578
	$2:10^2$	1.9531	0.5156
	$5:10^2$	4.8828	1.2890
	$1:10^3$	9.7656	2.5781

Table 6.5.1(b) Scaling Factors for Forces and Moments

Where $S_F = \frac{Charge}{Buffer} * \frac{0.264}{51.2} * SIGN$

Charge - Charge amplifier settings(Mechanical Units/V)
Buffer - Buffer Amplifier Settings(V/V)
SIGN - Direction Correction Factor

The full range of calculated scaling factors (S_F and S_M)derived from various combinations of charge and buffer amplifier settings are presented in Table 6.5.1(b). Note that, the direction correction factors are not included.

6.5.2. Centre of Pressure

The centre of pressure is an effective point where the resultant instantaneous force vector is applied. The coordinates of this position can be determined from the forces and moments recorded by the force plates. These coordinates are calculated relative to the origin of the force plate. They are as follows, (referring to Figure 6.5.2) :

At time (t),

$$X(t) = \frac{Mz(t) + Y * Fx(t)}{Fy(t)}$$

$$Z(t) = \frac{Y * Fz(t) - Mx(t)}{Fy(t)}$$

where $Y = 0.04\ m$ - this is the distance from the origin of the force plate to the ground where the load is being applied.

The centre of pressure through the stance phase can be plotted from the coordinates calculated. This will firstly demonstrate the progression of the force vector during the stance phase; secondly,it will show the

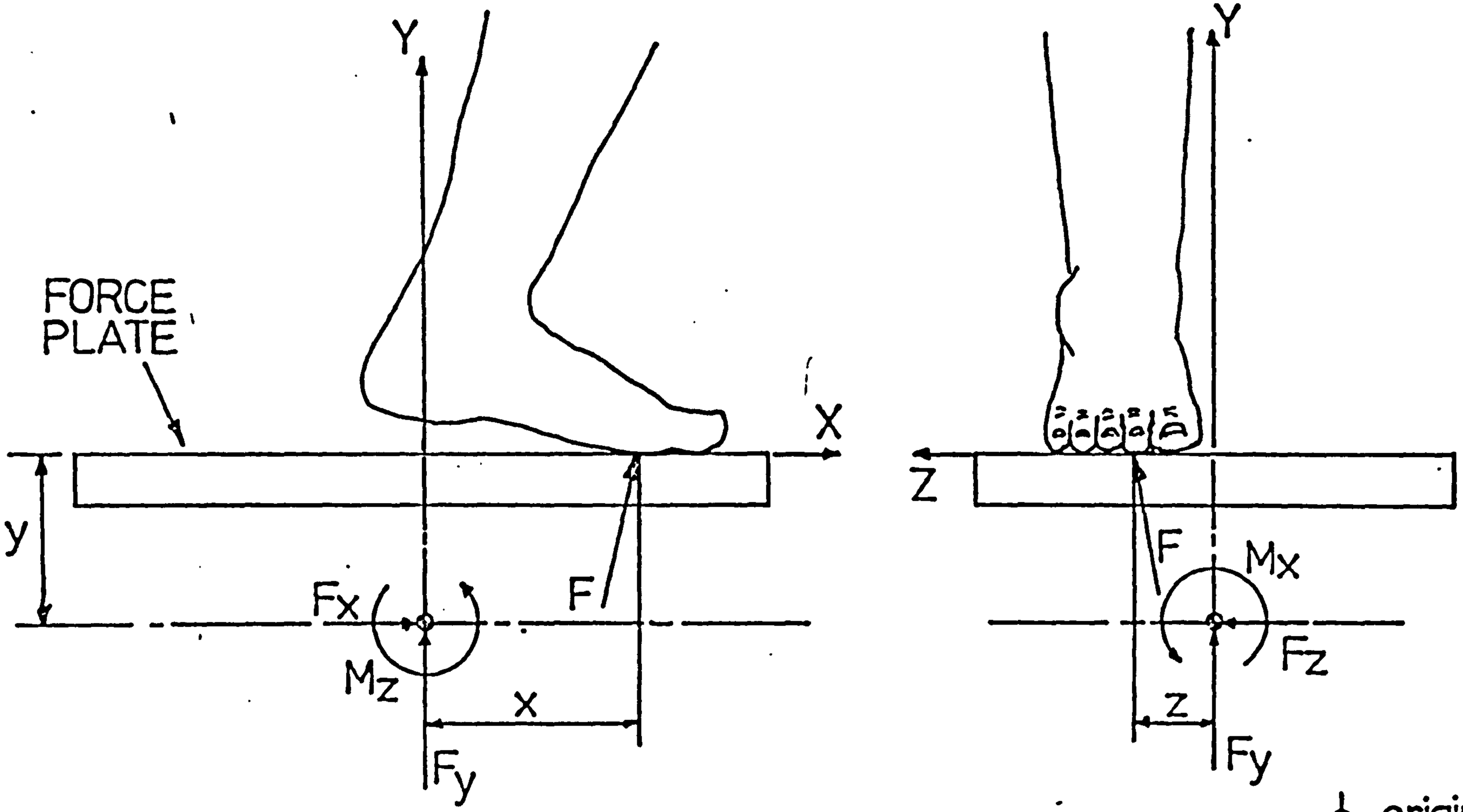

Figure 6.5.2 Diagrammatic representation of variables recorded by the force plate

relative loading of the foot and thirdly,the duration of loading over each area.

Centre of pressure can also be plotted against time to display different aspects of the data. The X-coordinate versus time plot is a straightforward one, which does not require any mathematical manipulation. The Z-coordinate versus time plot, requires the calculation of the mean of the Z-coordinates,

$$Z_{mean} = \sum_{t=1}^{n} Z(t)/n$$

Where n is the total number of points in the stance place.

Then referring all Z-coordinates to this mean, we have,

$$Z'(t) = Z(t) - Z_{mean}$$

Thus plotting $Z'(t)$ against time would describe the movement of the centre of pressure in the Z-coordinate.

The centre of pressure displacement versus time plot was developed to give a graphical representation which is independent of walking direction. The displacement coordinates are defined as follows :

$$D(t) = \sqrt{(X(t) - X_{ref})^2 + (Z(t) - Z_{ref})^2}$$

where X_{ref} is the first X-coordinate that exceeds the mean of the X-coordinate values, and

Z_{ref} is the corresponding Z-coordinate.

X_{ref} and Z_{ref} represent the reference point of the displacement calculation because the end points of the centre of pressure trace (i.e. heel strike and toe off) represent a transition period of high variability.

6.5.3. Force Vectors

Generation of these data would provide an overview of the ground reaction in simplistic graphical form. Superimposition of these data onto displacement data of the anatomical joint centres would give a better visual aid to kinetic analysis.

Force vector in the sagittal plane can be produced by Fx and Fy. The direction of the resultant is given as:

$$\theta_{xy} = \tan^{-1}\left[\frac{Fy}{Fx}\right]$$

and magnitude,

$$Fxy = \sqrt{Fy^2 + Fx^2}$$

Using information from the centre of pressure, particularly the X-coordinates, force vectors can then be plotted in the sagittal plane through the whole of stance phase. These sagittal plane force vectors have been demonstrated to be a useful tool in recognition of gait deviation, Boccardi et al (1976).

The transverse plane force vector can also be produced fairly easily from Fx and Fz. Again the direction of the force vector is given as :

$$\theta_{xz} = \tan^{-1}\left[\frac{Fx}{Fz}\right]$$

and the magnitude, $Fxz = \sqrt{Fx^2 + Fz^2}$

6.6 Kinetic Analysis

Ground reaction data can be related to the corresponding kinematic data to provide information that

allows definitive assessments. However, before any kinetic analysis can be made, anthropometric information of the body segments involved has to be determined. Hence, this section begins with the description of the methods used in determining the mass moment of inertia of the body segments. The calculation of the external loadings exerted on the joint centres of the lower limbs and the instantaneous energy levels of the body segments involved in ambulation is also presented.

6.6.1 Mass Moment of Inertia

The lower limb is divided into three segments; the thigh, which is defined as that section between the hip and knee joints; the shank, which is that section between the knee and ankle joints; and the foot.

The mass moment of inertia of the foot about its three principal axes has been shown to be very small and insignificant by Drillis and Contini (1966) and Chandler et al (1975). It has also been determined mathematically by Trnkoczy et al (1976) to be negligible. Therefore, in this analysis the mass moment of inertia of the foot will not be considered. However, it will be regarded together with the shank, because in locomotion the foot tends to move as a rigid body with the shank.

From the studies of Chandler et al (1975), it was clear that the values of the mass moment of inertia about the longitudinal axis were small. Hence it was decided that the effect of the inertial torque about the longitudinal axis in the analysis is to be ignored. The studies also showed that the mass moment of inertia about the Z-axis is approximately the same as that of the X-axis. Therefore, in this analysis, the two are assumed to be equal.

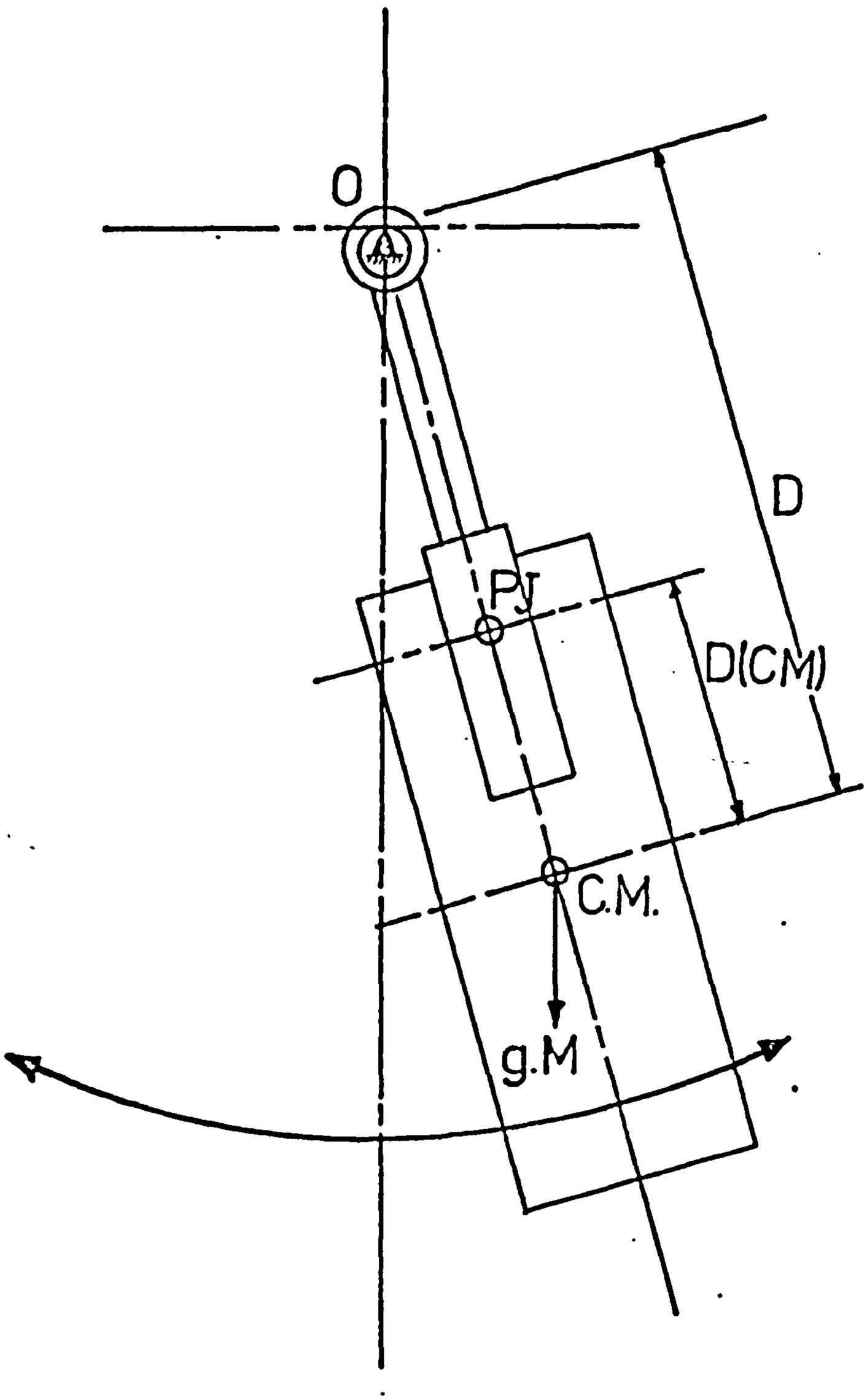

Figure 6.6.1 Compound pendulum Method of determining inertial effect of prosthesis

Two methods of derivation are used, since the one used for the normal limb cannot be applied to the prosthetic case.

a) Normal limb

The lower limb is regarded as two segments; (1) the thigh and (2) the shank and foot (which also includes the mass of the shoe).

Using the coefficients presented in Table 2.1, the following equation for the mass moment of inertia is adopted :

$$Mass\ of\ segment,\ Mseg_n = C_{1n} * Total\ Body\ Mass$$

where suffix "n" is used to denote the particular segment under consideration. Note also that for the shank/foot segment, $Mseg_s$ includes mass of shank, foot and shoe.

Distance from proximal joint to centre of mass (CM)

$$D(CM)_n = C_{2n} * Lseg_n$$

where $Lseg_n$ = Length of segment(n)

Radius of gyration, $R_n = C_{3n} * Lseg_n$

Hence, the mass moment of inertia about the proximal joint centre is

$$I(PJ) = Mseg_n(DC(CM)_n^2 + R_n^2)$$

b) Prosthetic Limb

The compound pendulum method of determining the mass moment of inertia was used (See Section 5.2.3. for details of method).

The equation used in the determination of the mass moment of inertia about the proximal joint is as follows:

$$I(PJ) = \frac{9.81 * Mass\ of\ Segment * D(CM) * T^2}{4\pi^2}$$

where $D(CM)$ = distance from proximal joint to centre of mass

T = period of oscillation (s)

Obviously, not all the limb can be easily suspended about its proximal joint, hence an alternative pivot must be used. However, this pivoting point must be rigidly connected to the segment.

Hence, referring to Figure 6.6.1, the mass moment of inertia about (O) is

$$I_o = \frac{9.81 * M * D * T^2}{4\pi^2}$$

where M= Total Mass of structure

D= Distance from pivot (O) to centre of mass

By using parallel axis theorem, the mass moment of inertia about the proximal joint can be calculated,

$$Icg = I_o - M * D^2$$

$$= I(PJ) - M*D(CM)^2$$

$$\therefore \quad I(PJ) = I_o - M(D^2 - D(CM)^2)$$

In both the cases (i.e. normal and prosthetic limbs) described above, the principal moments of inertia about the three axes are as follows :

$$Ixx = I(PJ)$$

$$Iyy = 0.0$$

$$Izz = I(PJ)$$

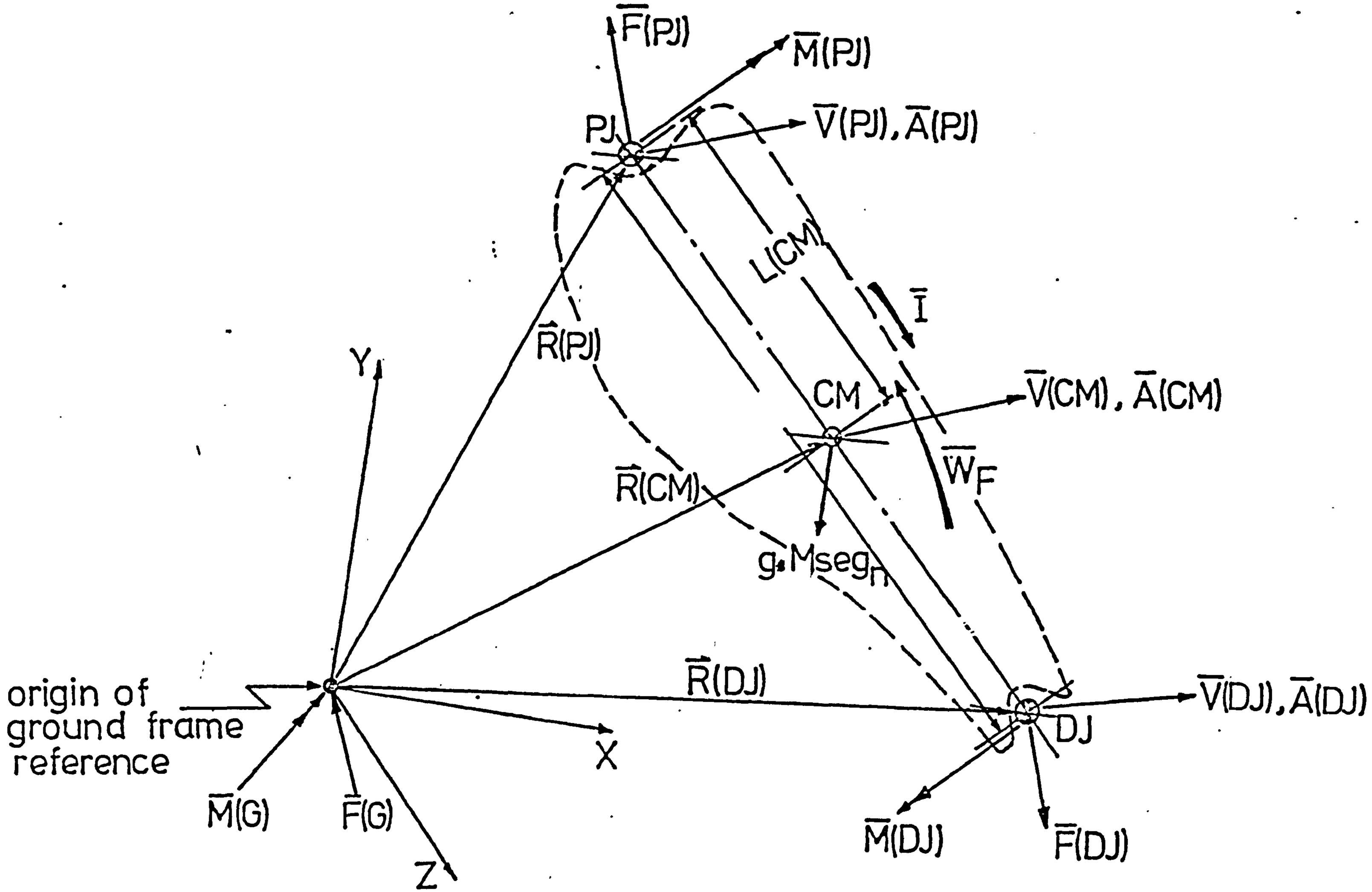

Figure 6.6.2. Resultant force and moment at proximal and distal joints of segment

6.6.2 Intersegmental Forces and Moments

Before any analysis can be performed, several assumptions have to be made :

1) Each segment is a rigid body
2) The location of the centre of mass remains fixed during locomotion
3) The mass moment of inertia of each segment is constant during locomotion.

The forces and moments recorded by the force plate are relative to the origin of the force plate frame of reference(FP). Referring them to the origin of the ground frame of reference (G), we have

$$\bar{F}(G) = \bar{F}(FP)$$
$$\bar{M}(G) = \bar{M}(FP) + \bar{D} * \bar{F}(FP)$$

where $\bar{D}$ is the vector relating the centre of the force plate to the origin of the ground frame of reference.

The following then, is a general solution for calculating the nett loads at the proximal joint :

Referring to Figure 6.6.2, the radius vector and linear acceleration of the centre of mass can be determined as follows :

$$\bar{R}(CM) = \bar{R}(DJ)*(1-L(CM)/L) + (L(CM)/L)*\bar{R}(PJ)$$
$$\bar{A}(CM) = \bar{A}(DJ)*(1-L(CM)/L) + (L(CM)/L)*\bar{A}(PJ)$$

The gravitational forces acting at the centre of mass are :

$$F(CM)_x = 0.0$$

$$F(CM)_y = g*Mseg_n$$

$$F(CM)_z = 0.0$$

Where, $g = 9.81\ m/s^2$

Therefore, the nett force acting at the proximal joint,

$$\bar{F}(PJ) = \left[\bar{F}(G) - \bar{F}(CM) - (Mseg_n * \bar{A}(CM)) \right]$$

The nett moment acting at the proximal joint, constitutes the following :

a) The rate of change of angular momentum, derived from the inertia effects :

Angular momentum,

$$\bar{H} = [I] * \bar{W}_M$$

Where $\bar{W}_M$ is the angular velocity vector

$[I]$ is the inertia matrix

which is $= \begin{bmatrix} Ixx & 0 & 0 \\ 0 & Iyy & 0 \\ 0 & 0 & Izz \end{bmatrix}$

Hence, the rate of change of angular momentum, relative to the moving system is given as :

$$\left[\frac{d\bar{H}}{dt} \right]_M = \begin{bmatrix} Ixx*\alpha xM - (Iyy-Izz)WyM*WzM \\ Iyy*\alpha yM - (Izz-Ixx)WzM*WxM \\ Izz*\alpha zM - (Ixx-Iyy)WxM*WyM \end{bmatrix}$$

Reference to this Euler's equation of motion, see Harrison (1978).

Referring these values to the fixed system, the

direction cosine matrix is used :

$$\left[\frac{d\bar{H}}{dt}\right]_F = [B] * \left[\frac{d\bar{H}}{dt}\right]_4$$

b) Moment due to gravitational and accelerational loads acting at the centre of mass, .

$$\bar{M}(CM) = (\bar{R}(CM) - \bar{R}(PJ)) * (Mseg_n * \bar{A}(CM) + \bar{F}(CM))$$

c) Moment due to external loads,

$$\bar{M}(EXT) = [(-\bar{R}(PJ)) * \bar{F}(G)] + \bar{M}(G)$$

Therefore, the nett moment acting at the proximal joint is,

$$\bar{M}(PJ) = \left\{\bar{M}(EXT) - \bar{M}(CM) - \left[\frac{d\bar{H}}{dt}\right]_F\right\}$$

6.6.3. Instantaneous Energy Levels

The instantaneous energy levels of each segment consist of the following :

a) The potential energy,

$$P.E. = g * Mseg_n * H(CM)$$

Where $H(CM)$ is the height of the segment (n) measured from the centre of mass (CM) to the ground.

b) The translational kinetic energy,

$$K.E._(T) = \frac{1}{2} * Mseg_n * \bar{V}(CM)_F^2$$

Where $V(CM)_F$ is the linear velocity vector of the centre of mass relative to the fixed axes system.

c) The rational kinetic energy,

$$K.E.(R) = \frac{1}{2} \cdot I \cdot \dot{W}_F^2$$

Therefore, the total instantaneous energy levels of the segment is :

$$E(TOT) = P.E. + K.E.(T) + K.E.(R)$$

The instantaneous energy levels of the whole leg can be determined by summing the energy levels of each segment.

The sum of the absolute energy changes over the time period yields the work done by the segment (or the whole leg) :

$$WD = \sum_{J=1}^{JMAX} |\Delta E(TOT)|$$

Where $JMAX$ is the total cycle.

CHAPTER 7

Results and Discussions

7.1. Discussion on Experimental Accuracy

It is recognised that in any comparative studies, the apparent differences in the results obtained should be representative of the true situation rather than the variation of errors inherent in the data acquisition processes.

Generally, the sources of errors can be categorised as systemic errors and random errors. Systemic errors are inherent in the measuring instrumentation and the analytical procedure. These errors are fairly consistent between tests, provided that they are performed under the same conditions. Therefore, the effects of this type of error on the differential results between tests should be minimal. However, the influence of systemic errors can be taken into account by estimating their magnitudes. Random errors on the other hand are more damaging and could invalidate data used in comparative studies. This type of error could be reduced by applying an appropriate digital filtering procedure to the data and also by averaging repeated results of the same test. Although these procedures do run the risk of concealing significant variations, extreme care can be taken to avoid this drawback.

The following sections will describe in detail the accuracy of the instruments and analytical procedure adopted in the project.

7.1.1. Force Plates System

The Kistler force plate is claimed to have an accuracy of $\pm 2\%$, if load is applied within the boundary of 400mm x 264mm on the force plate surface. Both the Kistler force plates used were calibrated by applying static loads on the plates in the three orthogonal

directions within the specified boundary. It was found that the results obtained for the three orthogonal forces were linear over the ranges considered. The overall accuracy was about ±3%. This value also takes into account the errors introduced through amplification and the analogue to digital conversion of the data. The resolution of the system is dependent on the settings of the transducer sensitivity range and also the range of the amplification. Cross-sensitivity between channels is claimed by the manufacturer to be about ±1.5%.

The dynamic frequency response of the force plate was claimed by the manufacturer to be 200 Hz minimal in the three orthogonal directions. This was checked by tapping the force plate with a small hammer, and by using an accelerometer and a spectral analyser, the dynamic impulse response was recorded. Table 7.1.1(a) shows the natural frequencies of both force plates in the three orthogonal directions. The value recorded for the vertical direction for force plate FP1 was 36% lower than that claimed by the manufacturer. The vertical and lateral directions for FP2 were about 10% lower.

Tests were also carried out with 70 kg dead weight on the surface of the force plates. The dynamic frequency response in the vertical direction, as expected, was reduced by approximately 35%. However, when a subject of 67 kg mass stood on the force plates, the dynamic frequency response increased by approximately 15%, and when the same subject walked over the force plates in the progressive direction, the dynamic frequency response was similar to the unloaded situation. Paul (1967) explained that although additional mass is added to the force plate as the subject steps onto it , the connection involves the joints of the body whose elastic stiffness depends on muscular tension and can therefore be regarded as negligibly small. This however still does

DIRECTION RECORDED	FORCE PLATE	
	FP1	FP2
X	351.9Hz	212.5Hz
Y	128.0Hz	185.0Hz
Z	232.5Hz	172.5Hz

Table 7.1.1(a) Natural frequencies of force plates in unloaded condition

not explain the increase in the frequency response when the subject is stationary on the force plate. The mechanics of this phenomenon are unclear and require further investigation .

Nevertheless, the force plates used are capable of picking up all the relevant signals during the walking event, since the maximum frequency, which occurs at heel strike is only 75 Hz (Simon et al 1981). The remainder of the force trace had been reported to have frequency components of 1 - 10 Hz.

7.1.2. Displacement Recording and Digitising Systems

The cine-photography technique is very susceptible to errors, these being due to the high degree of human intervention in the procedure. However, certain measures can be taken to minimise these errors.

Having personnel with good anatomical knowledge could avoid errors caused by misplacement of markers. However, errors caused by the relative movement between the skin marker and the underlying bony structure during locomotion would still be present. To determine the exact value of this type of error requires some kind of radiographic technique which is beyond the scope of this project. Nevertheless, the careful selection of bony anatomical landmarks, not covered by muscles, for the attachment of markers, would minimise the error. Body measurements taken may be another source of error, especially when measuring distances between two marker beads centres. A maximum error of 10mm can occur with marker beads of 10mm diameter, although only an estimated error of $\pm$2.5mm is expected.

It was suspected that when the cameras were running a small amount of rotational oscillations of the shutter

disc assembly took place. To check for its effects, the rotating shutter was exposed to stroboscopic flashes at the same frequency. All the cameras ran up to their working speed in within fractions of a second. The left and right cameras were observed to be fluctuating out of phase at an approximate range of 5 degrees, while the front camera at about 2 degrees. The magnitude of these errors is small and relatively insignificant when considering errors due to synchronisation of films. Films from the front and side cameras could be, at the worst,one frame out of phase, i.e. 20 ms. This was found to produce an error of 20mm in the direction of progression at the hip joint during level walking. The technique used in estimating the phase lag timing was capable of reducing the error by 75%. Furthermore, it was observed that the average phase lag time was about 10ms, therefore an error of 2.5mm can be estimated.

The digitiser used, trade-named DMAC, has a resolution of 0.1mm and its accuracy was found to be $\pm$0.1%. This was done by comparing the measured distance between two physical points on the DMAC table and the calculated distance was obtained by digitising the two points. In digitising a projected marker image, an error of up to 5mm can occur due to the misalignment of the cursor over the 10mm diameter marker centre. However, an error of approximately 2.0mm was found by digitising the marker image repeatedly. Another source of error in the digitising system is the distortion of the projected image; this could come from the camera and projector lenses, a distorted mirror and film distortion. None of these items can be checked individually.

The recording and digitising systems were also checked for their overall accuracy. A three-dimensional spatial calibration frame, with the same size of marker beads as those used in the project, was filmed by all the

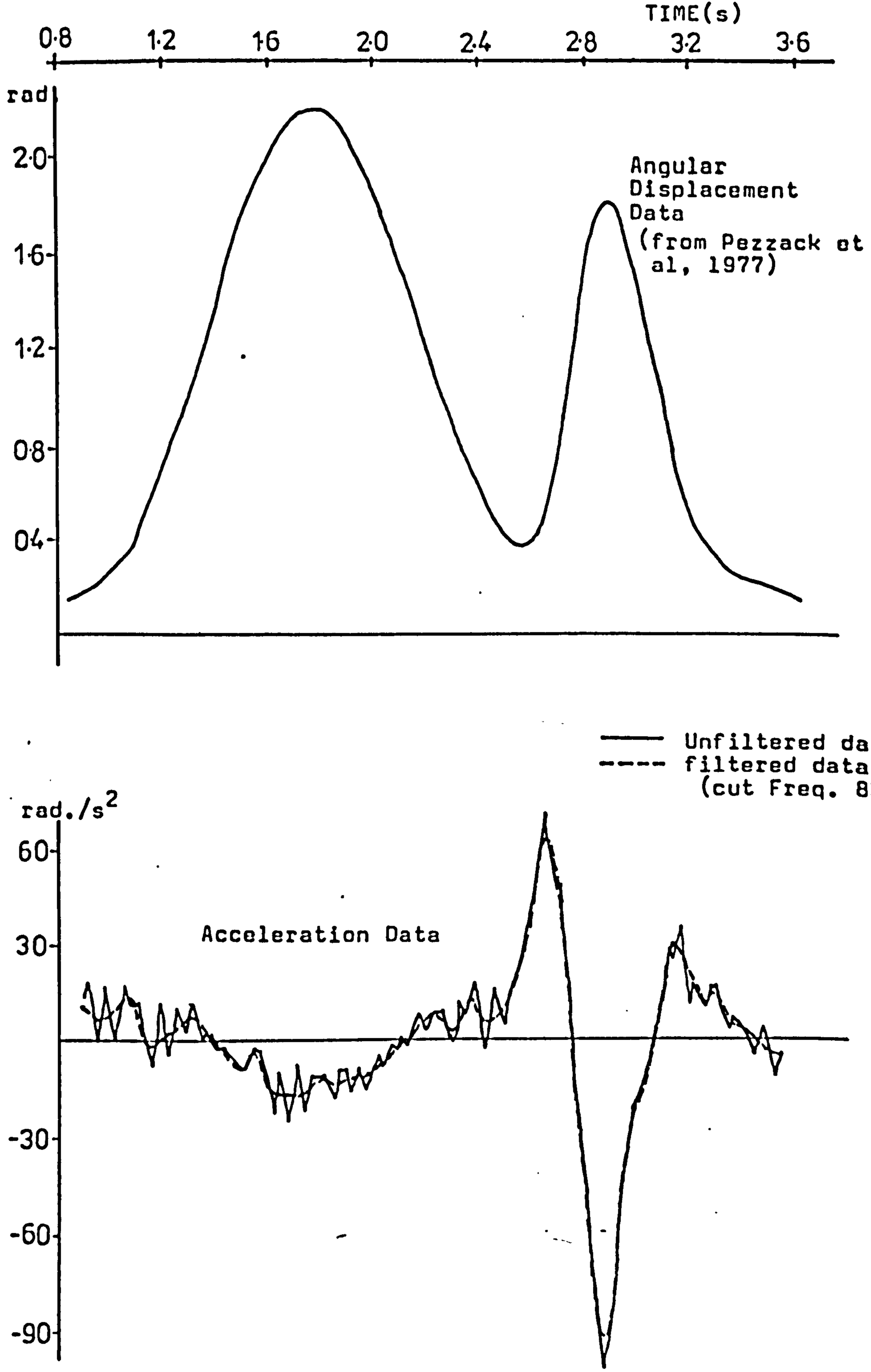

Figure 7.1.3(a) Comparison between the second derivatives of unfiltered and filtered displacement data

three cine-cameras simultaneously. The films were digitised and the "raw" data were processed by programs "COORDINATES" and "PARALLAX", the results of which were compared with the actual measured coordinates of the markers. An accuracy of approximately ±1.5% was found. It is recognised that the phase differences error is not included in the examination, since the calibration frame was stationary when being filmed. Moreover, the relative marker/skin movement during locomotion is also not considered. However, it does give an indication of the possible amount of error generated during the stance phase, where relative marker/skin movement is considerably small and phase differences do not have such a great effect.

7.1.3. Data Processing

The data smoothing process was found to have removed noise in a random fashion; it was observed that the process did not distort the data. The maximum amount of noise removed was 5mm. The digital filter and the numerical differentiator were also tested by applying them to a set of displacement data with known analogue acceleration, Pezzack et al (1977). However, this set of displacement data was contaminated with pseudo-random white noise (Gaussian distribution, standard deviation 0.006 rad) as suggested by Lanshammar (1982) before being employed for the test. Figure 7.1.3(a) shows the computed acceleration of filtered (8 Hz) data in comparison with the acceleration of unfiltered data. The results indicated that the procedure used is good enough to eliminate most of the random errors introduced.

Another source of errors in data processing can be in the assumptions made in the analysis. The assumption that no rotation of the shoulder in the sagittal plane took place, was shown to be reasonably acceptable, since only a very small amount was

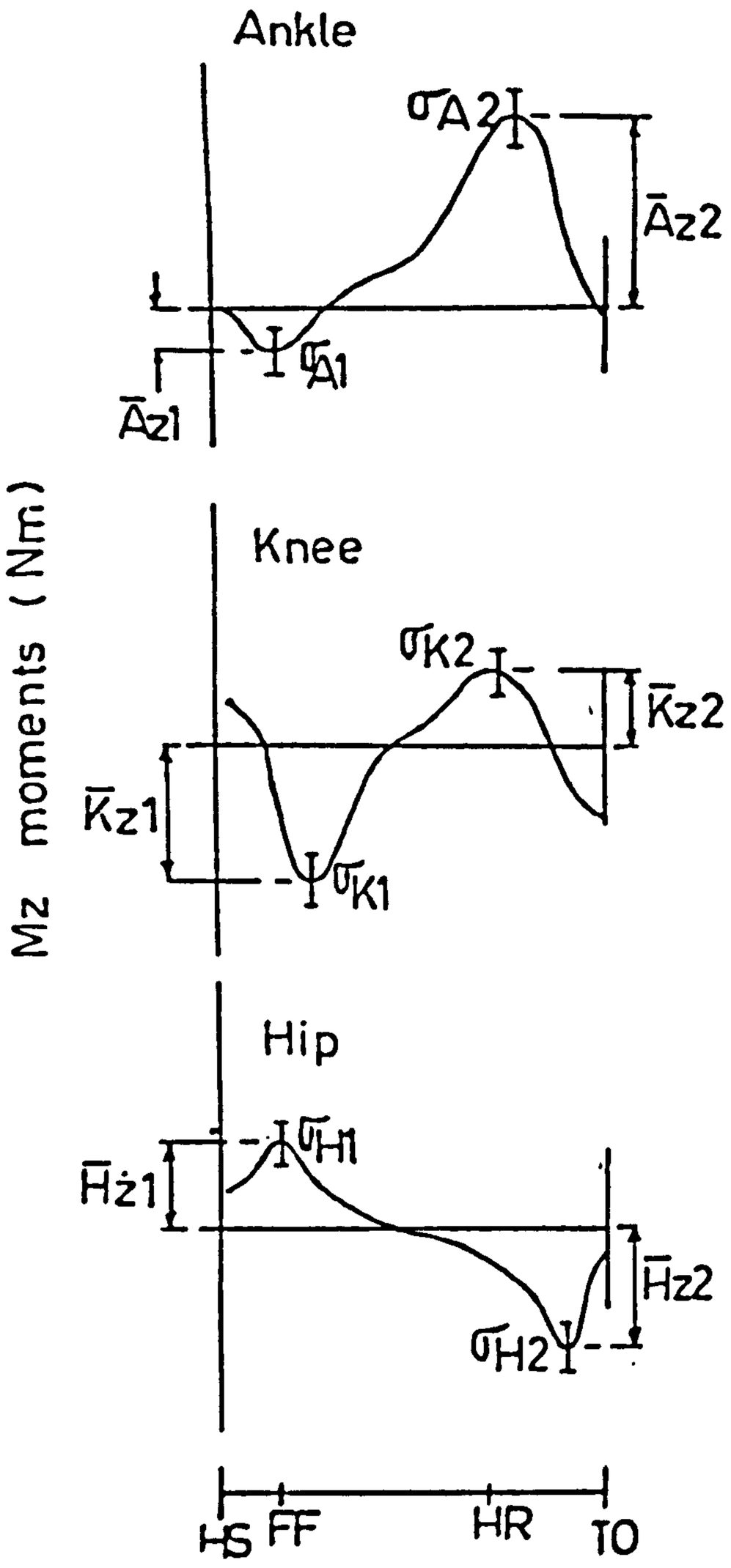

	Ankle		Knee		Hip	
	Āz1 (σA1)	Āz2 (σA2)	K̄z1 (σK1)	K̄z2 (σK2)	H̄z1 (σH1)	H̄z2 (σH2)
Normal(NSØØ1)						
-Left leg	-16.9 (2.7)	123.2 (3.5)	-44.1 (5.7)	45.9 (8.4)	89.4 (8.5)	-69.2 (7.2)
-Right leg	-17.3 (3.6)	100.1 (5.7)	-58.5 (11.3	37.0 (6.4)	78.4 (11.7)	-67.7 (5.8)
Above-knee(ARØØ1)						
SACH -Sound	-20.0 (4.5)	135.7 (4.5)	-36.3 (5.6)	61.3 (12.3)	165.7 (21.7)	-38.1 (5.9)
-Prosthetic	-32.9 (3.4)	78.8 (1.4)	0.9 (2.0)	34.4 (1.0)	5,.0 (8.7)	-59.1 (4.4)
Uniaxial-Sound	-19.9 (4.2)	138.4 (4.3)	-28.5 (12.5)	73.9 (7.6)	169.2 (21.4)	-26.7 (4.8)
-Prosthetic	-49.7 (9.0)	77.2 (1.0)	1.0 (1.9)	38.5 (3.1)	60.0 (14.6)	-58.2 (7.4)

Figure 7.1.4(a) Repeatability of Mz-Moments

observed from the displacement data. The main errors in kinetic calculation, besides the assumption made with regard to mass distribution in limb segments, were the inaccuracies in the body segment parameters used.

7.1.4. Repeatability

Table 7.1.4(a) shows the average maximum and minimum values of the Mz moments of the normal subject (NSØØ1) and the above-knee amputee (ARØØ1) during level walking. These average values were obtained from seven test walks performed under the same conditions.

The range of scatter in the variables recorded for the normal subject is similar to that of the above-knee amputee. For example, taking ±2 standard deviations, (viz 95% confidence level), the range of scatter is on average ±36% from the mean of the ankle plantar-flexion moment at early stance for both the normal subject and the above-knee amputee.

The range of scatter varies in magnitude when considering joint moments at different levels, and also, smaller moment values tend to have a greater range of scatter than larger moment values. At the ankle joint, the minimum Mz values has a greater range of scatter (±36% of the mean) than that of the maximum Mz values, i.e. ±6% of the mean. Although the maximum hip Mz moment, has approximately the same magnitude as the maximum ankle Mz moments, the scatter range is greater, i.e. ±25% of the mean.

Due to the high percentage of scatter, it is essential to check if comparison made between two values is significant. To do this the method of the standard error of difference is used. For example, the minimum ankle Mz moments of the above-knee amputee on the prosthetic

Patient Code	Mass (kg)	Size of Prosthetic foot	SACH foot		Uniaxial foot	
			Heel Compressibility	Heel Height (mm)	Plantar bumper stiffness	Heel Height (mm)
BRØØ2	64.0	26	medium	18	D42/3	25
BRØØ3	63.6	26	medium	18	D42/3	25
BRØØ4	70.0	27	medium	18	D42/3	25
BRØØ5	100.0	28	firm	18	D42/6	25
BRØØ7	75.8	28	medium	18	D42/4	25
BLØ12	74.6	27	medium	18	D42/4	25

Table 7.2(a) Selection of heel stiffness for Below-knee Amputee

Patient Code	Mass (kg)	Size of Prosthetic feet	SACH foot		Uniaxial foot	
			Heel Compressibility	Heel Height (mm)	Plantar bumper stiffness	Heel Height (mm)
ARØØ1	81.4	28	medium	18	D42/3	25
ALØØ6	81.5	27	medium	18	D42/4	25
ARØ1Ø	69.1	26	medium	18	D42/3	25
ARØ11	73.6	27	medium	18	Otto Bock's	25
ALØ13	95.5	27	firm	18	D42/5	25

Table 7.2(b) Selection of heel stiffness for Above-knee Amputee

side of the SACH and Uniaxial foot can be checked for significant difference. The difference between the two samples means is 16.8 Nm. The standard error of difference between the two samples is 14.0 Nm (i.e. 99.7% confidence limit). Therefore, the difference between the minimum ankle Mz moments of the SACH and the Uniaxial foot is significant. This method of checking for significant difference was used throughout the evaluation for other parameters as well.

The maximum hip Mz moments of the normal subject wereused to estimate the errors caused by the displacement data and force plate data,at the a 95% confidence level. The estimated error of the maximum hip Mz moment is ±12%. This value is within the total range of scatter of the maximum hip Mz moments (±25%).

7.2. Preliminary Assessment of Prosthetic Feet

Each patient was initially fitted with a SACH foot. The grade of the heel cushion was selected according to the mass of the patient as well as the consideration of his activity level. It is more or less a "trial and error" procedure. With an experienced prosthetist, usually a suitable heel cushion should be selected by the second trial. The criteria and procedure were also applied to the fitting of the Uniaxial foot. Tables 7.2.(a) and (b) show the preferred heel stiffness for the two types of prosthetic feet used on the below- and above-knee amputees, respectively. Three of the below-knee amputees showed preference for the medium grade SACH foot, even though their body mass exceeded that recommended by Radcliffe and Foort (1961), see Table 4.3.1(b). Furthermore, from the data collected, there is an indication that the guide to heel selection would not be suitable for the less-active amputees, who may require the soft grade SACH foot. Therefore, the guide has to be

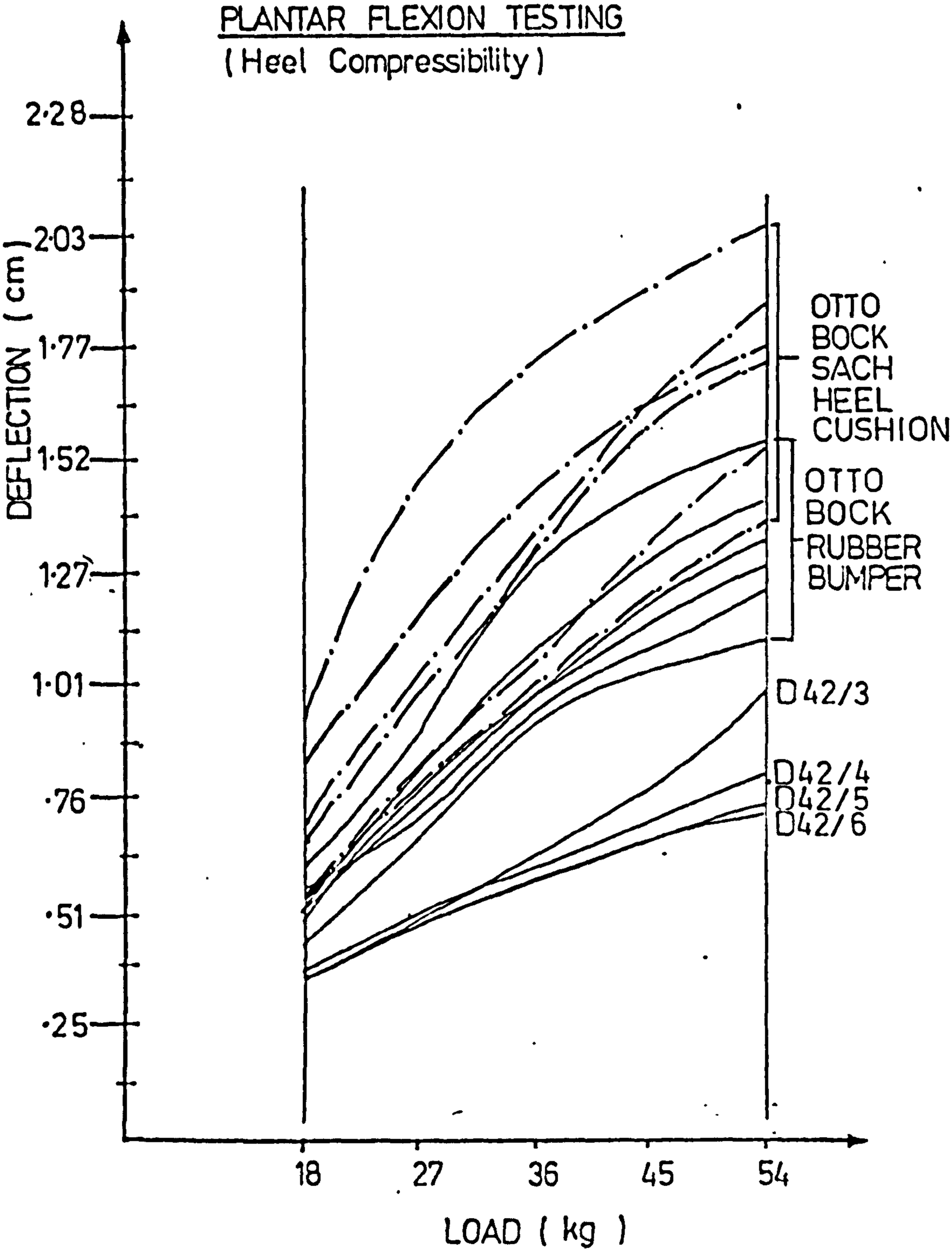

Figure 7.2(a) Plantar Flexion Testing

revised to include the level of activity as one of the basis of selection.

Figure 7.2(a) shows the load versus deformation curve of the plantar-flexion tests on both the SACH and Uniaxial foot. Due to the inadequacy of the Veterans Administration's classification of prosthetic ankle/foot assemblies, all the plantar rubber bumpers of the Uniaxial foot were classified as being "firm", although clearly they were of different stiffness. Therefore, it was decided that each patient should be fitted with all the available types of plantar rubber bumpers. From these fittings and the compression tests performed on mechanical testing machines, it was clear that the "Strathclyde" rubber bumpers are able to be classified more specifically. Samples D42/3 and D42/4, with Shore A hardness of 56^{o} and 60^{o} respectively, can be classified as "medium" Uniaxial grade, while samples D42/5 and D42/6, with Shore A hardness of 80^{o} and 85^{o} respectively can be classified as "firm" Uniaxial grade. The Otto Bock plantar rubber bumper was considered to be "soft" by most of the patients, this being distinctively evident during their gait when the prosthetic foot plantar-flexed rapidly immediately after heel contact. The range of bumper stiffness was adequate for all the patients tested.

It was observed that for a particular amputee the heel stiffness preferred for the Uniaxial foot was always more stiff than that of the SACH foot, according to the load versus deformation curve. This may be due to the different static load bearing characteristics of both feet. It is perhaps more appropriate to consider the ankle plantar-flexion moment versus the ankle angular displacement curve, which is more representative of the dynamic situation.

Fitting and subjective assessment were carried out by experienced prosthetists. No significant change was detected in the gait pattern of the patients when the two

types of prosthetic feet were fitted. Most of the gait deviations observed were consistent with the patients' usual manner of walking.

7.2.1. Patients' Comments

Below-knee Amputees

Patient BRØØ2 felt that the SACH foot gave a smoother ankle motion during the transition of weight from heel to toe during stance phase. Besides this, both prosthetic feet functioned satisfactorily. The patient's overall preference was for the SACH foot.

Patient BRØØ3 found that the "roll-over" during late stance provided by the Uniaxial foot was slightly better than that of the SACH foot. Otherwise, no significant difference was experienced between either type of prosthetic foot. However, the patient preferred the SACH foot because it "felt a lot better".

Patient BLØØ4 liked the plantar flexion action of the Uniaxial foot immediately after heel contact. He also expressed that it is aesthetically better looking than the SACH foot. Besides this, the patient found no other significant differences between the two feet. The patient's overall preference was for the Uniaxial foot.

Patient BRØØ5 found that the SACH foot was too rigid. He was delighted with the plantar-flexion action of the Uniaxial foot immediately after heel contact. He also expressed that the "roll-over" was better with the Uniaxial foot. The patient's overall preference was for the Uniaxial foot.

Patient BRØØ7 walked with an exceptionally good gait with either of the two prosthetic feet. He found no

significant difference between the two feet and thus he expressed no preference.

Patient BLØ12 expressed his delight in the functional aspect of the Uniaxial foot. Cushioning effect of the foot at heel impact and "roll-over" during late stance were found by him to be better than the SACH foot. He felt that he could walk at a faster pace and with more comfort on the Uniaxial foot. The patient's overall preference was for the Uniaxial foot because it felt "much more lively and natural".

An assessment of these comments from the below-knee amputees showed that there is no general preference for a particular type of prosthetic foot; three preferred the Uniaxial foot, two preferred the SACH foot and one had no preference. The three who preferred the Uniaxial foot were unanimous in expressing their delight at the plantar flexion action of the foot immediately after heel strike. Out of these three patients, two were convinced that the Uniaxial foot has definite advantages over the SACH foot. Apart from this, the remaining four amputees found no significant difference in function between the two types of foot.

Above-knee Amputees

Patient ARØØ1 felt that the SACH foot provided a smoother "roll-over" and better stability than the Uniaxial foot, although he expressed that he liked the cushioning effect of the Uniaxial foot during heel impact. The patient's overall preference was for the SACH foot, which he expressed without any hesitation.

Patient ALØØ6 liked the plantar-flexion action of the Uniaxial foot immediately after heel contact because it was "more natural looking". Although not much

difference was experienced with regard to the smoothness of ankle motion during the transition of weight from heel to toe during stance phase, the patient preferred the Uniaxial foot. His overall preference was for the Uniaxial foot.

Patient ARØ1Ø was very pleased with the cushioning effect provided by the Uniaxial foot during heel impact. He also felt that the "roll-over" with the Uniaxial foot was slightly better than that of the SACH foot. Other functional characteristics were very much the same with either types of prosthetic feet. The patient's overall preference was for the Uniaxial foot.

Patient ARØ11 found both prosthetic feet to be functionally satisfactory and acceptable. However, his overall preference was for the Uniaxial foot because he liked the plantar-flexion action immediately after heel strike.

Patient ALØ13 expressed that the cushioning effect of the Uniaxial foot at heel impact and the "roll-over" were not as good as the SACH foot. He felt more stable with the SACH foot than the Uniaxial foot. He also felt that the dorsiflexion stop of the Uniaxial foot coming into action had two distinct moves. Firstly, the ankle joint rotates until it hits the dorsiflexion stop and when it does, then the "roll-over" begins. This made him felt slightly insecure. The patient's overall preference was for the SACH foot.

Similar to the below-knee amputees' reactions, an assessment of the above-knee amputees' responses showed that there is no general preference for a particular prosthetic foot; three preferred the Uniaxial foot and two preferred the SACH foot.

The two amputees who preferred the SACH foot found

Patient Code	Prescribed Prosthetic Foot on Patient's own Prosthesis	Overall Preference
BR002	SACH	SACH
BR003	SACH	SACH
BL004	Uniaxial(wooden)	Uniaxial(Moulded)
BR005	SACH	Uniaxial(Moulded)
BR007	Uniaxial(wooden)	No preference
BL012	Uniaxial(Moulded)	Uniaxial(Moulded)

Table 7.2.1(a) Below-Knee Amputees

Patient Code	Prescribed Prosthetic Foot on Patient's own Prosthesis	Overall Preference
AR001	SACH	SACH
AL006	Uniaxial(Moulded)	Uniaxial(Moulded)
AR010	Uniaxial(wooden)	Uniaxial(Moulded)
AR011	Uniaxial(wooden)	Uniaxial(Moulded)
AL013	SACH	SACH

Table 7.2.1(b) Above-Knee Amputees

the ankle motion during the transition of weight from heel to toe much smoother and that also, the feeling of security in balance was greater than with the Uniaxial foot. Both amputees were not hesitant about their choice of the SACH foot. The three amputees who preferred the Uniaxial foot liked the plantar flexion action immediately after heel contact. One even expressed that the "roll-over" for the Uniaxial foot was better than that of the SACH foot.

The reactions of both the below- and above-knee amputees to prosthetic feet, as reported here, are different from the clinical experiences discussed in Section 4.3.2. These findings also varied from those reported by Fishman et al (1955). They presented the reactions of three below- and three above-knee amputees who found significant improvement with regard to the cushioning effect at heel impact and the smoothness of ankle motion with the SACH foot. Some improvement was also reported in socket comfort and security in balance over the conventional foot. The differences in reactions could be due to the smaller sample size of Fishman et al and also to the fact that the comparison was made against the conventional single-axis wooden foot.

Tables 7.2.1(a) and (b) show the prescribed prosthetic foot on the patient's own artificial limb and that preferred by him in the experiment. This comparison seems to indicate that the amputee's preference of a particular prosthetic foot corresponds to that with which he is already familiar. However, there are two exceptions and furthermore, those with a wooden single-axis foot prefer the moulded-type Uniaxial feet.

7.2.2. Prosthetists' Comments

With regard to the prosthetist's choice of fitting prosthetic feet, the two participating prosthetists had

slightly different preferences.

One of the prosthetists on the onset prefers to fit the SACH foot to both the below- and above-knee amputees. The rationale behind this preference is that it is much easier to fit and the maintenance requirement of it is almost nil. He believes that the SACH foot provides adequate function for the two levels of amputees. If the patient fails to respond satisfactorily to the SACH foot, for one reason or another, he would try the Uniaxial foot. He has found that some patients (both below- and above-knee amputees) perform better on the Uniaxial foot than with the SACH foot.

The other prosthetist prefers to fit all the below-knee amputees and those very active above-knee amputees, with the SACH foot. For all less-active above-knee amputees, the moulded Uniaxial foot is preferred. This is because this category of patients tends to walk very slowly and therefore requires foot-flat position quicker to provide stability.

Both prosthetists felt that the three grades of heel cushions available for the SACH foot are adequate for the range of below- and above-knee amputees. The only plantar bumper for the moulded Uniaxial foot of the modular type, supplied by the manufacturer, was found to be inadequate for even the sample of amputees used in this project. Both prosthetists were keen on the idea of having a range of rubber bumpers with varying stiffnesses for selection having found the performance of the "Strathclyde" rubber bumpers perfectly satisfactory.

Two other experienced prosthetists were asked to give their comments on the choice of prosthetic feet. One, a senior prosthetist,prefers to fit the SACH foot to almost all below-knee amputees and those very active above-knee amputees. However, most of the above-knee

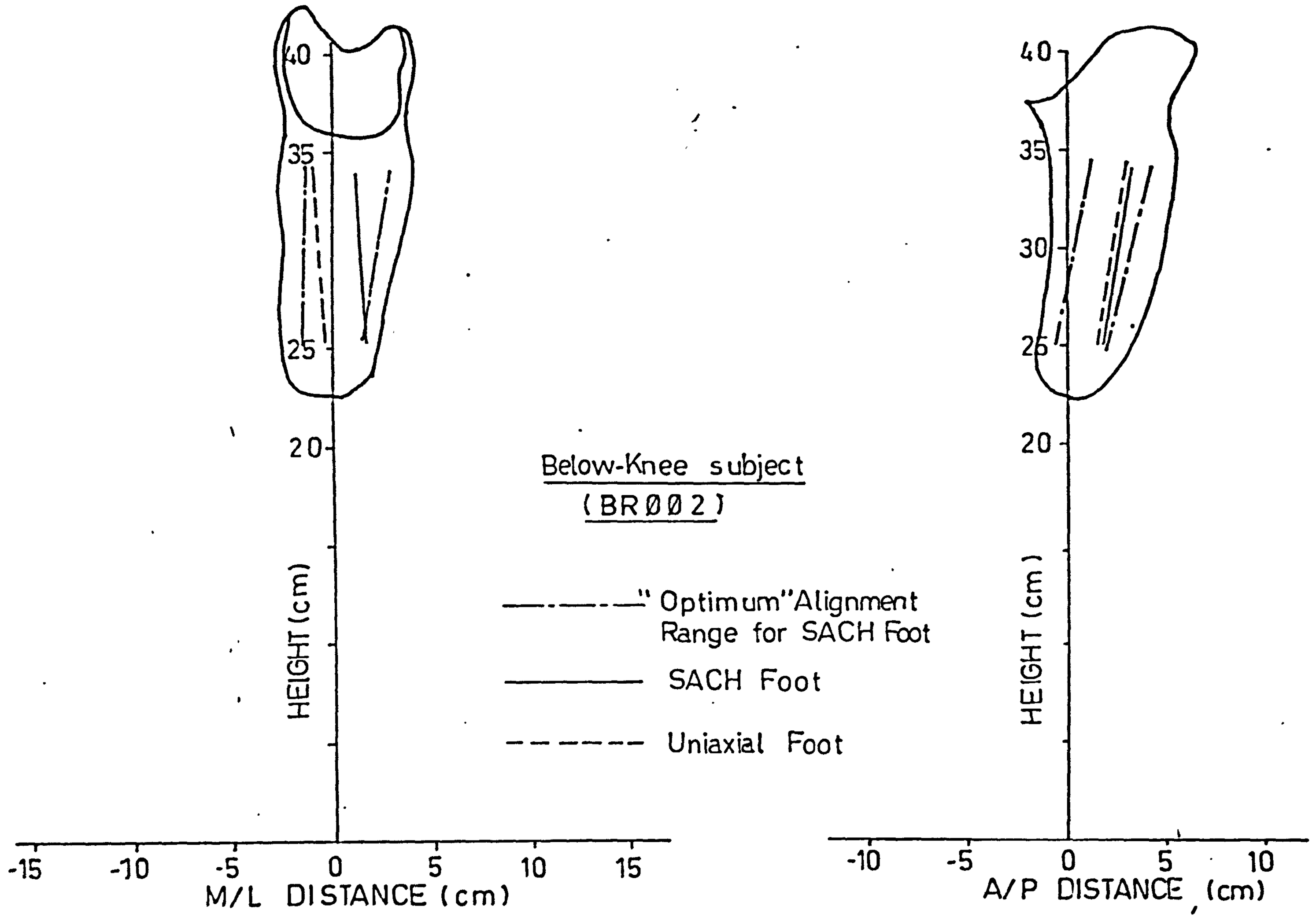

Figure 7.3.1(a) Alignment of Below-knee Prosthesis

amputees treated by him are enfeebled and are fairly unstable. The moulded Uniaxial feet are prescribed for this class of patient, since foot flat position with this type of foot can be achieved quickly to provide stability. The other prosthetist prefers to fit the SACH foot to both the below- and above-knee amputees. The reason given was that it is easier to fit and maintain. However, he would attempt to fit the Uniaxial foot to the inactive above-knee amputees, if stability is required.

7.3. Alignment Measurement Results

Tables C(1) and C(2) in Appendix (C), show the results of all the alignment measurements of the below- and above-knee prostheses, respectively. The definitions of the alignment parameters are also presented in Appendix (C). Presented together with the results of the alignment measurements are the ranges of "optimum" alignment obtained for each of the individual amputees. These "optimum" alignment ranges are the result of an on-going project towards the understanding of the patients' tolerance to dynamic alignment and an attempt to quantify "optimum" alignment, see Zahedi (1982). The prostheses used in the determination of these "optimum" alignment ranges were the same as those used in this project. Furthermore, the same prosthetists were also employed. However, these "optimum" alignment ranges were obtained with the SACH foot only. Nevertheless, the results compared well with those obtained in this project.

7.3.1. Below-knee Prostheses

Figure 7.3.1(a) shows the typical results of the alignment measurement of a right below-knee prosthesis plotted in the M/L and A/P planes. The "optimum" alignment ranges for this particular amputee are also

plotted in the diagrams. The alignments for the SACH and Uniaxial foot were included for comparison. Both alignments were observed to be within the "optimum" alignment range.

From Table C(1), the results obtained were found to be within the "optimum" alignment range in all of the below-knee prostheses measured, either with the SACH or the Uniaxial foot. On comparison of data obtained for the SACH and the Uniaxial feet, certain consistent differences were observed in all the prostheses. The most obvious one was the socket height, since the foot height of both prosthetic feet has a difference of about 1 cm. The socket height for the Uniaxial foot was found to be longer by 1.09 cm ($\pm$0.04). The Uniaxial foot tends to have a greater socket set out when compared with that of the SACH foot. The average difference is about 1.46cm. The SACH foot tends to toe-out more than the Uniaxial foot by an average value of 3.5^{o}.

The other alignment parameters which were considered did not show any significant difference when a comparison was made between SACH and Uniaxial foot. It must be noted that while there is no difference in the socket forward set between that of the SACH and Uniaxial foot, there is a difference in the distance between the axis of foot bolt/ankle and the heel. . This distance in the Uniaxial foot is longer by 1.5cm. The SACH foot, unlike the Uniaxial foot, has no articulating joint, therefore effectively the socket forward set of the SACH foot is posterior to that of the Uniaxial foot by 1.5cm.

These differences in alignment parameters suggest that when replacing either the SACH or the Uniaxial foot in the prosthesis, different alignment adjustments are necessary. These alignment changes have to be considered as an integral part of the differences in the SACH and

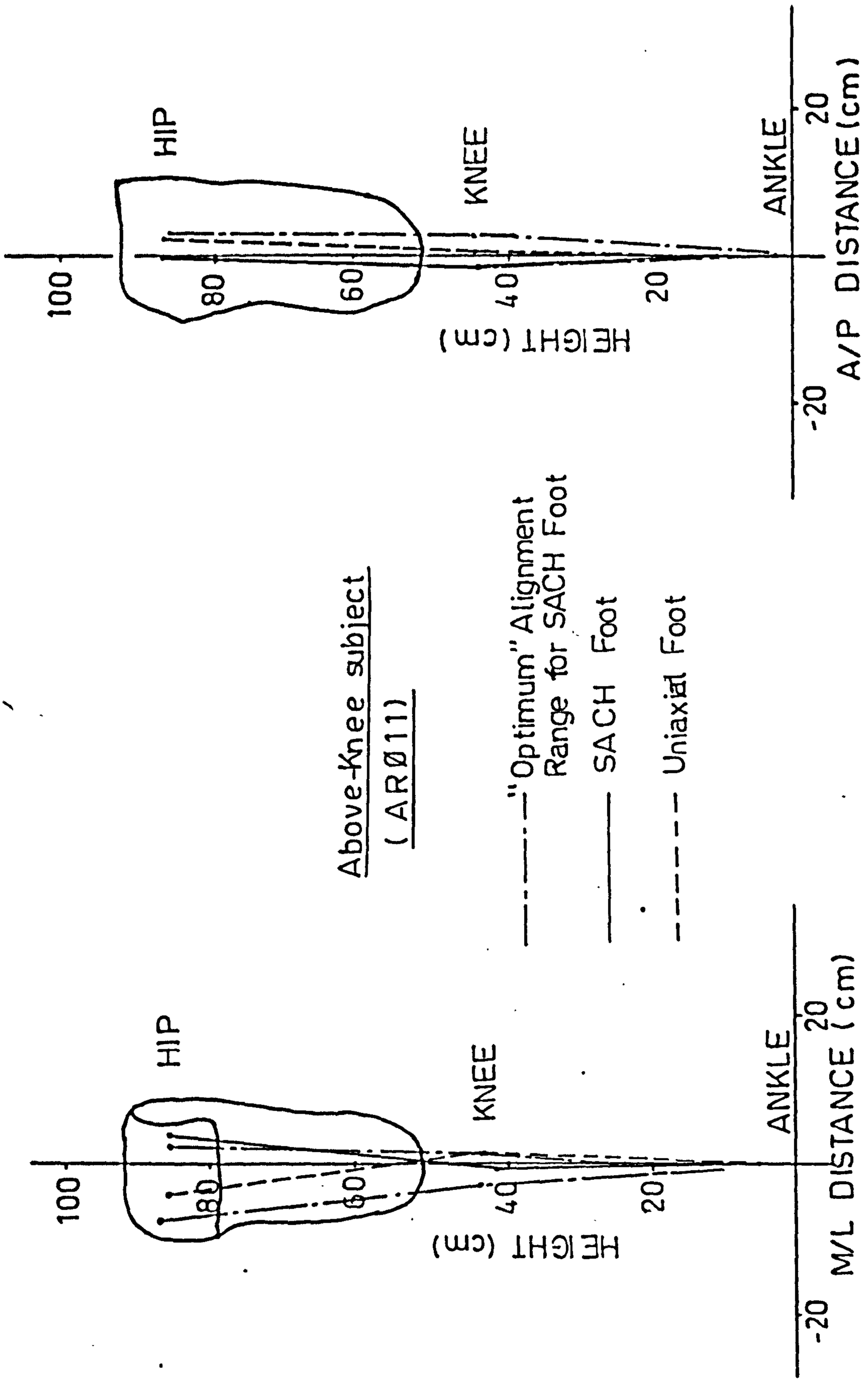

Figure 7.3.2(a) Alignment of Above-knee Prosthesis

the Uniaxial feet.

7.3.2. Above-knee Prostheses

Figure 7.3.2(a) shows the results of the alignment measurement of a right above-knee prosthesis plotted in the M/L and A/P planes. The "optimum" alignment ranges for this particular amputee are also plotted in the diagrams. Both the alignments of the prosthesis with SACH and Uniaxial foot were observed to be within the "optimum" alignment range.

Table C(2) shows that all the other alignments measured from the above-knee prostheses (with the SACH and Uniaxial foot) are also within the "optimum" alignment range. Comparison between results obtained for the SACH and the Uniaxial foot shows some consistent differences in all the prostheses. The socket height for the Uniaxial foot was on average 1.12cm ($\pm$0.16) greater than that of the SACH foot. This is due to the difference in foot height, as explained in the previous section. The toe-out with the SACH foot tends to be more than that of the Uniaxial foot by an average value of 2.46^{o}. This trend is consistent with that found in the below-knee alignment results. The socket flexion, with the Uniaxial foot, was found to be slightly more than that of the SACH foot. The average difference in value was 4.6^{o}.

The difference in the distance between the axis of the foot bolt/ankle and the heel of the SACH and Uniaxial foot was mentioned in the previous section. This difference meant that the knee set back and socket forward set of the SACH foot were now brought back by 1.5cm. The knee set back of the Uniaxial foot is therefore anterior to that of the SACH foot by 1.2cm. This difference is significant. The difference in the socket forward set after correction however, is not significant

Temporal Parameters of Walking Cycle	Time(s) mean (±1 S.C.)	Percent of Walking cycle(%)
Stance Phase (both limbs)	0.67 (0.03)	60.0
Swing Phase (both limbs)	0.45 (0.02)	40.0
Double Support Phase	0.09 (0.01)	8.0
Temporal Components of Stance Phase	Time(s) mean (±1 S.D.)	Percent of Stance Phase (%)
Heel-strike to Foot-flat	0.12 (0.01)	17.9
Foot-flat to Heel-rise	0.37 (0.02)	55.2
Heel-rise to Toe-off	0.18 (0.04)	26.9

Speed of Walking	1.465 m/s (± 0.086)
Cadence	114 steps per minute
Ratio of Swing to Stance	0.67

Table 7.4.1(a) Temporal Parameters of one Normal Subject

since it is within the scatter range.

All other alignment parameters considered did not show any significant difference when a comparison was made between the SACH and the Uniaxial feet.

7.4. Kinematic Results

7.4.1. Temporal Parameters

Table 7.4.1(a) shows the results of tests on a normal subject. Altogether, seven test walks were analysed. The temporal parameters of walking obtained were observed to be consistent with those presented by Murray et al (1964), see Figure 2.4.1(i). The preferred speed of walking varied from 1.381 m/s to 1.584 m/s. The average speed of walking was calculated to be 1.485 m/s with a standard deviation of 0.086 m/s. The corresponding average cadence was 114 steps per minute. The ratio of swing phase to stance phase is 0.67.

The temporal components of the stance phase are also presented. Slightly more than half the stance phase time was found to be spent during the period of foot-flat (FF) to heel-rise (HR). This long period of having the foot flat is to provide a broad base of support while the contralateral limb swings through to the next step. Therefore, this period is important as it offers stability to the body. The temporal parameters of the two limbs were observed to be very similar (0.02s difference). The average amount of variation in the temporal factors was found to be within 0.02 s.

Table 7.4.1(b) shows the average temporal parameters of six below-knee amputees. Between these six amputee subjects, a total of 24 test walks was analysed. The average preferred speed of walking for the

Temporal Parameters of Walking cycle	Time(s) mean (±1 S.D.)		Percent of Walking Cycle(%)	
	SACH	Uniaxial	SACH	Uniaxial
Stance Phase				
-Sound	0.696(0.08)	0.688(0.05)	60	62
Prosthetic	0.652(0.05)	0.665(0.03)	57	60
Swing Phase				
-Sound	0.463(0.04)	0.428(0.04)	40	38
Prosthetic	0.488(0.04)	0.445(0.03)	43	40
Double Support				
-Sound	0.100(0.03)	0.105(0.02)	8.6	9.4
Prosthetic	0.096(0.03)	0.123(0.02)	8.4	11.1
Temporal Components of Stance Phase	Time(s) mean (±1 S.D.)		Percent of Stance Phase (%)	
HS to FF				
-Sound	0.136(0.03)	0.144(0.01)	19.6	21.0
Prosthetic	0.292(0.05)	0.149(0.02)	44.5	22.4
FF to HR				
-Sound	0.372(0.06)	0.344(0.03)	53.6	50.1
Prosthetic	0.104(0.02)	0.292(0.03)	15.9	44.0
HR to TO				
-Sound	0.188(0.05)	0.200(0.04)	26.8	28.9
Prosthetic	0.256(0.03)	0.224(0.05)	39.6	33.6

	SACH	Uniaxial
Speed of Walking(m/s)	1.354(0.139)	1.36(0.095)
Ratio of Swing to Stance		
- Sound	0.67	0.62
Prosthetic	0.75	0.67

Table 7.4.1(b) Temporal Parameters of Below-knee Amputees

below-knee amputees was found to be the same whether they used the SACH or Uniaxial foot. The stance and swing phase timings were observed to be consistent with those presented by Breakey (1976), see Figure 3.3.1(d). The stance phase of the sound limb is longer than that of the prosthetic side and consequently the swing phase of the prosthetic side is longer than that of the sound side - this applied to both the SACH and Uniaxial foot. Thus, the symmetry in the parameters observed between the left and right leg of the normal subject is not apparent in the below-knee amputees. With the Uniaxial foot the stance phase times for both the sound and prosthetic limbs were 2 to 3% longer than those of the SACH foot.

The temporal components of the stance phase for the sound limb are similar to those of the normal subject. However, for the prosthetic limb there are significant differences. For the first period of stance phase, the Uniaxial foot demonstrated similar characteristic to the normal foot. This is due to the ability to plantar flex the foot about the hinge and the control of the rubber bumper, which simulates the pre-tibial muscles. With the SACH foot, this period extended to more than twice the normal time. This is because the rigid ankle prevents pivoting about the ankle axis. Therefore foot-flat position has to occur by compression of the heel cushion and forward movement of the knee joint. The delay in foot flat for the SACH foot does not affect the overall timing of the walking cycle. The total prosthetic stance phase duration with the SACH or Uniaxial foot was similar.

The second period of stance phase, tends to be shorter for the SACH foot, approximately 30% of the sound limb. This is due to the rigid ankle of the SACH foot. For the Uniaxial foot, this period is of

Temporal Parameters of Walking Cycle	Time(s) mean (±1 S.D.)		Percent of Walking Cycle(%)	
	SACH	Uniaxial	SACH	Uniaxial
Stance Phase				
-Sound	0.832(0.04)	0.835(0.04)	63	63
-Prosthetic	0.729(0.02)	0.721(0.03)	55	54
Swing Phase				
-Sound	0.492(0.04)	0.493(0.04)	37	37
-Prosthetic	0.594(0.05)	0.604(0.02)	45	46
Double Support				
-Sound	0.119(0.03)	0.110(0.03)	9.0	8.3
-Prosthetic	0.128(0.03)	0.131(0.04)	9.7	9.9
Temporal Components of Stance Phase	Time(s) mean (±1 S.D.)		Percent of Stance Cycle(%)	
HS to FF				
-Sound	0.156(0.03)	0.151(0.03)	18.8	18.1
-Prosthetic	0.245(0.02)	0.147(0.02)	33.6	20.4
FF to HR				
-Sound	0.256(0.09)	0.279(0.07)	30.0	33.1
-Prosthetic	0.118(0.03)	0.263(0.02)	15.7	36.5
Vaulting				
-Sound	0.179(0.01)	0.175(0.02)	21.6	20.4
HR to TO				
-Sound	0.245(0.03)	0.240(0.04)	29.6	28.4
-Prosthetic	0.374(0.04)	0.311(0.05)	50.7	43.1

	SACH	Uniaxial
Speed of Walking(m/s)	1.043(0.062)	1.043(0.062)
Ratio of Swing to Stance		
- Sound	0.59	0.59
- Prosthetic	0.81	0.84

Table 7.4.1(c) Temporal Parameters of Above-Knee Amputees

approximately the same duration as that for the sound limb. (approximately 85% of the normal).

The third and final period prepares the foot for toe-off. The SACH foot takes a slightly longer time to roll over the ball of the foot than the Uniaxial foot. This could be due to the different geometry of the keel at the distal section.

The ratio of swing to stance phase for the sound side is 0.67 for the SACH and 0.62 for the Uniaxial foot. These values are approximately those of the normal subject. For the prosthetic side with a SACH foot, the ratio is 0.75 and with a Uniaxial foot it is 0.67. This result suggests that with the SACH foot the prosthetic limb spent less time during stance phase which may be an indication of instability. This however is not substantiated by the reactions of the subjects and hence requires further confirmation from kinetic data.

Table 7.4.1(c) shows the averaged temporal parameters of five above-knee amputees. From these five above-knee amputees, altogether 28 test walks were analysed. The averaged preferred speed of walking for the above-knee amputees was found to be the same with either the SACH or Uniaxial foot. This value compared favourably with that presented by Murray et al (1980), see Figure 3.3.1(b). On comparison with those obtained for the below-knee amputees and the normal subject, the speed of walking for the above-knee amputee is slower by about 30%.

The temporal components of the walking cycle as shown, varied slightly in values with those reported by other investigators, see Figure 3.3.1(b). The stance and swing phase durations recorded in this project are shorter. This may be due to the fact that the above-knee

amputees used in this investigation are more active. Furthermore the scatter in the results seems much less than those reported previously.

There is no significant difference in the stance or swing phase timings between the SACH and Uniaxial foot for both the sound and prosthetic limbs. However, the stance phase for the prosthetic limb is much shorter than that of the sound limb. This is probably due to the relative weakness of the adductor muscles (as compared to the normal and below-knee subjects) of the above-knee amputees, resulting in lesser ability to control the pelvic tilt in the M/L plane after mid-stance. Therefore, the swing phase of the sound limb is shortened to assist or take over the control of the pelvis from the prosthetic limb.

The first and third periods of the stance phase of the sound limb are similar to those of the normal subject. However, the second period is divided into two sections, from foot-flat to heel-rise and "vaulting". On average, the above-knee amputees spent 20% of stance phase "vaulting". All the amputees are known to have "vault", through habit rather than a feeling of insecurity. The length of vaulting seems to be unaffected by the use of either type of prosthetic feet.

The first period of the stance phase of the prosthetic limb with a Uniaxial foot is similar to the normal, however the second period is much shorter. It is also shorter than that of below-knee amputees with a Uniaxial foot. This could be due to the inability of the above-knee amputee to control the ankle movement during this period resulting in having to pivot about the single-axis joint and therefore moving rapidly to engage the dorsiflexion stop. The third period of stance phase of the above-knee amputees with the Uniaxial foot

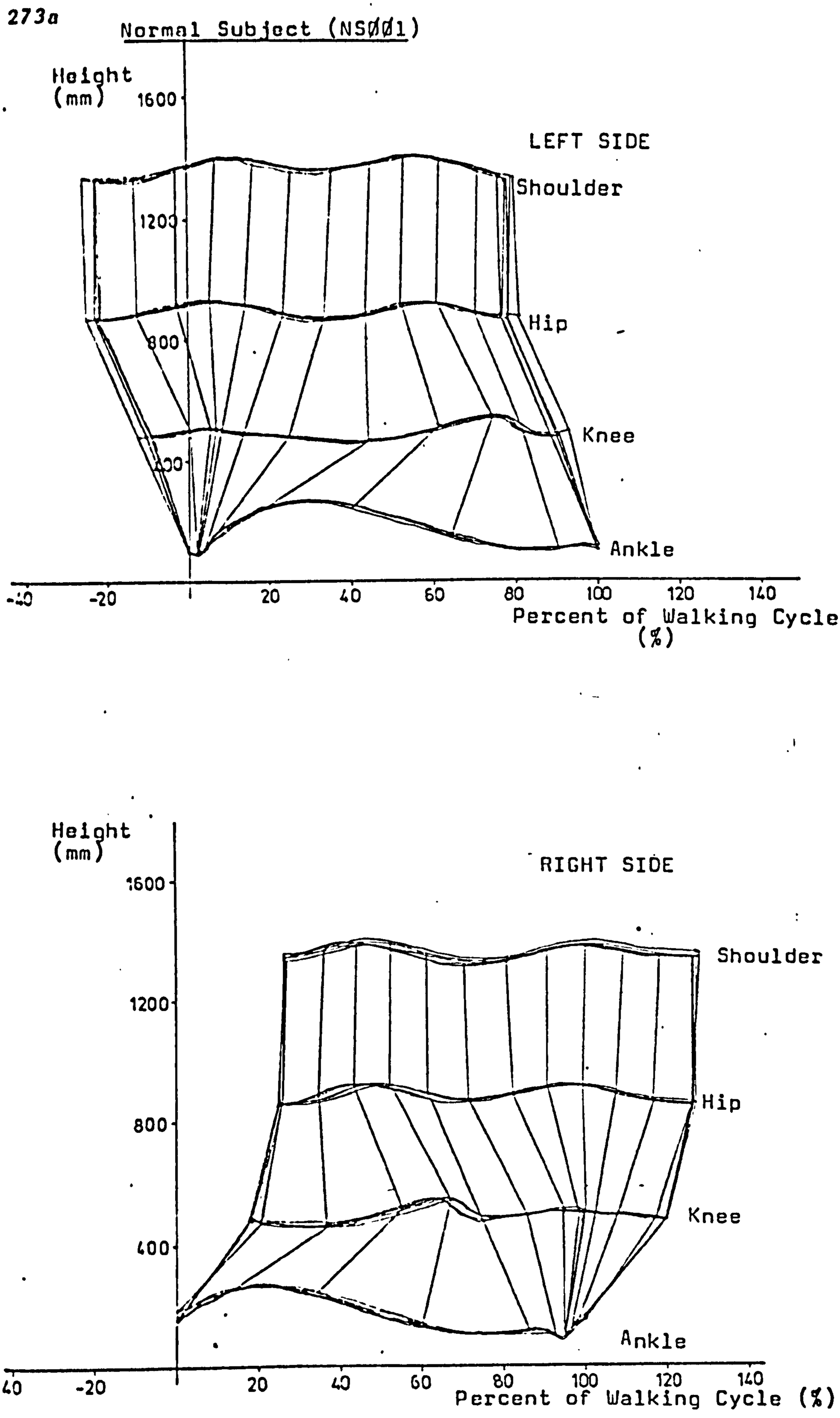

Figure 7.4.2(a) Stick Diagrams of Normal Subject

is much longer than that of the normal subject as well as the below-knee amputees with Uniaxial foot.

With the SACH foot, the first period of stance for the prosthetic side is longer than that of the normal subject. It is however, shorter than that of the below-knee amputee with SACH foot. This could be due to the alignment of the prosthesis, such that the angle of approach of the foot is less. Hence, the foot rolls to foot flat faster than that of the below-knee amputee. The second period of stance phase for the above-knee amputee with SACH foot is the same as that for the below-knee amputee with SACH foot; however the third period is very much longer.

7.4.2. Displacement Data

Stick Diagram

In order to assess the smoothness and aesthetic quality of gait, the trajectories of the joint centres of the lower limb and shoulder are considered. Furthermore, in discussing the problem of comparing the function of the SACH and Uniaxial feet with several experienced prosthetists, it was suggested that the hip and shoulder trajectories during level walking should be examined, as they might provide useful evaluation criteria.

Figure 7.4.2(a) shows the trajectories of the ankle, knee, hip and shoulder joint centres of a normal subject. Altogether seven test walks are superimposed one on top of the other. The range of scatter in the trajectories is approximately ±12 mm. This could be due to errors inherent in the recording and reduction systems and also the uncontrollable step to step variations, including speed of walking and step length changes. However, the overall pattern presented is consistent with those

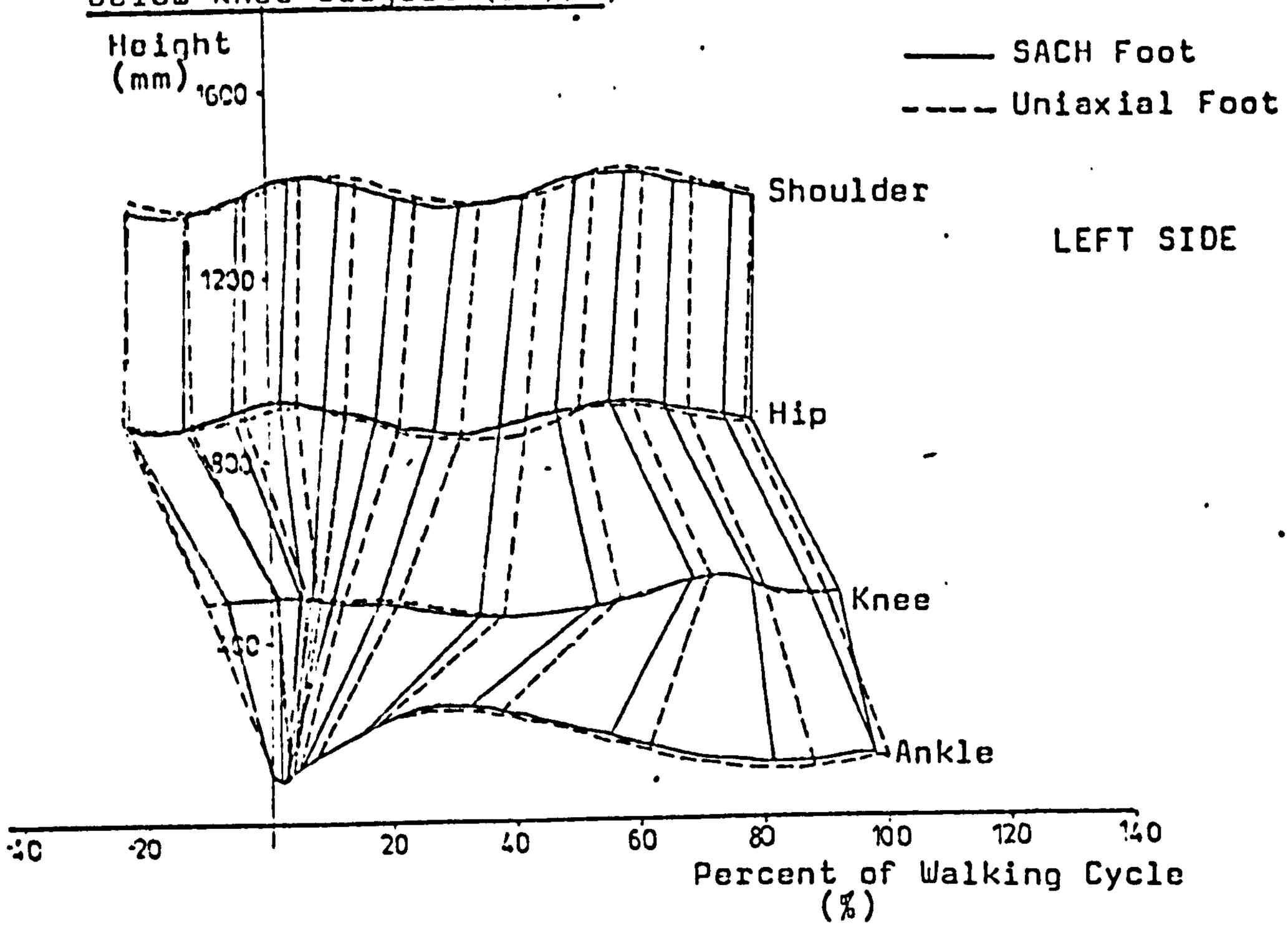

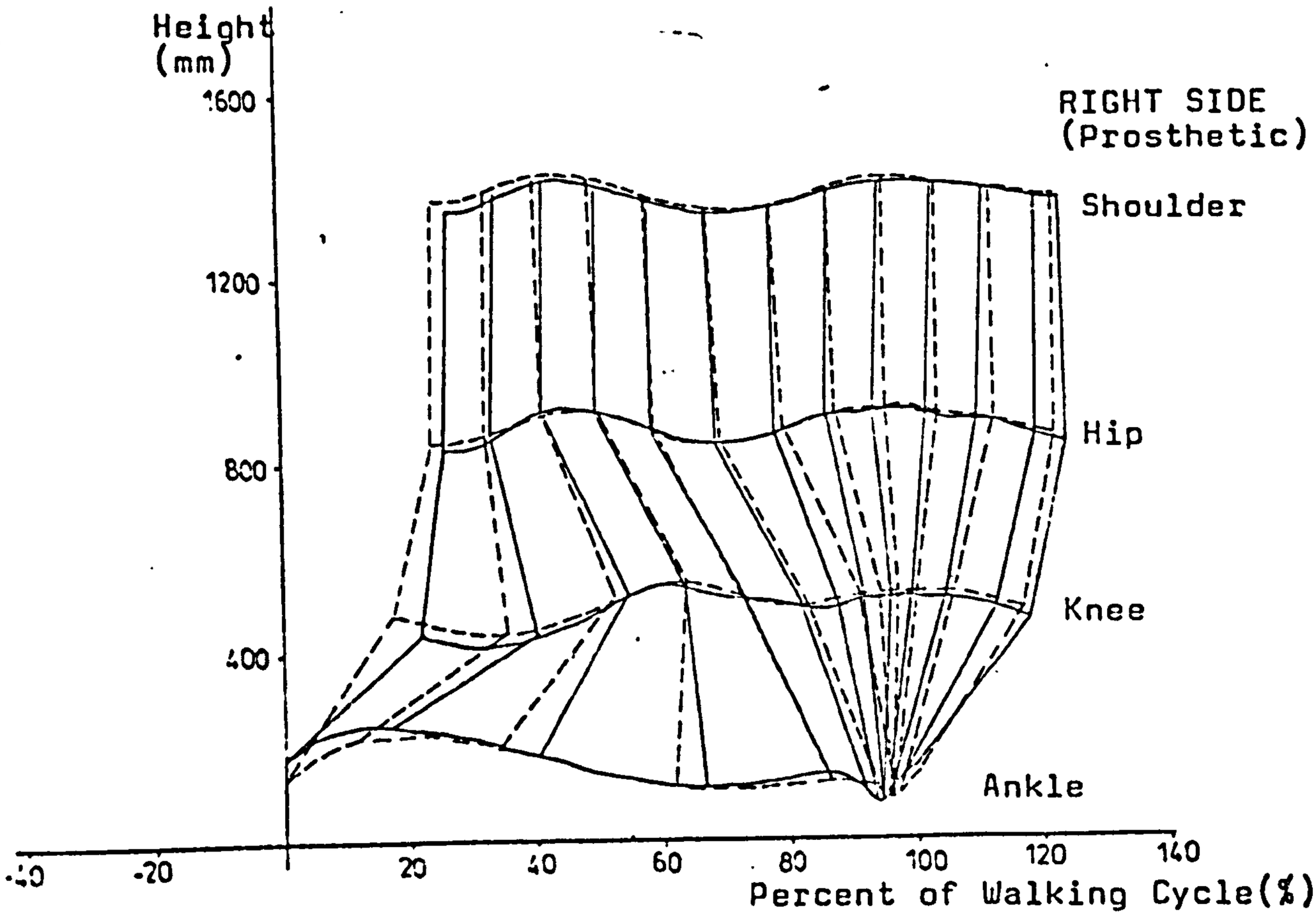

Figure 7.4.2(b) Typical Stick Diagram of Below-Knee Amputee

reported by other investigators, Murray et al (1964).

The curves demonstrate the typical two peaks in the hip and shoulder joint centres trajectories. The knee joint centre rises to a maximum, approximately 0.14 s before heel contact. The ankle joint centre rises to a maximum approximately 0.12s after toe-off. The flexing of the knee during stance phase prevents the body from elevating, thus maintaining the smooth trajectories of normal gait pattern.

Figure 7.4.2(b) shows the typical stick diagrams of a below-knee amputee. The curves are similar to those of the normal subject, except for the prosthetic side where the oscillating amplitudes are slightly less. Comparison between the SACH foot and Uniaxial foot showed no significant difference in the shapes of the curves. Any differences in values are within the ±12mm scatter range, which does not constitute a significant change.

Figure 7.4.2(c) shows the typical stick diagrams of an above-knee amputee. The trajectories differ significantly from those of the normal subject. The knee of the sound limb of the above-knee amputee is not raised as high as that of the normal or below-knee subjects. The trajectories of the hip and shoulder on the sound side show the two peak patterns although the peak associated with stance phase has a slightly higher amplitude. On the prosthetic side however, there is only one peak in the hip and shoulder trajectories, which is associated with the prosthetic swing phase. The amplitude of this peak is similar to that of the sound side during stance phase. This is recognised as being the vaulting action, inherent in the gait pattern of all the above-knee amputees tested. The absence of a trough before a second peak in the hip and shoulder trajectories is due to the prosthetic knee being fully extended and locked

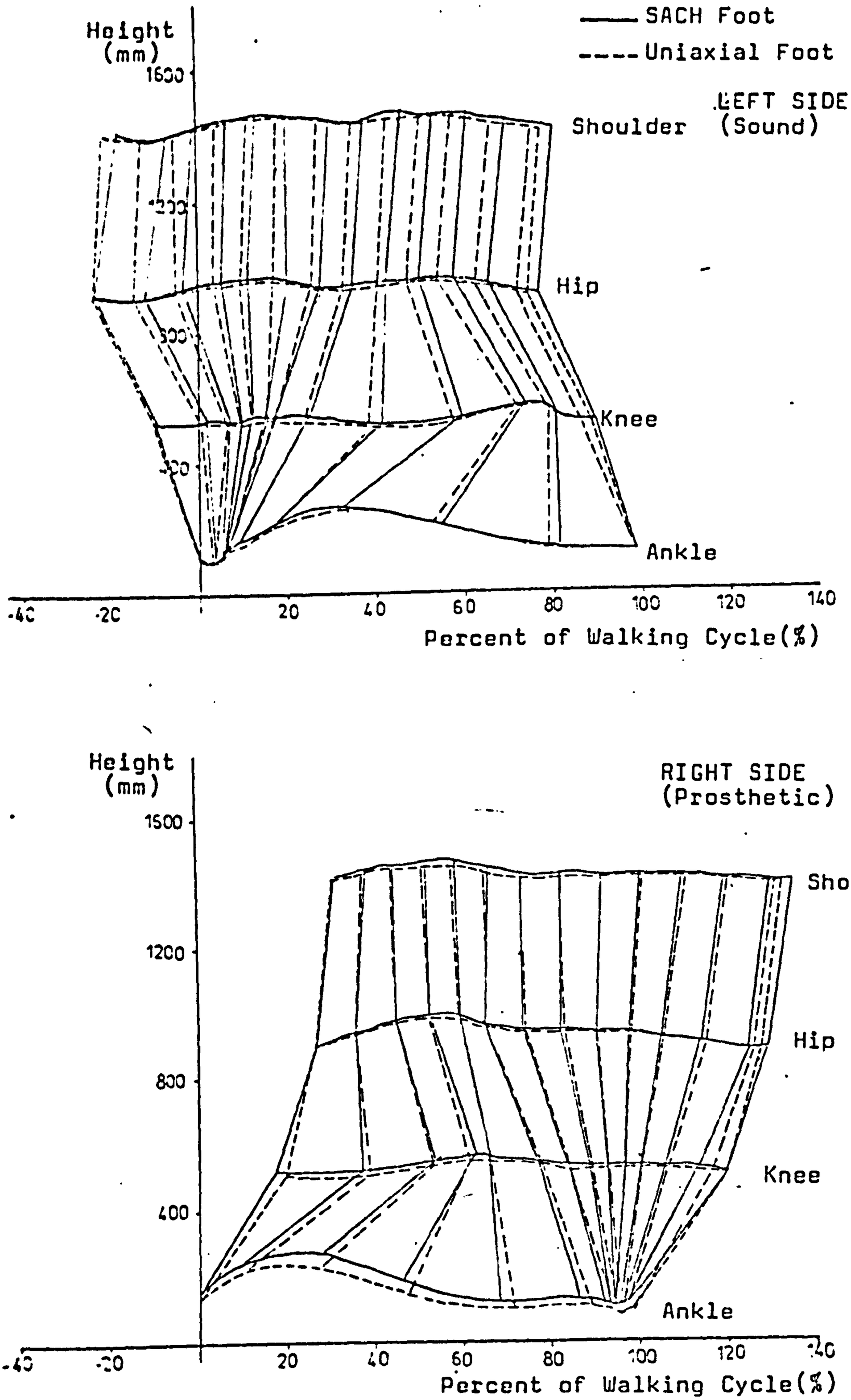

Figure 7.4.2(c) Typical Stick Diagrams of Above-knee Amputee

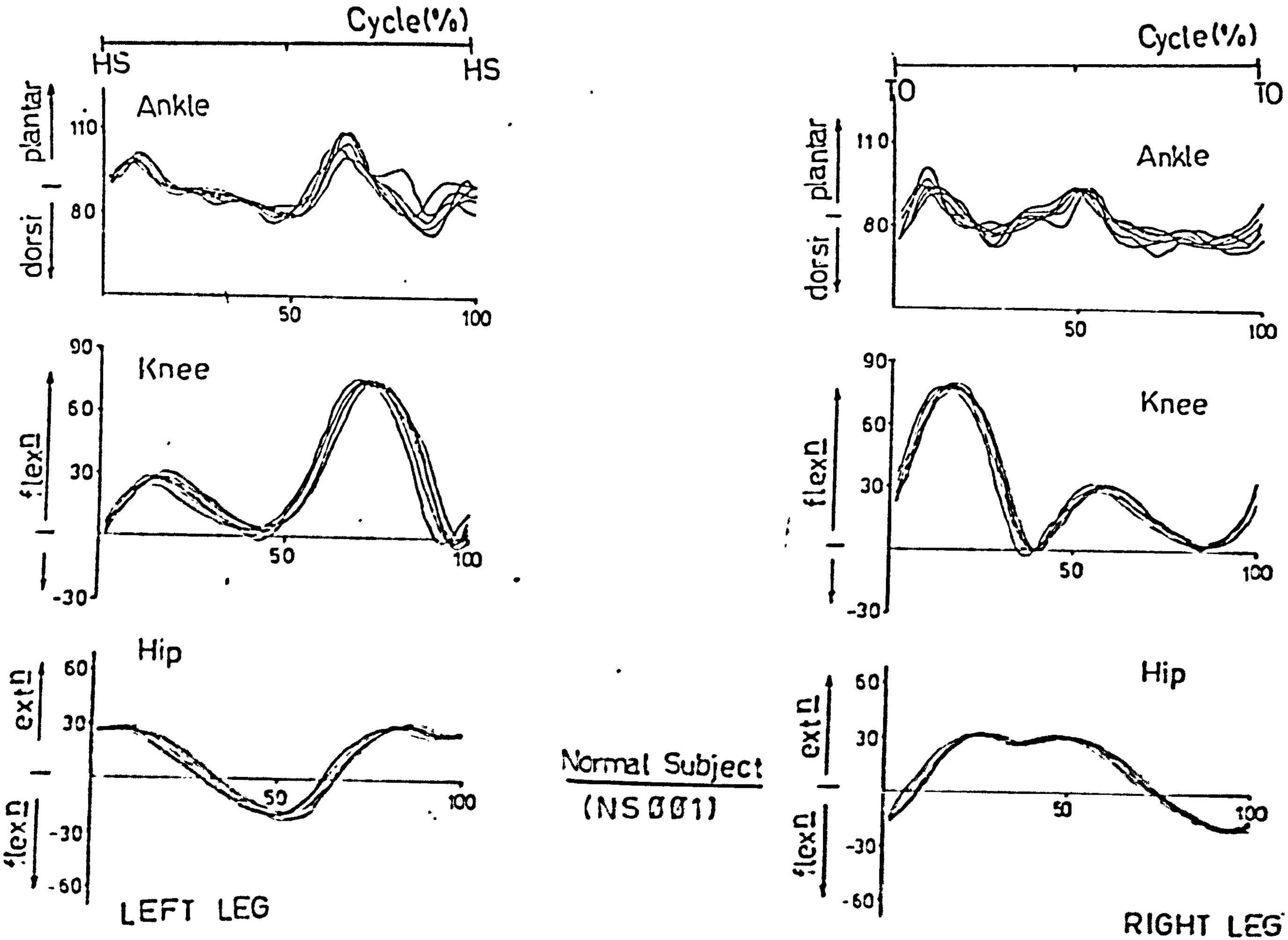

Figure 7.4.2(d) Angle-Time Diagrams of Normal Subject (NS001)

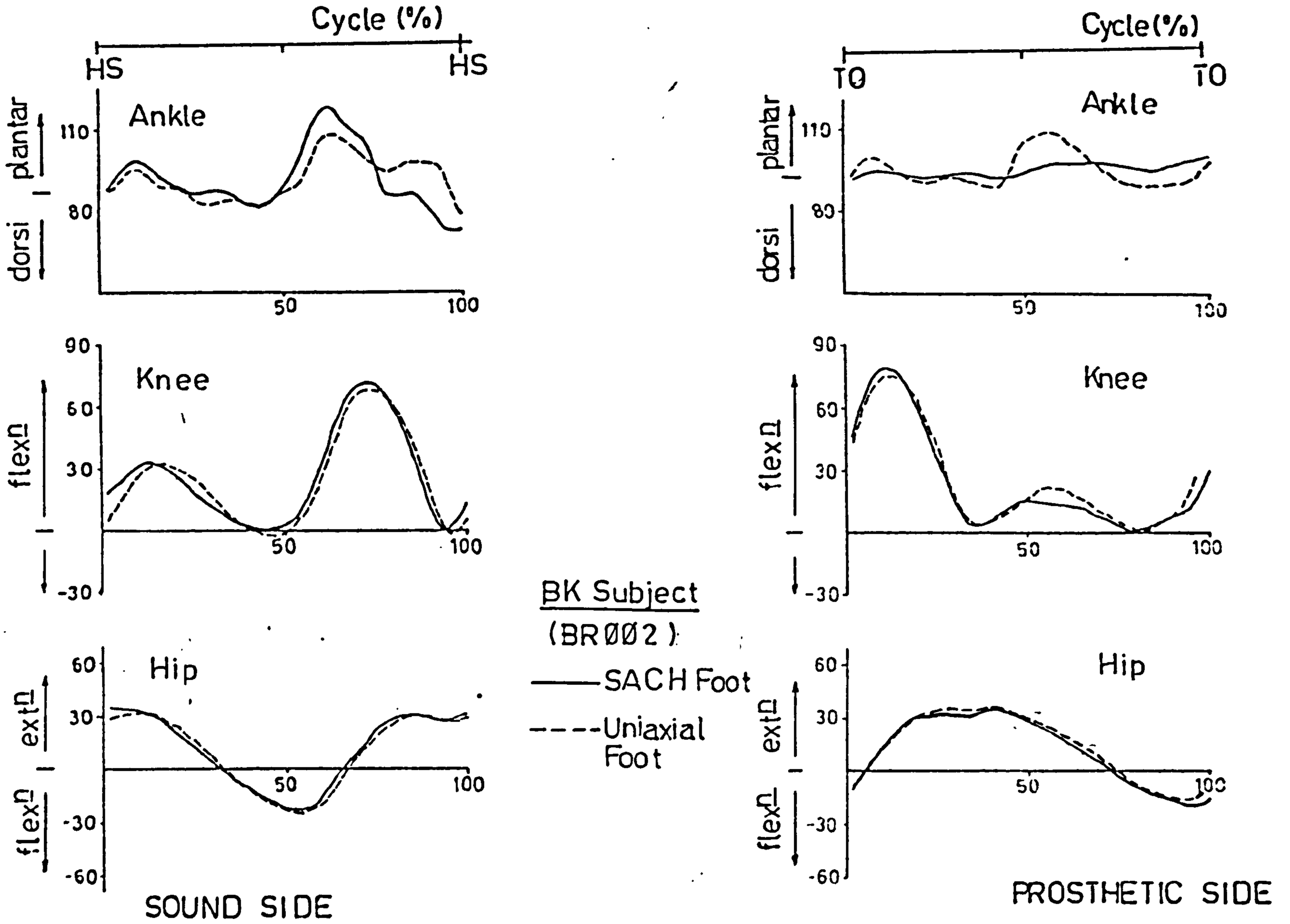

Figure 7.4.2(e) Typical Angle-Time Diagrams of Below-knee Amputee

during this period. Therefore, during stance phase, the extended locked knee of the prosthetic limb gives a pivoting compass effect.

Comparison between the SACH and Uniaxial foot gives no significant differences in the overall gait pattern of the above-knee amputees. Any magnitude differences are within the ±12mm scatter in the data, which cannot be regarded as significant.

Angle-Time Diagram

Figure 7.4.2(d) shows the angle-time diagrams of the normal subject. The general patterns of all the curves presented here are similar to those reported by Peizer et al (1969), although the magnitudes here are slightly larger. The range of scatter in the data presented is on average $\pm 7^{o}$. The foot is plantar-flexed after heel strike to about 15^{o} and then dorsiflexed to also about 15^{o} after mid-stance. Then it is plantar-flexed again to about 20^{o} to actively push off at toe-off. The knee flexion at stance phase is about 29^{o} and at swing phase about 76^{o}. The hip is flexed approximately 31^{o} and is extended to about 20^{o}.

Figure 7.4.2(e) shows the typical angle-time diagram of a below-knee amputee. The flexion-extension angles of the ankle, knee and hip joints on the sound side are fairly similar in feature to the normal subject. On the prosthetic side, the Uniaxial foot registered a plantar-flexion of between 10 to 15 degrees at heel strike. Apart from this angle, as expected, no other angular ankle movement was observed. With the SACH foot, only a small amount (about 5^{o}) of angular ankle movement was observed. The knee flexion during stance phase on the prosthetic side was approximately half that of the sound side. However, three amputees were found to have

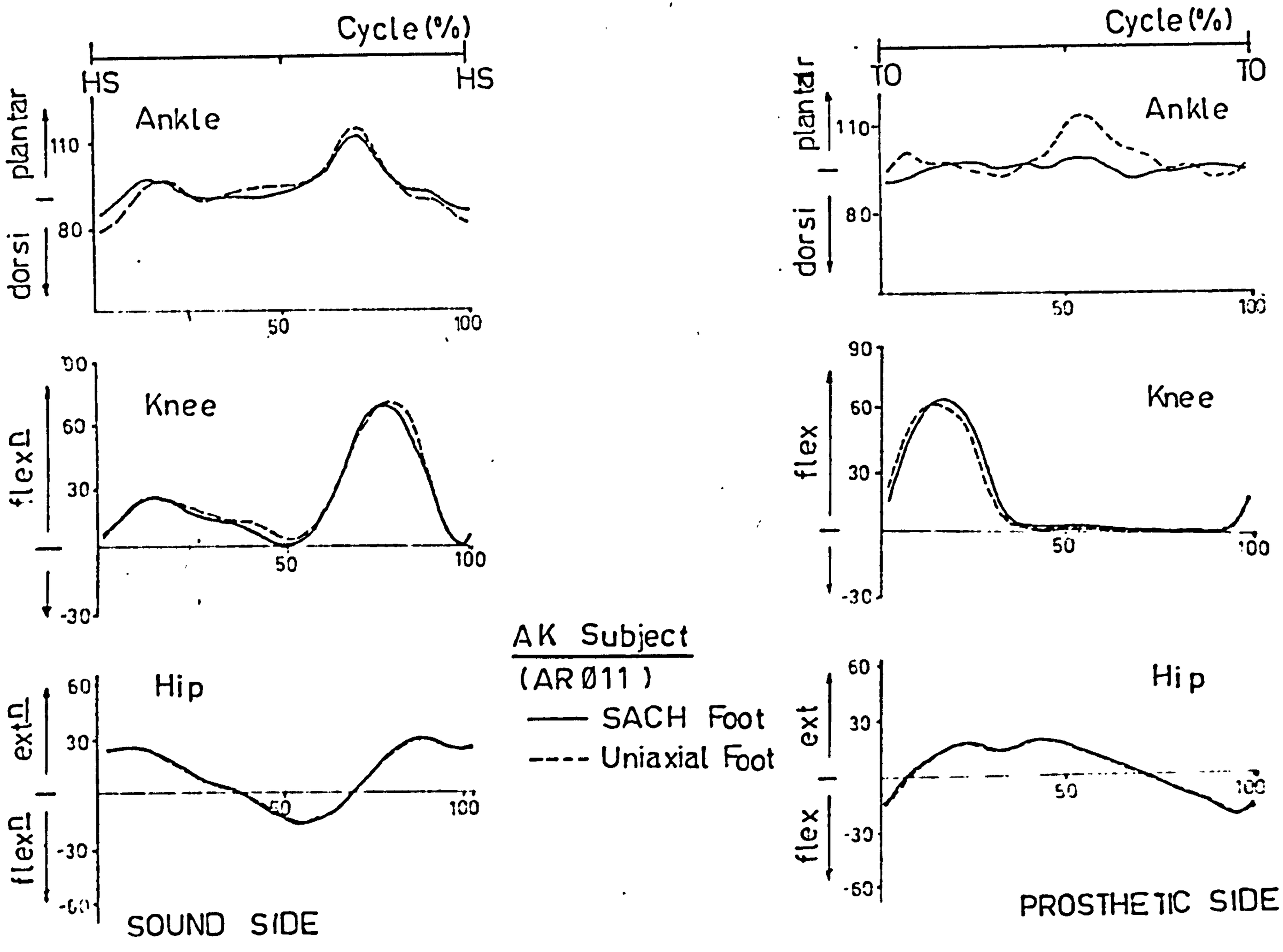

Figure 7.4.2(f) Typical Angle-Time Diagrams of Above-knee Amputee

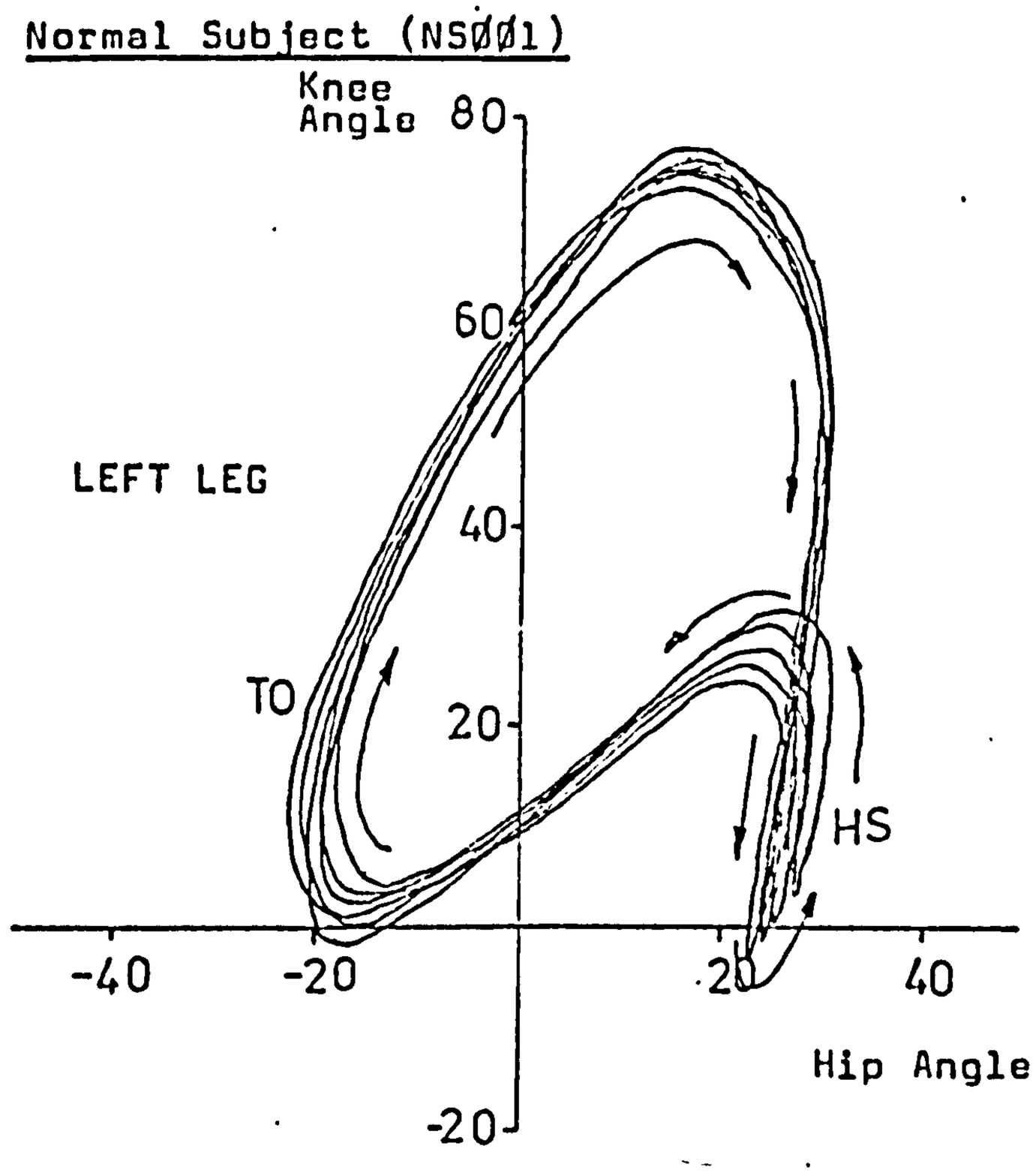

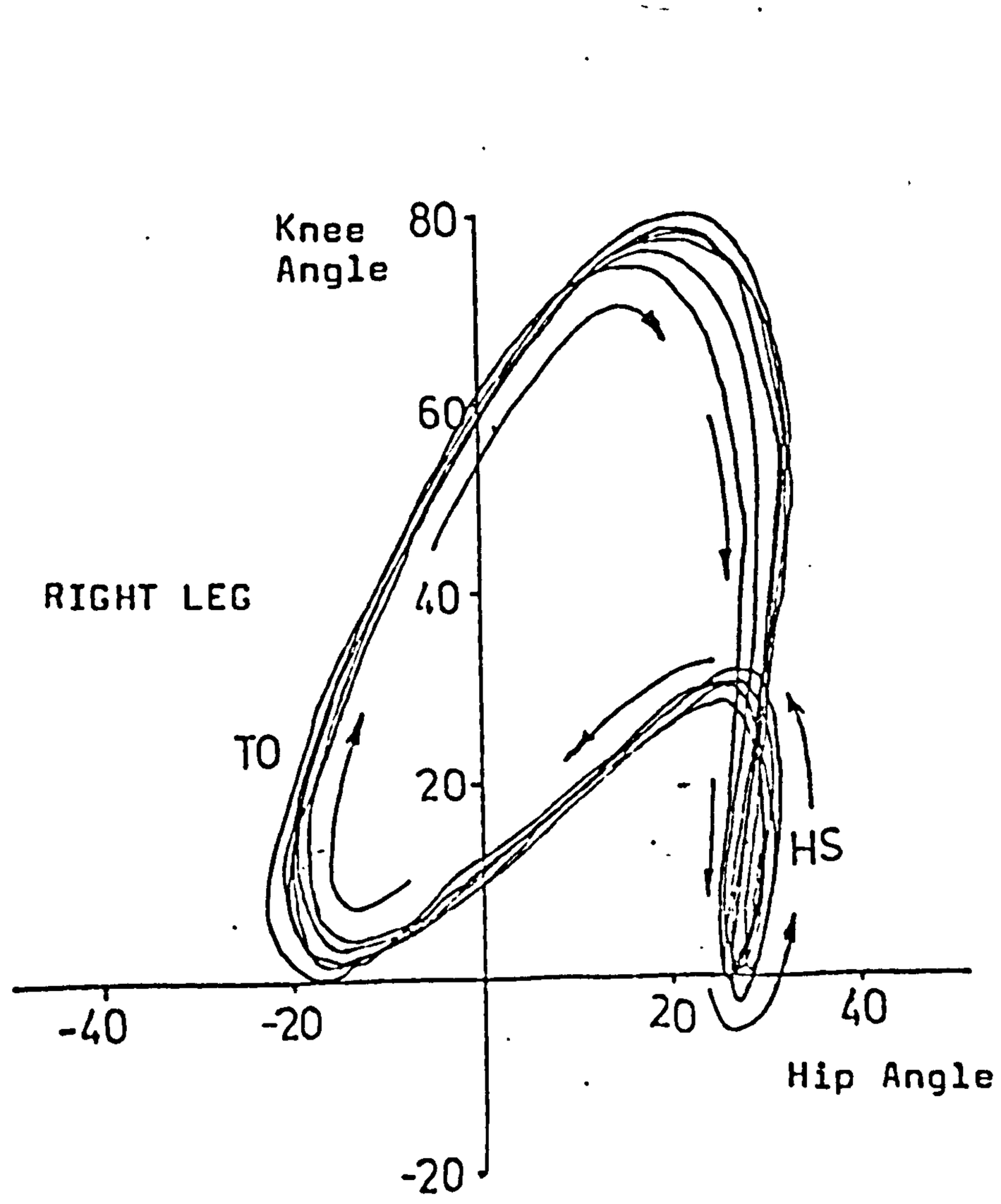

Figure 7.4.2(g) Angle-Angle Diagrams of Normal Subject

their flexion increased when they used the Uniaxial foot. The increase was approximately 6^{o}. These three amputees showed a preference for the Uniaxial foot. The hip angles on the prosthetic side showed less extension than on the sound side. Comparison between SACH and Uniaxial foot showed no significant difference in the hip angles.

Figure 7.4.2(f) shows the typical angle-time diagram of an above-knee amputee. The ankle, knee and hip angles for the sound limb have generally the same features as those of the normal subject. However all angles of mid-stance are lower, particularly at the knee level. This is probably due to "vaulting". On the prosthetic side, the knee flexion angles show significant differences. There is no knee flexion during stance phase, the prosthetic knee being fully extended and locked. Comparison between the SACH and the Uniaxial feet showed no significant difference in the angle-time diagrams of the above-knee amputees, except for the angular ankle movement on the prosthetic side, as discussed in the below-knee amputees' analysis.

Figure 7.4.2(g) shows the knee-hip angle-angle diagrams of the normal subject. The heel strike position is indicated in the figure as "HS" and following the arrow in a clockwise fashion, the knee flexion during stance is immediately evident. This knee flexion not only maintains the smoothness of gait but it also helps in shock absorption during impact. The knee then begins to extend as does the hip. The knee and hip are fully extended during late stance prior to toe-off.

During swing phase the hip and knee joints flex to carry the whole limb forward. As the swinging limb passes through mid-swing, the knee reaches its maximum flexion with the hip still flexing, after which the limb decelerates and the knee extends to brake the forward

Below-knee Subject (BR002)

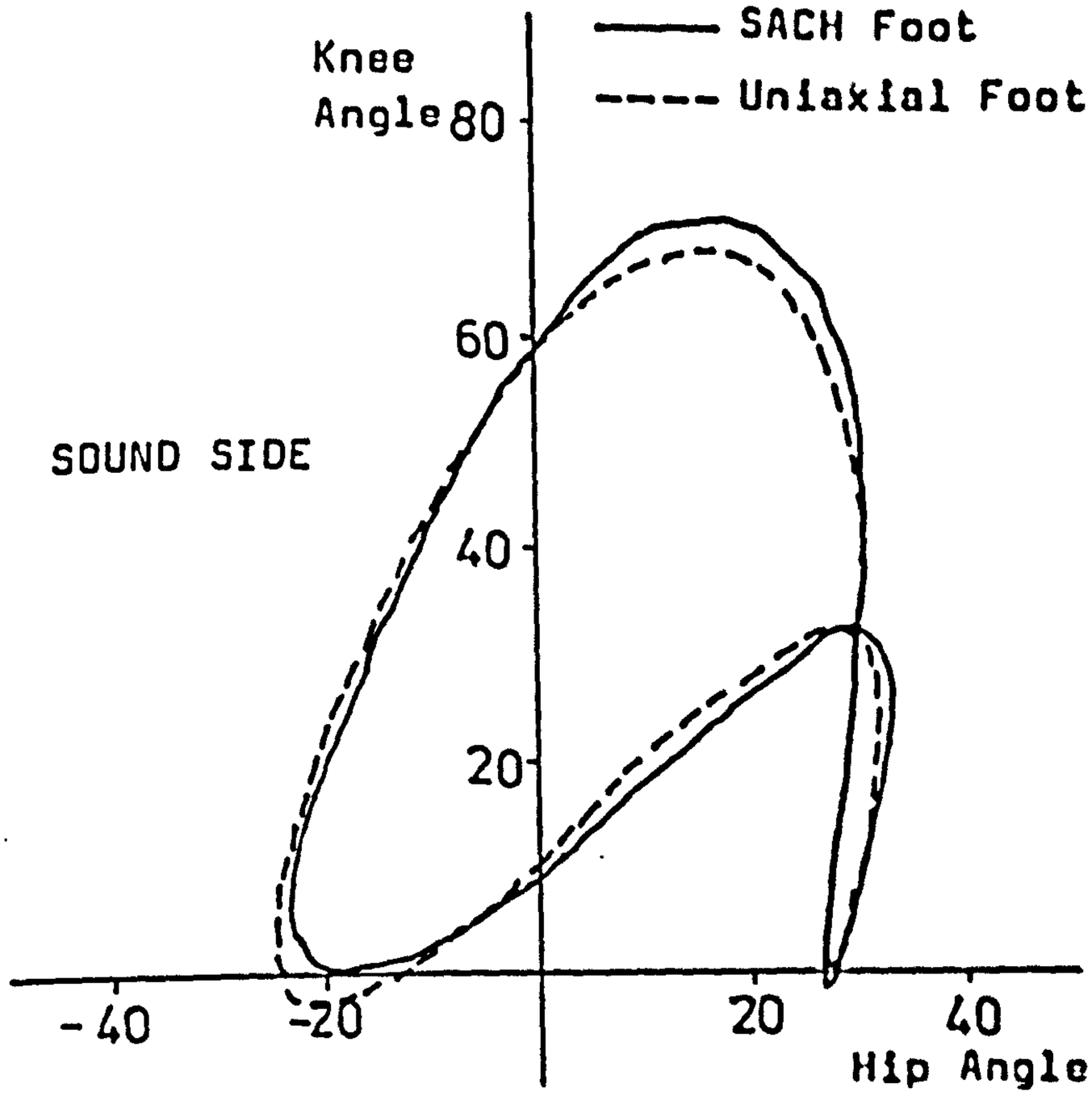

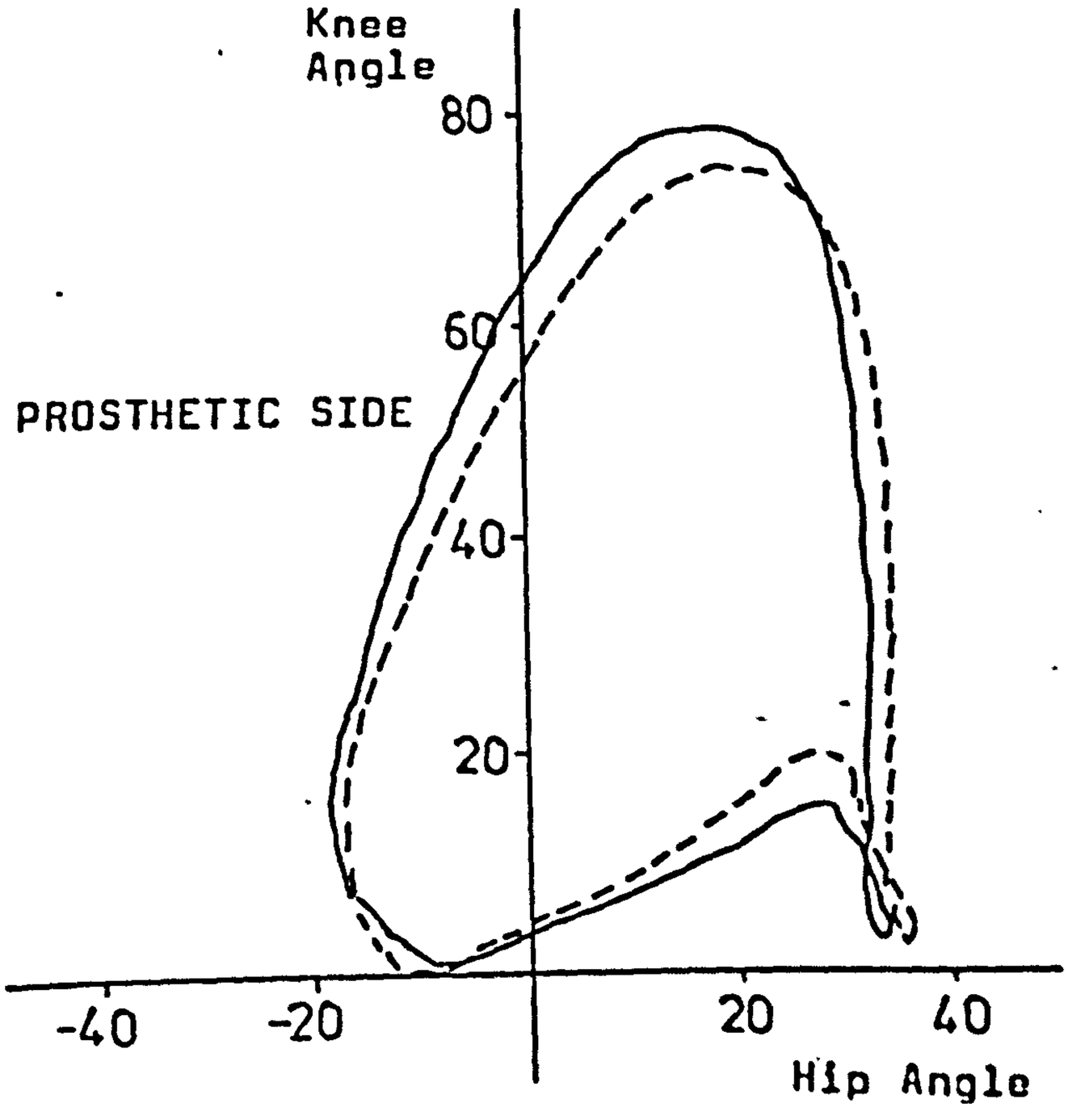

Figure 7.4.2(h) Typical Angle-angle diagrams of Below-knee Amputee

Above-knee Subject (ARØ11)

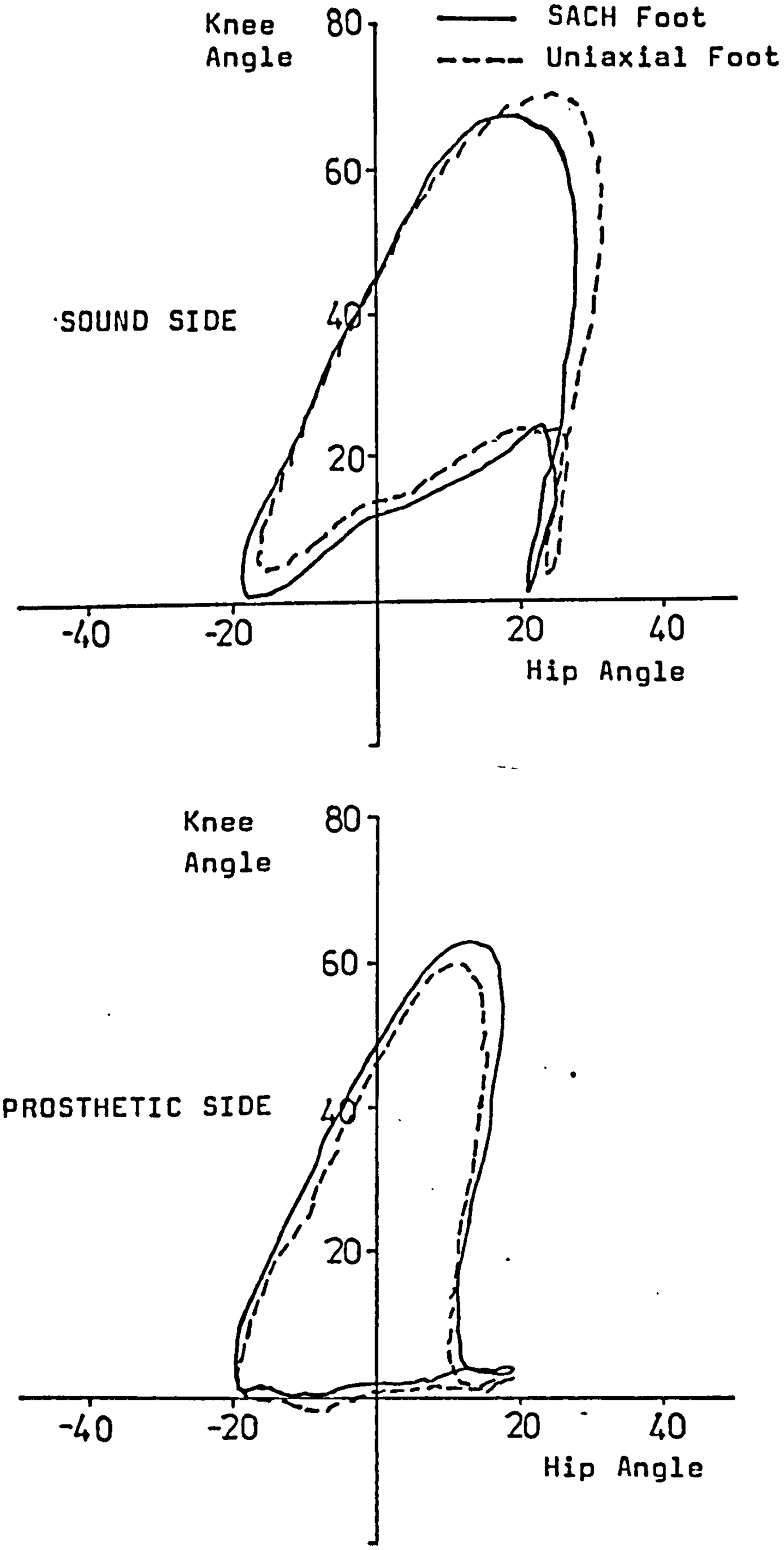

Figure 7.4.2(i) Typical Angle-angle diagrams of Above-knee Amputee

falling body at heel strike.

Figure 7.4.2(h) shows a typical angle-angle diagram of the below-knee amputee. The sound side showed a similar pattern to that of the normal subject. The prosthetic side showed a significant difference in the knee flexion during stance phase, in that it is lower than that recorded on the sound side, being approximately 12^{o} lower. This meant that the sound knee on the prosthetic side is not flexed enough to provide adequate shock absorption, although it should be noticed that the prosthetic foot has the requisite mechanism to compensate for this inadequacy. It was also observed that the late swing and early stance loop in the prosthetic side are different from those of the sound side. This suggests that the knee and hip joint motions are not as coordinated as those of the sound side, which may be due to weak muscular control in the knee because of amputation. Comparison of SACH foot and Uniaxial foot revealed that the latter produces a higher knee flexion during stance, approximately 6^{o}, in three of the six below-knee amputees. This slight difference is within the range of scatter, therefore it may not be significant.

Figure 7.4.2(i) shows a typical angle-angle diagram of the above-knee amputee. The knee-hip diagram of the sound side is on average much smaller than that of the normal subject, although the general feature is similar. The smaller magnitude in knee and hip flexion-extension is due to the amputee taking a shorter swing and a longer stance with the sound limb. Comparison between SACH and Uniaxial feet shows no significant difference. During stance phase no knee flexion is present at all. This is characteristic of all prosthetic limbs with a knee mechanism that has no provision for flexion during stance (i.e. stabilised knee unit). As the knee unit does not flex, the amputee is dependent on the heel of the

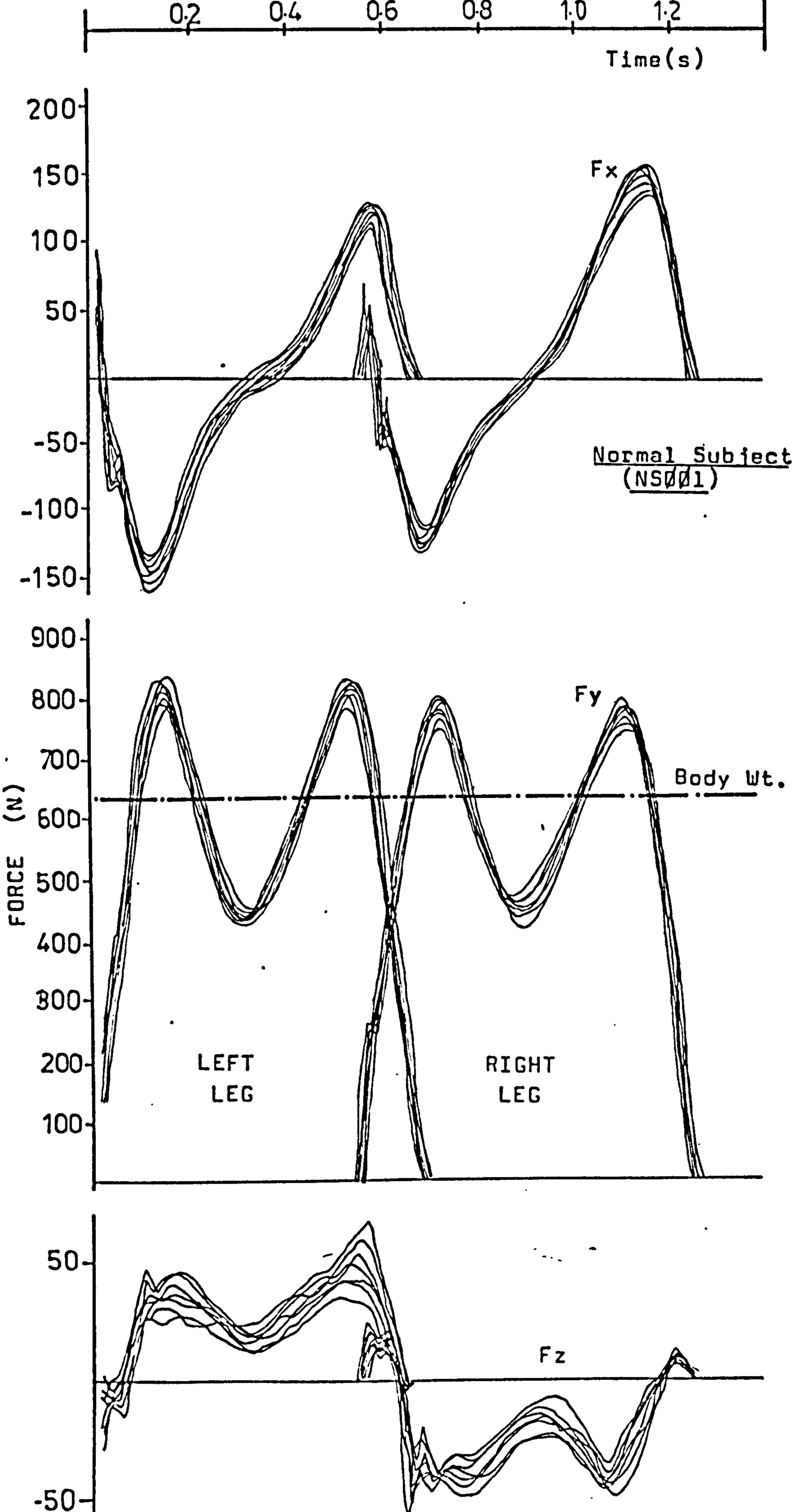

Figure 7.5.1(a) Ground-foot Forces on the Normal Subject

prosthetic foot to provide shock absorption, although some of the impact would undoubtedly be transmitted through to the stump. With the knee unit locked, the prosthetic limb pivots about the ankle joint of the Uniaxial foot or rolls over on the SACH foot. The prosthetic knee unit will begin to flex when the hip flexes prior to toe-off. The higher knee flexion on the prosthetic side is due to the long swing phase taken by the amputee. Comparison between the SACH foot and the Uniaxial foot showed no significant difference. The slight variation in magnitude is within the scatter range recorded.

7.5. Force Plate Results

7.5.1. Ground Reaction Data

Figure 7.5.1(a) shows the ground reaction data of a normal subject. The figure consists of the left and right force plate data obtained simultaneously. Altogether twelve sets of results are presented. The shapes of the curves are consistent with those reported by other investigators e.g. Cunningham (1950) and Paul (1967). The scatter in the fore and aft shear (Fx) was observed to be in the region of 17% (measured at the maximum values), for the vertical force (Fy) it is 6% and the lateral force (Fz) is approximately 38 percent. This range of scatter compared more favourably than that presented by Cunningham (1950), his results showed scatter of about 30% for Fx and Fy, and 60% for Fz. This larger scatter could be due to the less precise instrumentation used. The generally larger scatter of Fz is because the values obtained are very much lower.

The normal individual was tested on the same day twelve times. The source of scatter is from step to step variation. This comes in the form of different walking

	Left Leg		Right Leg	
	Average Values in Newtons (±1 S.D.)	Percent of body Weight (%)	Average Values in Newtons (±1 S.D.)	Percent of body Weight (%)
FX-Max.	122,7(10.9)	19	142.3(12.1)	22
-Min.	-143.4(14.8)	22	-130.2(7.8)	20
FY-1st Peak	797.1(23.9)	124	782.2(18.0)	122
Dip	439.2(24.7)	69	459.4(19.8)	72
2nd Peak	802.4(20.7	125	779.4(18.2)	122
FZ-Max	51.0(9.9)	8	-46.5(8.6)	7

Table 7.5.1(a) Maximum and Minimum Forces of Normal Subject

speeds and step lengths, both of which are very difficult to control accurately without affecting each other and also other physiological and psychological parameters.

The shapes of the three orthogonal forces recorded for the contralateral sides are similar, although the magnitudes are slightly different. Table 7.5.1(a) shows the average maximum and minimum values of these forces for the twelve test runs.

Figure 7.5.1(b) shows typical ground reaction data of a below-knee amputee. The shapes of the three orthogonal forces on the sound limb are similar to those of the normal subject. However, the magnitude in terms of percentage body weight is different. Table 7.5.1(b) shows the average maximum and minimum values of the ground reactions of the six below-knee amputees. Altogether 40 test walks were analysed.

The maximum Fx for the sound limb with either the SACH or Uniaxial foot is larger than that of the normal subject. This could be due to the compensatory action of the sound limb to overcome the deficient prosthetic ankle in order to maintain an approximately similar walking speed as that of the normal subject. The magnitudes of the fore and aft shear (Fx) on the prosthetic side are very much lower than those of the sound limb. The low positive value at late stance is an indication of the reduced push-off due to the absence of active plantar-flexion. The shape of the Fx curves during mid-stance is significantly different between the sound and prosthetic limbs. The sound limb, like that of the normal subject, transfers the weight from the heel to the ball of the foot continuously and smoothly. However, on the prosthetic side, the transition is neither continuous nor smooth. Comparison between SACH and Uniaxial foot showed a slightly different pattern of Fx at this transitional period as well,

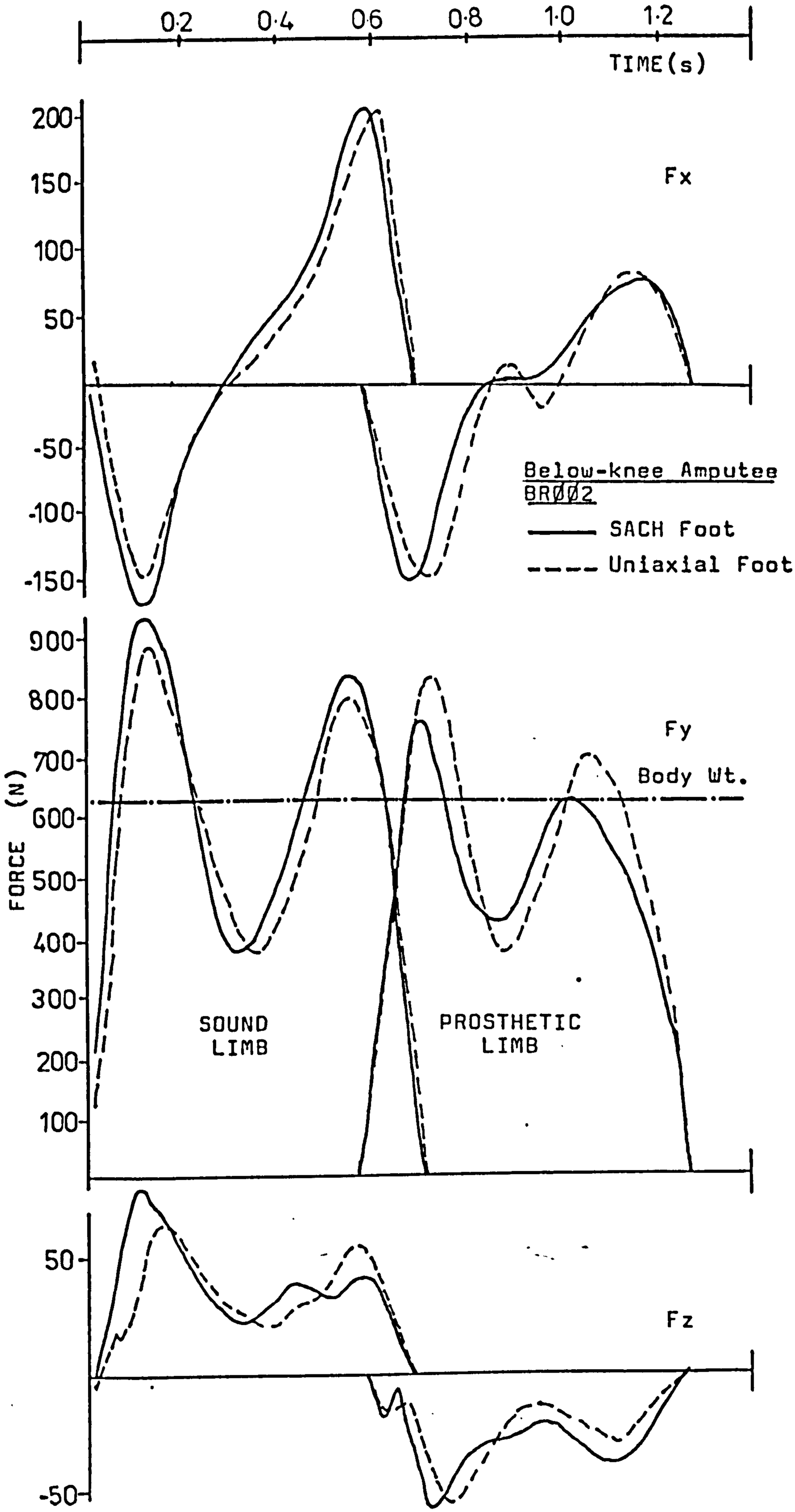

Figure 7.5.1(b) Typical Ground-Foot Forces acting on the Below-knee Amputee

suggesting that the working mechanism of both feet during this period is different. The abrupt transition of the Uniaxial foot is due to the initial restraining action of the dorsi-flexion stop. With the SACH foot, due to the rigid ankle and rocker-shaped wooden keel, the transition is slightly smoother. The average difference in Fx during this transition period between the SACH and Uniaxial feet is relatively small, approximately 15N. None of the below-knee amputees made any comment relating to this event; apparently the magnitude of the force is insignificant.

The magnitudes of the vertical force (Fy) on the prosthetic side are lower than those of the sound side. Comparison between SACH and Uniaxial foot showed that with the latter,the forces are more evenly distributed between the sound and prosthetic limbs. Results obtained from two other below-knee amputees showed a third peak during mid-stance on the prosthetic side with the SACH foot. The magnitude of this additional peak is about 85% body-weight. These two amputees had previously expressed that "roll-over" with Uniaxial foot was slightly better than with the SACH foot.

The lateral shear (Fz) of the sound limb is slightly larger than that of the normal subject. The difference is not significant when compared with the range of scatter recorded for this variable. On the prosthetic side, the Fz value is similar to that of the normal subject. A comparison between SACH and Uniaxial foot, as expected, showed no significant changes in the Fz of both the sound and prosthetic limb.

Figure 7.5.1(c) shows the typical ground reaction data of an above-knee amputee. The shapes and magnitudes of the three othrogonal forces of both the sound and prosthetic limbs are different from those of the normal

	Sound Leg		Prosthetic Leg	
	SACH	Uniaxial	SACH	Uniaxial
FX - Max	27.5	26.0	13.2	13.8
- Min	22.3	20.7	16.5	18.8
FY - 1st Peak	134.5	132.5	123.5	129.2
- Dip	69.3	69.7	75.3	73.8
- 2nd Peak	117.3	115.2	104.8	106.0
FZ - Max	10.2	9.2	8.3	8.2

All values are in percent of body weight

Table 7.5.1(b) Average maximum and minimum forces of six below-knee amputees

subject. Table 7.5.1(d) shows the average maximum and minimum mangitudes of the ground reactions of five above-knee amputees. Altogether 56 test walks were analysed.

The fore and aft shear (Fx) on the sound side shows an initial spike. This occurs just before foot flat at 0.04s. The reason for this spike is not clear. No unusual feature was observed from the kinematic data during this period. The Fx magnitudes of the sound limb are fairly similar to those of the normal subject. Comparison between SACH and Uniaxial foot showed no significant difference.

The vertical force (Fy) of the sound limb also shows a spike on the rise curve similar to that being described in the Fx curve. The slower walking speed and longer stance phase on the sound limb of the above-knee amputee produce a trough not as deep as that of the normal subject,approximately 10% of body weight higher. Another outstanding feature in the Fy curve of the sound limb that is significantly different from the normal subject, is the additional peak during mid-stance. This is due to the elevation of the centre of gravity of the body through "vaulting". This action is usually performed to compensate for the absence of knee and ankle control on the prosthetic side, to give sufficient clearance for the prosthetic limb to swing through without stubbing the toe, although, with proper alignment of the prosthesis sufficient clearance can be achieved without these deviations. However, amputees have been found to have this deviation in their gait out of habit and a feeling of insecurity. Comparison between the SACH and Uniaxial foot shows no significant difference. The shapes of these curves are different from those of the below-knee amputee. This is because the below-knee amputee still has the use of the intact knee to allow the prosthesis to perform in a fashion similar to that of the

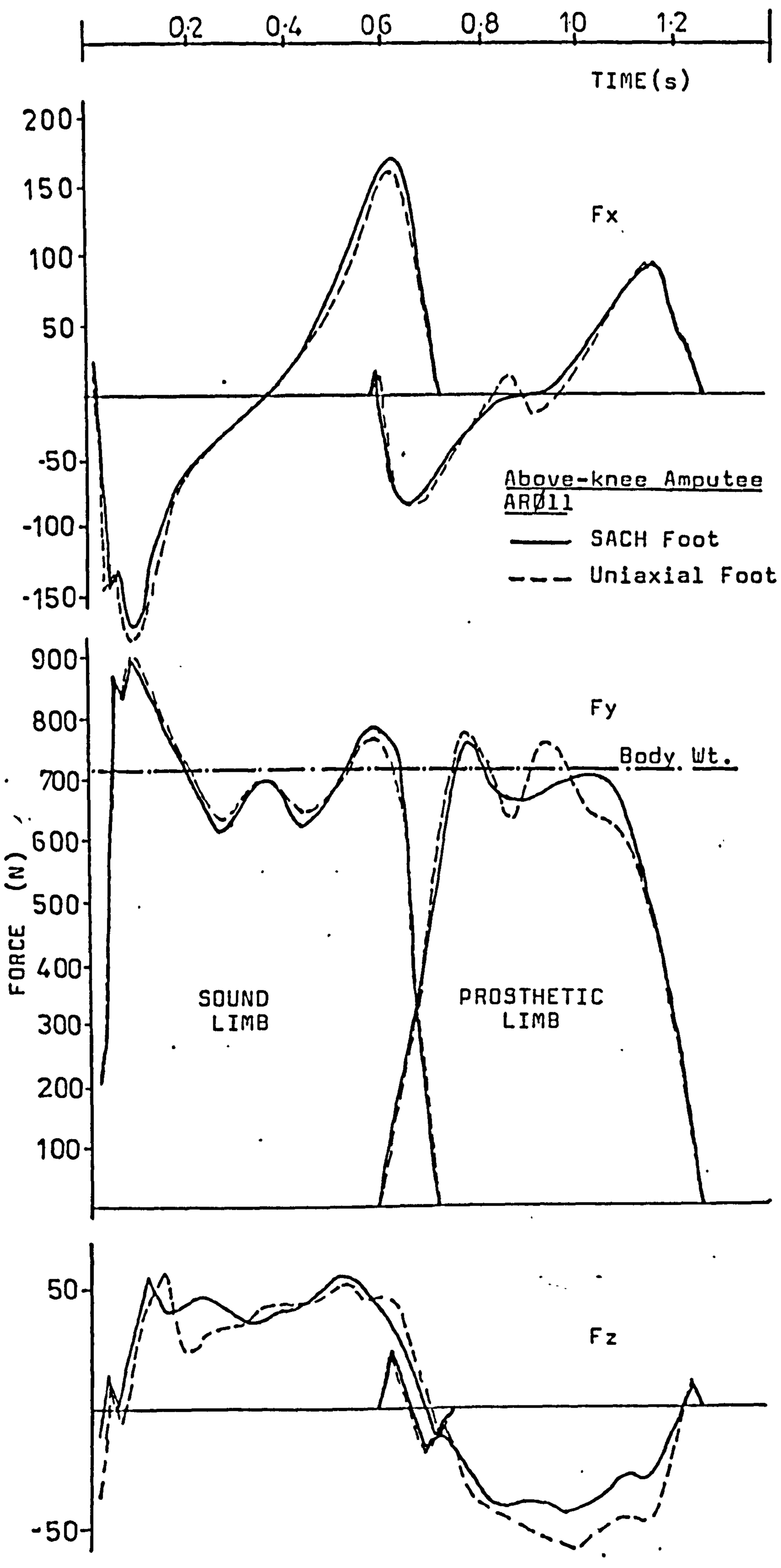

Figure 7.5.1(c) Typical Ground-Foot forces acting on the Above-Knee amputee

normal limb.

Comparison between SACH and Uniaxial foot shows distinct differences in the Fy curves, although the SACH foot shows the typical two peaks of the "normal" Fy curve, the second peak tends to be spread broadly over late stance. This is due to the rolling action provided by the ball of the SACH foot as the amputee rolls over with the fully extended prosthesis. The Uniaxial foot also shows two peaks in the Fy curve, except that the second peak occurs soon after mid-stance and then drops down to a step before the final decline. This could be due to the dorsiflexion stop being too stiff for the above-knee amputees, therefore resisting dorsiflexion and forcing heel rise to occur sooner than required. This then leads to an earlier roll over on the ball of the Uniaxial foot, thus producing the second peak soon after mid-stance. At late stance, the prosthetic knee is still fully extended and locked, therefore the foot is still loaded as evident from the Fy curve.

The design of the distal section of the Uniaxial foot is different from that of the SACH foot. The Uniaxial foot does not seem to have the rocker-type shape, and furthermore, the wooden keel is much shorter at the distal section, see Figure 5.2(b). Therefore, unless the dorsiflexion stop functions properly, the shape of the distal section of the Uniaxial foot could be part of the reason for the lack of smoothness in the curve. Unfortunately, the stiffness of the dorsiflexion stop in the type of Uniaxial foot used in the experiments cannot be changed. One method of overcoming the problem is to change the alignment of the prosthesis. However, there is a limit in making alignment adjustment. Only in one case, was it possible to give a satisfactory result through alignment changes. A typical two-peak Fy curve was obtained, in which the amputee subject commented that

	Sound Leg		Prosthetic leg	
	SACH	Uniaxial	SACH	Uniaxial
FX - Max	23.2	20.6	10.8	11.6
Min.	22.0	24.0	9.4	9.8
FY - 1st Peak	128.4	128.8	104.6	105.0
Min. Dip	79.6	81.0	87.2	85.6
2nd Peak	87.4	86.5	96.2	100.6
3rd Peak	117.2	116.6	-	-
FZ - Max.	9.0	9.8	8.4	9.2

All Values are in percent of body weight

Table 7.5.1(c) Average maximum and minimum forces of five above-knee amputees

the roll-over was slightly better than that of the SACH foot.

It seems therefore that provision must be made for the selection of a suitable stiffness of dorsiflexion stop in the Uniaxial foot, especially when prescribing for above-knee amputees. Furthermore, the distal section of the Uniaxial foot may require reconsideration.

The lateral shear (Fz) on the sound limb has similar maximum magnitudes to those of the below-knee amputees' sound limb, except that the shape is slightly different. Almost the same amount of Fz is applied throughout the stance phase. The shape of the Fz curve on the prosthetic side is also different. It is more rounded and reaches its maximum magnitude at about mid-stance. A comparison between SACH and Uniaxial feet shows no significant difference in the Fz of both the sound and prosthetic limbs.

The magnitudes of the fore and aft shear (Fx) and also the vertical force (Fy) on the prosthetic side are very much lower than those of the below-knee amputees' prosthetic limb. This is due to the slower speed of walking of the above-knee amputees and also the generally lower inertial effects of their prostheses.

The Fx curves on the prosthetic side are similar in shape to those of the below-knee amputees' prosthetic limb. The lower magnitude in the braking force is due to the reasons given above as well as the low deceleration of the prosthesis when it makes contact with the ground. Comparison between the SACH and Uniaxial feet revealed the same difference found in the Fx curve of the below-knee amputees' prosthetic side.

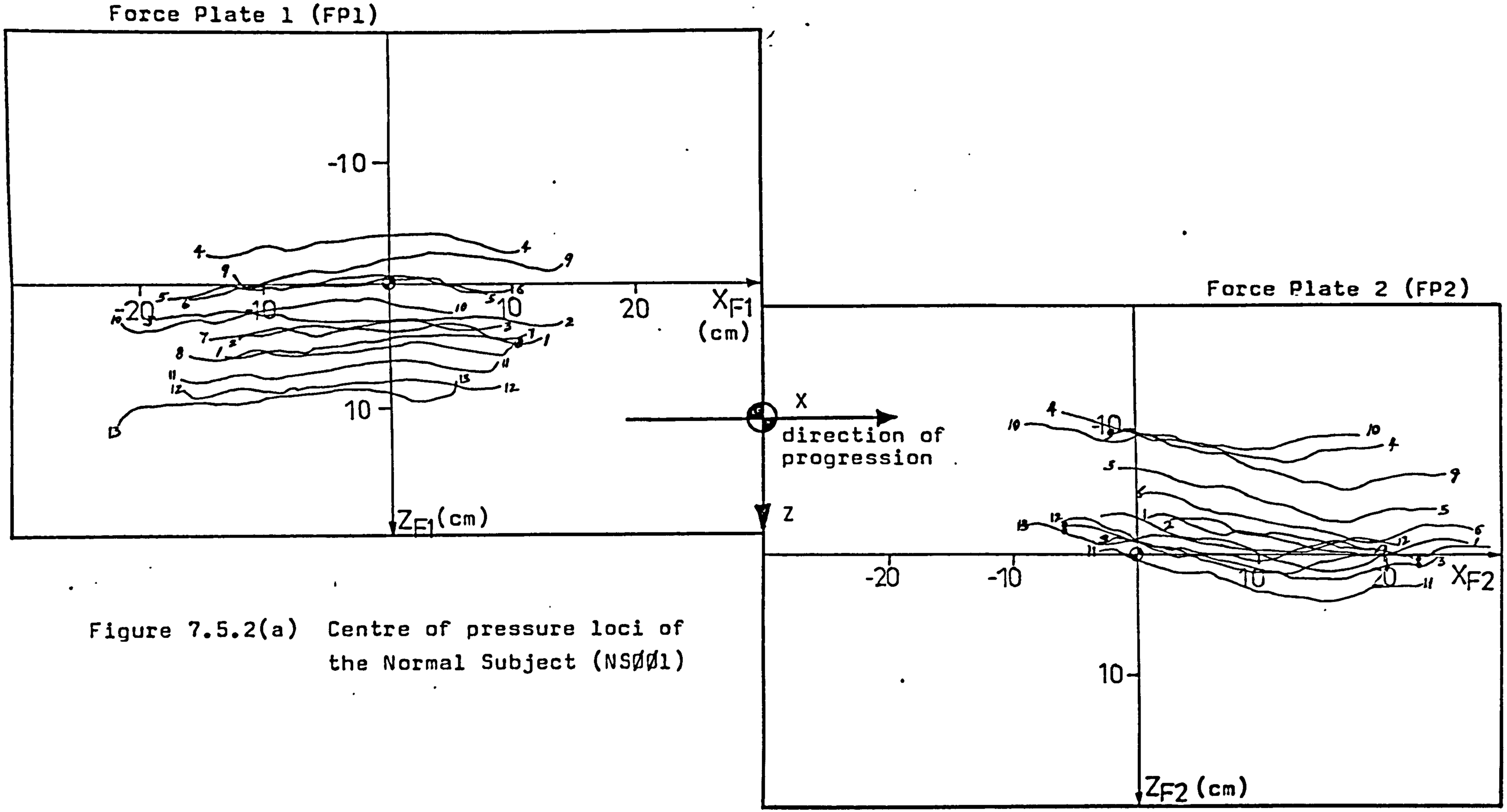

Figure 7.5.2(a) Centre of pressure loci of the Normal Subject (NSØØ1)

7.5.2. Centre of Pressure Plots

Figure 7.5.2(a) shows the traces of the centre of pressure recorded for a normal subject. All the lines shown are within the specified boundary of the force plates for accurate recording of the ground reactions.

The length of the centre of pressure line is dependent upon the length of the foot and also the manner in which the subject uses his foot during walking. For the normal subject tested, the length of the centre of pressure line of the left foot was 27.1cm (±0.4) and of the right foot, it was 26.2cm (±0.9). It is difficult however to quantify the centre of pressure by looking at its displacement display only. Another method used in describing the centre of pressure is by displacement-time diagram.

Figure 7.5.2(b) shows the displacement-time plot of the centre of pressure of the normal subject. The origin of the diagram was chosen to be at the mean of the centre of pressure points because it is a much more consistent position. Furthermore, only the absolute displacements of the centre of pressure points relative to the origin are plotted. In doing this, the plot gives a characterisitc shape, like that of the alphabet letter "V". It is also recognised that in choosing the origin, the time axis has to be re-organised. A time index is used in place of the real time scale and a negative time index stands for a time and position before the origin. The vertical axis of the diagram is normalised in terms of the length of the centre of pressure line.

The shapes of the curves on both legs of the normal subject are fairly similar. The left hand slope of the curve represents the rate at which the C.P. points progress towards the origin, while the right hand slope

Normal Subject (NSØØ1)

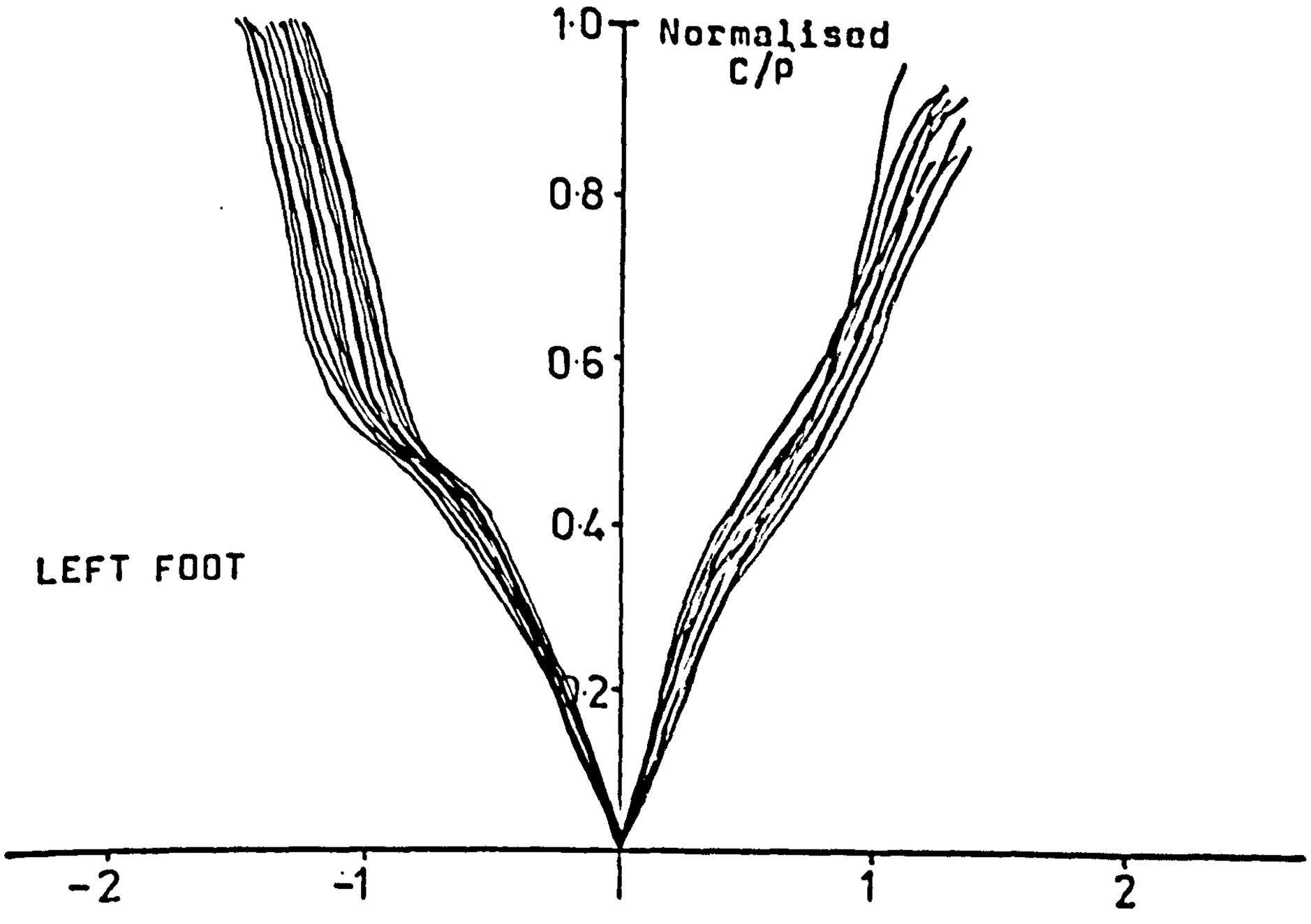

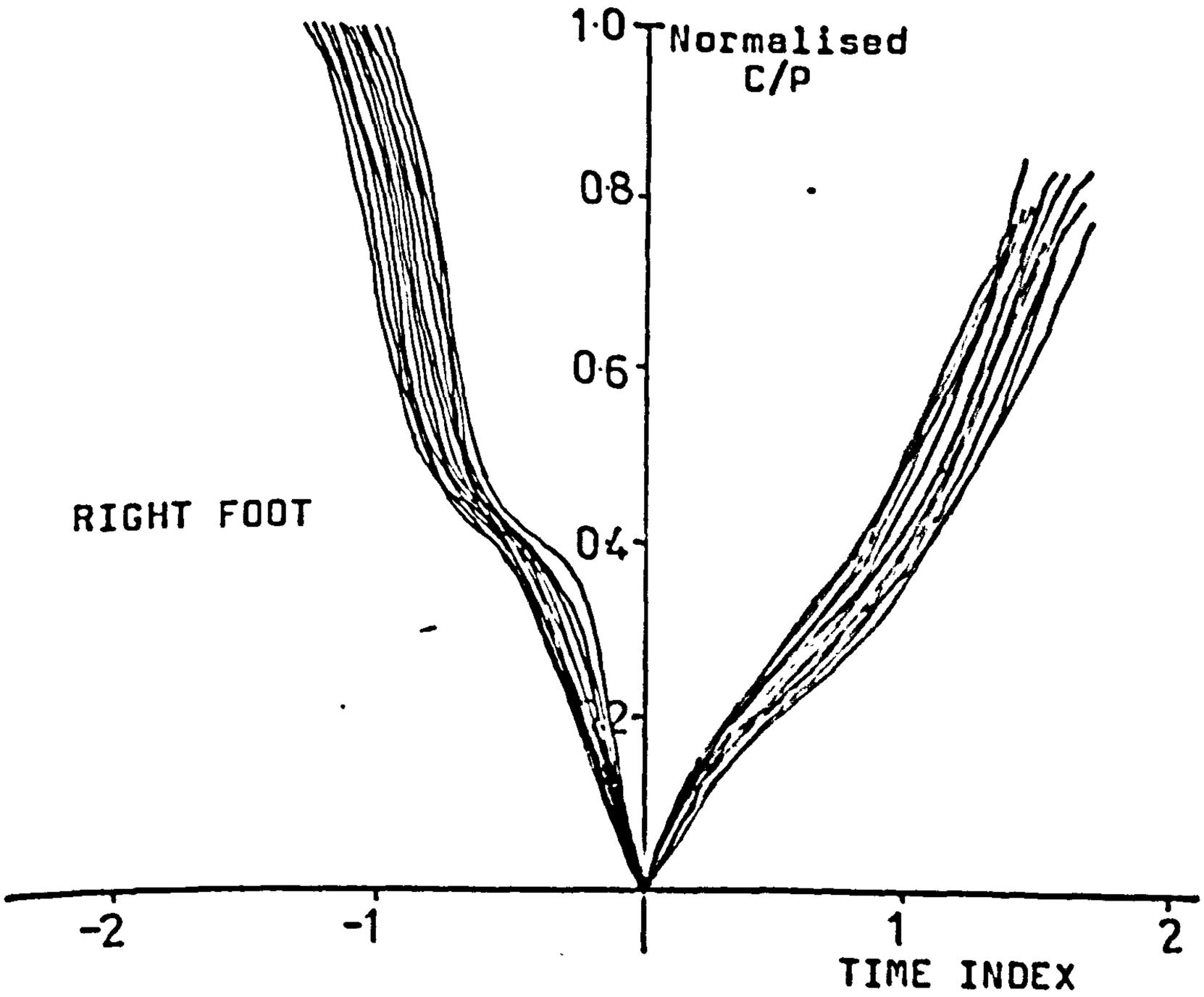

Figure 7.5.2(b) "V" Plots of the Normal Subject

Below-knee Subject (BR002)

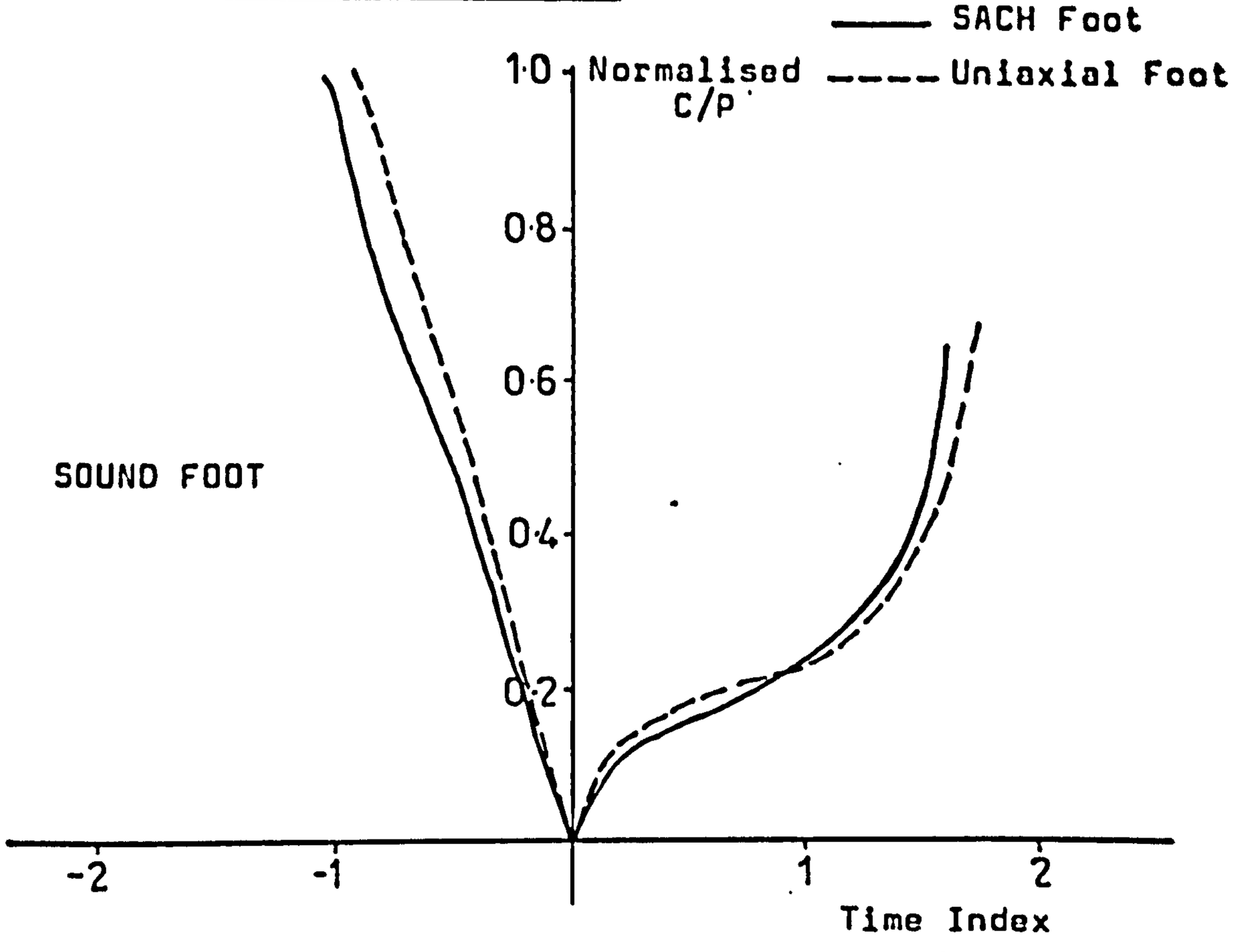

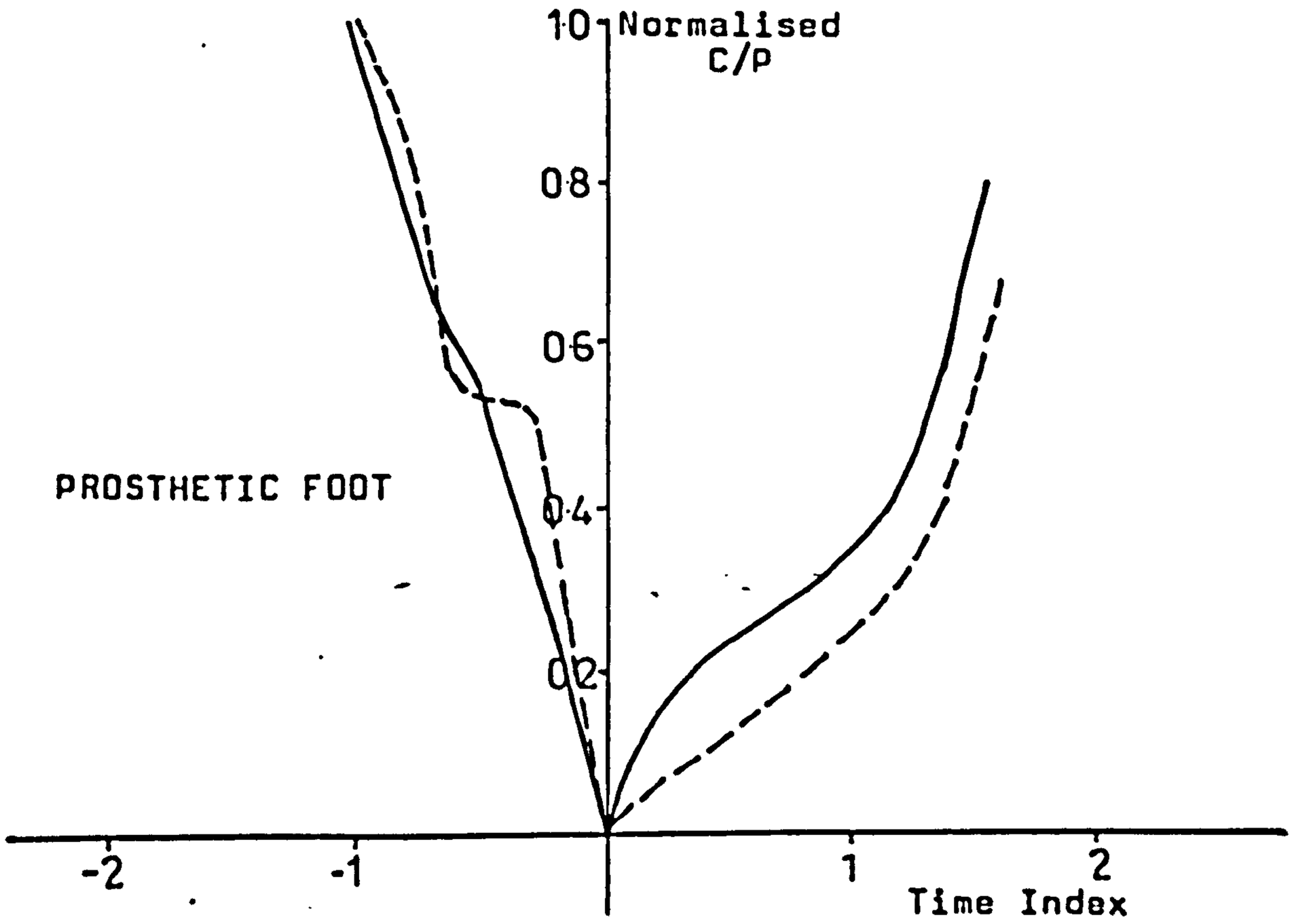

Figure 7.5.2(c) Typical "V" plots of Below-knee Amputee

gives the rate at which the C.P. points travel away from the origin. Note that the centre of pressure points only progress when the body is moving forward during stance phase. Therefore, further description of the centre of pressure progression is with reference to the moving foot.

For the normal subject, the centre of pressure initially progresses at about 6 units/s (i.e. 6 times the length of the centre of pressure length per second) towards the origin until foot-flat. Then the progression slows down to 1.5 units/s for about 0.08s before rising to 3 units/s towards the origin. The centre of pressure then travels away from the origin at a rate of 3 units/s.

Figure 7.5.2(c) shows the typical "V" plots of a below-knee amputee. For the sound limb, the rate of progression of the C.P. towards the origin is 4.5 units/s. Unlike the pattern of the normal individual, there is no slowing down of the progression. However, as it moves away from the origin, the rate of progression slows down to 0.8 unit/s. As it passes over the ball of the foot, the rate of progression rises to 6 units/s towards toe-off. The slowing down of the progression over the ball of the foot on the sound side is to allow the amputee to achieve control on the prosthetic side during early stance. Comparison of the SACH and Uniaxial feet shows no significant difference.

The "V" plots on the prosthetic side show a significant difference between the SACH and the Uniaxial foot. The rate of progression towards the origin with the SACH foot is 4.5 units/s; this drops to 1.7 unit/s for 0.04 s and then proceeds again at 4.5 units/s towards the origin. As for the Uniaxial foot, it progresses at 4.5 units/s to foot-flat and then drops to 0.3 unit/s for 0.12s before finally rising to 7.2 units/s towards the origin.

Above-knee Subject (AR011)

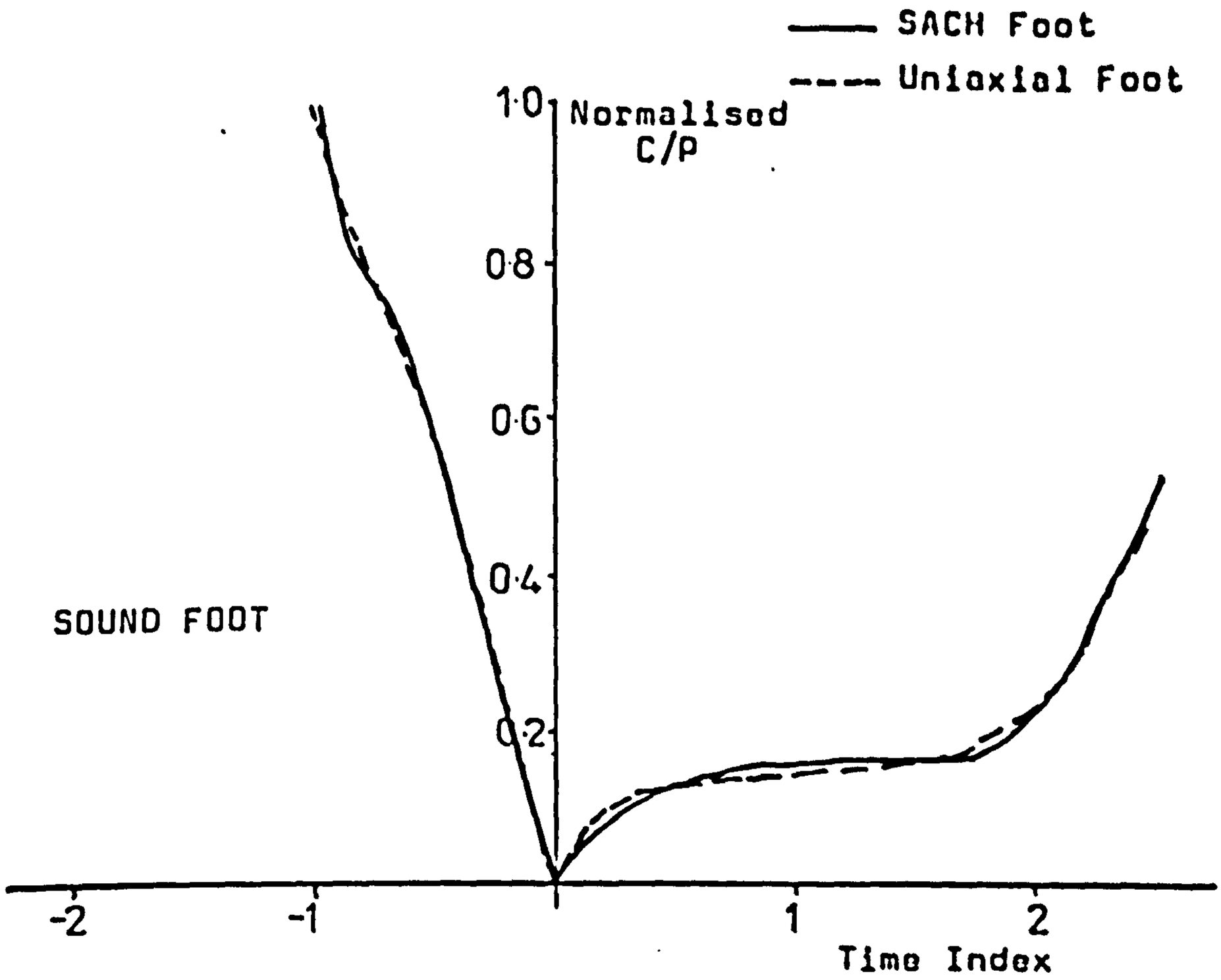

Figure 7.5.2(d) Typical "V" plots of Above-Knee Amputee

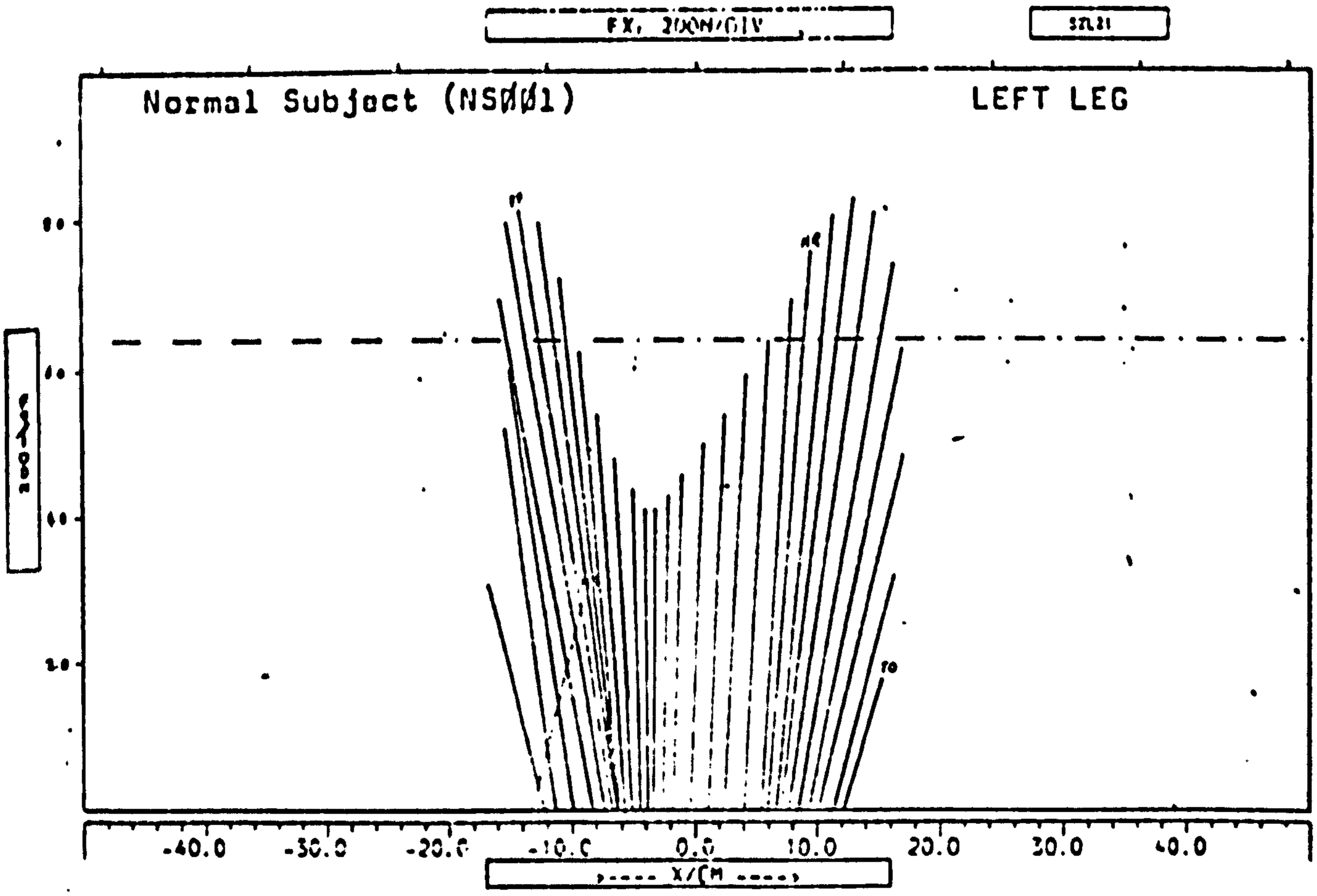

Figure 7.5.3(a) Typical Force Vector Diagram in X-Y Plane of the Normal Subject (NSØØ1)

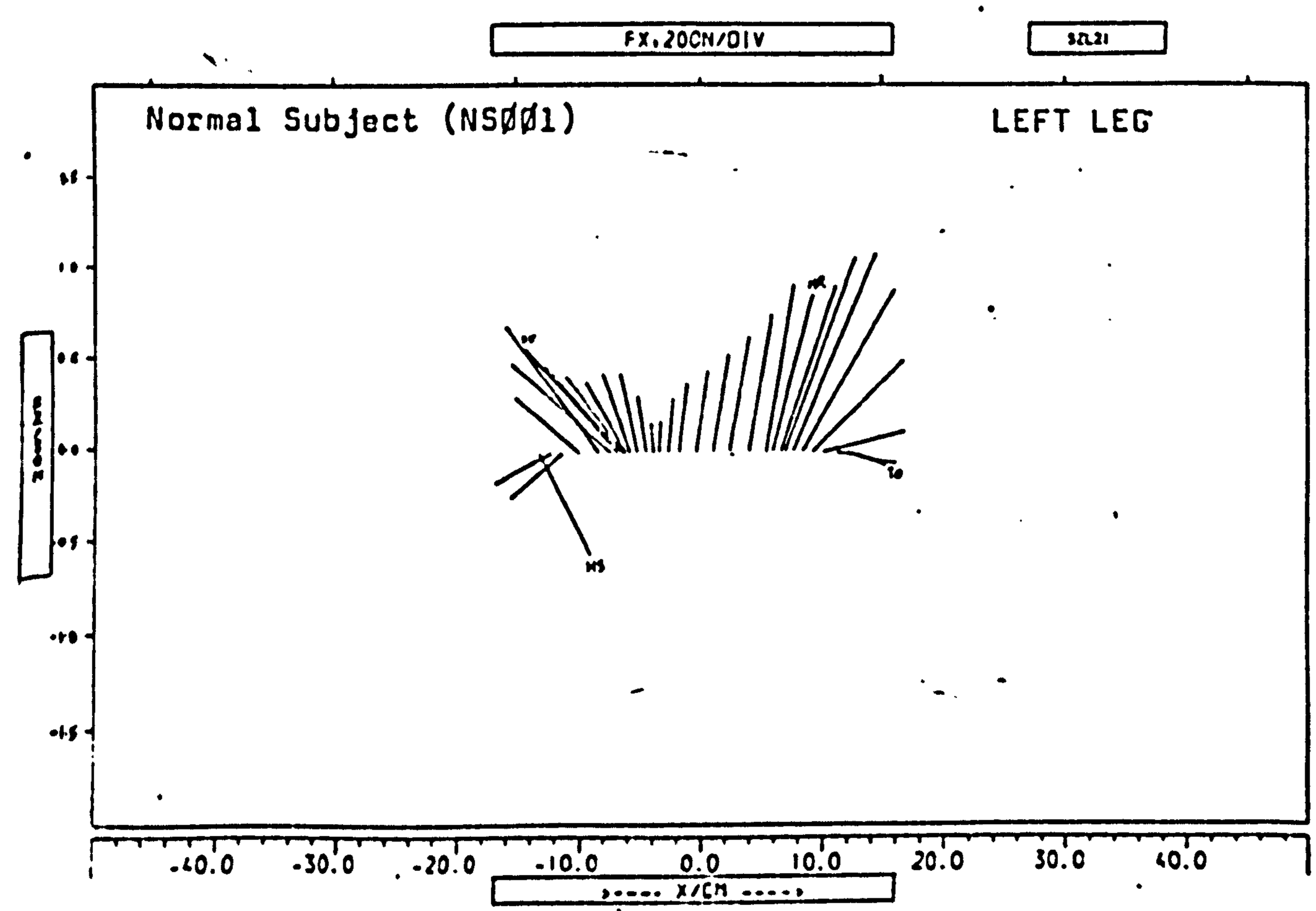

Figure 7.5.3(b) Typical Force Vector Diagram in X-Z Plane of the Normal Subject (NSØØ1)

The slowing down of the rate of progression to such a low value is due to the pivoting of the prosthetic limb about the hinge joint before it comes into contact with the dorsiflexion stop.

The rate of progression away from the origin is similar for the two prosthetic feet, moving gradually over the ball of the foot at 1.0 unit/s before rising to 4.7 units/s towards toe-off.

Figure 7.5.2(d) shows the typical "V" curves of the above-knee amputee. The rate of progression of the sound limb towards the origin is similar to that of the sound side of the below-knee amputee. However, the above-knee amputee moves away from the origin at a very low rate; 0.1 unit/s for 0.35 s before rising to 2.7 units/s towards toe-off. This long period of low progression rate is due to the vaulting action of the amputee during stance phase. Comparison between the SACH and Uniaxial feet shows no significant difference.

The "V" plots of the prosthetic side again show similar differences to those observed in the case of the below-knee amputee. The slowing down period on both prosthetic feet is slightly longer than that recorded for the below-knee amputee. This is because the above-knee amputee walks with a slower speed.

7.5.3. Force Vector Diagrams

Figure 7.5.3.(a) shows a typical force vector or "Butterfly" diagram in the sagittal plane of the left leg of a normal subject and Figure 7.5.3(b) shows the corresponding force vector diagram in the X-Z plane. The wide scatter range in Fz, which was discussed previously, was also manifested in this X-Z plane force vector diagram. However, in the normal it showed a consistent

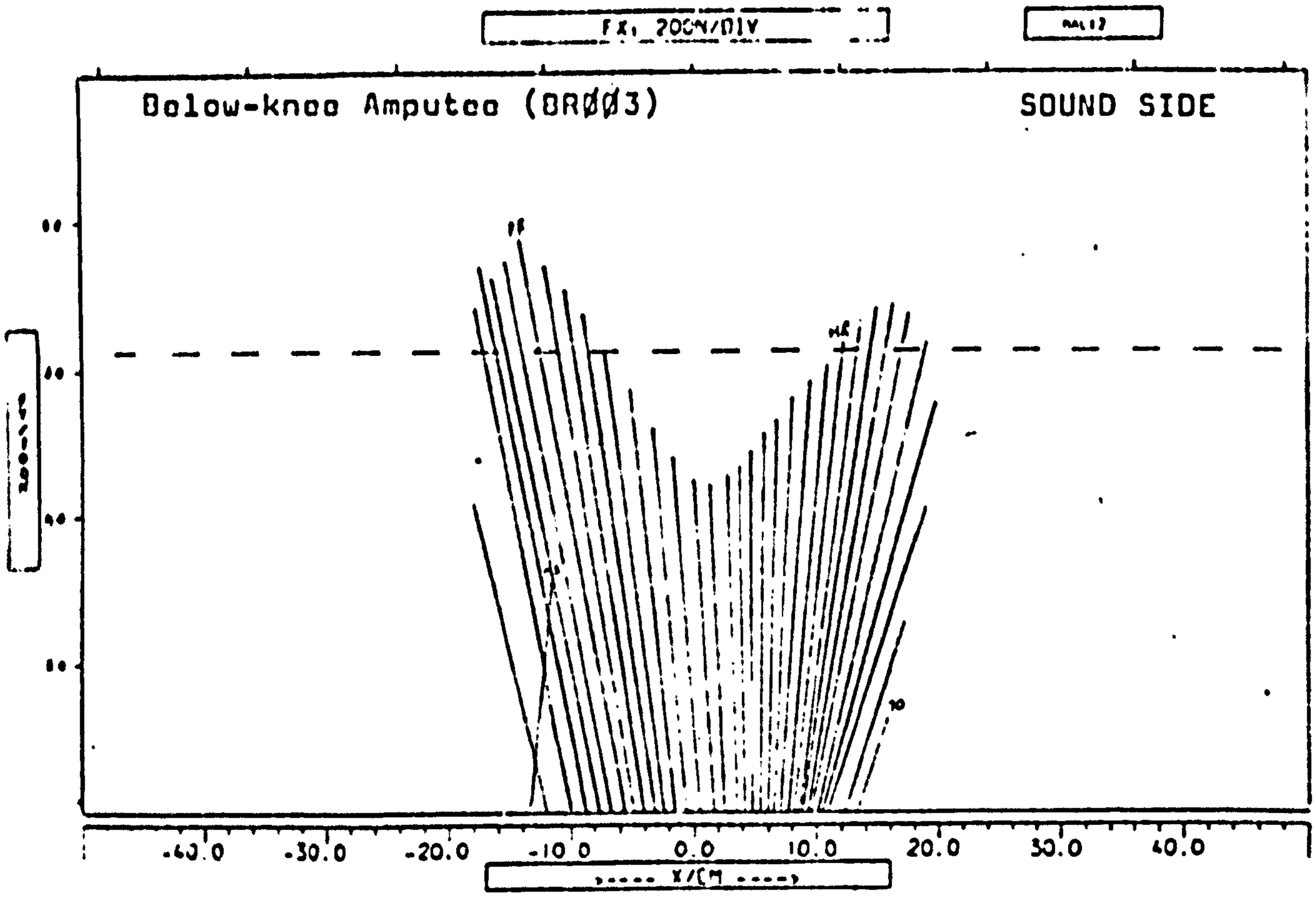

Figure 7.5.3(c) Typical Force Vector Diagram in X-Y Plane of Below-knee Amputee

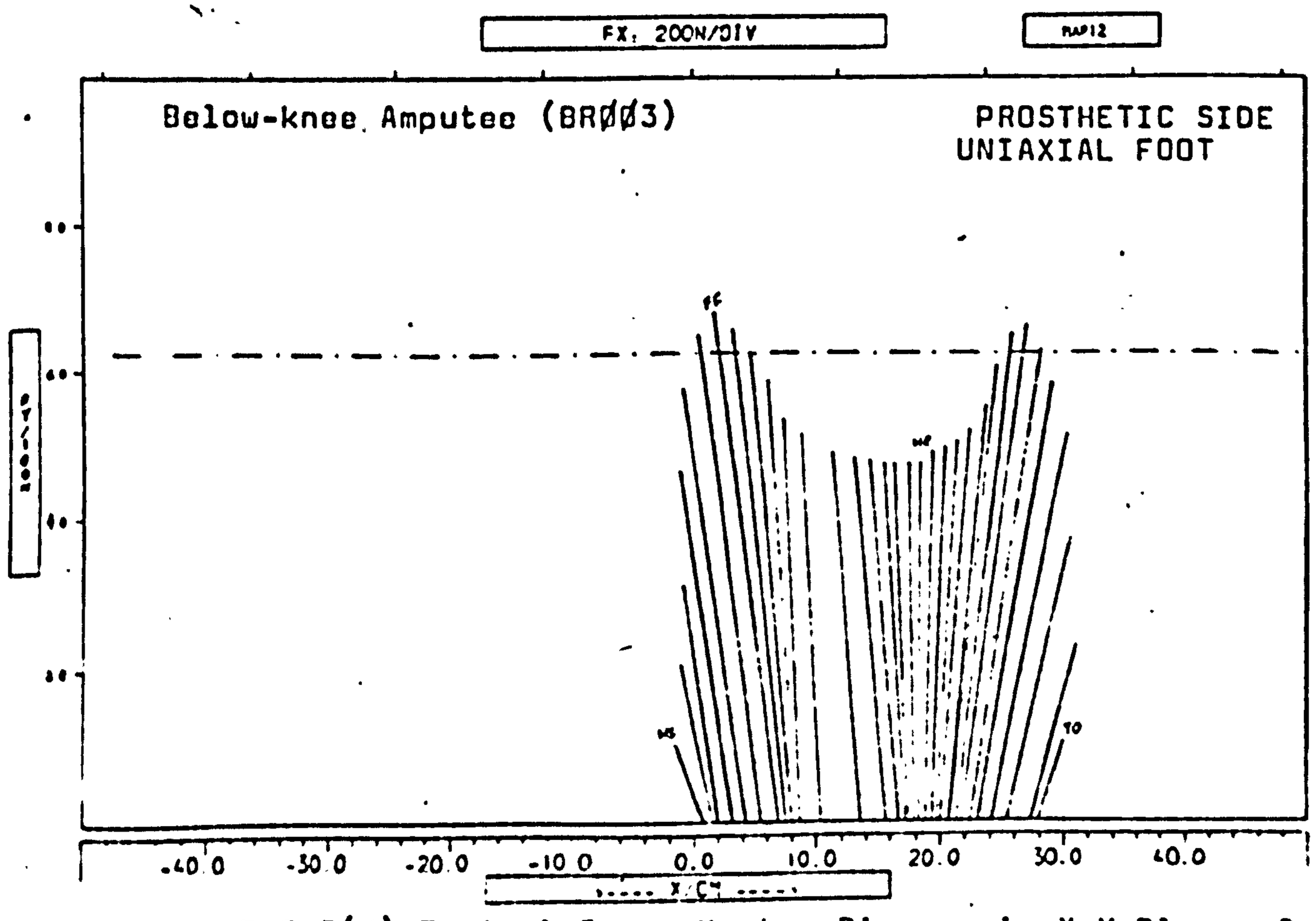

Figure 7.5.3(d) Typical Force Vector Diagram in X-Y Plane of Below-knee Amputee

trend of two peaks, one at foot-flat and the other at push-off.

Figure 7.5.3(c) shows the typical force vector diagram in the X-Y plane of the sound limb of a below-knee amputee. In this particular instance the amputee is wearing a Uniaxial foot. However, the pattern of the sound limb is similar whether the SACH or Uniaxial foot is used.

The diagram shows clearly the typical two peaks of the Fy-time curve. Unlike the normal subject, the below-knee amputee does not slow down his rate of progression of the C.P. points after foot-flat. The force vectors move with fairly evenly spaced intervals until about heel-rise. At this point, the foot slows down slightly to get over the ball of the foot for the push off.

Figure 7.5.3(d) shows the typical X-Y plane force vector diagram of the prosthetic limb with a Uniaxial foot for a below-knee amputee. Like the natural foot, the Uniaxial foot goes to foot flat at the first peak vector of the diagram, after which, the rate of progression slows down for the next four force vectors. This is due to the prosthetic limb pivoting freely about the hinge joint as it moves forward. In doing so, the load is transmitted through the joint and therefore the C.P. points are fairly close together. However, when the dorsiflexion stop comes into play, the force vector moves very rapidly forward. As it does the vector angulates in the anticlockwise direction instead of following the normal trend. This event is clearly shown in the Fx-time plot, see Figure 7.5.1(c). The relative change of angulation in the force vectors is very small, therefore the below-knee amputee would hardly notice the effects.

Figure 7.5.3(e) shows the typical X-Y plane force vector diagram of the prosthetic limb with a SACH foot,

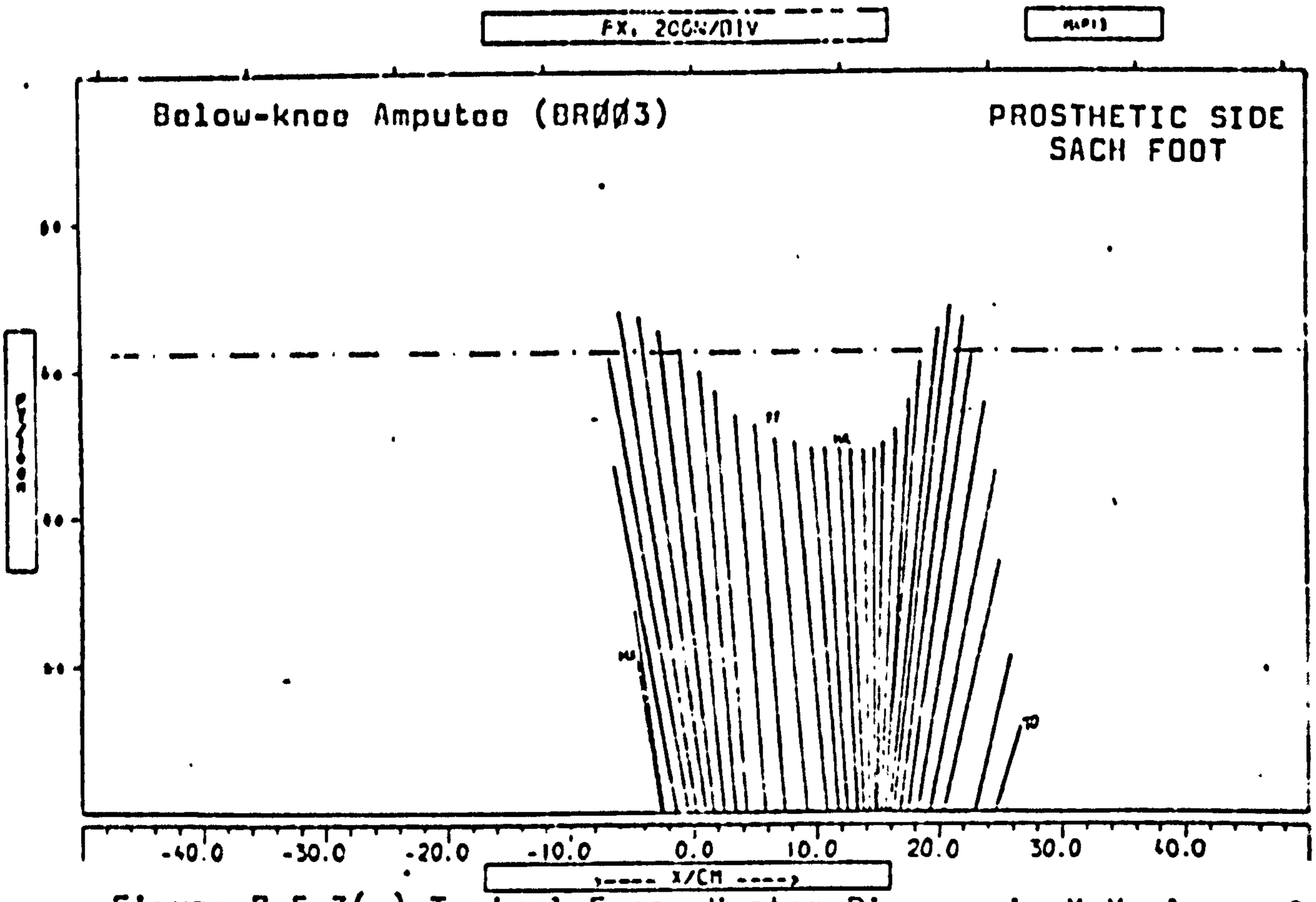

Figure 7.5.3(e) Typical Force Vector Diagram in X-Y plane of Below-knee Amputee

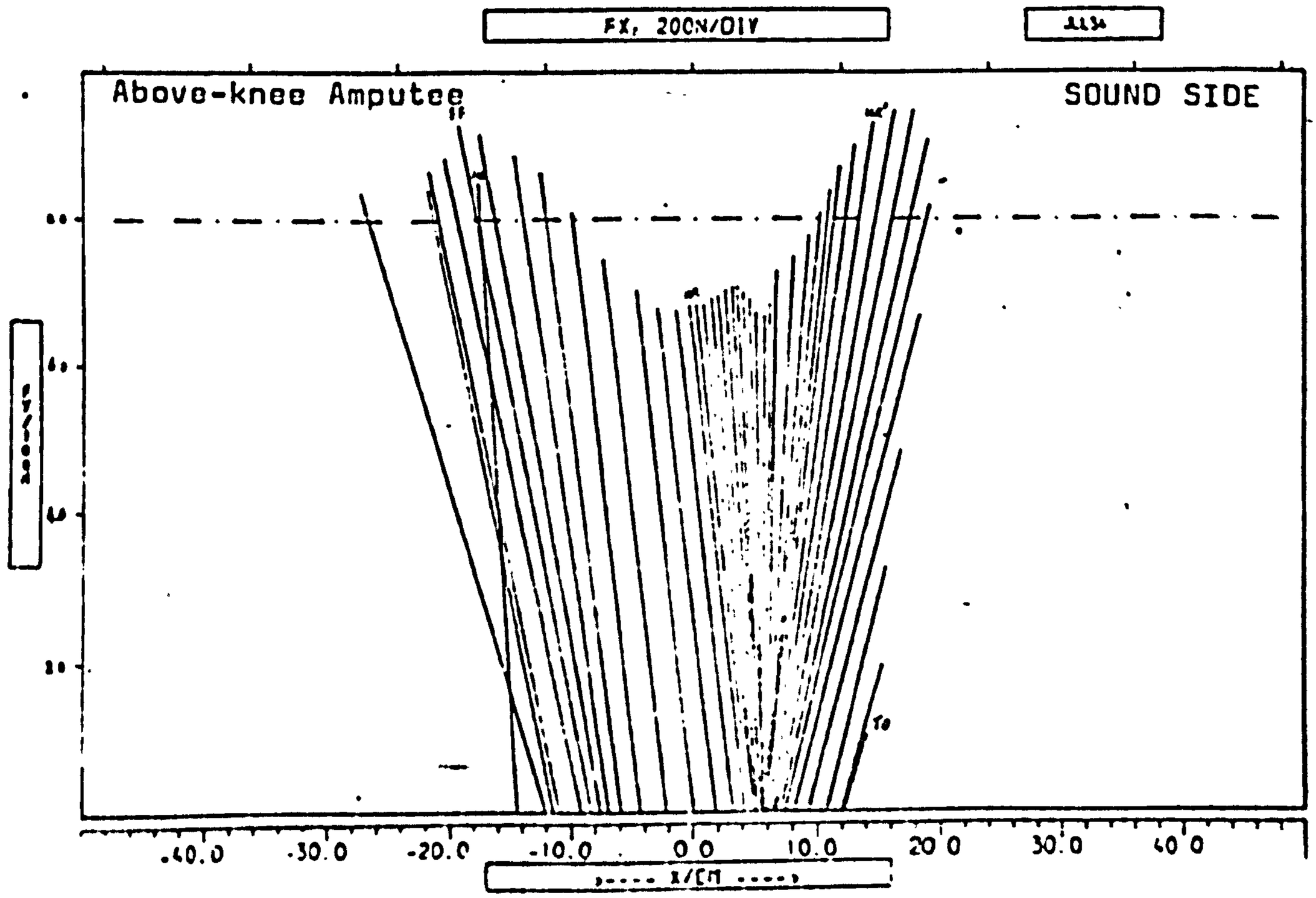

Figure 7.5.3(f) Typical Force Vector Diagram in X-Y Plane of Above-knee Amputee

for a below-knee amputee. Unlike that of the Uniaxial foot, the force vector of the SACH foot progresses with an even pace until about heel-rise. It is noticeable that the foot-flat position is achieved very much later with the SACH foot, approximately at mid-stance, and not with the first peak vector. The first peak vector in the SACH foot is associated with the complete compression of the heel cushion during early stance, therefore, the whole of the body weight is transferred to the prosthetic leg before foot-flat. This then poses the question of whether stability is impaired by the situation. In order to answer the question, the moments about the joint centres have to be considered.

The late stance pattern of both the SACH and the Uniaxial feet is similar. This is because the intact knee of the below-knee amputee is capable of controlling the roll-over and toe-off events with either prosthetic foot, even though the construction of the distal section of both feet is different.

Figure 7.5.3(f) shows the typical X-Y plane force vector diagram of the sound limb of an above-knee amputee. The different prosthetic foot has no effect on the pattern of the sound limb.

The diagram shows that the first peak vector occurs at foot-flat, a pattern similar to that of the normal subject. However, the rate of progression does not slow down until heel-rise. The first heel-rise (HR) is associated with vaulting and with it is the additional peak vector. Througout this event the progression of the force vector is considerably slowed down. Apparently the amputee is standing on the ball of his foot during this period. The second and ultimate heel rise (HR') is towards toe-off.

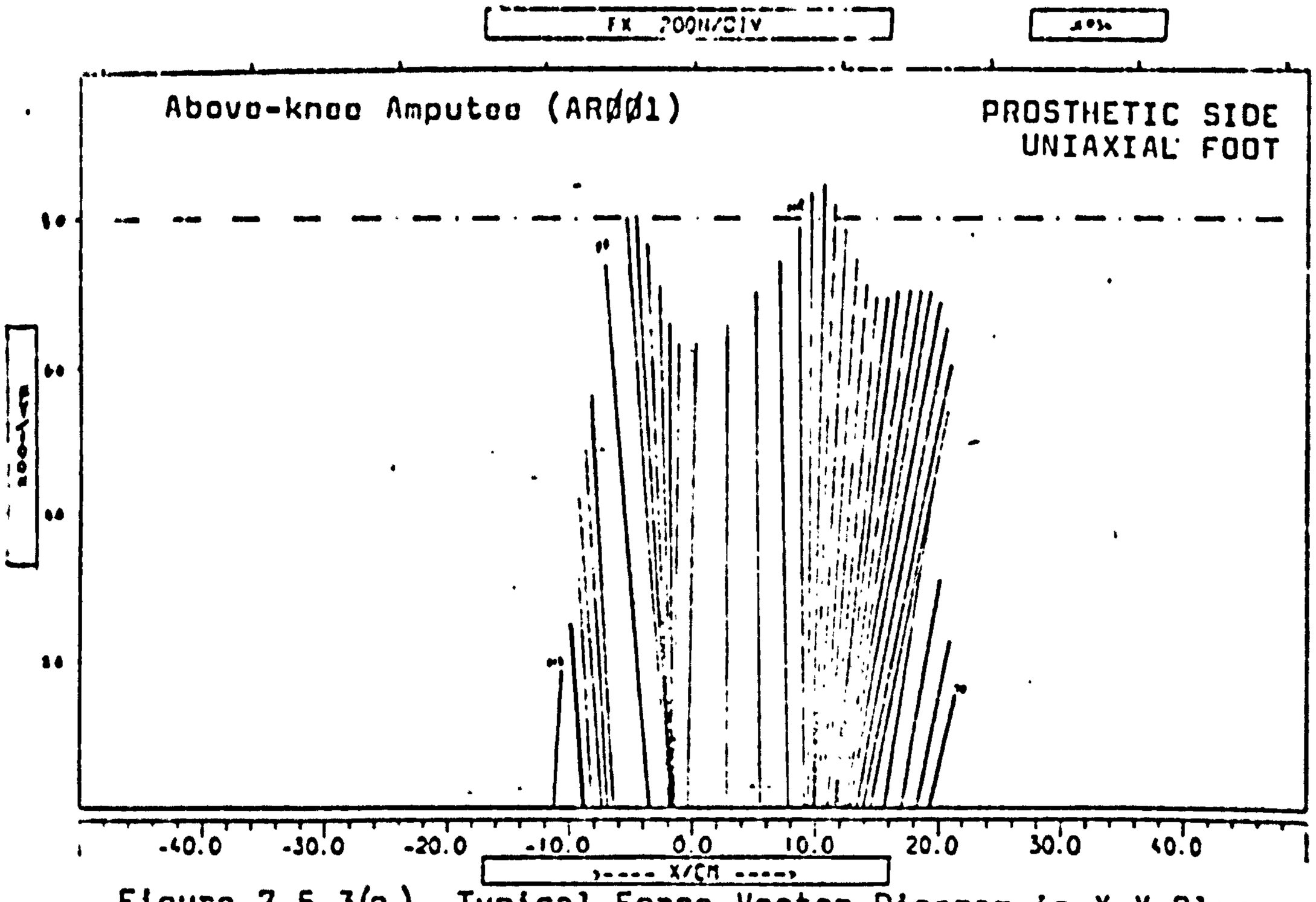

Figure 7.5.3(g) Typical Force Vector Diagram in X-Y Plane of Above-knee Amputee

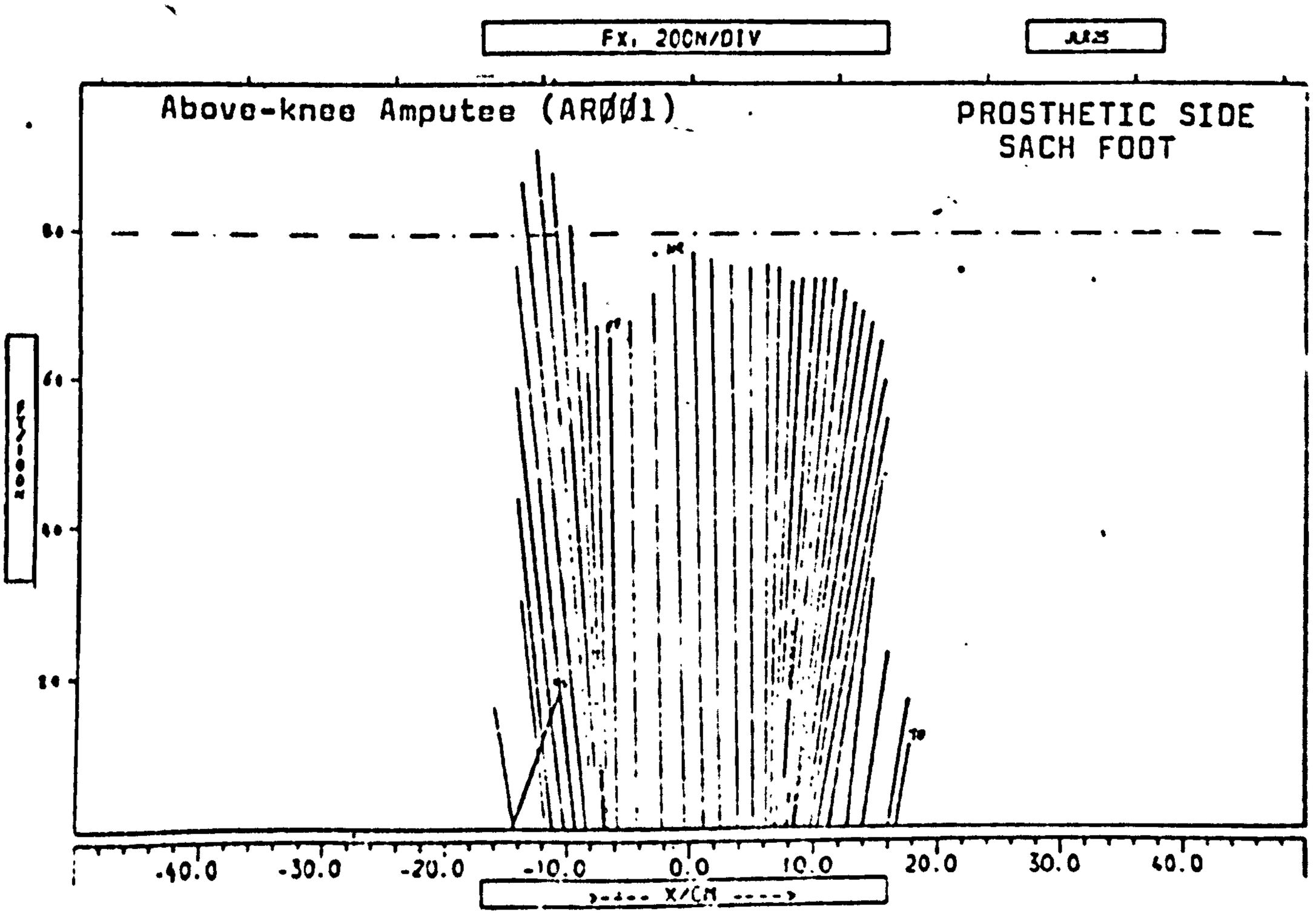

Figure 7.5.3(h) Typical Force Vector Diagram in X-Y Plane of Above-knee Amputee

Figure 7.5.3(g) shows the typical X-Y plane, force vector diagram, of the prosthetic limb with a Uniaxial foot, for an above-knee amputee. The foot-flat position occurs, with the first peak vector similar to that of the below-knee amputee with a Uniaxial foot, after which the progression force vector slows down, representing the free pivoting of the prosthetic limb about the hinge joint. However, it then rapidly moves to heel rise and to the second peak vector. Now the force vector progresses slowly about the ball of the foot maintaining a magnitude of about 80 percent body weight for a substantial amount of late stance. This apparently is due to the stiff dorsiflexion stop which forces an early heel rise and also the construction of the distal section of the Uniaxial foot which causes a delay in toe-off. The absence of the natural knee and ankle makes it difficult for the above-knee amputee to control these movements.

Figure 7.5.3(h) shows the typical X-Y plane force vector diagram, of the prosthetic limb with a SACH foot, of an above-knee amputee. The first part of the diagram is fairly similar to that of the below-knee amputee with a SACH foot. The first peak vector occurs well before the foot-flat event. Again, the stability during this period is questionable. The force vector then proceeds fairly rapidly to foot flat and heel-rise. After heel-rise the vector moves extremely slowly over the ball of the foot at fairly consistent magnitude of 80% of body weight. This must be due to the rolling action designed into the distal section of the SACH foot.

7.6. Kinetic Results

7.6.1. Intersegmental Moments

Figure 7.6.1(a), (b) and (c) show the moments about the three principal axes at the ankle, knee and hip joints of the contralateral sides of the normal subject.

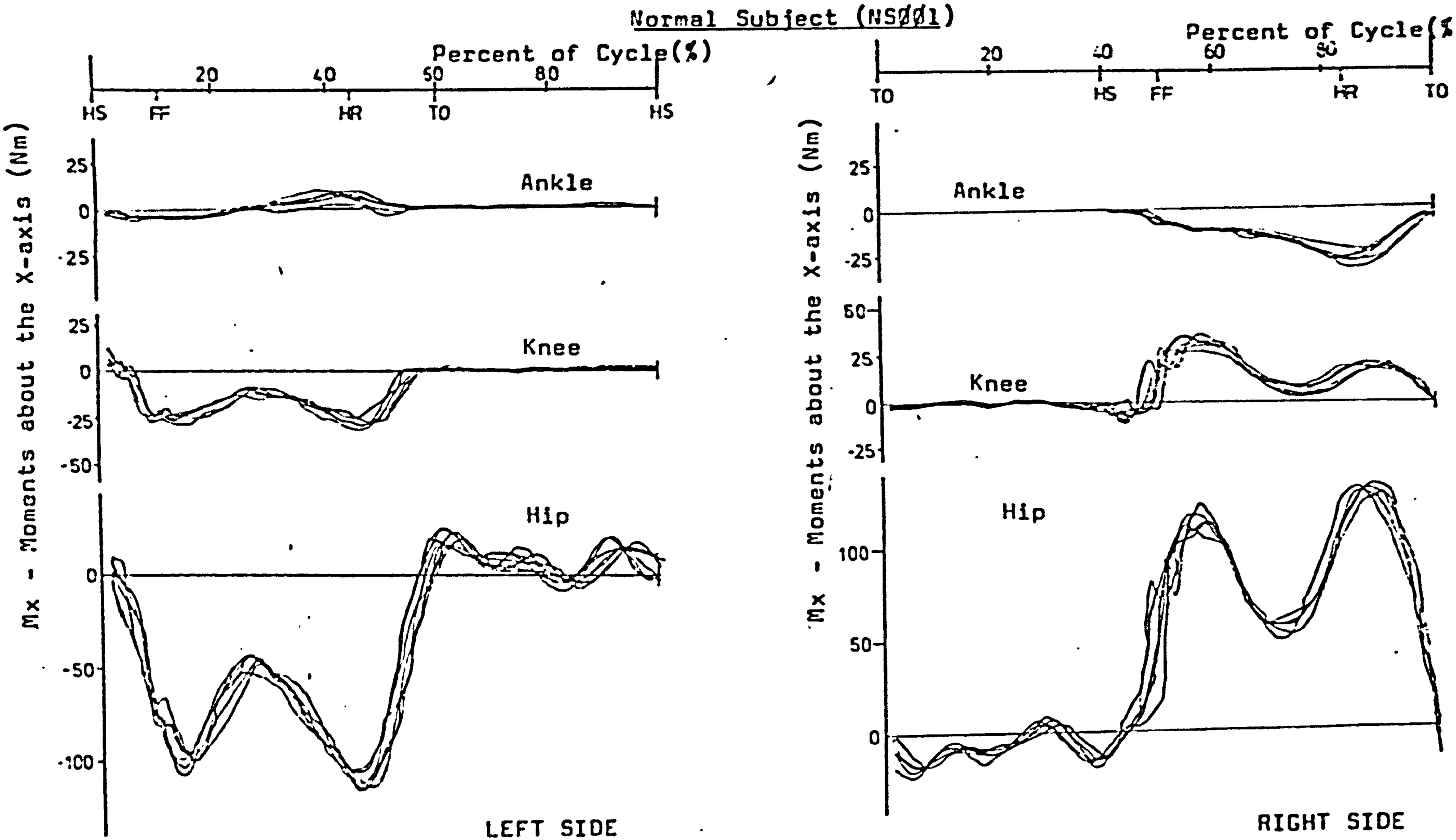

Figure 7.6.1(a) Moments about the X-axis of the Normal Subject

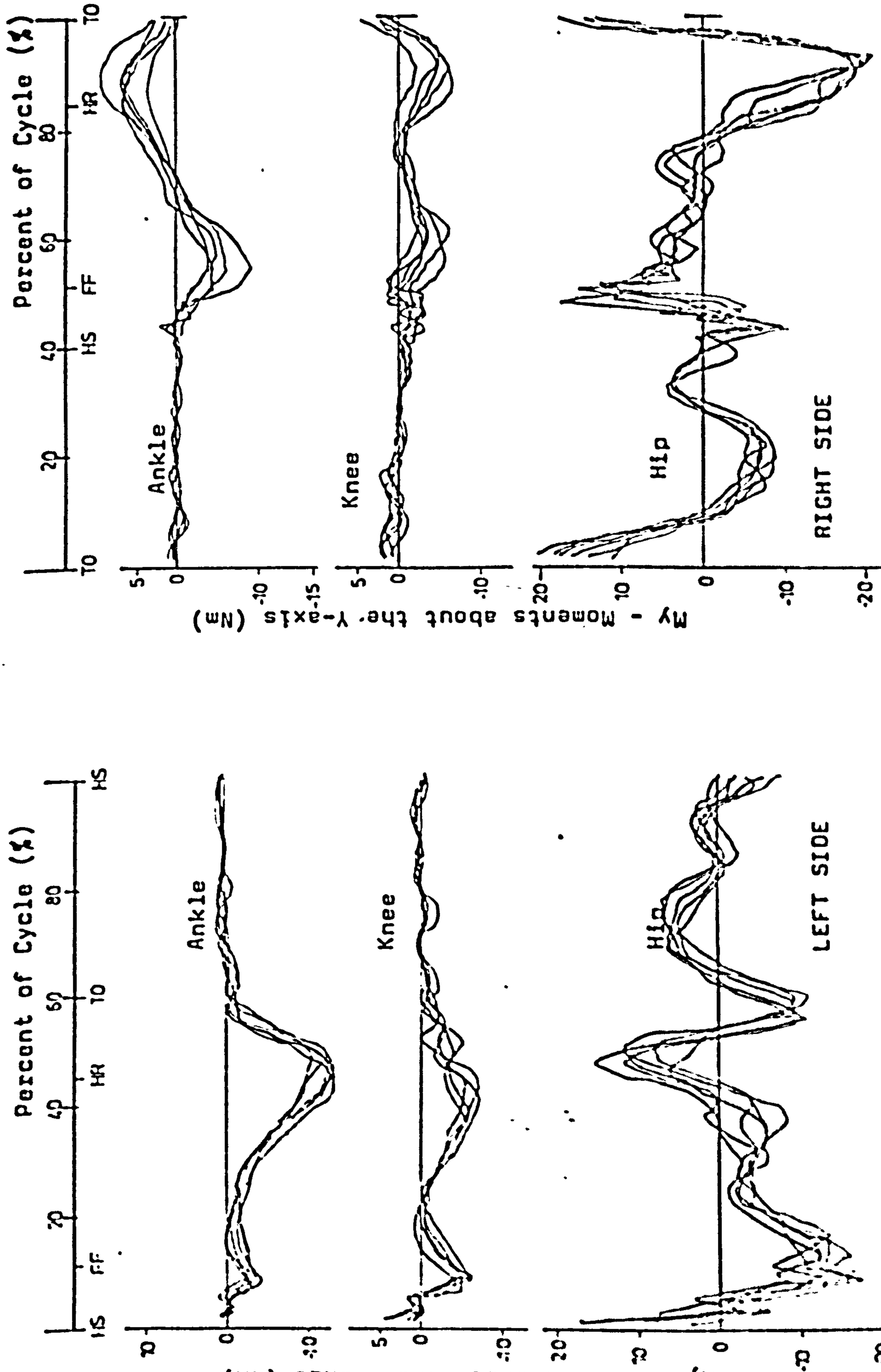

Normal Subject (USDDL)

Figure 7.6.1(b) Moments about the Y-axis of the Normal Subject

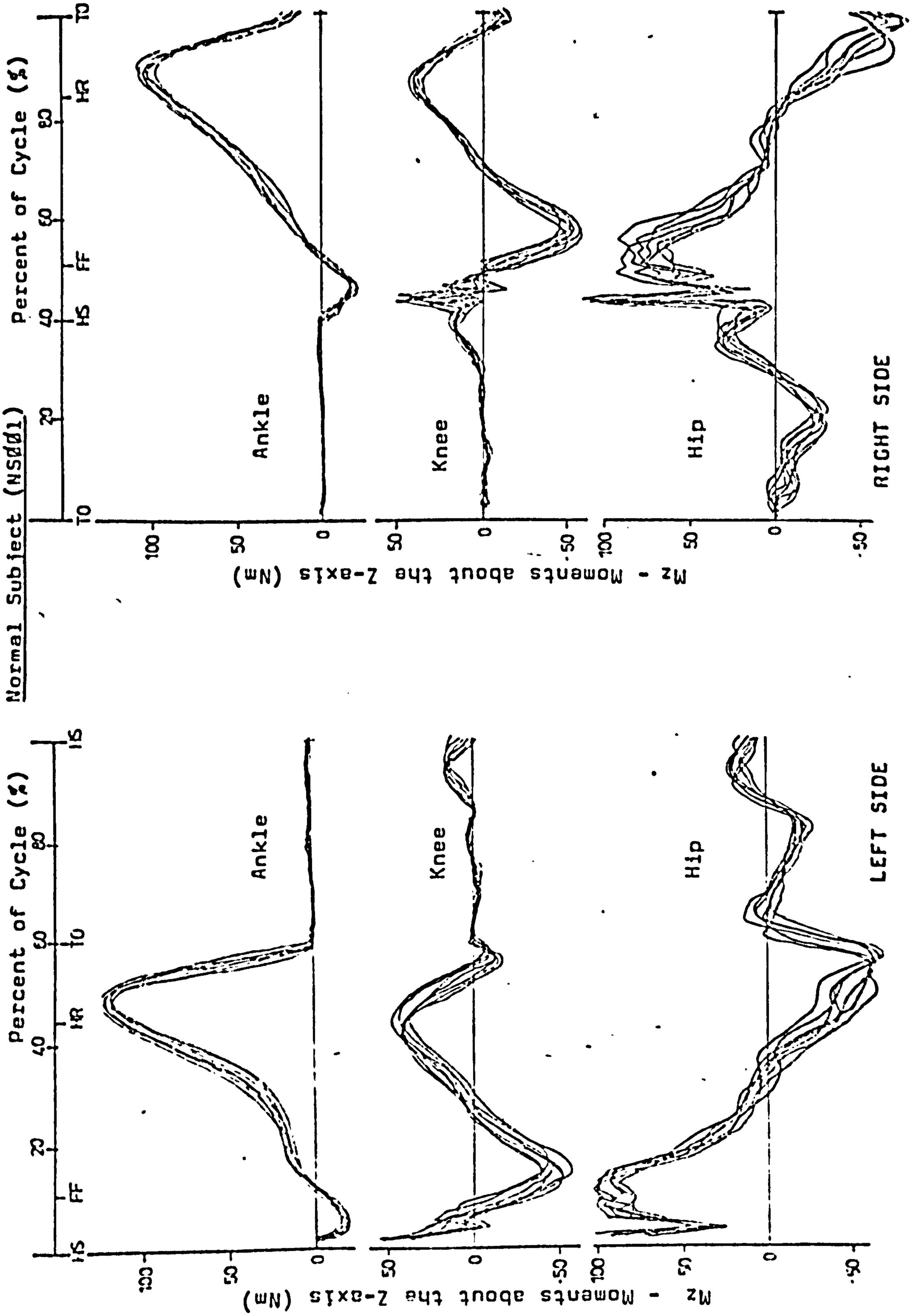

Figure 7.6.1(c) Moments about the Z-axis of the Normal Subject

The results obtained were useful in verifying the measuring system and the analytical procedure. The graphs shown were similar to those presented by other investigators, such as Bresler and Frankel (1951) and Paul (1970). The results were also useful in checking the repeatability of the system, the details of which were discussed in Section 7.1.4.

The hip moments about the three principal axes on the left and right legs were found to be highly symmetrical. The ankle and knee Mz moments and the knee Mx moments were also observed to be symmetrical. The ankle Mx moments were found to be different on the left and right legs. This difference was noticed to be consistent and therefore would be unlikely to be caused by errors in the measuring system. The magnitudes of the left ankle Mx moments are fairly small, hence the left foot is not greatly subjected to M/L movement. The magnitudes of the right ankle Mx moments are negative throughout stance phase, these moments tending to evert the right foot.

The ankle and knee My moments were found to be different on the left and right legs as well. Again, the differences were shown to be consistent. During early stance the ankle My moment on the left leg tends to rotate the foot medially with a magnitude of about 5.5 Nm, while the right My moment tends to rotate the foot laterally with a magnitude of about 2.5 Nm. During late stance, however, the directions of the ankle My moments on both legs were the same, i.e. tending to rotate the foot laterally, although the magnitudes were different. The average maximum left ankle My moment is 6.5 Nm, while that of the right is 14.4 Nm. The direction of the knee My moments on both legs was completely opposite, although the average maximum values are similar, i.e. 6 Nm. Cunningham (1952) had shown that in one normal subject, the ankle My moments were very variable on the contralateral sides as well as on the same leg. Therefore, the

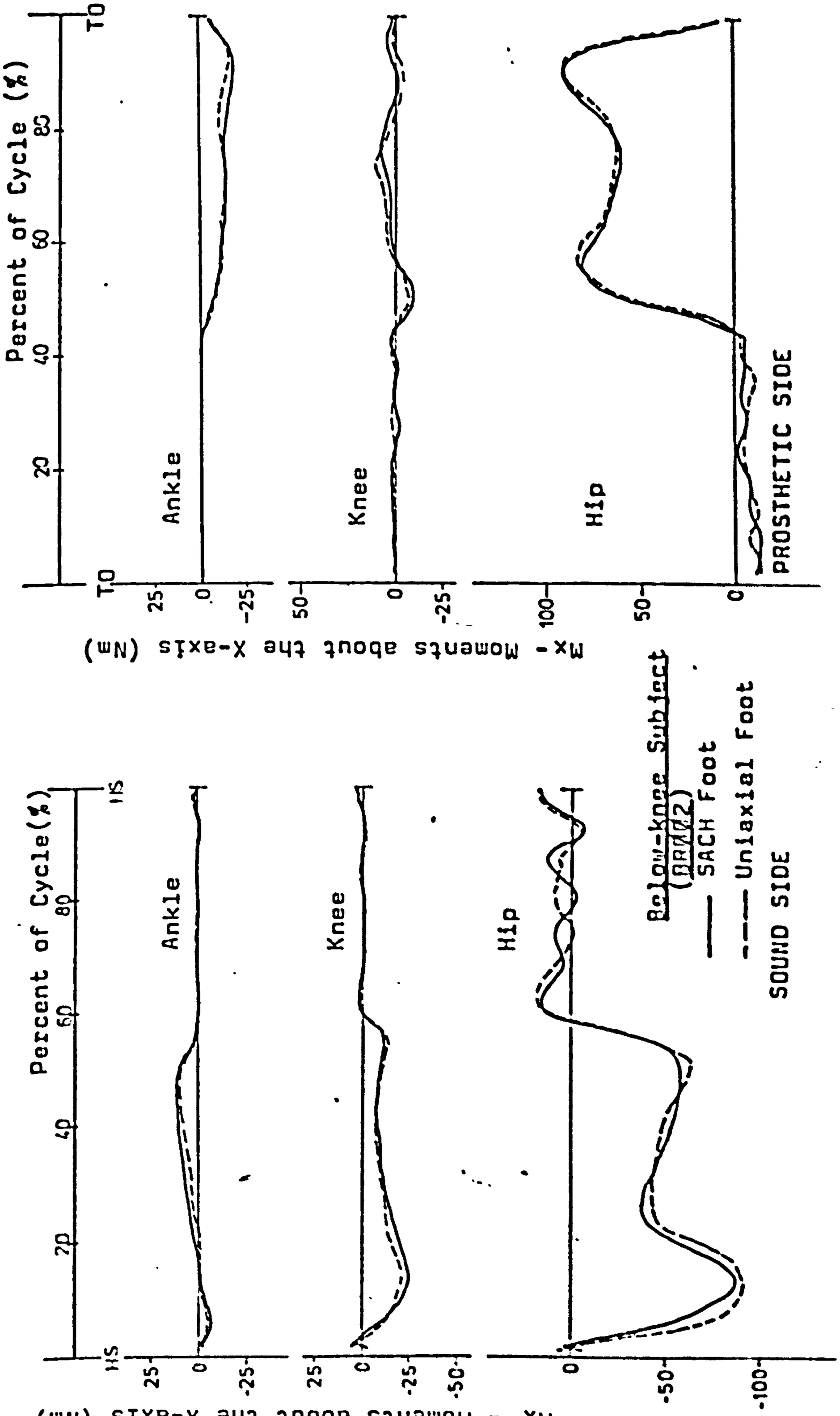

Figure 7.6.1(d) Typical Mx - Moments of Below-knee Amputee

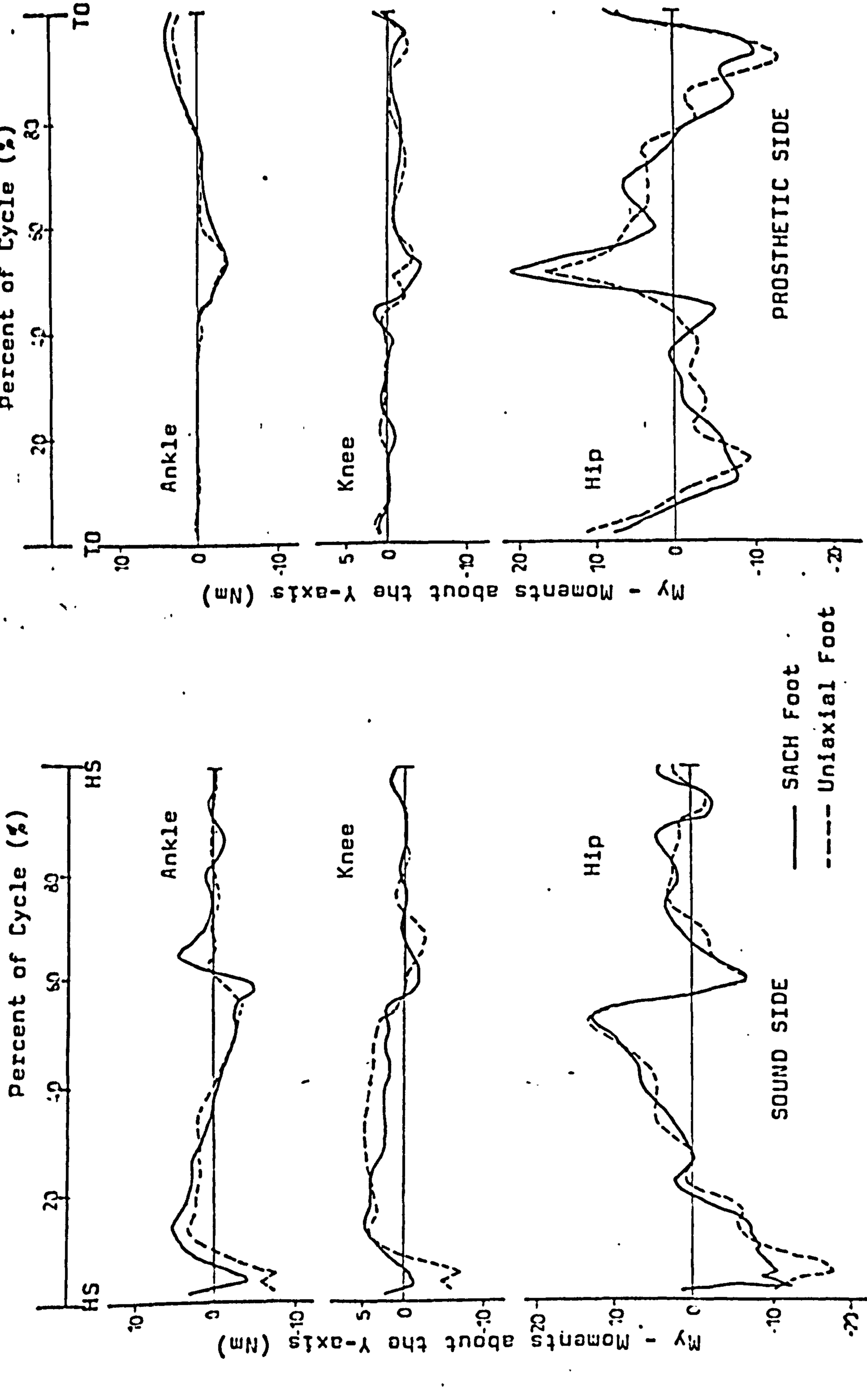

Figure 7.6.1(a) Typical My - moments of Below-knee Amputee

reason for the differences observed could be normal variability.

These "normal" results could be used as a reasonable standard of comparison when considering the results obtained for amputee subjects.

Figure 7.6.1(d), (e) and (f) show the typical moments about the three principal axes at the ankle, knee and hip joints of the contralateral sides of the below-knee amputee.

The ankle, knee and hip moments about the X and Z axes on the sound limb were found to be similar to those of the normal subject. The ankle and knee My moments were significantly different. This could be due to the prosthetic gait but in any case the magnitudes involved are very small. The hip My moment was found to be fairly similar to that of the normal subject. Comparison between the SACH and the Uniaxial feet showed no significant difference in the moments at the joints of the sound limb.

The ankle and knee Mx moments on the prosthetic side were observed to be different from those of the sound side. The magnitudes of the knee Mx moments were much smaller this must be due to the alignment of the prosthesis. The prosthetic foot was always set slightly on the lateral side relative to the knee joint. The negative ankle Mx moments tend to evert the prosthetic foot, however the magnitude recorded is fairly small. Note that both prosthetic feet had been shown to have a small amount of medio-lateral movement , see Section 5.2.1. A comparison between the SACH and the Uniaxial foot showed no significant difference in the Mx moments on the prosthetic side. No indication of M/L instability with the SACH foot was observed. This "instability" was previously suggested by the delayed foot flat event with

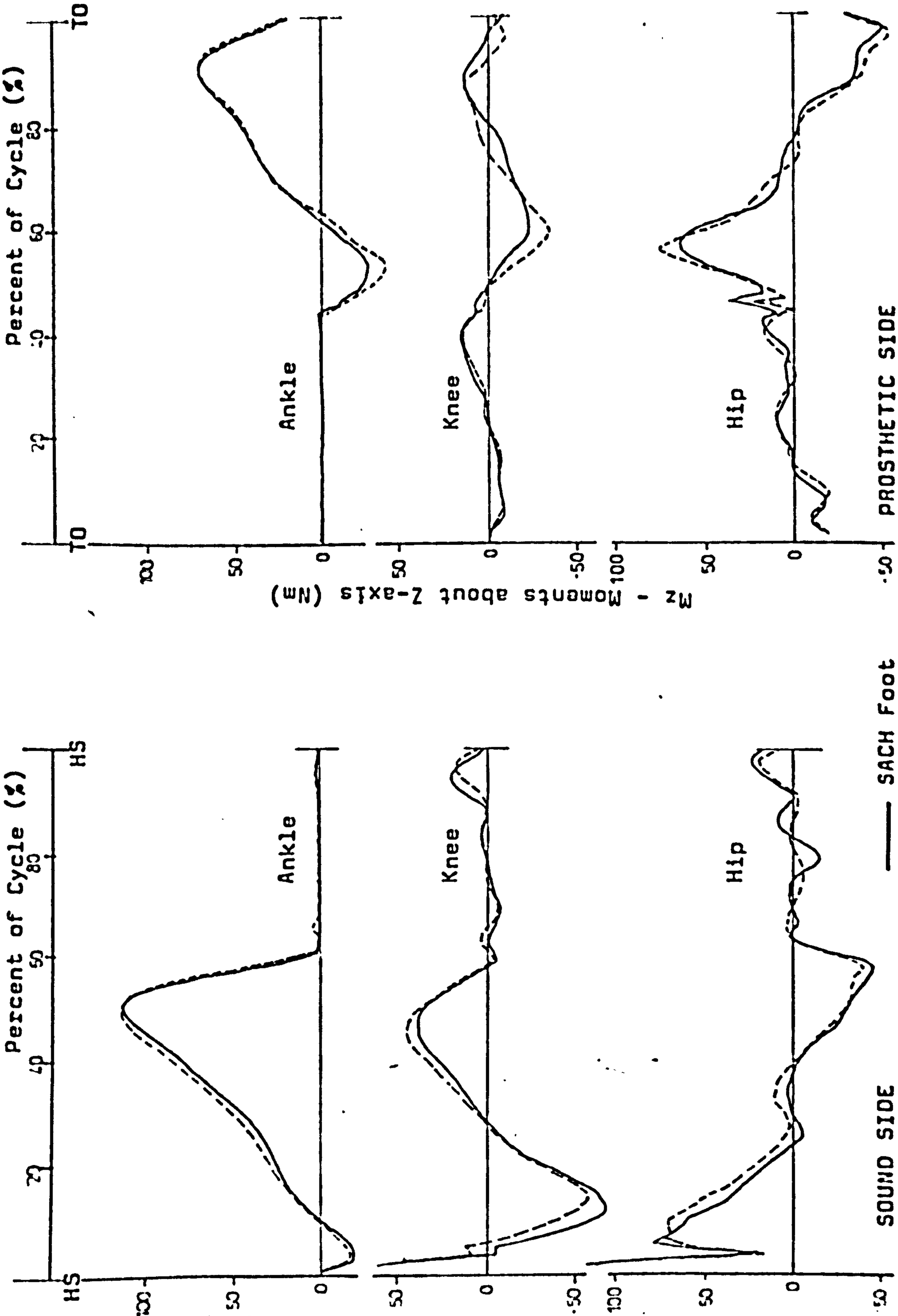

Figure 7.0.1(f) Typical Mz moments of Below-Knee Amputee

the SACH foot. It could be that the sound limb has compensated and provided stability to the prosthetic side during double support. The hip Mx moment on the prosthetic side was found to be similar to that of the sound side.

The My moment at the three joints on the prosthetic side was found to be similar to that of the sound side, although the magnitudes of the ankle and knee moments were generally lower and the hip moments were higher. Comparison between the SACH and the Uniaxial foot showed no significant difference in the My moments on the prosthetic side. This was as expected, since the design of the SACH and Uniaxial foot do not have any provision for axial rotation.

The Mz moments on the sound side were found to be similar to those of the normal and comparison between the SACH and Uniaxial feet showed no significant difference.

The shapes of the Mz moments on the prosthetic side were found to be similar to those of the sound side. The magnitudes of the hip Mz moments were also found to be similar, however the magnitudes of the ankle and knee Mz moments were generally lower, except for the ankle moments during early stance phase.

The ankle Mz moment during early stance tends to plantar flex the foot. The magnitude of this moment on the prosthetic side is about 1.5 times higher than that of the sound side. It was also noted that the magnitude with the Uniaxial foot is higher than that of the SACH foot by 27%. The reason for this could be due to the defined ankle position of the Uniaxial foot being 1.5cm forward (relative to the heel) when compared with the SACH foot. The low positive ankle Mx moments during late stance could be attributed to the lack of push off in

Above-knee Subject (ARØ11)

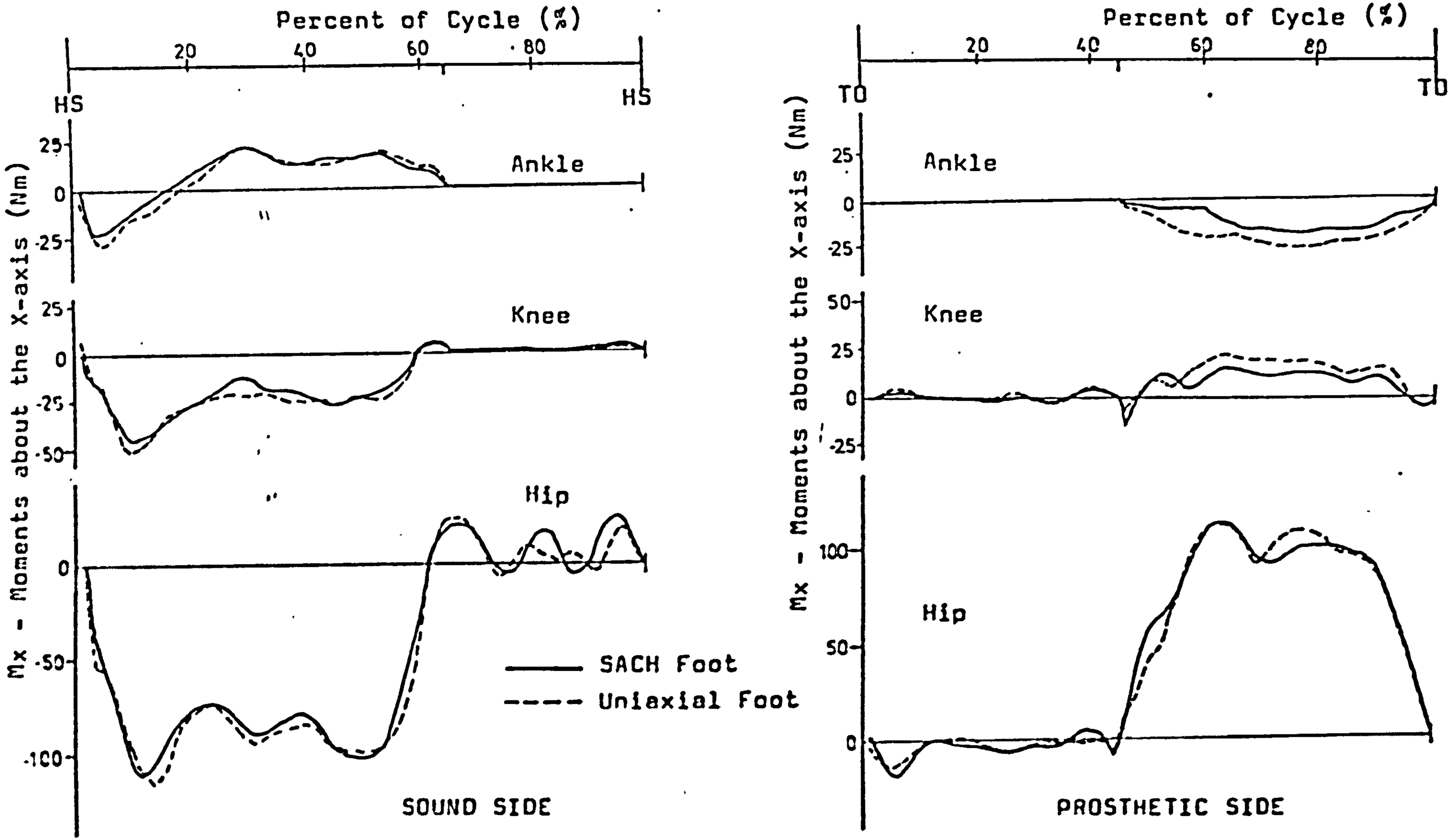

Figure 7.6.1(g) Typical Mx - moments of Above-knee Amputee

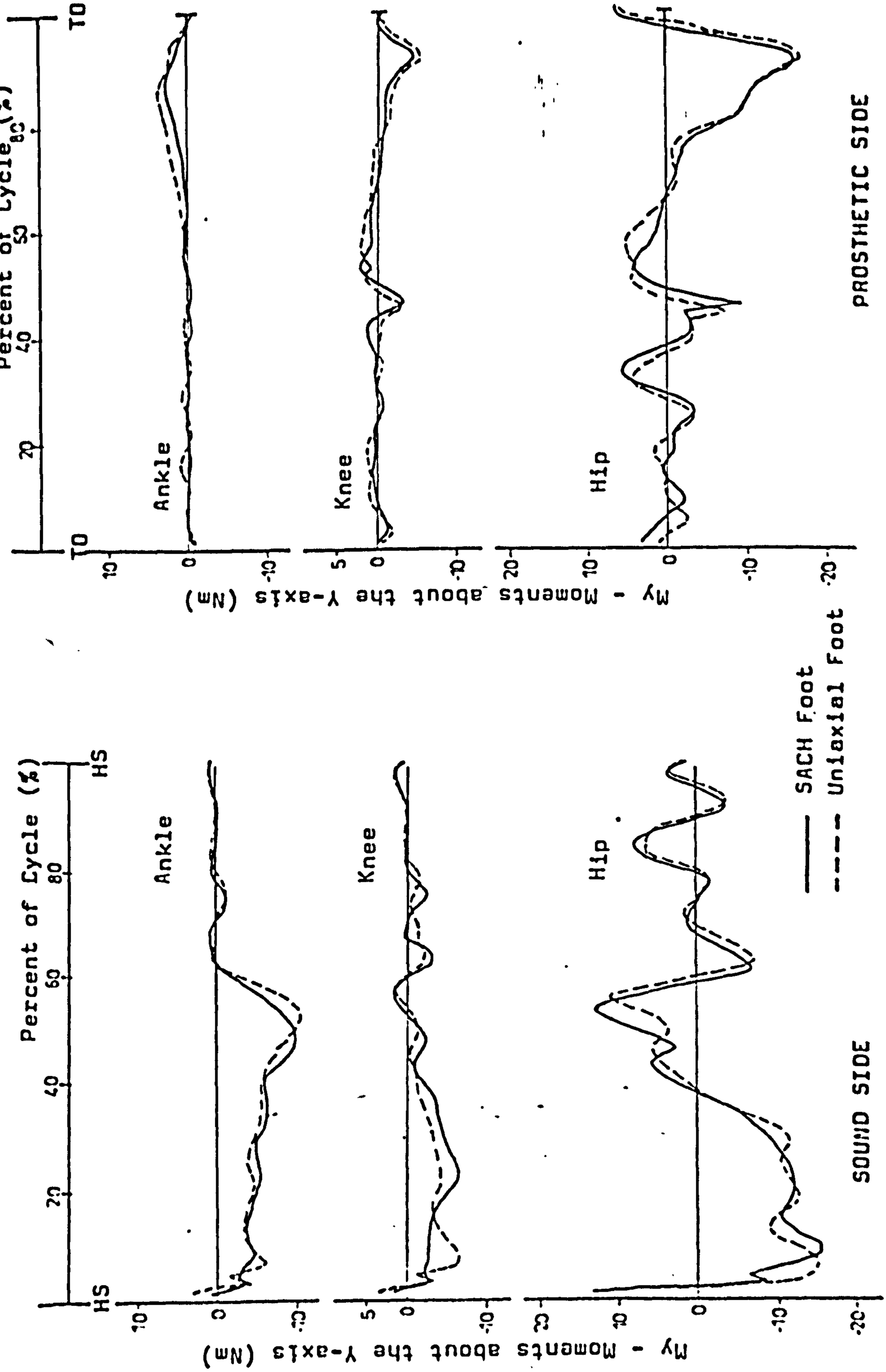

Figure 7.0.1(h) Typical My - moments of Above-knee Amputee

the prosthetic limb.

The lower knee Mz moments on the prosthetic side suggest that although the knee is still intact it does not have the same range of movement as that of the sound side during stance phase.

Figure 7.6.1 (g), (h) and (i) show the moments about the three principal axes at the ankle, knee and hip joints on the contralateral sides of the above-knee amputee.

The ankle, knee and hip Mx moments on the sound side are fairly similar to those of the below-knee amputee, except that the hip moment shows the characteristic three peaks of the corresponding Fy forces, the mid-peak being caused by "vaulting". The hip Mx moments on the prosthetic side during stance also reflect the corresponding Fy forces. Note that the curves are different for the SACH and Uniaxial foot, this being due to the different Fy force pattern reported previously. The ankle and knee Mx moments on the prosthetic side are fairly similar to those of the below-knee amputee. No indication of instability was observed, as suggested by the delayed foot flat of the SACH foot. A comparison between the SACH and the Uniaxial foot showed no significant difference. Any difference in magnitude is within the range of scatter.

The directions in which the My moments tend to rotate the segments on the sound leg are similar to those of the normal subject's left leg. On the prosthetic side, the My moments tend to rotate the segments in a similar direction to that of the below-knee amputee. As expected, no significant difference was found when comparing the SACH and Uniaxial foot, since no axial rotation is available in either prostheses.

Above-knee Subject (ARØ11)

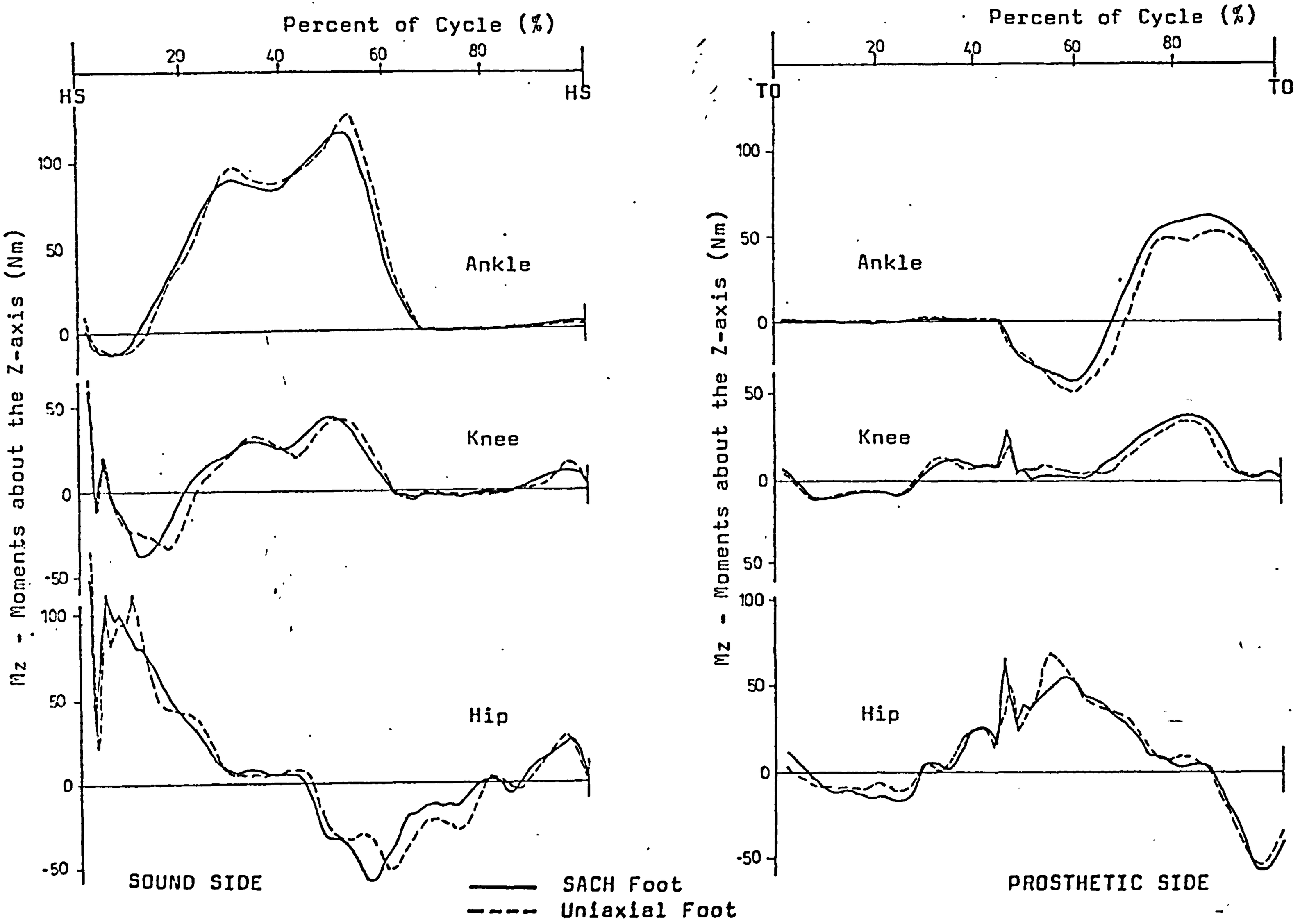

Figure 7.6.1(i) Typical Mz-moments of Above-knee Amputee

The Mz moments on the sound side are slighntly different from those of the normal. The ankle and knee Mz moments show an additional peak during the mid-stance period. This could be due to the "vaulting" action. The hip Mz moments show very low values during this event. A comparison between the SACH and Uniaxial foot shows no significant difference.

The ankle Mz moments on the prosthetic side are different from those of the sound side. The plantar-flexion moments during early stance are greater in magnitude. This is due to the absence of muscular control at the prosthetic ankle joint. The positive ankle Mz moments are lower because of the lack of push-off. The knee Mz moments show absolutely no flexion moments during stance. This is because the prosthetic knee unit used has no means of active control to provide stability, such as the Blatchford Stabilised Knee Unit. The knee unit therefore has to be set back, relative to the axis of the foot bolt to provide A/P stability during stance phase. The low magnitude of the hip flexion moment during early stance is an indication of the weaker muscular control in the stump when compared with that of the sound limb. A comparison between the SACH and the Uniaxial foot shows that the shape of the positive ankle Mz moment is different. The rounded curve of the SACH foot reflects the "smooth roll-over" pattern described earlier. While the two peak curve of the Uniaxial foot suggests difficulty in "roll-over", although the amplitude recorded is fairly small. However, there is one exception, it shows a "smooth roll-over" with the Uniaxial foot. It is therefore indicative that the alignment of the prosthesis and/or the stiffness of the dorsiflexion stop have to be critically adjusted to give a "smooth roll-over" during push off.

No other significant difference was observed in the

Normal Subject (NSØØ1)

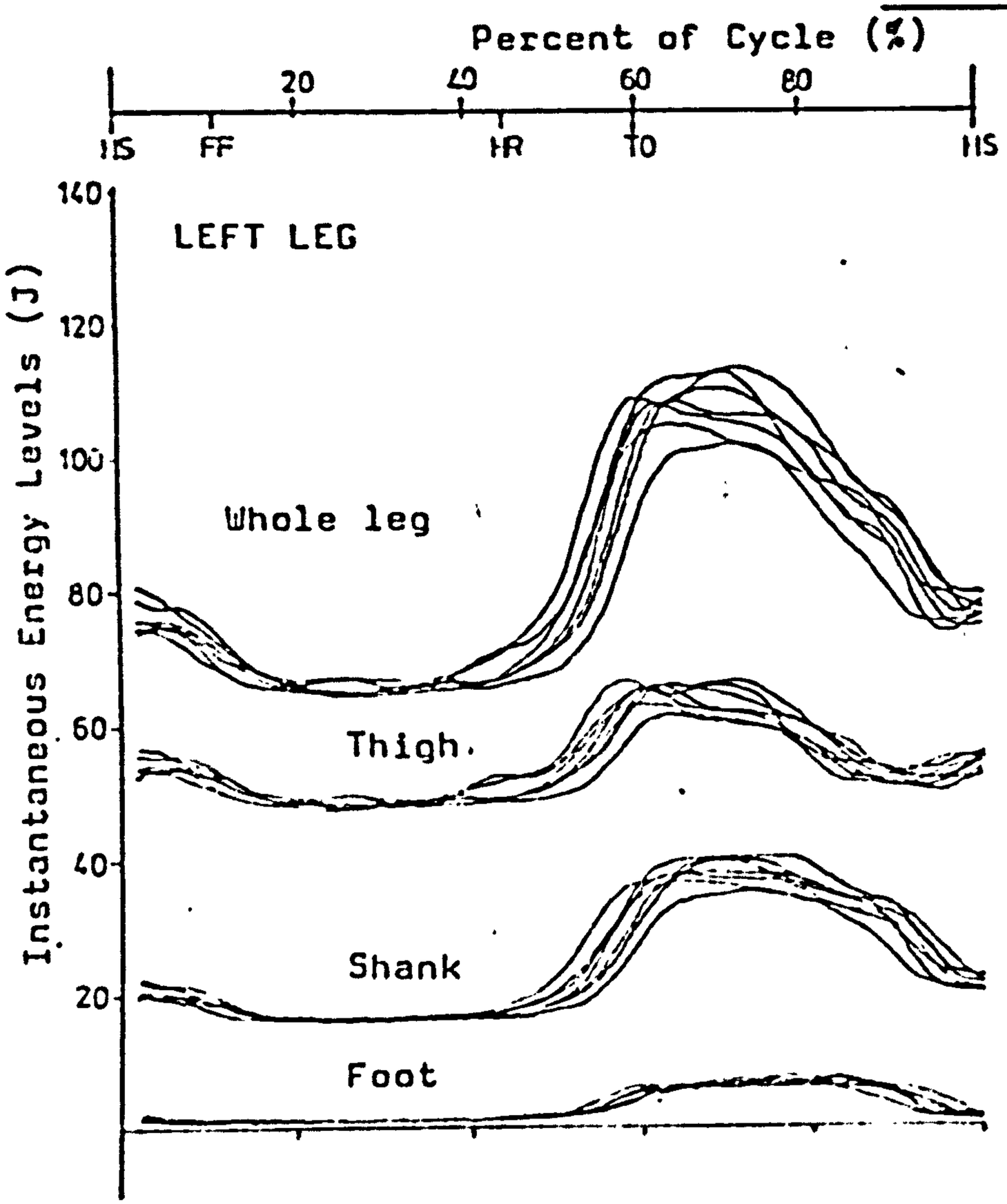

Figure 7.6.2(a) Instantaneous Energy Levels of the Normal Subject (left leg)

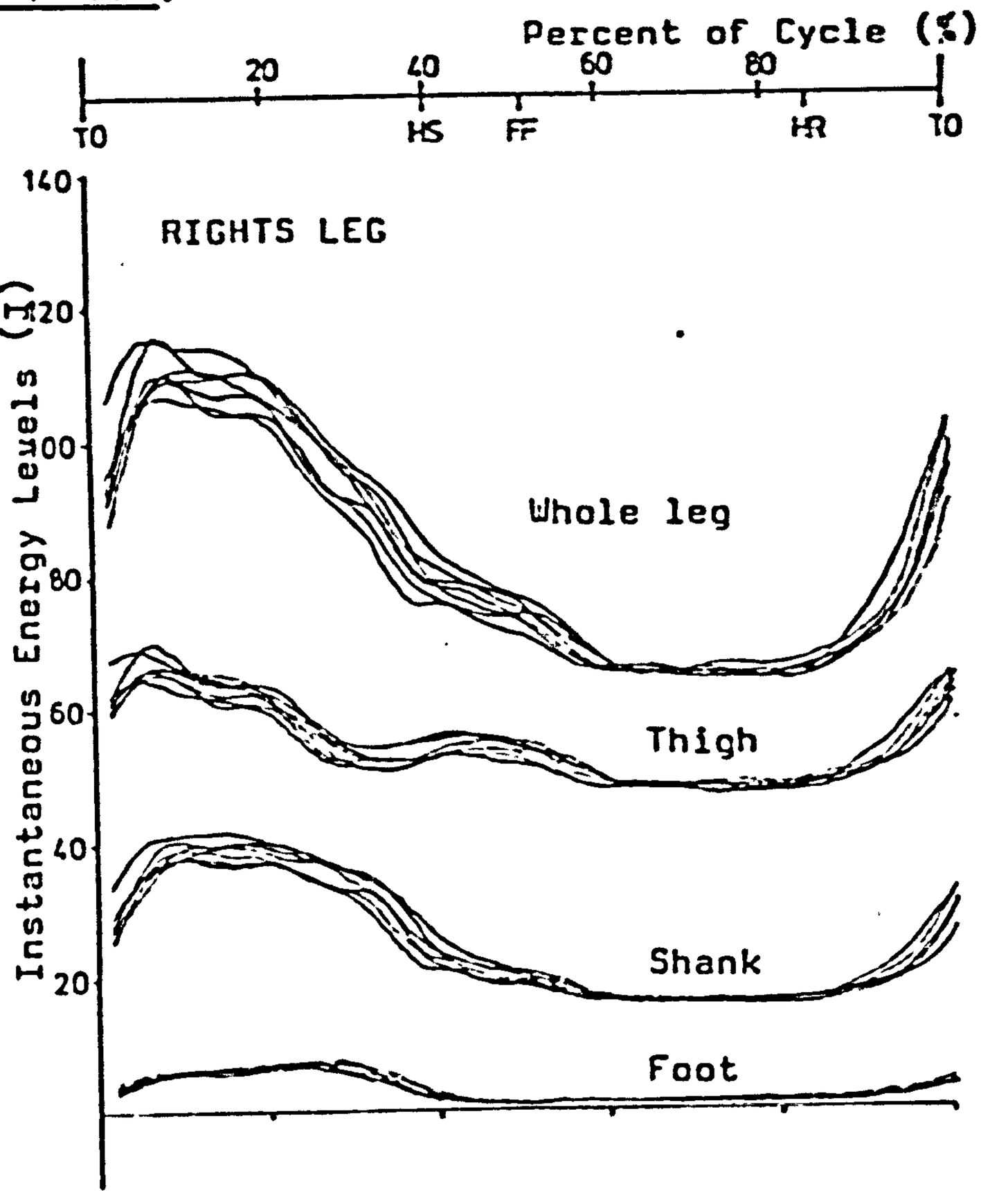

Figure 7.6.2(b) Instantaneous Energy Levels of the Normal Subject (Right leg)

Mz moments on the prosthetic side when comparing the SACH and Uniaxial feet. Any difference in magnitude is within the range of scatter.

7.6.2. Instantaneous Energy Levels

Figure 7.6.2(a) and (b) show the instantaneous energy levels of the left and right legs of the normal subject respectively. The instantaneous energy level is the summation of the potential and kinetic energies. Results from both legs are fairly similar in shape and magnitude.

The fluctuation in magnitude of the energy levels of each segment throughout the walking cycle are dependent on the height of the segment and the linear and angular velocities of the segment. The magnitude of the energy level is also directly proportional to the mass of the segment. The foot therefore, being relatively lighter and nearer to the ground has the lowest energy level.

The maximum instantaneous energy level of each segment occurs in the swing phase just after toe-off at maximum heel rise. This high magnitude is a combination of the increased elevation of the segment and its high velocity. Between foot-flat and heel-rise, the velocity of the segment is very low. Therefore the instantaneous energy levels during this period are effectively the potential energy of the segment; the magnitude of which can be regarded as being the baseline instantaneous energy level of that segment.

It can be seen from the figure that the energy level of the thigh drops approximately to its baseline value at late swing phase, prior to heel strike. This is because the thigh at this point is fully flexed and

Below-knee Subject (BRØØ2)

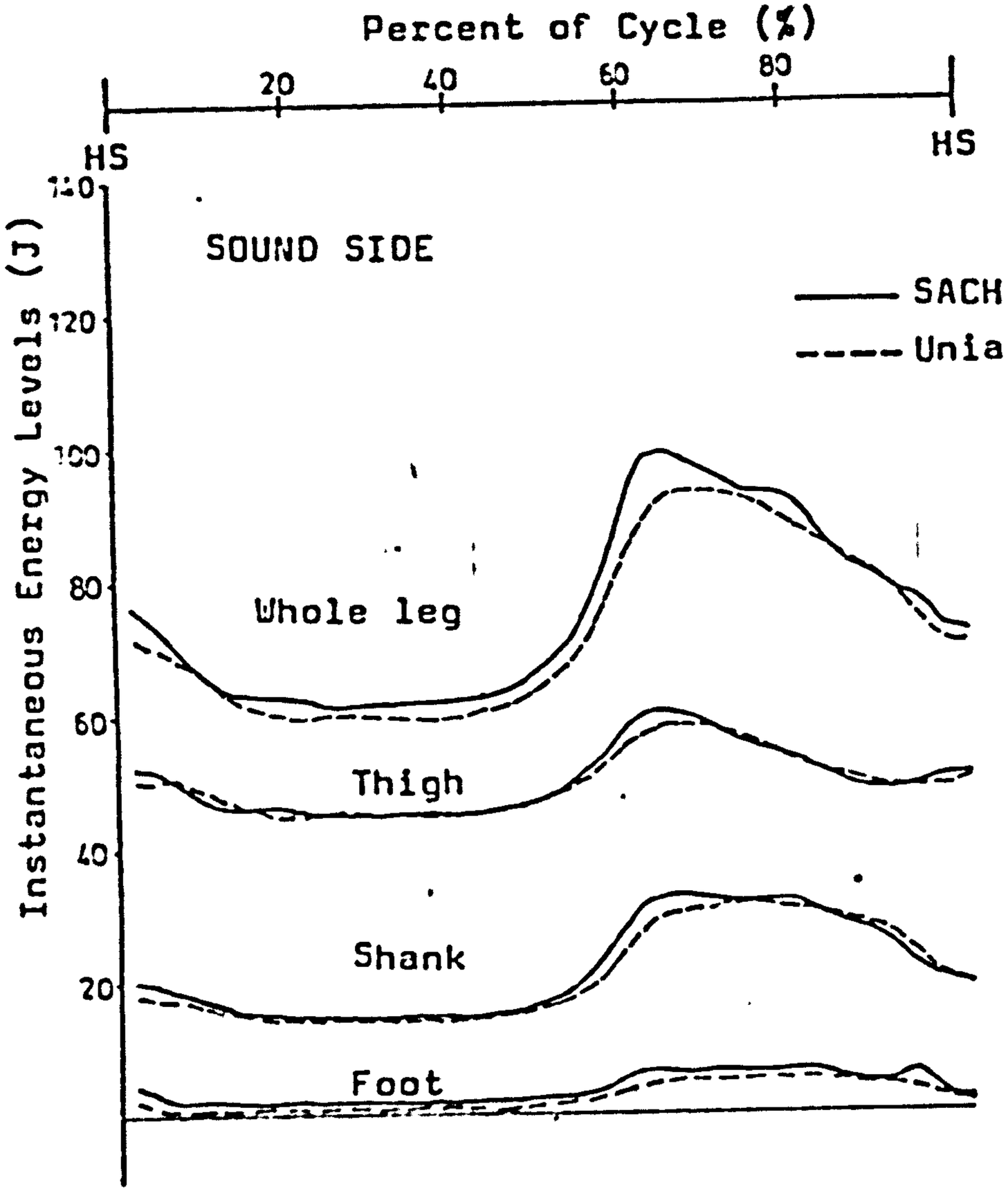

Figure 7.6.2(c) Typical energy levels of Below-knee Amputee (Sound Side)

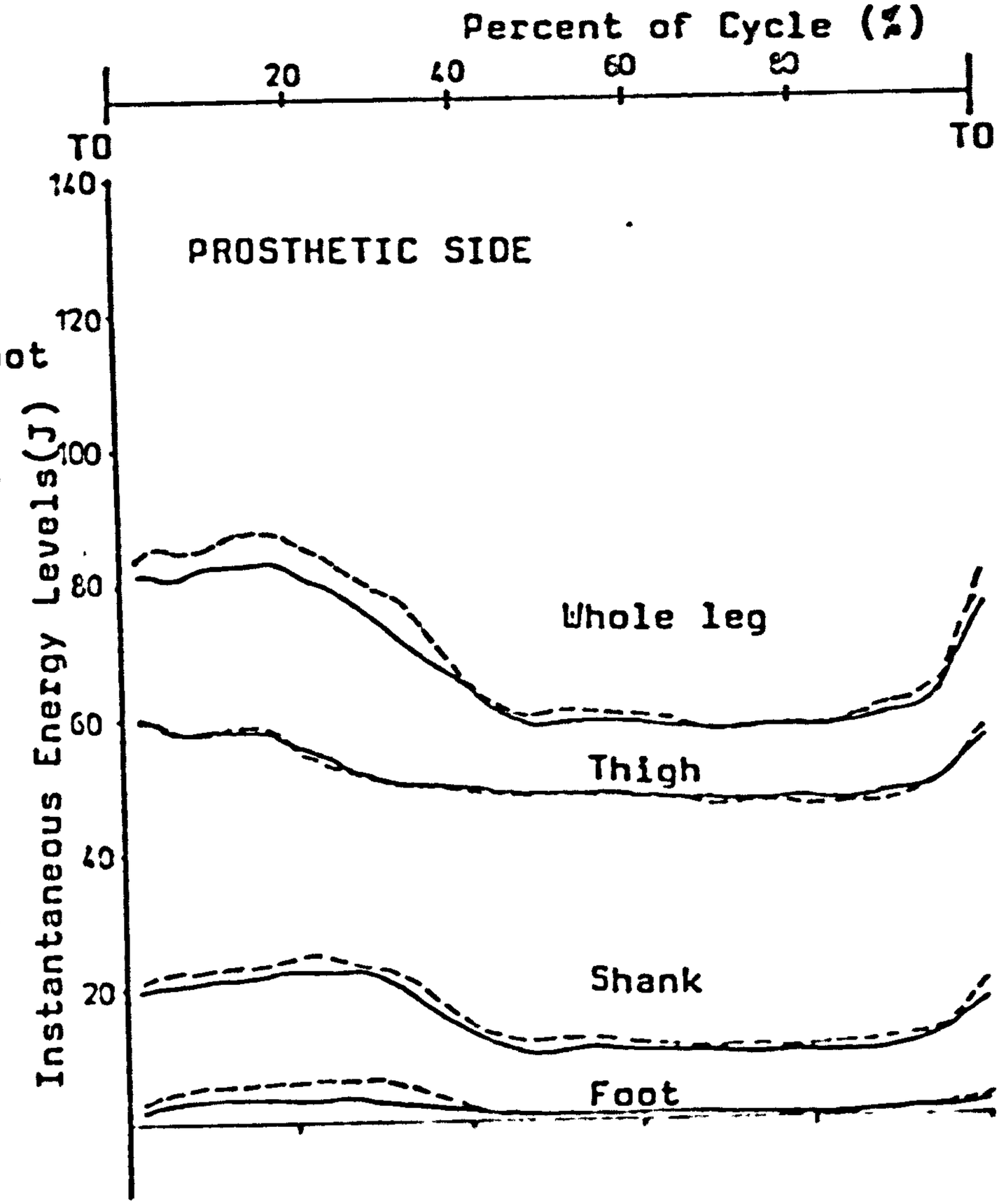

Figure 7.6.2(d) Typical Energy Levels of Below-knee Amputee (Prosthetic Side)

therefore has very low velocity.

The instantaneous energy level of the whole leg is obtained by summing up the energy levels of the segments. The work done by the whole leg per walking cycle can be calculated from the summation of the absolute energy changes over the walking cycle. The average result (with ±1 S.D.) obtained for the left leg of the normal subject is 92.6 joules (±8.6) and for the right it is 96.6 joules (±5.4), see Table 7.6(a).

Figure 7.6.2(c) and (d) show the typical energy levels of the sound and prosthetic side of the below-knee amputee, respectively.

The results of the sound side are similar in shape to those of the normal subject. The difference in magnitude is due to the difference in height and weight of each subject.

On the prosthetic side however the magnitudes obtained for the prosthetic shank are much lower than those of the sound shank. This is due to the mass of the prosthesis being lower and also due to the fact that the centre of mass is nearer to the ground. The magnitudes and shape of the thigh energy levels on the prosthetic side are fairly similar to those of the sound side. A comparison between the SACH and the Uniaxial foot shows no significant difference in the results of the prosthetic side nor in those of the sound side.

The average work done by the sound and prosthetic legs per walking cycle is as shown in Table 7.6.2(a). The results of the sound leg show a higher average work done per walking cycle than those of the prosthetic side. Furthermore, the work done per walking cycle with the Uniaxial foot is slightly higher than the SACH foot.

Above-knee Subject (AR011)

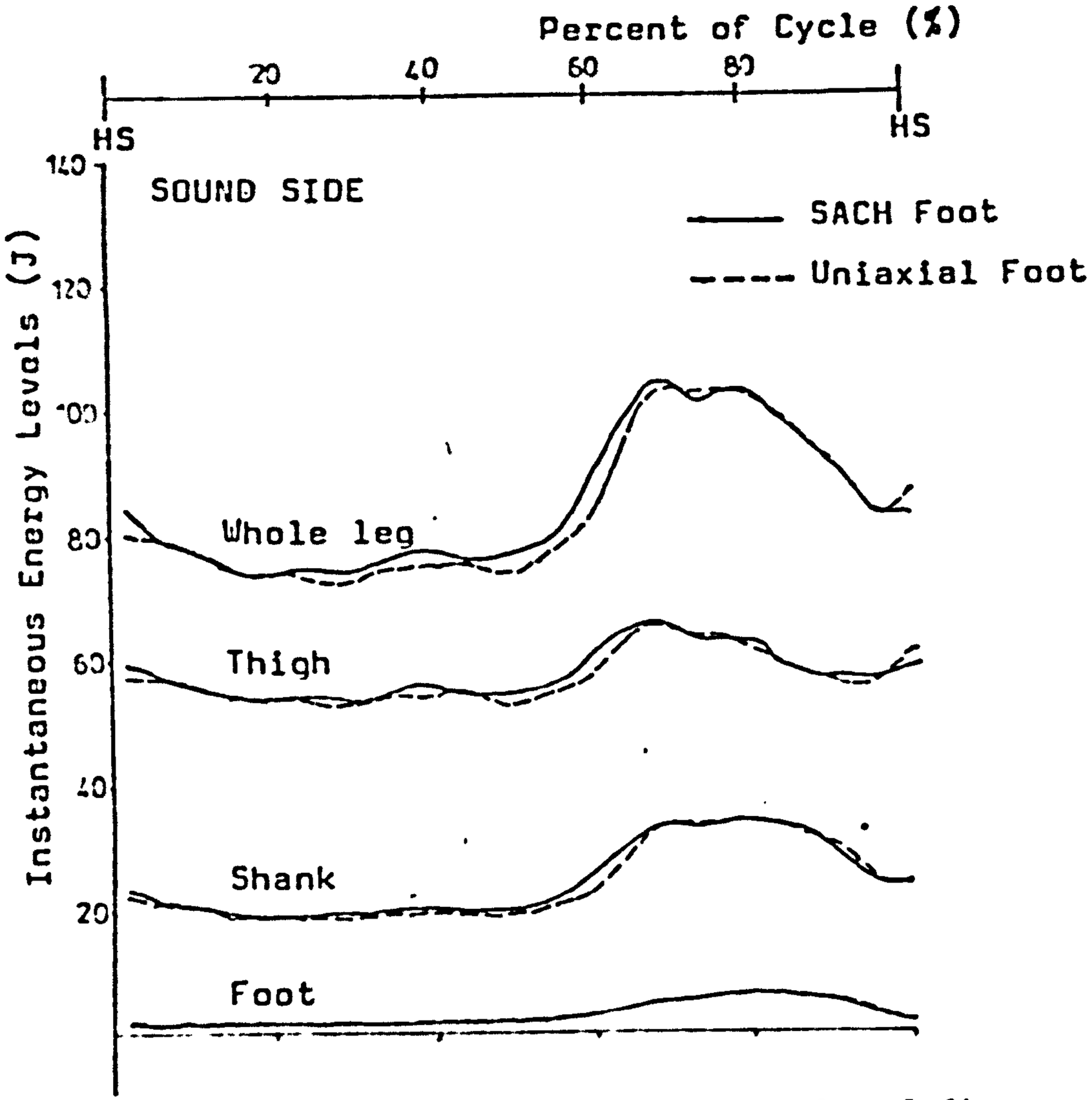

Figure 7.6.2(f) Typical Energy Levels of Above-knee Amputee (Sound Side)

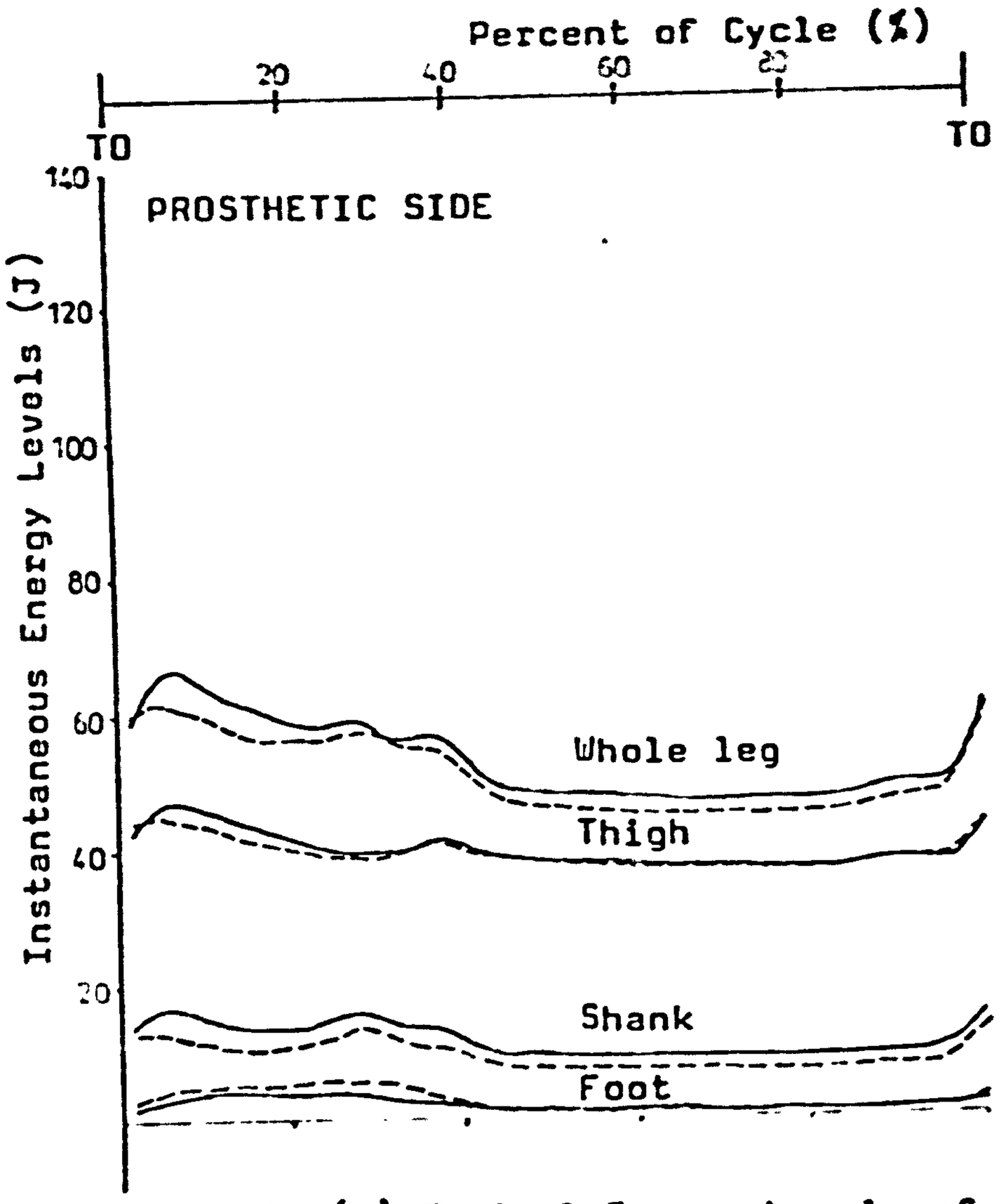

Figure 7.6.2(e) Typical Energy Levels of Above-knee Amputee (Prosthetic Side)

However, the range of scatter recorded is too great to show any significance in the differences obtained.

Figure 7.6.2(e) and (f) show the typical energy levels of the sound and prosthetic sides of the above-knee amputee.

The results from the sound side are similar in shape to those of the normal subject. The difference in magnitude is due to the height and weight of both subjects.

On the prosthetic side, the shapes and magnitudes of the energy levels are very different from those of the sound limb. The lower baseline values of the limb segments are due to the lower mass of the prosthesis and also due to the centre of mass being closer to the ground. The velocities of the prosthetic segments during swing phase are also fairly low. These are reflected in the energy levels of the segments. A comparison between the SACH and Uniaxial feet show no significant difference in the results of the prosthetic or those of the sound side.

The average work done by the sound and prosthetic limbs per walking cycle is as shown in Table 7.6.2(a). The results on the sound side show a higher value than those of the prosthetic side. On comparing the SACH and Uniaxial foot, no significant difference was observed.

Results from the normal subject show relatively similar values of work done by theleft and right legs over the walking cycle. The work done by the leg on the prosthetic side of the below-knee amputees over the walking cycle is 20 percent lower than that of the sound limb. For the above-knee amputees the work done per walking cycle on the prosthetic limb is 40 percent lower than that of the sound limb. The lower values recorded

Work done by leg per walking cycle(Joules) Mean (±1 S.D.)	Sound Side		Prosthetic Side	
	SACH	Uniaxial	SACH	Uniaxial
Below-Knee Amputees	100.0 (25.0)	105.8 (30.0)	76.6 (21.6)	85.9 (16.0)
Above-Knee Amputees	75.1 (16.3)	79.4 (17.3)	45.2 (4.6)	43.8 (5.32)
	Left Leg		Right Leg	
Normal Subject	92.6 (8.6)		96.6 (5.4)	

Table 7.6.2(a) Work Done by leg per Walking Cycle

for the prosthetic side are due to the relatively lower mass of the prostheses, as compared to that of the normal. The lower work done per walking cycle obtained for the above-knee amputees is due to the lower speed of walking, i.e. 1.043 m/s. The below-knee amputees walking at a faster speed of 1.36 m/s, fairly close to that of the normal subject (i.e. 1.465 m/s), had to do more work than the above-knee amputees.

CHAPTER 8

Conclusion and Recommendation for Future Work

Conclusion

The Otto Bock heel bumper stiffness supplied with the modular moulded-type Uniaxial foot were found to be too soft for most of the patients tested. The heel bumpers(of four different stiffnesses) moulded at the Bioengineering Unit were found to be acceptable to both patients and prosthetists.

The subjective comments of the patients showed that among the six below-knee amputees tested, three preferred the Uniaxial foot, two preferred the SACH foot and one had no specific preference. Among the five above-knee amputees tested, three preferred the Uniaxial foot while the remaining two preferred the SACH foot. No general trend of preference was observed between the performance of the SACH and Uniaxial feet in the choice made by the patients. However, the preferred prosthetic foot tends to correspond to that with which the patient is already familiar.

The Veterans Administration Standards and Specification for prosthetic ankle/foot assemblies was found to be inadequate in classifying the heel stiffness of the Uniaxial foot. All the rubber bumpers tested were classified merely as being "firm" when clearly they are of different stiffnesses.

The recommended heel stiffness of the SACH foot prescribed on the basis of type of amputation and body weight, presented by Radcliffe and Foort (1961), was found to be inadequate. For the below-knee amputees tested, the medium grade SACH foot was preferred even by patients whose body weight exceeded that of the recommendation. Furthermore, the guide does not make provision for amputees who require a soft grade SACH foot.

It was observed that for a particular amputee, the heel stiffness preferred for the Uniaxial foot was always more stiff than that of the preferred SACH foot according to the load versus deformation curve. This could be due to the different static load bearing characteristic of each prosthetic foot.

The alignment of the prostheses, whether with the SACH or Uniaxial foot, was found to be within the "optimum" alignment range (SACH foot) established in an on-going project in the Bioengineering Unit. Although there were indicative trends of differences in some of the alignment parameters measured, the stability characteristic of the patients was not altered.

The temporal components of the stance phase for the Uniaxial foot were found to be fairly similar to those of the normal subject but different from those of the SACH foot. Due to the rigid ankle, the SACH foot requires twice the time taken by the normal foot, to reach foot-flat position. These patterns were consistent in both the below and above-knee amputees.

The plantar-flexion angle during early stance with the Uniaxial foot was found to be in the region of 10^{o} to 15^{o}, in both the below-knee and above-knee amputees. This is fairly similar to that of the normal subject. Only a small amount of angular ankle movement was recorded on the SACH foot, i.e. approximately 5^{o}.

The ground to foot vertical force (Fy) on the prosthetic side of the above-knee amputee showed differences between the SACH and Uniaxial foot. The "broad" second peak of the SACH foot reflects the rocker-shaped design of the wooden keel in the SACH foot, which allows the patient to "roll-over" the ball of the foot fairly smoothly. With the Uniaxial foot, the second peak occurs

too soon, this suggests that the dorsiflexion stop is too stiff. Unfortunately, the dorsiflexion stop of the moulded Uniaxial foot used cannot be replaced. The design of the distal section of the Uniaxial foot could also have influenced the smoothness of the "roll-over". Only one patient was found to display the usual two-peak Fy curve with the Uniaxial foot after alignment changes.

The SACH foot, because of its rocker-shaped keel, produces a uniform rate of progression of the centre of pressure points as the foot moves from heel-strike to toe-off (referring to the "Butterfly" diagrams and "V" plots). With the Uniaxial foot, the rate of progression slows down during initial foot flat period. This is due to the pivoting effects of the whole body about the single-axis ankle joint. This event was also observed to be present in the normal subject, although the duration is not as long as that of the Uniaxial foot.

Kinetic analysis showed no indication of changes in the stability characteristics of the prosthetic gait whether using the SACH or Uniaxial foot. However, the positive ankle Mz moments of the above-knee amputees showed significant differences. The rounded curve of the SACH foot reflects the "smooth roll-over" pattern described earlier, while the two-peak curve of the Uniaxial foot suggests difficulty in "roll-over", although the amplitude recorded is fairly small. There was one exception. The same patient described previously, showed a "smooth roll-over" with the Uniaxial foot on the positive ankle Mz moments.

The results obtained show no conclusive evidence as to which prosthetic foot is functionally better for the amputee. Looking at foot action only, the Uniaxial foot seems to resemble the normal foot in function. However, when considering whole body action, the SACH

foot seems to function like that of the normal. Indications from both the kinematic and kinetic results suggest that with the selection of appropriate heel stiffness and proper alignment of the prosthesis, both prosthetic feet could be made to function similarly as far as whole body kinetics is concerned. This, however, is only indicative with active amputees.

Recommendation for Future Work

The followings are some ideas for future research in this area :

a) A statistical survey on the type of heel stiffness on both the SACH and Uniaxial foot prescribed to lower limb amputees. The information could be used to revise the existing guide proposed by Radcliffe and Foort (1961), for the selection of heel cushion stiffness of the SACH foot, and also provide a new guide for the selection of rubber bumper stiffness of the Uniaxial foot. However, the measure of heel stiffness should first and foremost be standardised. The "revised" guide should include selection of heel stiffness on the basis of level of amputation, body weight and level of activity of patient.

b) The Veterans Administration Standards and Specifications for prosthetic ankle/foot assemblies appears to be valid for the SACH foot only. The load versus deformation criterion used for testing plantar flexion is perhaps not the correct one. A revision of the current standards and specifications may be necessary. The ankle moment versus angular displacement may be a more appropriate criterion for testing the heel stiffness. There is also a need to clarify the definition of stiffness level for different prosthetic feet. This could be done by mechanical testing of prosthetic feet and then confirmed by subjective comments from patients and prosthetists.

BIBLIOGRAPHY

Amar J. (1916)
"Trottoir dynamographique"
Comt rend Acad d Sci 1916, 163, pp130-

American Academy of Orthopaedic Surgeons (1960)
"Orthopaedic Appliances Atlas, Vol. 2 - Artificial Limbs"
J.W. Edwards, Ann Arbor, Michigan

American Academy of Orthopaedic Surgeons (1981)
"Atlas on Limb Prosthetics : Surgical and Prosthetic Principles"
St. Louis : C.V. Mosby

Andrews B.J. (1975)
"Quantization effects in digital Kinematic Measurement and Data processing systems"
Internal Report, Bioengineering Unit, University of Strathclyde, Glasgow

Andrews B.J., Cappozzo A., and Gazzani G. (1981)
"A quantitative method for assessment of differentiation techniques used for locomotion analysis"
In: Computing in Medicine, Paul J.P. et al, MacMillan Press, U.K.

Andrews B.J., Thynn G., Nicol S.M., and Beale A.O. (1981)
"The Strathclyde TV/Computer system for 3-D Human motion analysis"
In: Computing in Medicine

Andriacchi T.P., Ogle J.A. and Galante J.D. (1977)
"Walking speed as a basis for normal and abnormal gait measurements"
J. Biomechanics, 10, pp 261-8

Asbelle C.C. and Canty T.J. (1957)
"A functional ankle (Cable) for Artificial legs"
Final Report, Navy Prosthetic Research Laboratory, U.S. Navy Hospital, Oakland, California.

Bajd T. and Kralj A. (1980)
"Simple kinematic gait measurements"
J. Biomed. Engng, 2(2), pp 129-132

Bartholomew S.H. (1952)
"Determination of Knee Moments during the swing phase of walking and physical constants of the human shank"
Series 11, Issue 19, Prosthetic Devices Research Project,University of California, Berkeley.

Baumann W. (1974)
"New Chronophotographic Methods for three-dimensional movement."
In: Biomechanics IV, Proceeding of the 4th International Seminar on Biomechanics, University Park, Pennsylvania, Editors: Nelson R.C. and Morehouse C.A.

Bernstein N.A. (1927)
"Die kymocyclographische Methode der Bewegungs - Untersuchung"
Hdb.d.biol. Arbeitsmethoden, 5(5a), Abderhalden.

Bernstein N.A. and Popova T.S. (1929)
"Untersuchung der Biodynanik des Klavieranschlags."
Arbeitsphysiologie, 1(5)

Bernstein N. (1934)
"The technique of the Study of Movements"
In: The Co-ordination and Regulation of Movements, Bernstein N., First English Edition, Pergamon Press, 1967

Bernstein N.A., Salzgeber O.A., Pavlenko P.O. and Gurvich N.A. (1936)
"Determination of location of the centres of gravity and mass of the limbs of the human body."
(in Russian)
All-Union Institute of Experimental Medicine, Moscow.

Berme N., Lawes P., Solomonidis S., and Paul J.P. (1976)
"A shorter pylon transducer for measurement of prosthetic forces and moments during amputee gait."
Engng in Med., 4(4), pp6-8.

Berme N., Purdey C.R., and Solomonidis S.E. (1978)
"Measurement of Prosthetic Alignment"
Prosthetics and Orthotics International, 2, pp 73-5.

Beveridge H. (1982)
PhD Thesis in Preparation University of Strathclyde, Glasgow.

Blanc Y. and Vadi P. (1981)
"An inexpensive but durable foot-switch for telemetered locomotion studies"
Biotelemetry Patient Monitg, 8, pp 240-5.

Boccardi S., Chiesa G. and Pedotti A. (1977)
"New procedure for evaluation of normal and abnormal gait."
Amer J Phys Med, 56, pp 163-182.

Bontrager E.L. (1980)
"Footswitch Redesign."
In: Annual reports of progress, Feb. 1980-Jan.1981, Rancho Los Amigos Rehab Eng. Centre, University of Southern California.

Borelli G.A. (1679)
"De Motu Animalium"
Lugdoni Batavorum

Braune W. and Fischer O. (1889)
"The centre of gravity of the human body as related to the equipment of the German infantryman." (in German)
Treat Math-Phys Class of the Royal Acad of Science of Saxony, 26, pp 561-

Braune W. and Fischer O. (1892)
"Determination of mass moments of inertia of the human body and its segment." (in German)
Treat Math-Phys Class of the Royal Acad of Science of Saxony, 18(8), pp 409-492.

Braune W. and Fischer O. (1895)
"Der Gang des Menschen" - Part I
Bei S. Hirzel, Leipzig

Breakey J. (1976)
"Gait of Unilateral below-knee amputees"
Orthotics and Prosthetics, 30(3), pp 17-24

Bresler B. (1951)
"Use of Energy Methods for Evaluation of Prostheses"
University of California, Berkeley

Bresler B. and Berry F.R. (1950)
"Energy characteristic of Normal and Prosthetic Ankle Joints"
Report Series 3, Issue 12, University of California, Berkeley, Prosthetic Devices Research Project

Bresler B. and Berry F.R. (1951)
"Energy and Power in the leg during normal level walking."
Report Series 11, Issue 15, University of California, Berkeley, Prosthetic Devices Research Project,

Bresler B. and Frankel J.P. (1950)
"The forces and moments in the Leg during level walking."
Trans Amer Soc Mech Eng, 72, pp 27-36

Bresler B., Radcliffe C.W. and Berry F.R. (1957)
"Energy and Power in the Legs of above-knee amputees during normal level walking."
Series 11, Issue 31, University of California, Berkeley.

Brown A.W.S. (1981)
"A microprocessor-based ultrasonic limb movement monitoring system."
J. Biomed Engn, 3, pp 275-280

Burgess E.W. and Matsen F.A. (1981)
"Determining Amputation levels in peripheral vascular disease" Review
J Bone Jt Surg, 63A, pp 1493-7

Campbell J.W. and Childs C.W. (1980)
"The SAFE foot"
Orthotics and Prosthetics, 34, pp 3-16

Cappozzo A., Maini M., Marchettim and Pedottia (1974)
"Analysis by hybrid computer of ground reactions in walking."
In: Biomechanics IV-Proc 4th Int Seminar on Biomechanics, University Park, Pennsylvania, Editors: Nelson R.C. and Morehouse C.A.

Cappozzo A., Figura F., Leot and Marchetti M. (1976)
"Biomechanical Evaluation of Above-knee Prostheses"
In: International Series on Biomechanics, Vol. 1A, Biomechanics V-A, Proceeding of the 5th Int. Congress of Biomechanics, Edited by Paavo V. Komi.

Cappozzo A. (1981)
"Analysis of the linear displacement of the head and trunk during walking at different speeds."
J. Biomechanics, 14, pp 411-425.

Carlet G. (1872)
"Essai experimental sur la locomotion humaine Étude de la marche."
Annal Scien Nat, Zool, 16

Carlson L.E., Dewar M. and Ackerley K. (1981)
"Agoniometer for simplified gait analysis."
In: Report 1981, Bioengineering Centre, Roehampton, London, Dept. of Mech. Engng, University College London.

Cavagna G., Saibene F. and Margaria R. (1961)
"A three directional accelerometer for analysing body movements."
J Appl Phys, 16, pp 191-

Cavagna G.A., Saibene F.R. and Margariar. (1963)
"External work in walking."
J. Appl Physiol, 18, pp 1-9

Chao E.Y.S. (1978)
"Experimental methods of joint kinematics."
In: CRC Handbk of Eng in Med and Biol. Vol. 1(B), pp 385-411

Chao E.Y.S., Rim K., Smidt G.L. and Johnston R.C. (1970)
"The application of 4x4 matrix method to the correction of measurements of hip joint rotations."
J. Biomechanics, 3, pp 459-471

Chao E.Y.S. (1977)
"Justification of goniometeric method as a means to evaluate joint replacement patients."
In: NIH-Gait Research Workshop,Children's Hospital Health Centre, San Diego, California..

Chandler R.F., Clauser C.E., McConville J.T., Reynolds H.M. and Young J.W. (1975)
"Investigation of inertia properties of the human body."
Report No. DOT HS-801 430/AMRL-TR-74-137, Aerospace Medical Division, Research Laboratory, Wright-Patterson Air Force Base.

Chatinier K. Du, Molen N.H. and Rozendal R.H. (1970)
"Step length, step frequency and temporal factors of the stride in human walking."
In: "Problems on the Evaluation of Gait-with special reference to the comparison of normal subjects with below-knee amputees."; by: Molen N.H.

Cheng I.S. (1974)
"Computer-television analysis of Biped locomotion."
PhD. Thesis, Ohio State University, Columbus, Ohio.

Chodera J.D. and Lord M. (1978)
"Pedobarographic foot-pressure measurements and their applications".
In: Disability-Proc seminar on Rehab of the disabled, Strathclyde Bioengineering Seminars, Editor: Kenedi R.M.K., Paul J.P. and Hughes J.

Clauser C.E., McConville J.T. and Young J.W. (1969)
"Weight, Volume and centre of Mass of Segments of the Human Body."
Report No. AMRL-TR-69-70, Aerospace Medical Division, Research Laboratory, Wright-Patterson Air Force Base, Ohio.

Close J.R. and Inman V.T. (1952)
"The action of the ankle joint"
Series 11, Issue 22, Prosthetic Devices Research Project, University of California, Berkeley.

Cohen A., Orin D.E. and Marsolais E.B. (1980)
"The gait laboratory force plate at the Cleveland V.A. Medical Centre"
BPR Spring, 10-33, pp 90-7

Contini R. (1972)
"Body Segment Parameters. Part II"
Artificial Limbs, 16(1), pp 1-19

Committee on Prosthetics Research and Development (1971)
"Cosmesis and Modular Limb Prostheses"
Report of a conference held in San Francisco, California, March 3-7, 1971, National Academy of Sciences, Washington, D.C.

Committee on Prosthetic Research and Development (1975)
Draft proposal for : "Standardisation of Gait Analysis Parameters and Data Reduction Techniques - A Task Force Report."
Distributed as minutes for limited distribution.

Cook T.M., Cozzens B.A. and Kenosian H. (1979)
"A technique for force-line visualization."
Rehab Engng Centre, Moss Rehab Hospital, Philadelphia, Pa 19141

Cousins S.J. (1975)
"A parallelogram chain designed to measure human joint motion."
M.Sc Thesis, University of British Columbia, Vancouver, Canada.

Crowninshield R.D. and Brand R.A. (1978)
"Kinematics and Kinetics of Gait"
In: CRC Handbook of Engineering in Medicine and Biology, Vol. 1(8), pp 413-425

Cummings V., March H., Steve L. and Robinson K.G. (1979)
"Energy costs of below-knee prostheses using two types of suspension."
Arch Phys Med Rehab., 60(7), pp 293-6

Cunningham D.M. (1950)
"Components of floor reactions during walking."
Report Series 11, Issue 14, University of California, Berkeley, Prosthetic Devices Research Project.

Cunningham D.M. and Brown G.W. (1952)
"Two devices for measuring the forces on the human body during walking."
Proc Soc Exp Stress Analysis, 9(2).

Daher R, (1973)
Personal Communication

Daher R.L., Nelson P.J., Heath J.B. and Peteleski N.(1974)
"Functional Evaluation of Artificial Feet by Load Vs. deflection Recordings"
Inter-clinic Information Bulletin, 13(4), pp 3-7.

Daher R.L. and Heath J.B. (1974)
"Durability testing of Artificial Feet in the Laboratory"
Inter-clinic Information Bulletin, 13(4),pp 11-17.

Daher R.L. (1975)
"Physical Response of SACH feet under laboratory Testing."
BPR Spring 10-23, pp 4-50.

Davies E.J., Friz B.R. and Clippinger F.W. (1970)
"Amputees and their prostheses"
Artificial limbs, 14(2), pp 19-48.

Day H.J.B. (1981)
"The assessment and description of amputee activity"
Prosthetic and Orthotics International, 5, pp 23-8

Dempster W.T. (1955)
"Space requirements of the seated operator"
USAF, WADC, Technical Report 55-159, Wright-Patterson Air Force Base, Ohio.

Department of Health and Social Security (1973)
"Lower Limb Modular Prostheses"
A report on an International Conference on Specification, Ascot, England - 1972.

Department of Health and Social Security Statistics and Research Division, (1976 and 1978)
Amputation Statistics for England, Wales and N. Ireland.

Dewar M., Carlson L., Smith D., Ackerley K., Hardgreaves G. and Wang D. (1981)
"A system for the clinical analysis of joint motion"
Report 1981, Bioengineering Centre, Roehampton, Dept. of Mech Engng, University College London.

Dorn W.S. and McCracken D.D. (1972)
"Numerical Methods with Fortran Case Studies"
John Wiley and Sons Inc.

Draganich L.F., Andriacchi T.P., Strongwater A.M., Galante J.O. (1980)
"Electronic measurement of instantaneous foot-floor contact patterns during gait"
J. Biomechanics, 13, pp 875-880.

Drillis R.J. (1958)
"Objective recording and biomechanics of pathological gait"
Ann New York Acad Sci, 74, pp 86-

Drillis R.J. (1958)
"The use of gliding cyclograms in the biomechanical analysis of movements"
Human Factors, 1(2)

Drillis R.J. and Contini R. (1966)
"Body Segment Parameters"
Technical Report No. 1166.03, New York University, School of Engineering and Science, Research Division.

Eberhart H. and Inman V. (1947) Editors
"Fundamental Studies of human locomotion and other information relating to design of artificial limbs"
University of California, Berkeley, Report to National Research Council, Committee on Artificial Limb - 2 Vol.

Eberhart H.D., Inman V.T., Rosenkranz G. and McKennon J.C. (1949)
"Summary Report of European Observations"
Report to Advisory Committee on Artificial limbs, Washington D.C., National Research Council.

Eberhart H.D., Inman V.T. and Bresler B. (1954)
"The principle elements in human locomotion."
In: Human Limbs and their Substitute, Klopsteg P.E. and Wilson P.D. et al.

Elftman H. (1934)
"A cinematic study of the distribution of pressure in the human foot"
Anatomical Record, 59, pp 481-491

Elftman H. (1938)
"The measurement of the external force in walking"
Science, 88, pp 152-

Elftmah H. (1939)
"The function of the muscles in locomotion"
Amer J Phys., 125, pp 357-366

Elftman H. (1939)
"Forces and energy changes in the leg during walking"
Amer J Phys., 125, pp 339-356

Elftman H. (1939)
"The rotation of the body in walking"
Arbeitsphysiologie, 10, pp 477-483

Elftman H. (1939)
"The Function of arms in walking."
Human Biol., 2, pp 529-535

Elftman H. (1939)
"The force exerted by the ground in walking"
Arbeitsphysiologie, 10, pp 485-491

Elftman H. (1960)
"The transverse tarsal joint and its control"
Clinical Orthopaedic, 16, pp 41-

Faulkner V. and Pritham C. (1973)
"A below-knee prosthesis with a porous socket"
Orthotics and Prosthetics, 27(1), pp 1-5

Felkel E.O. (1951)
"Determination of acceleration from displacement-time data"
Report Series 11, Issue 16, University of California Berkeley, Prosthetic Devices Research Project.

Fillauer C. (1968)
"Supracondylar wedge suspension of the PTB prosthesis"
Orthotics and Prosthetics, 22(2), pp 39-44

Finley F.R., Wirta R.W. and Hall M.G. (1972)
"Rehabilitation biomedical Engineering: orthotics design"
Final Report, Moss Rehabilitation Hospital, Social Adn Rehab. Service, Grant No. RD 23-P-55117/3

Fischer O. (1898-1904)
"Der Gang des Menschen"
Abh. d. Koeniql. Saechs. Gesellsch d. Wissensch. Math. Phys. D. (six parts)

Fischer S.V. and Gullickson G. (1978)
"Energy cost of ambulation in health and disability: a literature review"
Arch Phys Med and Rehab, 59(3), pp 124-133.

Fishman S. et al (1953)
"The functional and psychological suitability of an experimental hydraulic prosthesis for above-the-knee amputees"
Prosthetic Devices Study, New York University, Report No. 115.15

Fishman S. et al (1955)
"Evaluation of the Solid-Ankle Cushion-Heel foot"
Report No. 115.19, Prosthetic Devices Study, New York University.

Fishman S., Berger N. and Watkins D. (1975)
"A survey of prosthetic practice - 1973-1974"
Orthotics and Prosthetics, 29(3), pp 15-20

Freeborn C. (1980)
"Goniometric measurement via a sonic digitizer"
In: Annual reports of progress, Feb. 1980-Jan 1981
Rancho Los Amigos Rehab Eng Centre, University of Southern California.

Friedmann L.W. (1972)
"Amputations and prostheses in primitive cultures"
BPR Spring, 10-17, pp 105-138

Fulford G.E. and Hall M.J. (1968)
"Amputation and prostheses. A survey in N.W. Europe and North America"
Report on BLESMA Travelling Scholarship, Bristol, John Wright and Sons Ltd.

Furnee E.H. (1967)
"Hybrid instrumentation in prosthetic research"
Proc. 7th Int. Conf on Med and Biol Eng Stockholm.

Gabel R.H., Johnston R.C. and Crowninshield R.D. (1979)
"A gait analyzer/trainer instrumentation system"
J Biomechanics, 12, pp 543-9

Gage H. (1964)
"Accelerographic analysis of human gait"
ASME paper No 64-WA/HUF 8

Ganguli S. and Mukherjee P. (1973)
"A gait recording technique suitable for clinical use"
Biomed Engng, 8(2), pp 60-3

Garrison F.H. (1963)
"An introduction to the history of medicine"
Philadelphia, W.B. Saunders Co.

Garton W.T. (1979)
"Measurement of metabolic energy expediture in the disabled"
In: BRADU-Roehampton, London, Report 1979, D.H.S.S.

Glattly H.W. (1964)
"A statistical study of 12,000 new amputees"
South Med J, 57, pp 1373-

Gocht H., Radike R. and Schede (1920)
"Kunstliche Glieder" (Artificial Limbs)
Ferdinand Enke, Publisher, Stuttgart, (in German)

Godfrey C.M., Jousse A.T., Brett R. and Butler J.F.(1975)
"A comparison of some gait characteristics with six knee joints"
Orthotics and Prosthetics, 29(3), pp 33-38

Godfrey C.M., Brett R. and Jousse A.T. (1977)
"Foot Mass effect on gait in the prosthetic limb"
Arch Phys Med Rehab, 58(6):268-9

Gordon E.J. and Ardizzone J. (1960)
"Clinical Experience with the SACH foot prosthesis"
J.Bone Jt. Surg 42-A, pp 226-234

Grieve D.W. (1968)
"Gait pattern and the speed of walking"
Biomed Engng, 3, pp 119-

Grieve D.W. (1969)
"A device called the Polgon for the measurement of the orientation of parts of the body relative to a fixed external axis"
J. Physiol, 201, pp 70-

Grieve D.W. and Gear R.J. (1966)
"The relationships between length of stride, step frequency, time of swing and speed of walking for children and adults" Ergonomics, 9, pp 329-399

Grundy M.Tosh P.A., McLeish R.D. and Smidt G.L. (1975)
"An investigation of the centres of pressure under the foot while walking"
J Bone Jt Surg, 57(B), pp 98-103

Gunston F.H. (1971)
"Polycentric Knee arthroplasty"
J Bone Jt Surg, 53-B(2), pp 272-7

Hamming R.W. (1977)
"Digital Filters"
Prentice-Hall Signal Processing Series, Alan Oppenheim, Series Editor, Prentice-Hall, Inc., Englewood Cliffs, New Jersey.

Hargreaves P. and Scales J.T. (1975)
"Clinical assessment of gait using load measuring footwear"
Acta Orthop Scand, 46, pp 877-895

Harless E. (1860)
"The static moments of human limbs" (in German)
Treatise of the Math - Phys. Class of the Royal Acad of Science of Bavaria, 8(1), pp 69-96 and 257-294

Harrington I.J. (1974)
"Knee joint forces in Normal and Pathological Gait"
MSc Thesis, University of Strathclyde, Glasgow.

Harrison H.R. and Nettleton T. (1978)
"Principles of Engineering Mechanics"
Edward Arnold (Publishers) Ltd., London.

Hicks J.H. (1953)
"The mechanics of the foot : I - The joints"
J. Anat, 87, pp 345-357

Hicks J.H. (1954)
"The mechanics of the foot, II, The plantar Aponellrosis and the arch"
J. Anat, 88, pp 25-

Holden T.S. and Muncey R.W. (1953)
"Pressures on the human foot during walking"
Aust J Appl Sci, 4, pp 405-417

Huang C.T., Jackson J.R., Mobre N.B., Fine P.R., Kuhlemeier K.V, Traugh G .H. and Saunders P.T. (1979)
"Amputation: Energy Cost of Ambulation", Arch Phys Med Rehab, 60(1), pp 18-24

Inman V.T. (1976)
"The joints of the ankle"
The Williams and Wilkins Company Baltimore

Inman V.T., Raltson H.J. and Radcliffe C.W. (1981)
"Human Walking"
The Williams and Wilkins Company, Baltimore

Ishai G.A. (1975)
"Whole Body Gait Kinetics"
PhD. Thesis, University of Strathclyde, Glasgow

Isman R.E. and Inman V.T. (1969)
"Anthropometric studies of the Human Foot and Ankle"
BPR Spring, 10-11, pp97

Jacobs N.A., Skorecki J. and Charnley J. (1972)
"Analysis of the vertical component of force in normal and pathological gait"
J Biomechanics, 5, pp 11-34

James U. and ÖBERG K. (1973)
"Prosthetic gait pattern in Unilateral above-knee amputees"
Scand J Rehab Med, 5, pp 35-50

Jansen E. and Orbaer H. (1980)
"Reproducibility of gait measurement using the Lamoreux goniometer"
Pros Orth Int., 4, pp 159-161

Jarrett M.Q. (1976)
"Television-computer system for human locomotion analysis"
PhD Thesis, University of Strathclyde, Glasgow

Jarrett M.O. (1980)
"A clinical system for 3-dimensional Gait Analysis"
Biological Engineering Society, 20th Anniversary International Conference, London

Johnson F., Watts W.G. and Evans D.F. (1981)
"Goniometer for continuous recording of knee angle"
Med & Biol Eng & Comput., 19, pp 255-256

Johnston R.C. and Smidt G.L. (1969)
"Measurement of Hip Joint Motion during walking. Evaluation of an electrogoniometric Method"
J Bone Jt Surg, 51A, pp 1083-1094

Jones W.F. (1944)
"Structure and function as seen in the foot"
Pub. Bailliere, Tendell and Cox, London, England.

Jordan J.W. (1969)
"Direction Cosine Computational Error"
NASA TR-R-304

Jordan M.M. (1978)
"An interactive signal processing and analysis package for use in biomedical research"
PhD Theses, University of Strathclyde, Glasgow

Judge G. (1980)
"Survey of Knee Mechanisms for artificial legs"
BRADU 1977 to 1978, Revised 1980.

Karpovich P.V. and Karpovich G.P. (1959)
"Electrogoniometer: a new device for study of joints in action."
Fed Proc, 18, pp 79-

Kasvand T., Milner M and Rapley L.F. (1971)
"A computer-based system for the analysis of some aspects of human locomotion"
In: Human Locomotor Engineering, Proceedings of Conference at University of Sussex by Inst. Mech Engineers.

Kay H.W. et al (1957)
"Evaluation of the Navy Celastic Soft Socket for below-knee amputees"
Prosthetic Devices Study, New York University, Report No. 115.20.

Kay H.W. et al (1957)
"Evaluation of the Production Model SACH foot"
Report No. 115.23, Prosthetic Devices Study, New York University.

Kay H.W. and Newman J.D. (1973)
"Report of workshop on Below-knee and Above-knee Prostheses"
Orthotics and Prosthetics, 27(4), pp 9-25

Kay H.W. and Newman J.D. (1975)
"Relative incidence of new amputees. Statistical comparisons of 6,000 new amputations"
Orthotics and Prosthetics, 29, pp3-

Kettelkamp D.M., Johnson R.J., Smidt G.L., Chao E.Y.S. and Walker M. (1970)
"An electrogoniometric study of knee motion in normal gait"
J. Bone Jt Surg., 52A, pp 775-790

Kinzel G.L., Hall A.S. and Hillberry B.M. (1972)
"Measurement of the total motion between two body segments - 1. Analytical Development"
J. Biomechanics, 5, pp 93-105

Kirkpatrick G.S., Day E.E. and Lehmann J.F. (1969)
"Investigation of the performance of an ischial load bearing leg brace"
Exp Mech, 9, pp 31-5

Kistler A.G. of Switzerland (1977)
"Information Bulletin for electrical measurements of mechanical values"
Trade Literature, Number 15

Kljajic M. and Trnkoczy A. (1977)
"Ground reaction force measuring shoes"
In: Proc. 1st Mediterranean Conf Med and Biol. Engng, Sorrento, Sectionl, pp 57-60

Klopsteg P.E. and Wilson P.E. (1954)
"Human limbs and their substitutes"
Hafner Publishing Company, Reprinted 1968.

Kostuik J.P. and Gillespie R. (1981)
"Amputation surgery and rehabilitation. The Toronto experience"
Churchill Livingstone

Kuhn G.G. (1956)
"Typische Fehler beim Oberschenkelkunstbeinball"
(Typical Faults in Above-knee Prostheses)
Preisarbeit im Preisausschreiben des, Bundesministeriums fur Arbeit, Bonn

Kuo S.S. (1965)
"Numerical Methods and Computers"
Addison-Wesley, Reading, MA

Lamoreux L.W. (1971)
"Kinematic measurements in the study of human walking"
BPR Spring 1971, 10-15, pp 3-84

Lamoureux L.W. and Radcliffe C.W. (1977)
"Functional analysis of the UC-BL Shank axial rotation device"
Prosthetics and Orthotics International, 1(2), pp 114-8

Lanczos C. (1957)
"Applied Analysis"
Pitman, London

Lanshammar H. (1982)
On practical evaluation of differentiation techniques for human gait analysis
J. Biomechanics, 15, pp 99-106

Lauru L. (1957)
"Physiological study of motion"
Advanced management, 22, pp 17-24

LeBlanc M. (1973)
"Patient population and other estimates of prosthetics and orthotics in the U.S.A.
Orthotics and Prosthetics, 27, pp 38-

Liberson W.T. (1936)
"Une Nonvelle Application du Quartz Piezoelectrique: Piezoelectrographie de la Marche et des Mouvements Volontaires"
Paris, Le Travail Humain, 4, pp 1-7

Lindholm L.E. (1974)
"An Optoelectronic instrument for remote on-line movement monitoring"
In: Biomechanics IV, Proceedings of the 4th International seminar on Biomechanics, University Park, Pennsylvania, Editors: Nelson R.C. and Morehouse C.A.

Lippert F.G. (1973)
"The feasibility of photogrammetry as a clinical research tool"
J. Biomechanics, 6, pp 459-473

Litt B.D. and Nattress L.W (Jr)(1961)
"Report 1, Prosthetic services U.S.A. 1961"
American Orthotics and Prosthetics Association, Washington D.C.

Lovely D. (1981)
"Portable tape recorder system for prosthetic load data acquisition"
PhD. Thesis, University of Strathclyde, Glasgow

Lowe P.J. (1969)
"Knee mechanism performance in amputee activity"
PhD Thesis, University of Strathclyde, Glasgow.

Lyquist E. (1969)
"Recent variants of the PTB Prosthesis (PTS, KBM and Air-cushion Sockets)"
In: Prosthetic and Orthotic Practice; edited by Murdoch G. (1970)

McCollough N. and Snell R. (Co-chairman) (1977)
"Limb Prosthetics and Orthotics"
Report of a workshop, University of Miami, April3, 1977, Orthotics & Prosthetics, 31(4).

McDonald I (1961)
"Statistical studies of recorded energy expenditure of man. Part II, expenditure on walking related to weight, sex, age, height, speed and gradient"
Nutr Abstr Rev, 31, pp 739-762.

McDougall A. and Emmerson A. (1977)
"The preformed socket and modular assembly for primary amputees".
J.B. Jt. Surg., 59B(1), pp 77-9

McLeish R.D. and Arnold D.A. (1972)
"A foot-ground reaction force plate"
In: Joint British Comm for Stress Analysis, Proc Conf on Recording and Interpretation of Engng measurement, Institute of marine engineers.

Mann R.A. (1975)
"Biomechanics of the Foot"
In: American Academy of Orthopaedic Surgeons, Atlas of Orthotics : Biomechanical Principles and application. St. Louis, C.V. Mosby.

Mann R.A. and Inman V.T. (1964)
"Phasic activity of intrinsic muscles of the foot"
J Bone Jt Surg, 46A, pp 469-

Manter J.T. (1941)
"Movements of the subtalar and transverse tarsal joints"
Anat Rec., 96, pp 313-321

Marey J.E. (1873)
"De la locomotion terrestre chez tes bigedes et les quadrupedes"
J Anat Physiol, 9, pp 42-

Marey E.J. (1886)
"La methode graphique dans les sciences experimentales"
G. Masson, Paris, France.

Marsden J.P. and Montgomery S.R. (1972)
"An analysis of the dynamic characteristics of a force plate"
Measurement and Control, 5, pp 102-6

Mayott C.W., Weinstein A.M., Moyle D.D. and Bailey C.L. (1975)
"Computerised analysis of instant centres of the human knee"
28th ACEMB, New Orleans, Sept. 20-24 1975, 17, pp 156-

Meeh C. (1895)
Volummessungen des menschlichen Körpers and seiner einzelner Teile in der verschiedenen Altersstufen.
Ztschr. fur Biologie., 13, pp 125-147

Mital M.A. and Pierce D.S. (1971)
"Amputees and their prostheses"
Little, Brown and Company, Boston.

Miller D.I. and Nelson R.C. (1973)
"Biomechanics of Sport : A research Approach"
Lea and Febiger, Philadelphia

Milner M., Brennan P.K. and Wilberforce B.A. (1973)
"Stroboscopic polaroid photography in clinical studies of human locomotion"
S. Afr Med J., 9, pp 948-950

Milner M. (1977)
"An overview of the current status of existing gait laboratories"
In: NIH - Gait Research Workshop; Children's Hospital Health Centre, San Diego, California.

Mitchelson D.A. (1975)
"Recording of movement without photography"
In: Techniques for the analysis of human movement, The human movement series, Lepus Books

Mitchelson D. (1981)
In: Workshop on the Clinical, Application of Gait Analysis, Dundee, 30th March-1st April, 1981 (in press)

Mitchelson D.J. (1982)
Personal Communication

Miura M., Miyashita M., Matsui H. and Sodeyama H.(1974)
"Photographic method of analysing the pressure distribution of the foot against the ground"
In: Biomechanics IV, Proc 4th Int. Seminar on Biomechanics, University Park, Pennsylvannia; Editors : Nelson R.C. and Morehouse C.A.

Miyazaki S. and Iwakura H. (1978)
"Foot force measurement device for clinical assessment of pathological gait"
Med. and Biol. Engng and Comput., 16, pp 429-436

Molen N.H. and Boon W. (1972)
"Measurement of momentary velocity in the study of human gait"
J. Biomechanics, 5, pp 273-6

Molen N.H., Rozendal R.H., Faassen F. Van and Rijneveld H.M. (1973)
"Problems in the evaluation of the gait of below-knee amputees"
In: Problems on the Evaluation of gait with special reference to the comparison of normal subjects with below-knee amputees; edited by N.H. Molen.

Morris J.M. (1977)
"Biomechanics of the Foot and Ankle"
Clinical Orthopaedics 1977, 122, pp 10-17

Morris J.W. (1973)
"Accelerometry - A technique for the measurement of human body movements"
J. Biomechanics, 6, pp 729-736

Morrison J.B. (1967)
"The forces transmitted by the human knee joint during activity"
PhD. Thesis, University of Strathclyde, Glasgow.

Movement Techniques Limited (1982)
"CODA-3 Movement Monitoring Instrument"
Trade Literature

Mulby W.C. and Radcliffe C.W. (1960)
"An ankle-rotation device for prostheses" (UC-B ankle rotator - model Q74A)
Biomechanics Lab., University of California, San Francisco, Berkeley, Number 37.

Murdoch G. (1970)
"Prosthetic and Orthotic practice"
Base on a conf held in Dundee, June 1969.
London : E. Arnold.

Murphy E.F. (1954)
"The fitting of Below-knee Prostheses"
In: Human limbs and its substitutes, Klopsteg P.E. and Wilson P.D. et al., Hafner Publishing Co., Reprint 1968.

Murray M.P., Drought A.B. and Kory R.C. (1964)
"Walking Patterns of Normal men"
J. Bone Jt Surg., 46A(1), pp 335-360.

Murray M.P., Sepic S.B., Gardner G.M., and Mollinger L.A. (1980)
"Gait patterns of A/K amputees using constant - friction knee components"
BPR Fall, 10-34, pp 35-45

Muybridge E. (1882)
"The horse in motion, as shown by instantaneous photography"
London

Muybridge E. (1887)
"The human figure in motion"
New Edition 1955; Dover Publication, New York

Naeff M. and Pijkeren T. Van (1980)
"Dynamic Pressure measurements of the interface between residual limb and socket - the relationship between pressure distribution, comfort and brim shape"
BPR Spring, 10-33, pp 35-50

New York University (1955)
"Supplementary report - SACH foot"
Prosthetic Devices Study; New York University

New York University (1956)
"Report of Test of the SACH foot"
Prosthetic Devices Study; New York University

Nietert M. (1977)
"The human knee joint as a biomechanical problem"
Biomedizinische Technik, 22, pp 13-21

North J.P., Jones D., Govan N.A. and Hughes J. (1974)
"Performance measurement of the Jaipur foot"
World Congress of ISPO; Switzerland.

Northwestern Technological Institute (1947)
"A review of the literature, patents and manufacture items concerned with artificial legs, arms, arm harness, hand and hooks; Mechanical testing of legs."
Final Report to National Research Council, Committee on Artificial Limbs., N.T.I., Evanston, Illinois.

Oxford Medical Systems Ltd. (1980)
"Vicon System Technical Summary"
Trade Literature

Padgaonkar A.J., Krieger K.W. and King A.I. (1975)
"Measurement of angular acceleration of a rigid body using linear accelerometers"
J. Appl Mech., 42(3), pp 552-6

Paul J.P. (1967)
"Forces at the human hip joint"
PhD Thesis, University of Glasgow, Glasgow.

Paul J.P. (1970)
"The effect of walking speed on the force actions transmitted at the hip and knee joints"
Proc Royal Soc Med., 63(2), pp 200-2

Paul J.P. (1971)
"Comparison of EMG signals from leg muscles with the corresponding force actions calculated from walkpath measurements"
In: Human locomotor Engng., Proc. Conf at University of Sussex, Inst. Mech. Engineers, London.

Paul J.P. and Nicol A.C. (1981)
"Usability of the Selspot system for biomechanical data acquisition"
Report to the Scottish Home and Health Department (unpublished)

Pederson H.E. (1968)
"The problem of the geriatric amputee"
Artificial limbs, 12(1), pp 1-3

Pedotti A. (1977)
"Simple equipment used in clinical practice for evaluation of locomotion"
IEEE Trans Biomed Engng., BME-24, pp 456-461.

Peizer E. and Wright D.W. (1969)
"Human Locomotion"
In: "Prosthetic and Orthotic Practice"; Edited by Murdoch G. (1970)

Pepoe R. (1970)
Manual for automatic film scanner developed at Children's Hospital in Iowa city, Iowa, U.S.A.

Perry J, Bontgrager E. and Antonelli D. (1978)
"Foot switch definition of basic gait characteristics"
In: Disability - Strathclyde Bioeng. Seminars, Proc. Seminar on Rehab. of the disabled.; Edited by Kenedi R.M. Paul J.P., Hughes J.

Pezzack J.C., Norman R.W. and Winter D.A. (1977)
Technical Note : "An assessment of derivative determining techniques used for motion analysis"
J. Biomechanics, 10, pp 377-382

Pierquin L., Fajal G. and Paquin J.M. (1964)
"Prosthe'se Tibiale a'Emboitage Supracondylien"
Atlas d'Appareillage Prosthetique et Orthopedique.

Pipes L.A. (1963)
"Matrix Methods for Engineering"
Prentice-hall, Englewood Cliffs

Plagenhoef S. (1971)
"Patterns of human Motion - A cinematographic Analysis"
Englewood Cliffs, N.J., Prentice-hall.

Pritham C. (1979)
"Suspension of the Below-knee prosthesis : An overview"
Orthotics and Prosthetics, 33(2), pp 1-19

Program Guide G7 (1976)
"Selection and application of knee mechanisms"
Prosthetic and Sensory aids Service; Veterans Administration, Washington D.C., 1976.

Purdey C.R. (1977)
"Socket Axis Determination in Lower Limb Prosthetic Alignment"
MSc. Thesis, University of Strathclyde, Glasgow.

Racette W. and Breakey J.W. (1977)
"Clinical experience and functional considerations of axial rotators for the amputee"
Orthotics and Prosthetics, 31(2), pp 29-34

Radcliffe C.W. (1955)
"Functional considerations in the fitting of above-knee Prostheses"
Artificial limbs, 2(1)

Radcliffe C.W. (1962)
"The biomechanics of below-knee prostheses in normal, level, bi-pedal walking"
Artificial limbs, 6(2), pp 16-24

Radcliffe C.W. (1969)
"Biomechanics of Above-knee Prostheses"
In: Prosthetic and Orthotic Practice; Edited by Murdoch G. (1970)

Radcliffe C.W. (1969)
"Prosthetic knee mechanisms for above-knee amputees"
In: Prosthetic and Orthotic Practice, edited by G. Murdoch (1970)

Radcliffe C.W. and Foort J. (1961)
"The Patellar-tendon-bearing below-knee prosthesis"
Biomechanics Laboratory, California

Ralston H.J. (1958)
"Energy-speed relation and optimal speed during level walking"
Int Z Angen Physiol einschl Arbeitsphysiol, 17, pp 277-283

Ralston H.J. and Lukin L. (1969)
"Energy levels of human body segments during level walking"
Ergonomics, 12(1), pp 39-46

Redhead R.G. (1979)
"Total surface bearing self suspending above-knee sockets"
Prosthetics and Orthotics International, 3, pp 126-136

Reed D.J. and Reynold P.J. (1969)
"A joint angle detector"
J. Appl Physiol., 27, pp 745-8

Reed B., Wilson A.B. and Pritham C. (1979)
"Evaluation of an Ultralight below-knee prosthesis"
Orthotics and Prosthetics, 33(2), pp 45-53

Robertson D.G.E and Winter D.A. (1980)
"Mechanical energy operation, absorption and tra transfer amongst segments during walking"
J. Biomechanics, 13, pp 845-854

Root M.L., Orien W.P., Weed J.H. and Hughes R.J. (1971)
"Biomechanical examination of the foot. Vol. I"
Clinical Biomechanics Corpo., Los Angeles

Root M.L., Orient. W.P. and Weed J.H. (1977)
"Normal and abnormal function of the foot. Clinical Biomechanics. Vol II"
Clinical Biomechanics Corp., Los Angeles

Rubin G. and Byer J.L. (1973)
"A porous, flexible insert for the below-knee prosthesis"
Orthotics and Prosthetics, 27(3), pp 19-26

Rydell N.W. (1966)
"Forces acting on the femoral head prosthesis"
Acta Orthop Scand Suppl., 88

Ryker N.J. and Bartholomew S.H. (1951)
"Determination of Acceleration by use of accelerometers"
Report Series 11, Issue 17, University of California, Berkeley, Pros. Devices Res Project

Schwartz R.P. Heath A.L. and Wright J.N. (1933)
"Electrobasographic method of recording gait"
Arch surg, 27, pp 926-

Schwartz R.P. and Heath A.L. (1947)
"The definition of human locomotion on the basis of measurement with description of oscillographic method"
J Bone Jt Surg., 29(A), pp 203-

Selcom A.B. (1975)
Trade Literature on the Selspot system
Selective Electronic Company A.B.,Box 30, S-431 21, Mölndal, Sweden

Sethi P.K., Udawat M.P., Kasliwal S.C. and Chandra R. (1978)
"Vulcanised rubber foot for lower limb amputees"
Prosthetics and Orthotics International, 2, pp 125-136

Shoji H. (1977)
"The foot and ankle"
In: Musculo-skeletal Disorders; Regional Examination and Differential Diagnosis; edited by R.D. D'Ambrosia, Pub. J.B. Lippincott Co., pp 487-523.

Shore M. (1980)
"Footprint analysis in gait documentation: an instructional sheet format"
Phys. Ther, 60, pp 1163-7

Simon S.R. (1977)
"Techniques in gait research and management of data"
In: NIH; Gait Research Workshop; Children's Hospital Health Centre; San Diego, California

Simon S.R., Paul I.L., Mansour J., Munro M., Abernethy P.J. and Radin E.L. (1981)
"Peak dynamics force in human gait"
J. Biomechanics, 14, pp 817-822

Simon S.R. (1981)
In: Workshop on the Clinical, Application of Gait Analysis, Dundee, 30th March - 1st April, 1981 (in press)

Skorecki J. (1966)
"The design and construction of a new apparatus for measuring the vertical forces exerted in walking : a gait machine"
J. Strain Analysis, 1(5), pp 429-438

Slocum D.B. (1949)
"An atlas of amputations"
C.V. Mosby Co., St. Louis.

Smith K.U., McDermid C.D. and Shideman F.E. (1960)
"Analysis of the temporal components of motion in human gait"
Amer J Phys Med, 39, pp 142-

Solomonidis S.E.(editor)(1975)
"Modular Artificial Limbs, First report on a continuing programme of clinical and laboratory evaluation. Below-knee systems"
Scottish Home and Health Department

Solomonidis S.E.(editor)(1980)
"Modular Artificial limbs. Second report on a programme of clinical and laboratory evaluation. Above-knee systems."
Scottish Home and Health Department.

Soudan K., Audekercke R.V. and Martens M. (1979)
"Methods, idifficulties and inaccuracies in the study of human joint kinematics and pathokinematics by the instant axis concept. Example : the knee joint"
J. Biomechanics, 12, pp 27-33

Soudan K. and Dierckx P. (1979)
"Calculation of derivatives and fourier coefficients of human motion data, while using spline functions"
J. Biomechanics, 12, pp 21-6

Sowell T.T. (1981)
"A preliminary clinical evaluation of the Mauch hydraulic foot-ankle system"
Prosthetics and Orthotics International, 5(2), pp 87-91

Spolek G.A., Day E.E., Lippert F.G. and Kirkpatrick C.S. (1975)
"Ambulatory force measurement using an instrumented shoe system"
SESA, pp 271-4

Spolek G.A. and Lippert F.G. (1976)
"An instrumented shoe - a portable force measuring device"
J. Biomechanics, 9, pp 779-783

Staros A. (1963)
"Dynamic Alignment of Artificial legs with the Adjustable coupling"
Artificial limbs, 7(1), pp 31-43

Staros A. (1979)
"Economics of modular prostheses"
Prosthetics and Orthotics International, 3, pp 147-9

Staros A. and Goralnik T. (1981)
In: "Atlas on limb prosthetics: surgical and prosthetic principle" American academy of Orthopaedic Surgeons, St. Louis, C.V. Mosby.

Staros A. and Peizer E. (1972 & 1973)
Veterans Administration Prosthetic Centre Research Report, BPR 1972, 10-18, pp 226- ; BPR 1973, 10-19, pp 148-

Szulc J. (1982)
PhD. Thesis in preparation, University of Strathclyde, Glasgow

Tait J.H. and Rose G.K. (1979)
"The real time video vector display of ground reaction forces during ambulation"
J. Med Eng and Tech., 3(5), pp 252-5

Tibarewala D.N., Mukherjee P., Chakrabarty S. and Ganguli S. (1979)
"A digital gait recording technique"
J Med Engng and Tech., 3(3), pp 138-9

Tooth R. (1976)
"The Biomechanics of arthrodesis and arthroplasty in the human leg"
PhD Thesis, University of Strathclyde, Glasgow.

Townsend M.A., Izak M. and Jackson R.W. (1977)
"Total motion knee goniometry"
J. Biomechanics, 10, pp 183-193

Trappitt A.E. (1979)
"Load measuring system developed for patient orthosis tests"
PhD Thesis, University of Strathclyde, Glasgow

Trnkoczy A., Bajd T. and Malezic M. (1976)
"A dynamic model of the ankle joint under FES in free movement and isometric conditions"
J. Biomechanics, 9, pp 509-519

Veterans Administration Prosthetic Centre (1973)
"Standards and Specifications for Prosthetic foot/ankle assemblies"
VAPC-L-7007-2; Veterans Administration Central Office, Washington, D.C. 20420

Vitali M. (1969)
"The clinic Team : Hopes and Realities"
In: Prosthetics and Orthotics Practice; edited by G. Murdoch (1970)

Vitali M., Robinson K.P. , Andrews B.G. and Harris E.E. (1978)
"Amputations and Prostheses"
A. Bailliere Tindall Book; Pub. Cassel and Co. Ltd.

Waas R. (1969)
"A digital optical scanning system for kinematic analysis"
PhD. Thesis, Case Western Reserve University

Walker P.S., Shoji H. and Erkman M.J. (1972)
"The rotational axis of the knee and its significance to prosthesis design"
Clinical Orthopaedics, 89, pp 160-170

Wall J.C., Dhanenoran M. and Klenermal L. (1976)
"A method for measuring the temporal/distance factors of gait"
Biomed Eng, 11(12), pp 409-412

Wall J.C., Charteris J. and Hoare J.W. (1978)
"An automated on-line system for measuring the temporal patterns of foot/floor contact"
J. Med. Eng. & Tech., 4(2), pp 187-190.

Walt W.N. Van der and Wyndham C.H. (1973)
"An equation for prediction of energy expenditure of walking and running"
J Appl Physiol, 34, pp 559-563

Waters R.L., Perry J., Antonelli D. and Hislop H. (1976)
"Energy cost of walking of amputees : Influence of level of amputation"
J Bone Jt Surg., 58(A), pp 42-6

Warwick R. and Williams P.L. (1973)
"Grays Anatomy"
35th Edition, Longman : Edinburgh

Weber W. and Weber E. (1836)
"Mechanik der Menschlichen gehwerkzeuge"
Goettingen

Weiss M., Gielzynski A. and Wirski J. (1966)
"Myoplastic immediate fitting ambulation"
World Commission on Research in Rehabilitation, Tenth World congress of the Int. Soc. for Rehab. of the Disabled; Wiesbaden, Germany.

Whittle W.M. (1980)
"Kinematics of treadmill walking"
In: Oxford Orthopaedic Engineering Centre (UK), Annual Report No. 7.

Wilson A.B. Jr (1962)
"A Report on the SACH foot"
Prostheses, Braces and Technical Aids (International Technical and Medical Journal) No. 11, pp 5-8

Wilson J.B. Jr (1970)
"Limb prosthetics - 1970"
Artificial limbs, 14(1), pp 1-52

Wilson L.A., Lyquist E. and Radcliffe C.W. (1968)
"Air-cushion socket for Patellar-tendon-bearing below-knee prosthesis"
Technical Report 55, Department of Medicine and Surgery, Veterans Administration, Washington D.C.

Wilson A.B. Jr and Stills M. (1976)
"Ultra-light prostheses for below knee amputees"
Orthotics and Prosthetics, 30, pp 43-7

Winter D.A., Greenlaw R.K., Hobson D.A. (1972)
"Television - computer analysis of kinematics of human gait"
Comp Biomed Res., 5, pp 498-504

Winter D.A., Sidwall H.G. and Hobson D.A. (1974)
"Measurement and reduction of noise in kinematics of locomotion"
J. Biomechanics, 7, pp 157-9

Winter D.A., Quanbury A.D. and Reimer G.D. (1976)
"Analysis of instantaneous energy of normal gait"
J. Biomechanics, 9, pp 253-7

Winter D.A. (1979)
"Biomechanics of Human Movement"
Biomedical engineering and health systems; A wiley interscience publication.

Wirta R.W., Taylor D.R. and Finley F.R. (1970)
"Laboratory for kinesiologic analysis"
BPR, 10-13, pp 165-172

Woltring H.J. (1975)
"Single- and dual-axis lateral Photodetectors of rectangular shape"
LEEE Trans Electronic Devices, 22, pp 581-590 and 1101.

Woltring H.J. and Marsolais E.B. (1980)
"Optoelectric (Selspot) Gait measurement in two and three dimensional space - a preliminary report"
BPR ; 10-34, pp 46-52

Wright D.G., Desai S.M. and Henderson W.H. (1964)
"Action of the subtalar and ankle joint complex during the stance phase of walking"
J Bone Jt Surg., 46A(1)

Youm Y. and Yoon Y.S. (1979)
"Analytical development in investigation of wrist kinematics"
J. Biomechanics, 12(8), pp 613-

Zahedi S. (1982)
PhD Thesis in preparation; University of Strathclyde Glasgow

Zarrugh M.Y. (1981)
"Power requirements and mechanical efficiency of treadmill walking"
J. Biomechanics, 14(3), pp 157-165

Zarrugh M.Y., Todd F.N. and Ralston H.J. (1974)
"Optimization of energy expenditure during level walking"
Europ J Appl Physiol., 33, pp 293-306

Zarrugh M. and Radcliffe C.W. (1979)
"Computer generation of human gait kinematics"
J. Biomechanics,12, pp 99-110

Zuniga E.N. and Leavitt L.A. (1974)
"Analysis of Gait : A method of measurement"
Proc 4th Int Seminar Biomechanics; University Park, Pennsylvania; Editors: Nelson R.C. and Morehouse C.A.

APPENDIX (A)

Determination of Body Segment Parameters

Name of Investigator(s)(Year)	Number of Subjects	Type of Subject
Harless (1860)	2	Cadaver
Meeh (1884)	8	Living
Braune & Fischer (1889)	3	Cadaver
Fischer (1901)	1	Cadaver
Bernstein (1936)	76	Living
Dempster (1955)	8	Cadaver
Drillis & Contini (1966)	12	Living
Clauser et al (1969)	13	Cadaver
Contini (1972)	9	Living
Chandler et al (1975)	6	Cadaver

The coefficients C1, C2 and C3 obtained from the above investigators are presented in the following tables.

Note that the coefficients C2 and C3 for the foot were not derived consistently among the investigators. In this project, only those measured from the lateral malleolus were used. The key to the various points of measurement for the foot, listed in the tables are as follows :-

@ Measured from heel; segment length - heel to anterior point

+ Measured from ankle joint; segment length - undefined

* Measured from lateral malleolus; segment length - lateral malleolus to 5th metatarsar base.

Coefficient C1 :- Ratio of body segment mass to total body mass

	Thigh	Shank & Foot	Shank	Foot
Harless	0.1118	0.066	0.0439	0.0183
Meeh	0.0868	-	0.0468	0.0159
Braune & Fischer	0.1072	0.065	0.0478	0.0169
Fischer	0.1158	0.066	0.0527	0.0179
Bernstein	0.1221	-	0.0465	0.0145
Dempster	0.0990	0.061	0.0465	0.0145
Drillis & Contini	0.0946	-	0.042	0.0135
Clauser et al	0.103	0.058	0.043	0.015
Contini	0.0859	-	0.0423	0.0128
Chandler et al	0.1007	-	0.0411	0.013
Mean -	0.1027	0.0632	0.0453	0.0152
±1 S.D.	0.0119	0.0036	0.0035	0.0019

Coefficient C2 :- Ratio of distance between proximal joint and centre of mass of segment to total segment length

	Thigh	Shank & Foot	Shank	Foot*
Harless	0.467	-	0.36	0.46@
Braune & Fischer	0.44	0.519	0.42	0.434@
Bernstein	0.386	-	0.413	-
Dempster	0.433	0.433	0.433	0.5*
Drillis & Contini	0.410	0.450	0.393	0.445@
Clauser et al	0.37	-	0.37	0.45@
Contini	0.4355	-	0.4175	0.592+
Chandler et al	0.3935	-	0.4175	0.438@
Mean	0.4169	0.4673	0.403	0.50
±1 S.D.	0.0325	0.0455	0.0260	-

Coefficient C3 :- Ratio of radius of gyration to total segment length

	Thigh	Shank & Foot	Shank	Foot*
Braune & Fischer	0.30	-	0.30	0.30[@]
Dempster	0.323	0.416	0.302	0.475*
Drillis & Contini	0.23	0.29	0.27	-
Contini	0.281	0.334	0.281	-
Chandler et al	0.322	-	0.292	0.271[@]
Mean	0.2912	0.3467	0.289	0.475
±1 S.D.	0.0384	0.0639	0.0134	-

APPENDIX (8)

Bumper Rubber Composition

The rubber compounds used in manufacturing the plantar bumper of the Uniaxial foot were supplied by the Malaysian Rubber Producers' Research Association.

The following table shows the compound details and properties. The numbers 1 to 6 are as those designated by MRPRA as D42/1-6. It was noted that the actual hardness of the compounds did not tie up exactly with IRHD hardness figure on the table. MRPRA's explanation was that during compounding, small operator differences were inherent, e.g. longer rubber mastication times for some compounds over others, therefore, making it very difficult to be precise in replicating compounds.

Compounds D42/1 and D42/2 were supplied at the very late stage of the project, therefore they were not included in the evaluation.

	Parts by weight					
	1 36–45	2 46–55	3 56–65	4 66–75	5 76–85	6 86–95
Natural rubber (SMR 5CV)[1]	100	100	100	100	100	100
Zinc oxide	3	3	3	3	3	3
Zinc-2-ethylhexanoate	1	1	1	1	1	1
N-990, MT black	15					
N-762, SRF-LM-NS black		35	50			
N-550, FEF black				65	85	80
Whiting			30	30	70	120
Reinforcing resin[2]						10
Chlorinated wax[3]	5	5	5	5	5	5
Antidegradant[4]	3	3	3	3	3	3
N-Oxydiethylenebenzothiazole-2-sulphenamide	2	2	2	2	2	2
Tetrabutylthiuram disulphide	1·4	1·4	0·7	0·7	0·7	0·7
Sulphur	0·5	0·5	0·5	0·5	0·5	0·5
Mix properties						
Mooney scorch, t_5, 120°C, min	24·5	19·5	23	14	9·5	19·5
Monsanto *Rheometer*, 153°C						
scorch, t_{s1}, min	4·7	3·7	4	2·7	2·2	2·5
cure, t_c'(90)' min	9·7	8·7	8·2	5·7	5	6·5
Vulcanizate properties Cure: 20 min at 153°C						
Density, Mg'm³	1·02	1·08	1·29	1·26	1·39	1·49
Hardness[5], IRHD	38	48	58	70	83	90
Tensile strength, MPa	23 6	25·2	19·2	16·0	13·1	10·9
BS 2494, limits; [6]MPa, min.	*20*	*20*	*18*	*15*	*11*	*6*
Elongation at break, %	700	610	540	330	235	230
BS 2494, limits %, min.	*600*	*500*	*375*	*250*	*175*	*100*
Compression set, 70h at 23°C, %	3	4	4	5	5	11
BS 2494 limits; % max.	*10*	*10*	*10*	*15*	*15*	*15*
Compression set, 22h at 70°C, %	12	13	14	13	12	18
BS 2494 limits; %, max.	*25*	*25*	*25*	*25*	*25*	*25*
Water absorption, 7 days at 70°C, % vol	6·3	5·1	5·9	4·8	4·0	3·3
BS 2494 limits; % vol, max.	*8*	*8*	*8*	*8*	*8*	*8*
Air oven ageing resistance, 7 days at 70°C						
Change in hardness, IRHD	+2·5	+3	+3·5	+4	+2·5	+1
BS 2494 limits; IRHD, max.	*±5*	*±5*	*±5*	*±5*	*±5*	*±5*
Change in tensile strength	+5	−7	−2	−1	−4	−5
BS 2494 limits; %, max.	*±20*	*±20*	*±20*	*±20*	*±20*	*±20*
Change in elongation at break, %	−5	−8	−6	−2	−4	−6
BS 2494 limits; %, max.	*±20*	*±20*	*±20*	*±20*	*±20*	*±20*

1. Other high quality latex grades may be used
2. Phenol-formaldehyde resin, *Cellobond J1131H* (BP Chemicals).
3. *Cereclor 42* (ICI)—contains 42% chlorine.
4. N,N'-Di-(1,4-dimethylpentyl)-p-phenylenediamine, *Santoflex 77* (Monsanto).
5. For these vulcanizates the hardness change after 7th at 0°C is not more than 5 IRHD, as required in BS 2494.
6. For appropriate hardness range.

These ingredients in MRPRA formulations are designated by trade names: this indicates only that these were the materials used to develop the formulation and does not imply recommendation of specific trade materials. Chemically equivalent materials would normally be expected to give similar results

Table 8(1) Details and Properties of Rubber Compounds

APPENDIX (C)

Alignment Parameters

The alignment parameters used in the project are similar to those presented by Solomonidis et al (1980). Referring to Figure C(1), the alignment parameters are as follows :

Toe-out Angle
Knee height *
Knee set back *
Knee set out *
Knee M/L tilt *
Knee hyper-extension angle *
Socket forward set
Socket height
Socket set out
Socket flexion
Socket lateral tilt
Socket external rotation *

N.B. * Does not apply to below-knee prostheses.

Presented in Tables C(1) and C(2) are the alignment measurement of all the below- and above-knee prostheses, respectively, used in the project. The "optimum" alignment ranges of each prosthesis with SACH foot are also included. The measurement accuracies of each parameter are also given in the Tables.

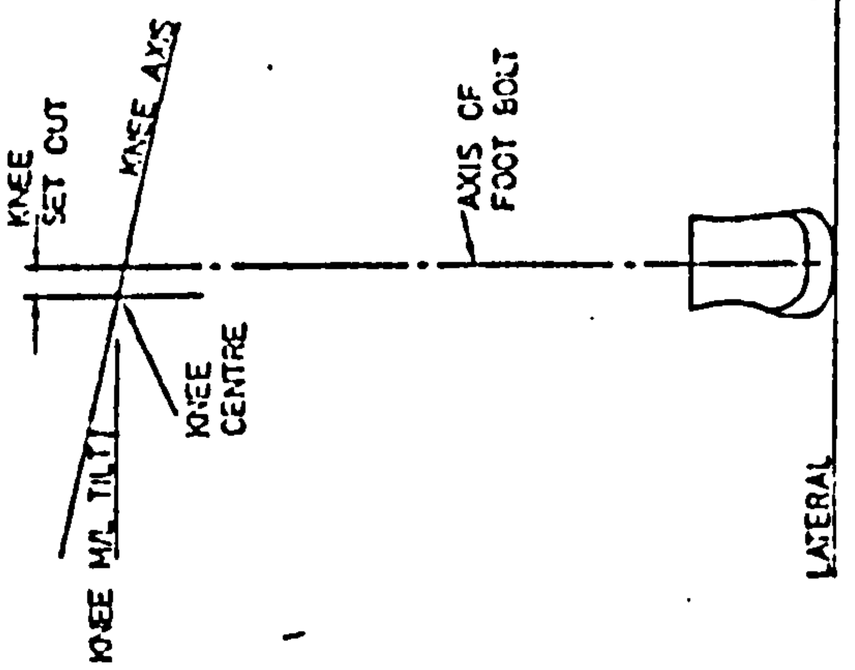

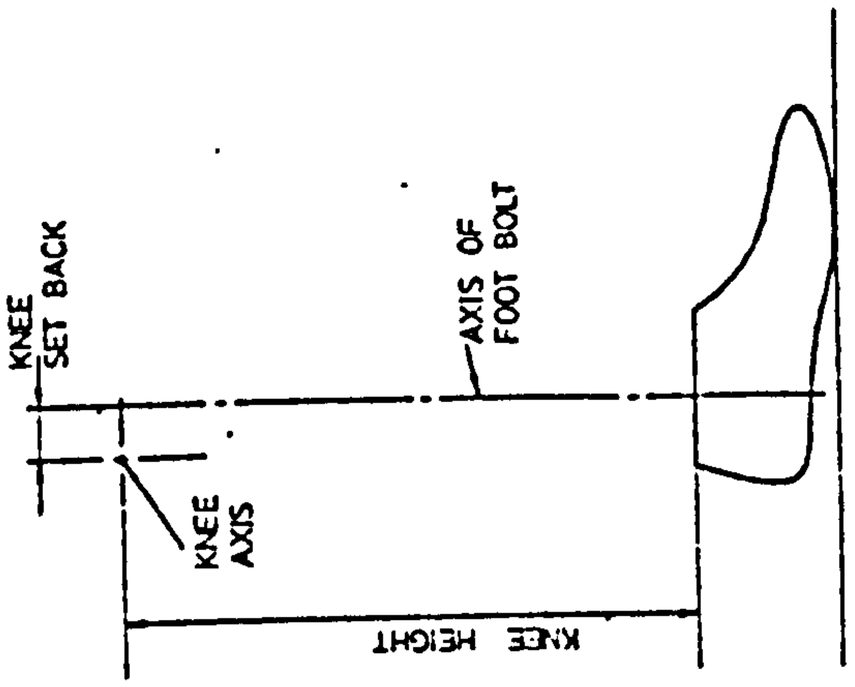

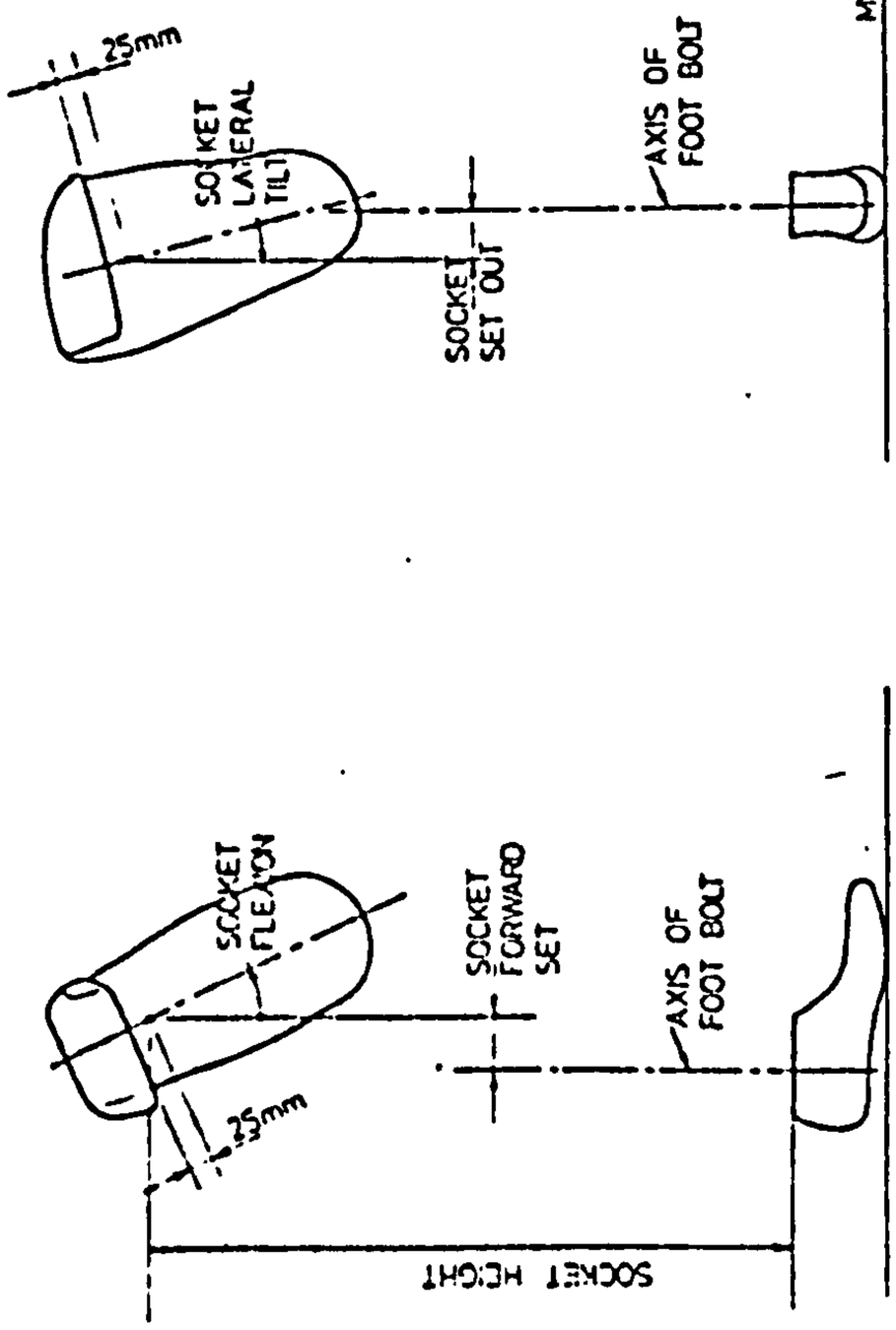

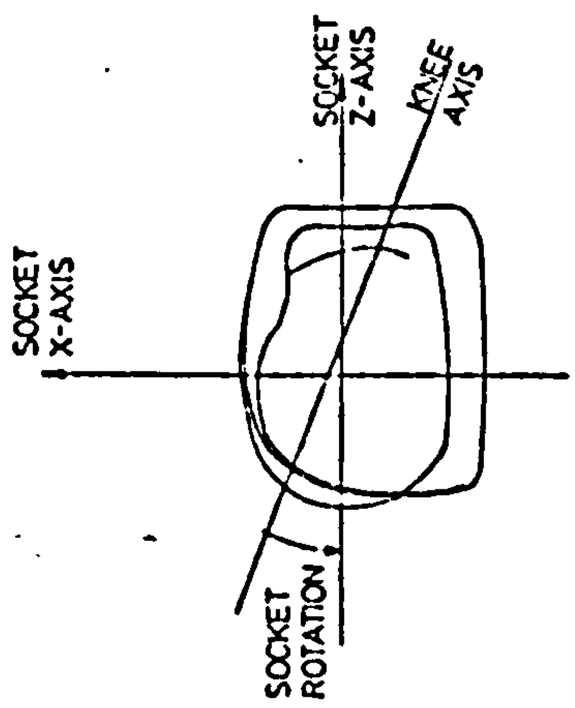

Figure C(1) Alignment Parameters
From Solomonidis et al (1980)

Patient		Socket Set Out (cm)	Socket Forward Set (cm)	Socket Lateral Tilt (deg)	Socket Flexion (deg)	Socket Height (cm)	Toe Out (deg)
BRØØ2	SACH	-1.03	2.8	6.0	5.0	33.65	5.0
	Uniaxial	-0.56	2.95	5.0	8.0	34.75	2.0
	Optimum	-1.91	0.50	-1.9	7.1	33.85	-7.59
	Range	1.78	3.29	10.8	13.7	34.55	5.42
BRØØ3	SACH	0.38	5.10	2.5	14.8	31.43	4.0
	Uniaixial	1.53	4.10	4.5	8.0	32.50	2.0
	Optimum	0.15	4.00	1.05	5.8	31.0	1.5
	Range	2.20	6.20	5.20	14.1	32.0	5.7
BLØØ4	SACH	-1.95	2.15	-6.0	5.0	29.93	9
	Uniaxial	2.00	1.70	-8.0	7.0	31.00	4
	Optimum	-2.18	1.75	-5.2	1.7	30.10	6
	Range	1.75	4.43	-14.7	7.5	30.20	14
BRØØ5	SACH	-0.63	2.90	8.0	4.0	37.40	10.0
	Uniaxial	-0.15	2.66	10.0	2.0	38.45	6.2
	Optimum	-2.30	2.35	-14.7	-0.9	38.10	6.14
	Range	1.02	4.58	16.7	6.4	38.45	14.97
BRØØ7	SACH	-1.68	2.40	3.5	8.0	32.35	3.5
	Uniaxial	-0.43	2.70	4.0	6.0	33.50	0.0
	Optimum	-2.25	2.04	3.8	2.2	31.35	4.35
	Range	0.94	2.74	7.7	8.2	33.75	0.0
	Accuracy	±0.035	±0.05	±0.05	±0.05	±0.045	±0.55

Table C(1) Alignment Results of Below-Knee Prostheses

		Socket Forward Set (cm)	Socket Flexion (deg)	Socket Set Out (cm)	Socket Lateral Tilt (deg)	Socket Rotation (deg)	Socket Height (cm)	Knee Set Back (cm)	Knee Hyper-Extn. (deg)	Knee Set Out (cm)	Knee M/L Tilt (deg)	Toe-Out (deg)	Knee Height (cm)
ARØØ1	SACH	2.1	2.0	-4.05	-12.0	-4	88.45	1.25	4.5	-0.75	-1.5	7.0	43.05
	Uniaxial	1.6	5.5	-0.13	-13.5	-4	89.85	0.65	1.5	2.8	6.5	5.0	44.20
	Optimum	0.2	-4.0	-8.5	-7.0	0	88.0	-0.8	-2.2	-4.5	-5.0	4.0	41.9
	Range	4.1	7.0	3.5	17.0	-7	90.1	1.8	6.5	1.9	2.5	11.0	44.5
ALØØ6	SACH	7.2	10	-0.2	0	4.8	72.0	3.8	10.0	-0.3	-3	8.9	42.5
	Uniaxial	4.5	8	2.8	5.4	2.9	73.0	2.0	6.0	0.3	3	4.9	48.6
	Optimum	8.0	14	-1.0	-3	7.2	71.8	2.8	7.0	1.8	5.2	9.6	41.6
	Range	6.1	5.1	-0.2	0.9	2.3	73.1	2.0	3.9	0.2	3.5	8.5	42.8
ARØ1Ø	SACH	0.8	-0.8	3.8	12.0	3.4	67.4	0.8	3.0	0.25	2	6.8	37.25
	Uniaxial	-1.2	3.5	2.0	6.9	5.2	68.4	0.9	4.0	-0.4	-1.5	4.8	38.8
	Optimum	4.8	8.0	4.1	17.0	4.2	68.9	1.8	5.0	1.0	3.5	8.5	36.9
	Range	-3.5	-1.2	-0.5	-1.8	1.8	68.0	0.4	0.5	-0.8	2.1	2.5	37.75
ARØ11	SACH	-2.2	5.0	2.0	12.5	7.0	74.8	-0.7	2.5	-1.8	-5.0	4.0	41.8
	Uniaxial	1.8	7.0	1.4	14.0	7.0	75.9	0.8	2	-2.2	-5.0	2.5	43.2
	Optimum	-4.0	11.0	1.8	15.0	9.0	74.9	2.0	6	-2.4	-7.0	8	41.75
	Range	2.1	-7.2	0.7	7.0	4.0	73.5	-0.9	1.2	-0.6	-2.9	0.0	42.10
ARØ13	SACH	0.8	-3.0	3.2	4.5	4.2	73.8	1.4	4.0	2.0	5.2	8.2	43.12
	Uniaxial	1.8	3.0	0.2	-1.2	2.1	74.9	0.8	2.8	1.4	4.1	5.4	47.80
	Optimum	3.8	7.0	2.2	1.4	6.2	74.4	1.2	3.2	0.0	0.2	12.1	43.6
	Range	-1.8	4.0	0.2	1.3	2.0	73.8	-0.6	-2.0	2.0	6.2	3.9	43.3
	Accuracy	±0.095	±0.8	±0.09	±0.8	±0.85	±0.05	±0.055	±0.15	±0.035	±0.15	±0.55	±0.035

Table C(2) Alignment Results of Above-Knee Prostheses

APPENDIX (D)

Computation

D(1) Introduction

The purpose of this Appendix is to describe the function and operation of computer programs used in performing the mathematical analysis in Chapter Six.

All the computer programs were written in the Fortran IV language, and were compiled into binary version before they could be used to process data. Associated with each program was a job control macro, written in George III operating commands. This enabled the use of a single line command to run the program and also to perform file handling procedure.

Raw force plate data were processed by program "BIOMECHANICS". This is a suite of programs written by Beveridge (1982). It was designed to assist in the analysis and interpretation of ground reaction data. Most of these programs included a graph plotting procedure of processed data. Only four of the programs from the suite were used in this project. These are described in the following sections. The main result file consists of the calibrated ground reaction data.

Raw displacement data were rationalised by programs "COORDINATES", "PARALLAX" and "FILTER". Three dimensional coordinates of joint centres and direction cosine matrices of body segments were calculated by program "JOINTS". Program "KINEMATICS" determined the linear velocities and accelerations of the joint centres as well as the angular velocities and accelerations of the body segments. Programs "COORDINATES", "PARALLAX", "JOINTS" and "KINEMATICS" were originally written by Ishai(1976). These were greatly modified to suit the present analytical procedure.

The final program "KINETICS" combines all the

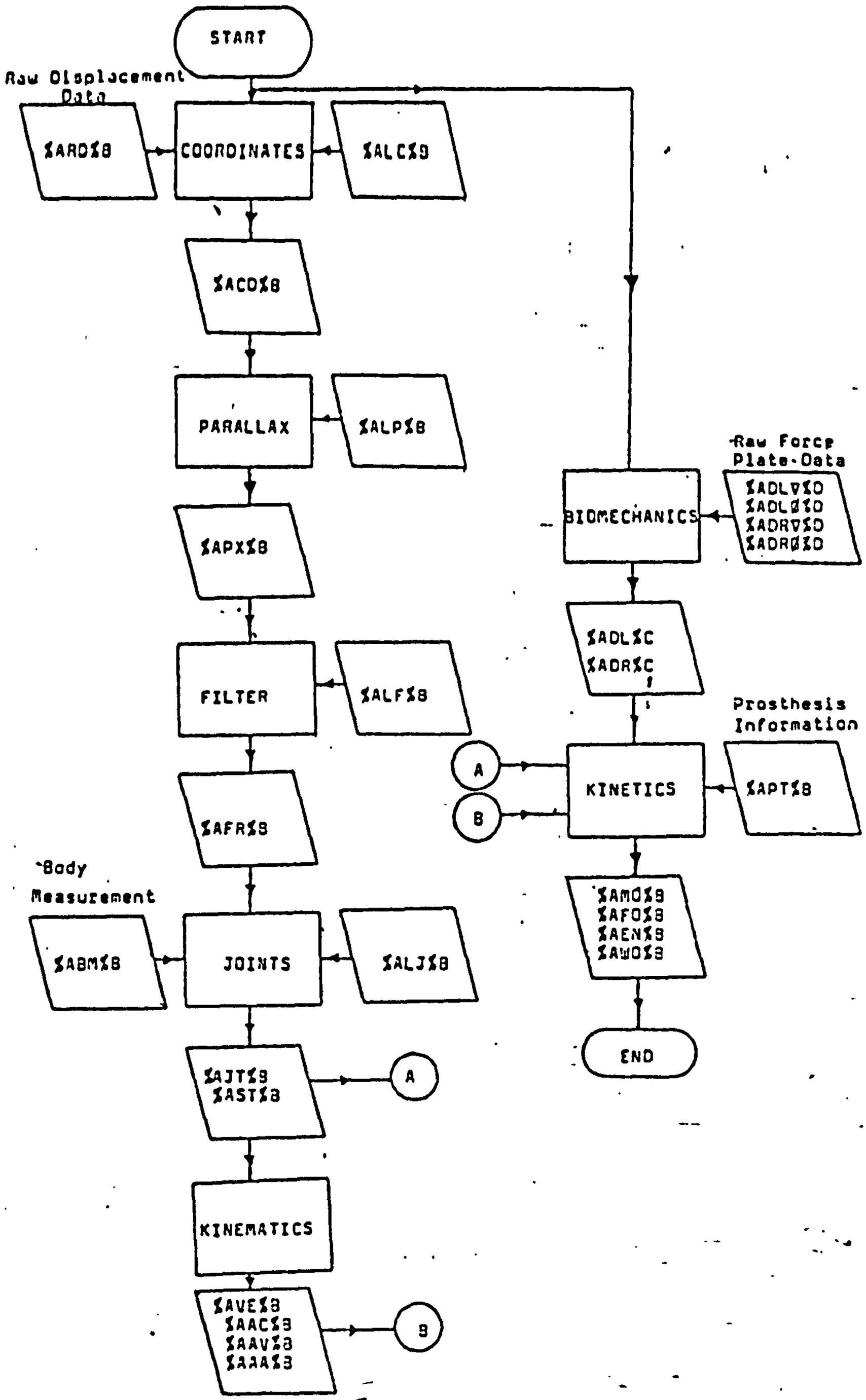

Figure D 1 Flow Diagram of main processing programs

relevant processed data to perform the dynamic analysis. Several peripheral programs were written to assist analysis and interpretation of the displacement data. Programs were also written to give graphical presentation of displacement data,ground reaction forces, intersegmental moments, energies and mechanical work. Standard GHOST software routines available in the ICL 1904s allowed much easier development of "plotting" programs.

Figure D1 shows an overview of the structural sequence of the main processing computer programs.

D(1.1) Standardised Filestore Notation

All the data stored on files in the computer has to be labelled such that each one has a unique filename, which can be easily identified and related to the various stages of computation. It must also be easy to handle. Beveridge (1981) suggested a filename of 12 characters, which is fairly flexible in its application. The following is a description of it being used in relation to this project.

The 12 characters are divided into 5 sections :

a) Section 1 consists of the first five characters, which are used to identify the specific subject under consideration.

The first two of these characters are letters of the alphabet, used to classify the subject into one of the three categories :

1) Normal Subject - NS
2) Below-Knee Amputee : Right - BR
   Left - BL
3) Above-Knee Amputee : Right - AR
   Left - AL

The next three characters are numbers, ranging from ØØ1 to 999 being ascribed to the subject.

b) Section 2 consists of three characters, which are used to specify the visit number. The first of these characters is the letter "V" and the rest are numbers, i.e. ranging from Ø1 to 99 visits.

c) Section 3 consists of two important characters (both letters of the alphabet) which are used to identify the types of data being stored.

Ground reaction data has the following notation : The first alphabet can either be "S", meaning a single force plate was used in the test walk, or "D", meaning two force plates were used concurrently in the test walk. The second alphabet is either "L" or "R", denoting left or right leg respectively. Therefore, "DL" would represent ground reaction data from the left leg obtained during a test walk utilising two force plates concurrently.

Kinematic and Kinetic data are denoted by abbreviation of their content. For example,

"RD" - Raw Displacement data
"CD" - Calibrated Displacement data
"AA" - Angular Acceleration data
"MO" - MOments at joints

As for files generated with data for checking purposes, the first letter used is "L" and the second letter identifies the program from which it was generated. For example, "LP" stands for data check file from program "PARALLAX".

The detail classification and notation are described in conjunction with the programs description section.

d) Section 4 consists of a single character. For the ground reaction data it is a number, which has the following significance :-

∇ (Blank)	-	Raw ground reaction data
Ø	-	Peripheral information data
1	-	Scaled ground reaction data

As for the kinematic data, it is a letter of the alphabet to identify the type of feet tested, i.e.

N	-	Normal subject
S	-	Amputee with SACH foot
U	-	Amputee with Uniaxial foot

e) Section 5 consists of a single character, a number which is used to identify the test walk. Up to 9 successful test walks per subject per visit can be recorded in this system of notation.

Each section or a combination of "neighbouring" sections can be represented by a masking parameter("%∇"; where ∇ is any alphabet) in the job control macro. This enables the facility for handling input and output data files in their standardised format.

The following is an illustration of its use in the project :

A left above-knee amputee has been ascribed a subject code number 13. Therefore section 1 of the file-name would be (ALØ13). He was on his second visit to the laboratory (i.e. VØ2) and has performed a successful test walk on the third run with a SACH foot.

The raw ground reaction data obtained would be stored in files "ALØ13VØ2DL∇3" for the left leg and "ALØ13VØ2DR∇3" for the right leg. These can be represented as "%ADL∇%N" and %ADR∇%N", where "%A" is "ALØ13VØ2"

and "%N" is "3". The calibrated left ground reaction data would be "ALØ13VØ2DL13" or "%ADL1%N".

For the raw displacement data, it would be stored in file "ALØ13VØ2RDS3" or "%ARDS%N". After being processed through program COORDINATES, the output data file is "ALØ13VØ2CDS3" or "%ACDS%N". This form of notation is used in the following sections to identify the input and output data files of each processing programs.

D(2) Force Plate data Processing Programs

D(2.1) "BIOMECHANICS"

This is a suite of computer programs designed to assist in the analysis and interpretation of ground reaction data. The program suite was developed in a semi-modular fashion with the view of introducing flexibility into the processing sequence within the bounds of a batch, in order to "pick and choose" those processing stages in the suite that are of interest. However, all raw data must be processed by the first program in the suite, as every other program depends on its output.

The following sections gives a brief description of the four programs in the suite that were employed in the processing of ground reaction acquired in this proje project. The running of the program suite is also briefly described. For further detail, the reader is recommended to consult Beveridge (1982).

"PROGCALF" is the first and main processing program in the suite. It was designed to perform the following function :-

a) Validify the format of the data in the entry files.

For ill-formatted data, an indication of the error is given to ease the problem of location of the "bad" data.

b) Correct the baseline shifts that exist due to the inaccuracies in the amplifications circuitry. The program estimates the shift factors of each channel and corrects the raw data accordingly.

c) Re-orientate the signal components with respect to the direction of walk and the arrangement of the two force plates. The direction of walk is coded and given in the entry "header information" file. The correct direction factors of the various channels from the two force plates are as given in Table 6.5.1(a). The program combines the two pieces of information and produces the appropriate direction factors. By applying these factors to the raw data, the correct orientation of the signal components is achieved.

d) Scale the signal components to their interpretable physical dimension. This is done by multiplying the re-orientated and baseline corrected data by the correct amplification factors and constants of force plate dimensions to obtain results expressed in Newtons and Newton-metres. See section 6.5.1 and Table 6.5.1(b).

e) Calculate the position of the centre of pressure from the Section 6.5.2. The vertical force component (Fy) is used to ensure that the beginning and end Fy values are sufficiently non-zero in order that poor co-ordinate estimates will not be generated. Therefore scanning windows were applied to the Fy signals. The size of these windows is determined as follows :-

Fore window size = 1 + Integer value of (sampling frequency/10).

Rear window size = Integer value of (sampling frequency/5).

Two input data files are required for the program, the header information file, "%A%BØ%N" and the raw ground reaction data file, "%A%BV%N", where "%B" could be either "DL" or "DR".

The file "%A%BV%N" consists of the baseline shifts of each channel followed by the raw ground reaction data with most of the baseline removed, giving mainly stance phase information. With this assumption, the program searches the Fy signals until two successive points exceed a specified threshold or the Forewindow is completely scanned. Failure to exceed the threshold implies poor data, resulting in processing being aborted. The threshold level can either be specified (in Header Information file) or a default of 2Ø "PDP12 units" is assumed. Once the threshold level is exceeded, centre of pressure calculation is performed until the rear window portion of the signal is reached. In this region, for the calculation to continue, the Fy signal has to exceed the stated threshold.

The generated results file is stored in "%A%B1%N". It consists of useful parameters and scaled, re-orientated ground reaction data with the corresponding centre of pressure. This file is then subsequently accessed by other processing programs in the suite for further computation.

"PROGFORCPLOT" generates the force-time and moment-time plots to provide a visual inspection of the computed data for any discrepancies and unusual characteristics. The horizontal axis of each plot is the stance phase time, normalised to allow comparison. The vertical axis of ea each plot has a default range, which can be rescaled to

suit signal amplitudes that exceed the default range.

"PROGCENTPLOT" generates three centre of pressure (CP) versus time plots displaying different aspects of the data. All plots have a normalised representation of the CP coordinates on the vertical axis, the three plots being X-coordinates(CP) versus time, Z-coordinates versus time and CP distance versus time. The derivation of the vertical CP coordinates was briefly discussed in Section 6.5.2(a).

"PROGVECTPLOT" also generates three plots; the first two are vector plots and the third is a centre of pressure plot. The generation of force vectors was described in Section 6.5.3. The first vector plot is Fy versus Fx and X-coordinate (CP). The vertical axis represents Fy and has a default range of 0 to 1000 Newtons. The horizontal axis is a combination of Fz versus Fx and X-coordinate (CP). The second vector plot is Fz versus Fx and X-coordinate (CP). The vertical axis represents Fz and has a default range of -100 to 100 Newtons. The horizontal axis is similar to the previous plot. The centre of pressure plot is different from those described previously. This CP plot is independent of time. The plot presents CP information as a line plot of X and Z coordinates. The axes of the plot is based on the force plate system, therefore it allows some degree of appreciation of where and how the foot made contact with the force plate.

Each of the four programs has an associated job control macro, which permits the processes to be run as background jobs. However, the initation of these job requests come from the overall job control macro. "RUNMAINCALF", which is also used interactively to check entry parameters "in situ", Figure D2.1 shows the chained job sequence of processing on the ICL 1904s computer.

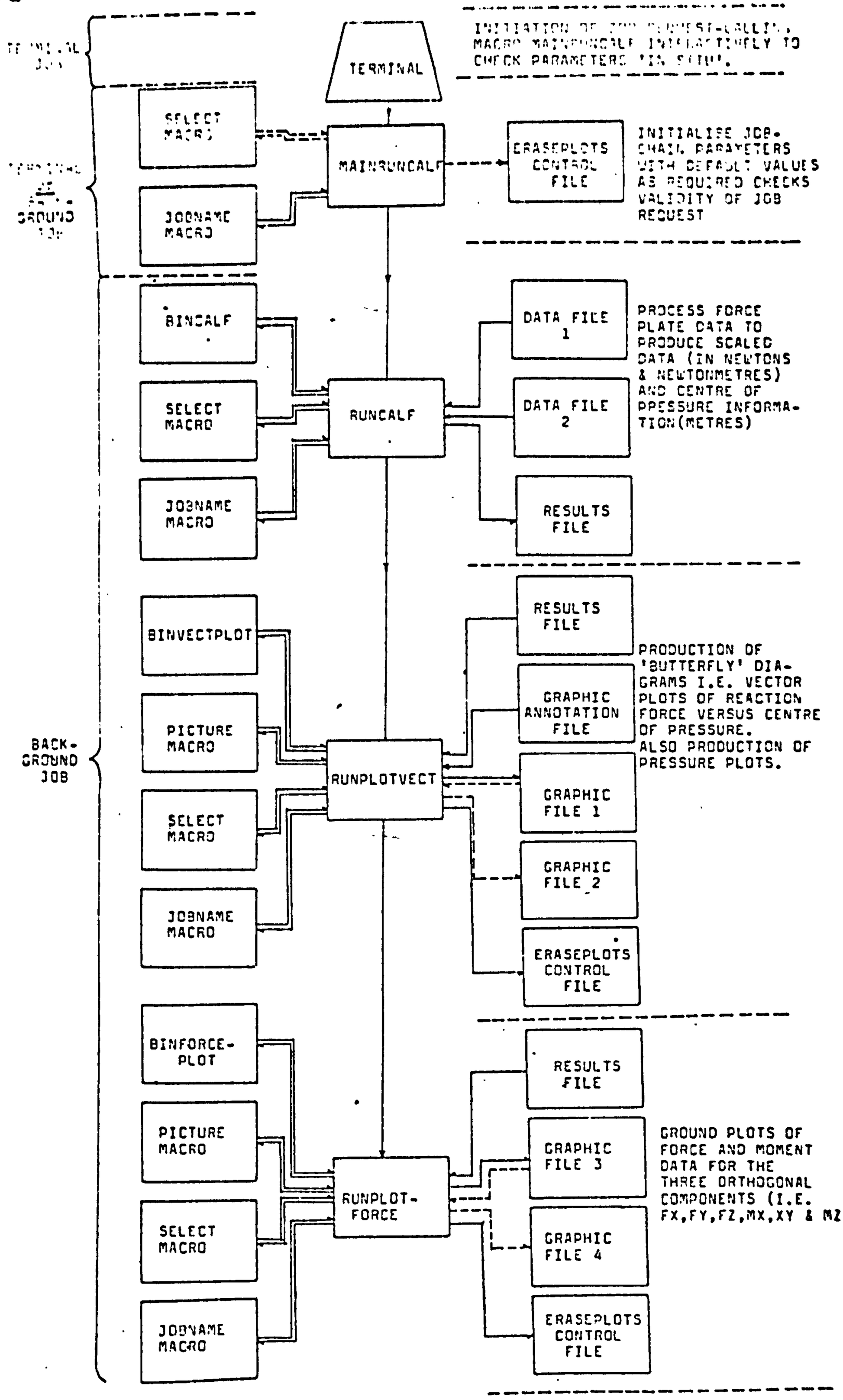

Figure D 2.1 Chained Job Sequence of Program BIOMECHANICS
(redrawn from Beveridge, 1982)

suit signal amplitudes that exceed the default range.

"PROGCENTPLOT" generates three centre of pressure (CP) versus time plots displaying different aspects of the data. All plots have a normalised representation of the CP coordinates on the vertical axis, the three plots being X-coordinates(CP) versus time, Z-coordinates versus time and CP distance versus time. The derivation of the vertical CP coordinates was briefly discussed in Section 6.5.2(a).

"PROGVECTPLOT" also generates three plots; the first two are vector plots and the third is a centre of pressure plot. The generation of force vectors was described in Section 6.5.3. The first vector plot is Fy versus Fx and X-coordinate (CP). The vertical axis represents Fy and has a default range of 0 to 1000 Newtons. The horizontal axis is a combination of Fz versus Fx and X-coordinate (CP). The second vector plot is Fz versus Fx and X-coordinate (CP). The vertical axis represents Fz and has a default range of -100 to 100 Newtons. The horizontal axis is similar to the previous plot. The centre of pressure plot is different from those described previously. This CP plot is independent of time. The plot presents CP information as a line plot of X and Z coordinates. The axes of the plot is based on the force plate system, therefore it allows some degree of appreciation of where and how the foot made contact with the force plate.

Each of the four programs has an associated job control macro, which permits the processes to be run as background jobs. However, the initation of these job requests come from the overall job control macro. "RUNMAINCALF", which is also used interactively to check entry parameters "in situ", Figure D2.1 shows the chained job sequence of processing on the ICL 1904s computer.

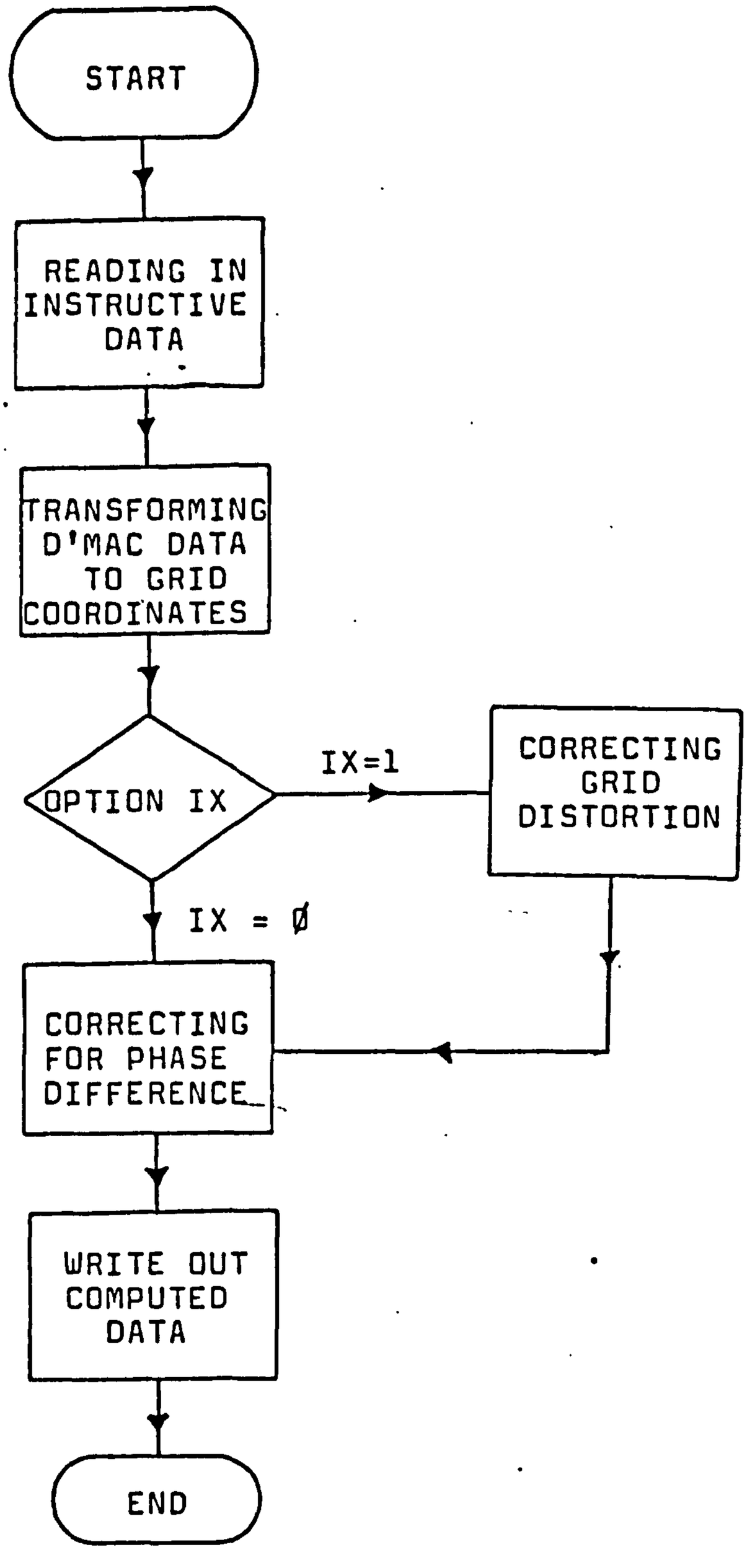

Figure D3.1(a) Flow Diagram of Program - "COORDINATES"

Data Preparation Form (1) for Stage (1) .... PROGRAM COORDINATES

Filename : ______________________

							Statement Format
[illegible]	[illegible]	[illegible]	[illegible]	[illegible]	[illegible]	[illegible]	7IØ
[illegible]	NAMAX	IIMAX1	IIMAX2	IIMAX3	JANGA	[illegible]	7IØ
AB?	HO?	T(1)	T(2)	T(3)	FCUT		6FØ.Ø
IX							IØ
DF?	[illegible]	CF	HF	HL	HR		6FØ.Ø
LTAIL1	LASIS	RTAIL1	RASIS				4IØ

ARRAY "MCODE" — 2IØ

1		
2		
3		
4		
5		
6		
7		
8		
9		
10		
11		
12		
13		
14		
15		
16		
17		
18		
19		
20		
21		
22		
23		
24		
25		
26		

ARRAY "NCHOS" — 2IØ

1		
2		
3		
4		
5		
6		

ARRAY "D" — FØ.Ø

1	
2	
3	
4	
5	
6	

∇	.	[illegible]	[illegible]	[illegible]	-	[illegible]	7A1

Figure D3.1(b) Data Preparation form for Program "COORDINATES" - File "[illegible]"

NGROUP : SUBJECT'S GROUP CODE

- Ø - Normal
- 1 - Below Knee Amputee
- 2 - Above Knee Amputee

NAMP : AMPUTATED SIDE CODE

- Ø - Normal
- 1 - Left Side
- 2 - Right Side

NPTNT : SUBJECT'S NUMBER

NDATE1 : DAY

NDATE2 : MONTH

NDATE3 : YEAR

NRUN : TEST NUMBER

NCASE : FILMING CASE DESCRIPTOR CODE

- 1 - Front, Left and Right Cameras were used
- 2 - Front and Left Cameras were used
- 3 - Front and Right Cameras were used

MAMAX : TOTAL NUMBER OF MARKERS USED (i.e. 26)

IIMAX(1) : TOTAL NUMBER OF MARKERS VIEWED BY THE FRONT CAMERA (i.e. 20)

IIMAX(2) : TOTAL NUMBER OF MARKERS VIEWED BY THE LEFT CAMERA (i.e. 13)

IIMAX(3) : TOTAL NUMBER OF MARKERS VIEWED BY THE RIGHT CAMERA (i.e. 13)

JAMAX : TOTAL NUMBER OF FRAMES (INCL. 'DUMMY' FRAMES) ANALYSED ONLY

NDMAX : TOTAL NUMBER OF MARKERS WHICH CAN ONLY BE VIEWED BY ONE CAMERA(i.e. 6)

AB : ACTUAL PHYSICAL DISTANCE BETWEEN THE TWO CALIBRATION MARKERS (A,B) ON THE GRID BOARD (in mm)

HØ : ACTUAL PHYSICAL HEIGHT OF THE MID-POINT OF AB, MEASURED FROM GROUND (in mm)

T(1) : PHASE LAG OF FRONT TO LEADING CAMERA (in ms)

T(2) : PHASE LAG OF LEFT TO LEADING CAMERA (in ms)

T(3) : PHASE LAG OF RIGHT TO LEADING CAMERA (in ms)

FCUT : CUTOFF FREQUENCY OF FILTER (in Hz)

IX : OPTION CODE FOR LENS DISTORTION CORRECTION

- Ø - BY PASS OPTION
- 1 - EXECUTE OPTION

DF, DL, DR : DISTANCES FROM THE FRONT, LEFT AND RIGHT CAMERAS RESPECTIVELY. TO THE ORIGIN OF THE GROUND FRAME OF REFERENCE (in mm)

HF, HL, HR : HEIGHT OF FRONT, LEFT AND RIGHT CAMERAS RESPECTIVELY FROM THE GROUND (in mm)

LTAIL1, LASIS : INDICES OF LEFT TAIL 1 AND A.S.I.S. RESPECITVELY

RTAIL1, RASIS : INDICES OF RIGHT TAIL 1 AND A.S.I.S. RESPECTIVELY

ARRAY "MCODE" : THIS IS A*MAMAX BY 2*(i.e. 26 x 2) MATRIX, WHICH IS USED FOR CODING THE SITUATION OF EACH MARKER

- 1st Column = 1, 2 or 3 - marker can be viewed by front and side camera, front camera only respectively
  4 - escape usual routine (only for pelvic tail(1) and spine markers)
- 2nd Column = Ø - if 1st Column is either 1 or 4
  Index of preceding adjacent marker, if 1st Column is either 2 or 3

ARRAY "NCHOS" : This is a*NDMAX BY 2*(i.e. 6 x 2) MATRIX, WHICH IS USED FOR CODING THE CHOSES OF CORRECT SOLUTION FOR MARKERS VIEWED BY ONLY ONE CAMERA

- 1st Column = 1, 2 or 3 - 'X', 'Y' or 'Z' coordinate respectively has two solutions
- 2nd Column = 1 - smaller value is correct
  2 - larger value is correct

ARRAY 'D' : THIS IS A*NDMAX BY 1*(i.e. 6 x 1) MATRIX CONTAINING THE DISTANCES BETWEEN MARKERS THAT COULD ONLY BE VIEWED BY ONE CAMERA AND ITS PRECEDING ADJACENT MARKERS

∇:XYZ - I : THESE ARE SYMBOLS WHICH WILL BE USED IN PROGRAM PARALLAX FOR PLOTTING THE TRAJECTORIES OF MARKERS (NOTE: ∇ MEANS BLANK SPACE)

N.B. If NDMAX = Ø, ARRAYS 'NCHOS' and 'D' will have no values, hence they will be omitted in the data file.

Figure D 3.1(c) Definition of Parameters listed in figure 3.1(b)

D(3) Displacement Data Rationalisation Programs

D(3.1) Program "COORDINATES"

This program performs the following functions, described mathematically in Section 6.2.1 and 6.2.2 :

a) Scaling the marker coordinates to real units and transforming them to relate to the ground frame of reference.

b) Correcting the phase difference between film frames of the cameras.

Also available in this program is an option to correct for fine lens distortion, described in Section 6.2.1. An option code (IX) is used to either by-pass or execute this sequence. However, for this option to be effective, the coordinates of the nearest grid junction associates with each body marker of every frame has to be included in the raw data.

The flow diagram of the program is presented in Figure D 3.1 (a). The Macro 'RUNCOOR' is used to run the program. A data preparation form, as shown in Figure D 3.1 (b), is used to collect information relevant to run program "COORDINATES", as well as programs "PARALLAX" and "FILTER". Only those parameters needed for the subsequent program are carried forward. Figure D 3.1 (c) gives the definition of the parameters listed in the Form.

Input and Output Data

The digitised marker coordinates are merged in the following fashion; data from the left camera are joined to the end of the data from the front camera and data from the left camera. At the beginning of each set of data is

						FORMAT
NGROUP	NAMP	NPTNT	NDATE1	NDATE2	NDATE3 NRUN	7IØ
NCASE	MAMAX	IIMAX(1)	IIMAX(2)	IIMAX(3)	JAMAX NDMAX	7IØ
AB	HD	T(1)	T(2)	T(3)	FCUT	6FØ.Ø
IX						IØ
DF	DL	DR	HF	HL	HR	6FØ.Ø
LTAIL1	LASIS	RTAIL1	RASIS			4IØ
ARRAY "MCODE"						2IØ
ARRAY "NCHOS"						2IØ
ARRAY "D"						FØ.Ø
.XYZ-1						7A1
1		- FRONT CAMERA CODE				IØ
Z_{G1}	Y_{G1}	⎫				
Z_{G2}	Y_{G2}	⎪				
Z_1	Y_1	⎪				
Z_2	Y_2	⎬ J=1			⎫	
.	.	⎪ .			⎪ FRONT CAMERA	
.	.	⎪ .			⎪ DATA	
Z_{26}	Y_{26}	⎭ .			⎭	
.	.	⎫				
.	.	⎬ J=JAMAX				
2		- LEFT CAMERA CODE				IØ
X_{G1}	Y_{G1}	⎫				2IØ
X_{G2}	Y_{G2}	⎪				
X_1	Y_1	⎬ J=1			⎫	
.	.	⎪ .			⎪ LEFT CAMERA	
.	.	⎪ .			⎪ DATA	
X_{13}	Y_{13}	⎭ .			⎭	
.	.	⎫				
.	.	⎬ J=JAMAX				
3		- RIGHT CAMERA CODE				IØ
X_{G1}	Y_{G1}	⎫				2IØ
X_{G2}	Y_{G2}	⎪				
X_{14}	Y_{14}	⎬ J=1			⎫	
.	.	⎪ .			⎪ RIGHT CAMERA	
.	.	⎪ .			⎪ DATA	
X_{26}	Y_{26}	⎭ .			⎭	
.	.	⎫				
.	.	⎬ J=JAMAX				

Figure D 3.1(d) Format of Files "%ARD%B"

a number used to identify the particular camera, from which the data comes.

The input data to this program, to be stored in file "%ARD%B", are generated by appending these raw displacement data to the end of the data collected in the form shown in Figure D 3.1 (b). The format to which these data are stored is as shown in Figure D 3.1 (d).

There are two output files from this program. One of them, "%ALC%B" was used to check that :-

1) None of the markers are missed when being digitised.

2) No extra marker is digitised.

3) The calibration markers digitised are correct and within the tolerance range.

This file is erased from store immediately after being listed on a line printer for examination.

The other output data file "%ACD%B", contains the transformed data and the peripheral information in the format required for entry into the next stage. See Section D(3.2) and Figure D 3.2 (b). Note that one "dummy" frame is eliminated at the beginning of the data from each camera after phase correction. Therefore, the maximum number of frames in the output data file "%ACD%B" is JMAX, i.e. (JAMAX-1).

D(3.2) Program "PARALLAX"

This program performs the parallax corrections on the transformed data from Stage (1), according to the mathematics in Section 6.2.3. It also computes the three dimensional spatial coordinates of all the markers

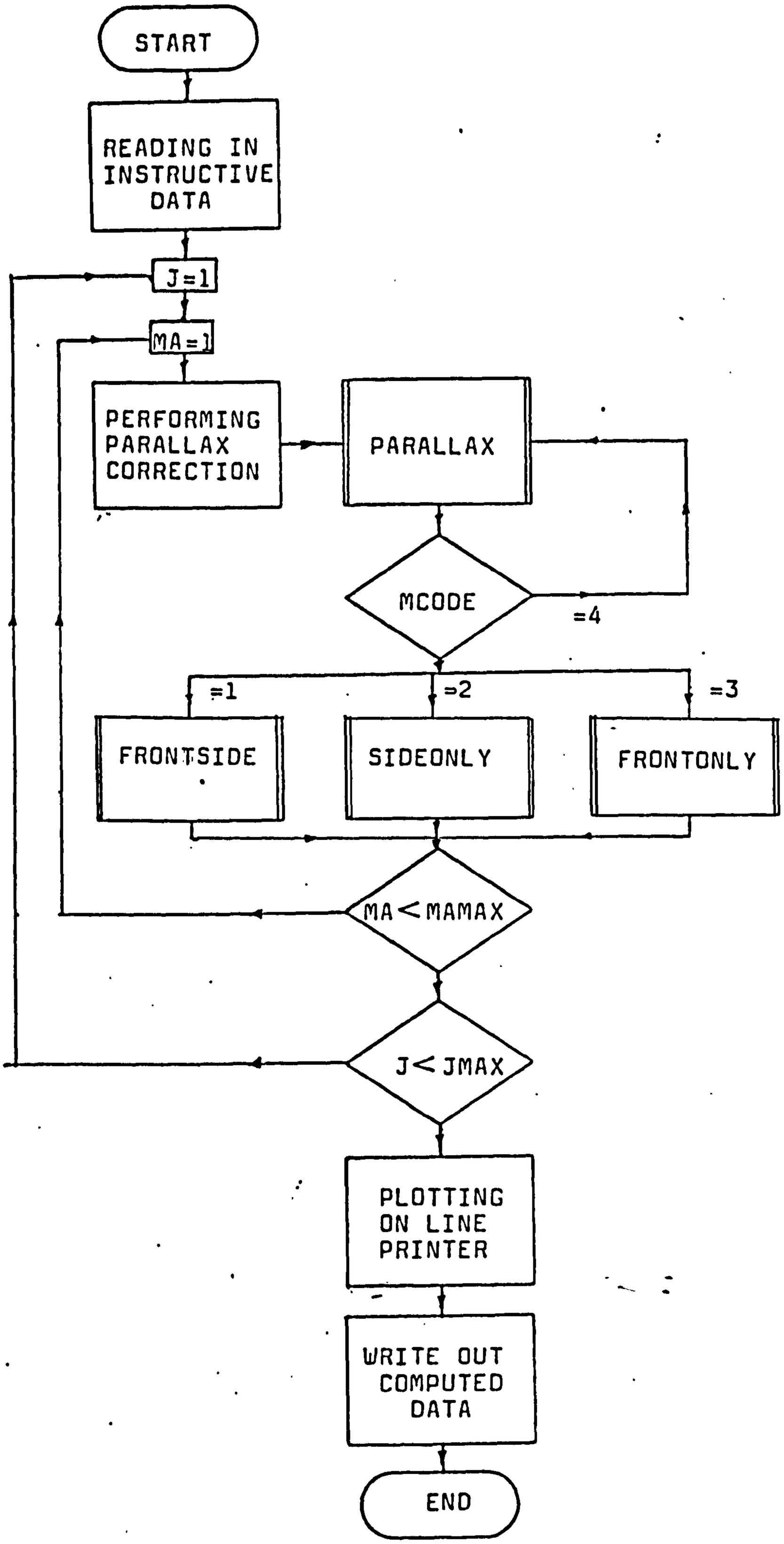

Figure D3.2(a) Flow Diagram of Program "PARALLAX"

relative to the origin of the ground frameeof reforenco.

A flow diagram of the program is presented in Figure D3.2(a). The macro used to run the program is "RUNPRLX".

Input and Output Data

The input data file "%ACD%B" is generated from the preceding program "COORDINATES". The structure of the file is featured in Figure D3.2(b).

Two output data files are created from this program. One is a data check file "%ALP%B", which allowed checks to be made on the calculated coordinates of markers seen by only one camera, in this case, the heel and tail markers. It also plots out the trajectories of all the markers to ensure that all the coordinates of the markers are in order. The file is erased immediately from store after a listing of it had been made.

The other output data file "%APX%B" contains the corrected data and some peripheral parameters in the format required for entry into the next stage. See Section D(3.3) and Figure D3.3(b).

Subroutine "PARLAX"

This is the major subroutine in the program. It uses the information available in the array "MCODE" to distinguish the category of each marker. In column one; if the value is "1", then the marker is directed to Subroutine "FRONTSIDE", and its corresponding value in column two will be zero.

If column one is "2" or "3", then the marker is directed either to subroutine "FRONTONLY" or subroutine

							FORMAT
NGROUP	NAMP	NPTNT	NRUN				4FØ
NCASE	MAMAX	IIMAX(1)	IIMAY(2)	IIMAX(3)	JMAX	NDMAX	7IØ
FCUT							FØ.Ø
DF	DL	DR	HF	H'	HR		6FØ.Ø
LTAIL1	'ASIS	RTAIL1	RASIS				4IØ
ARRAY "MCODE"							2IØ
ARRAY "NCHOS"							2IØ
ARRAY "D"							FØ.Ø
.XYZ-I							7A1

$$\left[\begin{matrix} Z_1(1) & Y_1(1) & \cdots & Z_1(7) & Y_1(7) \\ Z_2(1) & Y_2(1) & \cdots & Z_2(7) & Z_2(7) \\ \vdots & \vdots & \cdots & \vdots & \vdots \\ Z_{26}(1) & Y_{26}(1) & \cdots & Z_{26}(7) & Y_{26}(7) \end{matrix}\right]$$

7(2FØ.Ø)

$$\left[\begin{matrix} \vdots & \vdots & \cdots & Z_1(JMAX) & Y_1(JMAX) \\ \vdots & \vdots & \cdots & \vdots & \vdots \\ \vdots & \vdots & \cdots & Z_{26}(JMAX) & Y_{26}(JMAX) \end{matrix}\right]$$

— N=1 (FRONT)

$$\left[\begin{matrix} X_1(1) & Y_1(1) & \cdots & X_1(7) & Y_1(7) \\ \vdots & \vdots & \cdots & \vdots & \vdots \\ X_{13}(1) & Y_{13}(1) & \cdots & X_{13}(7) & Y_{13}(7) \end{matrix}\right]$$

$$\left[\begin{matrix} \vdots & \vdots & \cdots & X_1(JMAX) & Y_1(JMAX) \\ \vdots & \vdots & \cdots & \vdots & \vdots \\ \vdots & \vdots & \cdots & X_{13}(JMAX) & Y_{13}(JMAX) \end{matrix}\right]$$

— N=2 (LEFT)

$$\left[\begin{matrix} X_{14}(1) & Y_{14}(1) & \cdots & X_{14}(7) & Y_{14}(7) \\ \vdots & \vdots & \cdots & \vdots & \vdots \\ X_{26}(1) & Y_{26}(1) & \cdots & X_{26}(7) & Y_{26}(7) \end{matrix}\right]$$

$$\left[\begin{matrix} \vdots & \vdots & \cdots & X_{14}(JMAX) & Y_{14}(JMAX) \\ \vdots & \vdots & \cdots & \vdots & \vdots \\ \vdots & \vdots & \cdots & X_{26}(JMAX) & Y_{26}(JMAX) \end{matrix}\right]$$

— N=3 (RIGHT)

Figure D 3.2(b) Format of File "%ACD%B"

"SIDEONLY" respectively. The corresponding column two will be the number of the preceeding adjacent marker, the distance of which is stored in array "D". Since two solutions are obtained in these subroutines, information in array "NCHOS" gives the correct one.

The two pelvic tail markers which can only be seen from the side camera, have to be solved from the one associated pelvic spine marker. The pelvic tail marker 1 and pelvic spine marker are routed out of sequence by designating the number 4 to column one and zero to column two of array "MCODE". The pelvic spine marker was solved first by using subroutine "FRONTSIDE". The pelvic tail marker 1 was solved using subroutine "SIDEONLY" and the pelvic spine marker coordinates and its distance, stored in array "D".

Other Subroutines

Subroutine "FRONTSIDE" solves for the true spatial coordinates of a marker, that can be seen from the front and one of the side cameras, as described in Section 6.2.3(i).

Subroutine "FRONTONLY" solves for the true spatial coordinates of a marker, which can only be seen by the front camera. The calculation is based on the known distance of an adjacent marker, whose true coordinates were calculated previously, as described in Section 6.2.3(ii).

Subroutine "SIDEONLY" solves for the true spatial coordinates of a marker, which can only be seen by a side camera. The calculation again is based on a known distance of an adjacent marker, whose true coordinates were calculated previously, as described in Section 6.2.3(iii).

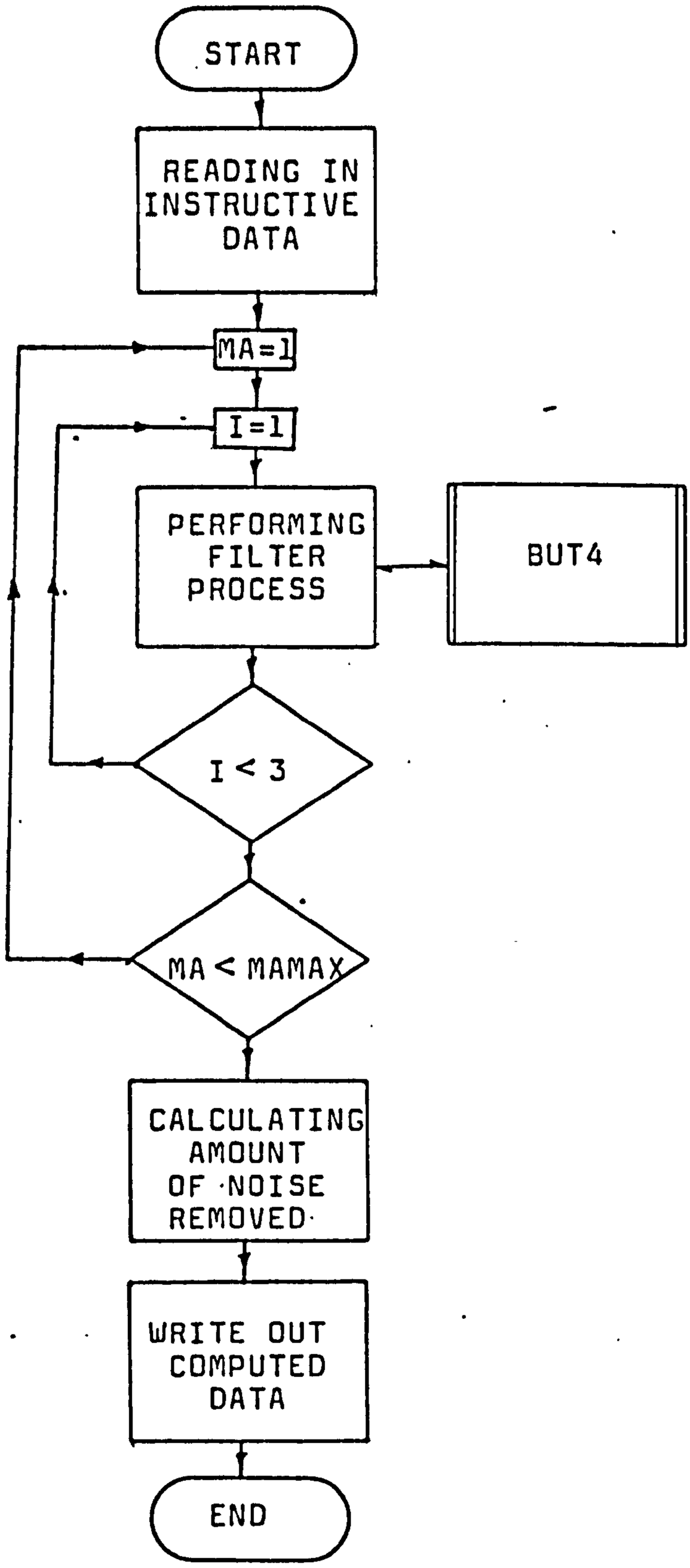

Figure D3.3(a) Flow Diagram of Program "FILTER"

	FORMAT
NGROUP NAMP NPTNT NRUN	4IØ
NCASE MAMAX JMAX	3IØ
FCUT	FØ.Ø
X_1 Y_1 Z_1	3FØ.Ø
X_2 Y_2 Z_2	
X_3 Y_3 Z_3	
X_4 Y_4 Z_4 — J=1	
X_5 Y_5 Z_5	
. . .	
: : :	
. . .	
X_{26} Y_{26} Z_{26}	
X_1 Y_1 Z_1	
. . .	
. . . — J=2	
. . .	
X_{26} Y_{26} Z_{26}	
X_1 Y_1 Z_1	
. . .	
. . . — J=JMAX	
. . .	
X_{26} Y_{26} Z_{26}	

Figure D 3.3(b) Format of File "%APX%8"

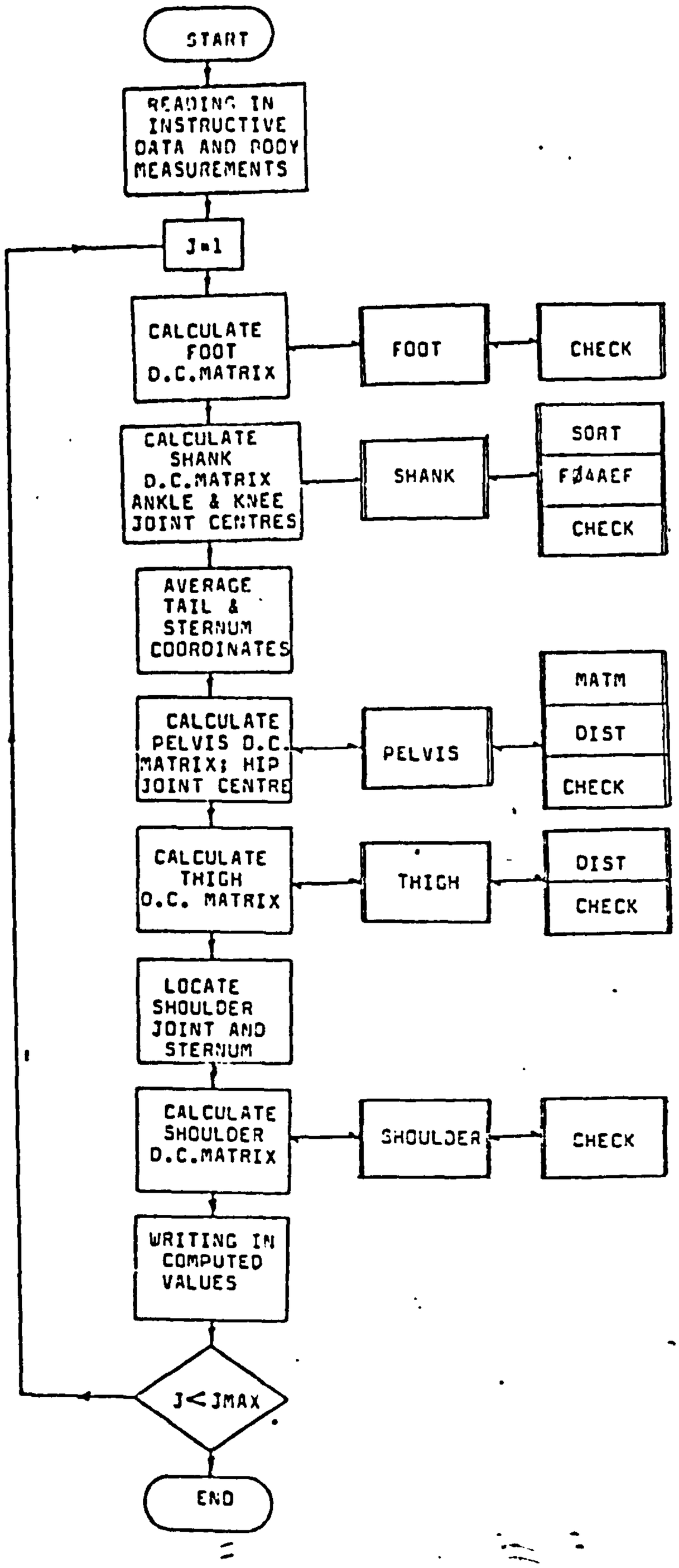

Figure D 3.4(a) Flow Diagram of Program "JOINTS"

D(3.3) Program "FILTER"

This program filters off the high frequency random noise in the data, as described in Section 6.2.4. The cut-off frequency of the digital filter can be chosen and specified in the input data file of program "COORDINATES" as parameter "FCUT". See Figure D3.1(b).

A flow diagram of the program is presented in Figure D3.3(a). The macro "RUNFITR" is used to run the program. Subroutine "BUT4" is the digital filter designed by Andrews (1975).

Input and Output Data

The input data file "%APX%B", generated by program "PARALLAX", has the format as shown in Figure D3.3(b).

There are 2 output data files, one is a data check file, "%ALF%B", which checks on the amount of data being removed. This file is erased after a listing is obtained. The other output data file, "%AFR%B" contains the smoothed data ready for entry into the next stage, the format of which is similar to file "%APX%B" in Figure D3.3(b), except that parameter "FCUT" is deleted.

D(3.4). Program "JOINTS"

This program calculates the spatial coordinates of the joint centres and direction cosine matrix of the segments described in Section 6.3.

Figure D3.4(a) shows the flow diagram of the program. The macro used to run the program is "RUNJNTS".

The analysis is carried out frame by frame, using several subroutines to perform the calculations.

Data Preparation Form (2) for Stage (4).....Prog. JOINTS

Filename : _____

						Statement Format
DFL	DFR	H	ST			4FØ.Ø
SL1	SL2	SL3	SL4	SL5		5FØ.Ø
SR1	SR2	SR3	SR4	SR5		5FØ.Ø
HX1	HYL	HZL	HXR	HYR	HZR	6FØ.Ø
DSL	DSR					2FØ.Ø
RP	RS					2FØ.Ø
JLMAX	JRMAX					2IØ

Figure D 3.4(b) Data Preparation Form for Program "JOINTS" - File "%ABM%B"

Input and Output Data

Two input data files are used in this program. File "%AFR%B", generated from the previous stage, program "FILTER", contains the filtered marker coordinates. The structure of the file was described in Section D(3.3). The second input data file "%ABM%B" consists of the required body measurements and other peripheral information. The format of the file is presented in Figure D3.4(b). The definitions of the parameters listed are given in Figure D3.4(c).

Three output data files are created by the program. There is the data check file "%ALF%B", which is immediately erased, after being listed on the line printer. The selection of the correct solution for the direction cosine "B11" of the shank can be checked. The variation of the shank lengths is listed to give an indication of accuracy. The coordinates of all the joint centres and direction cosine matrices of all the segments are presented. The determinant of each matrix is also calculated to check its orthogonality.

The two other output data files, "%AJT%B" and "%AST%B" contain the coordinates of all the joint centres and the direction cosine matrices of all the segments respectively. These two files are re-organised by using the editing commands of George 3 in "RUNJNTS", for entry into the next stage. The format of these files is given in Figure D3.5(b) and (c), respectively.

Subroutines

(i) Subroutine "SHANK" is used to determine the direction cosine of the shank as well as the knee and ankle joint centre, as described in Section 6.3.1. The frame number, coordinates of the tibial tuberosity, fibula head and

DFL, DFR	:	WIDTH OF LEFT AND RIGHT FOOT RESPECTIVELY AT ABOUT THE METATARSAL BREAK (see figure 5.3.4(b))(in mm)
H	:	LENGTH OF SHANK MARKERS (see figure 5.3.1(a))(in mm)
ST	:	SOCKET THICKNESS-ONLY WITH BELOW-KNEE PROSTHESIS(for all others, ST=Ø.Ø) (see figure 5.3.4(b))(in mm)
SL1 to SL5 SR1 to SR5	:	LEFT AND RIGHT SHANK DIMENSIONS RESPECTIVELY (see figure 5.3.4(b))(in mm) SL5/SR5-ONLY WITH UNIAXIAL FOOT (For all others, SL5/SR5=Ø.Ø)
HXL, HYL, HZL HXR,HYR,HZR	:	LOCATION OF LEFT AND RIGHT HIP JOINTS, RESPECTIVELY RELATIVE TO ASSOCIATED ANTERIOR SUPERIOR ILLIAC SPINE. (in mm)
DSL, DSR	:	A/P WIDTH OF LEFT AND RIGHT SHOULDER RESPECTIVELY(in mm)
RS	:	RATIO OF SHOULDER MARKERS
RP	:	RATIO OF PELVIC TAIL MARKERS
JLMAX, JRMAX	:	TOTAL NUMBER OF FRAMES IN THE LEFT AND RIGHT STRIDE RESPECTIVELY.

Figure D 3.4(c) Definitions of Parameters in File "%ABM%B"

lateral malleolus markers, the calculated shank dimensions and the code identifying the side being analysed are parameters required for entry into the subroutine. "SQRT" and "FØ4AEF" are subroutines from the computer library used by "SHANK". "SQRT" is used for determining the square root of a variable, while "FØ4AEF" is used to invert a matrix and multiply it by another matrix.

(ii) Subroutine "FOOT" is used to determine the direction cosine of the foot (see Section 6.3.2). The entry parameters are the frame number, coordinates of toe tip, 5th metatarsar base and mid-heel markers, ankle joint coordinates calculated from "SHANK", foot width, length of marker stalk and code for identifying the side being analysed. "DIST", which is a function used for calculating the distance between two points, and "SQRT" are employed by "FOOT".

(iii) Subroutine "PELVIS" determines the direction cosine of the pelvis and the coordinates of the hip joint centre according to Section 6.3.3. Entry parameters are the frame number, coordinates of the pelvic spine and tail markers, the location of the hip joint centre relative to the pelvic spine and the tail marker ratio. Subroutine "MATM" which performs matrix multiplication, "DIST" and "SQRT" are used in "PELVIS".

(iv) Subroutine "THIGH" determines the direction cosine of the thigh according to Section 6.3.4. The entry parameters are the frame number, the hip joint coordinates calculated from "PELVIS" and the knee joint coordinates calculated for "SHANK". "DIST and "SQRT" are also used.

(v) Subroutine "SHOULDER" determines the direction cosine of the shoulders and the coordinates of the shoulder

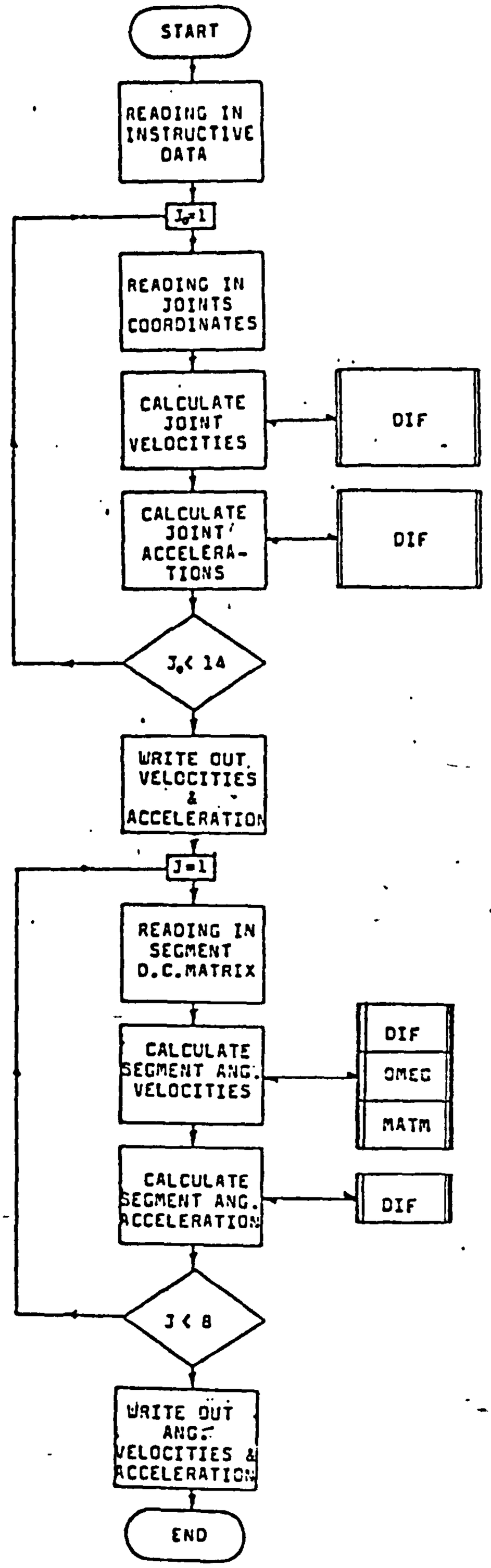

Figure D 3.5(a) Flow Diagram of Program "KINEMATICS"

joints. The entry parameters are the frame number, the shoulder and sternum markers and the dimension of the shoulders. "DIST" and "SQRT" are also used in this subroutine.

(vi) Subroutine "CHECK" is used to calculate the determinant of the direction cosine matrix of each segment. This is used to check the orthogonality of each matrix.

D(3.5) Program "KINEMATICS"

This program determines the linear velocities and accelerations of all the joint centres and also the angular velocities and accelerations of all the body segments. The equations used in the program were described in Section 6.4.1.

A flow diagram of the program is presented in Figure D3.5(a). The macro used to run this program is "RUNKMTS".

Input and Output data

The two input data files "%AJT%B" and "%AST%B" are generated from the previous program "JOINTS". The structure of these files is presented in Figures D3.5(b) and (c) respectively.

There are four output data files created from this program. The linear velocity and acceleration files, "%AVE%B" and "%AAC%B" respectively, contain data which are reduced by four and eight frames respectively per joint centre. The organisation of these files is similar to "%AJT%B", see Figure D3.5(b). The angular velocity and acceleration files, "%AAV%B" and "%AAA%B" respectively contain data which are reduced by four and eight frames

```
NGROUP      NAMP      NPTNT      NRUN
NCASE       MAMAX     JMAX

  X1(1)       Y1(1)       Z1(1)
  X1(2)       Y1(2)       Z1(2)
  X1(3)       Y1(3)       Z1(3)      ] JOINT=1
    .           .           .
    .           .           .
    .           .           .
  X1(JDMAX)   Y1(JDMAX)   Z1(JDMAX)  ]

  X2(1)       Y2(1)       Z2(1)
  X2(2)       Y2(2)       Z2(2)
    .           .           .
    .           .           .        ] JOINT=2
    .           .           .
  X2(JDMAX)   Y2(JDMAX)   Z2(JDMAX)  ]

                                        .
                                        .
                                        .
  X14(1)      Y14(1)      Z14(1)
    .           .           .
    .           .           .        ] JOINT=14
    .           .           .
  X14(JDMAX)  Y14(JDMAX)  Z14(JDMAX) ]
```

Note : For file %AJT%B, maximum frames, JDMAX=JMAX
%AVE%B, maximum frames, JDMAX=JMAX-4
%AAC%B, maximum frames, JDMAX=JMAX-8

Figure D 3.5(b) Format of Files "%AJT%B", "%AVE%B" and "%AAC%B"

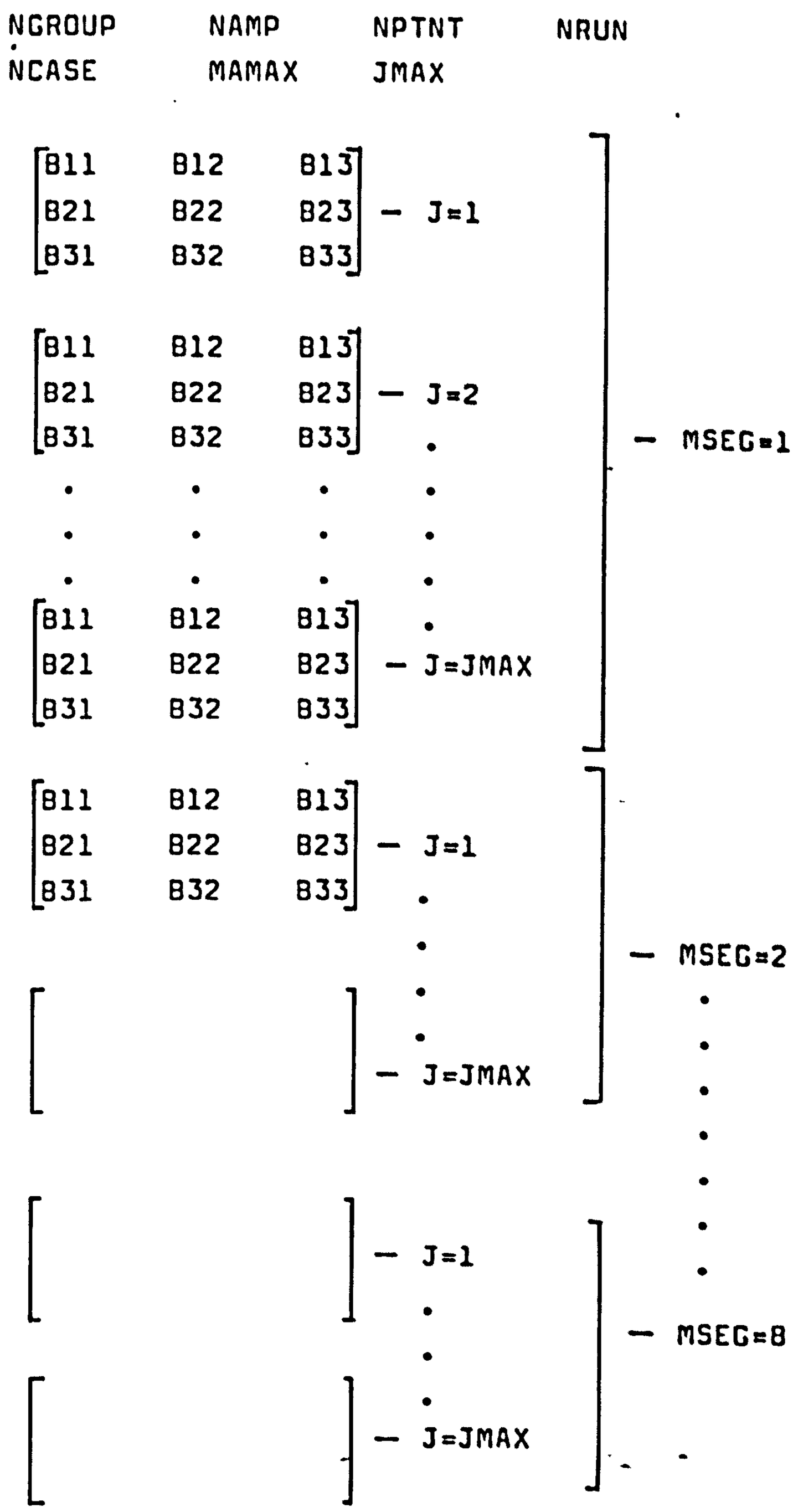

Figure D 3.5(c) Format of Files "%AST%8"

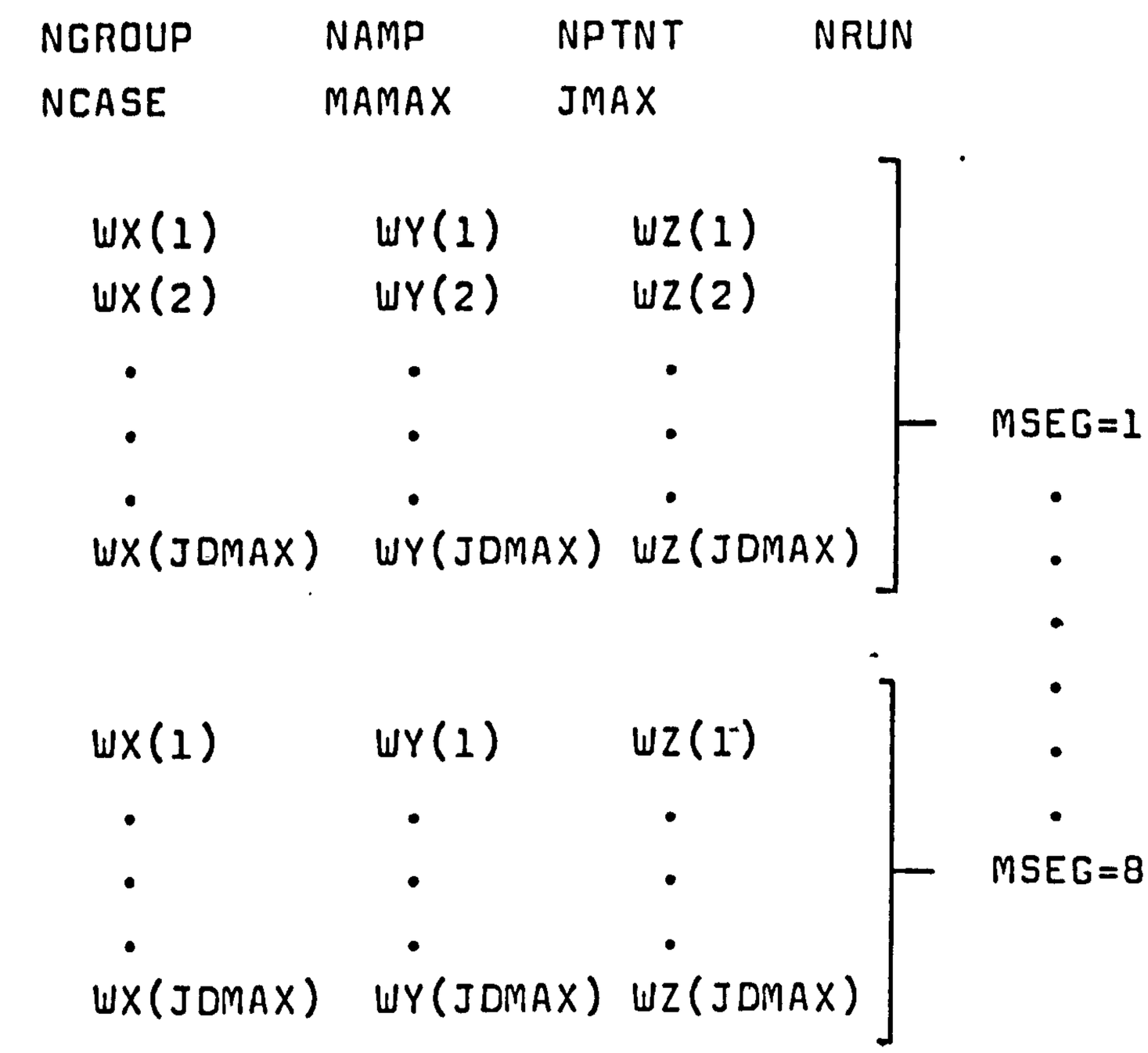

Note : %AAV%B - maximum frames, JDMAX=JMAX-4
%AAA%B - maximum frames, JDMAX=JMAX-8

Figure D3.5(d) Format of Files "%AAV%B" and "%AAA%B"

respectively per body segment. The organisation of these files is presented in Figure D3.5(d). These files are required for running the next stage, program "KINETICS".

Subroutines

Subroutine "DIF" is the numerical differentiator. The entry parameters are the data sampling time interval and the array of data. After differentiation, the total number of data will be reduced by four, viz two in the beginning and two at the end of the data. The first derivative (i.e. velocity) is obtained by using the displacement data and the second derivative(i.e. acceleration) is obtained by using the first derivative.

Subroutine "OMEG" is used to solve for the absolute angular velocity of each segment from its direction cosine matrix. See Section 6.4.1 for the mathematical derivation. Subroutine "MATM" is also used in this sequence.

D(4) Dynamic Analysis

D(4.1) Program "KINETICS"

This program performs the following calculations, as described in Section 6.6 :

a) body segment parameters

b) the external forces and intersegmental moments acting at the hip, knee and ankle joints of both legs.

c) the mechanical energy level of the thigh, shank and foot of both legs.

In the program, the force plates and kinematic data

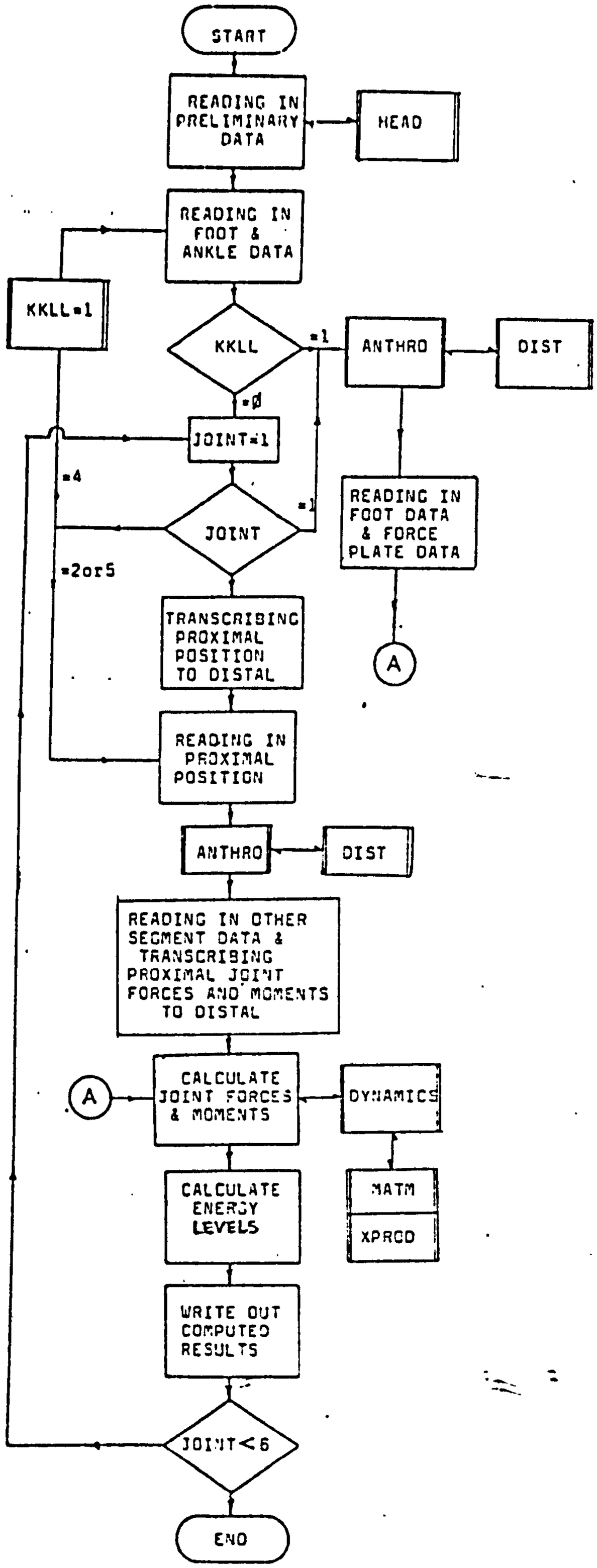

Figure D 4.1(a) Flow Diagram of Program "KINETICS"

are synchronised and related to make dynamic calculation possible. The flow diagram of the program is presented in Figure D4.1(a). The macro used to run the program is "RUNKNTS".

Input and Output Data

There are altogether nine input data files required for entry into the program; two sets of force plate data "%ADL%C" and "%ADR%C" from "BIOMECHANICS", joint centre coordinates "%ADJT%B" and D.C. matrix of segments "%AST%B" from "JOINTS", linear velocity and acceleration of joint centres, "%AVE%B" and "%AAC%B" respectively, and the angular velocity and acceleration of segments, "%AAV%B" and "%AAA%B" respectively from "KINEMATICS". Lastly, "%APT%B" which contains information on the physical properties of the prosthesis used. See Figure D4.1(b) and (c) for its format and definition of parameters, respectively.

Three output data files are generated from the program. "%AFO%B" and "%AMO%B" contain the external forces and the intersegmental moments respectively, exerted on and about the joint centres of the lower limbs of both legs. "%AEN%B" contains the instantaneous mechanical energy levels of the segments of the lower limbs of both legs.

Subroutines

(i) Subroutine "ANTHRO" determines the physical properties of each body segment when instructed. The parameters required are obtained as described in Section 6.6.1. The entry parameters are the coordinates of the proximal and distal joints of the segment, total body mass, mass of shoe, index of proximal joint, level and side of amputation and the physical properties of the prosthesis. The

Data Preparation Form (3) for Stage (6)... Program KINETICS

Filename : _____

			Statement Format
TOTM	SHOE		2FØ.Ø
FINT	FMAS	FDCM	3FØ.Ø
SINT	SMAS	SDCM	3FØ.Ø
TINT	TMAS	TDCM	3FØ.Ø

Figure D4.1(b) Data Preparation Form for Program "KINETICS" - File "%APT%B"

TOTM	-	Total Mass of body
SHOE	-	Mass of shoe
FINT, SINT, TINT	-	MASS MOMENT OF INERTIA OF PROSTHETIC FOOT, SHANK AND THIGH RESPECTIVELY
FMAS, SMAS, TMAS	-	MASS OF PROSTHETIC FOOT, SHANK AND THIGH RESPECTIVELY
FDCM, SDCM, TDCM	-	DISTANCE BETWEEN PROXIMAL JOINT OF PROSTHETIC SEGMENTS TO ITS CENTRE OF MASS

Figure D4.1(c) - Definition of parameters in file "%APT%B"

coefficients of body segment parameters presented in Section 2.1 are used for the unaffected limb. Function "DIST" is used by this subroutine.

(ii) Subroutine "DYNAMICS" calculates the external forces acting on the specified proximal joint and the inter-segmental moment about it. The entry parameters are the coordinates and acceleration of the proximal joint and centre of mass, the direction cosine matrix of the se segment, the angular velocity and acceleration of the segment, the physical properties of the segment (determined from subroutine "ANTHRO"), and the external forces and moments acting on the segment. The calculat-ions are based on the mathematics described in Section 6.6.2. Subroutine "XPROD" is used to perform the cross-product of two vectors. Subroutine "MATXM" and "DIST" are also used.

Listings of job control macro "RUNCOOR"

and program "COORDINATES"

DOCUMENT FUNCOOR

```
C SP N,(%A)(1,8)
1 SP V,(%A)(11,12)
2 SP N,(%A)(1,2)
3 SP T,(%A)(5)
4 LO BINCOOR
5 TIME 2MINS
6 AS *CR0,%A
7 AS *LP0,%NLC%V
8 AS *JP0,%NCD%V
9 RUN
10 LF %NLC%V,*LP
11 ER %NLC%V
12 IF HALTED (AH) -(R.DELETED (GG)), GO TO 1.OKAY
13 GO TO 1.NOTOKAY
14 1.OKAY
15 RJ TELEPX%"%T%V,RUNPHLY,PARAM(%NCD%V),HLS(JT 4MINS,MZ 45K)
16 DP 0,STAGE(1) EXECUTED SUCCESSFULLY,
17 EJ
18 1.NOTOKAY
19 DP 0,ERROR IN STAGE(1) :- PLEASE CHECK,
20 EJ NONE,RT(CHECKCOOR)
21 ****
22 DG
```

```
SCUPENT    COORDINATES

      'C
       1        PROGRAM C(COORDINATES)
       2        INPUT 6=CRC
       3        OUTPUT 5=IPC
       4        OUTPUT 7=TPC
       5        TRACE 2
       6        END
       7 C
       8 C  INPUT AND OUTPUT CHANNELS FOR PROG. COORDINATES
       9 C  I/P 6 - RAW DATA
      10 C  O/P 7 - SCALED MARKER COORDINATES
      11 C  O/P 5 - DATA CHECK FILE
      12 C
      13 C
      14 C  STAGE (1) ..... ADOPTED BY JAMES CON,RICENG UNIT
      15 C
      16 C  THIS PROGRAM PERFORMS THE FOLLOWING FUNCTIONS :-
      17 C     1.) TRANSFORMING D-RAC COORDINATES OF MARKERS TO THE GRID
      18 C         BOARD COORDINATES WITH ORIGIN AT GROUND REFERENCE
      19 C     2.) CORRECTING FOR PHASE DIFFERENCES BETWEEN EACH FRAME
      20 C         OF THE THREE CAMERAS
      21 C
      22 C  OPTION :- CORRECTING FOR LENS DISTORTION
      23 C
      24 C
      25 C    ***************************
      26        MASTER COORDINATES
      27 C    ***************************
      28 C
      29 C
      30        INTEGER STAIL,BASIS
      31        INTEGER BLANK,DOT,ZERO,VER1
      32        DIMENSION IMAX(3),MF(2),A(2,20,96,3)
      33        DIMENSION JVR(3)
      34        DIMENSION MCODE(20,2),D(4),MCPOS(6,2)
      35        DIMENSION JP(7),V(3),T(3),F1(50)
      36 C
      37 C
      38 C
      39 C
      40 C  NOMENCLATURE
      41 C  ************
      42 C
      43 C    NGROUP=PATIENTS' GROUP
      44 C         0 -- NORMAL
      45 C         1 -- BELOW KNEE AMPUTEE
      46 C         2 -- ABOVE KNEE AMPUTEE
      47 C
      48 C    NAMP = SIDE OF AMPUTATION
      49 C         0 -- NORMAL
      50 C         1 -- LEFT SIDE
      51 C         2 -- RIGHT SIDE
      52 C
      53 C    NPTNT = PATIENTS NUMBER
      54 C    NDATE1= DAY, NDATE2= MONTH, NDATE3= YEAR
      55 C    NRUN  = RUN NUMBER
      56 C
      57 C    NCASE = FILMING CASE DESCRIPTOR :-
      58 C         1 = FRONT,LEFT AND RIGHT CAMERAS USED
      59 C         2 = FRONT AND LEFT CAMERAS USED
      60 C         3 = FRONT AND RIGHT CAMERAS USED
      61 C
      62 C    MAPAX=TOTAL NUMBER OF MARKERS
      63 C      IMAX(1)= DIM. NO. OF MARKERS VIEWED BY FRONT CAMERA
      64 C      IMAX(2)= DIM. NO. OF MARKERS VIEWED BY LEFT CAMERA
      65 C      IMAX(3)= DIM. NO. OF MARKERS VIEWED BY RIGHT CAMERA
      66 C
      67 C    JMAX    = DIM. NUMBER OF FRAMES (INCL. DUMMY FRAMES)
      68 C    JMAX    = DIM. NUMBER OF FRAMES AFTER PHASING(I.E. JMAX-1)
      69 C
      70 C    NDMAX=TOTAL NUMBER OF FF AND SS CASES PER FRAME
      71 C     FF - CASES WHERE MARKERS CAN ONLY BE SEEN FROM THE FRONT CAMERA
      72 C     SS - CASES WHERE MARKERS CAN ONLY BE SEEN FROM THE SIDE CAMERA
      73 C    (IF ALL MARKERS CAN BE VIEWED BY ALL CAMERAS,THEN NDMAX=0)
      74 C
      75 C    AD,MCS GRID DIMENSIONS
      76 C     T(1)   = PHASE LAG OF FRONT TO LEADING CAMERA
      77 C     T(2)   = PHASE LAG OF LEFT TO LEADING CAMERA
      78 C     T(3)   = PHASE LAG OF RIGHT TO LEADING CAMERA
      79 C     FCUT   = CUT OFF FREQUENCY OF DIGITAL FILTER
      80 C
```

```
C OPTION CODE:( IX ) :-
C ---------------------
C    IX = LENS DISTORTION CORRECTION IDENTIFIER
C     IF IX = 0  --  BY-PASS OPTION
C              I.E GRID JUNCTION WERE NOT DIGITIZED
C         IX = 1  --  PERFORMS OPTION
C              I.E GRID JUNCTION NEAREST TO MARKER WERE DIGITIZED
C
C    DF, DL, DR = DISTANCES FROM THE FRONT, LEFT AND RIGHT
C                 CAMERAS TO THE ORIGIN OF THE GROUND
C                 COORDINATES SYSTEM
C    HF, HL, HR = HEIGHT OF FRONT , LEFT AND RIGHT CAMERAS
C                 FROM THE GROUND
C
C    LTAIL1,LASIS,RTAIL1,RASIS= INDICES OF LEFT TAIL1,A.S.I.S,
C      RIGHT TAIL1 AND A.S.I.S MARKERS, RESPECTIVELY
C
C    MCODE(MAMAX,2)=MARKER CODING MATRIX
C       1ST COL=1,2 OR 3=MARKER VIEWED BY FC+SC,FC ONLY OR SC ONLY,RESP.
C                4          =ESCAPE USUAL ROUTINE
C       2ND COL:WHEN MCODE(MA,1)=2 OR 3,MCODE(MA,2)=INDEX (MA) OF
C                / PREVIOUS MARKER AT A DISTANCE READ NEXT FROM D-ARRAY.
C                WHEN MCODE(MA,1)=1,MCODE(MA,2)=0.
C
C    NCHOS(NDMAX,2)=CHOSES CORRECT SOLUTION FOR XYZ IN FF AND SS CASES.
C       IN 1ST COL.1,2 OR 3 MEANS X,Y OR Z,RESP.,DETERMINES SOLUTION
C          IN 2ND COL:1=SMALLER VALUE IS CORRECT;2=LARGER VALUE IS CORRECT
C
C    D(NDMAX)=DISTANCES BETWEEN MARKERS,WHERE THE PROXIMAL MARKER IS A
C                 FF OR SS CASE
C ---------------------------------------------------------------------
C    A          = SIDE INDEX ; 1=FRONT, 2=LEFT, 3=RIGHT.
C    J          = FRAME INDEX.
C    I          = VIEWED-MARKER INDEX.
C    IXY        = GRID AXIS INDEX. 1=HORIZONTAL AXIS, 2=VERTICAL AXIS.
C    A          = ARRAY CONTAINING APPARENT COORDINATESOF MARKERS :
C                 DIMENSION OF A(IXY,I,J,N)= 2 *(MAXIMA(IIMAX(N)) *(JMAX+1) *3
C    ICODE      = FILMING SIDE IDENTIFIER
C    MF         = HORIZONTAL AND VERTICAL D-MAC COORDINATES
C ---------------------------------------------------------------------
C    BLANK,DOT,XXX,MINUS,VERT - THESE ARE SYMBOLS BEING USED
C      IN THE PLOTTING ROUTINE IN PROGRAM PARALLAX
C         TO CHECK THE SPATIAL DISPLACEMENT DATA
C ** ************************************
C READING IN PRILIMINARY DATA
C ** ************************************
      READ(6,14)NGROUP,NAME,NPINT,NDATE1,NDATE2,NDATE3,NRUN
      READ(6,14)NCASE,MAMAX,IIMAX,JMAX,NDMAX
      READ(6,16)PB,MC,I,FCUT
      READ(6,15)IX
      READ(6,16)DF,DL,DR,HF,HL,HR
      READ(6,545)LTAIL1,LASIS,RTAIL1,RASIS
      JMAX=JMAX-1
      WRITE(7,200)NGROUP,NAME,NPINT,NRUN
      WRITE(7,914)NCASE,MAMAX,IIMAX,JMAX,NDMAX
      WRITE(7,915)FCUT
      WRITE(7,916)DF,DL,DR,HF,HL,HR
      WRITE(7,920)LTAIL1,LASIS,RTAIL1,RASIS
      DO 540 IR=1,MAMAX
      READ(6,524)MCODE(IR,1),MCODE(IR,2)
      WRITE(7,921)MCODE(IR,1),MCODE(IR,2)
  540 CONTINUE
      IF(NDMAX.EQ.1)GOTO 542
      READ(6,524)((NCHOS(IR,MM),MM=1,2),IR=1,NDMAX)
      WRITE(7,921)((NCHOS(IR,MM),MM=1,2),IR=1,NDMAX)
      READ(6,535)(D(IR),IR=1,NDMAX)
      WRITE(7,923)(D(IR),IR=1,NDMAX)
  524 FORMAT(2I0)
  535 FORMAT(F10.0)
  545 FORMAT(4I0)
  923 FORMAT(F10.1)
  921 FORMAT(2I6)
  916 FORMAT(6F10.1)
  542 READ(6,1011)BLANK,DOT,XXX,MINUS,VERT
 1011 FORMAT(7A1)
      WRITE(7,1011)BLANK,DOT,XXX,MINUS,VERT
      WRITE(5,17)NGROUP
      WRITE(5,21)NAME
      WRITE(5,18)NPINT
      WRITE(5,19)NDATE1,NDATE2,NDATE3
      WRITE(5,20)NRUN
   14 FORMAT(7I0)
   15 FORMAT(I0)
   16 FORMAT(6F0.0)
   17 FORMAT(4H    1,12HGROUP NUMBER,I0)
   21 FORMAT(4H    2,12HSIDE OF AMPUTATION,I3)
   18 FORMAT(4H    3,14HPATIENT NUMBER,I7)
   19 FORMAT(4H    4,15HDATE OF EXPERIMENT,I2,I2,I5)
   20 FORMAT(4H    5,*HRUN NUMBER=,I1////)
  914 FORMAT(7I0)
  915 FORMAT(F10.1)
  920 FORMAT(4I0)
  200 FORMAT(1X,4I5)
C
```

```
C ****************************************************************
C READING CMAC DATA,TRANSFORM. INTO GRID COORDINATES
C  - STORING IN ARRAY A(IDV,I,J,N)
C ****************************************************************
C
      DO 52 N=1,2
      IF(NCASE.EQ.3)GOTO 161
      IF(N.NE.1.AND.N.NE.NCASE)GOTO 52
  161 READ(6,11)ICODE
      IF(ICODE.NE.N)GOTO 2002
 2002 WRITE(5,12)N,ICODE
      II=IIMAX(N)
      R=0.0
      DO 50 J=1,JAMAX
      READ(6,10)PF
      ZA=FLOAT(PF(1))
      YA=FLOAT(PF(2))
      READ(6,10)PF
      ZB=FLOAT(PF(1))
      YB=FLOAT(PF(2))
      F1(J)=SQRT((ZB-ZA)**2+(YB-YA)**2)
      WRITE(5,9000)J,ZA,ZB,F1(J)
 9000 FORMAT(5X,I4/3F10.2)
      F=AB/F1(J)
      R=R+F1(J)
      TG=(YB-YA)/(ZB-ZA)
      C=1.0/SQRT(1.0+TG**2)
      S=TG*C
      ZC=F*(ZA+ZB)/2.0
      YC=F*(YA+YB)/2.0
      DO 30 I=1,II
   67 READ(6,10)PF
      Z=F*FLOAT(PF(1))-ZC
      Y=F*FLOAT(PF(2))-YC
      A(1,I,J,N)= Z*C+Y*S
      A(2,I,J,N)=Y*C-Z*S
      IF(N.EQ.1.OR.N.EQ.2)A(1,I,J,N)=-A(1,I,J,N)
C
C ****************************************************
C OPTION IX OF THE FLOW CHART :-
C FOR THE CORRECTION OF GRID DISTORTION
C THROUGH THE CAMERA AND PROJECTOR LENS
C IF IX=0 ,BYPASS OPTION
C ****************************************************
C
      IF(IX.EQ.0)GOTO 50
      IF(KGR.EQ.2)GOTO 101
      GR1=A(1,I,J,N)
      GR2=A(2,I,J,N)
      KGR=2
      GOTO 67
  101 AR1 = A(1,I,J,N)
      AR2 = A(2,I,J,N)
      N1  = NINT(AR1/127.0)
      N2  = NINT(AR2/127.0)
      A(1,I,J,N) = GR1-AR1+127.0*FLOAT(N1)
      A(2,I,J,N) =GR2-AR2+127.0*FLOAT(N2)
   10 FORMAT(2I0)
   12 FORMAT(1X,' CHECKING DATA FORMAT/1X,2HN=,I2,4X,6HICODE=,I2///)
   11 FORMAT(I0)
   50 CONTINUE
      RA=R/JAMAX
      S=0.0
      DO 40 J=1,JAMAX
      S=S+(F1(J)-RA)**2
   40 CONTINUE
      SA=SQRT(S/JAMAX)
      WRITE(5,9001)RA,SA
 9001 FORMAT(//2X,16HAVERAGE LAB = ,F10.2/1X,15HSTD. DEV. = ,F10.6//)
   52 CONTINUE
C
```

```
C ****************************************
C CORRECTING FOR PHASE DIFFERENCE.:-
C    CT      =CYCLE TIME (=20 MSEC)
C    T(N)    = PHASE LAG OF N AND LEADING CAMERA
C     N=1   - FRONT CAMERA
C      =2   - LEFT CAMERA
C      =3   - RIGHT CAMERA
C ****************************************
C
      CT=20.0
      DO 53 N=1,3
      IF(NCASE.EQ.1)GOTO 148
      IF(N.NE.1.AND.N.NE.NCASE)GOTO 53
  148 DO 55 IXY=1,2
      DO 55 I=1,IIMAX(N)
      DO 55 J=1,JMAX
      JJ=J+1
      DELTA=(A(IXY,I,J,N)-A(IXY,I,JJ,N))*(T(N)/CT)
      A(IXY,I,J,N)=A(IXY,I,JJ,N)+DELTA
   55 CONTINUE
   53 CONTINUE
      DO 105 N=1,3
      IF(NCASE.EQ.1)GOTO 149
      IF(N.NE.NCASE.AND.N.NE.1)GOTO 105
  149 DO 104 J1=1,JMAX,7
      WRITE(7,908)
      J2=J1+6
      JP(1)=J1
      JP(2)=J1+1
      JP(3)=J1+2
      JP(4)=J1+3
      JP(5)=J1+4
      JP(6)=J1+5
      IF(J2.GE.JMAX)J2=JMAX
      JP(7)=J2
      J11=J1-((J1-1)/7)*7
      J22=J2-((J2-1)/7)*7
      DO 104 I=1,IIMAX(N)
      WRITE(7,910)((A(IXY,I,J,N),IXY=1,2),J=J1,J2)
  908 FORMAT(1X/)
  910 FORMAT(1X,7(2F12.4,1X))
  104 CONTINUE
  105 CONTINUE
      GOTO 2001
 2000 WRITE(5,2003)
 2003 FORMAT(1X,17HERROR IN RAW DATA/)
      GOTO 2002
 2001 STOP
      END
      FINISH
```

Listings of job control macro "RUNPRLX"

and program "PARALLAX"

```
DOCUMENT   RUNPRLX
        E SP N,(%A)(1,E)
        1 SP V,(%A)(11,12)
        2 SP M,(%A)(1,2)
        3 SP T,(%A)(5)
        4 LO BINPRLX
        5 TIME 4MINS
        6 AS *IR0,%A
        7 AS *LP0,%NLP%V(LIMITS00()
        8 AS *TP0,%NPX%V(LIMITS00()
        9 RUN
       10 LF %NLP%V,*LP
       11 ER %NLP%V
       12 IF HALTED (AH) OR DELETED (JC),GO TO 2.OKAY
       13 GO TO 2.NOTOKAY
       14 2.OKAY
       15 RJ TELEFR%M%T%V,FUNFITR,PARAM(%NPX%V),HLS(JT 4MINS)
       16 DP 0,STAGE(2) EXECUTED SUCCESSFULLY,
       17 EJ
       18 2.NOTOKAY
       19 DP 0,ERROR IN STAGE(2) - PLEASE CHECK,
       20 EJ NONE,RT(CHECKFRLX)
       21 ****
       22 DG
```

```
C


      PROGRAM (PARALLAX)
      INPUT 6=TR1
      OUTPUT 5=LP
      OUTPUT 7=TR1
      TRACE 2
      END
C
C INPUT AND OUTPUT CHANNELS FOR PROG. PARALLAX
C I/P 6 - SCALED MARKER COORDINATESDINATES(FROM PROG. COORD)
C O/P 7 - CORRECTED MARKER COORDINATES
C O/P 5 - DATA CHECK FILE
C
C
C STAGE(2) ............ ACCEPTED BY JAMES COM,RIDING. UINT
C
C THIS PROGRAM PERFORMS THE FOLLOWING FUNCTIONS:-
C   1) CORRECTS FOR THE PARALLAX ERRORS
C   2) GIVES THE MARKER COORDINATES IN THREE DIMENSIONS
C   3) PLOTS THE MARKER COORDINATES ON THE LINE PRINTER
C      FOR CHECKING PURPOSES
C
C ********************************
      MASTER PARALLAX
C ********************************
C
C
      REAL KPN,MI
      INTEGER RTAIL1,RBASIS
      INTEGER BLANK,DOT,XXX,VERT
      DIMENSION XXXX(119)
      DIMENSION MMN(13),E(3),DELT(3)
      DIMENSION LINE(61),XXX(3),XX(13),YY(13),ZZ(13)
      DIMENSION X(3)
      DIMENSION XYZ(3,26,31),A(2,2,9,3)
      DIMENSION IIMAX(3),MF(2)
      DIMENSION MCODE(26,2),NCHOS(6,2),D(6)
      COMMON/BLOCK2/DF,DL,DR,MF,ML,MR
C
C
C FOR NOMENCLATURE SEE STAGE(1),PROGRAM "COORDINATES"
C **********************************************
C
C
C READING IN PRELIMINARY DATA
C ****************************
C
C
      READ(6,200)NGROUP,NAMP,NPTNT,NRUN
      READ(6,14)NCASE,MAMAX,IIMAX,JMAX,NCMAX
      WRITE(7,200)NGROUP,NAMP,NPTNT,NRUN
      WRITE(7,200)NCASE,MAMAX,JMAX
      READ(6,15)FCUT
      WRITE(7,203)FCUT
      READ(6,16)DF,DL,DR,MF,ML,MR
      READ(6,201)LTAIL1,LBASIS,RTAIL1,RBASIS
      DO 540 IM=1,MAMAX
      READ(6,524)MCODE(IM,1),MCODE(IM,2)
  540 CONTINUE
      IF(NCMAX.EQ.0)GOTO 542
      READ(6,524)((NCHOS(IR,MM),MM=1,2),IR=1,NCMAX)
      READ(6,533)(D(IR),IR=1,NCMAX)
  542 READ(6,615)BLANK,DOT,XXX,MINUS,VERT
C
C CHECKING FOR THE TYPE OF FILMING SYSTEM(NCASE) BEING USED
C AND ALSO PREPARING DATA,WRITING IT IN ARRAY(A) FOR THE
C CORRECTION PROCESS
C
      DO 105 N=1,3
      IF(NCASE.EQ.1)GOTO 300
      IF(N.NE.NCASE.AND.N.NE.1)GOTO 105
  300 DO 104 J1=1,JMAX,7
      READ(6,902)
      J2=J1+6
      IF(J2.GE.JMAX)J2=JMAX
      DO 104 I=1,IIMAX(N)
      READ(6,910)((A(IXY,I,J,N),IXY=1,2),J=J1,J2)
  910 FORMAT(1X,7(2F8.4,1X))
  902 FORMAT(1X/)
  200 FORMAT(4I10)
  201 FORMAT(1X,4I5)
  202 FORMAT(1X,3I5)
  203 FORMAT(1X,F10.5)
  104 CONTINUE
  105 CONTINUE
   16 FORMAT(6F10.0)
   15 FORMAT(F10.0)
   14 FORMAT(7I10)
  915 FORMAT(2F10.0)
  615 FORMAT(7R1)
  524 FORMAT(2I10)
  533 FORMAT(F10.0)
C
```

```
C PERFORM PARALLAX CORRECTION
C **********************
C
C
      CALL PARLAX(JMAX,MAMAX,NOMAX,NCASE,IIMAX,
     1LASIS,LTAIL1,BASIS,RTAIL1,
     2PCODE,NCH(5,D,DOT,A,XYZ)
      WRITE(7,3)(((XYZ(IX,MA,J),IX=1,3),J=1,JMAX),MA=1,MAMAX)
    3 FORMAT(3(1E.1)
C
C GENERATION OF PLOTS ON LINE PRINTER FOR CHECKING PURPOSES
C ********************************************************
C
      DO 1 IM=1,119
      XXXX(IM)=ECT
    1 CONTINUE
      WRITE(5,5021)XXXX
 5021 FORMAT(119A1)
      WRITE(5,5022)
 5022 FORMAT(1X,///)
C
C
C STARTING TO WRITE AND GRAPH X,Y,Z.
C
      DO 615 MA=1,MAMAX
      KO(1)=-3.0
      KO(2)=-1.8
      KO(3)=-1.2
      DELT(1)=0.5
      DELT(2)=0.3
      DELT(3)=0.2
      DO 670 MK=1,3
      DO 669 NMK=1,13
      AMN(NMK)=KO(MK)+(NMK-1)*DELT(MK)
  669 CONTINUE
      WRITE(5,671)MK,KMN
  671 FORMAT(44),1HX,I1,13F5.1,2X,5HX10C))
  670 CONTINUE
      DO 625 NL=1,51
  625 LINE(NL)=ECT
      DO 629 NL=1,61,5
      LINE(NL)=VERT
  629 CONTINUE
      WRITE(5,621)LINE
  621 FORMAT(1X,2HMA,3X,1HJ,8X,1HX,10X,1HY,10X,1HZ,11X,51A1)
      DO 616 J=1,JMAX
      XYX=XYZ(1,MA,J)
      Y  =XYZ(2,MA,J)
      Z  =XYZ(3,MA,J)
      DO 617 K=1,61
  617 LINE(K)=PLUK
      DO 618 K=1,61,5
  618 LINE(K)=DOT
      KKX=NINT(XYX/100.0)
      IF(IABS(KKX).GE.30)KKX=30
      KX=31+KKX
C
      KKY=NINT(Y/60.0)
      IF(IABS(KKY).GE.30)KKY=30
      KY=31+KKY
C
      KKZ=NINT(Z/40.0)
      IF(IABS(KKZ).GE.30)KKZ=30
      KZ=31+KKZ
C
      LINE(KX)=XX(1)
      LINE(KY)=XY(2)
      LINE(KZ)=XX(3)
C
      WRITE(5,620)MA,J,(XYZ(IXYZ,MA,J),IXYZ=1,3),J,LINE
  620 FORMAT(1X,I2,1X,I3,3X,F8.1,3X,F8.1,3X,F8.1,5X,I3,3X,51A1)
  616 CONTINUE
      WRITE(5,24)
   24 FORMAT(///)
  615 CONTINUE
      STOP
      END
C
C
C
C ***************************************************
      SUBROUTINE PARLAX(JMAX,MAMAX,NOMAX,NCASE,IIMAX,
     1LASIS,LTAIL,BASIS,RTAIL,
     2PCODE,NCH(5,D,DOT,A,XYZ)
C ***************************************************
C
C THIS SUBROUTINE PREPARES DATA FOR PARALLAX CORRECTION
C
      INTEGER BASES
      INTEGER RTAIL,BASIS
      INTEGER BLANK,DOT,XXX,VERT
      DIMENSION XXXX(119)
      DIMENSION F(3)
      DIMENSION L(4)
      DIMENSION IIMAX(2)
      DIMENSION XYZ(3,26,50),A(2,20,90,3)
      DIMENSION PCODE(26,2),D(2),NCH05(5,3)
      DIMENSION XK(3),X1(3),X2(3)
      DIMENSION XXX(3)
C
```

```
      COMMON/BLOCK2/EF,EL,ER,MF,ML,MR
C
C PREPARING HEADER FOR LINE PRINTER PLOT
C
      DO 5100 KP=1,119
 5100 XXXX(KP)=ECT
      WRITE(5,5011)
      WRITE(5,5000)XXXX,XXXX
 5000 FORMAT(1H ,119A1/
     112X,54HJ   MA  IFR   IL  IL1   IR  IR1   IS  ND  NDT  ADDRESS  ,
     221X,57H   X1(1)     X1(2)     X1(3)     X2(1)   X2(2)   X2(3) N1,
     351X,2HN2/
     461X,119A1/)
C
      DO 505 J=1,JMAX
      WRITE(5,5010)
 5010 FORMAT(1X,/)
C
C INITIALISATION OF IDENTIFIERS FOR THE OPERATION OF PARALLAX CORRECTION
C
      ND=0
      ND1=0
      NDLT=0
      NDRT=0
      II =0
      IFR=0
      IL =0
      IL1=0
      IR =0
      IR1=0
      IS=0
C
C STARTING TO PERFORM CORRECTION - WITH ONE MARKER AT A TIME
C
      DO 508 MA=1,MAMAX
C
C ESCAPING USUAL ROUTINE WHEN MCODE(MA,1)=6
C
      IF(MCODE(MA,1).EQ.6)GOTO 525
C
C ***************
C ROUTINE SOLUTION
C ***************
C
      MMM=MCODE(MA,1)
      GOTO(507,514,513),MMM
C
C 'FRONTSIDE' CASE
C ================
C
  507 II=II+1
      IFR=IFR+1
      IF(II.GT.IIMAX(2))GOTO 511
      N=2
      IL=IL+1
      IS=IL
      GOTO 512
  511 N=3
      IR=IR+1
      IS=IR
  512 CALL FSCN(N,A(1,IFR,J,1),A(2,IFR,J,1),A(1,IS,J,N),A(2,IS,J,N),Y1)
      MAA=MA
      GOTO 501
C END OF 'FRONTSIDE'
C ==================
C
C
C 'FRONTONLY' CASE
C ----------------
C
  514 N=1
      II=II+1
      IFR=IFR+1
      ND=ND+1
      ND1=ND
      AA=A(1,IFR,J,N)
      BB=A(2,IFR,J,N)
      DO 527 III=1,3
      XX(III)=XYZ(III,MCODE(MA,2),J)
  527 CONTINUE
      CALL FF(N,AA,BB,D(ND),XX,X1,X2)
      MAA=MA
C END OF 'FRONTONLY'
C ------------------
C
      GOTO 509
C
```

```
C 'SIDEONLY' CASE
C **********
C
  512 II=II+1
      IF(II.GT.II*AX(2))GOTO 515
      N=2
      IL=IL+1
      IS=IL
      GOTO 528
  515 N=3
      IR=IR+1
      IS=IR
  528 ND=ND+1
      ND1=ND
      AA=A(1,IS,J,N)
      BB=A(2,IS,J,N)
      DO 529 III=1,3
      XK(III)=XYZ(III,MA(IFR,J)
  529 CONTINUE
      CALL SS(N,AA,BB,D(ND),XK,X1,X2)
      MAA=MA
C
C END OF 'SIDEONLY'
C **********
C
C SOLUTION CHOICE-CASES 'FRONTONLY' AND 'SIDEONLY'
C ** **********
C
      N1=NCHOS(ND1,1)
      N2=NCHOS(ND1,2)
  509 IF(X1(N1).EQ.X2(N1))GOTO 501
      IF(N2.EQ.1)GOTO 518
      IF(X1(N1).LT.X2(N1))GOTO 502
      GOTO 501
  518 IF(X1(N1).LT.X2(N1))GOTO 501
  502 DO 530 III=1,3
      XYZ(III,MA,J)=X2(III)
  530 CONTINUE
      IF(NMM.EQ.3)GOTO 550
      GOTO 506
  501 DO 531 III=1,3
      XYZ(III,MA,J)=X1(III)
  531 CONTINUE
      IF(NMM.NE.2)GOTO 506
  550 ADRES=509
      WRITE(5,5(4)J,MA,IFR,IL,IL1,IR,IR1,IS,NC,ND1,
     1ADRES,X1,X2,N1,N2
      GOTO 506
C END OF ROUTINE SOLUTION
C
C
C ** **********
C 'ESCAPE' SOLUTION
C ** **********
C ESCAPE FROM ROUTINE SOLUTION
C
  523 IF(MA.NE.LTAIL)GO TO 630
   31 II=II+1
      IL=IL+1
      ND=ND+1
      IL1=IL
      NDLT=ND
      GOTO 506
C
  630 IF(MA.NE.LBASIS)GO TO 507
   32 IFR=IFR+1
      IF(NCASE.EQ.1.AND.II.GT.II*AX(2))GOTO 40
      IF(NCASE.EQ.2)GOTO 40
      II=II+1
   40 IL=IL+1
      IS=IL
      N=2
      CALL FS(N,A(1,IFR,J,1),A(2,IFR,J,1),A(1,IS,J,N),A(2,IS,J,N),X1)
      ADRES=32
      WRITE(5,5(1)J,MA,IFR,IL,IL1,IR,IR1,IS,NC,ND1,
     1ADRES,X1
 5001 FORMAT(1H ,I2,9I5,I9,3X,3F9.1)
      DO 632 K=1,3
  632 XYZ(K,MA,J)=X1(K)
      ND1=NDLT
C
  605 DO 634 K=1,3
  634 XK(K)=X1(K)
      AA=A(1,IL1,J,N)
      BB=A(2,IL1,J,N)
      CALL SS(N,MA,BB,D(ND1),XK,X1,X2)
      MAA=LTAIL
      ADRES=605
      N1=NCHOS(ND1,1)
      N2=NCHOS(ND1,2)
      WRITE(5,5(4)J,MA,IFR,IL,IL1,IR,IR1,IS,NC,ND1,
     1ADRES,X1,X2,N1,N2
 5004 FORMAT(1H ,I2,9I5,I9,3X,3F9.1,1X,3F9.1,2I3)
      GOTO 509
C
C
```

```
  607 IF(MA.NE.MTAIL)GOTO 641
   33 II=II+1
      IR=IR+1
      ND=ND+1
      IR1=IR
      NDRT=ND
      GOTO 506
C
  641 IF(MA.NE.MASIS)GOTO 506
   34 N=3
      IFR=IFR+1
      IF(NCASE.EQ.1.AND.II.LT.IIMAX(2))GOTO 41
      IF(NCASE.EQ.3)GOTO 41
      II =II+1
   41 IR=IR+1
      IS =IR
      CALL FS(N,A(1,IFR,J,1),A(2,IFR,J,1),A(1,IS,J,N),A(2,IS,J,N),X1)
      ADRSS=34
      WRITE(6,F(3))J,MA,IFR,IL,IL1,IR,IR1,IS,ND,ND1,
     1ADRES,X1
      DO 642 K=1,3
  642 XY2(K,MA,J)=X1(K)
      ND1=NDRT
      DO 643 K=1,3
  643 XK(K)=X1(K)
      AA=A(1,IR1,J,N)
      BB=A(2,IR1,J,N)
      CALL SS(N,AA,BB,D(ND1),XK,Y1,X2)
      MAA=MTAIL
      ADRES=643
      N1=NCHOS(IE1,1)
      N2=NCHOS(IE1,2)
      WRITE(6,F(4))J,MA,IFR,IL,IL1,IR,IR1,IS,ND,ND1,
     1ADRES,Y1,X2,N1,N2
      GOTO 509
C KLUM - SEQUENCE TERMINATION POINT
  506 KLUM=506
C
C END OF ESCAPE SECTION
C
  508 CONTINUE
  509 CONTINUE
      RETURN
      END
C
C
C
C **********************************************
      SUBROUTINE FS(N,ZZ,YF,XX,YS,X)
C **********************************************
C
C THIS SUBROUTINE PERFORMS PARALLAX CORRECTION OF
C THOSE MARKERS THAT CAN BE VIEWED
C    FROM BOTH THE FRONT AND EITHER OF THE SIDE CAMERA
C N  - CAMERA NO
C ZZ - 'Z' COORDINATE FROM FRONT CAMERA
C YF - 'Y' COORDINATE FROM FRONT CAMERA
C XX - 'X' COORDINATE FROM SIDE CAMERA
C YS - 'Y' COORDINATE FROM SIDE CAMERA
C X  - SOLUTION ARRAY
C
      DIMENSION X(3)
      COMMON/BLOCK2/DF,DL,DR,HF,HL,HR
      IF(N.EQ.2)GOTO 152
      ZB=-ZZ
      DS=DR
      HS=HR
      GOTO 153
  152 DS=DL
      ZB=ZZ
      HS=HL
  153 X(1)=XX*DF*(DS+ZB)/(DF*DS+XX*ZB)
      X(2)=YF-X(1)*(YF-HF)/DF
      X(3)=ZB*(DF-X(1))/DF
      IF(N.EQ.2)GOTO 154
      X(3)=-X(3)
  154 RETURN
      END
C
C
C
```

```
C ****************************************************
      SUBROUTINE FF(N,ZZ,YF,D,XK,X1,X2)
C ****************************************************
C
C THIS SUBROUTINE PERFORMS PARALLAX CORRECTION ON
C THOSE MARKERS THAT CAN ONLY BE VIEWED
C     FROM THE FRONT CAMERA
C N,ZZ,YF - ARE DEFINED IN SUBROUTINE FS
C D  - DISTANCE OF AN ADJACENT MARKER
C XK - REAL COORDINATES OF ADJACENT MARKER
C X1,X2 - TWO SOLUTIONS DERIVED
C
      DIMENSION XK(3),X1(3),X2(3)
      COMMON/BLOCK2/DF,DL,DR,HF,HL,HR
      A=1.0+((YF-HF)/DF)**2+(ZZ/DF)**2
      B=XK(1)+(YF-HF)*(YF-XK(2))/DF+ZZ*(ZZ-XK(3))/DF
      C=(XK(1))**2+(YF-XK(2))**2+(ZZ-XK(3))**2-D**2
      DELTA=B**2-A*C
      IF(DELTA.GT.0.0)GOTO 157
      X1(1)=B/A
      X2(1)=B/A
      GOTO 158
  157 X1(1)=(B+SQRT(DELTA))/A
      X2(1)=(B-SQRT(DELTA))/A
  158 X1(2)=-(YF-HF)*X1(1)/DF+YF
      X2(2)=-(YF-HF)*X2(1)/DF+YF
      X1(3)=-ZZ*X1(1)/DF+ZZ
      X2(3)=-ZZ*X2(1)/DF+ZZ
      RETURN
      END
C
C
C
C ****************************************************
      SUBROUTINE SS(N,XX,YS,D,XK,X1,X2)
C ****************************************************
C
C THIS SUBROUTINE PERFORMS PARALLAX CORRECTION ON
C THOSE MARKERS THAT CAN BE VIEWED
C     FROM EITHER OF THE SIDE CAMERA
C N,XX,YS - ARE DEFINED IN SUBROUTINE FS
C D,XK,X1,X2 - ARE DEFINED IN SUBROUTINE FF
C
      DIMENSION XK(3),X1(3),X2(3)
      COMMON/BLOCK2/DF,DL,DR,HF,HL,HR
      IF(N.EQ.2)GOTO 160
      DS=DR
      HS=HR
      GOTO 161
  160 DS=DL
      HS=HL
  161 A=1.0+((YS-HS)/DS)**2+(XX/DS)**2
      IF(N.EQ.2)GOTO 2
      B=XK(3)+(YS-HS)*(YS-XK(2))/DS+XX*(XX-XK(1))/DS
      E=-1.0
      GOTO 3
    2 KLUM=2
      B=XK(3)-(YS-HS)*(YS-XK(2))/DS-XX*(XX-XK(1))/DS
      E=1.0
    3 KLUM=3
      C=(XK(3))**2+(YS-XK(2))**2+(XX-XK(1))**2-D**2
      DELTA=B**2-A*C
      IF(DELTA)[illegible],162
      X1(3)=B/A
      X2(3)=B/A
      GOTO 163
  162 X1(3)=(B+SQRT(DELTA))/A
      X2(3)=(B-SQRT(DELTA))/A
  163 X1(1)=E*XX*X1(3)/DS+XX
      X2(1)=E*XX*X2(3)/DS+XX
      X1(2)=E*(YS-HS)*X1(3)/DS+YS
      X2(2)=E*(YS-HS)*X2(3)/DS+YS
  164 RETURN
      END
      FINISH
```

Listings of job control macro "RUNFITR"

and program "FILTER"

DOCUMENT RUNFITR

```
C SP N,(%A)(1,8)
1 SP V,(%A)(11,12)
2 SP M,(%A)(1,2)
3 SP I,(%A)(5)
4 LO BINFITR
5 TIME 4MINS
6 AS *TRG,%A
7 AS *LPC,%NLF%V(LIMIT5000)
8 AS *TPG,%NER%V(LIMIT5000)
9 RUN
10 LF %NLF%V,*LP,NL
11 ER %NLF%V
12 IF HALTED (AH) OR DELETED (DC),GO TO 3.OKAY
13 GO TO 3.NOTOKAY
14 3.OKAY
15 RJ TELEJIT%M%I%V,RUNJNTS,PARAM(%NER%V),HLS(JT 3*MINS)
16 DP U,STAGE(3) EXECUTED SUCCESSFULLY,
17 EJ
18 3.NOTOKAY
19 DP D,ERROR IN STAGE(3) - PLEASE CHECK,
20 EJ NONE,RT(CHECKFITR)
21 ****
22 DG
```

```
      PROGRAM (FILTER)
      INPUT 6=TAPE)
      OUTPUT 5=TAPE
      OUTPUT 7=TAPE
      TRACE 2
      END
C C
C INPUT AND OUTPUT CHANNELS FOR PROG. FILTER
C I/P 6 - CORRECTED PARKER COORDINATES(FROM PROG. PARALLAX)
C O/P 7 - FILTERED MARKER COORDINATES
C O/P 5 - DATA CHECK FILE
C
C
C STAGE(3) ..... ADOPTED BY JAMES (OH,AIDENG, UNI
C
C THIS PROGRAM PERFORMS THE FOLLOWING FUNCTIONS:-
C    1) SMOOTHING MARKER COORDINATES
C ...2) CALCULATES AMOUNT OF NOISE REMOVED
C
C ***************
      PASTER FILTER
C ***************
C
C
C FOR NOMENCLATURE SEE STAGE(1),PROGRAM 'COORDINATES'
C **********************************************
C
      DIMENSION XYZ(3,24,50),FF1(3,90),FR(3,90)
      DIMENSION FF(90),FFD(90),FC(3),FS(3)
C
C READING IN INSTRUCTIVE DATA FROM INPUT FILE
C ***************************************
C
      READ(6,200)NGROUP,NAMP,NPOINT,NRUN
      READ(6,524)NCASE,PARAM,JMAX
      READ(6,15)FCUT
      WRITE(7,201)NGROUP,NAMP,NPOINT,NRUN
      WRITE(7,202)NCASE,PARAM,JMAX
  200 FORMAT(4I0)
  201 FORMAT(1X,4I5)
  202 FORMAT(1X,2I5)
  524 FORMAT(3I0)
C
C READING IN COORDINATES INTO ARRAY(FR)
C
      DO 61 PARAM=1,PARAM
      DO 62 J=1,JMAX
   62 READ(6,15)(FR(IX,J),IX=1,3)
   15 FORMAT(3F(.0)
C
C PERFORM FILTERING PROCESS,WITH ONE PARKER AT A TIME
C ***************************************************
C
      DO 51 IX=1,3
      FS(IX)=0.0
      FD(IX)=0.0
      DO 52 J=1,JMAX
   52 FF(J)=FR(IX,J)
      CALL BUTAWF(FF,JMAX,FCUT,0.02)
      DO 53 J=1,JMAX
      FFD(J)=FR(IX,J)-FF(J)
      FD(IX)=FD(IX)+FFD(J)
      XYZ(IX,PARAM,J)=FF(J)
   53 CONTINUE
      FD(IX)=FD(IX)/JMAX
      DO 54 J=1,JMAX
      FS(IX)=FS(IX)+(FFD(J)-FD(IX))**2
      FF1(IX,J)=FFD(J)
   54 CONTINUE
      FS(IX)=SQRT(FS(IX)/JMAX)
   51 CONTINUE
      WRITE(5,2)P1
      WRITE(5,6)((FF1(IX,J),IX=1,3),J=1,JMAX)
      WRITE(5,4)(FD(IX),IX=1,3)
      WRITE(5,4)(FS(IX),IX=1,3)
   60 CONTINUE
    2 FORMAT(1H1,'SM  MARKER NO  ',I3)
    4 FORMAT(1P,3E12.3)
      WRITE(7,3)(((XYZ(IX,PARAM,J),IX=1,3),PARAM=1,PARAM),J=1,JMAX)
    3 FORMAT(3F(.1)
      STOP
      END
C
C
```

```
      C ** ********************************
            SUBROUTINE BUT4(Q,N,FCUT,T)
      C ** ********************************
      C
      C THIS SUBROUTINE PERFORMS THE FILTERING PROCESS
      C
      C Q IS THE FILE; N IS NO. OF POINTS
      C FCUT IS CUTOFF FREQ.; T IS TIME INTERVAL
      C W1 IS THE RESULT FILE
      C TR IS THE TREND OF DATA
      C NOTE: TREND AND PEDESTAL REMOVED BEFORE FILTER,
      C       ADDED IN AFTER FILTERING PROCESS
      C
            DIMENSION C(13),Q(N),AD(130),W1(130),W(130)
            NR=N+20.0
            TR=Q(N)-Q(1)
            IF(FCUT.GE.1.0/(2.0*T))GOTO 17
            XPI=3.14159265
            T1=SIN(XPI*FCUT*T)
            T2=COS(XPI*FCUT*T)
            TT=T1/T2
            A=COS(XPI/2.0)*TT
            B=SIN(XPI/2.0)*TT
            C(1)=2*(A+B)
            C(2)=2*(A+B)**2
            C(3)=2*((A**2+B**2)*(A+B))
            C(4)=(A**2+B**2)**2
            C(5)=1+C(1)+C(2)+C(3)+C(4)
            C(6)=-4+4*C(4)-2*C(1)+2*C(3)
            C(7)=6+C*C(4)-2*C(2)
            C(8)=-4+2*C(1)-2*C(3)+4*C(4)
            C(9)=1-C(1)+C(2)*C(4)-C(3)
            DO 30 K44=N,130
         30 AD(K44)=0.0
            DO 2 L=1,N
            AD(L+4)=Q(L)-(L-1)*TR/(N-1)-Q(1)
          2 CONTINUE
            DO 9 L=1,4
            AD(L)=0.0
            W(L)=0.0
          9 CONTINUE
            N1=N+24
            DO 18 K=1,NR
            W(K+4)=(C(4)*(AD(K+4)+4*AD(K+3)+6*AD(K+2)+4*AD(K+1)
           *+AD(K))-(W(K+3)*C(6)+W(K+2)*C(7)+W(K+1)*C(8)+W(K)*
           *C(9)))/C(5)
         18 CONTINUE
            DO 37 JKJ=1,NR
         37 W(JKJ)=W(JKJ+4)
            DO 15 K=1,4
            K4=N1-K
            W1(K4+1)=0.0
            W(K4+1)=0.0
         15 CONTINUE
            DO 16 K=1,NR
            K5=N1-K
            W1(K5-3)=((C(4)*(W(K5-3)+4*W(K5-2)+6*W(K5-1)+
           *4*W(K5)+W(K5+1))-(W1(K5-2)*C(6)+W1(K5-1)*C(7)
           *+W1(K5)*C(8)+W1(K5+1)*C(9)))/C(5)
         16 CONTINUE
            DO 21 K=1,N
         21 W1(K)=W1(1)+(K-1)*TR/(N-1)+Q(1)
            DO 17 K=1,N
            Q(K)=W1(K)
         17 CONTINUE
            RETURN
            END
            FINISH
```

Listings of job control macro "RUNJNTS" and program "JOINTS"

```
DOCUMENT  RUNJNTS

C SP N,(%A)(1,8)
1 SP V,(%A)(11,12)
2 SP M,(%A)(1,2)
3 SP T,(%A)(5)
4 LO BINJNTS
5 TIME 3MINS
6 AS *CRO,%NBM%V
7 AS *TRO,%A
8 AS *LPO,%NLJ%V(LIMIT4000)
9 AS *TPO,%NEJ%V(LIMIT4000)
10 AS *TP1,%NES%V(LIMIT5000)
11 RUN
12 ER %NLJ%V
13 IF HALTED (AH) OR DELETED (CD),GO TO 4.OKAY
14 GO TO 4.NOTOKAY
15 4.OKAY
16 EDIT %NEJ%V,%NJT2V(LIMIT4000),EDITTPX
17 EDIT %NES%V,%NST2V(LIMIT5000),EDITTPB
18 ER %NEJ%V
19 ER %NES%V
20 RJT ELEW2M%T2V,SLNWALK2D,PARAM(%NJT2V)
21 DP D,STAGE(4) EXECUTED SUCCESSFULLY,
22 EJ
23 4.NOTOKAY
24 DP D,ERROR IN STAGE(4) - PLEASE CHECK,
25 EJ NONE,RT(CHECKJNTS)
26 ****
27 DS
```

```
      C       LIBRARY(EE,SUBROUPNAGE)
      1       PROGRAM EJOINTS)
      2       INPUT 4=CSE(
      3       INPUT 6=TSE(
      4       OUTPUT 5=LP(
      5       OUTPUT 7=IP(
      6       OUTPUT 8=TP(
      7       COPPICT
      8       TRACE 2
      9       END
     10 C
     11 C  INPUT AND OUTPUT CHANNELS FOR PROG. JOINTS
     12 C  I/P 4 - BODY MEASUREMENTS
     13 C  I/P 6 - FILTERED MARKER COORDINATES(FROM PROG. FILTER)
     14 C  O/P 7 - JOINT COORDINATES
     15 C  O/P 8 - SEGMENT D.C. MATRICES
     16 C  O/P 5 - DATA CHECK FILE
     17 C
     18 C
     19 C  STAGE (4) ..... ADOPTED AT JAMES COMPUTING UNIT .....
     20 C
     21 C  THIS PROGRAM PERFORMS THE CALCULATION OF :-
     22 C     1.) THE COORDINATES OF THE JOINT CENTRES
     23 C     2.) THE DIRECTION COSINE MATRIX OF THE SEGMENTS
     24 C
     25 C  ***********************
     26       MASTER JOINTS
     27 C  ***********************
     28 C
     29 C  FOR NOMENCLATURE SEE STAGE(1),PROGRAM 'COORDINATES'
     30 C  ***************************************************
     31 C  (OR ELSE THEY WILL BE DEFINED ALONG IN THE PROGRAM)
     32 C
     33       DIMENSION XJ(3,26),MJL(3),MJR(3),
     34      1  X1(3),X2(3),X3(3),X4(3),X5(3),X6(3),X7(3),X8(3),
     35      1X9(3),X10(3),X11(3),X12(3),X13(3),X14(3),R1(3,3),R2(3,3),
     36      2R3(3,3),R4(3,3),R5(3,3),R6(3,3),R7(3,3),R8(3,3)
     37       COMMON/JOINTS/XJ
     38 C  ---------------------------------------------------
     39 C
     40 C  READING IN HEADER INFO. FROM INPUT FILE MARKERS' COORDINATES
     41 C  ------------------------------------------------------------
     42 C
     43       READ(6,1)NGROUP,NAPP,NPTNT,NRUN
     44       WRITE(5,2)NGROUP,NAPP,NPTNT,NRUN
     45       WRITE(5,11)
     46       READ(6,3)NCASE,NMAX,JMAX
     47 C
     48 C  READING IN BODY MEASUREMENT FILE
     49 C  ****************************
     50       PI=3.14
     51 C  LEFT'S DATA - MARKER LENGTH(M) AND SOCKET THICKNESS(ST)
     52       READ(4,5)ELF,DRF,ST
     53       DFL=(DLF/2)*M
     54       DFR=(DRF/2)*M
     55 C  LEFT SHANK'S DATA
     56       READ(4,4)SL1,SL2,SL3,SL4,DLS
     57       IF(NGROUP.NE.2)GO TO 61
     58       IF(NGROUP.EQ.2.AND.NAPP.EQ.2)GOTO 61
     59       DL1=(SL1/2)*M
     60       DL2=(SL3/2)*M
     61       DL3=(SL2*2)
     62       DL4=SL4
     63       GOTO 70
     64    61 CL1=0.37*SL1*14.0
     65       CL2=0.75*SL1-21.0
     66       CL3=0.32*SL1*4.4
     67       DL4=SL4*0.0
     68       IF(NGROUP.EQ.1.AND.NAPP.EQ.1)GOTO 62
     69       DL1=SL2-CL1*M
     70       DL2=SL3-CL2*M
     71       DL3=    CL3*M
     72       GOTO 70
     73    62 DL1=SL2-ST-CL1*M
     74       DL2=(SL3/2)*M
     75       DL3=ST+CL2*M
     76 C  RIGHT SHANK'S DATA
     77    70 READ(4,4)SR1,SR2,SR3,SR4,DRS
     78       IF(NGROUP.NE.2)GOTO 63
     79       IF(NGROUP.EQ.2.AND.NAPP.EQ.2)GOTO 5
     80       DR1=(SR1/2)*M
     81       DR2=(SR2/2)*M
     82       DR3=(SR2*2)
     83       DR4=SR4
     84       GOTO 71
     85    63 CR1=0.37*SR1*14.0
     86       CR2=0.75*SR1-21.0
     87       CR3=0.32*SR1*4.4
     88       DR4=SR4*0.0
     89       IF(NGROUP.EQ.1.AND.NAPP.EQ.2)GOTO 64
     90       DR1=SR2-CR1*M
     91       DR2=SR3-CR2*M
     92       DR3=    CR3*M
```

```
      GOTO 71
   64 DR1=SR2-ST*CR1*H
      DR2=(SR3/2)*H
      DR3=ST*CR2*H
C LOCATION OF HIP RELATIVE TO PELVIC SPINE
   71 READ(4,4)HJL(1),HJL(2),HJL(3),HJR(1),HJR(2),HJR(3)
C WRITING IT IN VECTOR FORM
      DO 8 I=1,2
      HJL(I)=-HJL(I)
      HJR(I)=-HJR(I)
    8 CONTINUE
      HJR(3)=-HJR(3)
C SHOULDER'S DATA
      READ(4,5)DSL,DSR
C RATIOS TAIL(RF) AND SHOULDER(RS) MARKERS
      READ(4,5)RF,RS
C MAX. NO. OF FRAME OF LEFT(JLMAX) AND RIGHT(JRMAX) WALKING CYCLE
      READ(4,1)JLMAX,JRMAX
    5 FORMAT(4F10.0)
      WRITE(5,22)
      WRITE(5,30)DL1,DL2,DL3,DL4,DL5
      WRITE(5,30)DR1,DR2,DR3,DR4,DR5
      WRITE(7,7)NGROUP,NAPP,NPTNT,NRUN,NCASE,MAMAX,JMAX,JLMAX,JRMAX
      WRITE(8,7)NGROUP,NAPP,NPTNT,NRUN,NCASE,MAMAX,JMAX,JLMAX,JRMAX
    1 FORMAT(4I5)
    2 FORMAT(1H1,////////////////////5X,16HGROUP NUMBER   =,I4//1X,
     349X,16HAFFLICTED SIDE =,I4//1X,49X,16HPATIENT NUMBER =,I4//1X,
     449X,16HRUN NUMBER     =,I4)
   17 FORMAT(1H1,1X)
    3 FORMAT(3F10.0)
    4 FORMAT(6F10.0)
   31 FORMAT(1H ,5F10.1)
   32 FORMAT(19H   BODY MEASUREMENT)
    7 FORMAT(9I4)
C
C CALCULATION OF JOINTS COORDINATES AND SEGMENT DC MATRICES
C
C READING A SINGLE FRAME'S DATA FROM "MARKERS' COORDINATES" FILE
      DO 10 J=1,JMAX
      READ(6,11)((XJ(I,MA),I=1,3),MA=1,MAMAX)
   11 FORMAT(3F10.0)
C
C CALLING FOR APPROPRIATE SUBROUTINES.
C
      CALL SHANK(J,6,1,5,DL1,DL2,DL3,DL4,DL5,Z,B2,X3,X4,T2)
      CALL FOOT(J,2,3,4,X2,DFL,H,2,B1,X1,Y2,T1)
      CALL SHANK(J,21,26,22,DR1,DR2,DR3,DR4,DR5,3,B5,X8,X9,T5)
      CALL FOOT(J,23,24,25,X3,DFR,H,5,B4,X6,X7,T4)
      DO 18 I=1,2
      XJ(I,7)=(XJ(I,7)+XJ(I,13))/2.0
      XJ(I,9)=(XJ(I,9)+XJ(I,20))/2.0
      XJ(I,10)=(XJ(I,10)+XJ(I,16))/2.0
      XJ(I,11)=(XJ(I,11)+XJ(I,17))/2.0
   18 CONTINUE
      CALL PELVIS(J,8,19,9,7,B7,RP,HJL,HJR,X11,X5,X10,T7)
      CALL THIGH(J,X4,X5,B3,B2,T3)
      CALL THIGH(J,X9,X10,B6,B5,T6)
      DO 19 I=1,2
      XJ(I,10)=(XJ(I,10)-(XJ(I,10)-XJ(I,11))*RS)
      XJ(I,12)=(XJ(I,12)-(XJ(I,12)-XJ(I,10))*RS)
      XJ(I,14)=(XJ(I,14)-(XJ(I,14)-XJ(I,15))*RS)
   19 CONTINUE
      CALL SHOULDER(J,T6,12,14,B2,X14,X12,X13,DSL,DSR,T2)
      WRITE(7,12)X1,X2,X3,X4,X5,X6,X7,X8,X9,X10,X11,X12,X13,X14
      WRITE(8,12)((A1(L,K),L=1,3),K=1,3)
      WRITE(8,12)((B2(L,K),L=1,3),K=1,3)
      WRITE(8,12)((B3(L,K),L=1,3),K=1,3)
      WRITE(8,12)((B4(L,K),L=1,3),K=1,3)
      WRITE(8,12)((B5(L,K),L=1,3),K=1,3)
      WRITE(8,12)((B6(L,K),L=1,3),K=1,3)
      WRITE(8,12)((B7(L,K),L=1,3),K=1,3)
      WRITE(8,12)((B8(L,K),L=1,3),K=1,3)
      WRITE(5,30)
      WRITE(5,10)J
      WRITE(5,10)X1,X2,X3,X4,X5,X6,X7,X8,X9,X10,X11,X12,X13,X14
      WRITE(5,12)((A1(K,L),L=1,3),K=1,3)
      WRITE(5,30)T1
      WRITE(5,12)((B2(K,L),L=1,3),K=1,3)
      WRITE(5,30)T2
      WRITE(5,12)((B3(K,L),L=1,3),K=1,3)
      WRITE(5,30)T3
      WRITE(5,12)((B4(K,L),L=1,3),K=1,3)
      WRITE(5,30)T4
      WRITE(5,12)((B5(K,L),L=1,3),K=1,3)
      WRITE(5,30)T5
      WRITE(5,12)((B6(K,L),L=1,3),K=1,3)
      WRITE(5,30)T6
      WRITE(5,12)((B7(K,L),L=1,3),K=1,3)
      WRITE(5,30)T7
      WRITE(5,12)((B8(K,L),L=1,3),K=1,3)
      WRITE(5,30)T8
      WRITE(5,21)
   10 CONTINUE
   12 FORMAT(1H ,3F15.9)
```

```
   10 FORMAT(1X,'J4',I )
   18 FORMAT(1H ,F10.4,2X,F10.4,2X,F10.4)
   50 FORMAT(1X,'TF',F7.3)
   14 FORMAT(1H ,'(',I,')',1))
   12 FORMAT(1H ,F12.7)
   20 FORMAT(1H/)
   21 FORMAT(1H ,///)
      STOP
      END
C
C ****************************************************************
      SUBROUTINE FOOT(XJ,MA1,MA2,MA3,XA,DF,H,NSIDE,B,XH,XM,TF)
C ****************************************************************
C
C DETERMINES THE DIRECTION COSINE MATRIX OF FOOT
C MA1(XT) : INDEX OF TIP OF FOOT
C MA2(XM) : INDEX OF 5TH METATARSAR JOINT
C MA3(XH) : INDEX OF HEEL
C XA : ANKLE JOINT COORDINATES
C NSIDE  : 2 - LEFT FOOT BEING ANALYSE
C          3 - RIGHT FOOT BEING ANALYSE
C DF  : DISTANCE BETWEEN MA2 TO MID-LINE OF FOOT
C H   : LENGTH OF MARKERS
C B   : ARRAY CONTAINING THE D.C. MATRIX
C TF  : TEST FOR ORTHOGONALITY
C
      REAL L1,L2,L3,M1,M2,M3,N1,N2,N3
      DIMENSION XJ(3,20),XA(3),XT(3),XM(3),XH(3),B(3,3)
      COMMON/JNTS1/XJ
C
      DO 1 I=1,3
      XT(I)=XJ(I,MA1)
      XM(I)=XJ(I,MA2)
      XH(I)=XJ(I,MA3)
    1 CONTINUE
C
      DTH=DIST(XT,XH)
      L1=(XT(1)-XH(1))/DTH
      L2=(XT(2)-XH(2))/DTH
      L3=(XT(3)-XH(3))/DTH
      DAH=DIST(XA,XH)
      M1=(XA(1)-XH(1))/DAH
      M2=(XA(2)-XH(2))/DAH
      M3=(XA(3)-XH(3))/DAH
      DN=L1*M2-M1*L2
      GX=(L2*M3-M2*L3)
      GY=(L3*M1-M3*L1)
      DQ=SQRT(GX**2+GY**2+DN**2)
      B(3,3)=DN/DQ
      B(3,1)=GX/DQ
      B(3,2)=GY/DQ
C
C IF LEFT FOOT :- ADD DF
C IF RIGHT FOOT :- MINUS DF
C
      IF(NSIDE.EQ.2)GOTO 2
      DO 3 I=1,3
    3 XM(I)=XM(I)-DF*B(3,I)
      GOTO 4
    2 DO 5 I=1,3
    5 XM(I)=XM(I)+DF*B(3,I)
    4 DMH=DIST(XM,XH)
      DO 6 I=1,3
    6 B(1,I)=(XM(I)-XH(I))/DMH
      DM=B(3,3)*B(1,1)-B(3,1)*B(1,3)
      PX=(B(3,2)*B(1,3)-B(3,3)*B(1,2))
      PZ=(B(3,1)*B(1,2)-B(3,2)*B(1,1))
      DP=SQRT(PX**2+DM**2+PZ**2)
      B(2,2)=DM/DP
      B(2,1)=PX/DP
      B(2,3)=PZ/DP
C
C CHECK FOR ORTHOGONALITY
C
      CALL CHECK(B,TF)
C
C CALCULATE ACTUAL POSITION ON FOOT
C
      DO 7 I=1,3
      XH(I)=(XH(I)+H*B(1,I))
    7 CONTINUE
      RETURN
      END
C
C ****************************************************
      SUBROUTINE SHANK(J,MA1,MA2,MA3,D1,D2,D3,D4,D5,
     *NSIDE,R,XA,XK,TS)
C ****************************************************
C
C MA1:INDEX OF MARKER PLACED ON THE HEAD OF THE FIBULA.
C MA2:INDEX OF MARKER PLACED ON THE LATERAL MALLEOLUS.
C MA3:INDEX OF MARKER PLACED ON THE TIBIAL TUBERCSITY.
C NSIDE=2: THE LEFT SHANK IS BEING ANALYZED
C NSIDE=3: THE RIGHT SHANK IS BEING ANALYZED
C D1,D2,D3,D4,D5 - RELATED DIMENSIONS OF KNEE,SHANK AND ANKLE
C (FOR DETAIL SEE THESIS IN ANALYSIS OF SHANK)
C R - DIRECTION COSINE MATRIX OF SHANK
C XA - ANKLE COORDINATES
C XK - KNEE COORDINATES
C TS - TEST FOR ORTHOGONALITY OF MATRIX
```

```
      C
            REAL LX,L1,L2,PX,PY,PZ,NX,NY,NZ
            DIMENSION CO(3,1),XO(3,1)
            DIMENSION WKSP(3),AA(3,3),BB(3,1)
            DIMENSION XJ(3,20)
            DIMENSION XA(3),XK(3)
            DIMENSION B(3,3),BT(3,3),Q(3)
            DIMENSION V(3,3),W(3,3),C(3,3)
            COMMON/JNTSI/XJ
            AFA=1.0
            X1=XJ(1,M/1)
            Y1=XJ(2,M/1)
            Z1=XJ(3,M/1)
            X2=XJ(1,M/2)
            Y2=XJ(2,M/2)
            Z2=XJ(3,M/2)
            X3=XJ(1,M/3)
            Y3=XJ(2,M/3)
            Z3=XJ(3,M/3)
      C
      C FOR SOLVING RIGHT SHANK , CHANGE SIGNS OF DIMENSION.D1 AND.D2
      C
            IF(NSIDE.EQ.2)AFA=-1.0
      C
      C
      C SOLUTION FOR N
            DN= (X3-X1)*(Y3-Y2)-(Y3-Y1)*(X3-X2)
            AX=((Y3-Y2)*D1*AFA-(Y3-Y1)*D2*AFA)/DN
            BX=((Y3-Y2)*(Z1-Z3)+(Y3-Y1)*(Z3-Z2))/DN
            AY=(-(X3-X2)*D1*AFA+(X3-X1)*D2*AFA)/DN
            BY=((X3-X2)*(Z3-Z1)-(X3-X1)*(Z3-Z2))/DN
      C
            E= 1.0+AX**2+BY**2
            F=2.0*(AX*BX+AY*BY)
            G=-1.0+AX**2+AY**2
      C
            DIS=F**2-4.0*E*G
            IF(DIS.GE.0.0)GOTO 25
            DIS=0.0
         25 ANZ1=(-F+SQRT(DIS))/(2.0*E)
            ANZ2=(-F-SQRT(DIS))/(2.0*E)
            WRITE(5,90)ANZ1,ANZ2
         90 FORMAT(1H ,1X,5HANZ1=,F7.4,9X,5HANZ2=,F7.4)
            M1=1
            IF(ANZ1.LT.0.0)GOTO 28
            IF(ANZ1.GT.1.0)GOTO 28
            IF(ANZ1.EQ.ANZ2)GOTO 29
            GOTO 35
         28 M1=1
         35 IF(ANZ2.LT.0.0)GOTO 34
            IF(ANZ2.GT.1.0)GOTO 34
            IF(M1.NE.0)GOTO 36
      C
            WRITE(5,9)J,NSIDE
          9 FORMAT(1H ,25HMESSAGE FROM SHANK: AT J=,I3,
           1 18H, NSIDE=,I1,23H, TWO SOLUTIONS FOR NZ:,
           2 23OH THE CLOSEST TO 1.0 WAS CHOSEN)
            NZ=ANZ1
            IF(ANZ2.GT.ANZ1)NZ=ANZ2
            GOTO 37
         36 NZ=ANZ2
            GOTO 37
         34 IF(M1.EQ.0)GOTO 29
            WRITE(5,10)J,NSIDE
         10 FORMAT(1H ,25HMESSAGE FROM SHANK: AT J=,I3,
           1 13H, NSIDE=,I1,21H, NO SOLUTION FOR NZ:,
           2 23SHALL ELEMENTS OF B WERE SET TO 2.0,
           329H AND THOSE OF XO,XK TO 9999.9)
            DO 1 IX=1,3
            XO(IX)=9999.9
            XK(IX)=9999.9
            DO 1 JX=1,3
          1 B(IX,JX)=2.0
            GOTO 6
         29 NZ=ANZ1
         37 NY=AY*BY*NZ
            NX=AX*BX*NZ
      C
      C SOLUTION FOR L
      C
            DL=NY*(Z3-Z2)-NZ*(Y3-Y2)
            CY= -NZ*((Z3*D6)/DL
            DY=(-NX*(Z3-Z2)+NZ*(X3-X2))/DL
            CZ=  NY*((Z3*D5)/DL
            DZ=(NX*(Y3-Y2)-NY*(X3-X2))/DL
      C
            E= 1.0+DY**2+DZ**2
            F= 2.0*(CY*DY+CZ*DZ)
            G=-1.0+CY**2+CZ**2
      C
            DIS=F**2-4.0*E*G
            IF(DIS.GE.0.0)GOTO 38
            DIS=0.0
         38 ALX1=(-F+SQRT(DIS))/(2.0*E)
            ALX2=(-F-SQRT(DIS))/(2.0*E)
            WRITE(5,91)ALX1,ALX2
         91 FORMAT(1H ,1X,5HALX1=,F7.4,9X,5HALX2=,F7.4)
            M1=0
            IF(ALX1.LT.0.0)GOTO 5
```

```
      IF(ALX1.GT.1.0)GOTO 9
      IF(ALX1.EQ.ALX2)GOTO 16
      GOTO 15
    9 M1=1
   15 IF(ALX2.LT.-1.0)GOTO 11
      IF(ALX2.GT.1.0)GOTO 11
      IF(M1.EQ.0)GOTO 12
      LX=ALX2
      GOTO 42
   14 LX=ALX1
      GOTO 42
   11 IF(M1.NE.0)GOTO 13
      LX=ALX1
      GOTO 42
   13 WRITE(5,10)J,NSIDE
   10 FORMAT(1H ,25HMESSAGE FROM SHANKS AT J=,I3,
     19H, NSIDE=,I1,21H, NO SOLUTION FOR LX;,
     223HALL ELEMENTS OF B WERE SET TO 0.0,
     329H AND THOSE OF XA,XK TO 9999.9)
      GOTO 2
   12 WRITE(5,66)J,NSIDE
   66 FORMAT(1H ,25HMESSAGE FROM SHANKS AT J=,I3,
     19H, NSIDE=,I1,23H, TWO SOLUTIONS FOR LX;,
     222H THE CLOSEST TO 1.0 WAS CHOSEN)
      LX=ALX1
      IF(ALX2.GT.ALX1)LX=ALX2
   42 LY=CY+DY*LX
      LZ=CZ+DZ*LX
C
C SOLUTION FOR M
C
      MX=(LZ*NY-LY*NZ)
      MY=(LX*NZ-LZ*NX)
      MZ=(LY*NX-LX*NY)
C
C
C THE DIRECTION-COSINE MATRIX FOR THE SHANKS MOVING SYSTEM:
      B(1,1)=LX
      B(1,2)=LY
      B(1,3)=LZ
      B(2,1)=MX
      B(2,2)=MY
      B(2,3)=MZ
      B(3,1)=NX
      B(3,2)=NY
      B(3,3)=NZ
      CALL CHECK(B,TS)
C
C SOLVING FOR THE ANKLE RADIUS VECTOR XA.
      Q(1)=-D3+X3*B(1,1)+Y3*B(1,2)+Z3*B(1,3)
      Q(2)=    X2*B(2,1)+Y2*B(2,2)+Z2*B(2,3)
      Q(3)=D1*A1A+X1*B(3,1)+Y1*B(3,2)+Z1*B(3,3)
      DO 45 I=1,3
      QQ(I,1)=Q(I)
   45 CONTINUE
      IFAIL1=0
      CALL F04AEF(B,3,QQ,3,3,1,XX,3,WKSP,AA,3,BB,3,IFAIL1)
      DO 46 I=1,3
      XA(I)=XX(I,1)-D5*B(2,I)
   46 CONTINUE
C
C SOLUTION FOR THE UNKNOWN DISTANCES DK1,DK2,DK3.
      DK1=(X1-XA(1))*B(2,1)+(Y1-XA(2))*B(2,2)+(Z1-XA(3))*B(2,3)
      DK2=(XA(1)-X2)*B(1,1)+(XA(2)-Y2)*B(1,2)+(XA(3)-Z2)*B(1,3)
      DK3=(X3-XA(1))*B(2,1)+(Y3-XA(2))*B(2,2)+(Z3-XA(3))*B(2,3)
      DKK=DK1-DK3
      WRITE(5,65)DK1,DK2,DK3,DKK
   65 FORMAT(1H ,4HDK1=,F7.1,5X,4HDK2=,F7.1,5X,4HDK3=,F7.1,5X,
     110HDK1-DK3=,F7.1)
C
C SOLUTION FOR KNEE-RADIUSVECTOR XK.
      YKNEE=DK3+D6
      DO 47 I=1,3
      XK(I)=XA(I)+YKNEE*B(2,I)
   47 CONTINUE
    2 RETURN
      END
C
C ******************************************************************
      SUBROUTINE PELVIS(J,MA1,MA2,MA3,MA4,B,XP,HJL,HJR,RP,XLH,
     *XRH,TP)
C ******************************************************************
C
C DETERMINES THE DIRECTION COSINE MATRIX OF PELVIS
C AND CALCULATES THE HIP JOINTS COORDINATES
C MA1(X1) : INDEX OF LASIS
C MA2(X2) : INDEX OF RASIS
C MA3(X4) : INDEX OF TAIL(1)
C MA4(X5) : INDEX OF TAIL(2)
C X3  : EXTRAPOLATED POSITION ON THE SACRUM
C XP  : MID-POINT BETWEEN LASIS AND RASIS
C XLH : LEFT HIP JOINT COORDINATES
C XRH : RIGHT HIP JOINT COORDINATES
C RP  : RATIO OF TAIL MARKERS = 0.059
C HJL : LOCATION LEFT HIP REL. TO LASIS
C HJR : LOCATION RIGHT HIP REL. TO RASIS
C B   : ARRAY CONTAINING THE D.C. MATRIX
```

```
C TP   : TEST FOR ORTHOGONALITY OF MATRIX
C
      REAL L
      DIMENSION MJ(3,2*),X1(3),X2(3),X3(3),X4(3),X5(3),
     1X(3),XP(3),XLH(3),XRH(3),R(3,3),RT(3,3),XL(3),X*(3),
     2C(3,3),V(3,3),A(3,3),L(3),MJL(3),MJR(3),D(3)
      COMMON/JNTS*/XJ
C
      DO 1 I=1,3
      X1(I)=XJ(I,MA1)
      X2(I)=XJ(I,MA2)
      X4(I)=XJ(I,MA3)
      X5(I)=XJ(I,MA4)
    1 CONTINUE
      DO 2 I=1,3
      XP(I)=(X1(I)+X2(I))/2
      X3(I)=(X5(I)-(X5(I)-X4(I))*RP)
    2 CONTINUE
      D21=DIST(3,X1)
      D31=DIST(3,X1)
      DO 3 I=1,3
      R(3,I)=(X3(I)-X1(I))/D21
      L(I)=(X3(I)-X1(I))/D31
    3 CONTINUE
C
      DM=-(R(3,3)*L(1)-R(3,1)*L(3))
      PX=-(R(3,3)*L(3)-R(3,3)*L(2))
      PZ=-(R(3,2)*L(2)-R(3,2)*L(1))
      DP=SQRT(P**2+DM**2+PZ**2)
      R(2,2)=DM/DP
      R(2,1)=PX/DP
      R(2,3)=PZ/DP
      DL=R(2,2)*R(3,3)-R(2,3)*R(3,2)
      SY=(R(2,3)*R(3,1)-R(2,1)*R(3,3))
      SZ=(R(2,1)*R(3,2)-R(2,2)*R(3,1))
      DS=SQRT(DL**2+SY**2+SZ**2)
      R(1,1)=DL/DS
      R(1,2)=SY/DS
      R(1,3)=SZ/DS
C
C CHECK FOR ORTHOGONALITY OF MATRIX
C
      CALL CHECK(R,TP)
C
C TRANSPOSING MATRIX R INTO RT
C
      DO 5 I=1,3
      DO 5 IJ=1,3
      RT(I,IJ)=R(IJ,I)
    5 CONTINUE
C
C TRANSFORMING PELVIC MARKERS INTO THE PELVIS FRAME OF
C REFERENCE
C
      DO 4 I=1,3
      X1(I)=X1(I)-XP(I)
      X2(I)=X2(I)-XP(I)
    4 CONTINUE
      CALL MATM(RT,X1,XL,3,1,3)
      CALL MATM(RT,X2,XR,3,1,3)
C
C CALCULATE THE HIP JOINTS IN THE PELVIC SYSTEM
C
      DO 6 K=1,2
      IF(K.EQ.2)GOTO 8
      CALL MATM(RT,MJL,C,3,1,3)
      DO 10 I=1,3
   10 X(I)=XL(I)+C(I)
C
C TRANSFORM COORDINATES BACK TO GROUND REFERENCE
C
      CALL MATM(R,X,XLH,3,1,3)
      DO 7 I=1,3
    7 XLH(I)=XLH(I)+XP(I)
      GOTO 6
    8 CALL MATM(RT,MJR,C,3,1,3)
      DO 11 I=1,3
   11 X(I)=XR(I)+C(I)
C
C TRANSFORM COORDINATES BACK TO GROUND REFERENCE
C
      CALL MATM(R,X,XRH,3,1,3)
      DO 9 I=1,3
    9 XRH(I)=XRH(I)+XP(I)
C
    6 CONTINUE
      RETURN
      END
C
```

```
C ************************************
      SUBROUTINE THIGH(J,XK,XM,P,MS,TT)
C ************************************
C
C DETERMINE DIRECTION COSINE MATRIX OF THIGH
C XK : COORDINATE OF KNEE JOINT CENTRE
C XM : COORDINATE OF HIP JOINT CENTRE
C MS : D.C. MATRIX OF SHANK
C P  : D.C. MATRIX OF THIGH
C TT : TEST FOR ORTHOGONALITY
C
      DIMENSION XK(3),XM(3),A(3,3),BS(3,3)
C
C LENGTH OF THIGH = CHK
C
      CHK=DIST(XM,XK)
      DO 1 I=1,3
    1 A(2,I)=(XM(I)-XK(I))/CHK
      DN=P(2,2)*BS(1,1)-P(2,1)*BS(1,2)
      GX=(P(2,3)*BS(1,2)-P(2,2)*BS(1,3))
      GY=(P(2,1)*BS(1,3)-P(2,3)*BS(1,1))
      DG=SQRT(GX**2+GY**2+DN**2)
      B(3,3)=DN/DG
      B(3,1)=GX/DG
      B(3,2)=GY/DG
      DL=B(2,2)*B(3,3)-B(2,3)*B(3,2)
      SY=(B(2,3)*B(3,1)-B(2,1)*B(3,3))
      SZ=(B(2,1)*B(3,2)-B(2,2)*B(3,1))
      DS=SQRT(DL**2+SY**2+SZ**2)
      A(1,1)=DL/DS
      A(1,2)=SY/DS
      A(1,3)=SZ/DS
C
C CHECK FOR ORTHOGONALITY OF MATRIX
C
      CALL CHECK(P,TT)
      RETURN
      END
C
C ************************************************************
      SUBROUTINE SHOULDER(J,MA1,MA2,MA3,B,X1,X2,X3,DSL,DSR,T)
C ************************************************************
C
C DETERMINES THE DIRECTION COSINE MATRIX OF SHOULDER
C ORIGIN OF SHOULDER SYSTEM IS STERNUM
C MA1(X1) : INDEX OF STERNUM
C MA2(X2) : INDEX OF LEFT SHOULDER
C MA3(X3) : INDEX OF RIGHT SHOULDER
C DSL : WIDTH(A/P) OF LEFT SHOULDER
C DSR : WIDTH(A/P) OF RIGHT SHOULDER
C X1  : STERNUM COORDINATES
C X2  : LEFT SHOULDER JOINT
C X3  : RIGHT SHOULDER JOINT
C XS  : MID-POINT OF SHOULDER
C B   : D.C. MATRIX OF SHOULDER
C T   : TEST FOR ORTHOGONALITY OF MATRIX
C
      DIMENSION XJ(3,28),XS(3),X1(3),X2(3),X3(3),B(3,3),BL(3)
      COMMON/JOINT/XJ
C
      DO 1 I=1,3
      X1(I)=XJ(I,MA1)
      X2(I)=XJ(I,MA2)
      X3(I)=XJ(I,MA3)
    1 CONTINUE
      DO 3 I=1,3
      XS(I)=(X3(I)+X2(I))/2
    3 CONTINUE
      XS(2)=X1(2)
      D32=DIST(X3,X2)
      D1S=DIST(X1,XS)
      DO 2 I=1,3
      B(3,I)=(X3(I)-X2(I))/D32
      BL(I)=(X1(I)-XS(I))/D1S
    2 CONTINUE
C
      BP=B(3,3)*BL(1)-B(3,1)*BL(3)
      PX=(B(3,2)*BL(3)-B(3,3)*BL(2))
      PZ=(B(3,1)*BL(2)-B(3,2)*BL(1))
      DP=SQRT(BP**2+PX**2+PZ**2)
      B(2,2)=BP/DP
      B(2,1)=PX/DP
      B(2,3)=PZ/DP
C
      BL=(B(3,3)*B(2,2)-B(3,2)*B(2,3))
      SY=(B(3,1)*B(2,3)-B(2,1)*B(3,3))
      SZ=(B(2,1)*B(3,2)-B(2,2)*B(3,1))
      DS=SQRT(BL**2+SY**2+SZ**2)
      B(1,1)=BL/DS
      B(1,2)=SY/DS
      B(1,3)=SZ/DS
C
```

```
C LOCATING ACTUAL SHOULDER JOINT CENTRES
C
      DO 4 I=1,2
      X2(I)=X2(I)-((DSL/2)*B(2,I))
      X3(I)=X3(I)-((DSR/2)*B(2,I))
    4 CONTINUE
C
C CHECK FOR ORTHOGONALITY OF MATRIX
C
      CALL CHECK(B,T)
      RETURN
      END
C
C ***********************************
      SUBROUTINE MATP(V,W,C,MI,MJ,MK)
C ***********************************
C
C PERFORMS C(MI,MJ)=V(MI,MK)*W(MK,MJ)
C IMPORTANT :// C,V,W SHOULD BE DIMENSIONED IN
C   THE CALLING PROGRAM AS (3*3) ARRAYS.//
C
      DIMENSION C(MI,MJ),V(MI,MK),W(MK,MJ)
      DO 71 I=1,MI
      DO 71 J=1,MJ
      CC=0.0
      DO 72 K=1,MK
      CC=CC+V(I,K)*W(K,J)
   72 CONTINUE
      C(I,J)=CC
   71 CONTINUE
      RETURN
      END
C
C ***************************
      SUBROUTINE CHECK(E,TO)
C ***************************
C
C TO CHECK FOR ORTHOGONALITY OF DC MATRIX
C CALCULATES THE DETERMINANT OF THE MATRIX
C
      DIMENSION E(3,3)
      TA=B(1,1)*(B(2,2)*E(3,3)-E(3,2)*B(2,3))
      TB=B(2,1)*(B(1,2)*E(3,3)-B(3,2)*E(1,3))
      TC=B(3,1)*(E(1,2)*E(2,3)-B(2,2)*E(1,3))
      TO=TA-TB+TC
      RETURN
      END
C
C ************************
      FUNCTION DIST (A,B)
C ************************
C
C CALCULATES DISTANCE BETWEEN TWO POINTS
C
      DIMENSION A(3),B(3)
      DIMENSION R(3)
      D=0.0
      DO 107 I=1,3
      R(I)=(B(I)-A(I))**2
      D=D+R(I)
  107 CONTINUE
      DIST=SQRT(D)
      RETURN
      END
      FINISH
```

Listings of job control macro "RUNKNTS"

and program "KINEMATICS"

```
DOCUMENT   RUNKMTS

        0 SP N ,(%A)(1,8)
        1 SP V ,(%A)(11,12)
        2 SP M ,(%A)(1,2)
        3 SP T ,(%A)(5)
        4 LO B INKMTS
        5 TIME 4MINS
        6 AS * CR0,%A
        7 AS * CR1,%NSTZV
        8 AS * CP0,%NVEZV
        9 AS * CP1,%NACZV
       10 AS * CP2,%NAVZV
       11 AS * CP3,%NAAZV
       12 AS * LP0,%NLKZV
       13 RUN
       14 LF %NLKZV,*LP,NL
       15 ER %NLK%V
       16 IF HALTED-(AH)-(R=DELETED-(CO),GO TO 5.OKAY
       17 GO TO 5.NOTOKAY
       18 5.OKAY
       19 RJ TELEKN%M%TZV,RUNKNTS,PARAM(%A),HLS(JI 3MINS)
       20 ER %NCD%V
       21 ER %NPX%V
       22 ER %NER%V
       23 ER %NBM%V
       24 DP 0,STAGE(5) EXECUTED SUCCESSFULLY,
       25 EJ
       26 5.NOTOKAY
       27 DP 0,ERROR IN STAGE(5) - PLEASE CHECK,
       28 EJ NONE,RT(CHECKKMTS)
       29 ****
       30 DG
```

```
C
      PROGRAM (KINEMATICS)
      INPUT 2=CF0
      INPUT 3=CR1
      OUTPUT 4=CPC
      OUTPUT 5=CP1
      OUTPUT 6=CP2
      OUTPUT 7=CP3
      OUTPUT 8=LP4
      TRACE 2
      END
C
C
C  INPUT AND OUTPUT CHANNELS FOR PROC.KINEMATICS
C  I/P - 2 - JOINT COORDINATES
C  I/P - 3 - 'DC' MATRIX OF SEGMENT
C  O/P - 4 - LINEAR VELOCITY
C  O/P - 5 - LINEAR ACCELERATION
C  O/P - 6 - ANGULAR VELOCITY
C  O/P - 7 - ANGULAR ACCELERATION
C  O/P - 8 - DATA CHECK-PAR./*IN. VALUES
C
C
C  STAGE (S) ..... ADOPTED BY JAPES.GCH,BIDENG. UNIT
C
C  THIS PROGRAM CALCULATES THE LINEAR VELOCITIES AND ACCELERATION
C  OF THE JOINT CENTRES AND ALSO THE ANGULAR VELOCITIES AND
C  ACCELERATION OF THE SEGMENTS . ALL RESULTS ARE EXPRESSED RELATIVE
C  TO THE GROUND REFERENCE
C
C  **************************
      PASTER KINEMATICS
C  **************************
C
C  FOR NOMENCLATURE ,PLEASE SEE PREVIOUS PROGRAMS LISTING
C  ******************************************************
C
      DIMENSION L(90),AC(90),DX(3,90),DE(3,3,90)
      DIMENSION C(3,3),V(3,3),A(3,3)
      DIMENSION X(3,90),P(3,3,90),XD(3,90),WD(3,3,90)
      DIMENSION R(9),POS(90),VEL(90),T(3,3),TD(3,3),C*(3)
      DIMENSION CPE(3,90),OMED(3,90),ACC(90),ACE(90),AC(3,90)
C
C  READING IN HEADER INFORMATION FROM FILES JOINT COORDINATES AND
C  SEGMENT MATRICES GENERATED FROM PREVIOUS STAGE OF PROGRAMMING.
C  WRITING OUT USEFUL INFO. IN OUTPUT FILES
C  K - INTEGER ARRAY CONTAINING HEADER INFORMATION
C
      READ(2,1)HGROUP,NAPP,NPTNT,NRUN,NCASE,PAPAR,JMAX,JLMAX,JRMAX
      READ(3,1)K
      WRITE(4,2)K
      WRITE(5,2)K
      WRITE(6,2)K
      WRITE(7,2)K
C
C  JDMAX  - MAX. NUMBER OF FRAMES AFTER 1ST DERIVATION
C  JKMAX  - MAX. NUMBER OF FRAMES AFTER 2ND DERIVATION
C  DEL    - DATA SAMPLING INTERVAL(IN SEC)
      JDMAX=JMAX-4
      JKMAX=JMAX-2
      DEL=0.02
      WRITE(8,40)
C
C  SOLUTION OF VELOCITIES DATA
C
      DO 3 JNTS=1,14
      READ(2,10)((X(I,J),I=1,3),J=1,JMAX)
      WRITE(8,29)
      DO 5 I=1,3
      DO 6 J=1,JMAX
      POS(J)=X(I,J)
    6 CONTINUE
      CALL DIF(DEL,POS,JMAX,JDMAX,VEL)
      NMAX=0
      NMIN=0
      DO 7 JD=1,JDMAX
      XD(I,JD)=VEL(JD)
      NREF=IFIX(POS(JD))
      IF(NREF.GT.NMAX)GOTO 25
      IF(NREF.LT.NMIN)GOTO 24
      GOTO 7
   25 NMAX=NREF
      JD1=JD
      GOTO 7
   24 NMIN=NREF
      JD2=JD
    7 CONTINUE
      WRITE(8,20)JNTS,I,JD1,VEL(JD1),JD2,VEL(JD2)
    5 CONTINUE
      WRITE(4,18)((XD(I,JD),I=1,3),JD=1,JDMAX)
C
C  SOLUTION OF ACCELERATION DATA
C
```

```
      WRITE(8,22)
      DO 100 I=1,3
      DO 101 JD=1,JDMAX
      VEL(JD)=BB(I,JD)
100   CONTINUE
      CALL DIF(EEL,VEL,JDMAX,JKMAX,ACE)
      NMAX=0
      NMIN=0
      DO 102 JK=1,JKMAX
      AC(I,JK)=ACE(JK)
      NREF=IFIX(100*ACE(JK))
      IF(NREF.GT.NMAX)GOTO 27
      IF(NREF.LT.NMIN)GOTO 28
      GOTO 102
27    NMAX=NREF
      JK1=JK
      GOTO 102
28    NMIN=NREF
      JK2=JK
102   CONTINUE
      WRITE(8,20)JNTS,I,JK1,ACE(JK1),JK2,ACE(JK2)
101   CONTINUE
      WRITE(5,18)((AC(I,JK),I=1,2),JK=1,JKMAX)
3     CONTINUE
C
C  DIFFERENTIATING D.C. MATRICES
C
      WRITE(8,41)
      DO 15 NSEG=1,8
      READ(3,10)(((B(I,IJ,J),IJ=1,3),I=1,3),J=1,JMAX)
      DO 14 I=1,3
      DO 11 IJ=1,3
      DO 12 J=1,JMAX
      POS(J)=B(I,IJ,J)
12    CONTINUE
      CALL DIF(EEL,POS,JMAX,JDMAX,VEL)
      DO 13 JD=1,JDMAX
      BD(I,IJ,JD)=VEL(JD)
13    CONTINUE
11    CONTINUE
14    CONTINUE
C
C  SOLUTION FOR ANG VELOCITY
C
      DO 17 JD=1,JDMAX
      JJ=JD+2
      DO 16 I=1,3
      DO 15 IJ=1,3
      T(I,IJ)=B(I,IJ,JJ)
      TD(I,IJ)=BD(I,IJ,JD)
16    CONTINUE
      CALL OMEGA(T,TD,OM)
      DO 50 IK=1,3
50    OME(IK,JD)=OM(IK)
17    CONTINUE
      WRITE(6,18)((OME(IK,JD),IK=1,3),JD=1,JDMAX)
C
C  SOLUTION FOR ANG ACCELERATION
C
      DO 51 IK=1,3
      NMAX=0
      NMIN=0
      DO 52 JJ=1,JDMAX
      VEL(JJ)=OME(IK,JJ)
      NREF=IFIX(100*VEL(JJ))
      IF(NREF.GT.NMAX)GOTO 29
      IF(NREF.LT.NMIN)GOTO 30
      GOTO 52
29    NMAX=NREF
      JJ1=JJ
      GOTO 52
30    NMIN=NREF
      JJ2=JJ
52    CONTINUE
      WRITE(8,24)
      WRITE(8,20)NSEG,IK,JJ1,VEL(JJ1),JJ2,VEL(JJ2)
      CALL DIF(EEL,VEL,JDMAX,JKMAX,ACC)
      NMAX=0
      NMIN=0
      DO 53 JJ=1,JKMAX
      OMED(IK,JJ)=ACC(JJ)
      NREF=IFIX(100*ACC(JJ))
      IF(NREF.GT.NMAX)GOTO 31
      IF(NREF.LT.NMIN)GOTO 32
      GOTO 53
31    NMAX=NREF
      JJ1=JJ
      GOTO 53
32    NMIN=NREF
      JJ2=JJ
53    CONTINUE
      WRITE(8,24)
      WRITE(8,20)NSEG,IK,JJ1,ACC(JJ1),JJ2,ACC(JJ2)
51    CONTINUE
      WRITE(7,18)((OMED(IK,JJ),IK=1,3),JJ=1,JKMAX)
15    CONTINUE
```

```
    1 FORMAT(9I1)
    2 FORMAT(1H ,9I3)
   10 FORMAT(3F10.0)
   11 FORMAT(1H ,3F16.8)
   20 FORMAT(1X,3I5,F10.3,I5,F10.3)
   21 FORMAT(10H LIN. VEL.)
   22 FORMAT(12H LIN. ACCEL.)
   23 FORMAT(10H ANG. VEL.)
   24 FORMAT(12H ANG. ACCEL.)
   40 FORMAT(2X,6HJNTS,5H AXIS,3X,7HMAXIMUM,8X,7HMINIMUM)
   41 FORMAT(2X,6HNSEG,5H AXIS,3X,7HMAXIMUM,8X,7HMINIMUM)
      STOP
      END
C
C ****************************************
      SUBROUTINE DIF(DELTA,U,NA,NAD,AD)
C ****************************************
C
C THIS SUBROUTINE PERFORMS THE NUMERICAL DIFFERENTIATION
C TO OBTAIN VELOCITY OR ACCELERATION
C
C U    -ARRAY TO BE DIFFERENTIATED; DIMENSION = NA;
C        ARRAY SHOULD ALSO BE DIMENSIONED AT THE CALLING SEGMENT.
C AD   -THE RESULTING ARRAY; DIMENSION = NAD = NA-4
C        ARRAY SHOULD ALSO BE DIMENSIONED AT THE CALLING SEGMENT.
C DELTA-SAMPLING TIME INTERVAL
C
C
      DIMENSION U(NA),AD(NAD),B(5)
      DO 1 I=1,NAD
      DO 2 J=1,5
      K=I+J-1
      B(J)=U(K)
    2 CONTINUE
      AD(I)=(B(1)-8.0*B(2)+8.0*B(4)-B(5))/(12.0*DELTA)
    1 CONTINUE
      RETURN
      END
C
C ****************************************
      SUBROUTINE OMEG(TM,TMDOT,OMEGA)
C ****************************************
C
C
C SUBROUTINE SOLVES FOR THE ABSOLUTE ANGULAR VELOCITY - OMEGA
C IN TERMS OF THE FIXED  SYSTEM OF COORDINATES
C
C SUBROUTINE CALLS FOR MATM
C
C TM     - GIVEN TRANSFORMATION MATRIX (V(FIXED)=TM*V(MOVING))
C TMT    - TRANSPOSE OF TRANSFORMATION MATRIX(TM)
C TMDOT  - GIVEN DERIVATIVE OF MATRIX TM.
C
C
      DIMENSION TM(3,3),TMDOT(3,3),OMEGA(3)
      DIMENSION TMT(3,3),B(3,3)
      DIMENSION C(3,3),V(3,3),W(3,3)
      DIMENSION D(3,3)
C
C TRANSPOSING THE TRANSFORMATION MATRIX
C
      DO 1 I=1,3
      DO 1 J=1,3
      TMT(J,I)=TM(I,J)
    1 CONTINUE
C
C D=TMDOT*TMT
      CALL MATM(TMDOT,TMT,D,3,3,3)
C
C  OMEGA EXPRESSED IN THE FIXED SYSTEM.
      OMEGA(1)=D(3,2)
      OMEGA(2)=D(1,3)
      OMEGA(3)=D(2,1)
      RETURN
      END
C
C ****************************************
      SUBROUTINE MATM(V,W,C,MI,MJ,MK)
C ****************************************
C
C PERFORMS C(MI,MJ)=V(MI,MK)*W(MK,MJ)
C IMPORTANT :// C,V,W SHOULD BE DIMENSIONED IN
C    THE CALLING PROGRAM AS (3*3) ARRAYS. //
C
      DIMENSION C(MI,MJ),V(MI,MK),W(MK,MJ)
      DO 71 I=1,MI
      DO 71 J=1,MJ
      CC=0.0
      DO 72 K=1,MK
      CC=CC+V(I,K)*W(K,J)
   72 CONTINUE
      C(I,J)=CC
   71 CONTINUE
      RETURN
      END
```

Listings of job control macro "RUNKNTS"

and program "KINETICS"

```
DOCUMENT   RUNKNTS
        C SP N,(%A)(1,8)
        1 SP V,(%A)(11,12)
        2 SP U,(%A)(12)
        3 SP M,(%A)(1,2)
        4 SP I,(%A)(5)
        5 LO BINKNTS
        6 TIME 3MINS
        7 AS *CRC,%NPT%V
        8 AS *CR1,%A
        9 AS *CR2,%NST%V
       1C AS *CR3,%NAC%V
       11 AS *CR4,%NAV%V
       12 AS *CR5,%NAA%V
       13 AS *CR6,%NVE%V
       14 AS *TRC,%NDL1%U
       15 AS *TR1,%NDR1%U
       16 AS *LPC,%NFO%V
       17 AS *LP1,%NMO%V
       18 AS *LP2,%NEN%V
       19 RUN
       2C IF HALTED (AH) (F DELETED (DU),GOTO 6.OKAY
       21 GOTO 6.NOTOKAY
       22 6.OKAY
       23 RJ TELEMX%M%T%V,FUNMXPT,PARAM(%NMO%V)
       24 RJ TELEMY%M%T%V,FUNMYPT,PARAM(%NMO%V)
       25 RJ TELEMZ%M%T%V,FUNMZPT,PARAM(%NMO%V)
       26 RJ TELEFX%M%T%V,RUNFCPTX,PARAM(%NFO%V)
       27 RJ TELEFY%M%T%V,RUNFCPTY,PARAM(%NFO%V)
       28 RJ TELEFZ%M%T%V,RUNFCPTZ,PARAM(%NFO%V)
       29 RJ TELEEN%M%T%V,RUNENERGY,PARAM(%NEN%V)
       3C DP D,STAGE(6) EXECUTED SUCCESSFULLY,
       31 ER %NVE%V
       32 ER %NAC%V
       33 ER %NAA%V
       34 ER %NPT%V
       35 ER %NAV%V
       36 EJ
       37 6.NOTOKAY
       38 DP D,ERROR IN STAGE(6) - PLEASE CHECK,
       39 EJ NONE,RT(CHECKPNTS)
       4C ****
       41 DG
```

```
      PROGRAM(KINETICS)
      INPUT 1=CR0
      INPUT 2=CR1
      INPUT 3=CR2
      INPUT 4=CR3
      INPUT 5=CR4
      INPUT 6=CR5
      INPUT 7=CR6
      INPUT 8=TR0
      INPUT 9=TR1
      OUTPUT 10=LP0
      OUTPUT 11=LP1
      OUTPUT 12=LP2
      TRACE 2
      END
C
C INPUT AND OUTPUT CHANNELS FOR PROG. KINETICS
C I/P 1 - PATIENT'S INFORMATION
C I/P 2 - JOINT COORDINATES
C I/P 3 - "DC" MATRIX OF SEGMENT
C I/P 4 - LINEAR ACCELERATION
C I/P 5 - ANGULAR VELOCITY
C I/P 6 - ANGULAR ACCELERATION
C I/P 7 - LINEAR VELOCITY
C I/P 8 - FORCE PLATE ONE(LEFT)
C I/P 9 - FORCE PLATE TWO(RIGHT)
C O/P 10 - GROUND FORCE
C O/P 11 - JOINT MOMENT
C O/P 12 - ENERGY LEVEL OF SEGMENT
C
C
C STAGE (6) ............ ADOPTED BY JAMES GOH,BIOENG. UNIT
C
C THIS PROGRAM PERFORMS THE FOLLOWING FUNCTION :-
C     1.) CALCULATES THE EXTERNAL FORCES AND MOMENTS AT THE
C         HIP,KNEE AND ANKLE JOINTS OF BOTH LEGS
C     2.) CALCULATES THE ENERGY LEVEL   OF THE
C         THIGH,SHANK AND FOOT OF BOTH LEGS
C
C ***************************
C        MASTER KINETICS
C ***************************
C
C
C NOMENCLATURE
C ************
C JOINT INDEXING: AJ - 1,4 ; KJ - 2,5 ; HJ - 3,6
C NPTNT - PATIENT NO.
C NRUN  - TEST RUN NO.
C JMAX  - TOTAL NO. OF FILM FRAMES
C JDS   - NO. OF FRAMES IN SECOND DERIVATIVE
C JD    - NO. OF FRAMES IN FIRST DERIVATIVE
C JLMAX - TOTAL NO. OF FRAMES FOR LEFT WALKING CYCLE
C JRMAX - TOTAL NO. OF FRAMES FOR RIGHT WALKING CYCLE
C NGROUP   - AMPUTATION LEVEL: 0-NORMAL;1-B/K;2-A/K
C NAMP  - AMPUTATED SIDE: 0-NORMAL;1-LEFT;2-RIGHT
C TOTM  - TOTAL BODY MASS
C SHOE  - SHOE MASS
C SEGM  - SEGMENT MASS
C FINT,SINT,TINT -INERTIA OF PROSTHETIC FOOT,SHANK,THIGH
C FMAS,SMAS,TMAS -MASS OF PROSTHETIC FOOT,SHANK,THIGH
C FDCM,SDCM,TDCM -C.M. OF PROSTHETIC FOOT,SHANK,THIGH
C X,X1  - JOINT COORD. AT A PARTICULAR FRAME
C R,R1  - JOINT POSITION (PROXIMAL/DISTAL)
C A,A1  - ABS. ACCELERATION(PROXIMAL/DISTAL)
C V,V1  - LINEAR VELOCITY (PROXIMAL/DISTAL)
C RF    -POSITION OF IND. F.P. CENTRE TO CENTRE OF OVERALL
C            F.P. SYSTEM
C B     - "DC" MATRIX OF SEGMENT
C LOAD  - ARRAY CONTAINING THE 3 COMPONENTS OF JOINT FORCE
C            AT JDS FRAMES
C TORQ  - ARRAY WITH THE 3 JOINT MOMENT
C
C
      INTEGER AMP,SIDE
      REAL LOAD
      DIMENSION RL(9),R(3,3),RT(3,3),F(3),Z1(3),AD(3),
     1CRACT(3),FM1(3),FM(3),FM2(3),FM3(3),TK(3),FD(3),
     2W(3),WD(3),P(3,85),R1(3,85),A(3,85),A1(3,85),
     3AD1(3),P1(3,85),VA(85),TC(3),AJ(3),TO(3),LOAD(3,85),
     4WDP(3),WDM(3),DMP(3),DMM(3),FA1(3,85),FA2(3,85),
     5TORQ(3,85),V(3,85),V1(3,85),V2(3),VD1(3),V6(3),
     6PV1(3,85),PV2(3,85),TE(85),RF(3,85),
     7P1(3,85),BA(3),TK1(3),PF(3),GM(3,85),DV(3),
C
C READING INFORMATION FILE
C
      READ(1,2)TOTM,SHOE
      READ(1,3)FINT,FMAS,FDCM
      READ(1,3)SINT,SMAS,SDCM
      READ(1,3)TINT,TMAS,TDCM
    2 FORMAT(2F0.0)
    3 FORMAT(3F0.0)
```

391a

```
C
C  READING IN HEADER INFO. FROM FORCE PLATE FILES
C
      CALL HEAD(2,JL)
      CALL HEAD(6,JRR)
C
C  READING IN FIRST ROW FROM ALL OTHER FILES
C
      READ(2,5)(GROUP,NAMP,NPTNT,NRUN,NCASE,MAMAX,JMAX,
     *JLMAX,JRMAX
      READ(3,5)PL
      READ(4,5)PL
      READ(5,5)PL
      READ(6,5)PL
      READ(7,5)PL
      JD=JMAX-4
      JDD=JMAX-8
      JR=JDD-JRR
      WRITE(10,7)NPTNT,NRUN,JDD,JLMAX,JRMAX,TOTM
      WRITE(11,7)NPTNT,NRUN,JDD,JLMAX,JRMAX,TOTM
      WRITE(12,7)NPTNT,NRUN,JDD,JLMAX,JRMAX,TOTM
C
    5 FORMAT(9I0)
    7 FORMAT(1H ,5I5,F7.4)
      GOTO 101
  100 KKLL=1
C
C  STARTING TO READ FOOT POSITION(P1,P2)
C  AND ACCELERATION (FA1,FA2)
C
  101 DO 30 K=1,4
   30 READ(2,10)(DX(I),I=1,3)
      READ(2,10)((P1(I,J),I=1,3),J=1,JDD)
      READ(4,10)((FA1(I,J),I=1,3),J=1,JDD)
      DO 31 K=1,8
   31 READ(2,10)(DX(I),I=1,3)
      READ(2,10)((P2(I,J),I=1,3),J=1,JDD)
      READ(4,10)((FA2(I,J),I=1,3),J=1,JDD)
C
C  READING ANKLE POSITION(R1) AND ACCELERATION(A1)
C
      DO 32 K=1,8
   32 READ(2,10)(DX(I),I=1,3)
      READ(2,10)((R1(I,J),I=1,3),J=1,JDD)
      READ(4,10)((A1(I,J),I=1,3),J=1,JDD)
      DO 33 K=1,4
   33 READ(2,10)(DX(I),I=1,3)
C
C  READING VELOCITIES OF FOOT(FV1,FV2) AND ANKLE(V1)
      DO 34 K=1,2
   34 READ(7,10)(DX(I),I=1,3)
      READ(7,10)((FV1(I,J),I=1,3),J=1,JDD)
      DO 35 K=1,4
   35 READ(7,10)(DX(I),I=1,3)
      READ(7,10)((FV2(I,J),I=1,3),J=1,JDD)
      DO 36 K=1,4
   36 READ(7,10)(DX(I),I=1,3)
      READ(7,10)((V1(I,J),I=1,3),J=1,JDD)
      DO 37 K=1,2
   37 READ(7,10)(DX(I),I=1,3)
   10 FORMAT(3F8.4)
C
C  CONVERTING ALL DIMENSION TO METRE
C
      DIS=1.0
      DO 38 I=1,3
      DO 38 J=1,JDD
      P1(I,J)=P1(I,J)/1000.0
      P2(I,J)=P2(I,J)/1000.0
      FA1(I,J)=FA1(I,J)/1000.0
      FA2(I,J)=FA2(I,J)/1000.0
      FV1(I,J)=FV1(I,J)/1000.0
      FV2(I,J)=FV2(I,J)/1000.0
      R1(I,J)=R1(I,J)/1000.0
      A1(I,J)=A1(I,J)/1000.0
      V1(I,J)=V1(I,J)/1000.0
   38 CONTINUE
C
C  IF ANALYSING THE RIGHT FOOT GOTO LINE 102
C
      IF(KKLL.EQ.1)GOTO 102
C
C  STARTING TO SCAN JOINTS AND EXECUTE DYNAMIC
C  ANALYSIS
      DO 200 JOINT=1,6
      IF(JOINT.EQ.1)GOTO 102
      IF(JOINT.EQ.4)GOTO 150
      IF(JOINT.EQ.2.OR.JOINT.EQ.5)GOTO 151
C
C  TRANSCRIBING PROXIMAL TO DISTAL POSITION
C
      DO 39 J=1,JDD
      DO 39 I=1,3
      R1(I,J)=R(I,J)
      A1(I,J)=A(I,J)
      V1(I,J)=V(I,J)
   39 CONTINUE
      GOTO 151
C
```

```
C  ANTHROPOMETRY OF FOOT
C  **********************
C
   100 CALL ANTHRO(S1,P1,TOTP,SFOOT,SHOE,JOINT,NMAGUP,
      1NAMP,AA,BB,CC,T,DIS,FINT,FMAS,FDCM,JDD)
C
C  PREPARATION FOR DYNAMIC ANALYSIS
C
C  READING DC MATRIX(B),ANG. VEL.(W),ANG. ACC.(WD)
C
      DO 40 K=1,4
   40 READ(3,10)((B(I,J),J=1,3),I=1,3)
      DO 41 K=1,2
   41 READ(5,10)(W(I),I=1,3)
C  FRAME BY FRAME CALCULATION OF EXTERNAL LOAD
C
      DO 150 J=1,JDD
      READ(3,10)((B(I,IJ),IJ=1,3),I=1,3)
      READ(5,10)(W(I),I=1,3)
      READ(6,10)(WD(I),I=1,3)
      IF(JOINT.EQ.4)GOTO 43
      IF(J.GT.JL)GOTO 44
C
C  READING GROUND REACTION AND CENTRE OF PRESSURE(GRACT)
C
      READ(8,12)(GRACT(I),I=1,2)
      Z=-1.0
   12 FORMAT(2F6.3)
      GOTO 45
   43 IF(J.LE.JR)GOTO 44
      READ(9,12)(GRACT(I),I=1,2)
      Z=1.0
   45 FK1(1)=GRACT(1)
      FK1(2)=GRACT(2)
      FK1(3)=GRACT(3)
      RF(1)=Z*0.2
      RF(2)=-0.04
      RF(3)=Z*0.11
      CALL XPROD(RF,FK1,TK1)
      TK(1)=GRA(I(4)*TK1(1)
      TK(2)=GRA(I(5)*TK1(2)
      TK(3)=GRA(I(6)*TK1(3)
      GOTO 46
   44 DO 47 I=1,3
      FK1(I)=0.0
      TK(I)=0.0
   47 CONTINUE
C
C  CALCULATE C.G. POSITION(RG) AND ACCELERATION(AG)
C  AND VELOCITY(VG)
C
   46 DO 52 I=1,3
      RK1(I)=-R1(I,J)
      X(I)=P1(I,J)
      RA(I)=R1(I,J)
      RG(I)=X(I)+(1.0-(T/DIS))*(T/DIS)**A(I)
      AD(I)=FA1(I,J)
      AD1(I)=A1(I,J)
      AG(I)=AD(I)+(1.0-(T/DIS))*(T/DIS)*AD1(I)
      VA(I)=V1(I,J)
      VD(I)=FV1(I,J)
      VG(I)=VD(I)+(1.0-(T/DIS))*(T/DIS)*V0(I)
   52 CONTINUE
C
C  CALCULATION OF LOAD AT THE ANKLE JOINT
C  **************************************
C
      CALL DYNAMICS(RA,RG,AD,AG,B,W,WD,SEGM,AA,BB,CC,
     1FK1,RK1,TK,FO,TO)
C
C  CALCULATION OF ENERGY LEVEL(TE) AT FOOT
C
      VE=0.5*SEG**(VG(1)**2+VG(2)**2+VG(3)**2)
      TW=0.5*(AA*W(1)**2+BB*W(2)**2+CC*W(3)**2)
      TE(J)=SEG*9.81*RG(2)+TW+VE+TA
      DO 53 I=1,3
      EF(I,J)=FO(I)
      EM(I,J)=TO(I)
      LOAD(I,J)=FO(I)
      TORQ(I,J)=TO(I)
   53 CONTINUE
  150 CONTINUE
      WRITE(10,15)(((GF(I,J),I=1,3),J=1,JDD)
      WRITE(11,15)(((TORQ(I,J),I=1,3),J=1,JDD)
      WRITE(12,13)SEGM
      WRITE(12,14)(TE(J),J=1,JDD)
   15 FORMAT(1H ,3F10.3)
   16 FORMAT(1X,7(F10.4,1X))
   17 FORMAT(1X,80A1)
      DO 54 K=1,4
   54 READ(3,10)((B(I,J),J=1,3),I=1,3)
      DO 55 K=1,2
   55 READ(5,10)(W(I),I=1,3)
      IF(JOINT.EQ.1.OR.JOINT.EQ.4)GOTO 60
  151 DO 56 K=1,4
   56 READ(2,10)(DX(I),I=1,3)
```

```
      READ(2,10)((R(I,J),I=1,3),J=1,JDD)
      READ(4,10)((A(I,J),I=1,3),J=1,JDD)
      DO 57 K=1,4
   57 READ(2,10)(DX(I),I=1,3)
      DO 58 K=1,2
   58 READ(7,10)(DX(I),I=1,3)
      READ(7,10)((V(I,J),I=1,3),J=1,JDD)
      DO 59 K=1,2
   59 READ(7,10)(DX(I),I=1,3)
      DO 61 I=1,3
      DO 62 J=1,JDD
      R(I,J)=R(I,J)/100.0
      A(I,J)=A(I,J)/100.0
      V(I,J)=V(I,J)/100.0
   60 CONTINUE
      IF(JCINT.EQ.3.OR.JCINT.EQ.6)GOTO 107
C
C.ANTHROPOMETRY OF SHANK AND FOOT
C ***********************************
C
      CALL ANTHRO(R,R1,TOTM,SEGM,SHOE,JOINT,AGROUP,
     1NAPP,AA,BB,CC,T,DIS,SINT,SMAS,SDCM,JDD)
      GOTO 108
C
C ANTHROPOMETRY OF THIGH
C ***********************
C
  107 CALL ANTHRO(R,R1,TOTM,SEGM,SHOE,JOINT,AGROUP,
     1NAPP,AA,BB,CC,T,DIS,TINT,TMAS,TDCM,JDD)
  108 DO 62 K=1,4
   62 READ(3,10)((R(I,J),J=1,3),I=1,3)
      DO 63 K=1,2
   63 READ(5,10)(W(I),I=1,3)
C
      DO 64 J=1,JDD
      READ(3,10)((B(I,IJ),IJ=1,3),I=1,3)
      READ(5,10)(W(I),I=1,3)
      READ(6,10)(WD(I),I=1,3)
      IF(JCINT.EQ.3.OR.JCINT.EQ.6)GOTO 66
      DO 65 I=1,3
      RK1(I)=GF(I,J)
      TK(I)=GM(I,J)
      RK1(I)=2.*(-F(I,J)
   65 CONTINUE
      GOTO 69
   66 DO 68 I=1,3
      RK1(I)=LG(I,J)
      TK(I)=TORG(I,J)
      RK1(I)=R1(I,J)-R(I,J)
   68 CONTINUE
   69 DO 67 I=1,3
      X(I)=R(I,J)
      X1(I)=R1(I,J)
      AG(I)=X1(I)*(1.0-(T/DIS))+(T/DIS)*X(I)
      AD(I)=A(I,J)
      AD1(I)=A1(I,J)
      AG(I)=AD1(I)*(1.0-(T/DIS))+(T/DIS)*AD(I)
      VD(I)=V(I,J)
      VD1(I)=V1(I,J)
      VG(I)=VD1(I)*(1.0-(T/DIS))+(T/DIS)*VD(I)
   67 CONTINUE
C
C CALCULATION OF LOAD AT THE KNEE AND HIP JOINT
C **********************************************
C
      CALL DYNAMICS(X,RG,AD,AG,B,W,WD,SEGM,AA,BB,CC,
     1FK1,RK1,TK,FC,TC)
C
C CALCULATION OF ENERGY LEVEL(TE)  AT
C SHANK AND THIGH
C
      VE=0.5*SEGM*(VG(1)**2+VG(2)**2+VG(3)**2)
      TW=0.5*(AA*W(1)**2+BB*W(2)**2+CC*W(3)**2)
      TE(J)=SEGM*9.81*RG(2)+VE+TW
      DO 71 I=1,3
      LOAD(I,J)=FC(I)
      TORQ(I,J)=TC(I)
   71 CONTINUE
   64 CONTINUE
      WRITE(11,115)((TORQ(I,J),I=1,3),J=1,JDD)
      WRITE(12,117)SEGM
      WRITE(12,116)(TE(J),J=1,JDD)
      DO 73 K=1,4
   73 READ(3,10)((B(I,J),J=1,3),I=1,3)
      DO 74 K=1,2
   74 READ(5,10)(W(I),I=1,3)
  200 CONTINUE
      STOP
      END
C
C ***************************************************************
      SUBROUTINE DYNAMICS(RO,RG,AO,AG,B,WF,WDF,SEGM,AA,BB,
     1CC,FK1,RK1,TK,FC,TC)
```

```
C ******************************************************************
C
C RO,RC     -RADIUS VECTOR OF PROXIMAL JT./C.M.
C AO,AC     -ACCELERATION OF PROX. JT./C.M.
C RT,R      -SEGMENT "DC" MATRIX FIXED/MOVING
C WF,WM     -ANG. ACCELERATION FIXED/MOVING
C WDF,WDM   -DERIVATIVE OF WF AND WM
C DHF,DHM   -ANG MOMENTUM FIXED/MOVING
C SEGM      -SEGMENT MASS
C AA,BB,CC  -PRINCIPAL MOMENTS OF INERTIA ABOUT MOVING AXES
C R1         -POSITN OF DISTAL JT. REL. TO PROXIMAL JT.
C R2         -POSITN OF C.M. OF SEGMENT REL. TO PROXIMAL JT.
C FK1,FK2   -KNOWN FORCES
C TK        -KNOWN TORQUE
C FO        -CAL. NET FORCE AT PROX. JT.
C TO        -CAL. NET TORQUE
C
      DIMENSION RO(3),RC(3),AO(3),AC(3),R(3,3),RT(3,3),
     1R1(3),R2(3),FK1(3),FK2(3),TK(3),FO(3),TO(3),WF(3),
     2WDF(3),WDM(3),DHF(3),DHM(3),RES1(3),RES2(3),RES3(3),
     3WM(3)
C
C TRANSFORMATION OF ANG. VEL. AND ACC INTO MOVING FRAME
C
      DO 2 I=1,3
      DO 2 J=1,3
      RT(J,I)=R(I,J)
    2 CONTINUE
      CALL MATM(RT,WF,WM,3,1,3)
      CALL MATM(RT,WDF,WDM,3,1,3)
C CAL. ANG MOMENTUM VECTOR(DHM) IN MOVING FRAME
C
      DHM(1)=AA*WDM(1)-(BB-CC)*WM(2)*WM(3)
      DHM(2)=BB*WDM(2)-(CC-AA)*WM(3)*WM(1)
      DHM(3)=CC*WDM(3)-(AA-BB)*WM(1)*WM(2)
C TRANSFORMATION OF DHM INTO DHF (FIXED FRAME)
C
      CALL MATM(R,DHM,DHF,3,1,3)
C CAL. LOAD AT C.M.
C
      FK2(1)=0.0
      FK2(2)=9.81*SEGM
      FK2(3)=0.0
C
C THE NET FORCE AT THE PROXIMAL JOINT
      DO 3 I=1,3
      FO(I)=FK1(I)-FK2(I)-(SEGM*AC(I))
    3 CONTINUE
C
C THE NET TORQUE AT THE PROXIMAL JOINT
      DO 4 I=1,3
      R2(I)=RC(I)-RO(I)
    4 CONTINUE
      CALL XPROD(R2,AC,RES1)
      CALL XPROD(R1,FK1,RES2)
      CALL XPROD(R2,FK2,RES3)
      DO 5 I=1,3
      TO(I)=TK(I)-DHF(I)-(SEGM*RES1(I))+RES2(I)-RES3(I)
    5 CONTINUE
      RETURN
      END
C
C ***********************************
      SUBROUTINE MATM(V,W,C,MI,MJ,MK)
C ***********************************
C
      DIMENSION C(MI,MJ),V(MI,MK),W(MK,MJ)
      DO 71 I=1,MI
      DO 71 J=1,MJ
      CC=0.0
      DO 72 K=1,MK
      CC=CC+V(I,K)*W(K,J)
   72 CONTINUE
      C(I,J)=CC
   71 CONTINUE
      RETURN
      END
C
C ***********************************
      SUBROUTINE XPROD(PR1,PR2,RES)
C ***********************************
C
      DIMENSION PR1(3),PR2(3),RES(3)
      RES(1)=PR1(2)*PR2(3)-PR1(3)*PR2(2)
      RES(2)=PR1(3)*PR2(1)-PR1(1)*PR2(3)
      RES(3)=PR1(1)*PR2(2)-PR1(2)*PR2(1)
      RETURN
      END
C
C ******************************************************
      SUBROUTINE ANTHRO(P,R1,TOTM,SEGM,INDI,JOINT,AMP,
     1SIDE,A,B,C,T,S,XINT,XMAS,XCOM,JMAX)
C ******************************************************
C
C COMPUTES MASS PROPERTIES OF LIMB SEGMENTS
```

```
C
C  RO     -RADIUS VECTOR TO PROXIMAL JOINT - DATUM FRAME
C  RO1    -RADIUS VECTOR TO DISTAL JOINT - DATUM FRAME
C  TOTM   -TOTAL BODY MASS
C  SHOE   -MASS OF SINGLE SHOE
C  AMP     -LEVEL OF AMPUTATION
C  SIDE    -SIDE OF AMPUTATION
C  A,B,C  -PRINCIPAL MOMENTS OF INERTIA ABOUT MOVING AXES
C  SEGM   -MASS OF SEGMENT
C  T      -DISTANCE FROM PROX. JOINT TO C.M. OF SEGMENT
C  S      -LENGTH OF SEGMENT
C  C1,C2,C3 -BODY SEGMENT PARAMETERS COEFF.
C             C1 :- MASS COEFF.
C             C2 :- C.M. COEFF
C             C3 :- RAD. OF GYRATION COEFF. (ABOUT C.M.)
C  ICG    -MOMENT OF INERTIA OF SEGMENT ABOUT ITS C.M.
C  IGG    -MOMENT OF INERTIA OF SEGMENT ABOUT ITS
C           PROXIMAL JT. DUE TO CENTRIFUGAL EFFECT
C  IAJ    -MOMENT OF INERTIA OF FOOT ABOUT ANKLE JT.
C  IKJ    -MOMENT OF INERTIA OF SEGMENT ABOUT KNEE JT.
C  DKJCM  -DISTANCE OF KNEE JT. TO C.M OF PROS. SHANK
C  DKJHJ  -DISTANCE BETW. KNEE AND HIP JOINT
C  XINT   -MOMENT OF INERTIA OF PROTHESIS
C  XMAS   -MASS OF PROTHESIS
C  XDCM   -DISTANCE OF C.M. TO PROXIMAL JT
C
      INTEGER AMP,SIDE
      REAL IAJ,IKJ,ICG,IGG
      DIMENSION RO(3),R(3,85),R1(3,85),RO1(3)
      D=S
      S=0.0
      DO 21 J=1,JMAX
      DO 22 I=1,3
      RO(I)=R(I,J)
      RO1(I)=R1(I,J)
   22 CONTINUE
      S=S+DIST(RO,RO1)
   21 CONTINUE
      S=S/JMAX
      IF(JOINT.EQ.1.OR.JOINT.EQ.4)GOTO 1
      IF(JOINT.EQ.2.OR.JOINT.EQ.5)GOTO 2
      IF(JOINT.EQ.3.OR.JOINT.EQ.6)GOTO 3
      WRITE(9,20)
   20 FORMAT(1H ,17HJOINT INDEX ERROR/)
      GOTO 10
C
C  FOOT AND SHOE : ORIGIN: AJ
C
    1 IF(AMP.EQ.0.AND.SIDE.EQ.0)GOTO 4
      IF(JOINT.EQ.1.AND.SIDE.EQ.2)GOTO 4
      IF(JOINT.EQ.4.AND.SIDE.EQ.1)GOTO 4
      IAJ=XINT
      SEGM=XMAS+SHOE
      T=XDCM
      A=IAJ
      B=0.0
      C=A
      GOTO 10
    4 C1=0.0152
      C2=0.500
      C3=0.475
      SM=SHOE
      GOTO 5
C
C
C  SHANK,FOOT AND SHOE ; ORIGIN: KJ
    2 IF(AMP.EQ.0.AND.SIDE.EQ.0)GOTO6
      IF(JOINT.EQ.2.AND.SIDE.EQ.0)GOTO6
      IF(JOINT.EQ.5.AND.SIDE.EQ.1)GOTO6
      IKJ=XINT
      SEGM=XMAS+SHOE
      T=XDCM
      A=IKJ
      B=0.0
      C=A
      GOTO 10
    6 C11=0.0453
      C21=0.403
      C31=0.229
      C12=0.0153
      C22=0.500
      C32=0.475
      SM=SHOE
      SEGM1=(TOTM*C11)
      SEGM2=(TOTM*C12)+SM
      SEGM=SEGM1+SEGM2
      T1=S*C21
      T2=D*C22
      T=((SEGM1*T1)+SEGM2*(T2+S))/SEGM
      ICG=SEGM1*((C31*S)**2)+SEGM2*((C32*D)**2)
      IGG=SEGM1*((T-T1)**2)+SEGM2*((T2+S-T)**2)
      GOTO 8
C
```

```
      C  THIGH ; ORIGIN: MJ
         ! IF(A**.EQ.0.AND.SIDE.EQ.0)GOTO 7
           IF(A**.EQ.0.0)GOTO 7
           IF(JOINT.EQ.1.AND.SIDE.EQ.2)GOTO 7
           IF(JOINT.EQ.6.AND.SIDE.EQ.1)GOTO 7
           IKJ=JOINT
           SEG**=XMAS
           RKJMJ=S
           Y=RKJMJ-SEG**
           A=IKJ*SEGM*(RKJMJ*(RKJMJ-2.0*XBCM)
           R=0.0
           C=A
           GOTO 10
         7 C1=0.1027
           C2=0.4169
           C3=0.2912
           SM=0.0
      C
      C  CALCULATION OF MASS MOMENT OF INERTIA OF SEGMENT
      C
         5 SEGM=(TOT*C1)*SM
           T=S*C2
           IGG=SEGM*((T)**2)
           ICC=SEGM*((S*C3)**2)
           IF(JOINT.EQ.1.OR.JOINT.EQ.6)GOTO 8
           A=IGG+ICC
           B=0.223*ICG
           C=0.9115*ICG+ICG
           GOTO 10
         8 A=IGG+ICC
           B=0.0725*ICG
           C=A
           GOTO 10
         9 A=IGG+ICG
           B=0.1562*ICG
           C=A
        10 KLU=*10
           RETURN
           END
      C
      C  ***********************************
           FUNCTION DIST(A,B)
      C  ***********************************
      C
      C  CAL. DISTANCE BETW. TWO POINTS
      C
           DIMENSION A(3),B(3)
           DIMENSION R(3)
           D=0.0
           DO 107 I=1,3
           R(I)=(B(I)-A(I))**2
           D=D+R(I)
       107 CONTINUE
           DIST=SQRT(D)
           RETURN
           END
      C
      C  ***********************************
           SUBROUTINE HEAD(K,J)
      C  ***********************************
      C
      C  SUBROUTINE TO READ IN HEADER INFO OF FORCE PLATE
      C  FILES
      C
           DIMENSION BIG(5),SMALL(5)
           READ(K,1)HEAD,ICODE,XPAT
           READ(K,2)JHEAD,FLAG
           READ(K,3)BIG,FFA,FREQ,WT
           READ(K,4)ITAMP,IBAMP
           READ(K,3)C
           READ(K,3)ICALEX
           READ(K,4)JHEAD
           READ(K,3)(BIG(I),I=1,5)
           READ(K,3)(SMALL(I),I=1,5)
           READ(K,4)IHEAD
           READ(K,6)ICUTF,ISF
           READ(K,4)IUSER,J
           READ(K,6)IHEAD
         1 FORMAT(IC,F2,A5)
         2 FORMAT(I2,A7)
         3 FORMAT(5F(,,)
         4 FORMAT(3I()
           RETURN
           END
           FINISH
```